Chemical Constituents from the Endophytic Fungi: *Phomopsis* sp. PSU-A56, *Xylaria* sp. PSU-D14 and PSU-D65, *Eutypella scoparia* PSU-D44 and *Botryosphaeria mamane* PSU-M76 and the Wood-decayed Fungi: *Lachnum* sp. BCC 2424 and *Xylaria* sp. BCC 9653

Wipapan Pongcharoen

A Thesis Submitted in Fulfillment of the Requirements for the Degree of
Doctor of Philosophy in Organic Chemistry
Prince of Songkla University
2008

Thesis Title	Chemical Constituents from the Endophytic Fungi: *Phomopsis* sp. PSU-A56, *Xylaria* sp. PSU-D14 and PSU-D65, *Eutypella scoparia* PSU-D44 and *Botryosphaeria mamane* PSU-M76 and the Wood-decayed Fungi: *Lachnum* sp. BCC 2424 and *Xylaria* sp. BCC 9653
Author	Miss Wipapan Pongcharoen
Major Program	Organic Chemistry

Major Advisor

V. Rukachaisirikul.
(Prof. Dr. Vatcharin Rukachaisirikul)

Co-advisor

C. Karalai
(Assoc. Prof. Dr. Chatchanok Karalai)

Examining Committee :

P. Tuntiwachwuttikul ..... Chairperson
(Prof. Dr. Pittaya Tantiwachwuttikul)

V. Rukachaisirikul. ..... Committee
(Prof. Dr. Vatcharin Rukachaisirikul)

C. Karalai ..... Committee
(Assoc. Prof. Dr. Chatchanok Karalai)

K. Panthong ..... Committee
(Assist. Prof. Dr. Kanda Panthong)

The Graduate School, Prince of Songkla University, has approved this thesis as fulfillment of the requirements for the Degree of Doctor of Philosophy in Organic Chemistry

Krerkchai T.

(Assoc. Prof. Dr. Krerkchai Thongnoo)
Dean of Graduate School

ชื่อวิทยานิพนธ์	องค์ประกอบทางเคมีจากเชื้อราเอนโดไฟท์: *Phomopsis* sp. PSU-A56 *Xylaria* sp. PSU-D14 และ PSU-D65 *Eutypella scoparia* PSU-D44 และ *Botryosphaeria mamane* PSU-M76 และเชื้อราที่ย่อยสลายไม้: *Lachnum* sp. BCC 2424 และ *Xylaria* sp. BCC 9653
ผู้เขียน	นางสาววิภาพรรณ พงศ์เจริญ
สาขาวิชา	เคมีอินทรีย์
ปีการศึกษา	2550

บทคัดย่อ

งานวิจัยนี้เป็นการศึกษาองค์ประกอบทางเคมีจากเชื้อราเอนโดไฟท์จำนวน 5 ชนิด ได้แก่ *Phomopsis* sp. PSU-A56 *Xylaria* sp. PSU-D14 และ PSU-D65 *Eutypella scoparia* PSU-D44 และ *Botryosphaeria mamane* PSU-M76 และเชื้อราที่ย่อยสลายไม้จำนวน 2 ชนิด ได้แก่ *Lachnum* sp. BCC 2424 และ *Xylaria* sp. BCC 9653 โดยนำส่วนสกัดหยาบเอทิลอะซิเตทจากน้ำเลี้ยงเชื้อและ/หรือเซลล์ของเชื้อราดังกล่าว มาทำให้บริสุทธิ์ด้วยวิธีทางโครมาโทกราฟีสามารถแยกสารบริสุทธิ์ประเภทต่างๆได้ดังนี้

- สารใหม่ 4 สาร (**N2, N5, N6** และ **N7**) และสารที่มีการรายงานโครงสร้างแล้ว 3 สาร (**N1, N3** และ **N4**) จากส่วนสกัดหยาบน้ำเลี้ยงเชื้อราของ *Eutypella scoparia* PSU-D44
- สารใหม่ 5 สาร (**N9-N13**) และสารที่มีการรายงานโครงสร้างแล้ว 1 สาร (**N8**) จากส่วนสกัดหยาบน้ำเลี้ยงเชื้อราของ *Lachnum* sp. BCC 2424 และสาร **N9, N11** และ **N13** จากส่วนสกัดหยาบเซลล์เชื้อรา
- สารใหม่ 1 สาร (**N19**) และสารที่มีการรายงานโครงสร้างแล้ว 6 สาร (**N14-N18** และ **N20**) จากส่วนสกัดหยาบน้ำเลี้ยงเชื้อราของ *Botryosphaeria mamane* PSU-M76 และสารที่มีการรายงานโครงสร้างแล้ว 1 สาร (**N17**) จากส่วนสกัดหยาบเซลล์เชื้อรา
- สารใหม่ 1 สาร (**N26**) และสารที่มีการรายงานโครงสร้างแล้ว 7 สาร (**N21-N25, N27** และ **N28**) จากส่วนสกัดหยาบน้ำเลี้ยงเชื้อราของ *Xylaria* sp. BCC 9653 และสารที่มีการรายงานโครงสร้างแล้ว 4 สาร (**N29-N32**) จากส่วนสกัดหยาบเซลล์เชื้อรา
- สารใหม่ 2 สาร (**N34** และ **N35**) และสารที่มีการรายงานโครงสร้างแล้ว 2 สาร (**N33** และ **N36**) จากส่วนสกัดหยาบน้ำเลี้ยงเชื้อราของ *Xylaria* sp. PSU-D14

- สารที่มีการรายงานโครงสร้างแล้ว 2 สาร (**N37** และ **N38**) จากส่วนสกัดหยาบน้ำเลี้ยงเชื้อรา ของ *Xylaria* sp. PSU-D65
- สารที่มีการรายงานโครงสร้างแล้ว 5 สาร (**N39-N43**) จากส่วนสกัดหยาบน้ำเลี้ยงเชื้อราของ *Phomopsis* sp. PSU-A56

โครงสร้างของสารทั้งหมดวิเคราะห์โดยใช้ข้อมูลทางสเปกโทรสโกปี โดยเฉพาะ 1D และ 2D NMR สเปกโทรสโกปี และเปรียบเทียบข้อมูลกับสารที่มีการรายงานโครงสร้างแล้ว

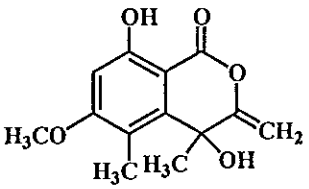

N1

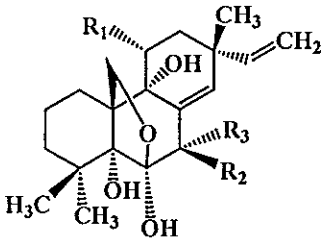

N2: R_1 = H, R_2+R_3 = O
N3: R_1 = OH, R_2+R_3= O
N4: R_1 = OH, R_2 = H, R_3 = OH

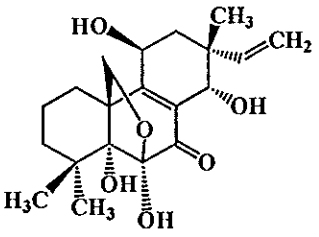

N5

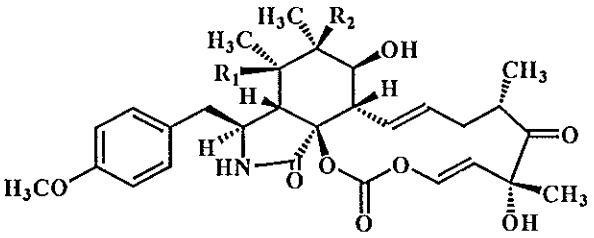

N6: R_1 = H, R_2 = OH
N7: R_1 = R_2 = double bond

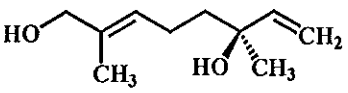

N8

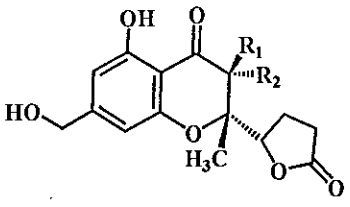

N9: R_1 = H, R_2 = H
N10: R_1 = CH_2COCH_3, R_2 = OH
N11: R_1 = OH, R_2 = H

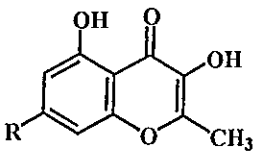

N12: R = CH_3
N13: R = CH_2OH

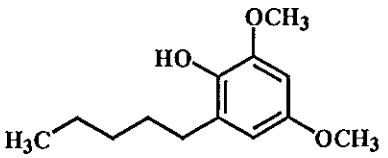

N14

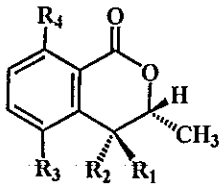

N15: $R_1 = R_2 = R_3 = H$, $R_4 = OH$
N17: $R_1 = R_3 = H$, $R_2 = R_4 = OH$
N18: $R_1 = R_4 = OH$, $R_2 = R_3 = H$
N21: $R_1 = R_2 = R_3 = H$, $R_4 = OCH_3$
N31: $R_1 = R_2 = H$, $R_3 = CO_2H$, $R_4 = OH$
N32: $R_1 = R_2 = H$, $R_3 = R_4 = OH$
N40: $R_1 = R_2 = H$, $R_3 = CO_2CH_3$, $R_4 = OH$

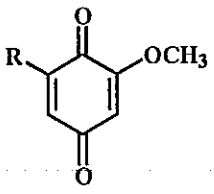

N16: R = pentyl
N41: $R = CH_3$

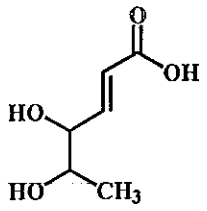

N20

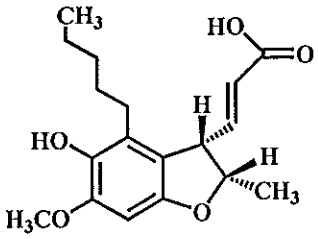

N19

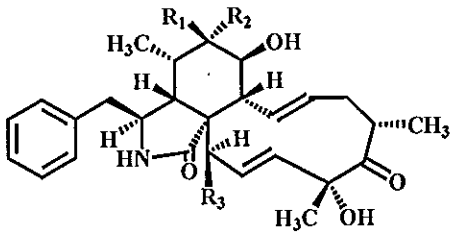

N22: $R_1+R_2 = CH_2$, $R_3 = OAc$
N23: $R_1 = OH$, $R_2 = CH_3$, $R_3 = OAc$
N24: $R_1+R_2 = CH_2$, $R_3 = OH$

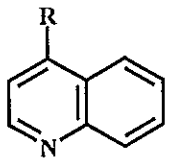

N25: R = CN
N28: R = CH=NOH

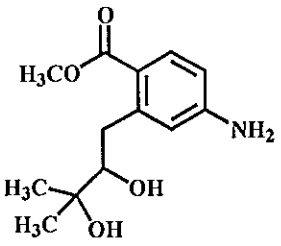

N26

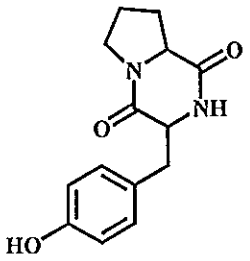

N27

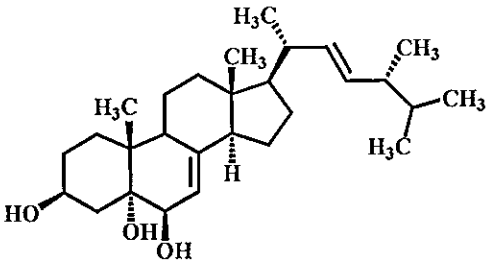

N29

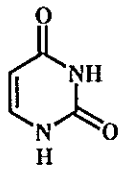

N30

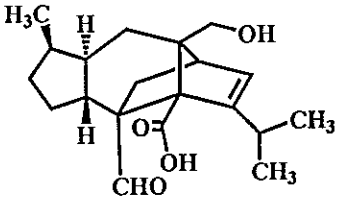

N33

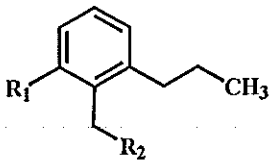

N34: R_1 = OH, R_2 = glu
N35: R_1 = glu, R_2 = OH

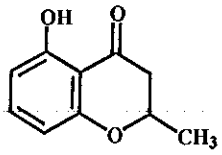

N36

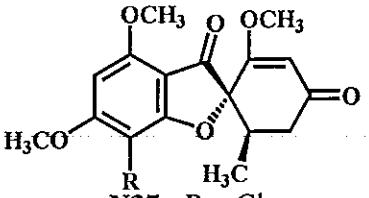

N37: R = Cl
N38: R = H

glu =

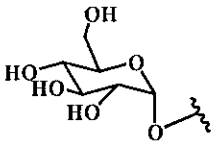

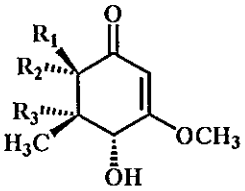

N39: R_1 = H, R_2+R_3 = epoxide
N42: R_1 = R_3 = OH, R_2 = H

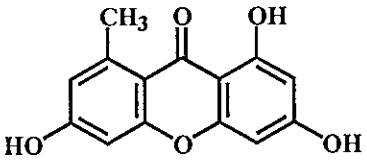

N43

Thesis Title	Chemical Constituents from the Endophytic Fungi: *Phomopsis* sp. PSU-A56, *Xylaria* sp. PSU-D14 and PSU-D65, *Eutypella scoparia* PSU-D44 and *Botryosphaeria mamane* PSU-M76 and the Wood-decayed Fungi: *Lachnum* sp. BCC 2424 and *Xylaria* sp. BCC 9653
Author	Miss Wipapan Pongcharoen
Major Program	Organic Chemistry
Academic Year	2007

ABSTRACT

This work involved chemical investigation of the ethyl acetate extracts from the culture broth and/or mycelia of five endophytic fungi, *Phomopsis* sp. PSU-A56, *Xylaria* sp. PSU-D14 and PSU-D65, *Eutypella scoparia* PSU-D44, and *Botryosphaeria mamane* PSU-M76, together with two wood-decayed fungi: *Lachnum* sp. BCC 2424 and *Xylaria* sp. BCC 9653. Each extract was subjected to various chromatographic techniques. Several types of compounds were isolated as follow.

- Four new (**N2**, **N5**, **N6** and **N7**) and three known (**N1**, **N3** and **N4**) compounds were isolated from the broth extract of *Eutypella scoparia* PSU-D44.
- Five new compounds (**N9-N13**) were isolated along with one known compound (**N8**) from the broth extract of *Lachnum* sp. BCC 2424. Compounds **N9**, **N11** and **N13** were also obtained from the mycelial extract.
- One new compound (**N19**) was isolated together with six known compounds (**N14-N18** and **N20**) from the broth extract of *Botryosphaeria mamane* PSU-M76. One additional known compound (**N17**) was obtained from the mycelial extract.
- One new compound (**N26**) was obtained along with seven known compounds (**N21-N25**, **N27** and **N28**) from the broth extract of *Xylaria* sp. BCC 9653 while four additional known compounds (**N29-N32**) were isolated from the mycelial extract.
- Two new (**N34** and **N35**) and two known (**N33** and **N36**) compounds were isolated from the broth extract of *Xylaria* sp. PSU-D14.

- Two known compounds (**N37** and **N38**) were obtained from the broth extract of *Xylaria* sp. PSU-D65.
- Five known compounds (**N39-N43**) were isolated from the broth extract of *Phomopsis* sp. PSU-A56.

The structures were identified by analysis of spectroscopic data, especially 1D and 2D NMR data, and comparison of the NMR data with those reported in the literatures.

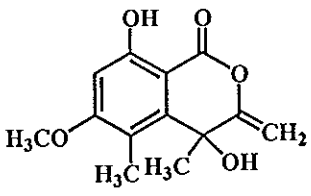

N1

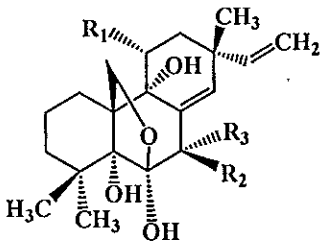

N2: R_1 = H, R_2+R_3 = O
N3: R_1 = OH, R_2+R_3= O
N4: R_1 = OH, R_2 = H, R_3 = OH

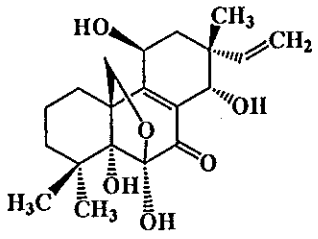

N5

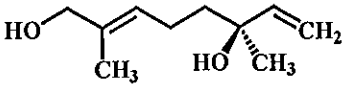

N8

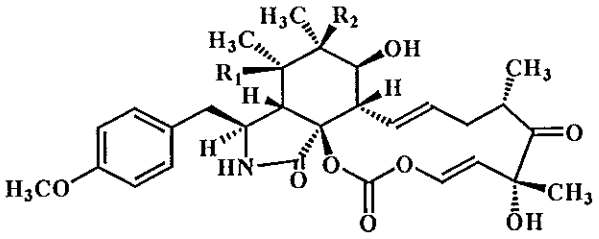

N6: R_1 = H, R_2 = OH
N7: R_1 = R_2 = double bond

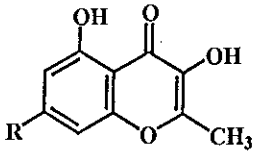

N12: R = CH_3
N13: R = CH_2OH

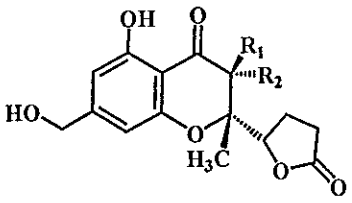

N9: R_1 = H, R_2 = H
N10: R_1 = CH_2COCH_3, R_2 = OH
N11: R_1 = OH, R_2 = H

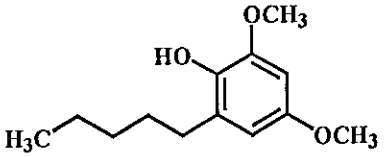

N14

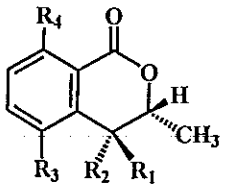

N15: $R_1 = R_2 = R_3 = H$, $R_4 = OH$
N17: $R_1 = R_3 = H$, $R_2 = R_4 = OH$
N18: $R_1 = R_4 = OH$, $R_2 = R_3 = H$
N21: $R_1 = R_2 = R_3 = H$, $R_4 = OCH_3$
N31: $R_1 = R_2 = H$, $R_3 = CO_2H$, $R_4 = OH$
N32: $R_1 = R_2 = H$, $R_3 = R_4 = OH$
N40: $R_1 = R_2 = H$, $R_3 = CO_2CH_3$, $R_4 = OH$

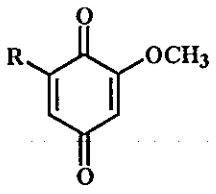

N16: R = pentyl
N41: R = CH_3

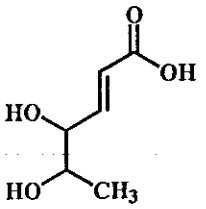

N20

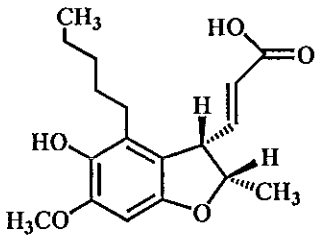

N19

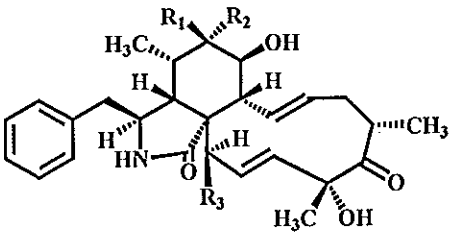

N22: $R_1+R_2 = CH_2$, $R_3 = OAc$
N23: $R_1 = OH$, $R_2 = CH_3$, $R_3 = OAc$
N24: $R_1+R_2 = CH_2$, $R_3 = OH$

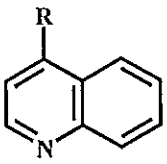

N25: R = CN
N28: R = CH=NOH

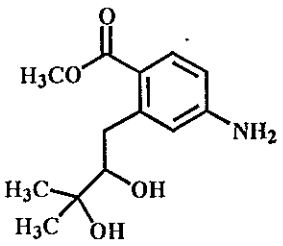

N26

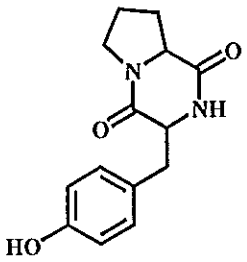

N27

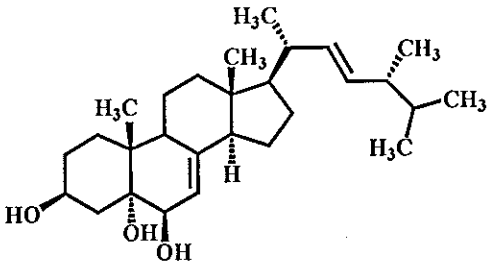

N29

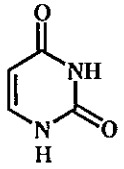

N30

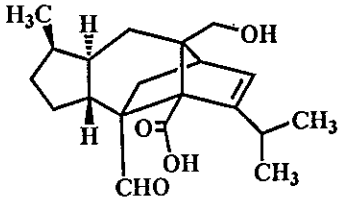

N33

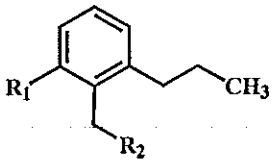

N34: R_1 = OH, R_2 = glu
N35: R_1 = glu, R_2 = OH

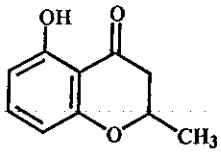

N36

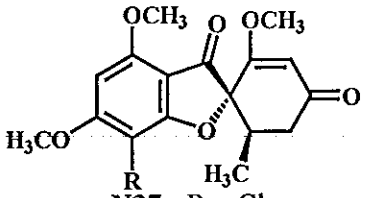

N37: R = Cl
N38: R = H

glu =

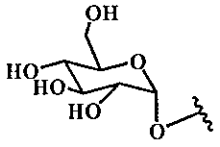

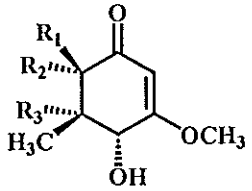

N39: R_1 = H, R_2+R_3 = epoxide
N42: R_1 = R_3 = OH, R_2 = H

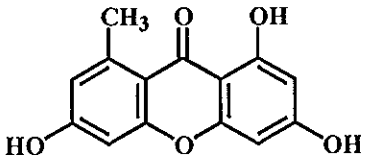

N43

ACKNOWLEDGEMENT

I wish to express my deepest and sincere gratitude to my supervisor, Professor Dr. Vatcharin Rukachaisirikul, for her valuable instruction, expert guidance and excellent suggestion. I would also like to express my appreciation to her for correction of my thesis.

My sincere thanks are expressed to Associate Professor Dr. Chatchanok Karalai, my co-advisor for his collaboration and to Professor Dr. Pittaya Tantiwachwuttikul and Assistant Professor Dr. Kanda Panthong for the valuable comments.

I would like to extend my appreciation to the staff of the Department of Chemistry, Faculty of Science, Prince of Songkla University, for making this thesis possible, to Dr. Yaowapa Sukpondma, the Department of Chemistry, Faculty of Science, Prince of Songkla University, for recording 300 and 500 MHz NMR spectra and to Associate Professor Dr. Souwalak Phongpaichit, the Department of Microbiology, Faculty of Science, Prince of Songkla University, and Dr. Masahiko Isaka, the National Center for Genetic Engineering and Biotechnology (BIOTEC), for the isolation and fermentation of the fungi.

I am grateful to the Royal Golden Jubilee Ph.D. Program of the Thailand Research Fund (Grant No. PHD/0218/2547) for a financial support. The Center for Innovation in Chemistry: Postgraduate Education and Research Program in Chemistry (PERCH-CIC), Commission on Higher Education, Ministry of Education, and the Graduate School, Prince of Songkla University are acknowledged for partial support.

Finally, none of this would have been possible without love and encouragement of my family and friends. I thank them all for their kindness and valuable advice. Everything will be always kept in my mind.

Wipapan Pongcharoen

THE RELEVANCE OF THE RESEARCH WORK TO THAILAND

Health problems caused by drug-resistant bacteria and fungi are increasing in many parts of the word including Thailand. An intensive search for newer and more effective antimicrobial agents and other bioactive compounds is needed. The culture extracts of the endophytic fungi: *Phomopsis* sp. PSU-A56, *Xylaria* sp. PSU-D14 and PSU-D65, *Eutypella scoparia* PSU-D44 and *Botryosphaeria mamane* PSU-M76 showed interesting biological activities while those of the wood-decayed fungi: *Lachnum* sp. BCC 2424 and *Xylaria* sp. BCC 9653 displayed interesting ^{1}H NMR spectral data. We were interested in searching for bioactive metabolites from these culture extracts with the hope that new compounds with significant biological activities will be isolated. Forty three compounds including thirteen new ones have been isolated from these fungi.

CONTENTS

CONTENTS (Continued)

CONTENTS (Continued)

CONTENTS (Continued)

CONTENTS (Continued)

LIST OF TABLES

LIST OF TABLES (Continued)

LIST OF TABLES (Continued)

LIST OF TABLES (Continued)

LIST OF TABLES (Continued)

LIST OF TABLES (Continued)

LIST OF TABLES (Continued)

LIST OF TABLES (Continued)

LIST OF TABLES (Continued)

LIST OF TABLES (Continued)

LIST OF TABLES (Continued)

LIST OF FIGURES

LIST OF FIGURES (Continued)

LIST OF FIGURES (Continued)

LIST OF FIGURES (Continued)

LIST OF ABBREVIATIONS AND SYMBOLS

s	=	*singlet*
d	=	*doublet*
t	=	*triplet*
q	=	*quartet*
m	=	*multiplet*
brs	=	*broad singlet*
brd	=	*broad doublet*
brdd	=	*broad doublet of doublet*
brt	=	*broad triplet*
dd	=	*doublet of doublet*
dt	=	*doublet of triplet*
dq	=	*doublet of quartet*
dm	=	*doublet of multiplet*
ddd	=	*doublet of doublet of doublet*
ddq	=	*doublet of doublet of quartet*
ddm	=	*doublet of doublet of multiplet*
td	=	*triplet of doublet*
qd	=	*quartet of doublet*
qt	=	*quartet of triplet*
δ	=	chemical shift relative to TMS
J	=	coupling constant
m/z	=	a value of mass divided by charge
°C	=	degree celcius
R_f	=	retention factor
g	=	gram
kg	=	kilogram
mg	=	milligram
μg	=	microgram
ml	=	milliliter

LIST OF ABBREVIATIONS AND SYMBOLS (Continued)

L	=	Liter
cm^{-1}	=	reciprocal centimeter (wavenumber)
nm	=	nanometer
ppm	=	part per million
λ_{max}	=	maximum wavelength
ν	=	absorption frequencies
ε	=	molar extinction coefficient
Hz	=	Hertz
MHz	=	megaHertz
$[\alpha]_D$	=	specific rotation
c	=	concentration
TLC	=	thin-layer chromatography
UV-S	=	Ultraviolet-short wavelength
FT-IR	=	Fourier Transform Infrared
MS	=	Mass Spectroscopy
LRMS	=	Low Resolution Mass Spectroscopy
HRMS	=	High Resolution Mass Spectroscopy
NMR	=	Nuclear Magnetic Resonance
1D NMR	=	One Dimensional Nuclear Magnetic Resonance
2D NMR	=	Two Dimensional Nuclear Magnetic Resonance
HMQC	=	Heteronuclear Multiple Quantum Coherence
HMBC	=	Heteronuclear Multiple Bond Correlation
DEPT	=	Distortionless Enhancement by Polarization Transfer
NOE	=	Nuclear Overhauser Effect
NOEDIFF	=	NOE Difference Spectroscopy
NOSEY	=	Nuclear Overhauser Enhanced Spectroscopy
COSY	=	Correlation Spectroscopy
TMS	=	tetramethylsilane
$CDCl_3$	=	deuterochloroform

LIST OF ABBREVIATIONS AND SYMBOLS (Continued)

Acetone-d_6	=	hexadeuteroacetone
ASA	=	anisaldehyde-sulphuric acid in acetic acid solution
CD_3OD	=	tetradeuteromethanol
$CHCl_3$	=	chloroform
DMSO-d_6	=	deuterodimethyl sulfoxide
CH_2Cl_2	=	dichloromethane
EtOH	=	ethanol
EtOAc	=	ethyl acetate
HCl	=	hydrochloric acid
H_2O	=	water
$MgSO_4$	=	magnesium sulfate
MeOH	=	methanol
$NaHCO_3$	=	sodium hydrogen carbonate
NaOH	=	sodium hydroxide
Na_2SO_4	=	sodium sulfate

PART I

CHEMICAL CONSTITUENTS FROM THE ENDOPHYTIC FUNGUS *EUTYPELLA SCOPARIA* PSU-D44

CHAPTER 1.1
INTRODUCTION

1.1.1 Introduction

In the course of our ongoing search for antimicrobial substances from plants and endophytic fungi, the ethyl acetate extract from the culture broth of the endophytic fungus *Eutypella scoparia* PSU-D44 exhibited antibacterial and antifungal activities against *S. aureus* ATCC 25923 and *Microsporum gypseum* SH-MU-4, respectively, with an equal MIC value of 500 μg/ml.

The endophytic fungus *E. scoparia* PSU-D44 was isolated from the leaves of *Garcinia dulcis*, collected in Songkhla Province, Thailand, in 2005. This fungus was deposited as PSU-D44 at the Department of Microbiology, Faculty of Science, Prince of Songkla University. Chemical investigation of the genus *Eutypella* has never been reported according to information from SciFinder Scholar database.

CHAPTER 1.2
EXPERIMENTAL

1.2.1 Chemicals and instruments

Melting points were recorded in °C and were measured on an electrothermal melting point apparatus (Electrothermal 9100). Infrared spectra (IR) were determined as neat on a Perkin Elmer 783 FTS165 FT-IR spectrometer. Ultraviolet (UV) absorption spectra were determined in methanol solution on a SHIMADZU UV-160A spectrophotometer. ^{1}H and ^{13}C NMR spectra were recorded on 300 or 500 MHz Bruker FTNMR Ultra Shield^{TM} spectrometer in deuterochloroform solution, unless otherwise stated, with tetramethylsilane (TMS) as internal standard. Mass spectra were obtained on a MAT 95 XL mass spectrometer (Thermofinnigan). Optical rotations were measured in methanol solution on a JASCO P-1020 polarimeter. Solvents for extraction and chromatography were distilled at their boiling point ranges prior to use except for light petroleum, chloroform, ethyl acetate and ethanol which were analytical grade reagent. Thin-layer chromatography (TLC) and precoated TLC were performed on silica gel 60 GF_{254} (Merck). Column chromatography (CC) was carried out on silica gel (Merck) type 100 (70-230 Mesh ASTM), reverse phase silica gel C-18 or Sephadex LH20.

1.2.2 Fermentation and extraction

The culture of the fungus *Eutypella scoparia* PSU-D44 (5 L) was filtered to separate into the filtrate and wet mycelia. The filtrate was extracted three times with an equal volume of EtOAc (300 ml). The EtOAc layer was dried over anhydrous Na_2SO_4 and evaporated to dryness under reduced pressure to afford a brown gum (212.1 mg). Because of low quantity of wet mycelia, it was not further investigated.

1.2.3 Purification of the broth extract

The ethyl acetate extract of the culture filtrate showed many UV-active spots on normal phase TLC with 30% ethyl acetate in light petroleum as a mobile phase (2 runs). Further separation was performed by column chromatography over silica gel using a gradient system of ethyl acetate-light petroleum followed by a gradient system of methanol-ethyl acetate. All fractions were examined by TLC, combined on the basis of their chromatogram characteristics and then evaporated to dryness under reduced pressure to afford eight fractions, as shown in **Table 1.**

Table 1 Fractions obtained from **the broth extract** by column chromatography over silica gel

Fraction	Eluent	Weight (mg)	Physical appearance
A	100% Light petroleum - 30% EtOAc/Light petroleum	14.3	Orange gum mixed with orange solid
B	40% EtOAc/Light petroleum	20.5	White solid
C	40% EtOAc/Light petroleum	11.2	Yellow solid
D	50% EtOAc/Light petroleum	5.5	Yellow gum
E	50-70% EtOAc/Light petroleum	38.5	Brown-orange gum mixed with orange solid
F	70% EtOAc/Light petroleum - 100% EtOAc	3.0	Orange solid
G	100% EtOAc - 5% MeOH/EtOAc	53.3	Brown-orange gum mixed with orange solid
H	10% MeOH/EtOAc - 100% MeOH	22.7	Dark-brown gum

Fraction A demonstrated two UV-active spots on normal phase TLC with the R_f values of 0.20 and 0.33 using 100% dichloromethane as a mobile phase. It was separated by precoated TLC using 100% dichloromethane as a mobile phase (2 runs) to give two bands.

Band 1 (N1) was obtained as a colorless gum (3.7 mg). Its chromatogram displayed one major UV-active spot on normal phase TLC with the R_f value of 0.30 using 100% dichloromethane as a mobile phase.

$[\alpha]_D^{29}$		+91.82 (c = 0.048, EtOH)
UV(MeOH) λ_{max} nm (log ε)		217 (3.55), 269 (3.24), 317 (3.04)
FT-IR (neat) ν_{cm-1}		3431 (O-H stretching), 1683 (C=O stretching)
^{1}H NMR ($CDCl_3$) (δ ppm) (300 MHz)		11.30 (*s*, 1H), 6.44 (*s*, 1H), 5.09 (*dd*, *J* = 2.1, 0.6 Hz, 1H), 4.96 (*dd*, *J* = 2.1, 0.6 Hz, 1H), 3.87 (*s*, 3H), 2.39 (*s*, 3H), 1.75 (*s*, 3H)
^{13}C NMR ($CDCl_3$) (δ ppm) (125 MHz)		166.41, 165.76, 163.17, 160.58, 142.33, 116.40, 98.52, 98.16, 95.45, 72.07, 55.96, 28.98, 11.95
DEPT (135°) ($CDCl_3$)	CH :	98.52
	CH_2 :	95.45
	CH_3 :	55.96, 28.98, 11.95
EIMS *m/z* (% relative intensity):		250 (18), 232 (5), 207 (100), 193 (14), 69 (13)

Band 2 (N2) was obtained as a white solid (4.4 mg), melting at 215.2-216.0 °C. Its chromatogram showed one UV-active spot on normal phase TLC with the R_f value of 0.13 using 100% dichloromethane as a mobile phase.

$[\alpha]_D^{29}$	+57.42 (c = 1.00, MeOH)
UV(MeOH) λ_{max} nm (log ε)	207 (3.17), 231 (3.31)
FT-IR (neat) ν_{cm-1}	3394 (O-H stretching), 1701 (C=O stretching)
^{1}H NMR ($CDCl_3$) (δ ppm) (300 MHz)	6.79 (*d*, *J* = 1.5 Hz, 1H), 5.87 (*dd*, *J* = 17.4, 10.5 Hz, 1H), 5.12 (*d*, *J* = 17.4 Hz, 1H), 5.07 (*d*, *J* = 10.5 Hz, 1H), 5.06 (*brs*, 1H), 4.04 (*d*, *J* = 9.9

		Hz, 1H), 3.73 (*d*, J = 9.9 Hz, 1H), 2.20 (*dt*, J = 13.5, 4.8 Hz, 1H), 2.08 (*m*, 2H), 1.71 (*m*, 2H), 1.60 (*m*, 1H), 1.55 (*m*, 1H), 1.48 (*m*, 1H), 1.43 (*s*, 3H), 1.24 (*m*, 1H), 1.19 (*s*, 3H), 1.16 (*s*, 3H)
^{13}C NMR ($CDCl_3$) (δ ppm) (75 MHz)		196.00, 150.53, 144.90, 134.96, 112.88, 104.31, 81.67, 74.62, 68.50, 49.31, 39.28, 37.38, 37.05, 29.47, 27.16, 26.97, 24.73, 23.52, 22.09, 17.46
DEPT (135°) ($CDCl_3$)	CH :	150.53, 144.90
	CH_2 :	112.88, 68.50, 37.38, 29.47, 27.16, 22.09, 17.46
	CH_3 :	26.97, 24.73, 23.52
EIMS *m/z* (% relative intensity):		330 (43), 257 (36), 228 (30), 215 (61), 187 (41), 167 (100), 149 (32), 121 (30), 91 (31), 69 (31)

Fraction B (N3) melted at 218.5-219.1 °C. Its chromatogram on normal phase TLC displayed one UV-active spot with the R_f value of 0.70 using 20% ethyl acetate in light petroleum as a mobile phase (2 runs).

$[\alpha]_D^{29}$	+131.13 (c = 0.101, $CHCl_3$)
UV(MeOH) λ_{max} nm (log ε)	231 (3.76)
FT-IR (neat) ν_{cm-1}	3394 (O-H stretching), 1703 (C=O stretching)
^{1}H NMR ($CDCl_3$) (δ ppm) (300 MHz)	6.80 (*d*, J = 1.8 Hz, 1H), 5.82 (*dd*, J = 17.4, 10.5 Hz, 1H), 5.66 (*brs*, 1H), 5.09 (*dd*, J = 17.4, 0.6 Hz, 1H), 5.07 (*dd*, J = 10.5, 0.6 Hz, 1H), 4.99 (*brs*, 1H), 4.13 (*d*, J = 10.2 Hz, 1H), 4.01 (*dd*, J = 11.7, 4.2 Hz, 1H), 3.70 (*d*, J = 10.2 Hz, 1H), 2.05 (*m*, 1H), 2.03 (*m*, 1H), 1.94 (*m*, 1H), 1.72 (*m*, 1H), 1.57 (*m*, 1H), 1.56 (*m*, 2H), 1.43 (*s*, 3H), 1.20 (*s*, 3H), 1.21 (*m*, 1H), 1.18 (*s*, 3H)
^{13}C NMR ($CDCl_3$) (δ ppm) (75 MHz)	196.70, 150.22, 144.04, 134.78, 113.05, 104.37, 81.57, 76.33, 68.62, 67.48, 51.12, 39.92, 39.80, 37.45, 37.29, 27.21, 25.87, 25.21, 23.66, 17.68

DEPT (135°) ($CDCl_3$) CH : 150.22, 144.04, 67.48
CH_2 : 113.05, 68.62, 39.92, 37.45, 25.21, 17.68
CH_3 : 27.21, 25.87, 23.66

Fraction C showed one major spot under UV-S on normal phase TLC using 20% ethyl acetate in light petroleum as a mobile phase (2 runs) with the same R_f value as **N3**. The ^1H NMR data indicated the presence of **N3** as a major component. Thus, no attempted investigation was performed.

Fraction D showed many inseparable UV-active spots on normal phase TLC using 20% ethyl acetate in light petroleum as a mobile phase (2 runs). Its ^1H NMR spectrum displayed none of major components. Therefore, no attempted investigation was performed.

Fraction E contained three UV-active spots on normal phase TLC with the R_f values of 0.25, 0.38 and 0.70 using 30% acetone in light petroleum as a mobile phase (3 runs). Further separation was performed by column chromatography over silica gel using a gradient system of acetone-light petroleum followed by a gradient system of methanol-acetone. All subfractions were examined by TLC, combined on the basis of their chromatogram characteristics and then evaporated to dryness under reduced pressure to afford six subfractions, as shown in **Table 2.**

Table 2 Subfractions obtained from **fraction E** by column chromatography over silica gel

Fraction	Eluent	Weight (mg)	Physical appearance
E-1	10-50% Acetone/Light petroleum	3.1	Yellow gum
E-2	50% Acetone/Light petroleum	4.2	Yellow solid
E-3	50% Acetone/Light petroleum	7.1	White solid

Table 2 Continued

Fraction	Eluent	Weight (mg)	Physical appearance
E-4	50% Acetone/Light petroleum	6.3	Yellow gum
E-5	50% Acetone/Light petroleum	5.1	Yellow gum
E-6	70% Acetone/Light petroleum - 100% MeOH	3.3	Yellow gum

Subfraction E-1 showed no definite spots under UV-S on normal phase TLC using 20% acetone in light petroleum as a mobile phase (5 runs). Its ^{1}H NMR spectrum displayed proton signals at high field region. Thus, it was not further investigated.

Subfraction E-2 displayed two UV-active spots on normal phase TLC with the R_f values of 0.13 and 0.45 using 20% acetone in light petroleum as a mobile phase (5 runs). The polar spot was identified as **N4** by comparison of TLC chromatogram. Thus, it was not further separated.

Subfraction E-3 (**N4**) melted at 215.5-216.8 °C. Its chromatogram showed only one UV-active spot on normal phase TLC with the R_f value of 0.13 using 20% acetone in light petroleum as a mobile phase (5 runs).

$[\alpha]_D^{29}$	+25.74 (c = 0.122, $CHCl_3$)
UV(MeOH) λ_{max} nm (log ε)	206 (3.46)
FT-IR (neat) ν_{cm-1}	3328 (O-H stretching)
^{1}H NMR ($CDCl_3$) (δ ppm) (300 MHz)	5.98 (*t*, *J* = 1.5 Hz, 1H), 5.82 (*dd*, *J* = 17.4, 10.5 Hz, 1H), 5.03 (*d*, *J* = 17.4 Hz, 1H), 4.98 (*brd*, *J* = 10.5 Hz, 1H), 4.59 (*d*, *J* = 2.1 Hz, 1H), 3.93 (*d*, *J* = 9.6 Hz, 1H), 3.83 (*dd*, *J* = 11.7, 4.8 Hz, 1H),

		3.30 (*d*, *J* = 9.3 Hz, 1H), 1.88 (*m*, 1H), 1.83 (*m*, 1H), 1.70 (*m*, 2H), 1.66 (*m*, 1H), 1.63 (*m*, 1H), 1.56 (*m*, 1H), 1.38 (*s*, 3H), 1.20 (*s*, 3H), 1.14 (*s*, 3H), 1.13 (*m*, 1H)
^{13}C NMR ($CDCl_3$) (δ ppm) (75 MHz)		146.61, 136.01, 132.68, 111.17, 106.26, 80.87, 77.24, 72.40, 68.04, 66.77, 49.95, 40.06, 38.18, 38.00, 37.72, 27.84, 24.89, 24.64, 24.19, 18.06
DEPT (135°) ($CDCl_3$)	CH :	146.61, 132.68, 72.40, 66.77
	CH_2 :	111.17, 68.04, 40.06, 37.72, 24.64, 18.06
	CH_3 :	27.84, 24.89, 24.19

Subfraction E-4 showed one major spot under UV-S on normal phase TLC with the R_f value of 0.13 using 20% acetone in light petroleum as a mobile phase (5 runs). When using 2% methanol in dichloromethane as a mobile phase (2 runs), the chromatogram showed three UV-active spots on normal phase TLC with the R_f values of 0.08, 0.20 and 0.33. Further purification by precoated TLC using 1% methanol in dichloromethane as a mobile phase (5 runs) afforded three bands.

Band 1 was obtained as a brown gum (0.8 mg). Its chromatogram showed one major spot under UV-S on normal phase TLC with the R_f value of 0.34 using 1% methanol in dichloromethane as a mobile phase (5 runs). Because of low quantity, it was not further purified.

Band 2 was obtained as a yellow gum (1.5 mg). Its chromatogram displayed one major spot under UV-S on normal phase TLC with the R_f value of 0.19 using 1% methanol in dichloromethane as a mobile phase (5 runs). The ^{1}H NMR data suggested that it was a mixture. Because of minute quantity, no attempted investigation was performed.

Band 3 (N5) was obtained as a yellow gum (1.3 mg), which displayed one spot under UV-S on normal phase TLC with the R_f value of 0.08 using 1% methanol in dichloromethane as a mobile phase (5 runs).

$[\alpha]_D^{29}$		+232.50 (c = 0.04, MeOH)
UV(MeOH) λ_{max} nm (log ε)		207 (3.99), 246 (3.91)
FT-IR (neat) ν_{cm-1}		3414 (O-H stretching), 1684 (C=O stretching)
^{1}H NMR ($CDCl_3$) (δ ppm) (300 MHz)		6.13 (*dd*, *J* = 17.7, 10.2 Hz, 1H), 5.34 (*dd*, *J* = 10.2, 0.9 Hz, 1H), 5.27 (*dd*, *J* = 17.7, 0.9 Hz, 1H), 5.06 (*brs*, 1H), 4.45 (*d*, *J* = 9.3 Hz, 1H), 4.43 (*m*, 1H), 4.42 (*dd*, *J* = 6.3, 4.8 Hz, 1H), 3.29 (*d*, *J* = 9.3 Hz, 1H), 2.65 (*m*, 2H), 2.24 (*dd*, *J* = 14.4, 4.8 Hz, 1H), 2.01 (*dd*, *J* = 14.4, 6.3 Hz, 1H), 1.74 (*m*, 2H), 1.60 (*m*, 1H), 1.56 (*s*, 3H), 1.32 (*m*, 1H), 1.27 (*s*, 3H), 1.03 (*s*, 3H)
^{13}C NMR ($CDCl_3$) (δ ppm) (125 MHz)		194.60, 164.63, 143.75, 132.29, 115.12, 104.93, 81.11, 70.40, 70.02, 64.53, 54.18, 40.07, 39.82, 37.59, 36.83, 27.95, 24.31, 24.13, 23.77, 17.78
DEPT (135°) ($CDCl_3$)	CH :	143.75, 70.02, 64.53
	CH_2 :	115.12, 70.40, 39.82, 37.59, 23.77
	CH_3 :	27.95, 24.31, 24.13
EIMS *m/z* (% relative intensity):		346 (6), 328 (56), 255 (46), 213 (49), 187 (70) 145 (46), 91 (60), 69 (100)

Subfraction E5 displayed three UV-active spots on normal phase TLC with the R_f values of 0.08, 0.20 and 0.33 using 2% methanol in dichloromethane as a mobile phase (2 runs). Further purification by precoated TLC using 1% methanol in dichloromethane as a mobile phase (5 runs) afforded three bands.

Band 1 was a yellow gum (0.2 mg) which showed one UV-active spot on normal phase TLC with the R_f value of 0.28 using 1% methanol in dichloromethane as a mobile phase (5 runs). The ^{1}H NMR data suggested that it was a mixture. Because of low quantity, it was not further purified.

Band 2 was a yellow gum (0.9 mg) which showed one UV-active spot on normal phase TLC with the R_f value of 0.17 using 1% methanol in

dichloromethane as a mobile phase (5 runs). The ^{1}H NMR data suggested that it was a mixture. Because of low quantity, it was not further separated.

Band 3 was obtained as a yellow gum (0.2 mg). Its chromatogram showed one major spot under UV-S on normal phase TLC with the R_f value of 0.05 using 1% methanol in dichloromethane as a mobile phase (5 runs). Its ^{1}H NMR spectrum displayed none of major components. Therefore, no attempted investigation was carried out.

Subfraction E6 showed no spots under UV-S on normal phase TLC using 20% acetone in light petroleum as a mobile phase (5 runs). Its ^{1}H NMR spectrum displayed none of major components. Therefore, further purification was not conducted.

Fraction F demonstrated a long tail under UV-S on normal phase TLC using 20% ethyl acetate in light petroleum as a mobile phase (2 runs). According to its ^{1}H NMR spectral data, this fraction was a mixture. Therefore, it was not further separated.

Fraction G contained three major UV-active spots on normal phase TLC with the R_f values of 0.15, 0.23 and 0.30 using 4% methanol in dichloromethane as a mobile phase. It was further separated by column chromatography over silica gel. Elution was conducted initially with pure dichloromethane, gradually enriched with methanol until pure methanol. Fractions, which contained similar components, were combined and evaporated to dryness under reduced pressure to give five subfractions, as shown in **Table 3**.

Table 3 Subfractions obtained from **fraction G** by column chromatography over silica gel

Fraction	Eluent	Weight (mg)	Physical appearance
G-1	100% CH_2Cl_2 - 4% MeOH/CH_2Cl_2	1.3	Yellow gum
G-2	4% MeOH/CH_2Cl_2	39.0	Yellow solid
G-3	4-6% MeOH/CH_2Cl_2	3.2	White solid
G-4	10-30% MeOH/CH_2Cl_2	7.4	Yellow gum
G-5	50% MeOH/CH_2Cl_2 - 100% MeOH	1.8	Yellow gum

Subfraction G-1 showed no definite spots under UV-S on normal phase TLC using 1% methanol in dichloromethane as a mobile phase (6 runs). Thus, it was not further investigated.

Subfraction G-2 displayed three major brown spots under UV-S on normal phase TLC with the R_f values of 0.25, 0.33 and 0.48 using 1% methanol in dichloromethane as a mobile phase (6 runs). Further chromatographic separation was performed by column chromatography over silica gel with pure dichloromethane, gradually enriched with methanol and finally with pure methanol. All subfractions were examined by TLC, combined on the basis of their chromatogram characteristics and then evaporated to dryness under reduced pressure to give six subfractions, as shown in **Table 4**.

Table 4 Subfractions obtained from **subfraction G-2** by column chromatography over silica gel

Subfraction	Eluent	Weight (mg)	Physical appearance
G-2-1	100% CH_2Cl_2 - 5% MeOH/CH_2Cl_2	0.7	Yellow gum

Table 4 Continued

Subfraction	Eluent	Weight (mg)	Physical appearance
G-2-2	5% MeOH/CH_2Cl_2	6.3	Yellow solid mixed with white solid
G-2-3	5-10% MeOH/CH_2Cl_2	10.9	White solid
G-2-4	10% MeOH/CH_2Cl_2	5.3	White solid mixed with white solid
G-2-5	10-30% MeOH/CH_2Cl_2	9.9	Yellow gum
G-2-6	50% MeOH/CH_2Cl_2 - 100% MeOH	2.0	Yellow gum

Subfraction G-2-1 showed no spots under UV-S on normal phase TLC using 100% dichloromethane (2 runs) followed by 2% methanol in dichloromethane as mobile phases (3 runs). Its ^{1}H NMR spectrum displayed none of major components. Thus, it was not further investigated.

Subfraction G-2-2 showed one major spot under UV-S on normal phase TLC with the R_f value of 0.43 using 100% dichloromethane (2 runs) followed by 2% methanol in dichloromethane (3 runs) as mobile phases. Its ^{1}H NMR spectral data and chromatogram on normal phase TLC indicated that it was **N6**.

Subfraction G-2-3 (N6) melted at 188.6-189.2 °C. Its chromatogram displayed one spot under UV-S on normal phase TLC with the R_f value of 0.43 using 100% dichloromethane (2 runs) followed by 2% methanol in dichloromethane (3 runs) as mobile phases.

$[\alpha]_D^{29}$	-52.67 (c = 0.17, MeOH)
UV(MeOH) λ_{max} nm (log ε)	205 (3.68), 224 (3.63), 276 (2.82), 283 (2.76)
FT-IR (neat) ν_{cm-1}	3272 (O-H stretching), 1764 and 1716 (C=O stretching)

^{1}H NMR ($CDCl_3$) (δ ppm) (300 MHz)		7.06 (*d*, *J* = 8.7 Hz, 2H), 6.87 (*d*, *J* = 8.7 Hz, 2H), 6.51 (*d*, *J* = 11.7 Hz, 1H), 6.11 (*brs*, 1H), 5.89 (*ddm*, *J* = 15.0, 9.9 Hz, 1H), 5.61 (*d*, *J* = 11.7 Hz, 1H), 5.23 (*ddd*, *J* = 15.0, 10.0, 3.6 Hz, 1H), 4.43 (*brs*, 1H), 3.79 (*s*, 3H), 3.68 (*m*, 1H), 3.00 (*dd*, *J* = 5.2, 2.7 Hz, 1H), 2.93 (*ddd*, *J* = 11.4, 6.9, 2.4 Hz, 1H), 2.85 (*td*, *J* = 13.5, 4.5 Hz, 1H), 2.67 (*m*, 1H), 2.65 (*m*, 1H), 2.64 (*m*, 1H), 2.62 (*m*, 1H), 2.29 (*dd*, *J* = 7.2, 5.2 Hz, 1H), 2.15 (*dm*, *J* = 13.8 Hz, 1H), 1.50 (*s*, 3H), 1.25 (*s*, 3H), 1.16 (*d*, *J* = 6.6 Hz, 3H), 1.11 (*d*, *J* = 7.2 Hz, 3H)
^{13}C NMR ($CDCl_3$) (δ ppm) (75 MHz)		211.71, 170.00, 158.90, 149.36, 142.15, 131.54, 130.54, 128.45, 127.93, 120.39, 114.34, 87.03, 77.00, 60.61, 57.26, 55.27, 53.75, 48.06, 45.89, 44.16, 40.80, 39.06, 35.83, 24.35, 20.07, 19.68, 13.21
DEPT (135°) ($CDCl_3$)	CH :	142.15, 131.54, 130.54, 128.45, 120.39, 114.34, 60.61, 53.75, 48.06, 45.89, 40.80, 35.83
	CH_2 :	44.16, 39.06
	CH_3 :	55.27, 24.35, 20.07, 19.68, 13.21
EIMS *m/z* (% relative intensity):		525 (12), 367 (86), 246 (100), 218 (24), 121(52)

Subfraction G-2-4 showed one UV-active spot on normal phase TLC with the R_f value of 0.43 using 100% dichloromethane (2 runs) followed by 2% methanol in dichloromethane (3 runs) as mobile phases. Its ^{1}H NMR spectral data and chromatogram on normal phase TLC indicated that it was **N6**.

Subfraction G-2-5 displayed two UV-active spots on normal phase TLC with the R_f values of 0.33 and 0.43 using 100% dichloromethane (2 runs) followed by 2% methanol in dichloromethane (3 runs) as mobile phases. Further purification by precoated TLC using 2% methanol in dichloromethane as a mobile phase (7 runs) afforded two bands.

Band 1 was a white solid (0.5 mg) which showed one UV-active spot on normal phase TLC with the R_f value of 0.50 using 2% methanol in dichloromethane as a mobile phase. Its ^{1}H NMR data indicated that it was **N6.**

Band 2 was a white solid (3.3 mg) which showed two UV-active spots on normal phase TLC with the R_f values of 0.43 and 0.50 using 2% methanol in dichloromethane as a mobile phase. Further purification by precoated TLC using 2% methanol in dichloromethane as a mobile phase (3 runs) afforded a white solid (**N7**) (1.6 mg), melting at 152.5-153.7 °C. Its chromatogram characteristic showed one UV-active spot on normal phase TLC with the R_f value of 0.45 using 2% methanol in dichloromethane (2 runs) as a mobile phase.

$[\alpha]_D^{29}$	+114.79 (c = 0.53, MeOH)
UV(MeOH) λ_{max} nm (log ε)	206 (3.95), 224 (3.85), 275 (3.16), 284 (3.12)
FT-IR (neat) ν_{cm-1}	3386 (O-H stretching), 1761 and 1716 (C=O stretching)
^{1}H NMR ($CDCl_3$) (δ ppm) (300 MHz)	7.00 (*d*, *J* = 8.7 Hz, 2H), 6.80 (*d*, *J* = 8.7 Hz, 2H), 6.60 (*d*, *J* = 11.7 Hz, 1H), 6.13 (*brdd*, *J* = 15.0, 10.5 Hz, 1H), 5.81 (*brs*, 1H), 5.59 (*d*, *J* = 11.7 Hz, 1H), 5.31 (*ddd*, *J* = 15.0, 11.1, 3.9 Hz, 1H), 4.42 (*brs*, 1H), 4.15 (*dd*, *J* = 5.7, 3.6 Hz, 1H), 3.81 (*brs*, 1H), 3.72 (*s*, 3H), 3.35 (*t*, *J* = 6.6 Hz, 1H), 2.87 (*m*, 1H), 2.81 (*m*, 1H), 2.78 (*m*, 2H), 2.73 (*m*, 1H), 2.70 (*m*, 1H), 1.61 (*brs*, 3H), 1.46 (*brs*, 3H), 1.44 (*s*, 3H), 1.11 (*d*, *J* = 6.6 Hz, 3H)
^{13}C NMR ($CDCl_3$) (δ ppm) (125 MHz)	211.51, 169.92, 158.69, 148.99, 142.48, 133.57, 131.66, 130.32, 129.40, 128.57, 125.35, 120.48, 114.31, 86.20, 76.63, 70.03, 59.17, 55.27, 49.96, 48.23, 43.23, 40.91, 39.02, 24.64, 20.17, 17.70, 13.94
DEPT (135°) ($CDCl_3$)	CH : 142.48, 133.57, 130.32, 129.40, 120.48, 114.31, 70.03, 59.17, 49.96, 48.23, 40.91

CH_2 : 43.23, 39.02

CH_3 : 55.27, 24.64, 20.17, 17.70, 13.94

EIMS *m/z* (% relative intensity): 525 (2), 367 (14), 350 (10), 246 (26), 228 (16), 121 (100), 81 (10), 69 (10)

Subfraction G-2-6 showed two spots under UV-S on normal phase TLC with the R_f values of 0.18 and 0.33 using 100% dichloromethane (2 runs) followed by 2% methanol in dichloromethane as mobile phases (3 runs). The ^1H NMR data indicated that it contained many compounds. Thus, it was not further separated.

Subfraction G-3 showed no definite spots under UV-S on normal phase TLC using 1% methanol in dichloromethane as a mobile phase (6 runs). Its ^1H NMR spectrum displayed none of major components. Therefore, further purification was not conducted

Subfraction G-4 displayed two spots under UV-S on normal phase TLC with the R_f values of 0.08 and 0.20 using 1% methanol in dichloromethane as a mobile phase (6 runs). It was further separated by column chromatography over Sephadex LH20. Elution was conducted with 50% methanol in dichloromethane. All subfractions were examined by TLC, combined on the basis of their chromatogram characteristics and then evaporated to dryness under reduced pressure to afford three subfractions, as shown in **Table 5**.

Table 5 Subfractions obtained from **subfraction G-4** by column chromatography over Sephadex LH20

Subfraction	Eluent	Weight (mg)	Physical appearance
G-4-1	50% MeOH/CH_2Cl_2	0.2	Pale-Yellow gum
G-4-2	50% MeOH/CH_2Cl_2	6.2	Yellow gum
G-4-3	50% MeOH/CH_2Cl_2	0.8	White solid

Subfraction G-4-1 demonstrated no spots under UV-S on normal phase TLC using 10% ethyl acetate in dichloromethane followed by 40% ethyl acetate in dichloromethane (5 runs) as mobile phases. Its ^{1}H NMR spectrum displayed none of major components and none of aromatic proton signals. Thus, it was not further investigated.

Subfraction G-4-2 displayed one UV-active spot on normal phase TLC with the R_f value of 0.33 using 10% ethyl acetate in dichloromethane followed by 40% ethyl acetate in dichloromethane (5 runs) as mobile phases. Its ^{1}H NMR spectrum indicated that it was a mixture. Therefore, no attempted separation was carried out.

Subfraction G-4-3 contained inseparable UV-active spots on normal phase TLC using 10% ethyl acetate in dichloromethane followed by 40% ethyl acetate in dichloromethane (5 runs) as mobile phases. Its ^{1}H NMR spectrum displayed none of major components. Thus, no further purification was carried out.

Subfraction G-5 showed no spots under UV-S on normal phase TLC using 1% methanol in dichloromethane as a mobile phase (6 runs). Its ^{1}H NMR spectrum displayed none of major components. Thus, further purification was not performed.

Fraction H displayed a long tail under UV-S on normal phase TLC using 20% ethyl acetate in light petroleum as a mobile phase (2 runs). Its ^{1}H NMR spectrum displayed none of major components. Therefore, it was not further separated.

CHAPTER 1.3
RESULTS AND DISCUSSION

Four new compounds (**N2, N5, N6** and **N7**) were isolated from the broth extract together with three known compounds (**N1, N3** and **N4**). The structures were identified by spectroscopic methods.

1.3.1 Compound N1

N1 was obtained as a colorless gum. The UV maximum absorption bands at λ_{max} 217, 269 and 371 nm indicated the presence of an isocoumarin chromophore. The IR spectrum showed absorption bands at 3431 and 1683 cm^{-1} for hydroxyl and carbonyl groups, respectively. The ^{1}H NMR spectrum (**Figure 1**) (**Table 6**) revealed the presence of proton signals for one chelated hydroxy proton (δ_H 11.30, *s*, 1H), one aromatic proton (δ_H 6.44, *s*, 1H), two geminal olefinic protons (δ_H 5.09, *dd*, J = 2.1 and 0.6 Hz, 1H and 4.96, *dd*, J = 2.1 and 0.6 Hz, 1H), one methoxyl group (δ_H 3.87, *s*, 3H), one aromatic methyl group (δ_H 2.39, *s*, 3H) and one oxyquaternary methyl group (δ_H 1.75, *s*, 3H). The ^{13}C NMR spectrum (**Figure 2**) (**Table 6**) contained 13 carbon signals of eight quaternary (δ_C 166.41, 165.76, 163.17, 160.58, 142.33, 116.40, 98.16 and 72.07), one methine (δ_C 98.52), one methylene (δ_C 95.45), one methoxyl (δ_C 55.96) and two methyl (δ_C 28.98 and 11.95) carbons. The chelated hydroxyl group which was placed at C-8 (δ_C 163.17), *ortho* to the carbonyl group, gave HMBC cross peaks (**Table 7**) with C-7 (δ_C 98.52) and C-8. The aromatic proton was then attributed to H-7, due to its correlation with C-7 in the HMQC spectrum. This was confirmed by its HMBC correlations with C-5 (δ_C 116.40), C-6 (δ_C 166.41), C-8 and C-8a (δ_C 98.16). Irradiation of H-7, in the NOEDIFF experiment, enhanced the signal of the methoxyl group at δ_H 3.87 (**Table 7**), indicating the attachment of the methoxyl group at C-6. A HMBC correlation between the methoxy protons and C-6 supported this assignment. The aromatic methyl group (Me-11), resonating at δ_H 2.39, was linked to C-5 on the basis of the HMBC cross

peaks between Me-11 with C-4a (δ_C 142.33), C-5 and C-6. The HMBC correlations of the oxyquaternary methyl protons (δ_H 1.75, Me-10) with C-3 (δ_C 160.58), C-4 (δ_C 72.07) and C-4a established the attachment of Me-10 at C-4 which was confirmed by signal enhancement of Me-11 upon irradiation of Me-10. The gem-disubstituted alkene moiety was connected to C-3, due to the HMBC correlations of the geminal olefinic protons (δ_H 5.09 and 4.96, H_{ab}-9) with C-3 and C-4. The chemical shift value of C-3, indicating that this carbon was an oxycarbon. Ring closure between the oxygen atom at C-3 and the carbonyl group to form a lactone ring was established according to the appearance of the carbonyl carbon at much higher field (δ_C 165.76). The observed optical rotation of **N1** ($[\alpha]_D^{29}$ +91.82, c = 0.048, EtOH) was almost identical to that of 4,8-dihydroxy-6-methoxy-4,5-dimethyl-3-methyleneisochroman-1-one ($[\alpha]_D^{29}$ +92.63, c = 0.048, EtOH). Therefore, **N1** was identified as 4,8-dihydroxy-6-methoxy-4,5-dimethyl-3-methyleneisochroman-1-one which was previously isolated from marine fungus *Halorosellinia oceanica.* (Chinworrungsee *et al.* 2002).

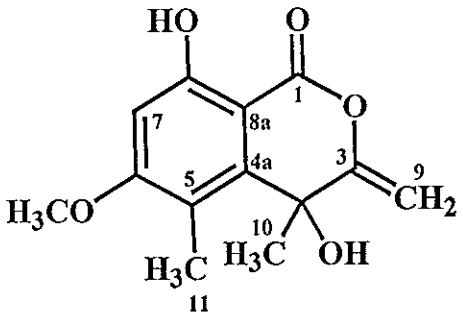

Table 6 The NMR data of **N1** in $CDCl_3$ and **4,8-dihydroxy-6-methoxy-4,5-dimethyl-3-methyleneisochroman-1-one** in acetone-d_6

Position	N1		4,8-Dihydroxy-6-methoxy-4,5-dimethyl-3-methyleneisochroman-1-one[a]	
	δ_H (mult., J_{Hz})	δ_C (C-Type)	δ_H (mult., J_{Hz})	δ_C (C-Type)
1	-	165.76 (C=O)	-	161.0 (C=O)
3	-	160.58 (C)	-	162.1 (C)
4	-	72.07 (C)	-	72.0 (C)
4a	-	142.33 (C)	-	144.0 (C)

Table 6 Continued

Position	N1		4,8-Dihydroxy-6-methoxy-4,5-dimethyl-3-methyleneisochroman-1-one[a]	
	δ_H (mult., J_{Hz})	δ_C (C-Type)	δ_H (mult., J_{Hz})	δ_C (C-Type)
5	-	116.40 (C)	-	117.0 (C)
6	-	166.41 (C)	-	166.0 (C)
6-OCH_3	3.87 (*s*)	55.96 (CH_3)	3.94 (*s*)	56.6 (CH_3)
7	6.44 (*s*)	98.52 (CH)	6.53 (*s*)	98.7 (CH)
8-OH	11.30 (*s*)	163.17 (C)	-	164.0 (C)
8a	-	98.16 (C)	-	100.3 (C)
9	a: 5.09 (*dd*, 2.1, 0.6)	95.45 (CH_2)	a: 5.12 (*brs*)	95.1 (CH_2)
	b: 4.96 (*dd*, 2.1, 0.6)	-	b: 4.88 (*brs*)	-
10	1.75 (*s*)	28.98 (CH_3)	1.67 (*s*)	20.1 (CH_3)
11	2.39 (*s*)	11.95 (CH_3)	2.40 (*s*)	10.1 (CH_3)

[a]Chinworrungsee *et al.* 2002

Table 7 The HMBC and NOE data of **N1** in $CDCl_3$

Position	HMBC	NOE
6-OCH_3	C-6	-
H-7	C-5, C-6, C-8, C-8a	6-OCH_3
8-OH	C-7, C-8	-
H_a-9	C-3, C-4, C-4a,	-
H_b-9	C-3, C-4, C-4a	-
Me-10	C-3, C-4, C-4a	Me-11
Me-11	C-4a, C-5, C-6	Me-10

1.3.2 Compound N3

N3 was isolated as a white solid, melting at 218.5-219.1 °C. The IR spectrum exhibited absorption bands at 3394 cm^{-1} for a hydroxyl group and 1703 cm^{-1} for a carbonyl group. The UV spectrum showed a maximum absorption band at λ_{max} 231 nm. The ^1H NMR spectrum (**Figure 3**) (**Table 8**) showed the characteristic signals of a β-olefinic proton at δ_H 6.80 (*d*, J = 1.8 Hz, 1H) of an α,β unsaturated carbonyl moiety, three olefinic protons of a monosubstituted alkene [δ_H 5.82 (*dd*, J = 17.4 and 10.5 Hz, 1H), 5.09 (*dd*, J = 17.4 and 0.6 Hz, 1H) and 5.07 (*dd*, J = 10.5 and 0.6 Hz, 1H)], two free hydroxy protons (δ_H 5.66, *brs*, 1H and 4.99, *brs*, 1H), one

oxymethine proton (δ_H 4.01, *dd*, J = 11.7 and 4.2 Hz, 1H), two nonequivalent oxymethylene protons (δ_H 4.13, *d*, J = 10.2 Hz, 1H and 3.70, *d*, J = 10.2 Hz, 1H) and three singlet methyl protons [δ_H 1.43 (*s*, 3H), 1.20 (*s*, 3H) and 1.18 (*s*, 3H)]. In addition, the ^{1}H NMR spectrum displayed signals for three sets of nonequivalent methylene protons [(δ_H 2.05, *m*, 1H and 1.94, *m*, 1H), (δ_H 2.03, *m*, 1H and 1.72, *m*, 1H) and (δ_H 1.57, *m*, 1H and 1.21, *m*, 1H)] and one set of equivalent methylene protons (δ_H 1.56, *m*, 2H). The presence of 20 resonances in the ^{13}C NMR spectrum (**Figure 4**) (**Table 8**) together with the appearance of three singlet methyl groups indicated that **N3** possessed a pimarane diterpene skeleton (Dettrakul *et al.*, 2003). The carbonyl carbon at δ_C 196.70 in the ^{13}C NMR spectrum supported the presence of the α,β-unsaturated ketone functional group. In the COSY spectrum, the methylene protons, H_2-2 (δ_H 1.56) (**Table 9**), were coupled with the methylene protons, H_{ab}-1 (δ_H 2.05 and 1.94), and the methylene protons, H_{ab}-3 (δ_H 1.57 and 1.21). In the HMBC spectrum, H_{ab}-3 (**Table 9**) showed cross peaks with C-2 (δ_C 17.68), C-4 (δ_C 37.29) and C-19 (δ_C 23.66) while the methyl protons of two methyl groups, Me-18 (δ_H 1.18) and Me-19 (δ_H 1.43), showed cross peaks with C-3 (δ_C 37.45) and C-5 (δ_C 81.57). These evidences suggested that both Me-18 and Me-19 were located at C-4. The lowfield-oxymethylene protons, H_{ab}-20 (δ_H 4.13 and 3.70), belonged to a hemiketal unit on the basis of their HMBC cross peaks with C-1 (δ_C 25.21), C-5, C-6 (δ_C 104.37) and C-9 (δ_C 76.33). The substituents at C-5, C-6 and C-9 were then assigned as the hydroxyl groups according to their ^{13}C chemical shifts. These resullts together with the HMBC cross peaks of 6-OH with C-5, C-6 and C-7 (δ_C 196.70) established the attachment of the carbonyl group at C-6. Furthermore, ^3J HMBC correlations of the β-olefinic proton (H-14) with C-7, C-15 (δ_C 144.04) and C-17 (δ_C 25.87) revealed that the β-carbon of the α,β-unsaturated carbonyl unit, Me-17 and the monosubstituted alkene moiety were attached at the same carbon, C-13 (δ_C 39.80). The oxymethine proton (δ_H 4.01, H-11) was coupled with the methylene protons (δ_H 2.03 and 1.72, H_{ab}-12) in the COSY spectrum. HMBC correlations of H-11/C-9 and C-10 (δ_C 51.12) and those of H_{ab}-12/C-13, C-14 (δ_C 150.22), C-15 and C-17 connected C-11 (δ_C 67.48) with C-9 and C-12 with C-13. Irradiation of the H-11, in

the NOEDIFF experiment, enhanced signals of H_b-20 and Me-17 (**Table 9**), suggesting that H-11, Me-17 and H_b-20 were located at the same side of the molecule. The X-ray analysis (**Figure 5**) confirmed these conclusions and further provided the absolute configuration of all chiral centers. The observed optical rotation of **N3** ($[\alpha]_D^{29}$ +131.13, c = 0.101, $CHCl_3$) was almost identical to that of diaporthein B ($[\alpha]_D^{31}$ +120.10, c = 0.106, $CHCl_3$), indicating that they possessed the same absolute configuration. Therefore, **N3** was diaporthein B, which was previously isolated from *Diaporthe* sp. BCC 6140 (Dettrakul *et al.*, 2003).

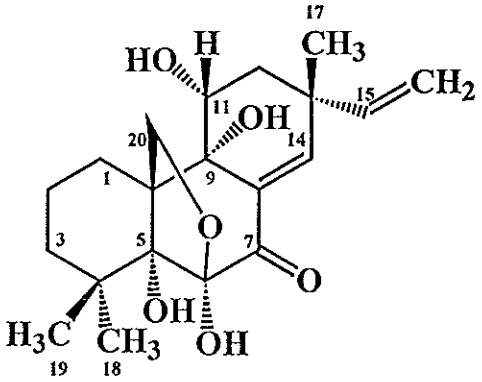

Table 8 The NMR data of **N3** and **diaporthein B** in $CDCl_3$

Position	N3		Diaporthein B[a]	
	δ_H (mult., J_{Hz})	δ_C (C-Type)	δ_H (mult., J_{Hz})	δ_C (C-Type)
1	a: 2.05 (*m*) b: 1.94 (*m*)	25.21 (CH_2)	a: 2.03 (*m*) b: 1.96 (*m*)	25.2 (CH_2)
2	1.56 (*m*)	17.68 (CH_2)	a: 1.68 (*m*) b: 1.62 (*m*)	17.6 (CH_2)
3	a: 1.57 (*m*) b: 1.21 (*m*)	37.45 (CH_2)	a: 1.55 (*m*) b: 1.23 (*m*)	37.5 (CH_2)
4	-	37.29 (C)	-	37.3 (C)
5-OH	-	81.57 (C)	-	81.9 (C)
6-OH	4.99 (*brs*)	104.37 (C)	-	104.1 (C)
7	-	196.70 (C=O)	-	196.2 (C=O)
8	-	134.78 (C)	-	134.7 (C)
9-OH	5.66 (*brs*)	76.33 (C)	-	76.2 (C)
10	-	51.12 (C)	-	51.1 (C)
11	4.01 (*dd*, 11.7, 4.2)	67.48 (CH)	4.03 (*dd*, 11.7, 4.1)	67.7 (CH)
12	a: 2.03 (*m*) b: 1.72 (*m*)	39.92 (CH_2)	a: 2.07 (*m*) b: 1.73 (*m*)	39.9 (CH_2)
13	-	39.80 (C)	-	40.1 (C)
14	6.80 (*d*, 1.8)	150.22 (CH)	6.81 (*d*, 1.8)	150.4 (CH)
15	5.82 (*dd*, 17.4, 10.5)	144.04 (CH)	5.82 (*dd*, 17.5, 10.7)	144.1 (CH)

Table 8 Continued

Position	N3		Diaporthein B[a]	
	δ_H (mult., J_{Hz})	δ_C (C-Type)	δ_H (mult., J_{Hz})	δ_C (C-Type)
16	a: 5.09 (*dd*, 17.4, 0.6) b: 5.07 (*dd*, 10.5, 0.6)	113.05 (CH_2)	5.09 (*m*)	113.1 CH_2)
17	1.20 (*s*)	25.87 (CH_3)	1.22 (*s*)	25.9 (CH_3)
18	1.18 (*s*)	27.21 (CH_3)	1.19 (*s*)	26.9 (CH_3)
19	1.43 (*s*)	23.66 (CH_3)	1.45 (*s*)	23.7 (CH_3)
20	a: 4.13 (*d*, 10.2) b: 3.70 (*d*, 10.2)	68.62 (CH_2)	a: 4.14 (*d*, 10.2) b: 3.71 (*d*, 10.2)	68.6 (CH_2)

[a]Dettrakul *et al.*, 2003.

Table 9 The HMBC, COSY and NOE data of **N3** in $CDCl_3$

Position	HMBC	COSY	NOE
H_{ab}-1	C-2, C-3, C-5, C-10, C-20	H_2-2	-
H_2-2	C-3, C-10	H_{ab}-1, H_{ab}-3	-
H_{ab}-3	C-2, C-4, C-19	H_2-2	-
6-OH	C-5, C-6, C-7	-	-
H-11	C-9, C-10, C-12	H_{ab}-12	H_b-12, Me-17, H_b-20
H_{ab}-12	C-9, C-11, C-13, C-14, C-15, C-17	H-11	-
H-14	C-7, C-8, C-9, C-12, C-15, C-17	-	H-15, H_{ab}-16, Me-17
H-15	C-12, C-13, C-14, C-17	H_{ab}-16	H_{ab}-12, H-14, Me-17
H_{ab}-16	C-13, C-15	H-15	H-14
Me-17	C-14, C-15	-	H-11, H-14, H-15
Me-18	C-3, C-5, C-19	-	-
Me-19	C-3, C-5, C-18	-	-
H_a-20	C-1, C-5, C-6, C-9, C-10	-	Me-18, Me-19, H_b-20

1.3.3 Compound N4

N4 was isolated as a white solid, melting at 215.5-216.8 °C. The IR spectrum exhibited an absorption band at 3328 cm^{-1} for a hydroxyl group. The UV spectrum showed a maximum absorption band at λ_{max} 206 nm which was lower than that found in **N3**. Its ^1H NMR spectrum (**Figure 6**) (**Table 10**) was similar to that of **N3** except for an addition signal of an oxymethine proton at δ_H 4.59 (*d*, J = 2.1 Hz, 1H). In addition, the olefinic proton, H-14 (δ_H 5.98), in **N4** displayed at much high field than that of **N3**. These suggested that the carbonyl group in **N3** was replaced by

an oxymethine group in **N4**. The ^{13}C NMR spectrum (**Figure 7**) (**Table 10**) supported the absence of the carbonyl carbon and the presence of an oxymethine carbon (δ_C 72.40). The HMBC correlations (**Table 11**) of H-7 (δ_H 4.59) with C-6 (δ_C 106.26), C-8 (δ_C 136.01) and C-14 (δ_C 132.68) confirmed the above conclusion. **N4** exhibited ^{1}H and ^{13}C NMR, HMQC and HMBC data identical to those of diaporthein A with a reported β-hydroxyl group at C-7 (Dettrakul *et al.*, 2003). The β-disposition of 7-OH has been assigned by comparison of its specific rotation with those of sphaeropsidins (Evidente *et al.*, 2002). However, in this investigation it was observed that the H-7 in the NOEDIFF experiment was strongly enhanced by irradiation of H-14 (**Table 11**), indicating that H-7 rather than 7-OH was located at the β-equatorial position. In addition, the remaining HMBC and NOEDIFF experiment confirmed that the location of all substituents and the absolute configuration of all chiral centers were identical to those of **N3**. **N4** gave almost identical optical rotation as diaporthein A ($[\alpha]_D^{29}$ of **N4** = +25.74, c = 0.122, $CHCl_3$ and $[\alpha]_D^{31}$ of diaporthein A = +25.80, c = 0.124, $CHCl_3$). Thus, **N4** was identified as diaporthein A, which was previously isolated from *Diaporthe* sp. BCC 6140 (Dettrakul *et al.*, 2003).

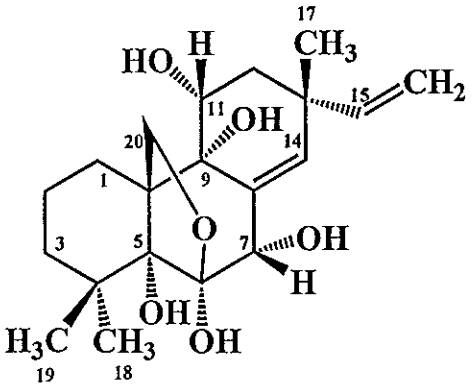

Table 10 The NMR data of **N4** and **diaporthein A** in $CDCl_3$

Position	N4		Diaporthein A[a]	
	δ_H (mult., J_{Hz})	δ_C (C-Type)	δ_H (mult., J_{Hz})	δ_C (C-Type)
1	a: 1.83 (*m*) b: 1.66 (*m*)	24.64 (CH_2)	a: 1.82 (*m*) b: 1.70 (*m*)	24.8 (CH_2)
2	1.56 (*m*)	18.06 (CH_2)	a: 1.67 (*m*) b: 1.61 (*m*)	18.0 (CH_2)
3	a: 1.63 (*m*) b: 1.13 (*m*)	37.72 (CH_2)	a: 1.69 (*m*) b: 1.22 (*m*)	37.8 (CH_2)

Table 10 Continued

Position	N4		Diaporthein A[a]	
	δ_H (mult., J_{Hz})	δ_C (C-Type)	δ_H (mult., J_{Hz})	δ_C (C-Type)
4	-	38.00 (C)	-	38.0 (C)
5	-	80.87 (C)	-	81.3 (C)
6	-	106.26 (C)	-	105.9 (C)
7	4.59 (*d*, 2.1)	72.40 (CH)	4.63 (*d*, 2.1)	73.3 (CH)
8	-	136.01 (C)	-	136.8 (C)
9	-	77.24 (C)	-	77.1(C)
10	-	49.95 (C)	-	50.1 (C)
11	3.83 (*dd*, 11.7, 4.8)	66.77 (CH)	3.86 (*dd*, 12.0, 4.2)	67.3 (CH)
12	a: 1.88 (*m*) b: 1.70 (*m*)	40.06 (CH_2)	a: 1.89 (*m*) b: 1.71 (*m*)	40.4 (CH_2)
13	-	38.18 (C)	-	38.3 (C)
14	5.98 (*t*, 1.5)	132.68 (CH)	5.99 (*dd*, 1.6, 1.7)	133.3 (CH)
15	5.82 (*dd*, 17.4, 10.5)	146.61 (CH)	5.85 (*dd*, 17.5, 10.7)	146.4 (CH)
16	a: 5.03 (*d*, 17.4) b: 4.98 (*brd*, 10.5)	111.17 (CH_2)	5.04 (*m*)	111.5 (CH_2)
17	1.14 (*s*)	24.89 (CH_3)	1.16 (*s*)	25.3 (CH_3)
18	1.20 (*s*)	27.84 (CH_3)	1.26 (*s*)	29.6 (CH_3)
19	1.38 (*s*)	24.19 (CH_3)	1.44 (*s*)	24.2 (CH_3)
20	a: 3.93 (*d*, 9.6) b: 3.30 (*d*, 9.6)	68.04 (CH_2)	a: 3.97 (*d*, 9.6) b: 3.36 (*d*, 9.6)	68.3 (CH_2)

[a]Dettrakul *et al.*, 2003.

Table 11 The HMBC and NOE data of **N4** in $CDCl_3$

Position	HMBC	NOE
H_{ab}-1	C-2, C-5, C-10	-
H_2-2	C-4	-
H_{ab}-3	C-5, C-10	-
H-7	C-6, C-8, C-14	H-14
H-11	C-10, C-12	H_b-20
H_{ab}-12	C-9, C-11, C-12, C-14, C-17	-
H-14	C-7, C-8, C-9, C-12, C-13, C-15	H-7, Me-17, H_b-20
H-15	C-12, C-13, C-14, C-17	H-14
H_{ab}-16	C-13, C-15	Me-17
Me-17	C-12, C-13, C-14, C-15	H-11, H-14, H-15, H_{ab}-16, H_b-20
Me-18	C-4, C-5, C-19	Me-19
Me-19	C-4, C-5, C-18	Me-18, H_a-20
H_a-20	C-1, C-5, C-6, C-9, C-10	Me-19, H_b-20
H_b-20	C-1, C-5, C-6, C-9, C-10	H-11, Me-17, H_a-20

1.3.4 Compound N2

N2 was obtained as a white solid, melting at 215.2-216.0 °C with $[\alpha]_D^{29}$ +57.42 (c = 1.00, MeOH). The UV and IR spectra were almost identical to those of **N3**. The molecular formula $C_{20}H_{28}O_5$ was deduced from the HREI-MS. The ^{1}H NMR spectral data (**Figure 9**) (**Table 12**) were similar to those of **N3** except that the oxymethine proton resonance (δ_H 4.01, *dd*, *J* = 11.7 and 4.2 Hz, 1H, H-11) in **N3** was replaced by the methylene proton signal (δ_H 1.71, *m*, 2H) in **N2**. Comparison of the ^{13}C NMR data (**Figure 10**) (**Table 12**) with those of **N3** showed analogy of the chemical shifts except for C-11 (δ_C 27.16) and C-12 (δ_C 29.47). The methylene protons were then attributed to H_2-11. This was confirmed by their HMBC cross peaks (**Table 12**) with C-8 (δ_C 134.96), C-9 (δ_C 74.62), C-12 and C-13 (δ_C 39.28). The absolute configuration was identical to that in **N3** according to NOEDIFF experiment of H_a-20 (δ_H 4.04, *d*, *J* = 9.9 Hz)/Me-19 (δ_H 1.43, *s*), H_b-20 (δ_H 3.73, *d*, *J* = 9.9 Hz)/H_2-11 and H_2-11/Me-17 (δ_H 1.16, *s*) (**Table 12**). Thus, **N2** was elucidated as a new pimarane diterpene derivative.

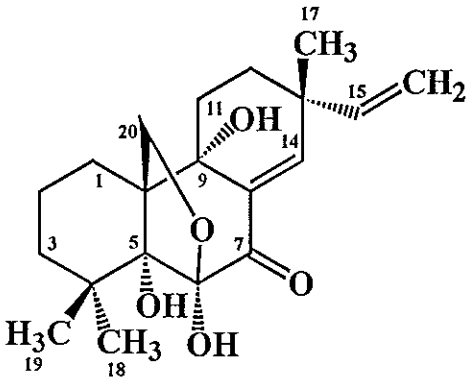

Table 12 The NMR data of **N2** in $CDCl_3$

Position	N2		HMBC	NOE
	δ_H (mult., J_{Hz})	δ_C (C-Type)		
1	2.08 (*m*)	22.09 (CH_2)	C-2, C-10, C-20	-
2	1.48 (*m*)	17.46 (CH_2)	C-10	-
3	a: 1.60 (*m*) b: 1.24 (*m*)	37.38 (CH_2)	C-2, C-4, C-5, C-10, C-19	-
4	-	37.05 (C)	-	-
5-OH	5.06 (*brs*)	81.67 (C)	-	-

Table 12 Continued

Position	N2		HMBC	NOE
	δ_H (mult., J_{Hz})	δ_C (C-Type)		
6	-	104.31 (C)	-	-
7	-	196.00 (C=O)	-	-
8	-	134.96 (C)	-	-
9	-	74.62(C)	-	-
10	-	49.31 (C)	-	-
11	1.71 (*m*)	27.16 (CH_2)	C-8, C-9, C-12, C-13	-
12	a: 2.20 (*dt*, 13.5, 4.8) b: 1.55 (*m*)	29.47 (CH_2)	C-11, C-13, C-15, C-17	-
13	-	39.28 (C)	-	-
14	6.79 (*d*, 1.5)	150.53 (CH)	C-7, C-8, C-9, C-12, C-15, C-17	Me-17
15	5.87 (*dd*, 17.4, 10.5)	144.90 (CH)	C-12, C-13, C-14, C-17	H-14, Me-17
16	a: 5.12 (*d*, 17.4) b: 5.07 (*d*, 10.5)	112.88 (CH_2)	C-13, C-15	H-15
17	1.16 (*s*)	24.73 (CH_3)	C-13, C-14, C-15	H-14, H-15, H_b-20
18	1.19 (*s*)	26.97 (CH_3)	C-3, C-4, C-5	Me-19
19	1.43 (*s*)	23.52 (CH_3)	C-4, C-5, C-18	Me-18, H_a-20
20	a: 4.04 (*d*, 9.9) b: 3.73 (*d*, 9.9)	68.50 (CH_2)	C-1, C-5, C-6, C-9, C-10	Me-19, H_b-20

1.3.5 Compound N5

N5 was obtained as a colorless gum with $[\alpha]_D^{29}$ +232.50, c = 0.04, MeOH). The UV spectrum showed a maximum absorption band at λ_{max} 246 nm while the hydroxyl and the carbonyl stretching frequencies in the IR spectrum were found in the region of 3414 and 1684 cm^{-1}, respectively. The HREI-MS showed the molecular formula $C_{20}H_{28}O_6$. The ^1H NMR data (**Figure 12**) (**Table 13**) were similar to those of **N3** except that the signal of the β-olefinic proton (δ_H 6.80, *d*, *J* = 1.8 Hz, 1H) of the α,β-unsaturated ketone in **N3** was replaced, in **N5**, by an oxymethine proton (δ_H 4.43, *m*, 1H). The oxymethine proton was attributed to H-14 on the basis of the ^3J HMBC cross peaks (**Table 13**) of H-14 with C-7 (δ_C 194.60), C-9 (δ_C 164.63), C-15 (δ_C 143.75) and C-17 (δ_C 24.31). The ^{13}C chemical shifts of C-8 (δ_C 132.29) and C-9

suggested the presence of a C_8-C_9 double bond. The absolute configuration of rings A and B was identical to that in **N3** according to NOEDIFF experiment (**Table 13**). Irradiation of H_b-20 (δ_H 3.29, *d*, J = 9.3 Hz, 1H) affected Me-17 (δ_H 1.03, *s*, 3H), but not H-11 (δ_H 4.42, *dd*, J = 6.3 and 4.8 Hz, 1H), indicating α-equatorial and β-axial location of H-11 and Me-17, respectively. The coupling constants derived from coupling between H-11 and H_a-12 (J = 4.8 Hz) and H_b-12 (J = 6.3 Hz) confirmed the α-equatorial position of H-11. Signal enhancement of H-14, upon irradiation of Me-17 in the NOEDIFF experiment, established the β-equatorial orientation of H-14. The absolute configuration of C-11 (δ_C 70.02) and C-14 (δ_C 64.53) was identical to that in sphaeropsidin E (Evidente *et al.*, 2002). Therefore, **N5** was assigned as a new pimarane diterpene derivative.

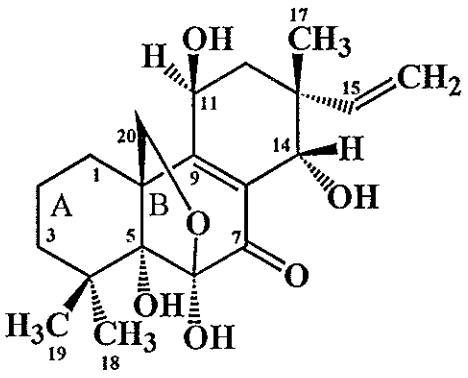

Table 13 The NMR data of **N5** in $CDCl_3$

Position	N5		HMBC	NOE
	δ_H (mult., J_{Hz})	δ_C (C-Type)		
1	1.74 (*m*)	23.77 (CH_2)	C-2, C-10, C-20	-
2	2.65 (*m*)	17.78 (CH_2)	-	-
3	a: 1.60 (*m*) b: 1.32 (*m*)	37.59 (CH_2)	C-2	-
4	-	36.83 (C)	-	-
5-OH	5.06 (*brs*)	81.11 (C)	C-5, C-6	-
6	-	104.93 (C)	-	-
7	-	194.60 (C=O)	-	-
8	-	132.29 (C)	-	-
9	-	164.63(C)	-	-
10	-	54.18 (C)	-	-

Table 13 Continued

Position	N5		HMBC	NOE
	δ_H (mult., J_{Hz})	δ_C (C-Type)		
11	4.42 (*dd*, 6.3, 4.8)	70.02 (CH)	C-8, C-9, C-10, C-12	H_b-12, Me-17
12	a: 2.24 (*dd*, 14.4, 4.8)	40.07 (CH_2)	C-9, C-11, C-13, C-14, C-15, C-17	-
	b: 2.01 (*dd*, 14.4, 6.3)	-	-	H-11, H_a-12, Me-17
13	-	39.82 (C)	-	-
14	4.43 (*m*)	64.53 (CH)	C-7, C-8, C-9, C-12, C-13, C-15, C-17	Me-17
15	6.13 (*dd*, 17.7, 10.2)	143.75 (CH)	C-12	-
16	a: 5.34 (*dd*, 10.2, 0.9)	115.12 (CH_2)	C-13, C-15	-
	b: 5.27 (*dd*, 17.7, 0.9)	-	-	-
17	1.03 (*s*)	24.31 (CH_3)	C-12, C-14, C-15	H-14, H_a-20
18	1.27 (*s*)	27.95 (CH_3)	C-3, C-4, C-5, C-19	Me-19
19	1.56 (*s*)	24.13 (CH_3)	C-3, C-4, C-5, C-18	Me-18, H_a-20
20	a: 4.45 (*d*, 9.3) b: 3.29 (*d*, 9.3)	70.40 (CH_2)	C-5, C-6, C-8, C-9, C-10	- Me-17, H_a-20

1.3.6 Compound N7

N7 was obtained as a white solid, melting at 152.5-153.7 °C, $[\alpha]_D^{29}$ +114.79 (c = 0.53, MeOH). The UV spectrum with maximum absorption bands at λ_{max} 224, 275 and 284 nm indicated that **N7** had a conjugated aromatic chromophore. A strong absorption band at 1761 cm^{-1} in the IR spectrum indicated the presence of a vinyl carbonate moiety while an absorption band at 1716 cm^{-1} was assigned to ketone and lactam carbonyl functional groups. The HREI-MS showed the molecular formula $C_{29}H_{35}NO_8$. The carbonyl carbon signals at δ_C 148.99, 169.92 and 211.51 were in agreement with the IR data. The ^1H (**Figure 15**) (**Table 14**) and ^{13}C NMR data (**Figure 16**) (**Table 14**) suggested that **N7** was structurally related to cytochalasin K (Steyn *et al.*, 1982). In the ^1H NMR spectrum, they differed only in the signal pattern of the phenyl ring attached at C-10. **N7** possessed a *para*-methoxybenzene ring

according to the presence of the characteristic proton resonances, δ_H 7.00 (*d*, *J* = 8.7 Hz, 2H), 6.80 (*d*, *J* = 8.7 Hz, 2H) and 3.72 (*s*, 3H). The absolute configuration was identical to that of cytochalasin K on the basis of the following NOEDIFF experiment (**Table 14**). Irradiation of H-3α (δ_H 3.35, *t*, *J* = 6.6 Hz, 1H) enhanced the signal intensity of only H-27 and H-31 (δ_H 7.00, *d*, *J* = 8.7 Hz, 2H), but not H-4 (δ_H 3.81, *brs*, 1H), indicating the *trans* relationship of H-3/H-4. Irradiation of H-8 (δ_H 2.81, *m*, 1H) affected the signal intensity of H-4, but not H-7 (δ_H 4.15, *dd*, *J* = 5.7 and 3.6 Hz, 1H) suggesting *cis* and *trans* relationship of H-4/H-8 and H-7/H-8, respectively. Upon irradiation of H-19 (δ_H 5.59, *d*, *J* = 11.7 Hz, 1H), the signal intensity of H-16 (δ_H 2.87, *m*, 1H) and Me-25 (δ_H 1.44, *s*, 3H) was enhanced, indicating the *cis* relationship of H-19/H-16 and H-19/Me-25. Therefore, **N7** was determined as a new methyl ether derivative of cytochalasin K.

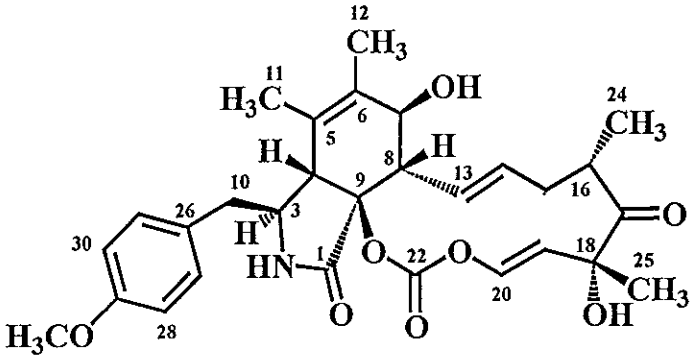

Table 14 The NMR data of **N7** in $CDCl_3$

Position	N7		HMBC	NOE
	δ_H (mult., J_{Hz})	δ_C (C-Type)		
1	-	169.92 (C=O)	-	-
2-NH	5.81 (*brs*)	-	-	-
3	3.35 (*t*, 6.6)	59.17 (CH)	C-1, C-5	Me-11, H-27
4	3.81 (*brs*)	48.23 (CH)	C-1, C-5, C-6, C-9	-
5	-	125.35 (C)	-	-
6	-	131.66 (C)	-	-
7	4.15 (*dd*, 5.7, 3.6)	70.03 (CH)	C-5	H-4, H-14
8	2.81 (*m*)	49.96 (CH)	C-1, C-7, C-9, C-13, C-14	-
9	-	86.20 (C)	-	-
10	2.78 (*m*)	43.23 (CH_2)	C-3, C-4, C-26, C-27	-

Table 14 Continued

Position	N7		HMBC	NOE
	δ_H (mult., J_{Hz})	δ_C (C-Type)		
11	1.46 (*brs*)	17.70 (CH_3)	C-4, C-5, C-6	-
12	1.61 (*brs*)	13.94 (CH_3)	C-5, C-6, C-7	Me-11
13	6.13 (*brdd*, 15.0, 10.5)	129.40 (CH)	-	-
14	5.31 (*ddd*, 15.0, 11.1, 3.9)	133.57 (CH)	C-8	H-8
15	a: 2.73 (*m*) b: 2.70 (*m*)	39.02 (CH_2)	C-13, C-14	-
16	2.87 (*m*)	40.91 (CH)	-	H-19, Me-24
17	-	211.51 (C=O)	-	-
18-OH	4.42 (*brs*)	76.63 (C)	-	-
19	5.59 (*d*, 11.7)	120.48 (CH)	C-18, C-20, C-25	H-16, H-20, Me-25
20	6.60 (*d*, 11.7)	142.48 (CH)	C-18, C-19, C-22	H-19
22	-	148.99 (C=O)	-	-
24	1.11 (*d*, 6.6)	20.17 (CH_3)	C-15, C-16, C-17	Me-25
25	1.44 (*s*)	24.64 (CH_3)	C-17, C-18, C-19	-
26	-	128.57 (C)	-	-
27, 31	7.00 (*d*, 8.7)	130.32 (CH)	C-10, C-29	H-3, H-28
28, 30	6.80 (*d*, 8.7)	114.31 (CH)	C-26, C-27, C-29	H-27, 29-OCH_3
29	-	158.69 (C)	-	-
29-OCH_3	3.72 (*s*)	55.27 (CH_3)	C-29	H-28

1.3.7 Compound N6

N6 was obtained as a white solid, melting at 188.6-189.2 °C with $[\alpha]_D^{29}$ -52.67, c = 0.17, MeOH. The UV and the IR data were similar to those of **N7**. The HREI-MS showed the molecular formula $C_{29}H_{37}NO_9$. The ^1H NMR spectrum (**Figure 18**) (**Table 15**) was similar to that of **N7** except for an additional signal of a methine proton (δ_H 2.29, *dd*, J = 7.2 and 5.2 Hz, 1H) in **N6**. In addition, signals of two methyl groups in the perhydroisoindolyl residue (Me-11, δ_H 1.11, *d*, J = 7.2 Hz, 3H and Me-12, δ_H 1.25, *s*, 3H) in **N6** resonated at higher field than those in **N7**. In the COSY spectrum (**Table 15**), the additional methine proton was coupled with Me-11. The HMBC cross peaks (**Table 15**) of Me-11 with C-4 (δ_C 48.06), C-5 (δ_C 35.83) and

C-6 (δ_C 57.27) and those of Me-12 with C-5, C-6 and C-7 (δ_C 60.61) indicated that they were located at C-5 and C-6, respectively. Consequently, the methine proton was attributed to H-5. The chemical shift of C-6 suggested the presence of a hydroxyl substituent at C-6. Signal enhancement of H-3α (δ_H 3.68, *m*, 1H) and Me-12 upon irradiation of Me-11 established their *cis* α-relationship. The absolute configuration of the macrocyclic ring was identical to that of **N7** on the basis of NOEDIFF experiment (**Table 15**). Therefore, **N6** was determined as a new cytochalasin derivative.

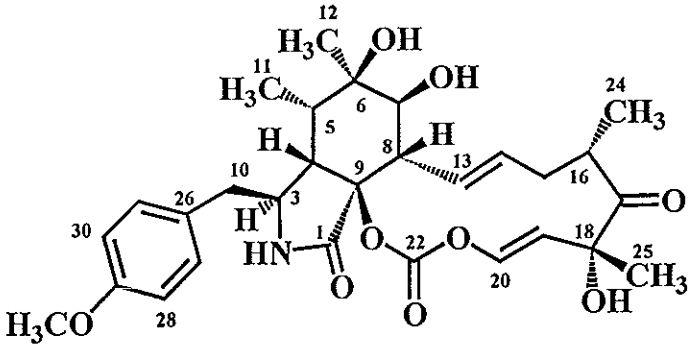

Table 15 The NMR data of **N6** in $CDCl_3$

Position	N6		HMBC	NOE
	δ_H (mult., J_{Hz})	δ_C (C-Type)		
1	-	170.00 (C=O)	-	-
2-NH	6.11 (*brs*)	-	-	-
3	3.68 (*m*)	53.75 (CH)	C-1, C-4, C-9, C-26	H-10, Me-11, Me-12, H-25
4	3.00 (*dd*, 5.2, 2.7)	48.06 (CH)	C-1, C-3, C-5, C-6, C-9, C-10	H-5, H-14, H-19
5	2.29 (*dd*, 7.2, 5.2)	35.83 (CH)	C-3, C-4, C-6, C-7, C-11, C-12	H-4, Me-11
6	-	57.27 (C)	-	-
7	2.65 (*m*)	60.61 (CH)	C-1	-
8	2.64 (*m*)	45.89 (CH)	C-1, C-9, C-13,C-14	-
9	-	87.03 (C)		-
10	a: 2.85 (*td*, 13.5, 4.5) b: 2.62 (*m*)	44.16 (CH_2)	C-3, C-4, C-26, C-27	H-3, H-4, H-27
11	1.11 (*d*, 7.2)	13.21 (CH_3)	C-4, C-5, C-6	H-3, H-5, Me-12
12	1.25 (*s*)	19.68 (CH_3)	C-5, C-6, C-7	H-3, Me-11

Table 15 Continued

Position	N6		HMBC	NOE
	δ_H (mult., J_{Hz})	δ_C (C-Type)		
13	5.89 (*ddm*, 15.0, 9.9)	128.45 (CH)	C-7, C-8	H-7
14	5.23 (*ddd*, 15.0, 10.0, 3.6)	131.54 (CH)	C-8, C-15	H-4, H-8, H_{ab}-15, H-19
15	a: 2.67 (*m*) b: 2.15 (*dm*, 13.8)	39.06 (CH_2)	C-13, C-14	- H-14, H_a-15, H-16, Me-24
16	2.93 (*ddd*, 11.4, 6.9, 2.4)	40.80 (CH)	C-24	H_b-15, H-19, Me-24
17	-	211.71 (C=O)	-	-
18-OH	4.43 (*brs*)	77.00 (C)	-	-
19	5.61 (*d*, 11.7)	120.39 (CH)	C-17, C-18, C-20, C-22, C-25	H-20
20	6.51 (*d*, 11.7)	142.15 (CH)	C-18, C-19, C-22	H-4, H-14, H-19, Me-25
22	-	149.36 (C=O)	-	-
24	1.16 (*d*, 6.6)	20.07 (CH_3)	C-15, C-16, C-17	H-16, Me-25
25	1.50 (*s*)	24.35 (CH_3)	C-17, C-18, C-19	Me-24
26	-	127.92 (C)	-	-
27, 31	7.06 (*d*, 8.7)	130.54 (CH)	C-10, C-29	-
28, 30	6.87 (*d*, 8.7)	114.34 (CH)	C-26, C-27, C-29	29-OCH_3
29	-	158.90 (C)	-	-
29-OCH_3	3.79 (*s*)	55.27 (CH_3)	C-29	-

PART II

CHEMICAL CONSTITUENTS FROM THE WOOD-DECAYED FUNGUS *LACHNUM* SP. BCC 2424

CHAPTER 2.1
INTRODUCTION

2.1.1 Introduction

The genus *Lachnum* is a rich source of biologically active secondary metabolites (**Table 16**). Chemical constituents isolated from the genus *Lachnum* are summarized in **Table 16** based on SciFinder Scholar database.

The fungus used in this study was collected on wood in leaf litter at Khao Yai National Park, Central Thailand, by Dr. Nigel. L. Hywel-Jones, the National Center for Genetic Engineering and Biotechnology (BIOTEC). On the basis of the DNA sequence data, it was identified as *Lachnum* sp., by Dr. Janet Jennifer Laungsaard, BIOTEC. This fungus was deposited in the BIOTEC Culture Collection as BCC 2424 on May 25, 1999.

Table 16 Compounds isolated from the *Lachnum* genus

Scientific name	Compound	Activity	References
L. papyraceum	(+)-Mycorrhizin A, **1** (+)-Chloromycorrhizin A, **2** (1′*E*)-Dechloromycorrhizin A, **3** Lachnumon, **4** Lachnumol A, **5**	Cytotoxic, nematicidal and antimicrobial	Stadler *et al.*, 1993a
	Lachnumon, **4** Lachnumol A, **5**	-	Stadler *et al.*, 1993b
	(1′*Z*)-Dechloromycorrhizin A, **6** Papyracon A, **7** Papyracon B, **8** Papyracon C, **9**	Antimicrobial, cytotoxic, nematicidal and phytotoxic	Stadler *et al.*, 1995a

Table 16 Continued

Scientific name	Compound	Activity	References
	Mycorrhizin B1, **10** Mycorrhizin B2, **11** Lachnumon B1, **12** Lachnumon B2, **13**		
	(+)-Mycorrhizin A, **1** (1′*E*)-Dechloromycorrhizin A, **3** (1′Z)-Dechloromycorrhizin A, **6** Papyracon A, **7** Papyracon B, **8** Papyracon C, **9**	Nematicidal and antimicrobial	Stadler *et al.*, 1995b
	Mycorrhizin B1, **10** Mycorrhizin B2, **11** Lachnumon B1, **12** Lachnomon B2, **13**	Nematicidal and antimicrobial	Stadler *et al.*, 1995c
	4-Chloro-6-hydroxymellein, **14** 4-Bromo-6-hydroxymellein, **15** 4-Chloro-6-methoxymellein, **16** 4-Chloro-5,6-dihydroxymellein, **17** 6-Hydroxymellein, **18** 6-Methoxymellein, **19**	Antimicrobial, cytotoxic, nematicidal and phytotoxic	Stadler *et al.*, 1995d
	4-Chloro-6-hydroxymellein, **14** 4-Bromo-6-hydroxymellein, **15** 4-Chloro-6-methoxymellein, **16** 4-Chloro-5,6-dihydroxymellein, **17**	Nematicidal and antimicrobial	Stadler *et al.*, 1995e
	Papyracon D, **20** 6-*O*-Methylpapyracon B, **21** 6-*O*-Methylpapyracon C, **22**	Antibioticl, nematicidal and cytotoxic	Shan *et al.*, 1996a

Table 16 Continued

Scientific name	Compound	Activity	References
	Lachnumfuran A, **23** Lachnumlactone A, **24** Chloromycorrhizinol A, **25**		
	Papyracillic acid, **26**	-	Shan *et al.*, 1996b Shan *et al.*, 1997a
	3,4-Dihydro-4,8-dihydroxy-6-methoxy-7-methyl-1(2*H*)-naphthalenone, **27** 6-*O*-Methylasparvenone, **28** 5-Hydroxy-7-methoxy-4,6-dimethylphthalide, **29** 2-Formyl-4-hydroxy-3-(hydroxymethyl)-6-methoxy-5-methylbenzoic acid, **30** 2-Formyl-3-(hydroxymethyl)-6-methoxy-5-methyl-4-[(3-methyl-2 butenyl)oxy]benzoic acid, **31** 1,7,8,9-Tetrahydro-1,9-dihydroxy-4-methoxy-5-methyl-8-(1-methylethenyl)-(1α,8α,9β)-3*H*-furo[3,4-*f*][1]-benzopyran-3-one, **32** 4-[(3-Methyl-2-butenyl)oxy]-6-methoxy-5-methyl-7-phthalidecarboxylic acid, **33**	Antimicrobial, phytotoxic and cytotoxic	Shan *et al.*, 1997b

Table 16 Continued

Scientific name	Compound	Activity	References
	4-[(3-Methyl-2-butenyl)oxy]-6-methoxy-5-methyl-7-phthalidecarboxylic acid methylester, **34**		

Structures of the metabolites from *Lachnum* genus

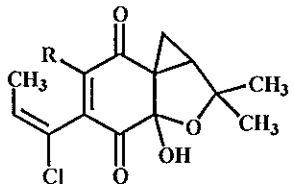

1: R = H : (+)-Mycorrhizin A
2: R = Cl : (+)-Chloromycorrhizin A

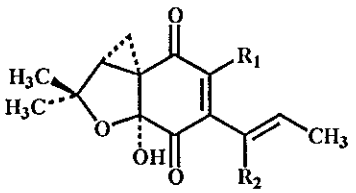

3: $R_1 = R_2 = H$: (1′*E*)-Dechloro-mycorrhizin A
10: $R_1 = H$, $R_2 = Br$: Mycorrhizin B1
11: $R_1 = Cl$, $R_2 = Br$: Mycorrhizin B2

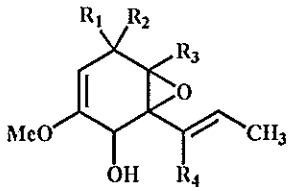

4: $R_1+R_2 = O$, $R_3 = R_4 = Cl$: Lachnumon
5: $R_1 = OH$, $R_2 = H$, $R_3 = R_4 = Cl$: Lachnumol A
12: $R_1+R_2 = O$, $R_3 = H$, $R_4 = Br$: Lachnumon B1
13: $R_1+R_2 = O$, $R_3 = Cl$, $R_4 = Br$: Lachnumon B2

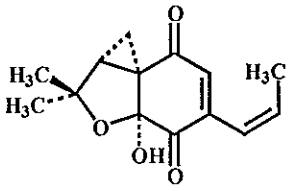

6: (1′Z)-Dechloromycorrhizin A

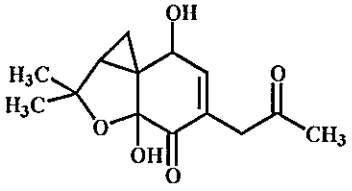

20: Papyracon D

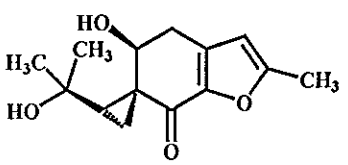

23: Lachnumfuran A

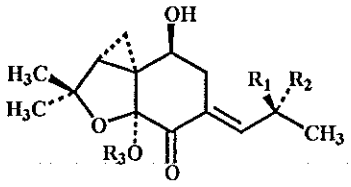

7: $R_1+R_2 = O$, $R_3 = H$: Papyracon A
8: $R_1 = OH$, $R_2 = H$, $R_3 = H$: Papyracon B
9: $R_1 = H$, $R_2 = OH$, $R_3 = H$: Papyracon C
21: $R_1 = OH$, $R_2 = H$, $R_3 = CH_3$: 6-*O*-Methylpapyracon B
22: $R_1 = H$, $R_2 = OH$, $R_3 = CH_3$: 6-*O*-Methylpapyracon C

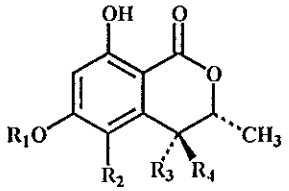

14: $R_1 = R_2 = R_4 = H$, $R_3 = Cl$: 4-Chloro-6-hydroxymellein
15: $R_1 = R_2 = R_4 = H$, $R_3 = Br$: 4-Bromo-6-hydroxymellein
16: $R_1 = CH_3$, $R_2 = R_4 = H$, $R_3 = Cl$: 4-Chloro-6-methoxymellein
17: $R_1 = R_4 = H$, $R_2 = OH$, $R_3 = Cl$: 4-Chloro-5,6-dihydroxymellein
18: $R_1 = R_2 = R_3 = R_4 = H$: 6-Hydroxymellein
19: $R_1 = CH_3$, $R_2 = R_3 = R_4 = H$: 6-Methoxymellein

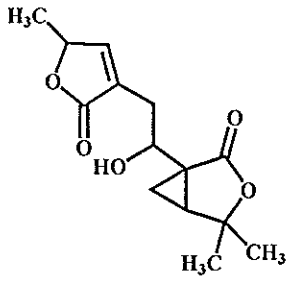

24: Lachnumlactone A

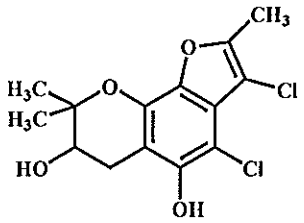

25: Chloromycorrhizinol A

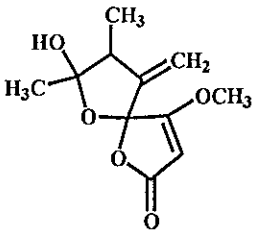

26: Papyracillic acid

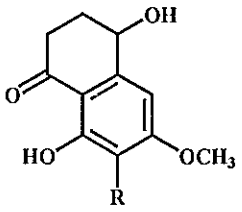

27: R = CH_3 : 3,4-Dihydro-4,8-dihydroxy- 6-methoxy-7-methyl-1(2*H*)-naphthalenone
28: R = CH_2CH_3 : 6-*O*-Methylasparvenone

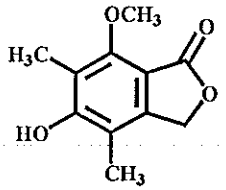

29: 5-Hydroxy-7-methoxy-4,6-dimethylphthalide

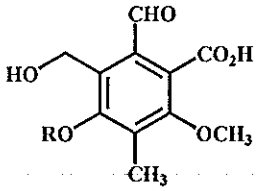

30: R = H : 2-Formyl-4-hydroxy-3-(hydroxymethyl)-6-methoxy-5-methylbenzoic acid

31: R = 3-methyl-2-butenyl : 2-Formyl-3-(hydroxymethyl)-6-methoxy-5-methyl-4-[(3-methyl-2-butenyl)oxy]benzoic acid

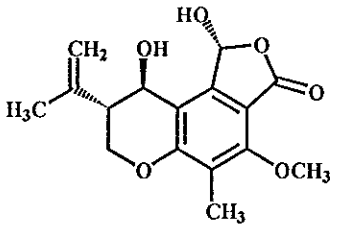

32: 1,7,8,9-Tetrahydro-1,9-dihydroxy-4-methoxy-5-methyl-8-(1-methylethenyl)-(1α,8α,9β)-3*H*-furo[3,4-*f*][1]-benzopyran-3-one

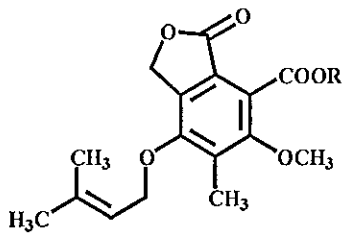

33: R = H : 4-[(3-Methyl-2-butenyl)oxy]-6-methoxy-5-methyl-7-phthalidecarboxylic acid

34: R = CH_3 : 4-[(3-Methyl-2-butenyl)oxy]-6-methoxy-5-methyl-7-phthalidecarboxylic acid methyl ester

CHAPTER 2.2
EXPERIMENTAL

2.2.1 Fermentation and extraction

The flask culture of the fungus *Lachnum* sp. BCC 2424 was filtered to separate into the filtrate and wet mycelia. The filtrate was extracted three times with an equal volume of EtOAc. The EtOAc layer was dried over anhydrous $MgSO_4$ and evaporated to dryness under reduced pressure to obtain a brown gum (572.4 mg). The wet mycelia were extracted twice with 500 ml of MeOH for 2 days. To the extract was added H_2O (50 ml), and the mixture washed with hexane (700 ml). The aqueous MeOH layer was concentrated under reduced pressure. The aqueous layer was extracted three times with an equal volume of EtOAc (700 ml). The EtOAc extract was dried over anhydrous $MgSO_4$ and then evaporated to dryness under reduced pressure to give a dark brown gum (250.8 mg).

2.2.2 Purification of the broth extract

The ethyl acetate extract of the culture filtrate showed four UV-active spots on normal phase TLC with the R_f values of 0.11, 0.13, 0.45 and 0.55 using 2% methanol in dichloromethane (3 runs) as a mobile phase. It was further separated by column chromatography over Sephadex LH20 using 100% MeOH as eluent. All fractions were examined by TLC, combined on the basis of their chromatogram characteristics and then evaporated to dryness under reduced pressure to give six fractions, as shown in **Table 17.**

Table 17 Fractions obtained from **the broth extract** by column chromatography over Sephadex LH20

Fraction	Eluent	Weight (mg)	Physical appearance
A	100% MeOH	4.4	Brown solid
B	100% MeOH	64.1	Brown gum
C	100% MeOH	146.5	Brown gum
D	100% MeOH	154.6	Brown-yellow gum
E	100% MeOH	57.7	Brown-orange solid
F	100% MeOH	32.7	Dark-brown gum

Fraction A showed no definite spots under UV-S on normal phase TLC using 2% methanol in dichloromethane as a mobile phase (2 runs). Its ^{1}H NMR spectrum displayed proton signals at high field region. Therefore, it was not further investigated.

Fraction B showed many spots under UV-S on normal phase TLC using 2% methanol in dichloromethane as a mobile phase (2 runs). Further separation by column chromatography over silica gel using a gradient system of methanol-dichloromethane was performed. All subfractions were examined by TLC, combined on the basis of their chromatogram characteristics and then evaporated to dryness under reduced pressure to afford four subfractions, as shown in **Table 18**.

Table 18 Subfractions obtained from **fraction B** by column chromatography over silica gel

Subfraction	Eluent	Weight (mg)	Physical appearance
B-1	100% CH_2Cl_2 - 5% MeOH/CH_2Cl_2	17.9	Yellow gum
B-2	5-7% MeOH/CH_2Cl_2	9.3	Yellow gum

Table 18 Continued

Subfraction	Eluent	Weight (mg)	Physical appearance
B-3	7-30% MeOH/CH_2Cl_2	12.8	Yellow gum mixed with yellow solid
B-4	50% MeOH/CH_2Cl_2 - 100% MeOH	23.8	Brown gum

Subfraction B-1 showed no spots under UV-S on normal phase TLC using 2% methanol in dichloromethane as a mobile phase (2 runs). According to the appearance of proton signals at high field in the ^{1}H NMR spectrum, it was not further studied.

Subfraction B-2 (N8) displayed one UV-active spot on normal phase TLC with the R_f value of 0.60 using 2% methanol in dichloromethane (2 runs) followed by 5% methanol in dichloromethane (3 runs) as mobile phases.

$[\alpha]_D^{26}$		+7.73 (c = 0.76, MeOH)
FT-IR (neat) ν_{cm-1}		3369 (O-H stretching), 1601 (C=C stretching)
^{1}H NMR ($CDCl_3$) (δ ppm) (300 MHz)		5.92 (*dd*, *J* = 17.4, 10.8 Hz, 1H), 5.42 (*triplet of sextet*, *J* = 7.0, 1.2 Hz, 1H), 5.22 (*dd*, *J* = 17.4, 1.2 Hz, 1H), 5.07 (*dd*, *J* = 10.8, 1.2 Hz, 1H), 3.99 (*q*, *J* = 0.9 Hz, 2H), 2.09 (*m*, 2H), 1.67 (*s*, 3H), 1.62 (*m*, 1H), 1.58 (*m*, 1H), 1.30 (*s*, 3H)
^{13}C NMR ($CDCl_3$) (δ ppm) (75 MHz)		144.88, 135.04, 125.95, 111.86, 73.32, 68.84, 41.73, 27.89, 22.33, 13.64
DEPT (135°) ($CDCl_3$)	CH :	144.88, 125.95
	CH_2 :	111.86, 68.84, 41.73, 22.33
	CH_3 :	27.89, 13.64

Subfraction B-3 demonstrated one major UV-active spot on normal phase TLC with the R_f value of 0.60 using 2% methanol in dichloromethane (2 runs) followed by 5% methanol in dichloromethane (3 runs) as mobile phases. Its ^{1}H NMR spectral data indicated the presence of **N8**. Therefore, no attempted investigation was carried out.

Subfraction B-4 showed no definite spots under UV-S on normal phase TLC using 2% methanol in dichloromethane (2 runs) followed by 5% methanol in dichloromethane (3 runs) as mobile phases. Its ^{1}H NMR spectrum displayed proton signals at high field region. Therefore, it was not further investigated.

Fraction C contained five major spots under UV-S on normal phase TLC with the R_f values of 0.05, 0.18, 0.40, 0.48 and 0.60 using 1% methanol in dichloromethane as a mobile phase. Further separation by column chromatography over silica gel using a gradient system of methanol-dichloromethane was performed. Fractions, which contained similar components, were combined and evaporated to dryness under reduced pressure to give eight subfractions, as shown in **Table 19**.

Table 19 Subfractions obtained from **fraction C** by column chromatography over silica gel

Subfraction	Eluent	Weight (mg)	Physical appearance
C-1	100% CH_2Cl_2 - 2% MeOH/CH_2Cl_2	9.2	Yellow gum
C-2	2-3% MeOH/CH_2Cl_2	7.2	Yellow gum
C-3	5% MeOH/CH_2Cl_2	22.7	Orange gum
C-4	10-20% MeOH/CH_2Cl_2	7.0	Orange gum
C-5	30% MeOH/CH_2Cl_2	4.7	Yellow gum
C-6	30% MeOH/CH_2Cl_2	5.0	Yellow gum
C-7	50-70% MeOH/CH_2Cl_2	36.9	Brown gum
C-8	80% MeOH/CH_2Cl_2 - 100% MeOH	23.7	Brown gum mixed with brown solid

Subfraction C-1 showed four spots under UV-S on normal phase TLC with the R_f values of 0.45, 0.53, 0.63 and 0.70 using 3% methanol in dichloromethane (3 runs) as a mobile phase. Further purification by precoated TLC with 100% dichloromethane as a mobile phase (7 runs) afforded four bands.

Band 1 was obtained as a yellow gum (1.5 mg). Its chromatogram showed two spots under UV-S on normal phase TLC with the R_f values of 0.43 and 0.78 using 0.5% methanol in dichloromethane as a mobile phase (2 runs). The ^1H NMR spectrum indicated that it was a mixture. Because of low quantity, it was not further purified.

Band 2 was a yellow gum (1.0 mg), which showed one spot under UV-S on normal phase TLC with the R_f value of 0.38 using 0.5% methanol in dichloromethane as a mobile phase (2 runs). The ^1H NMR spectrum indicated that it was a mixture. Therefore, no attempted separation was carried out.

Band 3 was obtained as a yellow solid (1.1 mg). Its chromatogram displayed one UV-active spot on normal phase TLC with the R_f value of 0.13 using 0.5% methanol in dichloromethane as a mobile phase (2 runs). The ^1H NMR spectrum suggested that it was a mixture. Therefore, no attempted investigation was performed.

Band 4 was obtained as an orange solid (2.0 mg). Its chromatogram contained one UV-active spot on normal phase TLC with the R_f value of 0.08 using 0.5% methanol in dichloromethane as a mobile phase (2 runs). The ^1H NMR spectrum suggested that it was a mixture. Thus, it was not further investigated.

Subfraction C-2 displayed one major UV-active spot on normal phase TLC with the R_f value of 0.45 using 3% methanol in dichloromethane (3 runs) as a mobile phase. Further purification by precoated TLC with 100% dichloromethane as a mobile phase (15 runs) afforded four bands.

Band 1 was obtained as a yellow solid (1.3 mg), which showed one spot under UV-S on normal phase TLC with the R_f value of 0.43 using 1% methanol in dichloromethane as a mobile phase (4 runs). The ^{1}H NMR spectrum indicated that it was not pure. Because of low quantity, it was not further investigated.

Band 2 was a yellow gum (1.0 mg), which showed one UV-active spot on normal phase TLC with the R_f value of 0.25 using 1% methanol in dichloromethane as a mobile phase (4 runs). The ^{1}H NMR spectrum indicated that it was a mixture. Therefore, no attempted separation was carried out.

Band 3 (N9) was a yellow gum (1.6 mg). Its chromatogram showed one spot under UV-S on normal phase TLC with the R_f value of 0.20 using 1% methanol in dichloromethane as a mobile phase (4 runs).

$[\alpha]_D^{26}$		+43.40 (c = 0.13, MeOH)
UV(MeOH) λ_{max} nm (log ε)		211 (3.64), 278 (3.36), 348 (2.77)
FT-IR (neat) ν_{cm-1}		3384 (O-H stretching), 1776 and 1642 (C=O stretching), 1573 (C=C stretching)
^{1}H NMR ($CDCl_3$) (δ ppm) (300 MHz)		11.57 (*s*, 1H), 6.52 (*brs*, 1H), 6.45 (*brs*, 1H), 4.63 (*brs*, 2H), 4.58 (*t*, J = 7.2 Hz, 1H), 2.98 (*d*, J = 17.1 Hz, 1H), 2.61 (*d*, J = 17.1 Hz, 1H), 2.60 (*m*, 2H), 2.32 (*m*, 2H), 1.43 (*s*, 3H)
^{13}C NMR ($CDCl_3$) (δ ppm) (125 MHz)		195.82, 176.10, 162.01, 158.90, 153.16, 106.92, 106.43, 105.29, 82.56, 80.85, 64.47, 42.85, 28.21, 22.34, 19.14
DEPT (135°) ($CDCl_3$)	CH :	106.43, 105.29, 82.56
	CH_2 :	64.47, 42.85, 28.21, 22.35
	CH_3 :	19.14
EIMS *m/z* (% relative intensity):		292 (19), 207 (100), 167 (35), 149 (55), 72 (37), 69 (25), 59 (58)

Band 4 (N10) was obtained as a yellow gum (1.9 mg). Its chromatogram showed one spot under UV-S on normal phase TLC with the R_f value of 0.15 using 1% methanol in dichloromethane as a mobile phase (4 runs).

$[\alpha]_D^{27}$		+51.43 (c = 0.035, MeOH)
UV(MeOH) λ_{max} nm (log ε)		281 (3.90), 354 (3.28)
FT-IR (neat) ν_{cm-1}		3367 (O-H stretching), 1775, 1731 and 1705 (C=O stretching), 1644 (C=C stretching)
^{1}H NMR ($CDCl_3$) (δ ppm) (500 MHz)		10.80 (*s*, 1H), 6.78 (*brs*, 1H), 6.53 (*q*, *J* = 1.5 Hz, 1H), 6.47 (*q*, *J* = 1.5 Hz, 1H), 5.36 (*dd*, *J* = 9.0, 7.0 Hz, 1H), 4.64 (*brs*, 2H), 2.86 (*d*, *J* = 16.5 Hz, 1H), 2.79 (*d*, *J* = 16.5 Hz, 1H), 2.60 (*m*, 2H), 2.45 (*s*, 3H), 2.44 (*m*, 2H), 1.26 (*s*, 3H)
^{13}C NMR ($CDCl_3$) (δ ppm) (125 MHz)		212.65, 195.51, 176.37, 162.36, 157.71, 153.27, 106.84, 105.22, 103.92, 84.28, 78.67, 77.72, 64.46, 39.08, 31.91, 27.96, 23.13, 12.77
DEPT (135°) ($CDCl_3$)	CH :	106.84, 105.22, 77.72
	CH_2 :	64.46, 39.08, 27.96, 23.13
	CH_3 :	31.91, 12.77
EIMS *m/z* (% relative intensity):		364 (26), 222 (39), 194 (46), 177 (80), 167 (100), 85 (45)

Subfraction C-3 showed two major spots under UV-S on normal phase TLC with the R_f values of 0.30 and 0.35 using 3% methanol in dichloromethane as a mobile phase (3 runs). Further purification by flash column chromatography over silica gel using a gradient system of dichloromethane-methanol was performed. Fractions, which contained similar components, were combined and evaporated to dryness under reduced pressure to give four subfractions, as shown in **Table 20.**

Table 20 Subfractions obtained from **subfraction C-3** by flash column chromatography over silica gel

Subfraction	Eluent	Weight (mg)	Physical appearance
C-3-1	100% CH_2Cl_2 - 3% MeOH/CH_2Cl_2	1.0	Yellow gum
C-3-2	3-5% MeOH/CH_2Cl_2	8.2	Yellow gum
C-3-3	5% MeOH/CH_2Cl_2	10.3	Orange gum
C-3-4	10-80% MeOH/CH_2Cl_2	3.1	Orange gum

Subfraction C-3-1 demonstrated no UV-active spots on normal phase TLC using 1% methanol in dichloromethane (6 runs) as a mobile phase. Its ^{1}H NMR spectrum displayed proton signals at high field region. Therefore, no attempted investigation was carried out.

Subfraction C-3-2 showed one major UV-active spot on normal phase with the R_f value of 0.33 TLC using 1% methanol in dichloromethane (6 runs) as a mobile phase. When using 20% ethyl acetate in light petroleum (3 runs) followed by 30% ethyl acetate in light petroleum (15 runs) as mobile phases, the chromatogram showed two UV-active spots on normal phase TLC with the R_f values of 0.31 and 0.54. Further purification by precoated TLC using 30% ethyl acetate in light petroleum as a mobile phase (21 runs) afforded two bands.

Band 1 (N11) was obtained as a yellow gum (2.5 mg), which displayed one spot under UV-S on normal phase TLC with the R_f value of 0.50 using 20% ethyl acetate in light petroleum as a mobile phase (12 runs).

$[\alpha]_D^{26}$	+27.10 (c = 0.22, MeOH)
UV(MeOH) λ_{max} nm (log ε)	211 (4.42), 244 (3.97), 279 (4.18), 346 (3.70)
FT-IR (neat) ν_{cm-1}	3388 (O-H stretching), 1734 and 1644 (C=O stretching), 1569 (C=C stretching)

^{1}H NMR ($CDCl_3$) (δ ppm) (300 MHz)		10.60 (*s*, 1H), 6.56 (*dt*, *J* = 1.2, 0.9 Hz, 1H), 6.48 (*dt*, *J* = 1.2, 0.9 Hz, 1H), 4.78 (*dd*, *J* = 7.8, 6.3 Hz, 1H), 4.65 (*t*, *J* = 0.9 Hz, 2H), 4.59 (*s*, 1H), 2.73 (*m*, 1H), 2.61 (*m*, 2H), 2.37 (*m*, 1H), 1.42 (*s*, 3H)
^{13}C NMR ($CDCl_3$) (δ ppm) (125 MHz)		196.36, 176.66, 161.19, 158.68, 154.35, 106.94, 106.05, 104.55, 84.30, 82.28, 71.30, 64.35, 28.27, 21.93, 13.43
DEPT (135°) ($CDCl_3$)	CH :	106.94, 106.05, 82.28, 71.30
	CH_2 :	64.35, 28.27, 21.93
	CH_3 :	13.43
EIMS *m/z* (% relative intensity):		308 (6), 284 (41), 223 (28), 185 (46), 133 (32), 81(28), 69 (61), 61 (43)

Band 2 was obtained as a yellow gum (3.8 mg), which showed one spot under UV-S on normal phase TLC with the R_f value of 0.38 using 20% ethyl acetate in light petroleum as a mobile phase (12 runs). The ^{1}H NMR spectrum suggested that it was a mixture. Therefore, no attempted investigation was performed.

Subfraction C-3-3 displayed two UV-active spots on normal phase TLC with the R_f values of 0.30 and 0.33 using 1% methanol in dichloromethane (6 runs) as a mobile phase. When using 20% ethyl acetate in light petroleum (3 runs) and 30% ethyl acetate in light petroleum (15 runs) as mobile phases, the chromatogram showed four UV-active spots on normal phase TLC with the R_f values of 0.31, 0.40, 0.54 and 0.65. Further purification by precoated TLC with 30% ethyl acetate in light petroleum as a mobile phase (21 runs) afforded two bands.

Band 1 was obtained as a yellow gum (4.1 mg), which displayed one spot under UV-S on normal phase TLC with the R_f value of 0.50 using 20% ethyl acetate in light petroleum as a mobile phase (12 runs). Its ^{1}H NMR spectral data indicated the presence of **N11**.

Band 2 was obtained as a yellow gum (5.6 mg), which showed one spot under UV-S on normal phase TLC with the R_f value of 0.38 using 20% ethyl acetate in light petroleum as a mobile phase (12 runs). The ^1H NMR spectrum suggested that it was a mixture. Therefore, no attempted investigation was carried out.

Subfraction C-3-4 showed no UV-active spots on normal phase TLC using 1% methanol in dichloromethane (6 runs) as a mobile phase. Its ^1H NMR spectrum displayed proton signals at high field region. Therefore, no attempted investigation was performed.

Subfraction C-4 demonstrated many UV-active spots on normal phase TLC using 3% methanol in dichloromethane (3 runs) as a mobile phase. Its ^1H NMR spectrum displayed proton signals at high field region. Thus, it was not further studied.

Subfraction C-5 displayed one major UV-active spot on normal phase TLC with the R_f value of 0.20 using 5% methanol in dichloromethane (3 runs) as mobile phase. Further purification by precoated TLC using 3% methanol in dichloromethane (5 runs) as a mobile phase afforded a yellow gum (2.2 mg), which displayed one spot under UV-S on normal phase TLC with the R_f value of 0.50 using 3% methanol in dichloromethane (5 runs) as a mobile phase. This compound was decomposed upon keeping in a $CDCl_3$ solution at 10° C for 7 days. Therefore, it was not further investigated.

Subfraction C-6 showed two UV-active spots on normal phase TLC with the R_f values of 0.15 and 0.20 using 5% methanol in dichloromethane (3 runs) as a mobile phase. Further purification by precoated TLC with 3% methanol in dichloromethane (5 runs) as a mobile phase afforded two bands.

Band 1 was obtained as a yellow gum (1.5 mg). Its chromatogram displayed one spot under UV-S on normal phase TLC with the R_f value of 0.50 using

3% methanol in dichloromethane (5 runs) as a mobile phase. Its ^{1}H NMR spectrum displayed proton signals at high field region. Thus, it was not further purified.

Band 2 was obtained as a yellow gum (1.3 mg), which showed one spot under UV-S on normal phase TLC with the R_f value of 0.30 using 3% methanol in dichloromethane (5 runs) as a mobile phase. The ^{1}H NMR spectrum suggested that it was a mixture. Therefore, no attempted purification was carried out.

Subfraction C-7 demonstrated a long UV-active spot using 3% methanol in dichloromethane (3 runs) followed by 5% methanol in dichloromethane (2 runs) as mobile phases. In addition, its chromatogram showed no definite spots after dipping the normal phase TLC in ASA reagent and subsequently heating. Its ^{1}H NMR spectrum displayed proton signals at high field region. Therefore, it was not further investigated.

Subfraction C-8 showed no UV-active spots on normal phase TLC using 3% methanol in dichloromethane (3 runs) followed by 5% methanol in dichloromethane (2 runs) as mobile phases and displayed no spots after dipping the normal phase TLC in ASA reagent and subsequently heating. Its ^{1}H NMR spectrum displayed proton signals at high field region. Therefore, no attempted investigation was carried out.

Fraction D showed four UV-active spots on normal phase TLC with the R_f values of 0.13, 0.20, 0.45 and 0.63 using 2% methanol in dichloromethane (3 runs) as a mobile phase. Further separation by column chromatography over silica gel using a gradient system of methanol-dichloromethane was performed. All subfractions were examined by TLC, combined on the basis of their chromatogram characteristics and then evaporated to dryness under reduced pressure to afford seven subfractions, as shown in **Table 21**.

Table 21 Subfractions obtained from **fraction D** by column chromatography over silica gel

Subfraction	Eluent	Weight (mg)	Physical appearance
D-1	100% CH_2Cl_2 - 2% MeOH/CH_2Cl_2	2.5	Yellow gum
D-2	2-5% MeOH/CH_2Cl_2	1.0	Yellow gum
D-3	5% MeOH/CH_2Cl_2	2.6	Orange solid
D-4	5% MeOH/CH_2Cl_2	11.3	Orange solid
D-5	10% MeOH/CH_2Cl_2	10.3	Yellow gum mixed with orange solid
D-6	10-20% MeOH/CH_2Cl_2	17.7	Orange-yellow gum
D-7	50% MeOH/CH_2Cl_2 - 100% MeOH	78.8	Brown gum mixed with brown solid

Subfraction D-1 showed no spots under UV-S on normal phase TLC using 5% methanol in dichloromethane as a mobile phase. Its ^{1}H NMR spectrum displayed proton signals at high field region. Thus, further purification was not performed.

Subfraction D-2 (N12) displayed one UV-active spot on normal phase TLC with the R_f value of 0.63 using 5% methanol in dichloromethane as a mobile phase.

UV(MeOH) λ_{max} nm (log ε)	245 (3.54), 277 (3.10), 342 (3.00)
FT-IR (neat) ν_{cm-1}	3346 (O-H stretching), 1639 (C=O stretching), 1596 (C=C stretching)
^{1}H NMR ($CDCl_3$) (δ ppm) (300 MHz)	11.58 (*s*, 1H), 6.71 (*brs*, 1H), 6.59 (*brs*, 1H), 5.78 (*brs*, 1H), 2.45 (*s*, 3H), 2.40 (*s*, 3H)
^{13}C NMR ($CDCl_3$) (δ ppm) (125 MHz)	175.28, 159.41, 155.84, 149.67, 146.75, 136.70, 110.95, 107.71, 107.28, 22.43, 15.09

DEPT (135°) ($CDCl_3$)	CH :	110.95, 107.71
	CH_3 :	22.43, 15.09
EIMS *m/z* (% relative intensity):		206 (100), 191 (23), 177 (23), 151 (26), 135 (23)

Subfraction D-3 displayed two UV-active spots on normal phase TLC with the R_f values of 0.30 and 0.63 using 5% methanol in dichloromethane as a mobile phase. According to its ^{1}H NMR data, it contained **N12** and **N13**. Because of low quantity, it was not further separated.

Subfraction D-4 (N13) melted at 148.5-149.2 °C. Its chromatogram showed one UV-active spot on normal phase TLC with the R_f value of 0.30 using 5% methanol in dichloromethane as a mobile phase.

UV(MeOH) λ_{max} nm (log ε)		245 (4.30), 344 (3.70)
FT-IR (neat) ν_{cm-1}		3346 (O-H stretching), 1639 (C=O stretching), 1600 (C=C stretching)
^{1}H NMR (Acetone-d_6) (δ ppm) (300 MHz)		12.10 (*s*, 1H), 7.85 (*brs*, 1H), 6.97 (*brs*, 1H), 6.70 (*brs*, 1H), 4.69 (*brs*, 2H), 2.43 (*s*, 3H)
^{13}C NMR (Acetone-d_6) (δ ppm) (75 MHz)		176.92, 160.81, 156.64, 152.17, 152.08, 138.09, 109.30, 107.76, 104.99, 63.89, 15.05
DEPT (135°) (Acetone-d_6)	CH :	107.76, 104.99
	CH_2 :	63.89
	CH_3 :	15.05
EIMS *m/z* (% relative intensity):		222 (100), 193 (29)

Subfraction D-5 showed two UV-active spots on normal phase TLC with the R_f values of 0.20 and 0.30 using 5% methanol in dichloromethane as a mobile phase. When using 50% ethyl acetate in light petroleum (2 runs) followed by 80% ethyl acetate in light petroleum (2 runs) as mobile phases, its showed three UV-active spots on normal phase TLC with the R_f values of 0.63, 0.78 and 0.85. Further purification by precoated TLC with 50% ethyl acetate in light petroleum (4 runs) as a mobile phase afforded three bands.

Band 1 was obtained as an orange-red solid (2.2 mg). Its chromatogram displayed one spot under UV-S on normal phase TLC with the R_f value of 0.60 using 50% ethyl acetate in light petroleum (3 runs) as a mobile phase. Its ^{1}H NMR spectral data and chromatogram on normal phase TLC indicated that it was **N13**.

Band 2 was obtained as a yellow solid (2.5 mg), which showed one spot under UV-S on normal phase TLC with the R_f value of 0.30 using 50% ethyl acetate in light petroleum (3 runs) as a mobile phase. The ^{1}H NMR spectrum suggested that it was a mixture. Because of low quantity, it was not further separated.

Band 3 was obtained as a yellow gum (3.1 mg). Its chromatogram showed one UV-active spot on normal phase TLC with the R_f value of 0.23 using 50% ethyl acetate in light petroleum (3 runs) as a mobile phase. Its ^{1}H NMR spectral data indicated that it was **N11**.

Subfraction D-6 showed three spots under UV-S on normal phase TLC with the R_f values of 0.55, 0.60 and 0.68 using 5% methanol in dichloromethane (3 runs) as a mobile phase. Further purification by precoated TLC with 3% methanol in dichloromethane (5 runs) as a mobile phase afforded three bands.

Band 1 was obtained as an orange solid (1.1 mg). Its chromatogram demonstrated one UV-active spot on normal phase TLC with the R_f value of 0.43 using 3% methanol in dichloromethane (2 runs) as a mobile phase. The ^{1}H NMR spectrum suggested that it was a mixture. Because of low quantity, it was not further separated.

Band 2 was obtained as a yellow gum (2.7 mg). Its chromatogram showed one spot under UV-S on normal phase TLC with the R_f value of 0.30 using 3% methanol in dichloromethane (2 runs) as a mobile phase. Its ^{1}H NMR spectral data indicated that it was **N11**.

Band 3 was an orange solid (1.5 mg). Its chromatogram displayed one spot under UV-S on normal phase TLC with the R_f value of 0.23 using 3% methanol in dichloromethane (2 runs) as a mobile phase. The ^1H NMR spectrum suggested that it was a mixture. Because of low quantity, it was not further investigated.

Subfraction D-7 displayed no UV-active spots on normal phase TLC using 5% methanol in dichloromethane (3 runs) as a mobile phase. Furthermore, its chromatogram showed no UV-active spots on reverse phase TLC using 50% methanol in water (2 runs) as a mobile phase. Its ^1H NMR spectrum displayed none of major components. Thus, it was not further isolated.

Fraction E contained many UV-active spots on normal phase TLC using 2% methanol in dichloromethane as a mobile phase (3 runs). Further separation by column chromatography over silica gel using a gradient system of methanol-dichloromethane was performed. All subfractions were examined by TLC, combined on the basis of their chromatogram characteristics and then evaporated to dryness under reduced pressure to afford four subfractions, as shown in **Table 22**.

Table 22 Subfractions obtained from **fraction E** by column chromatography over silica gel

Subfraction	Eluent	Weight (mg)	Physical appearance
E-1	100% CH_2Cl_2 - 5% MeOH/CH_2Cl_2	3.4	Yellow gum
E-2	5% MeOH/CH_2Cl_2	2.8	Orange solid
E-3	10-30% MeOH/CH_2Cl_2	9.3	Orange solid
E-4	30% MeOH/CH_2Cl_2	40.6	Orange-brown gum

Subfraction E-1 showed no spots under UV-S on normal phase TLC using 2% methanol in dichloromethane (3 runs) as a mobile phase. Its ^1H NMR spectrum displayed proton signals at high field region. Therefore, no attempted investigation was performed.

Subfraction E-2 displayed one orange spot on normal phase TLC with the R_f value of 0.60 using 2% methanol in dichloromethane (3 runs) as a mobile phase. Its ^1H NMR spectrum displayed proton signals at high field region. Therefore, it was not further purified.

Subfraction E-3 contained many inseparable spots under UV-S on normal phase TLC using 5% methanol in dichloromethane (3 runs) as a mobile phase. Its ^1H NMR spectrum displayed none of major components. Therefore, no attempted purification was carried out.

Subfraction E-4 showed no spots under UV-S on normal phase TLC using 5% methanol in dichloromethane (3 runs) as a mobile phase and displayed no UV-active spots on reverse phase TLC using 30% methanol in water (5 runs) followed by 50% methanol in water (2 runs) as mobile phases. The ^1H NMR spectrum indicated that it contained none of major components. Therefore, further purification was not conducted.

Fraction F demonstrated no spots under UV-S on normal phase TLC using 2% methanol in dichloromethane as a mobile phase (2 runs). Its ^1H NMR spectrum displayed none of major components. Thus, this fraction was not further separated.

2.2.3 Purification of the mycelial extract

The crude material showed three UV-active spots on normal phase TLC with the R_f values of 0.45, 0.55 and 0.64 using 2% methanol in dichloromethane (3 runs) as a mobile phase. It was further separated by column chromatography over Sephadex LH20 using 100% MeOH as eluent. All fractions were examined by TLC, combined on the basis of their chromatogram characteristics and then evaporated to dryness under reduced pressure to give five fractions, as shown in **Table 23.**

Table 23 Fractions obtained from **the mycelial extract** by column chromatography over Sephadex LH20

Fraction	Eluent	Weight (mg)	Physical appearance
MA	100% MeOH	64.5	Yellow gum
MB	100% MeOH	133.6	Yellow gum
MC	100% MeOH	12.4	Brown gum
MD	100% MeOH	13.7	Brown gum
ME	100% MeOH	24.1	Dark-brown gum

Fraction MA showed two spots with the R_f values of 0.60 and 0.76 after dipping the normal phase TLC in ASA reagent and subsequently heating using 2% methanol in dichloromethane (2 runs) as a mobile phase. The ^{1}H NMR spectrum indicated that the major components might be a mixture of long chain hydrocarbons. Therefore, no attempted investigation was carried out.

Fraction MB contained many inseparable spots after dipping the normal phase TLC in ASA reagent and subsequently heating using 2% methanol in dichloromethane (2 runs) as a mobile phase. This fraction was not further investigated because its ^{1}H NMR spectrum indicated that it was a mixture of long chain hydrocarbons.

Fraction MC displayed two UV-active spots on normal phase TLC with the R_f values of 0.08 and 0.38 using 2% methanol in dichloromethane (2 runs) as a mobile phase. Further purification by precoated TLC with 5% methanol in dichloromethane (8 runs) followed by 10% methanol in dichloromethane (4 runs) as mobile phases afforded three bands.

Band 1 was obtained as a yellow gum (4.4 mg). Its chromatogram demonstrated one UV-active spot on normal phase TLC with the R_f value of 0.73 using 2% methanol in dichloromethane (3 runs) followed by 5% methanol in dichloromethane (2 runs) as mobile phases. Its ^{1}H NMR spectral data indicated that it was **N9**.

Band 2 was a yellow gum (3.7 mg). Its chromatogram showed one spot under UV-S on normal phase TLC with the R_f value of 0.20 using 2% methanol in dichloromethane (3 runs) followed by 5% methanol in dichloromethane (2 runs) as mobile phases. The ^{1}H NMR spectrum suggested that it was a mixture. Because it was obtained in low quantity, it was not further investigated.

Band 3 was a yellow gum (2.5 mg). Its chromatogram displayed one UV-active spot with the R_f value of 0.05 using 2% methanol in dichloromethane (3 runs) followed by 5% methanol in dichloromethane (2 runs) as mobile phases. The ^{1}H NMR spectrum suggested that it was a mixture. Thus, it was not further purified.

Fraction MD showed four UV-active spots on normal phase TLC with the R_f values of 0.10, 0.15, 0.33 and 0.38 using 2% methanol in dichloromethane (2 runs) as a mobile phase. Further purification by precoated TLC with 5% methanol in dichloromethane (8 runs) followed by 10% methanol in dichloromethane (7 runs) as mobile phases afforded four bands.

Band 1 was obtained as a color less (1.5 mg). Its chromatogram demonstrated one UV-active spot on normal phase TLC with the R_f value of 0.80 using 2% methanol in dichloromethane (3 runs) followed by 5% methanol in dichloromethane (2 runs) as mobile phases. Its ^{1}H NMR spectrum displayed proton signals at high field region. Therefore, it was not further purified.

Band 2 was a yellow gum (3.8 mg), which showed one spot under UV-S on normal phase TLC with the R_f value of 0.70 using 2% methanol in dichloromethane (3 runs) followed by 5% methanol in dichloromethane (2 runs) as mobile phases. Its ^{1}H NMR spectrum suggested that it was **N13.**

Band 3 was a yellow gum (2.6 mg). Its chromatogram displayed one UV-active spot with the R_f value of 0.65 using 2% methanol in dichloromethane (3 runs) followed by 5% methanol in dichloromethane (2 runs) as mobile phases. Its ^{1}H NMR spectrum suggested that it was **N11.**

Band 4 was obtained as a yellow gum (2.9 mg). Its chromatogram displayed one UV-active spot on normal phase TLC with the R_f value of 0.10 using 2% methanol in dichloromethane (3 runs) followed by 5% methanol in dichloromethane (2 runs) as mobile phases. The ^1H NMR spectrum suggested that it was a mixture. Therefore, no attempted purification was performed.

Fraction ME showed no UV-active spots on normal phase TLC using 2% methanol in dichloromethane (2 runs) as a mobile phase and displayed no spots after dipping the normal phase TLC in ASA reagent and subsequently heating. Thus, it was not further isolated.

CHAPTER 2.3
RESULTS AND DISCUSSION

Five new compounds (**N9**, **N10**, **N11**, **N12** and **N13**) were isolated from the broth extract together with one known compound (**N8**). In addition, compounds **N9**, **N11** and **N13** were also obtained from the mycelial extract. The structures were identified by spectroscopic methods.

2.3.1 Compound N8

N8 was obtained as a yellow gum. The UV spectrum showed no absorption bands in the region of 200-400 nm, indicating the absence of a conjugation chromophore. The IR spectrum showed an absorption band at 3369 cm^{-1} for a hydroxyl group. The ^1H NMR spectrum (**Figure 20**) (**Table 24**) showed the characteristic signals of three olefinic protons of a monosubstituted alkene [δ_H 5.92 (*dd*, J = 17.4 and 10.8 Hz, 1H), 5.22 (*dd*, J = 17.4 and 1.2 Hz, 1H) and 5.07 (*dd*, J = 10.8 and 1.2 Hz, 1H)], one olefinic proton of a trisubstituted alkene (δ_H 5.42, *triplet of sextet*, J = 7.0 and 1.2 Hz, 1H), one oxymethylene group (δ_H 3.99, *s*, 2H), two methylene groups [δ_H 2.09 (*m*, 2H), 1.62 (*m*, 1H) and 1.58 (*m*, 1H)], one oxyquaternary methyl group (δ_H 1.30, *s*, 3H) and one vinylic methyl group (δ_H 1.67, *s*, 3H). The ^{13}C NMR spectrum (**Figure 21**) (**Table 24**) showed two methine (δ_C 144.88 and 125.95), four methylene (δ_C 111.86, 68.84, 41.73 and 22.33) and two methyl (δ_C 27.89 and 13.64) carbons. In the COSY spectrum (**Table 25**), the methylene protons, H_2-4 (δ_H 2.09), were coupled with the olefinic proton, H-3 (δ_H 5.42), and the methylene protons, H_{ab}-5 (δ_H 1.62 and 1.58). Furthermore, H-3 showed cross peaks in the COSY spectrum with the vinylic methyl group Me-9 (δ_H 1.67) and oxymethylene protons, H_2-1 (δ_H 3.99). These results established structural unit 1. HMBC cross peaks (**Table 25**) of H_2-1 with C-2 (δ_C 135.04), C-3 (δ_C 125.95) and C-9 (δ_C 13.64) and those of Me-9 with C-1 (δ_C 68.84), C-2 and C-3 supported the assigned structural unit 1. Irradiation of H_2-1, in the NOEDIFF experiment, enhanced signal

intensity of H-3 and Me-9 (δ_H 1.67) (**Table 25**), indicating *E* configuration of double bond between C-2 and C-3.

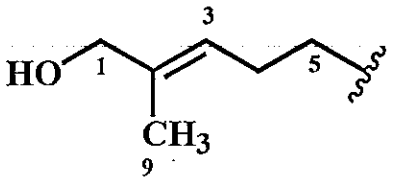

Structural unit 1

The unit 1 and the monosubstituted alkene were jointed together with a quaternary carbon (C-6, δ_C 73.32) according to ^3J HMBC cross peaks of the oxyquaternary methyl protons, Me-10 (δ_H 1.30), with C-5 (δ_C 41.73), C-6 and C-7 (δ_C 144.88). The chemical shift of C-6 suggested that it was an oxycarbon. The observed optical rotation of **N8** ($[\alpha]_D^{26}$ +7.73, c = 0.76, MeOH) was almost identical to that of (2*E*,6*S*)-2,6-dimethyl-2,7-octadien-1,6-diol ($[\alpha]_D^{23}$ +7.59, c = 0.76, MeOH) (Morikawa *et al.*, 2004). This indicated that C-6 in **N8** also had *S* configuration. Therefore, **N8** was identified as (2*E*,6*S*)-2,6-dimethyl-2,7-octadien-1,6-diol, a known compound which was previously isolated from *Nicotiana tobacum* L. (Behr *et al.*, 1978).

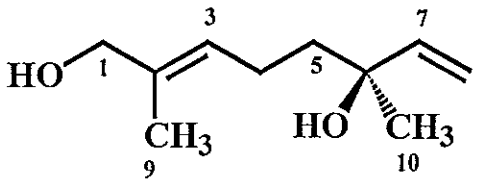

Table 24 The NMR data of **N8** in $CDCl_3$ and **(2*E*,6*S*)-2,6-dimethyl-2,7-octadien-1,6-diol** in CD_3OD

Position	N8		(2*E*,6*S*)-2,6-Dimethyl-2,7-octadien-1,6-diol[a]	
	δ_H (mult., J_{Hz})	δ_C (C-Type)	δ_H (mult., J_{Hz})	δ_C (C-Type)
1	3.99 (*s*)	68.84 (CH_2)	3.90 (*s*)	69.0 (CH_2)
2	-	135.04 (C)	-	135.9 (C)
3	5.42 (*triplet of sextet*, 7.0, 1.2)	125.95 (CH)	5.38 (*tq*, 7.0, 1.0)	126.9 (CH)
4	2.09 (*m*)	22.33 (CH_2)	2.07 (*m*)	23.4 (CH_2)
5	a: 1.62 (*m*) b: 1.58 (*m*)	41.73 (CH_2)	1.54 (*m*)	43.1 (CH_2)
6-OH	-	73.32 (C)	-	73.8 (C)
7	5.92 (*dd*, 17.4, 10.8)	144.88 (CH)	5.91 (*dd*, 18.0, 11.0)	146.3 (CH)
8	a: 5.22 (*dd*, 17.4, 1.2) b: 5.07 (*dd*, 10.8, 1.2)	111.86 (CH_2)	a: 5.19 (*dd*, 18.0, 2.0) b: 5.03 (*dd*, 11.0, 2.0)	112.1 (CH_2)
9	1.67 (*s*)	13.64 (CH_3)	1.63 (*brs*)	13.7 (CH_3)
10	1.30 (*s*)	27.89 (CH_3)	1.25 (*s*)	27.7 (CH_3)

[a] Morikawa *et al.*, 2004.

Table 25 The HMBC, COSY and NOE data of **N8** in $CDCl_3$

Position	HMBC	COSY	NOE
H_2-1	C-2, C-3, C-9	H-3, H_2-4, Me-9	H-3, Me-9
H-3	C-1, C-4, C-9	H_2-1, H_2-4, Me-9	H_2-1, H_{ab}-5
H_2-4	C-2, C-3, C-5	H_2-1, H-3, H_{ab}-5	-
H_{ab}-5	C-3, C-6, C-7, C-10	H_2-4	-
H-7	C-6, C-10	H_a-8, H_b-8	H_b-8
H_a-8	C-6, C-7	H-7, H_b-8	-
H_b-8	C-6, C-7	H-7, H_a-8	H-7, H_a-8
Me-9	C-1, C-2, C-3	H_2-1, H-3	-
Me-10	C-5, C-6, C-7	-	-

2.3.2 Compound N12

N12 was obtained as a yellow gum. The HREI-MS showed the molecular formula $C_{11}H_{10}O_4$, indicating that **N12** had seven degrees of unsaturation, which was consistent with apparent chromone absorption bands at λ_{max} 245, 277, and 342 nm in the UV spectrum. The IR spectrum exhibited hydroxyl and conjugated carbonyl absorption bands at 3346 and 1639 cm^{-1}, respectively. The ^1H NMR spectrum (**Figure 23**) (**Table 26**) showed resonances for one chelated hydroxy proton (δ_H 11.58, *s*, 1H), two aromatic protons (δ_H 6.71, *brs*, 1H and 6.59, *brs*, 1H), one hydroxy proton (δ_H 5.78, *brs*, 1H) and two methyl groups (δ_H 2.45, *s*, 3H and 2.40, *s*, 3H). The ^{13}C NMR spectrum (**Figure 24**) (**Table 26**) showed signals indicating one carbonyl (δ_C 175.28), six quaternary (δ_C 159.41, 155.84, 149.67, 146.75, 136.70 and 107.43), two methine (δ_C 110.95 and 107.71) and two methyl (δ_C 22.43 and 15.09) carbons. The chelated hydroxyl group that was placed at C-5 (δ_C 159.41), *peri* position to the carbonyl group, gave HMBC cross peaks (**Table 26**) with C-4a (δ_C 107.43), C-5 and C-6 (δ_C 110.95). The aromatic proton at δ_H 6.59 was attributed to H-6, due to its correlation with C-6 in the HMQC spectrum and ^3J HMBC correlations with the C-4a, C-8 (δ_C 107.71) and C-10 (δ_C 22.43). HMQC correlations from the methyl protons at δ_H 2.40 to C-10 and from the other aromatic proton at δ_H 6.71 to C-8 indicated the location of the methyl group and the aromatic proton at C-7 (δ_C 146.8) and C-8, respectively. Irradiation of Me-10, in the NOEDIFF experiment, enhanced the intensity of H-6 and H-8 resonances (**Table 26**), supporting the above assignments. The other hydroxyl group was located at C-3 (δ_C 136.70), on the basis of HMBC correlations from the hydroxy proton (δ_H 5.78) to C-2 (δ_C 149.67) C-3 and C-4 (δ_C 175.28). HMBC correlations between the remaining methyl protons at δ_H 2.45 with C-2 and C-3 established the attachment of the methyl group at C-2. Therefore, **N12** was assigned as 3,5-dihydroxy-2,7-dimethylchromen-4-one, a new 3-hydroxy derivative of altechromone A (Kimura *et al.*, 1992).

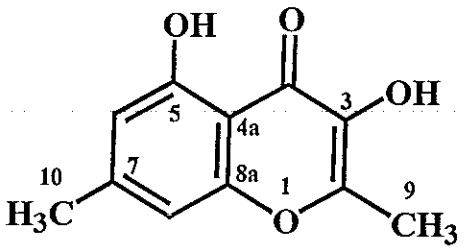

Table 26 The NMR data of **N12** in $CDCl_3$

Position	N12		HMBC Correlation	COSY	NOE
	δ_H (mult., J_{Hz})	δ_C (C-Type)			
2	-	149.67 (C)	-	-	-
3-OH	5.78 (*brs*)	136.70 (C)	C-2, C-3, C-4	-	-
4	-	175.28 (C)	-	-	-
4a	-	107.28 (C)	-	-	-
5-OH	11.58 (*s*)	159.41 (C)	C-4a, C-5, C-6	-	-
6	6.59 (*brs*)	110.95 (CH)	C-4a, C-5, C-8, C-10	H-8, H-10	H-10
7	-	146.75 (C)	-	-	-
8	6.71 (*brs*)	107.71 (CH)	C-4a, C-6, C-8a, C-10	H-6, H-10	H-10
8a	-	155.84 (C)	-	-	-
9	2.45 (*s*)	15.09 (CH_3)	C-2, C-3	-	-
10	2.40 (*s*)	22.43 (CH_3)	C-6, C-7, C-8	-	H-6, H-8

2.3.3 Compound N13

N13 was obtained as an orange solid, melting at 148.5-149.2 °C. The molecular formula $C_{11}H_{10}O_5$ deduced by HREI-MS was higher than that of **N12** by one additional oxygen atom. The UV and IR spectra were almost identical to those of **N12**. The ^1H (**Figure 26**) (**Table 27**) and ^{13}C (**Figure 26**) (**Table 27**) NMR spectral data were similar to those of **N12**. The difference between **N12** and **N13** was that the C-10 signal, observed as a methyl carbon signal (δ_C 24.43) in **N12**, was observed as an oxymethylene carbon signal (δ_C 63.89) in **N13**. The replacement of Me-10 in **N12** with H_2-10 resonating at δ_H 4.69 (*brs*) in **N13** was supported by signal enhancement of H-6 (δ_H 6.70, *brs*) and H-8 (δ_H 6.97, *brs*) in the NOEDIFF experiment after

irradiation of H_2-10 (**Table 27**). Thus, **N13** was elucidated as 3,5-dihydroxy-7-hydroxymethyl-2-methylchromen-4-one, a new 7-hydroxymethyl derivative of **N12**.

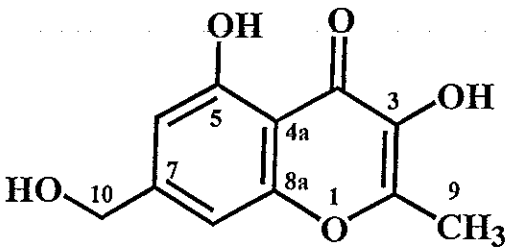

Table 27 The NMR data of **N13** in acetone-d_6

Position	N13		HMBC	COSY	NOE
	δ_H (mult., J_{Hz})	δ_C (C-Type)			
2	-	152.17 (C)	-	-	-
3-OH	7.85 (*brs*)	138.09 (C)	-	-	-
4	-	176.92 (C)	-	-	-
4a	-	109.30 (C)	-	-	-
5-OH	12.10 (*s*)	160.81 (C)	C-4a, C-5, C-6	-	-
6	6.70 (*brs*)	107.76 (CH)	C-4a, C-5, C-8, C-10	H-8, H-10	H-10
7	-	152.08 (C)	-	-	-
8	6.97 (*brs*)	104.99 (CH)	C-4a, C-6, C-8a, C-10	H-6, H-10	H-10
8a	-	156.64 (C)	-	-	-
9	2.43 (*s*)	15.05 (CH_3)	C-2, C-3	-	-
10	4.69 (*brs*)	63.89 (CH_2)	C-6, C-8	H-6, H-8	H-6, H-8

2.3.4 Compound N9

N9 was obtained as a yellow gum with $[\alpha]_D^{26}$ +43.40 (c = 0.13, MeOH). The molecular formula $C_{15}H_{16}O_6$ was determined by HREI-MS. The UV spectrum showed bands at 211, 278 and 348 nm, while the IR spectrum displayed bands at 3384, 1776 and 1642 cm^{-1} characteristic for hydroxyl, γ-lactone carbonyl and conjugated ketone carbonyl groups, respectively. In the ^{13}C NMR spectrum (**Figure 30**) (**Table 28**), carbon resonances at δ_C 176.19 and 195.82 supported the presence of the γ-lactone and ketone carbonyl groups. The ^1H NMR spectrum (**Figure 29**) (**Table 28**) exhibited resonances for one hydrogen-bonded hydroxyl group (δ_H 11.57, *s*, 1H),

two aromatic protons (δ_H 6.52, *brs*, 1H and 6.45, *brs*, 1H), two hydroxymethyl protons (δ_H 4.63, *brs*, 2H), one oxymethine proton (δ_H 4.58, *t*, J = 7.2 Hz, 1H), three methylene groups [δ_H 2.98 (*d*, J = 17.1 Hz, 1H), 2.61 (*d*, J = 17.1 Hz, 1H), 2.60 (*m*, 2H) and 2.32 (*m*, 2H)] and one oxyquaternary methyl group (δ_H 1.43, *s*, 3H). HMBC (**Table 28**) and NOEDIFF (**Table 28**) results indicated that **N9** possessed the left-hand aromatic ring identical to **N13**. The nonequivalent methylene protons at δ_H 2.98 and 2.61 were attributed to H_{ab}-3 of the chromanone skeleton due to their correlations with C-2 (δ_C 80.85), C-4 (δ_C 195.82) and C-9 (δ_C 19.14) in the HMBC spectrum. A HMQC cross peak from the oxyquaternary methyl protons resonating at δ_H 1.43 to C-9 and HMBC correlations from the methyl protons to C-2 and C-3 (δ_C 42.85) revealed the linkage of the methyl group at C-2 of the chromanone unit. In the COSY spectrum (**Table 28**), the methylene protons at δ_H 2.32 (H_2-4′) were coupled with the methylene protons at δ_H 2.60 (H_2-3′) and the oxymethine proton at δ_H 4.58 (H-5′). These results together with a ^3J HMBC cross-peak from H-5′ to the carbonyl carbon at δ_C 176.10 (C-2′) confirmed the presence of the γ-lactone moiety. Bond formation between C-5′ of the γ-lactone unit and C-2 of the chromanone skeleton was established on the basis of ^3J HMBC correlations of H-5′/C-3 and C-9. The NOEDIFF experiment of H-5′/Me-9 and H_a-3 (δ_H 2.98) and those of Me-9/H-5′ and H_b-3 (δ_H 2.61) (**Table 28**) revealed that both H-5′ and Me-9 had the β-orientation. Accordingly, **N9** was elucidated as 5-hydroxy-7-hydroxymethyl-2-methyl-2-(2-oxo-tetrahydrofuran-5-yl)-chroman-4-one, a new chromanone derivative.

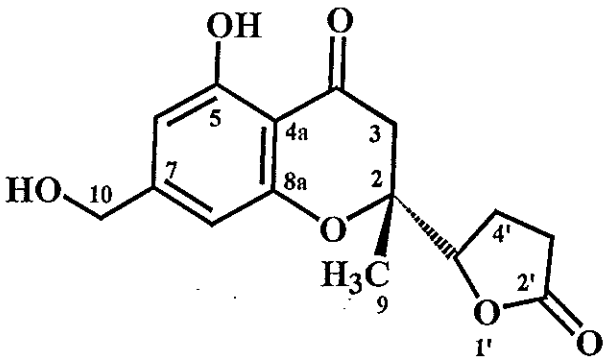

Table 28 The NMR data of **N9** in $CDCl_3$

Position	N9		HMBC Correlation	COSY	NOE
	δ_H (mult., J_{Hz})	δ_C (C-Type)			
2	-	80.85 (C)	-	-	-
3	a: 2.98 (*d*, 17.1)	42.85 (CH_2)	C-2, C-4, C-9	H_b-3	-
	b: 2.61 (*d*, 17.1)	-	-	H_a-3	-
4	-	195.82 (C)	-	-	-
4a	-	106.92 (C)	-	-	-
5-OH	11.57 (*s*)	162.01 (C)	C-4a, C-5	-	-
6	6.52 (*brs*)	106.43 (CH)	C-5, C-8, C-10	H-8, H-10	H-10
7	-	153.16 (C)	-	-	-
8	6.45 (*brs*)	105.29 (CH)	C-4a, C-8a, C-10	H-6, H-10	H-10
8a	-	158.90 (C)	-	-	-
9	1.43 (*s*)	19.14 (CH_3)	C-2, C-3, C-5′	-	H_b-3, H-5′
10	4.63 (*brs*)	64.47 (CH_2)	C-7, C-8, C-8a	H-6, H-8	H-6, H-8
2′	-	176.10 (C)	-	-	-
3′	2.60 (*m*)	28.21 (CH_2)	C-2′, C-4′, C-5′	H_2-4′	-
4′	2.32 (*m*)	22.34 (CH_2)	C-2, C-3′, C-5′	H_2-3′, H-5′	-
5′	4.58 (*t*, 7.2)	82.56 (CH)	C-3, C-9, C-2′, C-4′	H_2-4′	Me-9, H_2-4′, H_a-3

2.3.5 Compound N11

N11 was obtained as a yellow gum with $[\alpha]_D^{26}$ +27.10 (c = 0.22, MeOH). The HREI-MS showed the molecular formula $C_{15}H_{16}O_7$, 16 mass units higher than that of **N9**. The UV and IR spectra were almost identical to those of **N9**, indicating the presence of an identical chromophore. The ^1H NMR spectral data (**Figure 32**) (**Table 29**) were similar to those of **N9**, except for the replacement of H_{ab}-3 (δ_H 2.98 (*d*, *J* = 17.1 Hz, 1H and 2.61, *d*, *J* = 17.1 Hz, 1H) resonances in **N9** with an oxymethine signal (δ_H 4.59, *s*, 1H) in **N11**, thus revealing the location of the oxymethine proton at C-3 (δ_C 71.30). This assignment was confirmed by HMBC correlations from H-3 to C-2 (δ_C 84.30), C-4 (δ_C 196.36), C-9 (δ_C 13.43) and C-5′ (δ_C 82.27). Irradiation of H-5′ (δ_H 4.78, *dd*, *J* = 7.8 and 6.3 Hz, 1H), in the NOEDIFF experiment, enhanced only the signal intensity of Me-9 (δ_H 1.42) (**Table 29**), suggesting that H-5′, Me-9 and 3-OH were β-oriented. Therefore, **N11** was assigned

as 3,5-dihydroxy-7-hydroxymethyl-2-methyl-2-(2-oxotetrahydrofuran-5-yl)chroman-4-one, a new 3-hydroxy derivative of **N9**.

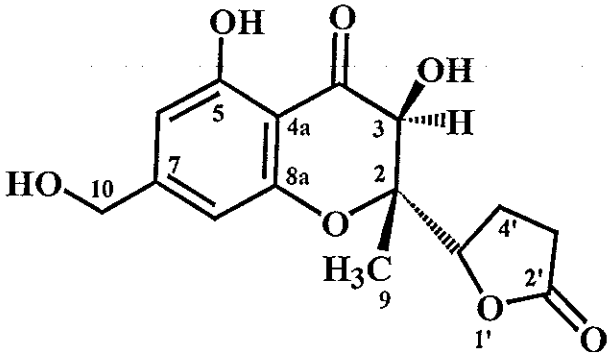

Table 29 The NMR data of **N11** in $CDCl_3$

Position	N11		HMBC	COSY	NOE
	δ_H (mult., J_{Hz})	δ_C (C-Type)			
2	-	84.30 (C)	-	-	-
3	4.59 (*s*)	71.30 (CH)	C-5′, C-2, C-4, C-9	H-9	-
4	-	196.36 (C)	-	-	-
4a	-	104.55 (C)	-	-	-
5-OH	10.60 (*s*)	161.19 (C)	C-4a, C-5, C-6		-
6	6.56 (*dt*, 1.2, 0.9)	106.94 (CH)	C-4a, C-5, C-8, C-10	H-8, H-10	H-10
7	-	154.35 (C)	-	-	-
8	6.48 (*dt*, 1.2, 0.9)	106.05 (CH)	C-4a, C-6, C-8a, C-10	H-6, H-10	H-10
8a	-	158.68 (C)	-	-	-
9	1.42 (*s*)	13.43 (CH_3)	C-5′, C-2, C-3	-	H-5′
10	4.65 (*t*, 0.9)	64.35 (CH_2)	C-6, C-7	-	H-6, H-8
2′	-	176.66 (C)	-	-	-
3′	a: 2.73 (*m*) b: 2.61 (*m*)	28.27 (CH_2)	C-2, C-2′	H_{ab}-4′, H-5′	-
4′	a: 2.61 (*m*) b: 2.37 (*m*)	21.93 (CH_2)	C-2, C-9, C-2′, C-5′	H_{ab}-3′, H-5′	-
5′	4.78 (*dd*, 7.8, 6.3)	82.27 (CH)	C-2′, C-4′	H_{ab}-3′, H_{ab}-4′	Me-9

2.3.6 Compound N10

N10 was obtained as a yellow gum with the $[\alpha]_D^{27}$ +51.43 (c = 0.035, MeOH). The UV and IR spectra were similar to those of **N11**, with an additional ketone carbonyl stretching frequency at 1731 cm^{-1}. The HREI-MS showed the molecular formula $C_{18}H_{20}O_8$. The ^1H (**Figure 35**) (**Table 30**) and ^{13}C NMR (**Figure 36**) (**Table 30**) data were similar to those of **N11**, implying that **N11** and **N10** had a similar chromanone unit with a γ-lactone moiety attached at C-2 (δ_C 84.28). The differences were the replacement of the methine unit (δ_H 4.59, δ_C 71.30) in **N11** with an oxyquaternary carbon (δ_C 78.67) in **N10**, thus revealing the absence of the hydrogen atom at C-3 (δ_C 78.67). In addition, the ^1H and ^{13}C NMR spectra displayed additional resonances belonging to one methylene unit [(δ_H 2.86, *d*, *J* = 16.5 Hz, 1H and 2.79, *d*, *J* =16.5 Hz, 1H, H_{ab}-11) and (δ_C 39.08, C-11)], one methyl group [(δ_H 2.45, *s*, 3H, Me-13) and (δ_C 31.91, C-13)], and one ketone carbonyl carbon (δ_C 212.65, C-12). The HMBC correlations (**Table 30**) from H_{ab}-11 to C-2, C-3, C-4 (δ_C 195.51), and C-12 and from Me-13 to C-12 linked a 2-propanoyl group at C-3. This assignment was further supported by the HMBC cross-peaks between 3-OH (δ_H 6.78, *brs*) with C-2, C-3, and C-11. The orientation of 3-OH and the 2-propanoyl group at the α- and β-positions, respectively, was established due to the following NOEDIFF experiment: Me-9 (δ_H 1.26, *s*, 3H)/H_{ab}-11 and H-5′ (δ_H 5.36, *dd*, *J* = 9.0 and 7.0 Hz, 1H)/3-OH (**Table 30**). Therefore, **N10** was assigned as 3,5-dihydroxy-7-hydroxymethyl-2-methyl-3-(2-oxopropyl)-2-(2-oxotetrahydrofuran-5-yl)chroman-4-one, a new chromanone derivative.

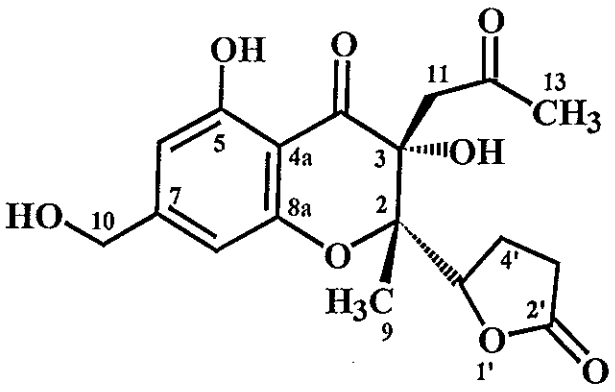

Table 30 The NMR data of **N10** in $CDCl_3$

Position	N10		HMBC	COSY	NOE
	δ_H (mult., J_{Hz})	δ_C (C-Type)			
2	-	84.28 (C)	-	-	-
3-OH	6.78 (*brs*)	78.67 (C)	C-2, C-3, C-11	-	-
4	-	195.51 (C=O)	-	-	-
4a	-	103.92 (C)	-	-	-
5-OH	10.80 (*s*)	162.36 (C)	C-4a, C-5, C-6	-	-
6	6.53 (*q*, 1.5)	106.84 (CH)	C-4a, C-5, C-8, C-10	H-8, H-10	H-10
7	-	153.27 (C)	-	-	-
8	6.47 (*q*, 1.5)	105.22 (CH)	C-4a, C-6, C-8a, C-10	H-6, H-10	H-10
8a	-	157.71 (C)	-	-	-
Me-9	1.26 (*s*)	12.77 (CH_3)	C-2, C-3, C-5′	-	H_{ab}-11
10	4.64 (*brs*)	64.46 (CH_2)	C-6, C-7, C-8	H-6, H-8	H-6, H-8
11	a: 2.86 (*d*, 16.5)	39.08 (CH_2)	C-2, C-3, C-4, C-12	H_b-11	-
	b: 2.79 (*d*, 16.5)		C-2, C-3, C-4, C-12	H_a-11	-
12	-	212.65 (C=O)	-	-	-
Me-13	2.45 (*s*)	31.91 (CH_3)	C-11, C-12	-	-
2′	-	176.37 (C=O)	-	-	-
3′	2.60 (*m*)	27.96 (CH_2)	C-2′, C-4′, C-5′	H-4′	-
4′	2.44 (*m*)	23.13 (CH_2)	C-2′, C-3′, C-5′	H-3′, H-5′	-
5′	5.36 (*dd*, 9.0, 7.0)	77.72 (CH)	C-2	H-4′	-

PART III

CHEMICAL CONSTITUENTS FROM THE ENDOPHYTIC FUNGUS *BOTRYOSPHAERIA MAMANE* PSU-M76

CHAPTER 3.1
INTRODUCTION

3.1.1 Introduction

The genus *Botryosphaeria* is a rich source of various types of compounds (**Table 31**). Some of them exhibited a wide range of biological activities (**Table 31**). Chemical constituents isolated from the genus *Botryosphaeria* are summarized in **Table 31** based on SciFinder Scholar database.

The endophytic fungus *B. mamane* PSU-M76 was isolated from the leaves of *Garcinia mangostana*, collected in Suratthani Province, Thailand in 2005. This fungus was deposited as PSU-M76 at the Department of Microbiology, Faculty of Science, Prince of Songkla University. The ethyl acetate extract from the culture broth of this fungus exhibited interesting antibacterial activity against *Staphylococcus aureus* ATCC25923 (SA) and methicillin-resistant *S. aureus* SK1 (MRSA) and antifungal activity against *Microsporum gypseum* clinical isolate with the MIC values of 32, 64 and 8 μg/ml, respectively.

Table 31 Compounds isolated from the *Botryosphaeria* genus

Scientific name	Compound	Activity	References
B. berengeriana	Macrophorin A, **35** Macrophorin E, **36** Macrophorin G, **37** Macrophorin F, **38**	Antifungal	Sassa *et al.*, 1998
B. obtusa	Tyrosol, **39** (*R*)-(-)-Mellein, **40** *cis*-(-)-4-Hydroxymellein, **41**	-	Venkatasubba-iah and Chilton 1990

Table 31 Continued

Scientific name	Compound	Activity	References
	(*R*)-5-Hydroxymellein, **42** 4-Hydroxybenzaldehyde, **43**		
B. rhodina	Tyrosol, **39** Ergosterol, **44** Lasiodiplodin, **45** Inosin, **46**	Inhibition of photophos-phorylation and electron transport chain	Veiga *et al.*, 2007

Structures of the metabolites from *Botryosphaeria* genus

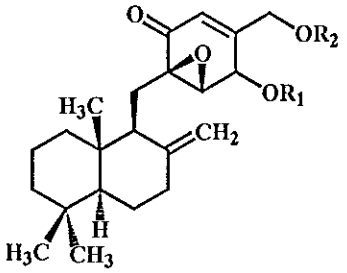

35: $R_1 = R_2 = H$: Macrophorin A

36: $R_1 = H$, $R_2 =$ 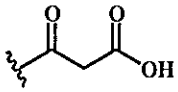 : Macrophorin E

37: $R_1 =$ 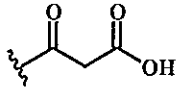 , $R_2 =$ H : Macrophorin G

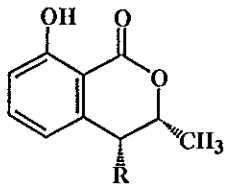

40: R = H : (*R*)-(-)-Mellein
41: R = OH : *cis*-4-Hydroxymellein

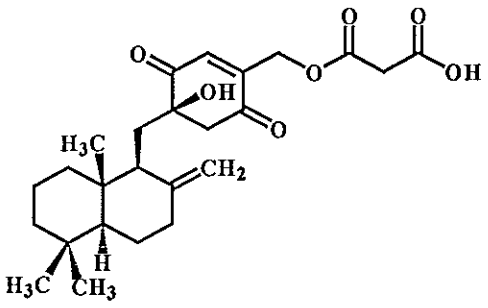

38: Macrophorin F

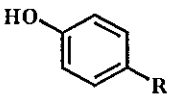

39: R = CH_2CH_2OH : Tyrosol
43: R = CHO : 4-Hydroxybenzaldehyde

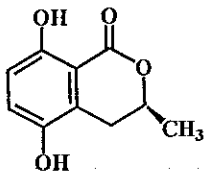

42: (*R*)-5-Hydroxymellein

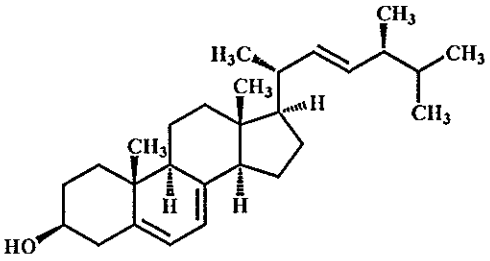

44: Ergosterol

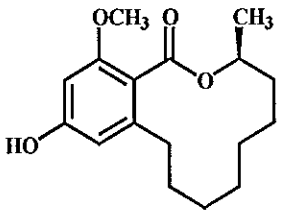

45: Lasiodiplodin

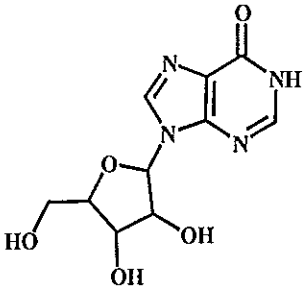

46: Inosin

CHAPTER 3.2
EXPERIMENTAL

3.2.1 Fermentation and extraction

The fermentation and the extraction of the culture broth were performed using the same procedure as those of *Eutypella scoparia* PSU-D44 to obtain a brown gum (320.0 mg). The wet mycelia were extracted twice with 300 ml of MeOH for 2 days. The aqueous MeOH layer was concentrated under reduced pressure. To the extract was added H_2O (50 ml), and the mixture washed with hexane (300 ml). The aqueous layer was extracted three times with an equal volume of the EtOAc (300 ml), dried over anhydrous Na_2SO_4 and then evaporated to dryness under reduced pressure to give a dark brown gum (190.0 mg).

3.2.2 Purification of the broth extract

The ethyl acetate extract of the culture filtrate showed nine UV-active spots on normal phase TLC with the R_f values of 0.10, 0.18, 0.23, 0.28, 0.35, 0.53, 0.63, 0.70 and 0.93 using 3% methanol in dichloromethane (2 runs) as a mobile phase. It was further separated by column chromatography over Sephadex LH20 using 100% MeOH as eluent. Fractions, which contained similar components, were combined and evaporated to dryness under reduced pressure to give four fractions, as shown in **Table 32.**

Table 32 Fractions obtained from **the broth extract** by column chromatography over Sephadex LH20

Fraction	Eluent	Weight (mg)	Physical appearance
A	100% MeOH	9.1	Brown gum
B	100% MeOH	54.7	Dark-brown gum

Table 32 Continued

Fraction	Eluent	Weight (mg)	Physical appearance
C	100% MeOH	220.9	Dark-brown gum
D	100% MeOH	35.2	Brown gum

Fraction A showed no spots under UV-S on normal phase TLC using 5% methanol in dichloromethane as a mobile phase (2 runs). Its ^{1}H NMR spectrum displayed proton signals at high field region. Therefore, it was not further investigated.

Fraction B showed no spots under UV-S on normal phase TLC using 5% methanol in dichloromethane as a mobile phase (2 runs). In addition, its chromatogram showed a long tail after dipping the normal phase TLC in ASA reagent and subsequently heating. It was further separated by column chromatography over Sephadex LH20 using 100% MeOH as eluent. All subfractions were examined by TLC, combined on the basis of their chromatogram characteristics and then evaporated to dryness under reduced pressure to afford four subfractions, as shown in **Table 33**.

Table 33 Subfractions obtained from **fraction B** by column chromatography over Sephadex LH20

Subfraction	Eluent	Weight (mg)	Physical appearance
B1	100% MeOH	3.0	Brown solid
B2	100% MeOH	10.7	Brown gum
B3	100% MeOH	34.0	Brown gum
B4	100% MeOH	4.8	Dark-brown gum

Subfraction B1 showed no UV-active spots on normal phase TLC using 7% methanol in dichloromethane (2 runs) as a mobile phase and showed no definite spots after dipping the normal phase TLC in ASA reagent and subsequently heating. Its ^{1}H NMR spectrum displayed proton signals at high field region. Therefore, no attempted investigation was carried out.

Subfraction B2 showed two pale UV-active spots on normal phase TLC with the R_f values of 0.13 and 0.23 using 7% methanol in dichloromethane (2 runs) as a mobile phase and showed a long tail under UV-S on reverse phase TLC using 50% methanol in water as a mobile phase. Further purification by precoated TLC using 7% methanol in dichloromethane (2 runs) followed by 10% methanol in dichloromethane (4 runs) as mobile phases afforded two bands.

Band 1 was obtained as a brown gum (2.7 mg), which displayed one spot under UV-S on normal phase TLC with the R_f value of 0.25 using 10% methanol in dichloromethane (4 runs) as a mobile phase. The ^{1}H NMR spectrum suggested that it was a mixture. Therefore, no attempted investigation was carried out.

Band 2 was obtained as a brown gum (3.5 mg), which showed one spot under UV-S on normal phase TLC with the R_f value of 0.13 using 10% methanol in dichloromethane (4 runs) as a mobile phase. Its ^{1}H NMR spectrum displayed proton signals at high field region. Therefore, no attempted investigation was performed.

Subfraction B3 showed four pale UV-active spots on normal phase TLC with the R_f values of 0.10, 0.38, 0.73 and 0.90 using 7% methanol in dichloromethane (2 runs) as a mobile phase and showed no definite UV-active spots on reverse phase TLC using 50% methanol in water as a mobile phase. Further purification by precoated TLC using 7% methanol in dichloromethane (2 runs) followed by 10% methanol in dichloromethane (4 runs) as mobile phases afforded four bands.

Band 1 was obtained as a yellow gum (4.5 mg), which displayed one spot under UV-S on normal phase TLC with the R_f value of 0.93 using 10% methanol in dichloromethane (4 runs) as a mobile phase. The ^{1}H NMR spectrum showed proton signals at high field region. Thus, it was not further investigated.

Band 2 was obtained as a yellow gum (4.2 mg), which showed one spot under UV-S on normal phase TLC with the R_f value of 0.75 using 10% methanol

in dichloromethane (4 runs) as a mobile phase. Its ^{1}H NMR spectrum displayed proton signals at high field region. Therefore, no attempted investigation was performed.

Band 3 was obtained as a yellow gum (3.9 mg), which displayed one spot under UV-S on normal phase TLC with the R_f value of 0.38 using 10% methanol in dichloromethane (4 runs) as a mobile phase. The ^{1}H NMR spectrum suggested that it was a mixture. Therefore, no attempted investigation was carried out.

Band 4 was obtained as a brown gum (8.8 mg), which displayed no spots under UV-S on normal phase TLC using 10% methanol in dichloromethane (4 runs) as a mobile phase and showed one spot with the R_f value of 0.15 after dipping the normal phase TLC in ASA reagent and subsequently heating. The ^{1}H NMR spectrum showed none of major proton signals. Thus, it was not further investigated.

Subfraction B4 showed no UV-active spots on normal phase TLC using 7% methanol in dichloromethane (2 runs) as a mobile phase and showed no definite spots after dipping the normal phase TLC in ASA reagent and subsequently heating. In addition, its chromatogram showed a long tail under UV-S on reverse phase TLC using 50% methanol in water as a mobile phase. Its ^{1}H NMR spectrum displayed proton signals at high field region. Therefore, no attempted investigation was performed.

Fraction C contained four spots under UV-S on normal phase TLC with the R_f values of 0.18, 0.38, 0.60 and 0.75 using 100% dichloromethane as a mobile phase. Further separation by column chromatography over silica gel using a gradient system of methanol-dichloromethane was performed. Subfractions, which contained similar components, were combined and evaporated to dryness under reduced pressure to give ten subfractions, as shown in **Table 34**.

Table 34 Subfractions obtained from **fraction C** by column chromatography over silica gel

Subfraction	Eluent	Weight (mg)	Physical appearance
C1	100% CH_2Cl_2	1.0	Colorless gum
C2	100% CH_2Cl_2	3.0	Yellow gum
C3	100% CH_2Cl_2	4.8	Yellow solid
C4	100% CH_2Cl_2	7.3	Yellow gum
C5	100% CH_2Cl_2 - 5% MeOH/CH_2Cl_2	33.1	Brown-yellow gum
C6	5% MeOH/CH_2Cl_2	4.2	Orange solid mixed with orange gum
C7	10% MeOH/CH_2Cl_2	52.4	Brown gum
C8	10-30% MeOH/CH_2Cl_2	16.1	Brown gum mixed with brown solid
C9	30-60% MeOH/CH_2Cl_2	50.8	Brown gum
C10	60% MeOH/CH_2Cl_2 - 100% MeOH	33.1	Brown gum

Subfraction C1 demonstrated no UV-active spots on normal phase TLC using 100% dichloromethane (2 runs) as a mobile phase. Its ^{1}H NMR spectrum displayed proton signals at high field region. Therefore, no attempted investigation was carried out.

Subfraction C2 (N14) displayed one UV-active spot on normal phase TLC with the R_f value of 0.75 using 100% dichloromethane (2 runs) as a mobile phase.

UV(MeOH) λ_{max} nm (log ε)	227 (3.51), 289 (3.29)
FT-IR (neat) ν_{cm-1}	3393 (O-H stretching), 1606 (C=C stretching)

^{1}H NMR ($CDCl_3$) (δ ppm) (300 MHz)		6.35 (*d*, *J* = 2.7 Hz, 1H), 6.29 (*d*, *J* = 2.7 Hz, 1H), 5.25 (*s*, 1H), 3.86 (*s*, 3H), 3.76 (*s*, 3H), 2.61 (*t*, *J* = 7.5 Hz, 2H), 1.36 (*m*, 6H), 0.87 (*t*, *J* = 6.6 Hz, 3H)
^{13}C NMR ($CDCl_3$) (δ ppm) (125 MHz)		152.66, 146.65, 137.43, 128.63, 105.65, 96.54, 55.95, 55.73, 31.72, 29.70, 29.52, 22.59, 14.07
DEPT (135°) ($CDCl_3$)	CH :	105.65, 96.54
	CH_2 :	31.72, 29.70, 29.52, 22.59
	CH_3 :	55.95, 55.73, 14.07

Subfraction C3 (N15) melted at 56.1-56.7 °C. Its chromatogram showed one spot under UV-S on normal phase TLC with the R_f value of 0.68 using 100% dichloromethane (2 runs) as a mobile phase.

$[\alpha]_D^{27}$		-114.29 (c = 0.07, $CHCl_3$)
UV(MeOH) λ_{max} nm (log ε)		246 (3.76), 314 (3.58)
FT-IR (neat) ν_{cm-1}		3365 (O-H stretching), 1652 (C=O stretching), 1606 and 1553 (C=C stretching)
^{1}H NMR ($CDCl_3$) (δ ppm) (300 MHz)		11.06 (*s*, 1H), 7.44 (*t*, *J* = 8.1 Hz, 1H), 6.92 (*d*, *J* = 8.1 Hz, 1H), 6.72 (*d*, *J* = 8.1 Hz, 1H), 4.77 (*tq*, *J* = 7.2, 6.6 Hz, 1H), 2.96 (*d*, *J* = 7.2 Hz, 2H), 1.56 (*d*, *J* = 6.6 Hz, 3H)
^{13}C NMR ($CDCl_3$) (δ ppm) (75 MHz)		169.93, 162.21, 139.38, 136.12, 117.87, 116.24, 108.30, 76.07, 34.61, 20.74
DEPT (135°) ($CDCl_3$)	CH :	136.12, 117.87, 116.24, 76.07
	CH_2 :	34.61
	CH_3 :	20.74
EIMS *m/z* (% relative intensity):		178 (89), 160 (100), 149 (48), 134 (93), 106 (36), 78 (43)

Subfraction C4 showed two major UV-active spots on normal phase TLC with the R_f values of 0.38 and 0.50 using 70% dichloromethane in light petroleum as a mobile phase. Further purification by precoated TLC using 30% dichloromethane in light petroleum followed by 40% dichloromethane in light petroleum as mobile phases afforded three bands.

Band 1 was obtained as a yellow solid (0.8 mg), which displayed one spot under UV-S on normal phase TLC with the R_f value of 0.43 using 50% dichloromethane in light petroleum as a mobile phase. Its ^{1}H NMR data indicated the presence of **N15**.

Band 2 was obtained as a yellow gum (1.7 mg), which showed one spot under UV-S on normal phase TLC with the R_f value of 0.33 using 50% dichloromethane in light petroleum as a mobile phase. The ^{1}H NMR spectrum suggested that it was a mixture. Therefore, no attempted investigation was carried out.

Band 3 was obtained as a yellow gum (2.6 mg). Its chromatogram displayed one spot under UV-S on normal phase TLC with the R_f value of 0.28 using 50% dichloromethane in light petroleum as a mobile phase. The ^{1}H NMR spectrum suggested that it was a mixture. Thus, it was not further purified.

Subfraction C5 displayed two UV-active spots on normal phase TLC with the R_f values of 0.35 and 0.53 using 100% dichloromethane (2 runs) as a mobile phase. Further separation by column chromatography over silica gel using a gradient system of methanol-dichloromethane was performed. All subfractions were examined by TLC, combined on the basis of their chromatogram characteristics and then evaporated to dryness under reduced pressure to afford five subfractions, as shown in **Table 35**.

Table 35 Subfractions obtained from **subfraction C5** by column chromatography over silica gel

Subfraction	Eluent	Weight (mg)	Physical appearance
C5-1	100% CH_2Cl_2	5.0	Pale-yellow gum
C5-2	100% CH_2Cl_2	7.1	Yellow solid
C5-3	100% CH_2Cl_2	5.3	Brown solid
C5-4	2-5% MeOH/CH_2Cl_2	4.2	Brown gum
C5-5	10-80% MeOH/CH_2Cl_2	8.8	Brown gum

Subfraction C5-1 showed no UV-active spots on normal phase TLC using 100% dichloromethane (2 runs) as a mobile phase. Its ^{1}H NMR spectrum displayed proton signals at high field region. Therefore, no attempted investigation was carried out.

Subfraction C5-2 (N16) melted at 63.8-64.5 °C. Its chromatogram showed one spot under UV-S on normal phase TLC with the R_f value of 0.55 using 100% dichloromethane (2 runs) as a mobile phase.

UV(MeOH) λ_{max} nm (log ε)	267 (3.64)
FT-IR (neat) ν_{cm-1}	1679 and 1652 (C=O stretching), 1602 (C=C stretching)
^{1}H NMR ($CDCl_3$) (δ ppm) (300 MHz)	6.51 (*td*, J = 2.4, 1.5 Hz, 1H), 5.90 (*d*, J = 2.4 Hz, 1H), 3.84 (*s*, 3H), 2.45 (*td*, J = 8.1, 1.5 Hz, 2H), 1.54 (*m*, 2H), 1.37 (*m*, 2H), 1.34 (*m*, 2H), 0.92 (*t*, J = 6.9 Hz, 3H)
^{13}C NMR ($CDCl_3$) (δ ppm) (75 MHz)	187.70, 182.13, 158.86, 147.59, 132.88, 107.08, 56.26, 31.35, 28.66, 27.38, 22.34, 13.89
DEPT (135°) ($CDCl_3$)	CH : 132.88, 107.08 CH_2 : 31.35, 28.66, 27.38, 22.34 CH_3 : 56.26, 13.89

Subfraction C5-3 showed one major spot under UV-S on normal phase TLC with the R_f value of 0.55 using 100% dichloromethane (2 runs) as a mobile phase. Further purification by precoated TLC using 50% dichloromethane in light petroleum (8 runs) as a mobile phase afforded two bands.

Band 1 was obtained as a yellow solid (2.9 mg), which displayed one spot under UV-S on normal phase TLC with the R_f value of 0.53 using 50% dichloromethane in light petroleum (3 runs) as a mobile phase. Its ^{1}H NMR spectral data indicated the presence of **N16**.

Band 2 was obtained as a purple solid (1.7 mg), which showed one spot under UV-S on normal phase TLC with the R_f value of 0.38 using 50% dichloromethane in light petroleum (3 runs) as a mobile phase. Its ^{1}H NMR spectrum displayed proton signals at high field region. Thus, it was not further purified.

Subfraction C5-4 displayed two spots under UV-S on normal phase TLC with the R_f values of 0.50 and 0.55 using 100% dichloromethane (2 runs) as a mobile phase. Further purification by precoated TLC using 50% dichloromethane in light petroleum (12 runs) as a mobile phase afforded two bands.

Band 1 was obtained as a yellow solid (1.8 mg). Its chromatogram displayed one spot under UV-S on normal phase TLC with the R_f value of 0.53 using 50% dichloromethane in light petroleum (3 runs) as a mobile phase. Its ^{1}H NMR spectral data indicated the presence of **N16**.

Band 2 was obtained as a yellow gum (1.6 mg), which showed one spot under UV-S on normal phase TLC with the R_f value of 0.46 using 50% dichloromethane in light petroleum (3 runs) as a mobile phase. The ^{1}H NMR spectrum suggested that it was a mixture. Therefore, no attempted purification was carried out.

Subfraction C5-5 demonstrated no UV-active spots using 100% dichloromethane (2 runs) as a mobile phase. In addition, its chromatogram showed no definite spots after dipping the normal phase TLC in ASA reagent and subsequently heating. Its ^{1}H NMR spectrum displayed proton signals at high field region. Therefore, it was not further investigated.

Subfraction C6 showed no UV-active spots on normal phase TLC using 100% dichloromethane (2 runs) followed by 5% methanol in dichloromethane (5 runs) as mobile phases. Its ^{1}H NMR spectrum displayed none of aromatic proton signals. Therefore, no attempted investigation was carried out.

Subfraction C7 contained one major spot under UV-S on normal phase TLC with the R_f value of 0.68 using 5% methanol in dichloromethane (5 runs) as a mobile phase. Further separation by column chromatography over silica gel using a gradient system of methanol-dichloromethane was performed. Subfractions, which contained similar components, were combined and evaporated to dryness under reduced pressure to give five subfractions, as shown in **Table 36.**

Table 36 Subfractions obtained from **subfraction C7** by column chromatography over silica gel

Subfraction	Eluent	Weight (mg)	Physical appearance
C7-1	100% CH_2Cl_2	2.5	Dark-brown solid
C7-2	100% CH_2Cl_2 - 8% MeOH/CH_2Cl_2	27.1	Brown gum
C7-3	8% MeOH/CH_2Cl_2	8.1	Brown gum
C7-4	8-30% MeOH/CH_2Cl_2	16.8	Brown gum
C7-5	50% MeOH/CH_2Cl_2 - 100% MeOH	11.0	Brown gum

Subfraction C7-1 showed no spots under UV-S on normal phase TLC using 1% methanol in dichloromethane (2 runs) as a mobile phase. Its ^{1}H NMR

spectrum displayed proton signals at high field region. Thus, further purification was not performed.

Subfraction C7-2 demonstrated two overlapping UV-active spots on normal phase TLC using 1% methanol in dichloromethane (2 runs) as a mobile phase. It was further separated by column chromatography over Sephadex LH20 using 100% MeOH as eluent. All subfractions were examined by TLC, combined on the basis of their chromatogram characteristics and then evaporated to dryness under reduced pressure to afford three subfractions, as shown in **Table 37.**

Table 37 Subfractions obtained from **subfraction C7-2** by column chromatography over Sephadex LH20

Subfraction	Eluent	Weight (mg)	Physical appearance
C7-2-1	100% MeOH	2.9	Yellow gum
C7-2-2	100% MeOH	7.4	Yellow gum
C7-2-3	100% MeOH	14.3	Yellow gum

Subfraction C7-2-1 showed no UV-active spots on normal phase TLC using 1% methanol in dichloromethane (2 runs) as a mobile phase. Its ^{1}H NMR spectrum displayed proton signals at high field region. Therefore, no attempted investigation was carried out.

Subfraction C7-2-2 (N17) showed one UV-active spot on normal phase TLC with the R_f value of 0.43 using 1% methanol in dichloromethane (2 runs) as a mobile phase.

$[\alpha]_D^{29}$	-25.53 (c = 0.04, $CHCl_3$)
UV(MeOH) λ_{max} nm (log ε)	245 (3.26), 314 (3.14)
FT-IR (neat) ν_{cm-1}	3395 (O-H stretching), 1661 (C=O stretching), 1611 (C=C stretching)

^{1}H NMR ($CDCl_3$) (δ ppm) (300MHz)		10.99 (*s*, 1H), 7.52 (*dd*, *J* = 8.4, 7.2 Hz, 1H), 7.02 (*dd*, *J* = 8.4, 0.9 Hz, 1H), 6.92 (*dt*, *J* = 7.2, 0.9 Hz, 1H), 4.70 (*qd*, *J* = 6.6, 2.1 Hz, 1H), 4.57 (*brd*, *J* = 2.1 Hz, 1H), 1.59 (*d*, *J* = 6.6 Hz, 3H)
^{13}C NMR ($CDCl_3$) (δ ppm) (75 MHz)		169.19, 162.08, 140.53, 136.77, 118.51, 118.28, 106.84, 78.21, 67.23, 15.99
DEPT (135°) ($CDCl_3$)	CH :	136.77, 118.51, 118.28, 78.21, 67.23
	CH_3 :	15.99
EIMS *m/z* (% relative intensity):		194 (96), 150 (95), 122 (100), 93 (19), 65 (25)

Subfraction C7-2-3 displayed two overlapping UV-active spots on normal phase TLC using 1% methanol in dichloromethane (2 runs) as a mobile phase. Further separation by column chromatography over Sephadex LH20 using 100% MeOH as eluent was performed. Subfractions, which contained similar components, were combined and evaporated to dryness under reduced pressure to give five subfractions, as shown in **Table 38.**

Table 38 Subfractions obtained from **subfraction C7-2-3** by column chromatography over Sephadex LH20

Subfraction	Eluent	Weight (mg)	Physical appearance
C7-2-31	100% MeOH	2.4	Yellow gum
C7-2-32	100% MeOH	2.1	Yellow gum
C7-2-33	100% MeOH	6.5	Yellow gum
C7-2-34	100% MeOH	0.7	Yellow gum
C7-2-35	100% MeOH	0.9	Yellow gum

Subfraction C7-2-31 showed no spots under UV-S on normal phase TLC using 100% dichloromethane (5 runs) as a mobile phase. Its ^{1}H NMR spectrum displayed proton signals at high field region. Thus, further purification was not performed.

Subfraction C7-2-32 displayed one spot under UV-S on normal phase TLC with the R_f value of 0.45 using 100% dichloromethane (5 runs) as a mobile phase. Its ^1H NMR spectral data indicated the presence of **N17.**

Subfraction C7-2-33 displayed two overlapping UV-active spots on normal phase TLC using 100% dichloromethane (5 runs) as a mobile phase. Further separation by column chromatography over Sephadex LH20 using 100% MeOH as eluent was performed. All subfractions were examined by TLC, combined on the basis of their chromatogram characteristics and then evaporated to dryness under reduced pressure to afford three subfractions, as shown in **Table 39.**

Table 39 Subfractions obtained from **subfraction C7-2-33** by column chromatography over Sephadex LH20

Subfraction	Eluent	Weight (mg)	Physical appearance
C7-2-33-1	100% MeOH	0.7	Yellow gum
C7-2-33-2	100% MeOH	3.7	Yellow gum
C7-2-33-3	100% MeOH	2.0	Yellow gum

Subfraction C7-2-33-1 contained one spot under UV-S on normal phase TLC with the R_f value of 0.50 using 100% dichloromethane (8 runs) as a mobile phase. Its ^1H NMR spectral data indicated the presence of **N17.**

Subfraction C7-2-33-2 displayed two overlapping UV-active spots on normal phase TLC using 100% methanol (8 runs) as a mobile phase. Further separation by column chromatography over Sephadex LH20 using 100% MeOH as eluent was performed. Subfractions, which contained similar components, were combined and evaporated to dryness under reduced pressure to give three subfractions, as shown in **Table 40.**

Table 40 Subfractions obtained from **subfraction C7-2-33-2** by column chromatography over Sephadex LH20

Subfraction	Eluent	Weight (mg)	Physical appearance
C7-2-33-21	100% MeOH	0.5	Yellow gum
C7-2-33-22	100% MeOH	2.4	Yellow gum
C7-2-33-23	100% MeOH	0.7	White solid

Subfraction C7-2-33-21 showed one spot under UV-S on normal phase TLC with the R_f value of 0.43 using 100% dichloromethane (7 runs) as a mobile phase. Its ^{1}H NMR spectral data indicated the presence of **N17**.

Subfraction C7-2-33-22 displayed two overlapping UV-active spots on normal phase TLC using 100% dichloromethane (7 runs) as a mobile phase. Because of low quantity, it was not further purified.

Subfraction C7-2-33-23 (N18) melted at 109.7-110.3 °C. Its chromatogram showed one UV-active spot on normal phase TLC with the R_f value of 0.40 using 100% dichloromethane (7 runs) as a mobile phase.

$[\alpha]_D^{29}$	+28.80 (c = 1.00, MeOH)
UV(MeOH) λ_{max} nm (log ε)	244 (3.25), 314 (3.14)
FT-IR (neat) ν_{cm-1}	3398 (O-H stretching), 1662 (C=O stretching), 1610 (C=C stretching)
^{1}H NMR ($CDCl_3$) (δ ppm) (500 MHz)	10.99 (*s*, 1H), 7.55 (*dd*, *J* = 8.5, 7.5 Hz, 1H), 7.03 (*d*, *J* = 7.5 Hz, 1H), 7.01 (*d*, *J* = 8.5 Hz, 1H), 4.64 (*m*, 1H), 4.62 (*m*, 1H), 1.53 (*d*, *J* = 6.6 Hz, 3H)
^{13}C NMR ($CDCl_3$) (δ ppm) (125 MHz)	168.56, 162.08, 141.14, 136.87, 117.87, 116.15, 106.50, 79.91, 69.22, 17.92
DEPT (135°) ($CDCl_3$)	CH : 136.87, 117.87, 116.15, 79.91, 69.22 CH_3 : 17.92

Subfraction C7-2-33-3 contained one spot under UV-S on normal phase TLC with the R_f value of 0.45 using 100% dichloromethane (8 runs) as a mobile phase. Its ^{1}H NMR spectral data indicated the presence of **N18**.

Subfraction C7-2-34 displayed one spot under UV-S on normal phase TLC with the R_f value of 0.38 using 100% dichloromethane (5 runs) as a mobile phase. Its ^{1}H NMR spectral data indicated the presence of **N18**.

Subfraction C7-2-35 showed no spots under UV-S on normal phase TLC using 100% dichloromethane (5 runs) as a mobile phase. Its ^{1}H NMR spectrum displayed none of major proton signals. Therefore, no attempted investigation was carried out.

Subfraction C7-3 showed two spots under UV-S on normal phase TLC with the R_f values of 0.20 and 0.35 using 1% methanol in dichloromethane (2 runs) as a mobile phase. Further purification by precoated TLC using 0.5% methanol in dichloromethane (6 runs) as a mobile phase afforded three bands.

Band 1 was obtained as a yellow gum (3.0 mg). Its chromatogram displayed one spot under UV-S on normal phase TLC with the R_f value of 0.38 using 1% methanol in dichloromethane as a mobile phase. Its ^{1}H NMR spectral data and chromatogram on normal phase TLC indicated that it was **N17**.

Band 2 was obtained as a yellow solid (1.5 mg), which showed one spot under UV-S on normal phase TLC with the R_f value of 0.30 using 1% methanol in dichloromethane as a mobile phase. The ^{1}H NMR spectrum suggested that it was a mixture. Because of low quantity, it was not further separated.

Band 3 was obtained as a white solid (2.3 mg). Its chromatogram showed one UV-active spot on normal phase TLC with the R_f value of 0.22 using 1% methanol in dichloromethane as a mobile phase. The ^{1}H NMR spectrum suggested that it was not pure. Because of low quantity, it was not further investigated.

Subfraction C7-4 demonstrated two spots under UV-S on normal phase TLC with the R_f values of 0.21 and 0.35 using 1% methanol in dichloromethane (2 runs) as a mobile phase. Further purification by precoated TLC using 0.5% methanol in dichloromethane (7 runs) as a mobile phase afforded two bands.

Band 1 was obtained as a yellow gum (5.5 mg). Its chromatogram displayed one spot under UV-S on normal phase TLC with the R_f value of 0.36 using 0.5% methanol in dichloromethane as a mobile phase. Its ^{1}H NMR spectral data indicated that it was **N17**.

Band 2 was obtained as a yellow solid (7.2 mg), which showed one spot under UV-S on normal phase TLC with the R_f value of 0.18 using 0.5% methanol in dichloromethane as a mobile phase. The ^{1}H NMR spectrum suggested that it was a mixture. Further purification by precoated TLC using 100% dichloromethane as a mobile phase (5 runs) afforded two bands.

Band 2-1 was obtained as a white solid (3.5 mg). Its chromatogram characteristic showed one UV-active spot on normal phase TLC with the R_f value of 0.43 using 0.2% methanol in dichloromethane (2 runs) as a mobile phase. The ^{1}H NMR data indicated that it contained many compounds. Thus, it was not further purified.

Band 2-2 was obtained as a yellow solid (1.7 mg), which showed one UV-active spot on normal phase TLC with the R_f value of 0.30 using 0.2% methanol in dichloromethane (2 runs) as a mobile phase. The ^{1}H NMR spectrum suggested that it was a mixture. Therefore, no attempted investigation was performed.

Subfraction C7-5 showed no distinct spots under UV-S on normal phase TLC using 5% methanol in dichloromethane (2 runs) as a mobile phase. Its ^{1}H NMR spectrum displayed none of aromatic proton signals. Therefore, further purification was not conducted.

Subfraction C8 demonstrated two spots under UV-S on normal phase TLC with the R_f values of 0.25 and 0.48 using 5% methanol in dichloromethane (5 runs) as a mobile phase. When using 20% ethyl acetate in light petroleum (3 runs) and 40% ethyl acetate in light petroleum (3 runs) as mobile phases, the chromatogram showed three UV-active spots on normal phase TLC with the R_f values of 0.20, 0.43 and 0.80. Further purification by precoated TLC using 40% ethyl acetate in light petroleum (6 runs) as a mobile phase afforded three bands.

Band 1 was a yellow gum (2.5 mg), which showed one spot under UV-S on normal phase TLC with the R_f value of 0.60 using 20% ethyl acetate in light petroleum (6 runs) as a mobile phase. The ^{1}H NMR spectrum indicated that it was a mixture. Therefore, no attempted separation was carried out.

Band 2 (N19) was obtained as a white solid (3.8 mg) and melted at 149.6-150.0 °C. Its chromatogram showed one UV-active spot on normal phase TLC with the R_f value of 0.33 using 20% ethyl acetate in light petroleum (6 runs) as a mobile phase.

$[\alpha]_D^{29}$	+22.22 (c = 0.24, MeOH)
UV(MeOH) λ_{max} nm (log ε)	300 (3.45)
FT-IR (neat) ν_{cm-1}	3392 (O-H stretching), 1684 (C=O stretching), 1605 and 1554 (C=C stretching)
^{1}H NMR ($CDCl_3$) (δ ppm) (500 MHz)	6.96 (*dd*, *J* = 15.5, 9.0 Hz, 1H), 6.32 (*s*, 1H), 5.79 (*d*, *J* = 15.5 Hz, 1H), 4.85 (*dq*, *J* = 9.0, 6.5 Hz, 1H), 3.90 (*t*, *J* = 9.0 Hz, 1H), 3.84 (*s*, 3H), 2.55 (*m*, 1H), 2.37 (*m*, 1H), 1.55 (*m*, 1H), 1.48 (*m*, 1H), 1.40 (*d*, *J* = 6.5 Hz, 3H), 1.31 (*m*, 4H), 0.87 (*t*, *J* = 7.0 Hz, 3H)
^{13}C NMR ($CDCl_3$) (δ ppm) (125 MHz)	168.83, 152.31, 148.29, 146.76, 137.89, 126.16, 121.91, 118.23, 92.01, 82.78, 56.19, 48.14, 32.07, 28.98, 27.30, 22.54, 16.43, 13.99

DEPT (135°) ($CDCl_3$) CH : 148.29, 121.91, 92.01, 82.78, 48.14

CH_2 : 32.07, 28.98, 27.30, 22.54

CH_3 : 56.19, 16.43, 13.99

EIMS *m/z* (% relative intensity): 320 (100), 275 (9), 231 (16)

Band 3 was obtained as a yellow solid (5.4 mg). Its chromatogram displayed one UV-active spot on normal phase TLC with the R_f value of 0.15 using 20% ethyl acetate in light petroleum (6 runs) as a mobile phase. Its ^1H NMR spectrum displayed proton signals at high field region. Therefore, further purification was not performed.

Subfraction C9 appeared as a long tail under UV-S on normal phase TLC using 10% methanol in dichloromethane as a mobile phase (2 runs). Furthermore, its chromatogram showed many UV-active spots on reverse phase TLC using 50% methanol in water (2 runs) as a mobile phase. Further separation by column chromatography over reverse phase silica gel was performed. Elution was conducted initially with 30% methanol in water and gradually enriched with methanol until pure methanol. Subfractions, which contained similar components, were combined and evaporated to dryness under reduced pressure to give four subfractions, as shown in **Table 41**

Table 41 Subfractions obtained from **subfraction C9** by column chromatography over reverse phase silica gel

Subfraction	Eluent	Weight (mg)	Physical appearance
C9-1	30% MeOH/H_2O	24.5	Brown gum
C9-2	50-70% MeOH/H_2O	9.9	Brown gum
C9-3	70% MeOH/H_2O	10.1	Brown gum
C9-4	100% MeOH	6.0	Brown gum mixed with brown solid

Subfraction C9-1 showed no definite spots under UV-S on normal phase TLC using 5% methanol in dichloromethane as a mobile phase (5 runs). Furthermore, its chromatogram showed no UV-active spots on reverse phase TLC using 50% methanol in water as a mobile phase. Its ^{1}H NMR spectrum displayed none of major signals. Therefore, further investigation was not conducted.

Subfraction C9-2 displayed a long tail under UV-S on normal phase TLC using 5% methanol in dichloromethane as a mobile phase (5 runs). Its chromatogram showed many UV-active spots on reverse phase TLC using 50% methanol in water as a mobile phase. Its ^{1}H NMR spectrum displayed proton signals at high field region. Thus, further isolation was not performed.

Subfraction C9-3 showed a long tail under UV-S on normal phase TLC using 5% methanol in dichloromethane as a mobile phase (5 runs). When using 50% ethyl acetate in light petroleum (3 runs) and 100% ethyl acetate (2 runs) as mobile phases, the chromatogram showed many UV-active spots on normal phase TLC. Therefore, further purification was not carried out.

Subfraction C9-4 showed no spots under UV-S on normal phase TLC using 5% methanol in dichloromethane as a mobile phase (5 runs). Its ^{1}H NMR spectrum indicated none of major components. Therefore, no attempted investigation was carried out.

Subfraction C10 contained many spots under UV-S on normal phase TLC using 10% methanol in dichloromethane as a mobile phase (2 runs). Furthermore, its chromatogram showed no distinct UV-active spots on reverse phase TLC using 50% methanol in water (2 runs) as a mobile phase. Further separation by column chromatography over Sephadex LH20 using 100% MeOH as eluent was performed. Subfractions, which contained similar components, were combined and evaporated to dryness under reduced pressure to give three subfractions, as shown in **Table 42.**

Table 42 Subfractions obtained from **subfraction C10** by column chromatography over Sephadex LH20

Subfraction	Eluent	Weight (mg)	Physical appearance
C10-1	100% MeOH	5.9	Yellow gum
C10-2	100% MeOH	11.5	Yellow gum
C10-3	100% MeOH	13.6	Yellow gum

Subfraction C10-1 showed no spots under UV-S on normal phase TLC using 5% methanol in dichloromethane as a mobile phase (3 runs). Its ^{1}H NMR spectrum indicated none of major components. Therefore, no attempted investigation was performed.

Subfraction C10-2 showed many spots under UV-S on normal phase TLC using 5% methanol in dichloromethane as a mobile phase (3 runs). Further separation by column chromatography over Sephadex LH20 using 100% MeOH as eluent was performed. All subfractions were examined by TLC, combined on the basis of their chromatogram characteristics and then evaporated to dryness under reduced pressure to afford four subfractions, as shown in **Table 43.**

Table 43 Subfractions obtained from **subfraction C10-2** by column chromatography over Sephadex LH20

Subfraction	Eluent	Weight (mg)	Physical appearance
C10-2-1	100% MeOH	2.0	Colorless gum
C10-2-2	100% MeOH	1.8	Yellow gum
C10-2-3	100% MeOH	7.1	Yellow gum
C10-2-4	100% MeOH	0.5	Yellow gum

Subfraction C10-2-1 showed one major spot under UV-S on normal phase TLC with the R_f value of 0.23 using 50% ethyl acetate in light petroleum as a mobile phase. Its ^{1}H NMR spectral data indicated the presence of **N20** as a major

component together with other components. Because of low quantity, it was not further purified.

Subfraction C10-2-2 (N20) showed one UV-active spot on normal phase TLC with the R_f value of 0.23 using 50% ethyl acetate in light petroleum as a mobile phase.

$[\alpha]_D^{29}$	+73.11 (c = 0.90, $CHCl_3$)
FT-IR (neat) ν_{cm-1}	3372 (O-H stretching), 1749 (C=O stretching), 1607 (C=C stretching)
^{1}H NMR ($CDCl_3$+CD_3OD) (δ ppm) (300 MHz)	6.96 (*dd*, J = 15.6, 4.8 Hz, 1H), 6.07 (*dd*, J = 15.6, 1.2 Hz, 1H), 4.23 (*dd*, J = 4.8, 3.9 Hz, 1H), 3.88 (*qd*, J = 6.3, 3.9 Hz, 1H), 1.15 (*d*, J = 6.3 Hz, 3H)
^{13}C NMR ($CDCl_3$+CD_3OD) (δ ppm) (125 MHz)	168.63, 146.94, 122.07, 74.53, 69.87, 17.34
DEPT (135°) ($CDCl_3$+CD_3OD) CH :	146.94, 122.07, 74.53, 69.87
CH_3 :	17.34

Subfraction C10-2-3 showed one major spot under UV-S on normal phase TLC with the R_f value of 0.23 using 50% ethyl acetate in light petroleum as a mobile phase. Further separation by column chromatography over Sephadex LH20 using 100% MeOH as eluent was performed. All subfractions were examined by TLC, combined on the basis of their chromatogram characteristics and then evaporated to dryness under reduced pressure to afford three subfractions, as shown in **Table 44**.

Table 44 Subfractions obtained from **subfraction C10-2-3** by column chromatography over Sephadex LH20

Subfraction	Eluent	Weight (mg)	Physical appearance
C10-2-31	100% MeOH	0.4	Yellow gum
C10-2-32	100% MeOH	6.0	Yellow gum
C10-2-33	100% MeOH	0.5	Yellow gum

Subfraction C10-2-31 showed no spots under UV-S on normal phase TLC using 50% ethyl acetate in light petroleum as a mobile phase. Its ^{1}H NMR spectrum displayed proton signals at high field region. Therefore, no attempted investigation was carried out.

Subfraction C10-2-32 showed one spot under UV-S on normal phase TLC with the R_f value of 0.23 using 50% ethyl acetate in light petroleum as a mobile phase. Its ^{1}H NMR spectral data indicated that it was **N20.**

Subfraction C10-2-33 showed no definite spots under UV-S on normal phase TLC using 50% ethyl acetate in light petroleum as a mobile phase. Because of low quantity, it was not further isolated.

Subfraction C10-2-4 showed no spots under UV-S on normal phase TLC using 50% ethyl acetate in light petroleum as a mobile phase. Because of low quantity, it was not further investigated.

Subfraction C10-3 showed no definite spots under UV-S on normal phase TLC using 5% methanol in dichloromethane as a mobile phase (3 runs). Its ^{1}H NMR spectrum showed none of aromatic proton signals. Therefore, further investigation was not conducted.

Fraction D demonstrated no definite UV-active spots using 5% methanol in dichloromethane (2 runs) as a mobile phase. In addition, its chromatogram showed no

spots after dipping the normal phase TLC in ASA reagent and subsequently heating. Its ^{1}H NMR spectrum indicated none of major components. Therefore, it was not further investigated.

3.2.3 Purification of the mycelial extract

The crude material showed six UV-active spots on normal phase TLC with the R_f values of 0.28, 0.35, 0.53, 0.63, 0.70 and 0.93 using 3% methanol in dichloromethane (2 runs) as a mobile phase. It was further separated by column chromatography over Sephadex LH20 using 100% MeOH as eluent. All fractions were examined by TLC, combined on the basis of their chromatogram characteristics and then evaporated to dryness under reduced pressure to give six fractions, as shown in **Table 45**.

Table 45 Fractions obtained from **the mycelial extract** by column chromatography over Sephadex LH20

Fraction	Eluent	Weight (mg)	Physical appearance
MA	100% MeOH	97.1	Brown solid
MB	100% MeOH	25.6	Dark-brown gum
MC	100% MeOH	49.2	Dark-brown gum mixed with brown solid
MD	100% MeOH	14.5	Dark-brown gum
ME	100% MeOH	9.1	Brown gum
MF	100% MeOH	17.5	Dark-brown gum mixed with brown solid

Fraction MA showed no definite spots after dipping the normal phase TLC in ASA reagent and subsequently heating using 10% ethyl acetate in light petroleum (2 runs) as a mobile phase. The ^{1}H NMR spectrum indicated that the major components might be a mixture of long chain hydrocarbons. Further investigation by column chromatography over silica gel was performed. Elution was conducted with gradient

systems of ethyl acetate-light petroleum and methanol-ethyl acetate. Subfractions, which contained similar components, were combined and evaporated to dryness under reduced pressure to give three subfractions, as shown in **Table 46.**

Table 46 Subfractions obtained from **fraction MA** by column chromatography over silica gel

Subfraction	Eluent	Weight (mg)	Physical appearance
MA-1	10-50% EtOAc/Light petroleum	13.1	Brown solid
MA-2	70% EtOAc/Light petroleum	13.2	Dark-brown gum
MA-3	90% EtOAc/Light petroleum - 100% MeOH	58.5	Dark-brown gum mixed with brown solid

Subfraction MA-1 showed a long tail after dipping the normal phase TLC in ASA reagent and subsequently heating using 30% ethyl acetate in light petroleum (2 runs) as a mobile phase. Its ^{1}H NMR spectrum displayed proton signals at high field region. Therefore, it was not further investigated.

Subfraction MA-2 showed a long tail after dipping the normal phase TLC in ASA reagent and subsequently heating using 30% ethyl acetate in light petroleum (2 runs) as a mobile phase. The ^{1}H NMR spectrum indicated that it contained no major components. Therefore, it was not further investigated.

Subfraction MA-3 showed no definite spots after dipping the normal phase TLC in ASA reagent and subsequently heating using 30% ethyl acetate in light petroleum (2 runs) as a mobile phase. The ^{1}H NMR spectrum indicated that the major components might be a mixture of long chain hydrocarbons. Therefore, no attempted investigation was carried out.

Fraction MB contained many inseparable spots after dipping the normal phase TLC in ASA reagent and subsequently heating using 10% ethyl acetate in light petroleum (2 runs) as a mobile phase. This fraction was not further investigated because its ^{1}H NMR spectrum indicated that it was a mixture of long chain hydrocarbons.

Fraction MC displayed four UV-active spots on normal phase TLC with the R_f values of 0.13, 0.40, 0.70 and 0.80 using 10% ethyl acetate in light petroleum (2 runs) as a mobile phase. Further separation by column chromatography over silica gel was performed. Elution was conducted with gradient systems of ethyl acetate-light petroleum and methanol-ethyl acetate. Subfractions, which contained similar components, were combined and evaporated to dryness under reduced pressure to give seven subfractions, as shown in **Table 47**.

Table 47 Subfractions obtained from **fraction MC** by column chromatography over silica gel

Subfraction	Eluent	Weight (mg)	Physical appearance
MC1	2-30% EtOAc/Light petroleum	5.1	Colorless gum
MC2	30-50% EtOAc/Light petroleum	1.8	Yellow gum
MC3	50% EtOAc/Light petroleum	5.4	Brown-orange gum
MC4	50-70% EtOAc/Light petroleum	1.5	Brown gum
MC5	70% EtOAc/Light petroleum - 100% EtOAc	5.2	Brown gum
MC6	2-5% MeOH/EtOAc	4.2	Yellow solid
MC7	10-80% MeOH/EtOAc	22.5	Dark-brown gum

Subfraction MC1 showed no spots on normal phase TLC using 2% ethyl acetate in light petroleum as a mobile phase. Its ^{1}H NMR spectrum showed none of aromatic proton signals. Therefore, it was not further investigated.

Subfraction MC2 showed two spots on normal phase TLC with the R_f values of 0.25 and 0.43 using 5% ethyl acetate in light petroleum as a mobile phase. The ^{1}H NMR spectrum indicated that it was a mixture of **N14** and **N16**. Therefore, it was not further purified.

Subfraction MC3 displayed one spot with the R_f value of 0.25 together with two overlapping spots under UV-S on normal phase TLC using 5% ethyl acetate in light petroleum as a mobile phase. The ^{1}H NMR spectral data and chromatogram on normal phase TLC indicating the presence of a mixture of **N14, N17** and **N18**. Therefore, it was not further investigated.

Subfraction MC4 showed one major spot on normal phase TLC with the R_f value of 0.25 using 5% ethyl acetate in light petroleum as a mobile phase. The ^{1}H NMR spectrum indicated the presence of **N14** as a major component.

Subfraction MC5 showed two spots on normal phase TLC with the R_f values of 0.35 and 0.13 using 10% ethyl acetate in light petroleum followed by 30% ethyl acetate in light petroleum as mobile phases. Further purification by precoated TLC using 30% ethyl acetate in light petroleum (3 runs) followed by 50% ethyl acetate in light petroleum (2 runs) as mobile phases afforded two bands.

Band 1 was a yellow gum (1.6 mg), which showed one spot under UV-S on normal phase TLC with the R_f value of 0.30 using 40% ethyl acetate in light petroleum (3 runs) as a mobile phase. The ^{1}H NMR spectrum indicated that it was a mixture. Because of low quantity, it was not further purified.

Band 2 was a yellow gum (3.1 mg), which showed one spot under UV-S on normal phase TLC with the R_f value of 0.08 using 40% ethyl acetate in light petroleum (3 runs) as a mobile phase. The ^{1}H NMR spectrum indicated that it was a mixture. Therefore, no attempted separation was carried out.

Subfraction MC6 showed one major spot on normal phase TLC with the R_f value of 0.25 using 10% ethyl acetate in light petroleum followed by 30% ethyl acetate in light petroleum (5 runs) as mobile phases. Further purification by precoated TLC using 50% ethyl acetate in light petroleum (5 runs) as a mobile phase afforded a white solid (2.0 mg). Its chromatogram characteristic displayed one spot on normal phase TLC with the R_f value of 0.20 using 50% ethyl acetate in light petroleum (2 runs) as a mobile phase. The ^{1}H NMR data indicated that it contained many compounds. Thus, it was not further purified.

Subfraction MC7 showed a long tail under UV-S on normal phase TLC using 50% ethyl acetate in light petroleum (5 runs) as a mobile phase. Its ^{1}H NMR spectrum indicated none of major components. Therefore, further investigation was not conducted.

Fraction MD showed three UV-active spots on normal phase TLC with the R_f values of 0.13, 0.23 and 0.65 using 10% ethyl acetate in light petroleum (2 runs) as a mobile phase. Further purification by precoated TLC with 5% ethyl acetate in light petroleum (5 runs) as a mobile phase afforded four bands.

Band 1 was obtained as a yellow gum (2.9 mg). Its chromatogram demonstrated one UV-active spot on normal phase TLC with the R_f value of 0.63 using 5% ethyl acetate in light petroleum as a mobile phase. Its ^{1}H NMR spectrum displayed proton signals at high field region. Therefore, it was not further purified.

Band 2 was obtained as a white solid (3.5 mg), which showed one spot under UV-S on normal phase TLC with the R_f value of 0.20 using 5% ethyl acetate in light petroleum as a mobile phase. Its ^{1}H NMR spectrum suggested that it contained **N18** as a major component.

Band 3 was a yellow gum (2.0 mg). Its chromatogram displayed one UV-active spot with the R_f value of 0.10 using 5% ethyl acetate in light petroleum as a mobile phase. Its ^{1}H NMR spectrum suggested that it was **N17**.

Band 4 was obtained as a brown gum (4.2 mg). Its chromatogram displayed one UV-active spot on normal phase TLC with the R_f value of 0.05 using 5% ethyl acetate in light petroleum as a mobile phase. Its ^1H NMR spectrum showed none of aromatic proton signals. Thus, it was not further isolated.

Fraction ME showed three UV-active spots on normal phase TLC with the R_f values of 0.18, 0.60 and 0.63 using 10% ethyl acetate in light petroleum (2 runs) as a mobile phase. Further purification by precoated TLC with 5% ethyl acetate in light petroleum (5 runs) followed by 10% ethyl acetate in light petroleum (5 runs) as mobile phases afforded three bands.

Band 1 was obtained as a colorless gum (0.7 mg). Its chromatogram demonstrated one UV-active spot on normal phase TLC with the R_f value of 0.60 using 5% ethyl acetate in light petroleum as a mobile phase (5 runs). The ^1H NMR spectrum indicated that it was a mixture. Because of low quantity, it was not further purified.

Band 2 was obtained as a yellow gum (0.6 mg), which showed one spot under UV-S on normal phase TLC with the R_f value of 0.58 using 5% ethyl acetate in light petroleum (5 runs) as a mobile phase. The ^1H NMR spectrum indicated that it was a mixture. Because of low quantity, it was not further purified.

Band 3 was a yellow gum (5.2 mg). Its chromatogram displayed one UV-active spot with the R_f value of 0.18 using 5% ethyl acetate in light petroleum as a mobile phase. Its ^1H NMR spectrum suggested that it was a mixture of **N17** and **N18**. Therefore, it was not further investigated.

Fraction MF showed no spots under UV-S on normal phase TLC using 10% ethyl acetate in light petroleum (2 runs) followed by 30% ethyl acetate in light petroleum (2 runs) as mobile phases (5 runs). Furthermore, its chromatogram showed no UV-active spots on reverse phase TLC using 50% methanol in water as a mobile phase. Its ^1H NMR spectrum displayed none of aromatic proton signals. Therefore, no further investigation was pursued.

CHAPTER 3.3
RESULTS AND DISCUSSION

One new compound (**N19**) was isolated from the broth extract together with six known compounds (**N14-N18** and **N20**). In addition, compound **N17** was also obtained from the mycelial extract. The structures were identified by spectroscopic methods.

3.3.1 Compound N14

N14 was obtained as a yellow gum. The UV spectrum showed maximum absorption bands at 227 and 289 nm, indicating the presence of a benzene chromophore. Its IR spectrum exhibited an absorption band due to a hydroxyl group at 3393 cm^{-1}. The ^1H NMR spectrum (**Figure 37**) (**Table 48**) showed the characteristic signals for two *meta*-aromatic protons (δ_H 6.35, *d*, J = 2.7 Hz, 1H and 6.29, *d*, J = 2.7 Hz, 1H), one hydroxyl group (δ_H 5.25, *s*, 1H), two methoxyl groups (δ_H 3.86, *s*, 3H and 3.76, *s*, 3H) and one pentyl unit [δ_H 2.61 (*t*, J = 7.5 Hz, 2H), 1.36 (*m*, 6H) and 0.87 (*t*, J = 6.6 Hz, 3H)]. The hydroxy proton (1-OH) gave HMBC correlations (**Table 48**) with C-1 (δ_C 137.43), C-2 (δ_C 146.65) and C-6 (δ_C 128.63). The methoxyl group resonating at δ_H 3.86 and the pentyl side chain were then located at C-2 and C-6, respectively, on the basis of the following ^3J HMBC correlations: 2-OCH_3/C-2 and H_2-7(δ_H 1.36)/C-1, C-5 (δ_C 105.65) and C-6. Two *meta*-aromatic protons, resonating at δ_H 6.35 and 6.29, were attributed to H-3 and H-5, respectively, due to HMBC correlations of H-3/C-1, C-2, C-4 (δ_C 152.66) and C-5 and those of H-5/C-1, C-3 (δ_C 96.54) and C-4. The other methoxyl group (δ_H 3.76) was attached at C-4 on the basis of a HMBC correlation between 4-OCH_3 with C-4. Signal enhancement of both methoxyl resonances after irradiation of H-3 (**Table 48**) in the NOEDIFF experiment confirmed the assigned location. The attachment of the pentyl group at C-6 was supported by signal enhancement of H-5 upon irradiation of H_2-7 in the

NOEDIFF experiment. Thus, **N14** was elucidated as 2,4-dimethoxy-6-pentylphenol which was synthesized in 1983 (Srebnik and Mechoulam, 1983).

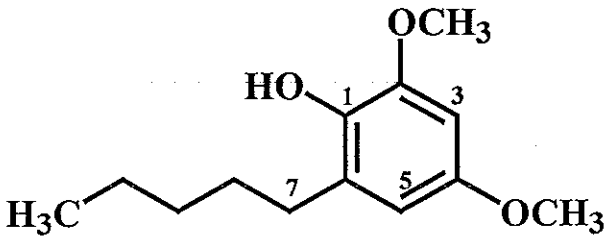

Table 48 The NMR data of **N14** and **2,4-dimethoxy-6-pentylphenol** in $CDCl_3$

Position	N14		HMBC	NOE	2,4-Dimethoxy-6-pentylphenol [a]
	δ_H (mult., J_{Hz})	δ_C (C-Type)			δ_H (mult., J_{Hz})
1-OH	5.25 (*s*)	137.43 (C)	C-1, C-2, C-6	-	5.29 (*s*)
2	-	146.65 (C)	-	-	-
2-OCH_3	3.86 (*s*)	55.95 (CH_3)	C-2	H-3	3.84 (*s*)
3	6.35 (*d*, 2.7)	96.54 (CH)	C-1, C-2, C-4, C-5	2-OCH_3, 4-OCH_3	6.30 (*m*)
4	-	152.66 (C)	-	-	-
4-OCH_3	3.76 (*s*)	55.73 (CH_3)	C-4	H-3, H-5	3.75 (*s*)
5	6.29 (*d*, 2.7)	105.65 (CH)	C-1, C-3, C-4	4-OCH_3	6.30 (*m*)
6	-	128.63 (C)	-	-	-
7	1.36 (*m*)	29.52 (CH_2)	C-1, C-5, C-6	H-5	1.42 (*m*)
8	1.36 (*m*)	31.72 (CH_2)	-	-	1.42 (*m*)
9	1.36 (*m*)	29.70 (CH_2)	-	-	1.42 (*m*)
10	2.61 (*t*, 7.5)	22.59 (CH_2)	-	-	2.63 (*t*, 6.6)
11	0.87 (*t*, 6.6)	14.07 (CH_3)	-	-	0.89 (*t*, 6.0)

[a] Srebnik and Mechoulam, 1983.

3.3.2 Compound N15

N15 was obtained as a yellow solid, melting at 56.1-56.7 °C. The UV spectrum showed maximum absorption bands at λ_{max} 247 and 314 nm. The IR spectrum exhibited absorption bands at 3365 cm^{-1} for a hydroxyl group and at 1652 cm^{-1} for a carbonyl group. The LREI-MS (**Figure 39**) showed the molecular formula $C_{10}H_{10}O_3$. The ^1H NMR spectral data (**Figure 40**) (**Table 49**) consisted of signals for one chelated hydroxyl group (δ_H 11.06, *s*, 1H), three aromatic protons of a 1,2,3-

trisubstituted benzene [δ_H 7.44 (*t*, *J* = 8.1 Hz, 1H), 6.92 (*d*, *J* = 8.1 Hz, 1H) and 6.72 (*d*, *J* = 8.1 Hz, 1H)], one oxymethine proton (δ_H 4.77, *tq*, *J* = 7.2 and 6.6 Hz, 1H), one methylene group (δ_H 2.96, *d*, *J* = 7.2 Hz, 2H) and one methyl group (δ_H 1.56, *d*, *J* = 6.6 Hz, 3H). The ^{13}C NMR spectrum (**Figure 41**) (**Table 49**) showed one ester carbonyl (δ_C 169.93), three quaternary (δ_C 162.21, 139.38 and 108.30), three methine (δ_C 136.12, 117.87 and 116.24), one oxymethine (δ_C 76.07), one methylene (δ_C 34.61) and one methyl (δ_C 20.74) carbons. Its spectroscopic data were similar to those of mellein. The chelated hydroxyl group which was placed at C-8 (δ_C 162.21), *peri* position to the carbonyl group, gave HMBC cross peaks (**Table 50**) with C-7 (δ_C 116.24), C-8 and C-8a (δ_C 108.30). The aromatic proton at δ_H 6.92 was then assigned as H-7 due to its correlation with C-7 in the HMQC spectrum and its HMBC correlations with the C-1 (δ_C 169.93), C-5 (δ_C 117.87), C-8 and C-8a. The remaining aromatic protons resonating at δ_H 6.72 and 7.44 were then attributed to H-5 and H-6, respectively, on the basis of their multiplicity and coupling constants. The ^3J HMBC correlations of H-5 with C-4 (δ_C 34.61), C-7 and C-8a indicated that the methylene group (δ_H 2.96, H_2-4) was linked at C-4a (δ_C 139.38) of the aromatic ring. The COSY spectrum revealed that H_2-4 was coupled with the oxymethine proton (H-3, δ_H 4.77) which was further coupled with Me-9 (δ_H 1.56). The chemical shifts of C-1 (δ_C 169.93) and C-3 (δ_C 76.04) constructed a lactone ring. Thus, **N15** was identified as mellein. The observed optical rotation of **N15** ($[\alpha]_D^{27}$ -114.29, c = 0.07, $CHCl_3$) was almost identical to that of (*R*)-(-)-mellein ($[\alpha]_D^{26}$ -101.30, c = 0.07, $CHCl_3$), indicating that they possessed the same configuration at C-3. Therefore, **N15** was (*R*)-(-)-mellein, which was previously isolated from *Aspergillus melleus* (Dimitriadis *et al.*, 1997).

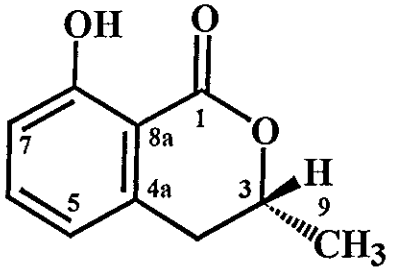

Table 49 The NMR data of **N15** and **(*R*)-(-)-mellein** in $CDCl_3$

Position	**N15**		**(*R*)-(-)-Mellein**[a]	
	δ_H (mult., J_{Hz})	δ_C (C-Type)	δ_H (mult., J_{Hz})	δ_C (C-Type)
1	-	169.93 (C=O)	-	169.9 (C=O)
3	4.77 (*tq*, 7.2, 6.6)	76.07 (CH)	4.73 (*m*)	76.1 (CH)
4	2.96 (*d*, 7.2)	34.61 (CH_2)	2.93 (*d*, 7.3)	34.6 (CH_2)
4a	-	139.38 (C)	-	139.3 (C)
5	6.72 (*d*, 8.1)	117.87 (CH)	6.89 (*d*, 8.3)	117.9 (CH)
6	7.44 (*t*, 8.1)	136.12 (CH)	7.41 (*m*)	136.1 (CH)
7	6.92 (*d*, 8.1)	116.24 (CH)	6.69 (*d*, 7.3)	116.2 (CH)
8-OH	11.06 (*s*)	162.21 (C)	11.03 (*s*)	162.1 (C)
8a	-	108.30 (C)	-	108.2 (C)
9	1.56 (*d*, 6.6)	20.74 (CH_3)	1.53 (*d*, 6.3)	20.8 (CH_3)

[a] Dimitriadis *et al.*, 1997.

Table 50 The HMBC and NOE data of **N15** in $CDCl_3$

Position	HMBC	NOE
H-3	C-4a, C-9	Me-9
H-4	C-3, C-4a, C-5, C-8a, C-9	H-3, H-5, Me-9
H-5	C-1, C-4, C-4a, C-6, C-7, C-8a	H-4, H-6
H-6	C-4a, C-5, C-8	-
H-7	C-1, C-5, C-8, C-8a	H-6
8-OH	C-7, C-8, C-8a	-
Me-9	C-3, C-4	H-3, H-4

3.3.3 Compound N17

N17 was obtained as a yellow gum. The UV spectrum showed maximum absorption bands at λ_{max} 245 and 314 nm. The IR spectrum was similar to that of **N15**. The ^1H NMR spectral data (**Figure 42**) (**Table 51**) were similar to those of **N15** except that the methylene protons (δ_H 2.96, *d*, J = 7.2 Hz, 2H) of **N15** were replaced, in **N17**, by an oxymethine proton (δ_H 4.57, *brd*, J = 2.1 Hz, 1H). The oxymethine proton was attributed to H-4 due to its HMBC correlations (**Table 52**) with C-3 (δ_C 78.21), C-4a (δ_C 140.53), C-5 (δ_C 118.28), C-8a (δ_C 106.84) and C-9 (δ_C 15.99). The small coupling constant (2.1 Hz) between H-3 and H-4 indicated that both

protons had *cis* relationship. **N17** gave almost identical rotation to *cis*-4-hydroxymellein, $[\alpha]_D^{29}$ of **N17** = -25.53 (c = 0.04, $CHCl_3$) and $[\alpha]_D$ of *cis*-4-hydroxymellein = -27.50 (c = 0.04, $CHCl_3$) (Garson *et al.*, 1984). Therefore, **N17** was assigned as *cis*-4-hydroxymellein which was previously isolated from *Uvaria hamiltonii* (Asha *et al.*, 2004).

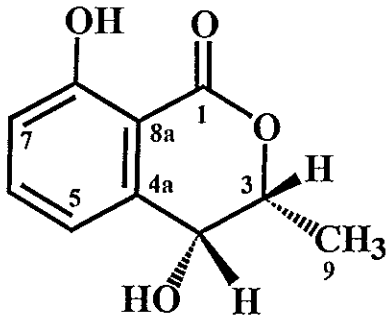

Table 51 The NMR data of **N17** and ***cis*-4-hydroxymellein** in $CDCl_3$

Position	N17		*cis*-4-Hydroxymellein [a]	
	δ_H (mult., J_{Hz})	δ_C (C-Type)	δ_H (mult., J_{Hz})	δ_C (C-Type)
1	-	169.19 (C=O)	-	162.0 (C=O)
3	4.70 (*qd*, 6.6, 2.1)	78.21 (CH)	4.67 (*qd*, 6.5, 1.5)	77.9 (CH)
4	4.57 (*brd*, 2.1)	67.23 (CH)	4.55 (*brs*)	67.1 (CH)
4a	-	140.53 (C)	-	140.8 (C)
5	6.92 (*dt*, 7.2, 0.9)	118.28 (CH)	6.90 (*d*, 7.0)	118.1 (CH)
6	7.52 (*dd*, 8.4, 7.2)	136.77 (CH)	7.47 (*t*, 7.0)	137.0 (CH)
7	7.02 (*dd*, 8.4, 0.9)	118.51 (CH)	7.01 (*d*, 7.0)	118.4 (CH)
8-OH	10.99 (*s*)	162.08 (C)	11.01 (*s*)	162.0 (C)
8a	-	106.84 (C)	-	106.9 (C)
9	1.59 (*d*, 6.6)	15.99 (CH_3)	1.56 (*d*, 6.5)	15.9 (CH_3)

[a] Asha *et al.*, 2004.

Table 52 The HMBC, COSY and NOE data of **N17** in $CDCl_3$

Position	HMBC	COSY	NOE
H-3	C-4, C-4a, C-9	H-4, Me-9	H-4, Me-9
H-4	C-3, C-4a, C-5, C-8a, C-9	H-3	H-3, H-5, Me-9
H-5	C-1, C-4a, C-6, C-7, C-8a	H-4, H-6, H-7	H-4, H-6
H-6	C-4a, C-7, C-8	H-5, H-7	H-5, H-7
H-7	C-1, C-5, C-8, C-8a	H-5, H-6	H-6
8-OH	C-7, C-8, C-8a	-	-
Me-9	C-3, C-4	H-3	H-3

3.3.4 Compound N18

N18 was obtained as a white solid, melting at 109.7-110.3 °C. The UV and IR spectra were almost identical to those of **N17**. The ^{1}H NMR spectral data (**Figure 44**) (**Table 53**) were similar to those of **N17** with the differences in chemical shift and multiplicity of H-3 and H-4. HMBC data in **Table 54** suggested the identical location of all substituents. Therefore, **N18** had the same structure as **N17** but differed in the absolute stereochemistry of C-3 (δ_C 79.91) and C-4 (δ_C 69.22). Irradiation of Me-9 (δ_H 1.53, *d*, *J* = 6.6 Hz, 3H) affected the signal intensity of H-4 (δ_H 4.64, *m*, 1H), indicating *cis* and *trans* relationship of H-4/Me-9 and H-3/H-4, respectively. The observed optical rotation of **N18** ($[\alpha]_D^{29}$ +28.80, c = 1.00, MeOH) was almost identical to that of *trans*-4-hydroxymellein ($[\alpha]_D^{23}$ +23.30, c = 1.00, MeOH) (Izawa *et al.*, 1989), supporting above conclusion. Therefore, **N18** was assigned as *trans*-4-hydroxymellein, which was previously isolated from *Uvaria hamiltonii* (Asha *et al.*, 2004).

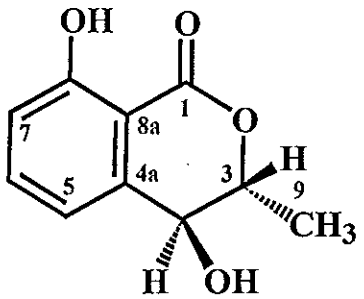

Table 53 The NMR data of **N18** and ***trans*-4-hydroxymellein** in $CDCl_3$

Position	N18		*trans*-4-Hydroxymellein[a]	
	δ_H (mult., J_{Hz})	δ_C (C-Type)	δ_H (mult., J_{Hz})	δ_C (C-Type)
1	-	168.56 (C=O)	-	161.96 (C=O)
3	4.62 (*m*)	79.91 (CH)	4.58 (*dq*, 4.5, 7.0)	79.8 (CH)
4	4.64 (*m*)	69.22 (CH)	4.60 (*brs*)	69.1 (CH)
4a	-	141.14 (C)	-	141.0 (C)
5	7.03 (*d*, 7.5)	116.15 (CH)	7.00 (*d*, 8.5)	116.1 (CH)
6	7.55 (*dd*, 8.5, 7.5)	136.87 (CH)	7.52 (*t*, 8.5)	136.7 (CH)
7	7.01 (*d*, 8.5)	117.87 (CH)	6.97 (*d*, 8.5)	117.8 (CH)
8-OH	10.99 (*s*)	162.08 (C)	10.97 (*s*)	161.96 (C)
8a	-	106.50 (C)	-	106.7 (C)
9	1.53 (*d*, 6.6)	17.92 (CH_3)	1.49 (*d*, 6.5)	17.8 (CH_3)

[a] Asha *et al.*, 2004.

Table 54 The HMBC, COSY and NOE data of **N18** in $CDCl_3$

Position	HMBC	COSY	NOE
H-3	C-1, C-4, C-4a	H-4, Me-9	Me-9
H-4	C-3, C-4a, C-5, C-8a	H-3	H-5, Me-9
H-5	C-4, C-7, C-8a	H-6	H-4
H-6	C-4a, C-8	H-5, H-7	H-5, H-7
H-7	C-5	H-6	H-6
8-OH	C-7, C-8, C-8a	-	-
Me-9	C-3, C-4	H-3	H-3, H-4

3.3.5 Compound N16

N16 was obtained as a yellow solid, melting at 63.8-64.5 °C. The UV spectrum showed a maximum absorption band of a *p*-quinone moiety at λ_{max} 267 nm (Rukachaisirikul *et al.*, 2003). The IR spectrum exhibited absorption bands at 1679 and 1652 cm^{-1} for conjugated ketone carbonyl groups. The ^1H NMR spectral data (**Figure 46**) (**Table 55**) consisted of signals for two olefinic protons [δ_H 6.51 (*td*, J = 2.4 and 1.5 Hz, 1H) and 5.90 (*d*, J = 2.4 Hz, 1H)], one methoxyl group (δ_H 3.84, *s*, 3H) and one pentyl group [δ_H 2.45 (*td*, J = 8.1 and 1.5 Hz, 2H), 1.54 (*m*, 2H), 1.37 (*m*, 2H), 1.34 (*m*, 2H) and 0.92 (*t*, J = 6.9 Hz, 3H)]. The ketone carbonyl carbons at δ_C 187.70 and 182.13, in the ^{13}C NMR spectrum (**Figure 47**) (**Table 55**), supported the presence of the quinone moiety. Two olefinic protons were attributed to H-3 (δ_H 5.90) and H-5 (δ_H 6.51) on the basis of HMBC correlations (**Table 56**) of H-3/C-1 (δ_C 182.13), C-2 (δ_C 158.86), C-4 (δ_C 187.70) and C-5 (δ_C 132.88) and those of H-5/C-1 and C-3 (δ_C 107.08). These results together with ^3J correlations of the methylene protons, H_2-7 (δ_H 2.45), of the pentyl moiety with C-1 and C-5 linked the pentyl unit at C-6 (δ_C 147.59). Consequently, the methoxyl group (δ_H 3.84) was located at C-2 (δ_C 158.86). This was confirmed by its HMBC correlation with C-2. Irradiation of 2-OCH_3, in the NOEDIFF experiment, enhanced the signals of H-3 (**Table 56**), thus supporting the assignment. Therefore, **N16** was identified as primin, which was previously isolated from *Miconia lepidota* (Gunatilaka *et al.*, 2001).

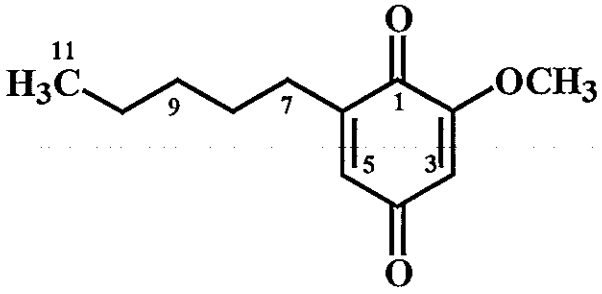

Table 55 The NMR data of **N16** and **primin** in $CDCl_3$

Position	N16		Primin	
	δ_H (mult., J_{Hz})	δ_C (C-Type)	δ_H[a] (mult., J_{Hz})	δ_C[b] (C-Type)
1	-	182.13 (C=O)	-	182.2 (C=O)
2	-	158.86 (C)	-	158.9 (C)
2-OCH_3	3.84 (*s*)	56.26 (CH_3)	3.76 (*s*)	56.4 (CH_3)
3	5.90 (*d*, 2.4)	107.08 (CH)	5.71 (*d*, 2.5)	107.0 (CH)
4	-	187.70 (C=O)	-	187.8 (C=O)
5	6.51 (*td*, 2.4, 1.5)	132.88 (CH)	6.30 (*m*)	132.0 (CH)
6	-	147.59 (C)	-	147.7 (C)
7	2.45 (*td*, 8.1, 1.5)	28.66 (CH_2)	2.34 (*t*, 7.5)	28.8 (CH_2)
8	1.54 (*m*)	27.38 (CH_2)	1.13-1.63 (*m*)	27.5(CH_2)
9	1.37 (*m*)	31.35 (CH_2)	1.13-1.63 (*m*)	31.5 (CH_2)
10	1.34 (*m*)	22.34 (CH_2)	1.13-1.63 (*m*)	22.4 (CH_2)
11	0.92 (*t*, 6.9)	13.89 (CH_3)	0.92 (*t*, 7.5)	13.9 (CH_3)

[a] Bieber *et al.*, 1990.
[b] Gunatilaka *et al.*, 2001.

Table 56 The HMBC and NOE data of **N16** in $CDCl_3$

Position	HMBC	NOE
2-OCH_3	C-2	H-3
H-3	C-1, C-2, C-4, C-5	2-OCH_3
H-5	C-1, C-3, C-7	H-7, H-8
H-7	C-1, C-5, C-6, C-8, C-9	H-5, H-8
H-8	C-6, C-7, C-9, C-10	H-5, H-7
H-9	C-7, C-10, C-11	-
H-10	C-9, C-11	-
H-11	C-9, C-10	-

3.3.6 Compound N19

N19 was obtained as a white solid, melting at 149.6-150.0 °C with $[\alpha]_D^{29}$ +22.22 (c = 0.24, MeOH). The UV spectrum showed a maximum absorption band at λ_{max} 300 nm. The IR spectrum exhibited absorption bands at 3392 cm^{-1} for a hydroxyl group and 1684 cm^{-1} for a carbonyl group of an α,β-unsaturated carboxylic acid. The HREI-MS spectrum showed the molecular formula $C_{18}H_{24}O_5$. The ^1H NMR spectrum (**Figure 49**) (**Table 57**) displayed typical signals of two *trans*-olefinic protons of the α,β-unsaturated carboxylic acid (δ_H 6.96, *dd*, J = 15.5 and 9.0 Hz, 1H and 5.79, *d*, J = 15.5 Hz, 1H), one aromatic proton (δ_H 6.32, *s*, 1H), one oxymethine proton (δ_H 4.85, *dq*, J = 9.0 and 6.5 Hz, 1H), one methine proton (δ_H 3.90, *t*, J = 9.0 Hz, 1H), one methoxyl group (δ_H 3.84, *s*, 3H), one pentyl side chain [δ_H 2.55 (*m*, 1H), 2.37 (*m*, 1H), 1.55 (*m*, 1H), 1.48 (*m*, 1H), 1.31 (*m*, 4H) and 0.87 (*t*, J = 7.0 Hz, 3H)] and one secondary methyl group (δ_H 1.40, *d*, J = 6.5 Hz, 3H). The carbonyl carbon signal at δ_C 168.83, in the ^{13}C NMR spectrum (**Figure 50**) (**Table 57**), supported the presence of the α,β-unsaturated carboxylic acid. The aromatic proton at δ_H 6.32 (*s*, 1H) was assigned as H-7. Irradiation at H-7 in the NOEDIFF experiment (**Table 57**) enhanced the signal intensity of the methoxyl group, thus indicating the attachment of the methoxyl group at C-6 (δ_C 146.76). HMBC correlations (**Table 57**) of H-7/C-3a (δ_C 118.23), C-5 (δ_C 137.89), C-6 and C-7a (δ_C 152.31) and those of the methylene protons of the pentyl moiety (δ_H 2.55 and 2.37, H_{ab}-12)/C-3a, C-4 (δ_C 126.16) and C-5 established the linkage of the pentyl group at C-4. In the COSY spectrum (**Table 57**), The methine proton at δ_H 3.90 (H-3) was coupled with the oxymethine proton at δ_H 4.85 (H-2) and the downfield *trans*-olefinic proton (δ_H 6.96, H-9) of the α,β-unsaturated carboxylic acid. H-2 was further coupled with the methyl protons at δ_H 1.40 (Me-8). HMBC cross peak of H-3/C-3a and C-7a established the linkage of the methine group carrying the 1-oxysubstituted ethyl group and *trans* α,β-unsaturated carboxylic acid moiety at C-3a. According to the chemical shifts of both C-2 (δ_C 82.78) and C-7a and the molecular formula, these carbons were joined together with an ether linkage to form a dihydrobenzofuran skeleton. Since there was no other signal in the ^1H NMR spectrum, the substituent at C-5 must be a hydroxyl group. This

hydroxycarbon resonated at much higher field due to the resonance effect of two oxysubstituents at C-6 and C-7a. Irradiation of H-3 in the NOEDIFF experiment enhanced signal intensity of H-2, indicating their *cis* relationship. Therefore, **N19** was determined as a new dihydrobenzofuran derivative.

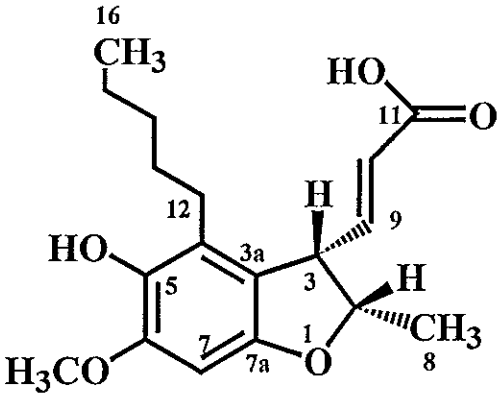

Table 57 The NMR data of **N19** in $CDCl_3$

Position	N19		HMBC	COSY	NOE
	δ_H (mult., J_{Hz})	δ_C (C-Type)			
2	4.85 (*dq*, 9.0, 6.5)	82.78 (CH)	C-9	H-3, H-8	H-3, H-8
3	3.90 (*t*, 9.0)	48.14 (CH)	C-3a, C-7a, C-9, C-10	H-2, H-9	H-2, H-10
3a	-	118.23 (C)	-	-	-
4	-	126.16 (C)	-	-	-
5-OH	-	137.89 (C)	-	-	-
6	-	146.76 (C)	-	-	-
6-OCH_3	3.84 (*s*)	56.19 (CH_3)	C-6	-	H-7
7	6.32 (*s*)	92.01 (CH)	C-3a, C-5, C-6, C-7a	-	6-OCH_3
7a	-	152.31 (C)	-	-	-
8	1.40 (*d*, 6.5)	16.43 (CH_3)	C-2, C-3	H-2	H-2
9	6.96 (*dd*, 15.5, 9.0)	148.29 (CH)	C-3, C-3a, C-11	H-3, H-10	-
10	5.79 (*d*, 15.5)	121.91 (CH)	C-3, C-11	H-9	H-3
11	-	168.83 (C=O)	-	-	-
12	a: 2.55 (*m*)	27.30 (CH_2)	C-3a, C-4	H_b-12, H_{ab}-13	H_b-12
	b: 2.37 (*m*)	-	C-4, C-5, C-13	H_a-12, H_{ab}-13	H_a-12
13	a: 1.55 (*m*)	28.98 (CH_2)	C-14	-	-
	b: 1.48 (*m*)	-	-	-	-

Table 57 Continued

Position	N19		HMBC	COSY	NOE
	δ_H (mult., J_{Hz})	δ_C (C-Type)			
14	1.31 (*m*)	32.07 (CH_2)	C-13, C-15	-	-
15	1.31 (*m*)	22.54 (CH_2)	C-14	H-16	H-16
16	0.87 (*t*, 7.0)	13.99 (CH_3)	C-14, C-15	H-15	-

3.3.7 Compound N20

N20 was obtained as a yellow gum with $[\alpha]_D^{29}$ +73.11 (c = 0.90, $CHCl_3$). The UV spectrum showed no absorption bands in the region of 200-400 nm. The IR spectrum exhibited absorption bands at 3372 cm^{-1} for a hydroxyl group and 1749 cm^{-1} for a carboxylic carbonyl group. The ^1H NMR spectrum (**Figure 51**) (**Table 58**) showed characteristic signals for *trans*-olefinic protons of an α,β-unsaturated carboxylic acid [δ_H 6.96 (*dd*, J = 15.6 and 4.8 Hz, 1H) and 6.07 (*dd*, J = 15.6 and 1.2 Hz, 1H)], two oxymethine protons [δ_H 4.23 (*dd*, J = 4.8 and 3.9 Hz, 1H) and 3.88 (*qd*, J = 6.3 and 3.9 Hz, 1H)] and one secondary methyl group [δ_H 1.15 (*d*, J = 6.3 Hz, 3H)]. The carbonyl carbon signal at δ_C 168.63, in the ^{13}C NMR spectrum (**Figure 52**) (**Table 58**), supported the presence of the α,β-unsaturated carboxylic acid. In the COSY spectrum (**Table 58**), the downfield *trans*-olefinic proton (δ_H 6.96, H-3) of the α,β-unsaturated carboxylic acid was coupled with the other *trans*-olefinic proton (δ_H 6.07, H-2) and the oxymethine proton (δ_H 4.23, H-4). The oxymethine proton at δ_H 3.88 (H-5) was coupled with H-4 and the secondary methyl protons (δ_H 1.15, Me-6). These data established either diol or epoxide functional group at C-4 (δ_C 74.53) and C-5 (δ_C 69.87). Since H-4 (δ_H 3.22) and H-5 (δ_H 2.98) of 4,5-epoxy-2-hexanoic acid (Curci *et al.*, 1980) resonated at much higher field, **N20** was assigned as 4,5-dihydroxy-2-hexenoic acid which was previously reported as a synthetic compound (Jaime *et al.*, 1991).

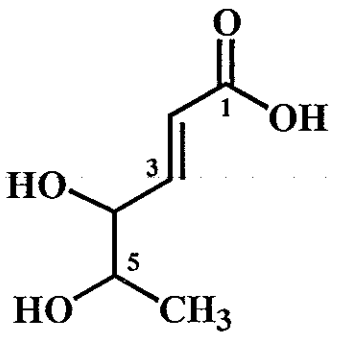

Table 58 The NMR data of **N20** in $CDCl_3$+CD_3OD

Position	N20		HMBC	COSY	NOE
	δ_H (mult., J_{Hz})	δ_C (C-Type)			
1	-	168.63 (C)	-	-	-
2	6.07 (*dd*, 15.6, 1.2)	122.07 (CH)	C-1, C-4	H-3	H-4
3	6.96 (*dd*, 15.6, 4.8)	146.94 (CH)	C-1, C-2, C-4	H-2, H-4	H-4, Me-6
4	4.23 (*dd*, 4.8, 3.9)	74.53 (CH)	C-2, C-3, C-5, C-6	H-3, H-5	H-2, H-3, H-5, Me-6
5	3.88 (*qd*, 6.3, 3.9)	69.87 (CH)	C-3, C-6	H-4, Me-6	H-4, Me-6
6	1.15 (*d*, 6.3)	17.34 (CH_3)	C-4, C-5	H-5	H-4, H-5

PART IV

CHEMICAL CONSTITUENTS FROM THE WOOD-DECAYED FUNGUS *XYLARIA* SP. BCC 9653

CHAPTER 4.1
INTRODUCTION

4.1.1 Introduction

The genus *Xylaria* is a rich source of various types of compounds (**Table 59**). Some of them exhibited a wide range of biological activities (**Table 59**). Chemical constituents isolated from the genus *Xylaria* are summarized in **Table 59** based on SciFinder Scholar database.

The wood-decayed fungus *Xylaria* sp. BCC 9653 was collected on an unidentified wood in Bala-Hala Wildlife Sanctuary, Naratiwat Province, on 14 May 2001, by Mr. Prasert Srikitikulchai. This fungus was deposited at the BIOTEC Culture Collection as BCC 9653 on 16 July 2001.

Table 59 Compounds isolated from the *Xylaria* genus

Scientific name	Compound	Activity	References
X. berteri	Berteric acid, **47**	-	Adeboya *et al.*, 1995
X. cubensis	Cytochalasin D, **48** Cubensic acid, **49**	Antibiotics	Edwards *et al.*, 1991
X. euglossa	Xylactam, **50** Penochalasin B, **51** Neoechinulin A, **52**	-	Wang *et al.*, 2005
X. grammica	Grammicin, **53** γ-Pyrone-3-acetic acid, **54**	-	Edwards *et al.*, 2001
X. hypoxylon	19,20-Epoxycytochalasin C, **55** 19,20-Epoxycytochalasin N, **56** 19,20-Epoxycytochalasin D, **57** 19,20-Epoxycytochalasin R, **58**	-	Espada *et al.*, 1997

Table 59 Continued

Scientific name	Compound	Activity	References
	18-Deoxy-19,20-epoxycytochalasin R, **59** 18-Deoxy-19,20-epoxycytochalasin Q, **60** 19,20-Epoxycytochalasin Q, **61** Cytochalasin Q, **62** Cytochalasin R, **63**		
X. intracolorata	Coloratin A, **64** Coloratin B, **65**	Antimicrobial	Quang *et al.*, 2006
X. longiana	Longianone, **66** (*R*)-(-)-Mellein, **40** A mixture of 4-hydroxymellein, **41, 67**	-	Edwards *et al.*, 1999
X. longipes	Xylaramide, **68** Tyrosol, **39** 2,5-Furandimethanol, **69** Piliformic acid, **70**	Antifungal	Schneider *et al.*, 1996
X. mellisii	Mellisol, **71** 1,8-Dihydroxynaphthol 1-*O*-α-glucopyranoside, **72** (-)-5-Carboxymellein, **73** Cytochalasin C, **74** Cytochalasin D, **48**	Anti-herpes simplex virus-type 1 and cytotoxicity	Pittayakhajon wut *et al.*, 2005
X. multiplex	Multiplolide A, **75** Multiplolide B, **76**	Antifungal	Boonphong *et al.*, 2001
X. obovata	19,20-Epoxycytochalasin Q, **61** Deacetyl 19,20-epoxycytochalasin Q, **77**	Cytotoxicity	Dagne *et al.*, 1994

Table 59 Continued

Scientific name	Compound	Activity	References
X. obovata	19,20-Epoxycytochalasin C, **55** 18-Deoxy-19,20-epoxycytochalasin Q, **60** 19,20-Epoxycytochalasin Q, **61** Cytochalasin Q, **62** Deacetyl 19,20-epoxycytochalasin Q, **77** Deacetyl 19,20-epoxycytochalasin C, **78** Xylobovide, **79** 4,6,10,12-Tridecatetraene-2,8-diol, **80** Clonostachydiol, **81** (+)-Phaseolinone, **82** (*E*)-Methyl-3-(4-methoxy-phenoxy)-propenoate, **83**	Cytotoxicity, antibiotic, anthelmintic and phytotoxic	Abate *et al.*, 1997
X. persicaria	Xylarenal A, **84** Xylarenal B, **85**	Affinity for mouse NPY receptors	Smith *et al.*, 2002
Xylaria sp.	Dihydromaldoxin, **86** Isodihydromaldoxin, **87** Dechlorodihydromaldoxin, **88** Maldoxone, **89** Maldoxin, **90**	-	Adeboya *et al.*, 1996a
	Xylarin, **91**	Antifungal	Schneider *et al.*, 1995
	Integric acid, **92**	Anti-HIV	Singh *et al.*, 1999

Table 59 Continued

Scientific name	Compound	Activity	References
Xylaria sp.	19,20-Epoxycytochalasin Q, **61**	CCR 5 antagonistic	Jayasuriya *et al.*, 2004
	2-Hydroxy-6-methyl-8-methoxy-9-oxo-9*H*-xanthene-1-carboxylic acid, **93** 2-Hydroxy-6-hydroxymethyl-8-methoxy-9-oxo-9*H*-xanthene-1-carboxylic acid, **94**	Antimicrobial	Healy *et al.*, 2004
	3-Chloro-4-hydroxyphenyl-acetamide, **95** 3-Chloro-4-hydroxyphenyl-acetic acid, **96**	-	Davis *et al.*, 2005a
	7-Hydroxy-3-(hydroxymethyl)-1-methoxy-9*H*-xanthen-9-one, **97** 2,5-Dihydroxy-8-methoxy-6-methyl-9-oxo-9*H*-xanthene -1-carboxylic acid, **98**	-	Davis *et al.*, 2006
	(-)-Xylariamide A, **99**	Toxicity	Davis 2005b
	Xyloallenolide A, **100** 3-[4-(2,3-Butadienyloxy)-phenyl]-2-propenoic acid, **101** Eucalyptene A methyl ester, **102**	-	Lin *et al.*, 2001a
	Xyloketal A, **103** Xyloketal B, **104** Xyloketal C, **105** Xyloketal D, **106**	Acetyl choline esterase inhibitor	Lin *et al.*, 2001b

Table 59 Continued

Scientific name	Compound	Activity	References
Xylaria sp.	Xyloketal E, **107** 1-(2,4-Dihydroxyphenyl)-ethanone, **108**		
	Ergosterol, **44** Piliformic acid, **70** (-)-5-Carboxymellein, **73** α-Glycerol monopalmitate, **109** *p*-Hydroxybenzoic acid, **110** Protocatechuic acid methyl ester, **111** 4-Hydroxy-2-methoxy-acetophenone, **112** Cerevisterol, **113**	- -	Wu *et al.*, 2002
	Xyloketal G, **114**	-	Wu *et al.*, 2005a
	Xyloketal F, **115**	L-calcium channel blocking	Wu *et al.*, 2005b
	Xyloketal H, **116**	-	Liu *et al.*, 2006a
	(3*S*)-7-Hydroxymellein, **117**	-	Liu *et al.*, 2006b
	Cytochalasin D, **48** 2-Hexyl-3-methylbutanedioic acid, **118** Griseofulvin, **119** 7-Dechlorogriseofulvin, **120** Cytochalasin B, **121**	Antifungal	Cafeu *et al.*, 2005

Table 59 Continued

Scientific name	Compound	Activity	References
	Piliformic acid, **70**	-	Liu *et al.*, 2006c
	Kolokoside A, **122** Kolokoside B, **123** Kolokoside C, **124** Kolokoside D, **125** 19,20-Epoxycytochalasin N, **56**	Antibacterial	Deyrup *et al.*, 2007
	19,20-Epoxycytochalasin Q, **61** (+)-Phaseolinone, **82** (-)-Depudecin, **126** (+)-Phomenone, **127** (*E*)-Methyl 3-(4-methoxyphenoxy)propenoate, **128**	Antiplasmodial	Isaka *et al.*, 2000
Xylaria spp.	Cameronic acid, **129** Malaysic acid, **130**	-	Adeboya *et al.*, 1995
X. telfairii	threo-Telfairic acid, **131** erythro-Telfairic acid, **132** 2,3-Didehydrotelfairic anhydride, **133**	-	Adeboya *et al.*, 1996b

Structures of the metabolites from *Xylaria* genus

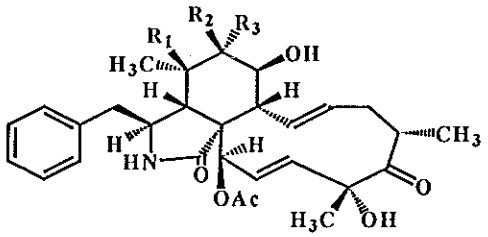

48: R_1 = H, R_2+R_3 = CH_2 : Cytochalasin D
74: R_1 = R_2 = double bond, R_3 = CH_3 : Cytochalasin C

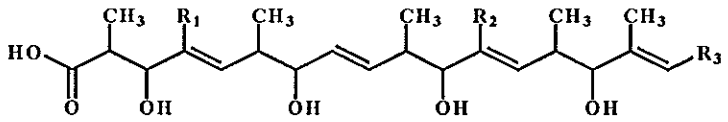

47: R_1 = H, R_2 = CH_3, R_3 = 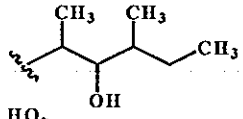 : Berteric acid

49: R_1 = CH_3, R_2 = H, R_3 = 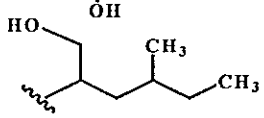 : Cubensic acid

129: R_1 = R_2 = H, R_3 = 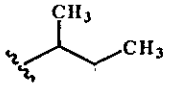 : Cameronic acid

130: R_1 = R_2 = H, R_3 = 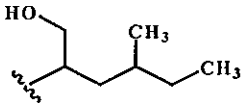 : Malaysic acid

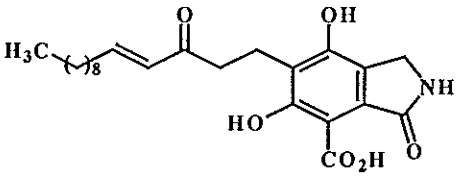

50: Xylactam

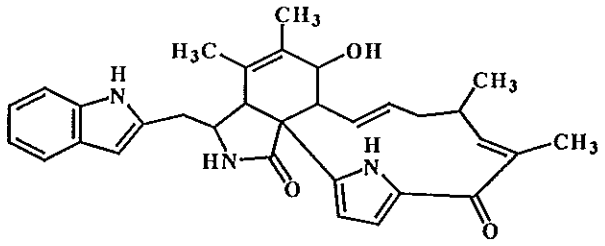

51: Penochalasin B

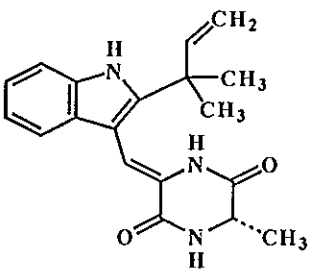

52: Neoechinulin A

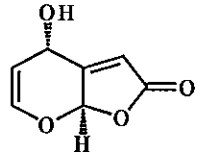

53: Grammicin

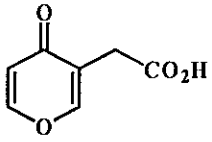

54: γ-Pyrone-3-acetic acid

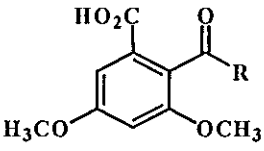

64: R = 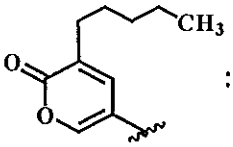 : Coloratin A

65: R = OCH_3 : Coloratin B

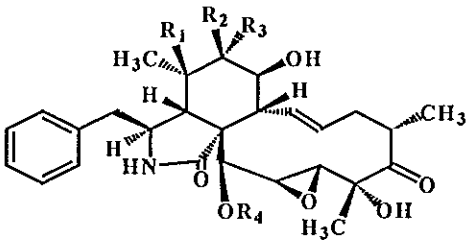

55: R_1 = R_2 = double bond, R_3 = CH_3, R_4 = Ac: 19,20-Epoxycytochalasin C
56: R_1 = R_2 = epoxide, R_3 = CH_3, R_4 = Ac: 19,20-Epoxycytochalasin N
57: R_1 = H, R_2+R_3 = CH_2, R_4 = Ac : 19,20-Epoxycytochalasin D
78: R_1 = R_2 = double bond, R_3 = CH_3, R_4 = H: Deacetyl 19,20-epoxycytochalasin C

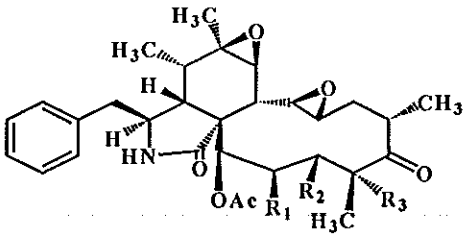

58: $R_1 = R_2$ = epoxide, R_3 = OH : 19,20-Epoxycytochalasin R
59: $R_1 = R_2$ = epoxide, R_3 = H : 18-Deoxy-19,20-epoxycytochalasin R
63: $R_1 = R_2$ = double bond, R_3 = OH : Cytochalasin R

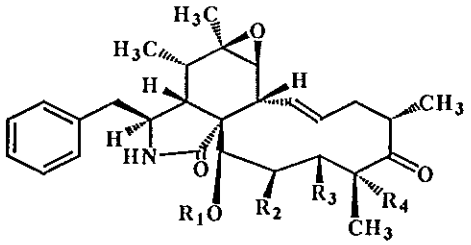

60: R_1 = Ac, $R_2 = R_3$ = epoxide, R_4 = H : 18-Deoxy-19,20-epoxycytochalasin Q
61: R_1 = Ac, $R_2 = R_3$ = epoxide, R_4 = OH : 19,20-Epoxycytochalasin Q
62: R_1 = Ac, $R_2 = R_3$ = double bond, R_4 = OH : Cytochalasin Q
77: R_1 = H, $R_2 = R_3$ = epoxide, R_4 = OH : Deacetyl 19,20-epoxycytochalasin Q

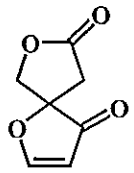

66: Longianone

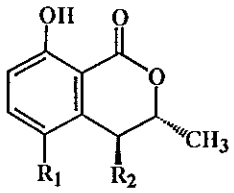

67: R_1 = H, R_2 = OH
: *trans*-(-)-4-Hydroxymellein
73: $R_1 = CO_2H$, R_2 = H
: (-)-5-Carboxymellein

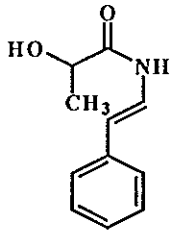

68: Xylaramide

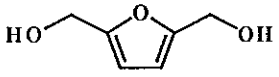

69: 2,5-Furandimethanol

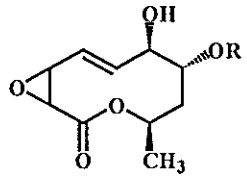

75: R = H: Multiplolide A
76: R = 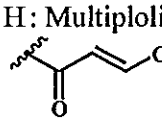 : Multiplolide B

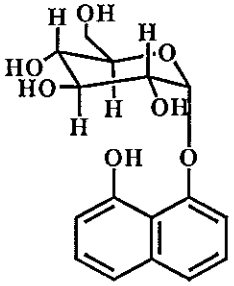

72: 1,8-Dihydroxynaphthol
1-*O*-α-glucopyranoside

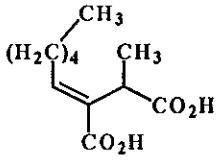

70: Piliformic acid

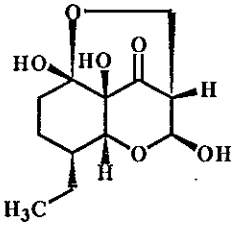

71: Mellisol

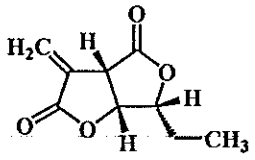

79: Xylobovide

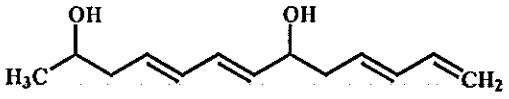

80: 4,6,10,12-Tridecatetraene-2,8-diol

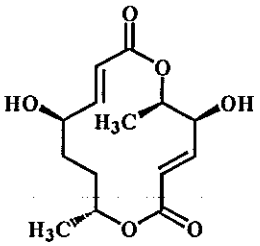

81: Clonostachydiol

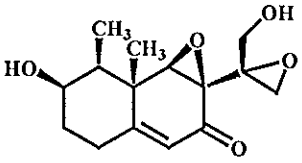

82: (+)-Phaseolinone

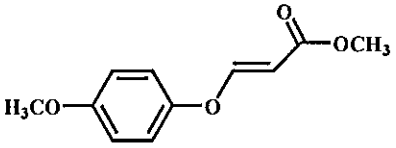

83: (*E*)-methyl-3-(4-methoxy-phenoxy)-propenoate

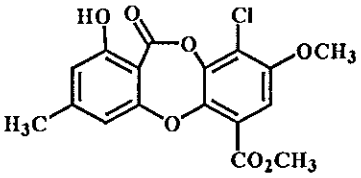

89: Maldoxone

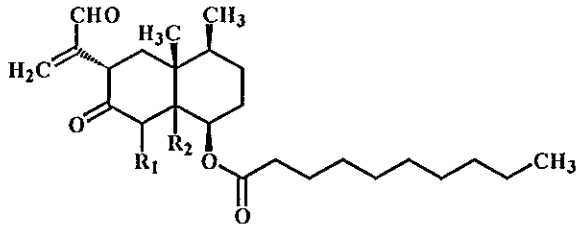

84: $R_1 = R_2$ = double bond : Xylarenal A
85: $R_1 = R_2$ = epoxide : Xylarenal B

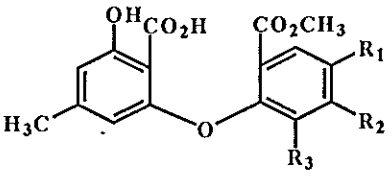

86: $R_1 = OCH_3$, $R_2 = Cl$, $R_3 = OH$:Dihydromaldoxin
87: $R_1 = OH$, $R_2 = Cl$, $R_3 = OCH_3$:Isodihydromaldoxin
88: $R_1 = OCH_3$, $R_2 = H$, $R_3 = OH$:Dechlorodihydromaldoxin

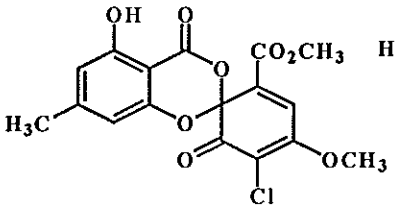

90: Maldoxin

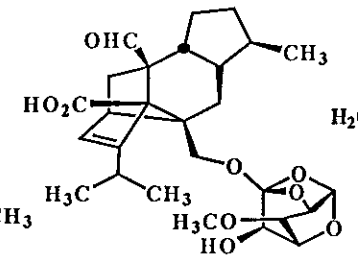

91: Xylarin

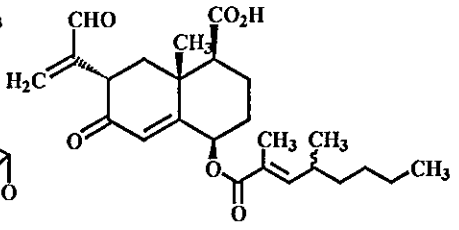

92: Integric acid

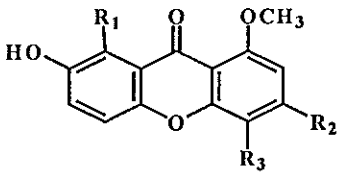

93: $R_1 = CO_2H$, $R_2 = CH_3$, $R_3 = H$: 2-Hydroxy-6-methyl-8-methoxy-9-oxo-9*H*-xanthene-1-carboxylic acid

94: $R_1 = CO_2H$, $R_2 = CH_2OH$, $R_3 = H$: 2-Hydroxy-6-hydroxymethyl-8-methoxy-9-oxo-9*H*-xanthene-1-carboxylic acid

97: $R_1 = R_3 = H$, $R_2 = CH_2OH$: 7-Hydroxy-3-(hydroxymethyl)-1-methoxy-9*H*-xanthen-9-one

98: $R_1 = CO_2H$, $R_2 = CH_3$, $R_3 = OH$: 2,5-Dihydroxy-8-methoxy-6-methyl-9-oxo-9*H*-xanthene-1-carboxylic acid

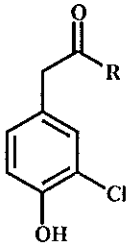

95: R = NH_2 : 3-Chloro-4-hydroxyphenylacetamide

96: R = OH : 3-Chloro-4-hydroxyphenylacetic acid

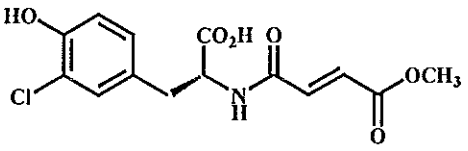

99: (-)-Xylariamide A

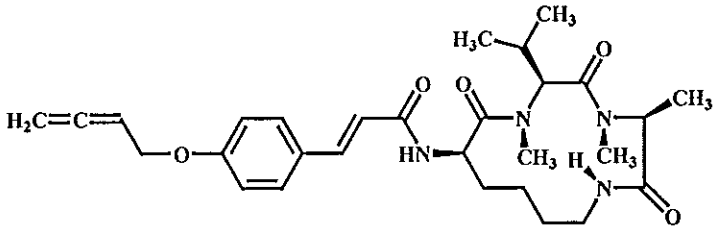

100: Xyloallenolide A

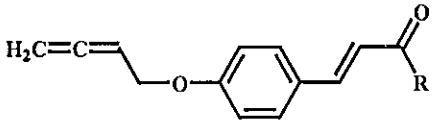

101: R = OH : 3-[4-(2,3-Butadienyloxy)phenyl]-2-propenoic acid

102: R = OCH_3 : Eucalyptene A methyl ester

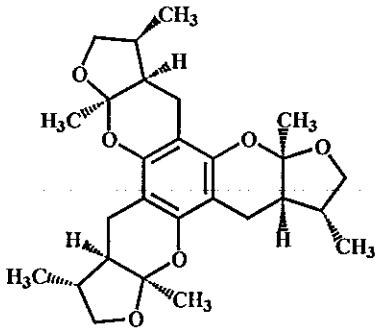

103: Xyloketal A

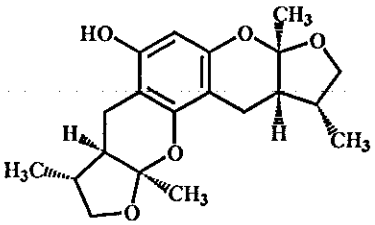

104: Xyloketal B

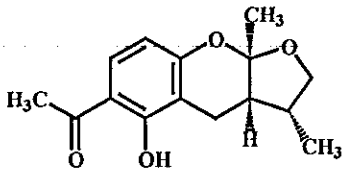

106: Xyloketal D

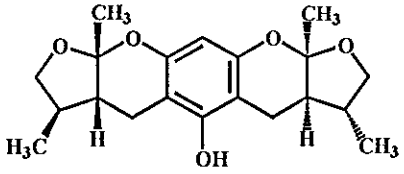

105: Xyloketal C

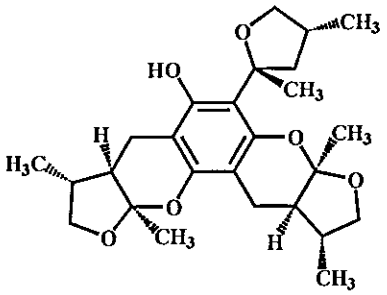

107: Xyloketal E

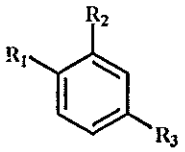

108: R_1 = Ac, R_2 = R_3 = OH : 1-(2,4-Dihydroxyphenyl)ethanone
110: R_1 = CO_2H, R_2 = H, R_3 = OH : *p*-Hydroxybenzoic acid
111: R_1 = R_2 = OH, R_3 = CO_2CH_3 : Protacatechuic acid methyl ester
112: R_1 = Ac, R_2 = OCH_3, R_3 = OH : 4-Hydroxy-2-methoxyacetophenone

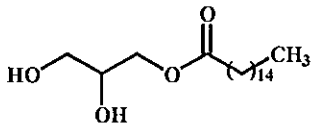

109: α-Glycerol monopalmitate

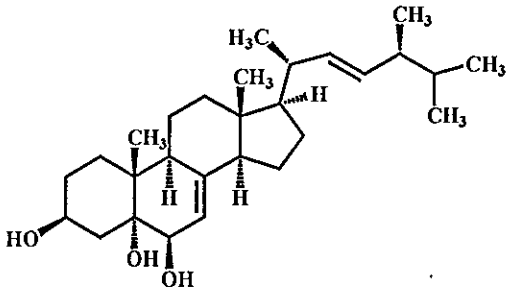

113: Cerevisterol

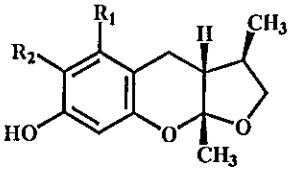

114: R_1 = H, R_2 = Ac : Xyloketal G
116: R_1 = OH, R_2 = H : Xyloketal H

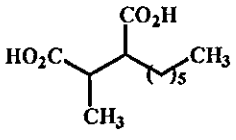

118: 2-Hexyl-3-methylbutanedioic acid

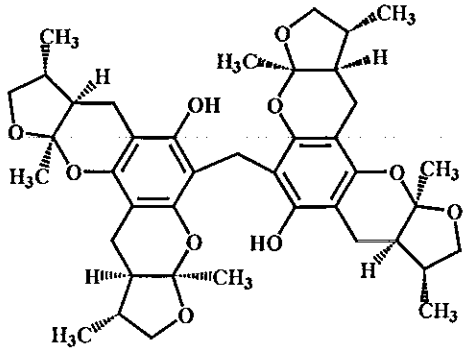

115: Xyloketal F

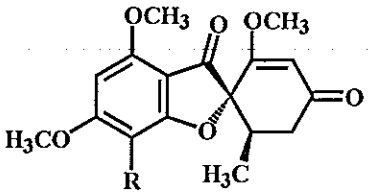

119: R = Cl : Griseofulvin

120: R = H : 7-Dechlorogriseofulvin

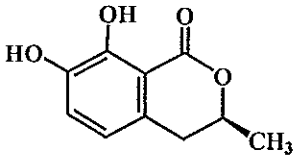

117: (3*S*)-7-Hydroxymellein

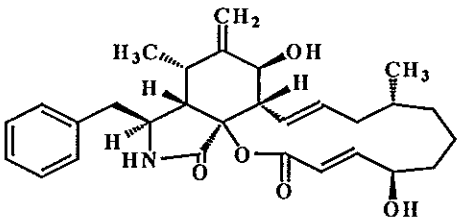

121: Cytochalasin B

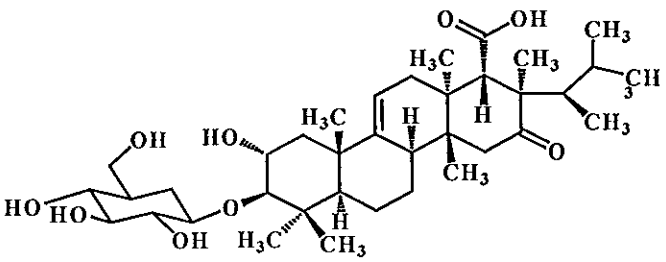

122: Kolokoside A

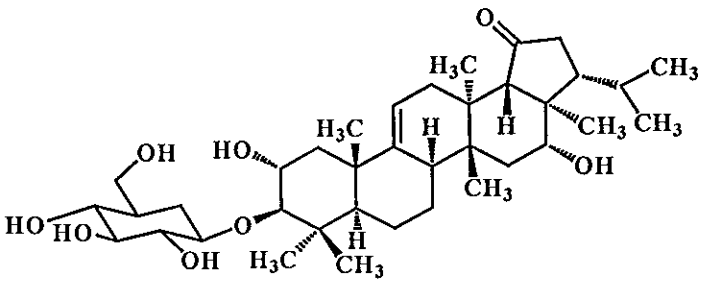

123: Kolokoside B

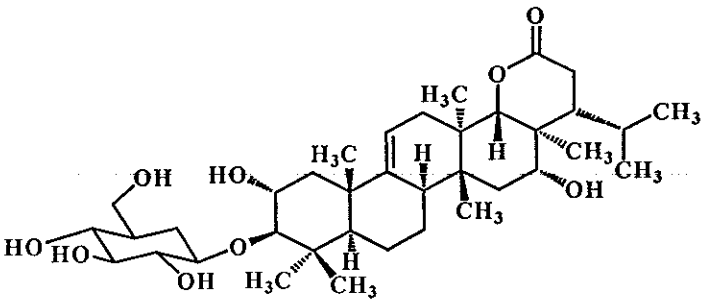

124: Kolokoside C

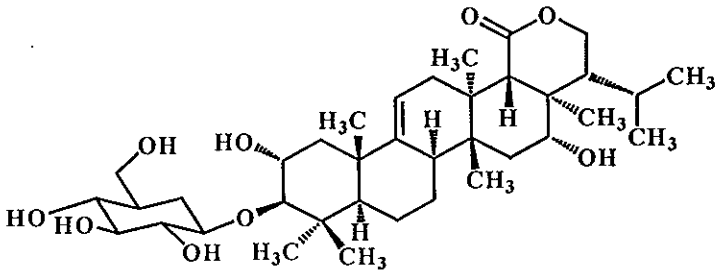

125: Kolokoside D

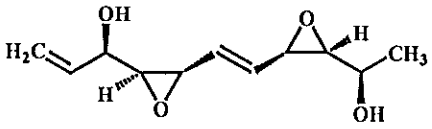

126: (-)-Depudecin

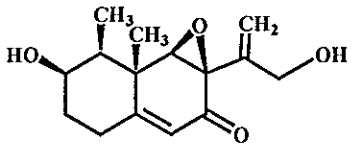

127: (+)-Phomenone

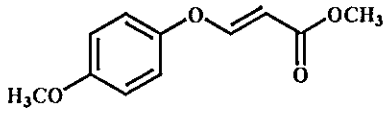

128: (*E*)-Methyl 3-(4-methoxyphenoxy)propenoate

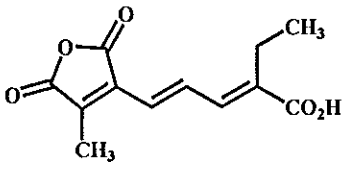

133: 2,3-Didehydrotelfairic anhydride

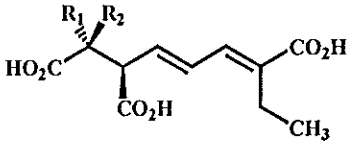

131: $R_1 = CH_3$, $R_2 = H$: threo-Telfairic acid
132: $R_1 = H$, $R_2 = CH_3$: erythro-Telfairic

CHAPTER 4.2
EXPERIMENTAL

4.2.1 Fermentation and extraction

The fermentation and extraction was performed using the same procedure as those of *Lachnum* sp. BCC 2424. The crude EtOAc extracts from the culture broth and mycelia were obtained in 560.0 mg and 522.1 mg, respectively, both as a brown gum.

4.2.2 Purification of the broth extract

The broth extract was further separated by column chromatography over Sephadex LH20 using 100% MeOH as eluent. All fractions were examined by TLC, combined on the basis of their chromatogram characteristics and then evaporated to dryness under reduced pressure to afford five fractions, as shown in **Table 60**.

Table 60 Fractions obtained from **the broth extract** by column chromatography over Sephadex LH20

Fraction	Eluent	Weight (mg)	Physical appearance
A	100% MeOH	16.9	Brown gum mixed with brown solid
B	100% MeOH	405.0	Brown solid
C	100% MeOH	98.6	Brown solid
D	100% MeOH	34.4	Pale-brown solid
E	100% MeOH	4.0	Dark-brown gum

Fraction A showed no definite spots under UV-S on normal phase TLC using 100% dichloromethane as a mobile phase (2 runs). Its ^{1}H NMR spectrum displayed proton signals at high field region. Therefore, it was not further investigated.

Fraction B showed five spots under UV-S on normal phase TLC with the R_f values of 0.08, 0.10, 0.35, 0.58 and 0.73 using 100% dichloromethane as a mobile phase (2 runs) with. Further separation by column chromatography over silica gel using a gradient system of methanol-dichloromethane was performed. All subfractions were examined by TLC, combined on the basis of their chromatogram characteristics and then evaporated to dryness under reduced pressure to afford six subfractions, as shown in **Table 61.**

Table 61 Subfractions obtained from **fraction B** by column chromatography over silica gel

Subfraction	Eluent	Weight (mg)	Physical appearance
B1	100% CH_2Cl_2 - 7% MeOH/CH_2Cl_2	7.3	Yellow gum
B2	7-20% MeOH/CH_2Cl_2	188.1	Yellow gum mixed with yellow solid
B3	30-50% MeOH/CH_2Cl_2	31.2	Yellow gum
B4	70% MeOH/CH_2Cl_2	56.5	Yellow gum mixed with yellow solid
B5	70-80% MeOH/CH_2Cl_2	74.4	Brown-yellow gum
B6	100% MeOH	6.8	Brown gum

Subfraction B1 displayed no definite spots under UV-S on normal phase TLC using 100% dichloromethane as a mobile phase. According to the appearance of proton signals at high field, it was not further studied.

Subfraction B2 contained five major spots under UV-S on normal phase TLC with the R_f values of 0.50, 0.58, 0.68, 0.83 and 0.92 using 100% dichloromethane as a mobile phase (2 runs). Further separation by column chromatography over silica gel using a gradient system of methanol-dichloromethane was performed. Subfractions, which contained similar components, were combined and evaporated to dryness under reduced pressure to give five subfractions, as shown in **Table 62.**

Table 62 Subfractions obtained from **subfraction B2** by column chromatography over silica gel

Subfraction	Eluent	Weight (mg)	Physical appearance
B2-1	100% CH_2Cl_2 - 5% MeOH/CH_2Cl_2	1.0	Yellow gum
B2-2	5% MeOH/CH_2Cl_2	1.8	Yellow gum
B2-3	5-20% MeOH/CH_2Cl_2	116.2	Pale-yellow gum mixed with yellow solid
B2-4	20% MeOH/CH_2Cl_2	60.5	Pale-yellow gum mixed with yellow solid
B2-5	30% MeOH/CH_2Cl_2 - 100% MeOH	3.0	Yellow gum

Subfraction B2-1 showed no spots under UV-S on normal phase TLC using 100% dichloromethane as a mobile phase. Because of low quantity, it was not further purified.

Subfraction B2-2 (N21) displayed one UV-active spot on normal phase TLC with the R_f value of 0.40 using 100% dichloromethane as a mobile phase.

$[\alpha]_D^{27}$ -232.73 (c = 0.50, $CHCl_3$)

UV(MeOH) λ_{max} nm (log ε) 243 (3.18), 306 (2.99)

FT-IR (neat) ν_{cm-1}	1730 (C=O stretching), 1599 (C=C stretching)
^{1}H NMR ($CDCl_3$) (δ ppm) (300 MHz)	7.45 (*dd*, J = 8.7, 7.2 Hz, 1H), 6.92 (*d*, J = 8.7 Hz, 1H), 6.79 (*d*, J = 7.2 Hz, 1H), 4.56 (*qt*, J = 6.3, 4.2 Hz, 1H), 3.95 (*s*, 3H), 2.87 (*d*, J = 4.2 Hz, 2H), 1.48 (*d*, J = 6.3 Hz, 3H)
^{13}C NMR ($CDCl_3$) (δ ppm) (75 MHz)	162.57, 161.26, 141.95, 134.39, 119.17, 113.93, 110.91, 74.08, 56.17, 36.11, 20.69
DEPT (135°) ($CDCl_3$)	CH : 134.39, 119.17, 110.91, 74.08 CH_2 : 36.11 CH_3 : 56.17, 20.69

Subfraction B2-3 demonstrated two UV-active spots on normal phase TLC with the R_f values of 0.40 and 0.53 using 1% methanol in dichloromethane (3 runs) as a mobile phase. Further separation by column chromatography over silica gel using a gradient system of methanol-dichloromethane was performed. Subfractions, which contained similar components, were combined and evaporated to dryness under reduced pressure to give five subfractions, as shown in **Table 63.**

Table 63 Subfractions obtained from **subfraction B2-3** by column chromatography over silica gel

Subfraction	Eluent	Weight (mg)	Physical appearance
B2-3-1	100% CH_2Cl_2 - 3% MeOH/CH_2Cl_2	2.0	Yellow gum
B2-3-2	3% MeOH/CH_2Cl_2	58.5	Yellow gum
B2-3-3	3-5% MeOH/CH_2Cl_2	31.5	White solid
B2-3-4	5% MeOH/CH_2Cl_2	5.3	Yellow gum
B2-3-5	5-10% MeOH/CH_2Cl_2 - 100% MeOH	7.0	Yellow gum

Subfraction B2-3-1 displayed no spots under UV-S on normal phase TLC using 100% dichloromethane as a mobile phase. According to the appearance of proton signals at high field, it was not further investigated.

Subfraction B2-3-2 showed two UV-active spots on normal phase TLC with the R_f values of 0.55 and 0.70 using 4% methanol in dichloromethane as a mobile phase (2 runs). It was further separated by column chromatography over Sephadex LH20 using 100% MeOH as eluent. All subfractions were examined by TLC, combined on the basis of their chromatogram characteristics and then evaporated to dryness under reduced pressure to afford four subfractions, as shown in **Table 64.**

Table 64 Subfractions obtained from **subfraction B2-3-2** by column chromatography over Sephadex LH20

Subfraction	Eluent	Weight (mg)	Physical appearance
B2-3-21	100% MeOH	0.3	Colorless gum
B2-3-22	100% MeOH	10.3	White solid
B2-3-23	100% MeOH	45.7	White solid
B2-3-24	100% MeOH	0.5	Colorless gum

Subfraction B2-3-21 showed no UV-active spots on normal phase TLC using 2% methanol in dichloromethane as a mobile phase (3 runs). Because of low quantity, it was not further investigated.

Subfraction B2-3-22 (N22) melted at 267.0-267.3 °C and displayed one UV-active spot on normal phase TLC with the R_f value of 0.28 using 2% methanol in dichloromethane as a mobile phase (3 runs).

$[\alpha]_D^{27}$ -31.05 (c = 0.33, $CHCl_3$)

UV(MeOH) λ_{max} nm (log ε) 237 (3.45)

FT-IR (neat) ν_{cm-1}	3400 (O-H stretching), 1738, 1695 and 1638 (C=O stretching), 1606 (C=C stretching)
^{1}H NMR ($CDCl_3$) (δ ppm) (300 MHz)	7.32 (*td*, J = 8.1, 1.5 Hz, 1H), 7.27 (*m*, 2H), 7.13 (*dd*, J = 8.1, 1.5 Hz, 2H), 6.10 (*dd*, J = 15.6, 2.4 Hz, 1H), 5.69 (*dd*, J = 15.6, 9.9 Hz, 1H), 5.63 (*t*, J = 2.4 Hz, 1H), 5.60 (*brs*, 1H), 5.34 (*ddd*, J = 15.6, 10.5, 4.8 Hz, 1H), 5.30 (*brs*, 1H), 5.14 (*dd*, J = 15.6, 2.4 Hz, 1H), 5.09 (*brs*, 1H), 3.81 (*d*, J = 10.8 Hz, 1H), 3.24 (*m*, 1H), 2.85 (*m*, 1H), 2.83 (*m*, 1H), 2.75 (*m*, 1H), 2.74 (*m*, 1H), 2.68 (*m*, 1H), 2.51 (*dd*, J = 12.6, 10.5 Hz, 1H), 2.26 (*s*, 3H), 2.15 (*dd*, J = 6.6, 3.6 Hz, 1H), 2.02 (*dd*, J = 12.6, 4.8 Hz, 1H), 1.51 (*s*, 3H), 1.20 (*d*, J = 6.9 Hz, 3H), 0.94 (*d*, J = 6.6 Hz, 3H)
^{13}C NMR ($CDCl_3$) (δ ppm) (75 MHz)	210.27, 173.50, 169.68, 147.58, 137.23, 134.12, 132.30, 130.61, 129.09, 128.93, 127.63, 127.09, 114.43, 77.71, 77.12, 69.84, 53.57, 50.90, 50.00, 47.00, 45.29, 42.34, 37.75, 32.67, 24.18, 20.82, 19.37, 13.65
DEPT (135°) ($CDCl_3$)	CH : 134.12, 132.30, 130.61, 129.09, 128.93, 127.63, 127.09, 77.71, 69.84, 53.57, 50.00, 47.00, 42.34, 32.67
	CH_2 : 114.43, 45.29, 37.75
	CH_3 : 24.18, 20.82, 19.37, 13.65

Subfraction B2-3-23 demonstrated two UV-active spots on normal phase TLC with the R_f values of 0.28 and 0.45 using 2% methanol in dichloromethane (3 runs) as a mobile phase. Further separation by column chromatography over silica gel using a gradient system of methanol-dichloromethane was performed. Subfractions, which contained similar components, were combined and evaporated to dryness under reduced pressure to give four subfractions, as shown in **Table 65**.

Table 65 Subfractions obtained from **subfraction B2-3-23** by column chromatography over silica gel

Subfraction	Eluent	Weight (mg)	Physical appearance
B2-3-231	100% CH_2Cl_2 - 3% MeOH/CH_2Cl_2	0.3	Colorless gum
B2-3-232	3% MeOH/CH_2Cl_2	4.1	White solid
B2-3-233	3-5% MeOH/CH_2Cl_2	5.6	White solid
B2-3-234	5% MeOH/CH_2Cl_2	34.9	White solid

Subfraction B2-3-231 showed no UV-active spots on normal phase TLC using 2% methanol in dichloromethane as a mobile phase (2 runs). Because of low quantity, it was not further investigated.

Subfraction B2-3-232 (N23) melted at 259.7-260.5 °C and showed one UV-active spot on normal phase TLC with the R_f value of 0.65 using 2% methanol in dichloromethane as a mobile phase (4 runs).

$[\alpha]_D^{27}$	-38.20 (c = 0.80, MeOH)
UV(MeOH) λ_{max} nm (log ε)	237 (3.77)
FT-IR (neat) ν_{cm-1}	3393 (O-H stretching), 1736, 1698 and 1642 (C=O stretching), 1607 (C=C stretching)
^{1}H NMR ($CDCl_3$) (δ ppm) (300 MHz)	7.28 (*m*, 1H), 7.23 (*m*, 2H), 7.12 (*dd*, *J* = 6.6, 1.5 Hz, 2H), 6.03 (*dd*, *J* = 15.6, 2.4 Hz, 1H), 5.77 (*dd*, *J* = 15.6, 9.6 Hz, 1H), 5.74 (*t*, *J* = 2.4 Hz, 1H), 5.67 (*s*, 1H), 5.20 (*ddd*, *J* = 15.6, 10.8, 4.8 Hz, 1H), 5.07 (*dd*, *J* = 15.6, 2.4 Hz, 1H), 3.53 (*brt*, *J* = 8.4 Hz, 1H), 2.73 (*d*, *J* = 7.2 Hz, 2H), 2.67 (*d*, *J* = 5.7 Hz, 1H), 2.65 (*m*, 1H), 2.47 (*dd*, *J* = 9.9, 5.7 Hz, 1H), 2.40 (*m*, 1H), 2.18 (*s*, 3H), 2.05 (*dd*, *J* = 5.7, 2.4 Hz, 1H), 1.90 (*m*, 1H), 1.66

	(*m*, 1H), 1.45 (*s*, 3H), 1.14 (*d*, J = 6.6 Hz, 3H), 1.13 (*s*, 3H), 0.83 (*d*, J = 7.2 Hz, 3H)
^{13}C NMR ($CDCl_3$) (δ ppm) (75 MHz)	210.41, 174.53, 169.73, 136.97, 131.84, 131.80, 130.86, 129.16, 128.97, 127.68, 127.14, 77.76, 75.85, 62.54, 57.04, 55.09, 54.08, 50.65, 45.88, 45.15, 42.28, 37.92, 36.82, 24.23, 20.76, 19.58, 19.31, 12.55
DEPT (135°) ($CDCl_3$)	CH : 131.84, 131.80, 130.86, 129.16, 128.97, 127.68, 127.14, 75.85, 62.54, 54.08, 50.65, 45.15, 42.28, 36.82
	CH_2 : 45.88, 37.92
	CH_3 : 24.23, 20.76, 19.58, 19.31, 12.55

Subfraction B2-3-233 displayed two UV-active spots on normal phase TLC with the R_f values of 0.45 and 0.65 using 2% methanol in dichloromethane as a mobile phase (4 runs). Its ^{1}H NMR spectral data and chromatogram on normal phase TLC indicated that it was a mixture of **N22** and **N23**.

Subfraction B2-3-234 showed one major spot under UV-S on normal phase TLC with the R_f value of 0.45 using 2% methanol in dichloromethane as a mobile phase (4 runs). Its ^{1}H NMR data suggested that it was **N22**.

Subfraction B2-3-24 showed no definite spots under UV-S on normal phase TLC using 2% methanol in dichloromethane as a mobile phase (3 runs). Because of low quantity, it was not further purified.

Subfraction B2-3-3 showed one UV-active spot on normal phase TLC with the R_f value of 0.55 using 4% methanol in dichloromethane as a mobile phase (2 runs). Its ^{1}H NMR spectral data and chromatogram on normal phase TLC indicated that it was **N22**.

Subfraction B2-3-4 showed no definite spots under UV-S on normal phase TLC using 4% methanol in dichloromethane as a mobile phase (2 runs). According to the appearance of proton signals at high field, it was not further investigated.

Subfraction B2-3-5 displayed no spots under UV-S on normal phase TLC using 4% methanol in dichloromethane as a mobile phase (2 runs). Its ^{1}H NMR spectrum displayed none of major components. Thus, no attempted separation was performed.

Subfraction B2-4 demonstrated three UV-active spots on normal phase TLC with the R_f values of 0.30, 0.43 and 0.53 using 1% methanol in dichloromethane (3 runs) as a mobile phase. Further separation by column chromatography over silica gel using a gradient system of methanol-dichloromethane was performed. Fractions, which contained similar components, were combined and evaporated to dryness under reduced pressure to give three subfractions, as shown in **Table 66.**

Table 66 Subfractions obtained from **subfraction B2-4** by column chromatography over silica gel

Subfraction	Eluent	Weight (mg)	Physical appearance
B2-4-1	100% CH_2Cl_2 - 5% MeOH/CH_2Cl_2	1.9	Yellow gum
B2-4-2	5-10% MeOH/CH_2Cl_2	30.7	White solid
B2-4-3	20-70% MeOH/CH_2Cl_2	22.8	Yellow gum

Subfraction B2-4-1 displayed many spots under UV-S on normal phase TLC using 4% methanol in dichloromethane (4 runs) as a mobile phase. According to the appearance of proton signals at high field, it was not further studied.

Subfraction B2-4-2 showed one UV-active spot on normal phase TLC with the R_f value of 0.45 using 4% methanol in dichloromethane as a mobile phase (4 runs). Its ^1H NMR spectral data indicated that it was **N22.**

Subfraction B2-4-3 showed one major UV-active spot on normal phase TLC with the R_f value of 0.30 using 4% methanol in dichloromethane as a mobile phase (4 runs). It was further separated by column chromatography over Sephadex LH20 using 100% MeOH as eluent. All subfractions were examined by TLC, combined on the basis of their chromatogram characteristics and then evaporated to dryness under reduced pressure to afford four subfractions, as shown in **Table 67.**

Table 67 Subfractions obtained from **subfraction B2-4-3** by column chromatography over Sephadex LH20

Subfraction	Eluent	Weight (mg)	Physical appearance
B2-4-31	100% MeOH	0.5	Colorless gum
B2-4-32	100% MeOH	2.6	Colorless gum
B2-4-33	100% MeOH	14.8	Colorless gum
B2-4-34	100% MeOH	4.4	Pale-yellow gum

Subfraction B2-4-31 showed no UV-active spots on normal phase TLC using 2% methanol in dichloromethane (3 runs) as a mobile phase. Because of low quantity, it was not further investigated.

Subfraction B2-4-32 displayed one spot under UV-S on normal phase TLC with the R_f value of 0.53 using 2% methanol in dichloromethane (3 runs) as a mobile phase. When using 50% ethyl acetate in light petroleum (2 runs) as a mobile phase, the chromatogram showed two UV-active spots on normal phase TLC with the R_f values of 0.55 and 0.62. Further purification by precoated TLC with 50% ethyl acetate in light petroleum as a mobile phase (3 runs) afforded a colorless gum, **N24** (2.0 mg). Its chromatogram characteristic showed one UV-active spot on normal

phase TLC with the R_f value of 0.23 using 50% ethyl acetate in light petroleum as a mobile phase.

$[\alpha]_D^{27}$	+23.70 (c = 0.23, EtOH)
UV(MeOH) λ_{max} nm (log ε)	235 (3.38)
FT-IR (neat) ν_{cm-1}	3370 (O-H stretching), 1708 and 1638 (C=O stretching), 1607 (C=C stretching)
^{1}H NMR ($CDCl_3$) (δ ppm) (500 MHz)	7.31 (*t*, *J* = 7.0 Hz, 1H), 7.25 (*m*, 2H), 7.12 (*d*, *J* = 7.0 Hz, 2H), 6.21 (*dd*, *J* = 16.0, 2.5 Hz, 1H), 5.65 (*dd*, *J* = 15.0, 10.5 Hz, 1H), 5.45 (*brs*, 1H), 5.42 (*dd*, *J* = 16.0, 2.5 Hz, 1H), 5.31 (*s*, 1H), 5.27 (*ddd*, *J* = 15.0, 11.0, 5.5 Hz, 1H), 5.11 (*s*, 1H), 4.71 (*brs*, 1H), 4.07 (*brs*, 1H), 3.79 (*d*, *J* = 10.5 Hz, 1H), 3.29 (*ddd*, *J* = 8.5, 4.5, 4.0 Hz, 1H), 2.88 (*dd*, *J* = 14.0, 4.0 Hz, 1H), 2.84 (*t*, *J* = 10.5 Hz, 1H), 2.72 (*ddq*, *J* = 11.5, 2.0, 6.5 Hz, 1H), 2.57 (*m*, 1H), 2.56 (*m*, 1H), 2.48 (*ddd*, 13.0, 11.5, 11.0), 2.00 (*ddd*, *J* = 13.0, 5.5, 2.0 Hz, 1H), 1.90 (*m*, 1H), 1.54 (*s*, 3H), 1.19 (*d*, *J* = 6.5 Hz, 3H), 1.10 (*d*, *J* = 6.5 Hz, 1H),
^{13}C NMR ($CDCl_3$) (δ ppm) (125 MHz)	210.00, 175.00, 148.22, 137.32, 137.01, 133.67, 131.09, 129.19, 128.90, 127.16, 127.15, 113.99, 77.21, 76.52, 69.76, 54.32, 53.48, 50.22, 45.64, 45.39, 42.37, 37.72, 32.91, 24.24, 19.38, 13.81
DEPT (135°) ($CDCl_3$)	CH : 137.01, 133.67, 131.09, 129.19, 128.90, 127.16, 76.52, 69.76, 53.48, 50.22, 45.64, 42.37, 32.91
	CH_2 : 113.99, 45.39, 37.72
	CH_3 : 24.24, 19.38, 13.81

Subfraction B2-4-33 showed one UV-active spot on normal phase TLC with the R_f value of 0.28 using 2% methanol in dichloromethane as a mobile phase (3 runs). When using 50% ethyl acetate in light petroleum (2 runs) as a mobile phase, the chromatogram showed two UV-active spots on normal phase TLC with the

R_f values of 0.10 and 0.20. Further purification by precoated TLC with 50% ethyl acetate in light petroleum as a mobile phase (8 runs) afforded two bands.

Band 1 was obtained as a colorless gum (3.8 mg), which showed one spot under UV-S on normal phase TLC with the R_f value of 0.22 using 50% ethyl acetate in light petroleum as a mobile phase (2 runs). The ^{1}H NMR data suggested that it was a mixture. Because of low quantity, it was not further investigated.

Band 2 was obtained as a pale-yellow gum (7.3 mg), which showed one spot under UV-S on normal phase TLC with the R_f value of 0.15 using 50% ethyl acetate in light petroleum as a mobile phase (2 runs). The ^{1}H NMR data suggested that it was a mixture. Further separation by column chromatography over Sephadex LH20 using 100% MeOH as eluent was performed. Fractions, which contained similar components, were combined and evaporated to dryness under reduced pressure to give three subfractions, as shown in **Table 68.**

Table 68 Subfractions obtained from **subfraction B2-4-33 band 2** by column chromatography over Sephadex LH20

Subfraction	Eluent	Weight (mg)	Physical appearance
SB2-1	100% MeOH	1.2	Colorless gum
SB2-2	100% MeOH	4.5	Colorless gum
SB2-3	100% MeOH	1.3	Colorless gum

Subfraction SB2-1 displayed no definite spots under UV-S on normal phase TLC using 2% methanol in dichloromethane as a mobile phase (3 runs). According to the appearance of proton signals at high field, it was not further investigated.

Subfraction SB2-2 showed one spots under UV-S on normal phase TLC with the R_f value of 0.23 using 2% methanol in dichloromethane as a mobile phase (3

runs). Its ^{1}H NMR spectrum displayed none of major components. Thus, it was not further purified.

Subfraction SB2-3 displayed no definite spots under UV-S on normal phase TLC using 2% methanol in dichloromethane as a mobile phase (3 runs). Because of low quantity, it was not further investigated.

Subfraction B2-4-34 showed a long tail under UV-S on normal phase TLC using 2% methanol in dichloromethane as a mobile phase (3 runs). When using 50% ethyl acetate in light petroleum (2 runs) as a mobile phase, the chromatogram showed two UV-active spots on normal phase TLC with the R_f values of 0.20 and 0.33. Further purification by precoated TLC with 50% ethyl acetate in light petroleum as a mobile phase (8 runs) afforded two bands.

Band 1 was obtained as a colorless gum (1.6 mg), which showed one spot under UV-S on normal phase TLC with the R_f value of 0.20 using 50% ethyl acetate in light petroleum as a mobile phase (2 runs). The ^{1}H NMR data suggested that it was a mixture. Because of low quantity, it was not further investigated.

Band 2 was obtained as a yellow gum (2.1 mg), which showed one spot under UV-S on normal phase TLC with the R_f value of 0.13 using 50% ethyl acetate in light petroleum as a mobile phase (2 runs). The ^{1}H NMR data suggested that it was not pure. Because of low quantity, it was not further purified.

Subfraction B2-5 displayed a long tail on normal phase TLC using 2% methanol in dichloromethane (3 runs) as a mobile phase. Its ^{1}H NMR spectrum displayed none of major components. Thus, further investigation was not conducted.

Subfraction B3 showed two UV-active spots on normal phase TLC with the R_f values of 0.50 and 0.60 using 4% methanol in dichloromethane (2 runs), 6% methanol in dichloromethane (2 runs) and 10% methanol in dichloromethane as mobile phases. It was further separated by column chromatography over Sephadex

LH20 using 100% MeOH as eluent. Fractions, which contained similar components, were combined and evaporated to dryness under reduced pressure to give three subfractions, as shown in **Table 69.**

Table 69 Subfractions obtained from **subfraction B3** by column chromatography over Sephadex LH20

Subfraction	Eluent	Weight (mg)	Physical appearance
B3-1	100% MeOH	13.0	Yellow gum
B3-2	100% MeOH	16.3	Yellow gum mixed with yellow solid
B3-3	100% MeOH	1.5	Yellow gum

Subfraction B3-1 showed two UV-active spots on normal phase TLC with the R_f values of 0.40 and 0.48 using 4% methanol in dichloromethane (5 runs) as a mobile phase and demonstrated many spots after dipping the normal phase TLC in ASA reagent and subsequently heating. The ^1H NMR data indicated that it was a mixture of **N22, N23** and other components. Therefore, it was not further purified.

Subfraction B3-2 showed a long tail under UV-S on normal phase TLC using 4% methanol in dichloromethane as a mobile phase (5 runs). When using 50% ethyl acetate in light petroleum (6 runs) as a mobile phase, the chromatogram showed five UV-active spots on normal phase TLC with the R_f values of 0.25, 0.38, 0.50, 0.63 and 0.73. Further separation by column chromatography over silica gel using gradient systems of ethyl acetate in light petroleum follow by methanol in ethyl acetate was performed. Fractions, which contained similar components, were combined and evaporated to dryness under reduced pressure to give four subfractions, as shown in **Table 70.**

Table 70 Subfractions obtained from **subfraction B3-2** by column chromatography over silica gel

Subfraction	Eluent	Weight (mg)	Physical appearance
B3-2-1	30-70% EtOAc/Light petroleum	2.2	Pale-yellow gum
B3-2-2	100% EtOAc - 5% MeOH/EtOAc	2.9	Yellow gum
B3-2-3	5-50% MeOH/EtOAc	6.4	Yellow gum
B3-2-4	70% MeOH/EtOAc - 100% MeOH	3.7	Yellow gum

Subfraction B3-2-1 displayed many inseparable spots under UV-S on normal phase TLC using 60% ethyl acetate in light petroleum (4 runs) as a mobile phase. According to the appearance of proton signals at high field, it was not further investigated.

Subfraction B3-2-2 showed two spots after dipping the normal phase TLC in ASA reagent and subsequently heating with the R_f values of 0.23 and 0.30 using 60% ethyl acetate in light petroleum (4 runs) as a mobile phase. Its ^1H NMR spectrum displayed none of major components. Thus, no attempted separation was conducted.

Subfraction B3-2-3 displayed many spots under UV-S on normal phase TLC using 60% ethyl acetate in light petroleum (4 runs) as a mobile phase. Further separation by column chromatography over Sephadex LH20 using 100% MeOH as eluent was performed. Fractions, which contained similar components, were combined and evaporated to dryness under reduced pressure to give three subfractions, as shown in **Table 71**.

Table 71 Subfractions obtained from **subfraction B3-2-3** by column chromatography over Sephadex LH20

Subfraction	Eluent	Weight (mg)	Physical appearance
B3-2-31	100% MeOH	2.4	Colorless gum
B3-2-32	100% MeOH	2.7	Pale-yellow gum
B3-2-33	100% MeOH	0.9	Pale-yellow gum

Subfraction B3-2-31 displayed no UV-active spots and showed no spots after dipping the normal phase TLC in ASA reagent and subsequently heating using 6% methanol in dichloromethane (2 runs) as a mobile phase. Its ^{1}H NMR spectrum showed none of aromatic proton signals. Therefore, it was not further investigated.

Subfraction B3-2-32 showed many spots under UV-S on normal phase TLC using 6% methanol in dichloromethane (2 runs) as a mobile phase. The ^{1}H NMR data suggested that it was a mixture. Therefore, it was not further purified.

Subfraction B3-2-33 displayed no UV-active spots on normal phase TLC using 6% methanol in dichloromethane (2 runs) as a mobile phase. Its ^{1}H NMR spectrum showed none of major components. Thus, no attempted investigation was conducted.

Subfraction B3-2-4 displayed no UV-active spots on normal phase TLC using 60% ethyl acetate in light petroleum (4 runs) as a mobile phase. Its ^{1}H NMR spectrum displayed none of major components. Therefore, further investigation was not performed.

Subfraction B3-3 showed no definite spots under UV-S on normal phase TLC using 4% methanol in dichloromethane as a mobile phase (5 runs). Therefore, it was not further investigated.

Subfraction B4 showed three UV-active spots on normal phase TLC with the R_f values of 0.38, 0.48 and 0.55 using 4% methanol in dichloromethane (2 runs), 6% methanol in dichloromethane (2 runs) and 10% methanol in dichloromethane as mobile phases. It was further separated by column chromatography over Sephadex LH20 using 100% MeOH as eluent. Fractions, which contained similar components, were combined and evaporated to dryness under reduced pressure to give three subfractions, as shown in **Table 72.**

Table 72 Subfractions obtained from **subfraction B4** by column chromatography over Sephadex LH20

Subfraction	Eluent	Weight (mg)	Physical appearance
B4-1	100% MeOH	7.2	Yellow gum
B4-2	100% MeOH	35.3	Yellow gum
B4-3	100% MeOH	13.0	Yellow gum

Subfraction B4-1 showed one major UV-active spot on normal phase TLC with the R_f value of 0.45 using 6% methanol in dichloromethane (4 runs) as a mobile phase. Its ^{1}H NMR spectrum displayed proton signals at high field region. Thus, no attempted investigation was carried out.

Subfraction B4-2 showed many inseparable UV-active spots on normal phase TLC using 6% methanol in dichloromethane (4 runs) as a mobile phase. Its ^{1}H NMR spectrum demonstrated none of major components. Thus, no attempted separation was performed.

Subfraction B4-3 displayed a long tail under UV-S on normal phase TLC using 6% methanol in dichloromethane (4 runs) as a mobile phase. Its ^{1}H NMR spectrum displayed none of aromatic proton signals. Thus, further purification was not conducted.

Subfraction B5 showed a long tails under UV-S on normal phase TLC using 4% methanol in dichloromethane (2 runs), 6% methanol in dichloromethane (2 runs) and 10% methanol as mobile phases and displayed four UV-active spots on reverse phase TLC with the R_f values of 0.05, 0.13, 0.53 and 0.70 using 50% methanol in water (3 runs) as a mobile phase. Further separation by column chromatography over reverse phase silica gel was performed. Elution was conducted initially with 50% methanol in water and gradually enriched with methanol until pure methanol. Subfractions, which contained similar components, were combined and evaporated to dryness under reduced pressure to give four subfractions, as shown in **Table 73.**

Table 73 Subfractions obtained from **subfraction B5** by column chromatography over reverse phase silica gel

Subfraction	Eluent	Weight (mg)	Physical appearance
B5-1	50% MeOH/H_2O	19.2	Yellow gum
B5-2	50% MeOH/H_2O	17.0	Yellow gum
B5-3	50-70% MeOH/H_2O	18.7	Yellow gum
B5-4	70% MeOH/H_2O - 100% MeOH	14.8	Yellow gum

Subfraction B5-1 showed two minor spots under UV-S on normal phase TLC with the R_f values of 0.08 and 0.18 using 5% methanol in dichloromethane (2 runs) and 8% methanol in dichloromethane (2 runs) as mobile phases and displayed no UV-active spots on reverse phase TLC using 50% methanol in water as a mobile phase. The ^1H NMR spectrum displayed none of major components. Therefore, further investigation was not conducted.

Subfraction B5-2 showed no spots under UV-S on normal phase TLC using 5% methanol in dichloromethane (2 runs) and 8% methanol in dichloromethane (2 runs) as mobile phases and displayed a long tail under UV-S on reverse phase TLC

using 50% methanol in water as a mobile phase. The ^{1}H NMR spectrum showed none of major components. Thus, further separation was not carried out.

Subfraction B5-3 contained four UV-active spots on normal phase TLC with the R_f values of 0.08, 0.18, 0.38 and 0.50 using 5% methanol in dichloromethane (2 runs) and 8% methanol in dichloromethane (2 runs) as mobile phases. The ^{1}H NMR spectrum displayed none of major signals. Thus, further separation was not investigated.

Subfraction B5-4 demonstrated a long tail on normal phase TLC using 5% methanol in dichloromethane (2 runs) and 8% methanol in dichloromethane (2 runs) as mobile phases. The ^{1}H NMR data suggested none of major components. Thus, no further investigation was pursued.

Subfraction B6 showed no definite spots on normal phase TLC using 4% methanol in dichloromethane (2 runs), 6% methanol in dichloromethane (2 runs) and 10% methanol in dichloromethane as mobile phases. The ^{1}H NMR spectrum showed none of major components. Therefore, it was not further investigated.

Fraction C contained eight spots under UV-S on normal phase TLC with the R_f values of 0.08, 0.10, 0.20, 0.42, 0.58, 0.70, 0.88 and 0.95 using 100% dichloromethane as a mobile phase. Further separation by column chromatography over silica gel using a gradient system of methanol-dichloromethane was performed. Fractions, which contained similar components, were combined and evaporated to dryness under reduced pressure to give nine subfractions, as shown in **Table 74.**

Table 74 Subfractions obtained from **fraction C** by column chromatography over silica gel

Subfraction	Eluent	Weight (mg)	Physical appearance
C1	100% CH_2Cl_2	2.9	Colorless gum
C2	100% CH_2Cl_2	1.2	Yellow solid
C3	2-6% MeOH/CH_2Cl_2	3.5	Yellow solid
C4	10% MeOH/CH_2Cl_2	11.9	Yellow gum
C5	10-15% MeOH/CH_2Cl_2	7.0	Yellow gum
C6	15-30% MeOH/CH_2Cl_2	10.0	Yellow gum
C7	30% MeOH/CH_2Cl_2	9.6	Yellow gum
C8	30-70% MeOH/CH_2Cl_2	37.5	Brown-yellow gum
C9	70% MeOH/CH_2Cl_2 - 100% MeOH	3.7	Brown gum

Subfraction C1 demonstrated no UV-active spots on normal phase TLC using 100% dichloromethane as a mobile phase. Its ^{1}H NMR spectrum displayed proton signals at high field region. Thus, no attempted investigation was carried out.

Subfraction C2 (N25) melted at 102.5-102.9 °C. Its chromatogram displayed one UV-active spot on normal phase TLC with the R_f value of 0.45 using 100% dichloromethane as a mobile phase.

UV(MeOH) λ_{max} nm (log ε)	214 (3.07), 229 (3.05), 240 (2.93), 265 (2.65), 314 (2.54), 327 (2.44)
FT-IR (neat) ν_{cm-1}	1608 and 1579 (C=C stretching)
^{1}H NMR ($CDCl_3$) (δ ppm) (500 MHz)	9.06 (*d*, J = 4.5 Hz, 1H), 8.23 (*dd*, J = 8.5, 1.0 Hz, 1H), 8.22 (*dd*, J = 8.5, 1.0 Hz, 1H), 7.89 (*td*, J = 8.5, 1.0 Hz, 1H), 7.79 (*td*, J = 8.5, 1.0 Hz, 1H), 7.75 (*d*, J = 4.5 Hz, 1H)

^{13}C NMR ($CDCl_3$) (δ ppm)		149.42, 148.20, 131.17, 130.45, 129.21, 125.06,
(125 MHz)		124.98, 124.79, 118.80, 115.50
DEPT (135°) ($CDCl_3$)	CH :	149.42, 131.17, 130.45, 129.21, 124.98, 124.79

Subfraction C3 showed no spots under UV-S on normal phase TLC using 100% dichloromethane (2 runs) as a mobile phase. Its ^{1}H NMR spectrum displayed proton signals at high field region. Thus, further purification was not performed.

Subfraction C4 displayed three spots under UV-S on normal phase TLC with the R_f values of 0.13, 0.25 and 0.38 using 3% methanol in dichloromethane (2 runs) as a mobile phase. When using 60% ethyl acetate in light petroleum (2 runs) as a mobile phase, the chromatogram showed five UV-active spots on normal phase TLC with the R_f values of 0.10, 0.15, 0.20, 0.33 and 0.53. Further purification by precoated TLC using 50% ethyl acetate in light petroleum (3 runs) as a mobile phase afforded five bands.

Band 1 was obtained as a colorless gum (1.0 mg), which showed one spot under UV-S on normal phase TLC with the R_f value of 0.48 using 50% ethyl acetate in light petroleum as a mobile phase. The ^{1}H NMR data suggested that it was a mixture. Because of low quantity, it was not further separated.

Band 2 (N26) was obtained as a colorless gum (4.6 mg), which showed one spot under UV-S on normal phase TLC with the R_f value of 0.28 using 50% ethyl acetate in light petroleum as a mobile phase.

$[\alpha]_D^{27}$	-19.17 (c = 0.90, $CHCl_3$)
UV(MeOH) λ_{max} nm (log ε)	223 (4.81), 251 (4.35), 334 (4.02)
FT-IR (neat) ν_{cm-1}	3371 (O-H stretching), 1686 (C=O stretching), 1618 (C=C stretching)
^{1}H NMR ($CDCl_3$) (δ ppm) (500 MHz)	7.81 (*d*, *J* = 8.1 Hz, 1H), 6.56 (*d*, *J* = 1.5 Hz, 1H), 6.52 (*dd*, *J* = 8.1, 1.5 Hz, 1H), 3.86 (*s*, 3H), 3.62

		(*dd*, *J* = 10.5, 2.4 Hz, 1H), 2.80 (*dd*, *J* = 13.5, 2.4 Hz, 1H), 2.50 (*dd*, *J* = 13.5, 10.5 Hz, 1H), 1.29 (*s*, 3H), 1.26 (*s*, 3H)
^{13}C NMR ($CDCl_3$) (δ ppm) (125 MHz)		168.10, 150.61, 145.71, 131.70, 117.40, 117.15, 109.50, 78.62, 72.64, 51.46, 38.35, 26.45, 23.82
DEPT (135°) ($CDCl_3$)	CH :	131.70, 117.40, 117.15, 78.62
	CH_2 :	38.35
	CH_3 :	51.46, 26.45, 23.82
EIMS *m/z* (% relative intensity):		253 (67), 195 (56), 163 (57), 135 (100), 120 (49), 100 (63)

Band 3 was obtained as a yellow gum (0.6 mg), which showed one spot under UV-S on normal phase TLC with the R_f value of 0.18 using 50% ethyl acetate in light petroleum as a mobile phase. The ^{1}H NMR data suggested that it was a mixture. Because of low quantity, it was not further investigated.

Band 4 was obtained as a yellow gum (0.8 mg), which showed one spot under UV-S on normal phase TLC with the R_f value of 0.13 using 50% ethyl acetate in light petroleum as a mobile phase. The ^{1}H NMR data suggested that it was not pure. Therefore, it was not further purified.

Band 5 was obtained as a pale-yellow gum (4.1 mg), which showed two spots under UV-S on normal phase TLC with the R_f values of 0.28 and 0.38 using 70% ethyl acetate in light petroleum as a mobile phase. Further purification by precoated TLC using 60% ethyl acetate in light petroleum (7 runs) as a mobile phase afforded two bands.

Band 5-1 was obtained as a colorless gum (1.6 mg). Its chromatogram displayed one spot under UV-S on normal phase TLC with the R_f value of 0.33 using 70% ethyl acetate in light petroleum (3 runs) as a mobile phase. The ^{1}H NMR data suggested that it was a mixture. Thus, no attempted purification was carried out.

Band 5-2 was obtained as a colorless gum (1.8 mg), which showed one spot under UV-S on normal phase TLC with the R_f value of 0.25 using 70% ethyl acetate in light petroleum (3 runs) as a mobile phase. The ^{1}H NMR spectrum displayed that it was a mixture. Thus, further purification was not performed.

Subfraction C5 showed one major spot under UV-S on normal phase TLC with the R_f value of 0.25 using 50% ethyl acetate in light petroleum as a mobile phase (6 runs). Further purification by precoated TLC using 50% ethyl acetate in light petroleum (7 runs) as a mobile phase afforded a yellow gum (4.2 mg). Its chromatogram displayed one spot under UV-S on normal phase TLC with the R_f value of 0.15 using 50% ethyl acetate in light petroleum as a mobile phase (5 runs). Its ^{1}H NMR spectral data and chromatogram on normal phase TLC indicated that it was not pure. Therefore, further purification by precoated TLC using 60% ethyl acetate in light petroleum (7 runs) as a mobile phase gave **N27** as a yellow gum (2.5 mg), which showed one UV-active spot on normal phase TLC with the R_f value of 0.10 using 70% ethyl acetate in light petroleum (4 runs) as a mobile phase.

$[\alpha]_D^{27}$	-88.59 (c = 0.50, MeOH)
UV(MeOH) λ_{max} nm (log ε)	222 (5.47), 275 (4.69), 284 (3.63)
FT-IR (neat) ν_{cm-1}	3370 (O-H stretching), 1657, 1644 (C=O stretching), 1605 (C=C stretching)
^{1}H NMR ($CDCl_3$) (δ ppm) (500 MHz)	7.08 (*d*, *J* = 8.5 Hz, 2H), 6.80 (*d*, *J* = 8.5 Hz, 2H), 5.70 (*s*, 1H), 4.22 (*dd*, *J* = 10.0, 3.5 Hz, 1H), 4.08 (*t*, *J* = 8.0 Hz, 1H), 3.64 (*m*, 1H), 3.57 (*td*, *J* = 13.0, 3.0 Hz, 1H), 3.51 (*dd*, *J* = 14.5, 3.5 Hz, 1H), 2.74 (*dd*, *J* = 14.5, 10.0 Hz, 1H), 2.34 (*m*, 1H), 2.02 (*m*, 1H), 1.97 (*m*, 1H), 1.90 (*m*, 1H)
^{13}C NMR ($CDCl_3$) (δ ppm) (125 MHz)	169.45, 165.13, 155.26, 130.34, 127.57, 116.15, 59.14, 56.23, 45.42, 35.98, 28.35, 22.52
DEPT (135°) ($CDCl_3$)	CH : 130.34, 116.15, 59.14, 56.23 CH_2 : 45.42, 35.98, 28.35, 22.52

Subfraction C6 contained three spots under UV-S on normal phase TLC with the R_f values of 0.33, 0.45 and 0.50 using 7% methanol in dichloromethane (3 runs) as a mobile phase. Further purification by precoated TLC using 7% methanol in dichloromethane (4 runs) as a mobile phase afforded three bands.

Band 1 was obtained as a colorless gum (0.5 mg). Its chromatogram displayed one spot under UV-S on normal phase TLC with the R_f value of 0.48 using 7% methanol in dichloromethane (2 runs) as a mobile phase. The ^1H NMR data suggested that it was a mixture. Because of low quantity, it was not further separated.

Band 2 was obtained as a colorless gum (3.2 mg), which showed one spot under UV-S on normal phase TLC with the R_f value of 0.41 using 7% methanol in dichloromethane (2 runs) as a mobile phase. When using 70% ethyl acetate in light petroleum (5 runs) as a mobile phase, the chromatogram showed one major UV-active spot on normal phase TLC with the R_f value of 0.35 and many inseparable spots. Purification by precoated TLC using 60% ethyl acetate in light petroleum (7 runs) as a mobile phase afforded a colorless gum (1.7 mg), which showed one UV-active spot on normal phase TLC with the R_f value of 0.25 using 60% ethyl acetate in light petroleum (4 runs) as a mobile phase. The ^1H NMR data suggested that it was a mixture. Thus, further purification was not conducted.

Band 3 was obtained as a colorless gum (5.3 mg). The chromatogram showed one UV-active spot on normal phase TLC with the R_f value of 0.28 using 7% methanol in dichloromethane (2 runs) as a mobile phase. When using 70% ethyl acetate in light petroleum (5 runs) as a mobile phase, the chromatogram showed two UV-active spots on normal phase TLC with the R_f values of 0.13 and 0.25. Further, purification by precoated TLC using 60% ethyl acetate in light petroleum (7 runs) as a mobile phase afforded two bands.

Band 3-1 was obtained as a colorless gum (0.7 mg). The chromatogram displayed one spot under UV-S on normal phase TLC with the R_f value of 0.23 using 70% ethyl acetate in light petroleum (4 runs) as a mobile phase.

Its ^{1}H NMR spectrum showed proton signals at high field region. Because of low quantity, it was not further investigated.

Band 3-2 was obtained as a colorless gum (2.8 mg), which showed one spot under UV-S on normal phase TLC with the R_f value of 0.13 using 70% ethyl acetate in light petroleum (4 runs). The ^{1}H NMR data suggested that it was a mixture. Thus, no attempted investigation was carried out.

Subfraction C7 demonstrated two spots under UV-S on normal phase TLC with the R_f values of 0.20 and 0.48 using 7% methanol in dichloromethane (3 runs) as a mobile phase. Further purification by precoated TLC using 5% methanol in dichloromethane (4 runs) followed by 8% methanol in dichloromethane (3 runs) as mobile phases afforded two bands.

Band 1 was a yellow gum (1.2 mg), which showed one spot under UV-S on normal phase TLC with the R_f value of 0.45 using 8% methanol in dichloromethane (2 runs) as a mobile phase. Its ^{1}H NMR spectrum displayed none of major components. Thus, no attempted separation was performed.

Band 2 was obtained as a yellow gum (5.5 mg) and showed one UV-active spot on normal phase TLC with the R_f value of 0.21 using 8% methanol in dichloromethane (2 runs) as a mobile phase. When using 70% ethyl acetate in light petroleum (3 runs) as a mobile phase, the chromatogram showed two UV-active spots with the R_f values of 0.18 and 0.30. Further purification by precoated TLC using 60% ethyl acetate in light petroleum (8 runs) as a mobile phase afforded two bands.

Band 2-1 was obtained as a yellow gum (1.8 mg), which showed one spot under UV-S on normal phase TLC with the R_f value of 0.30 using 70% ethyl acetate in light petroleum (2 runs) as a mobile phase. The ^{1}H NMR data suggested that it was a mixture. Therefore, further purification was not performed.

Band 2-2 was obtained as a yellow gum (2.6 mg). Its chromatogram showed one UV-active spot on normal phase TLC with the R_f value of 0.15 using 70% ethyl acetate in light petroleum (2 runs) as a mobile phase. The ^1H NMR data suggested that it was not pure. Thus, no attempted investigation was carried out.

Subfraction C8 displayed many UV-active spots on normal phase TLC using 10% methanol in dichloromethane (2 runs) as a mobile phase. It was further separated by column chromatography over Sephadex LH20 using 100% MeOH as eluent. Fractions, which contained similar components, were combined and evaporated to dryness under reduced pressure to give four subfractions, as shown in **Table 75.**

Table 75 Subfractions obtained from **subfraction C8** by column chromatography over Sephadex LH20

Subfraction	Eluent	Weight (mg)	Physical appearance
C8-1	100% MeOH	3.4	Yellow gum
C8-2	100% MeOH	6.0	Yellow gum
C8-3	100% MeOH	24.4	Yellow gum mixed with yellow solid
C8-4	100% MeOH	2.8	Yellow gum

Subfraction C8-1 demonstrated no spots under UV-S on normal phase TLC using 10% methanol in dichloromethane as a mobile phase (3 runs). Its ^1H NMR spectrum showed none of aromatic proton signals. Thus, further purification was not performed.

Subfraction C8-2 displayed three spots under UV-S on normal phase TLC with the R_f values of 0.20, 0.25 and 0.43 using 10% methanol in dichloromethane as a mobile phase (3 runs). Its ^1H NMR spectrum displayed none of major components. Therefore, further investigation was not conducted.

Subfraction C8-3 showed a long tail under UV-S on normal phase TLC using 10% methanol in dichloromethane as a mobile phase (3 runs). Its chromatogram characteristic appeared as a long tail on reverse phase TLC using 40% methanol in water as a mobile phase. The ^{1}H NMR spectrum displayed none of major components. Therefore, further purification was not carried out.

Subfraction C8-4 showed many inseparable spots under UV-S on normal phase TLC using 10% methanol in dichloromethane as a mobile phase (3 runs). Its ^{1}H NMR spectrum displayed none of major components. Because of low quantity, it was not further separated.

Subfraction C9 showed no definite spots under UV-S on normal phase TLC using 7% methanol in dichloromethane as a mobile phase (3 runs). The ^{1}H NMR spectrum showed none of major components. Thus, no attempted investigation was performed.

Fraction D displayed a long tail under UV-S on normal phase TLC using 100% dichloromethane as a mobile phase (2 runs). Furthermore, its chromatogram showed three UV-active spots on reverse phase TLC with the R_f values of 0.18, 0.30 and 0.88 using 50% methanol in water as a mobile phase. Further separation by column chromatography over reverse phase silica gel was performed. Elution was conducted initially with 50% methanol in water and gradually enriched with methanol until pure methanol. Fractions, which contained similar components, were combined and evaporated to dryness under reduced pressure to give five subfractions, as shown in **Table 76.**

Table 76 Subfractions obtained from **fraction D** by column chromatography over reverse phase silica gel

Subfraction	Eluent	Weight (mg)	Physical appearance
D1	50% MeOH/H_2O	2.7	Yellow gum
D2	50% MeOH/H_2O	11.5	Yellow gum
D3	50-70% MeOH/H_2O	4.5	Yellow gum
D4	70% MeOH/H_2O	6.7	Yellow gum mixed with yellow solid
D5	100% MeOH	5.5	Yellow gum

Subfraction D1 showed many spots under UV-S on normal phase TLC using 4% methanol in dichloromethane (2 runs) and 6% methanol in dichloromethane (3 runs) as mobile phases. Its ^{1}H NMR spectrum displayed proton signals at high field region. Therefore, further investigation was not conducted.

Subfraction D2 demonstrated four spots under UV-S on normal phase TLC with the R_f values of 0.10, 0.25, 0.45 and 0.65 using 4% methanol in dichloromethane (2 runs) and 6% methanol in dichloromethane (3 runs) as mobile phases. Further purification by precoated TLC using 5% methanol in dichloromethane (3 runs), 6% methanol in dichloromethane (3 runs) followed by 10% methanol in dichloromethane (2 runs) as mobile phases afforded four bands.

Band 1 was a pale-yellow gum (1.5 mg), which showed one spot under UV-S on normal phase TLC with the R_f value of 0.63 using 10% methanol in dichloromethane (2 runs) as a mobile phase. The ^{1}H NMR data suggested that it was a mixture. Thus, no attempted separation was performed.

Band 2 was obtained as a yellow gum (2.0 mg). Its chromatogram showed one UV-active spot on normal phase TLC with the R_f value of 0.38 using 10% methanol in dichloromethane (2 runs) as a mobile phase. The ^{1}H NMR data suggested that it was not pure. Thus, no attempted investigation was carried out.

Band 3 was obtained as a yellow gum (1.7 mg), which showed one spot under UV-S on normal phase TLC with the R_f value of 0.20 using 10% methanol in dichloromethane (2 runs) as a mobile phase. The ^1H NMR data suggested that it was a mixture. Thus, it was not further purified.

Band 4 was obtained as a yellow gum (3.3 mg). Its chromatogram showed one UV-active spot on normal phase TLC with the R_f value of 0.08 using 10% methanol in dichloromethane (2 runs) as a mobile phase. The ^1H NMR data suggested that it was a mixture. Therefore, it was not further investigated.

Subfraction D3 displayed many inseparable spots under UV-S on normal phase TLC using 4% methanol in dichloromethane (2 runs) followed by 6% methanol in dichloromethane (3 runs) as mobile phases. Its ^1H NMR spectrum displayed none of major components. Therefore, further investigation was not conducted.

Subfraction D4 showed two UV-active spots on normal phase TLC with the R_f values of 0.23 and 0.48 using 2% methanol in dichloromethane as a mobile phase (3 runs). Further purification by precoated TLC using 2% methanol in dichloromethane (4 runs) as a mobile phase afforded two bands.

Band 1 was obtained as a pale-yellow solid (1.0 mg), which showed one spot under UV-S on normal phase TLC with the R_f value of 0.48 using 2% methanol in dichloromethane (2 runs) as a mobile phase. The ^1H NMR data suggested that it was a mixture. Thus, no attempted separation was performed.

Band 2 (N28) was obtained as a white solid (5.2 mg) and melted at 182.0-182.6 °C. Its chromatogram showed one UV-active spot on normal phase TLC with the R_f value of 0.20 using 2% methanol in dichloromethane (2 runs) as a mobile phase.

UV(MeOH) λ_{max} nm (log ε)	222 (5.30), 236 (5.31), 311 (4.94), 330 (4.72)
FT-IR (neat) ν_{cm-1}	3392 (O-H stretching), 1609, 1580 and 1553 (C=C stretching)
^{1}H NMR ($CDCl_3$+CD_3OD) (δ ppm) (300 MHz)	8.86 (*d*, *J* = 4.5 Hz, 1H), 8.77 (*s*, 1H), 8.45 (*dd*, *J* = 8.4, 1.2 Hz, 1H), 8.12 (*dd*, *J* = 8.4, 1.2 Hz, 1H), 7.80 (*ddd*, *J* = 8.4, 6.6, 1.2 Hz, 1H), 7.72 (*d*, *J* = 4.5 Hz, 1H), 7.64 (*ddd*, *J* = 8.4, 6.6, 1.2 Hz, 1H)
^{13}C NMR ($CDCl_3$+CD_3OD) (δ ppm) (75 MHz)	153.45, 152.02, 150.04, 141.54, 133.78, 133.10, 131.37, 129.41, 128.10, 123.05
DEPT (135°) ($CDCl_3$+CD_3OD) CH :	153.45, 150.04, 133.78, 133.10, 131.37, 128.10, 123.05
EIMS *m/z* (% relative intensity):	172 (100), 155 (49), 128 (34), 101 (23)

Subfraction D5 showed no spots under UV-S on normal phase TLC using 4% methanol in dichloromethane (2 runs) as a mobile phase. The ^{1}H NMR spectrum showed none of aromatic proton signals. Thus, no attempted investigation was carried out.

Fraction E showed no spots under UV-S on normal phase TLC using 100% dichloromethane (2 runs) as a mobile phase. Furthermore, its chromatogram showed no UV-active spots on reverse phase TLC using 50% methanol in water as a mobile phase. Its ^{1}H NMR spectrum displayed none of major components. Thus, no further investigation was pursued.

4.2.3 Purification of the mycelial extract

The crude material was separated by column chromatography over Sephadex LH20 using 100% MeOH as eluent. All fractions were examined by TLC, combined on the basis of their chromatogram characteristics and then evaporated to dryness under reduced pressure to give five fractions, as shown in **Table 77**.

Table 77 Fractions obtained from **the mycelial extract** by column chromatography over Sephadex LH20

Fraction	Eluent	Weight (mg)	Physical appearance
MA	100% MeOH	196.4	Brown-yellow gum
MB	100% MeOH	223.8	Yellow gum mixed with yellow solid
MC	100% MeOH	87.3	Yellow gum mixed with yellow solid
MD	100% MeOH	11.2	Yellow gum
ME	100% MeOH	3.1	Yellow gum

Fraction MA displayed a long tail after dipping the normal phase TLC in ASA reagent and subsequently heating using 10% methanol in dichloromethane (3 runs) as a mobile phase. The ^{1}H NMR data indicated that the major components might be a mixture of long chain hydrocarbons. Therefore, it was not further investigated.

Fraction MB contained three UV-active spots on normal phase TLC with the R_f values of 0.23, 0.65 and 0.90 using 10% methanol in dichloromethane (3 runs) as a mobile phase. This fraction was separated by column chromatography over silica gel using a gradient system of methanol-dichloromethane. All subfractions were examined by TLC, combined on the basis of their chromatogram characteristics and then evaporated to dryness under reduced pressure to give six subfractions, as shown in **Table 78.**

Table 78 Subfractions obtained from **fraction MB** by column chromatography over silica gel

Subfraction	Eluent	Weight (mg)	Physical appearance
MB-1	100% CH_2Cl_2 - 10% MeOH/CH_2Cl_2	5.8	Colorless gum

Table 78 Continued

Subfraction	Eluent	Weight (mg)	Physical appearance
MB-2	10% MeOH/CH_2Cl_2	67.4	Pale-yellow gum mixed with yellow solid
MB-3	10-40% MeOH/CH_2Cl_2	30.3	Yellow gum
MB-4	40% MeOH/CH_2Cl_2	10.4	Yellow gum
MB-5	40-60% MeOH/CH_2Cl_2	32.1	Yellow gum
MB-6	60% MeOH/CH_2Cl_2-100% MeOH	70.8	Brown-yellow gum

Subfraction MB-1 showed no spots after dipping the normal phase TLC in ASA reagent and subsequently heating using 2% methanol in dichloromethane (3 runs) as a mobile phase. This fraction was not further investigated because its ^{1}H NMR data indicated that it was a mixture of long chain hydrocarbons.

Subfraction MB-2 appeared as a long tail under UV-S on the normal phase TLC using 2% methanol in dichloromethane (3 runs) as a mobile phase. When using 20% ethyl acetate in light petroleum (5 runs) as a mobile phase, the chromatogram showed many spots after dipping the normal phase TLC in ASA reagent and subsequently heating. Further separation by column chromatography over Sephadex LH20 using 100% MeOH as eluent was performed. Subfractions, which contained similar components, were combined and evaporated to dryness under reduced pressure to give five subfractions, as shown in **Table 79.**

Table 79 Subfractions obtained from **subfraction MB-2** by column chromatography over Sephadex LH20

Subfraction	Eluent	Weight (mg)	Physical appearance
MB-21	100% MeOH	11.7	Yellow gum
MB-22	100% MeOH	8.4	White-yellow solid

Table 79 Continued

Subfraction	Eluent	Weight (mg)	Physical appearance
MB-23	100% MeOH	38.7	White-yellow solid
MB-24	100% MeOH	4.7	Yellow gum
MB-25	100% MeOH	2.5	Yellow gum

Subfraction MB-21 showed no spots under UV-S on normal phase TLC using 2% methanol in dichloromethane (3 runs) as a mobile phase. Its ^{1}H NMR spectrum displayed proton signals at high field region. Therefore, it was not further investigated.

Subfraction MB-22 showed one major spot under UV-S on normal phase TLC with the R_f value of 0.38 using 2% methanol in dichloromethane (3 runs) as a mobile phase. The ^{1}H NMR data indicated the presence of **N22** as a major component. Therefore, it was not further purified.

Subfraction MB-23 displayed many spots under UV-S on normal phase TLC using 2% methanol in dichloromethane (3 runs) as a mobile phase. Further separation by column chromatography over Sephadex LH20 using 100% MeOH as eluent was performed. All subfractions were examined by TLC, combined on the basis of their chromatogram characteristics and then evaporated to dryness under reduced pressure to afford four subfractions, as shown in **Table 80.**

Table 80 Subfractions obtained from **subfraction MB-23** by column chromatography over Sephadex LH20

Subfraction	Eluent	Weight (mg)	Physical appearance
MB-231	100% MeOH	2.3	Yellow gum
MB-232	100% MeOH	12.3	White-yellow solid
MB-233	100% MeOH	20.5	Yellow solid
MB-234	100% MeOH	2.7	Yellow gum

Subfraction MB-231 showed no spots under UV-S on normal phase TLC using 20% ethyl acetate in light petroleum and 50% ethyl acetate in light petroleum (2 runs) as mobile phases. Its ^{1}H NMR spectrum showed none of aromatic proton signals. Therefore, it was not further investigated.

Subfraction MB-232 showed one spot under UV-S on normal phase TLC with the R_f value of 0.70 using 20% ethyl acetate in light petroleum and 50% ethyl acetate in light petroleum (2 runs) as mobile phases. Its chromatogram characteristic displayed one major spot with the R_f value of 0.58 after dipping the normal phase TLC in ASA reagent and subsequently heating. The ^{1}H NMR data indicated that it was a mixture of **N22** and **N23**. Therefore, it was not further purified.

Subfraction MB-233 showed many spots after dipping the normal phase TLC in ASA reagent and subsequently heating using 20% ethyl acetate in light petroleum and 50% ethyl acetate in light petroleum (2 runs) as mobile phases. Its ^{1}H NMR spectral data indicated the presence of **N22** as a major component. Therefore, further investigation was not conducted.

Subfraction MB-234 showed no definite spots after dipping the normal phase TLC in ASA reagent and subsequently heating using 20% ethyl acetate in light petroleum and 50% ethyl acetate in light petroleum (2 runs) as mobile phases. Its ^{1}H NMR spectrum showed none of major components. Thus, no further investigation was pursued.

Subfraction MB-24 showed many spots under UV-S on normal phase TLC using 2% methanol in dichloromethane (3 runs) as a mobile phase. The ^{1}H NMR spectral data and chromatogram on normal phase TLC indicated the presence of a mixture of **N22, N23** and other components. Therefore, it was not further separated.

Subfraction MB-25 showed no spots under UV-S on normal phase TLC using 2% methanol in dichloromethane (3 runs) as a mobile phase. Its ^{1}H NMR

spectrum showed none of major components. Thus, no attempted investigation was carried out.

Subfraction MB-3 appeared as a long tail under UV-S on the normal phase TLC using 2% methanol in dichloromethane (3 runs) as a mobile phase. When using 20% ethyl acetate in light petroleum (5 runs) as a mobile phase, the chromatogram showed three spots with the R_f values of 0.08, 0.15 and 0.35 after dipping the normal phase TLC in ASA reagent and subsequently heating. Further separation by column chromatography over Sephadex LH20 using 100% MeOH as eluent was performed. Subfractions, which contained similar components, were combined and evaporated to dryness under reduced pressure to give three subfractions, as shown in **Table 81**.

Table 81 Subfractions obtained from **subfraction MB-3** by column chromatography over Sephadex LH20

Subfraction	Eluent	Weight (mg)	Physical appearance
MB-31	100% MeOH	1.2	Colorless gum
MB-32	100% MeOH	27.3	Yellow gum mixed with white solid
MB-33	100% MeOH	0.7	Yellow gum

Subfraction MB-31 showed no spots after dipping the normal phase TLC in ASA reagent and subsequently heating using 2% methanol in dichloromethane (3 runs) as a mobile phase. Its ^{1}H NMR spectrum showed none of aromatic proton signals. Therefore, it was not further investigated.

Subfraction MB-32 was separated into two parts: a white solid (4.2 mg) (**N29**) and a yellow solution (**MB-32s**), upon standing at room temperature. **N29** melted at 247.8-248.1 °C and showed one spot with the R_f value of 0.13 after dipping the normal phase TLC in ASA reagent and subsequently heating using 50% ethyl acetate in light petroleum (2 runs) as a mobile phase.

$[\alpha]_D^{27}$	-77.75 (c = 0.16, pyridine)
UV(MeOH) λ_{max} nm (log ε)	247 (2.92)
FT-IR (neat) ν_{cm-1}	3362 (O-H stretching)
^{1}H NMR ($CDCl_3$) (δ ppm) (300 MHz)	5.35 (*brd*, *J* = 3.0 Hz, 1H), 5.23 (*dd*, *J* = 15.0, 6.0 Hz, 1H), 5.16 (*dd*, *J* = 15.0, 6.0 Hz, 1H), 4.08 (*m*, 1H), 3.63 (*brs*, 1H), 2.14 (*dd*, *J* = 12.0, 9.0 Hz, 1H), 2.06 (*m*, 1H), 1.97 (*m*, 1H), 1.92 (*m*, 1H), 1.87 (*m*, 2H), 1.78 (*m*, 2H), 1.66 (*m*, 2H), 1.58 (*m*, 2H), 1.55 (*m*, 2H), 1.48 (*m*, 1H), 1.44 (*m*, 1H), 1.33 (*m*, 1H), 1.30 (*m*, 1H), 1.26 (*m*, 2H), 1.09 (*s*, 3H), 1.02 (*d*, *J* = 9.0 Hz, 3H), 0.91 (*d*, *J* = 9.0 Hz, 3H), 0.84 (*d*, *J* = 6.0 Hz, 3H), 0.82 (*d*, *J* = 6.0 Hz, 3H), 0.60 (*s*, 3H)
^{13}C NMR ($CDCl_3$) (δ ppm) (75 MHz)	144.01, 135.37, 132.19, 117.54, 75.97, 73.67, 67.74, 55.99, 54.76, 43.77, 43.45, 42.81, 40.39, 39.45, 39.22, 37.15, 33.08, 32.96, 30.85, 29.69, 22.89, 22.05, 21.11, 19.95, 19.63, 18.83, 17.59, 12.33
DEPT (135°) ($CDCl_3$)	CH : 135.37, 132.19, 117.54, 73.67, 67.74, 55.99, 54.76, 43.77, 42.81, 40.39, 33.08
	CH_2 : 39.45, 39.22, 32.96, 30.85, 29.69, 22.89, 22.05
	CH_3 : 21.11, 19.95, 19.63, 18.83, 17.59, 12.33

A yellow solution (**MB-32s**) showed many inseparable spots after dipping the normal phase TLC in ASA reagent and subsequently heating using 2% methanol in dichloromethane (3 runs) as a mobile phase. When using 40% ethyl acetate in light petroleum (2 runs) as a mobile phase, the chromatogram showed six spots with the R_f values of 0.08, 0.20, 0.33, 0.48, 0.60 and 0.70 after dipping the normal phase TLC in ASA reagent and subsequently heating. Further separation by column chromatography over Sephadex LH20 using 100% MeOH as eluent was performed. All subfractions were examined by TLC, combined on the basis of their

chromatogram characteristics and then evaporated to dryness under reduced pressure to afford three subfractions, as shown in **Table 82.**

Table 82 Subfractions obtained from **subfraction MB-32s** by column chromatography over Sephadex LH20

Subfraction	Eluent	Weight (mg)	Physical appearance
MB-32s-1	100% MeOH	3.0	Yellow gum
MB-32s-2	100% MeOH	13.4	Yellow gum mixed with yellow solid
MB-32s-3	100% MeOH	6.4	Yellow gum

Subfraction MB-32s-1 showed no definite spots under UV-S on normal phase TLC using 4% methanol in dichloromethane (5 runs) as a mobile phase. The ^{1}H NMR data indicated that it was a mixture. Thus, it was not further investigated.

Subfraction MB-32s-2 showed many inseparable spots under UV-S on normal phase TLC using 4% methanol in dichloromethane (5 runs) as a mobile phase. The ^{1}H NMR spectrum showed none of major proton signals. Thus, no attempted investigation was performed.

Subfraction MB-32s-3 showed many UV-active spots on normal phase TLC using 4% methanol in dichloromethane (5 runs) as a mobile phase. The ^{1}H NMR spectrum showed none of major components. Therefore, it was not further purified.

Subfraction MB-33 showed no spots after dipping the normal phase TLC in ASA reagent and subsequently heating using 2% methanol in dichloromethane (3 runs) as a mobile phase. Because of low quantity, it was not further investigated.

Subfraction MB-4 demonstrated two spots under UV-S on normal phase TLC with the R_f values of 0.10 and 0.20 using 5% methanol in dichloromethane (2 runs) as a mobile phase. Further purification by precoated TLC using 4% methanol in dichloromethane (2 runs) followed by 7% methanol in dichloromethane (5 runs) as mobile phases afforded two bands.

Band 1 was a yellow gum (3.8 mg), which showed one spot under UV-S on normal phase TLC with the R_f value of 0.38 using 10% methanol in dichloromethane (2 runs) as a mobile phase. Its ^{1}H NMR data suggested that it was a mixture. Thus, no attempted separation was performed.

Band 2 was a yellow gum (2.3 mg), which displayed one spot under UV-S on normal phase TLC with the R_f value of 0.28 using 10% methanol in dichloromethane (2 runs) as a mobile phase. Its ^{1}H NMR data suggested that it was a mixture. Therefore, it was not further purified.

Subfraction MB-5 displayed four spots under UV-S on normal phase TLC with the R_f values of 0.08, 0.28, 0.35 and 0.40 using 10% methanol in dichloromethane (3 runs) as a mobile phase. Further separation by column chromatography over Sephadex LH20 using 100% MeOH as eluent was performed. All subfractions were examined by TLC, combined on the basis of their chromatogram characteristics and then evaporated to dryness under reduced pressure to afford four subfractions, as shown in **Table 83**.

Table 83 Subfractions obtained from **subfraction MB-5** by column chromatography over Sephadex LH20

Subfraction	Eluent	Weight (mg)	Physical appearance
MB-51	100% MeOH	0.8	Colorless gum
MB-52	100% MeOH	22.5	Yellow gum
MB-53	100% MeOH	5.3	Yellow gum
MB-54	100% MeOH	1.2	Colorless gum

Subfraction MB-51 showed no UV-active spots on normal phase TLC using 8% methanol in dichloromethane (5 runs) as a mobile phase. Because of low quantity, it was not further investigated.

Subfraction MB-52 showed many spots under UV-S on normal phase TLC using 8% methanol in dichloromethane (5 runs) as a mobile phase. Its ^{1}H NMR spectrum showed none of major components. Thus, no attempted investigation was carried out.

Subfraction MB-53 displayed many inseparable spots under UV-S on normal phase TLC using 8% methanol in dichloromethane (5 runs) as a mobile phase and showed no UV-active spots on reverse phase TLC using 40% methanol in water as a mobile phase. Its ^{1}H NMR spectrum showed none of major signals. Thus, it was not further investigated.

Subfraction MB-54 showed no definite UV-active spots on normal phase TLC using 8% methanol in dichloromethane (5 runs) as a mobile phase. Because of low quantity, it was not further purified.

Subfraction MB-6 displayed many inseparable UV-active spots on normal phase TLC using 10% methanol in dichloromethane (3 runs) as a mobile phase. It was further separated by column chromatography over Sephadex LH20 using 100% MeOH as eluent. Subfractions, which contained similar components, were combined and evaporated to dryness under reduced pressure to afford four subfractions, as shown in **Table 84**.

Table 84 Subfractions obtained from **subfraction MB-6** by column chromatography over Sephadex LH20

Subfraction	Eluent	Weight (mg)	Physical appearance
MB-61	100% MeOH	0.6	Yellow gum
MB-62	100% MeOH	15.9	Yellow gum mixed with yellow solid
MB-63	100% MeOH	30.5	Yellow gum mixed with yellow solid
MB-64	100% MeOH	23.5	Yellow gum

Subfraction MB-61 showed no spots under UV-S on normal phase TLC using 6% methanol in dichloromethane (4 runs) as a mobile phase. Because of low quantity, it was not further investigated.

Subfraction MB-62 showed many spots under UV-S on normal phase TLC using 6% methanol in dichloromethane (4 runs) as a mobile phase. Its ^{1}H NMR spectrum showed none of major proton signals. Therefore, it was not further separated.

Subfraction MB-63 showed many inseparable spots under UV-S on normal phase TLC using 6% methanol in dichloromethane (4 runs) as a mobile phase and showed no UV-active spots on reverse phase TLC using 40% methanol in water as a mobile phase. Its ^{1}H NMR spectrum showed none of major components. Thus, no attempted investigation was carried out.

Subfraction MB-64 showed many spots under UV-S on normal phase TLC using 6% methanol in dichloromethane (4 runs) as a mobile phase and showed many UV-active spots on reverse phase TLC using 40% methanol in water as a mobile phase. Its ^{1}H NMR spectrum showed none of major components. Thus, no attempted investigation was performed.

Fraction MC displayed four UV-active spots on normal phase TLC with the R_f values of 0.08, 0.30, 0.60 and 0.80 using 10% methanol in dichloromethane (3 runs) as a mobile phase. Further separation by column chromatography over Sephadex LH20 using 100% MeOH as eluent was performed. All subfractions were examined by TLC, combined on the basis of their chromatogram characteristics and then evaporated to dryness under reduced pressure to afford four subfractions, as shown in **Table 85.**

Table 85 Subfractions obtained from **subfraction MC** by column chromatography over Sephadex LH20

Subfraction	Eluent	Weight (mg)	Physical appearance
MC-1	100% MeOH	4.7	Colorless gum
MC-2	100% MeOH	49.4	Yellow gum mixed with yellow solid
MC-3	100% MeOH	17.5	Yellow gum mixed with yellow solid
MC-4	100% MeOH	15.2	Yellow solid

Subfraction MC-1 showed no UV-active spots on normal phase TLC using 4% methanol in dichloromethane (2 runs) as a mobile phase. This fraction was not further investigated because its ^{1}H NMR data indicated the presence of a mixture of long chain hydrocarbons.

Subfraction MC-2 was precipitated upon standing at room temperature to give a white solid (24.0 mg) (**N30**) and a yellow solution (**MC-2s**). **N30** melted at 311.2-311.8 °C and showed one UV-active spot on normal phase TLC with the R_f value of 0.18 using 4% methanol in dichloromethane (2 runs) as a mobile phase.

$[\alpha]_D^{27}$	+47.00 (c = 0.79, $CHCl_3$)
UV(MeOH) λ_{max} nm (log ε)	258 (4.27)
FT-IR (neat) ν_{cm-1}	1657 and 1622 (C=O stretching)
^{1}H NMR (CD_3OD) (δ ppm) (300 MHz)	7.40 (*d*, *J* = 7.5 Hz, 1H), 5.62 (*d*, *J* = 7.5 Hz, 1H)
^{13}C NMR (CD_3OD) (δ ppm) (75 MHz)	164.98, 151.18, 141.14, 99.35
DEPT (135°) (CD_3OD)	CH : 141.14, 99.35

A yellow solution (**MC-2s**) showed many UV-active spots on normal phase TLC using 4% methanol in dichloromethane (2 runs) as a mobile phase. It was further acetylated with acetic anhydride (3.0 ml) and pyridine (0.5 ml). The mixture was stirred at room temperature for 24 hours. To the extract was added H_2O (15 ml), and the reaction mixture was extracted with ethyl acetate (3×20 ml). The ethyl acetate layer was consecutively washed with 10% hydrochloric acid (3×20 ml) and 10% sodium bicarbonate (3×20 ml). The combined ethyl acetate extracts were washed with water (2×20 ml) and dried over anhydrous Na_2SO_4, filtered and evaporated under reduced pressure to yield a yellow gum (30.5 mg), which showed many inseparable UV-active spots on normal phase TLC using 4% methanol in dichloromethane (2 runs) as a mobile phase. The ^{1}H NMR data indicated none of major components. Thus, no attempted purification was carried out.

Subfraction MC-3 displayed two UV-active spots on normal phase TLC with the R_f values of 0.20 and 0.45 using 4% methanol in dichloromethane (2 runs) as a mobile phase. It was further separated by column chromatography over Sephadex LH20 using 100% MeOH as eluent. Subfractions, which contained similar components, were combined and evaporated to dryness under reduced pressure to afford three subfractions, as shown in **Table 86.**

Table 86 Subfractions obtained from **subfraction MC-3** by column chromatography over Sephadex LH20

Subfraction	Eluent	Weight (mg)	Physical appearance
MC-31	100% MeOH	2.9	Colorless gum
MC-32	100% MeOH	11.2	Yellow gum mixed with yellow solid
MC-33	100% MeOH	2.7	Yellow gum

Subfraction MC-31 showed no UV-active spots on normal phase TLC using 6% methanol in dichloromethane (4 runs) as a mobile phase. Its ^{1}H NMR spectrum showed none of aromatic proton signals. Thus, it was not further isolated.

Subfraction MC-32 showed four UV-active spots on normal phase TLC with the R_f values of 0.05, 0.20, 0.38 and 0.60 using 6% methanol in dichloromethane (4 runs) as a mobile phase. Further purification by precoated TLC using 6% methanol in dichloromethane (5 runs) as a mobile phase afforded four bands.

Band 1 was a white solid (1.5 mg), which showed one spot under UV-S on normal phase TLC with the R_f value of 0.63 using 6% methanol in dichloromethane (5 runs) as a mobile phase. Its ^{1}H NMR spectral data indicated that it was **N28**.

Band 2 (N31) was obtained as a white solid (2.3 mg) and melted at 245.5-246.3 °C, which showed one spot under UV-S on normal phase TLC with the R_f value of 0.50 using 6% methanol in dichloromethane (5 runs) as a mobile phase.

$[\alpha]_D^{27}$ -52.55 (c = 0.02, MeOH)

UV(MeOH) λ_{max} nm (log ε) 218 (5.51), 248 (4.94), 318 (4.53)

FT-IR (neat) ν_{cm-1}		3365 (O-H stretching), 1712 and 1661 (C=O stretching), 1606 and 1550 (C=C stretching)
^{1}H NMR (CD_3OD) (δ ppm) (300 MHz)		7.90 (*d*, *J* = 8.7 Hz, 1H), 6.84 (*d*, *J* = 8.7 Hz, 1H), 4.68 (*m*, 1H), 3.74 (*dd*, *J* = 17.4, 3.3 Hz, 1H), 2.97 (*dd*, *J* = 17.4, 11.7 Hz, 1H), 1.49 (*d*, *J* = 6.3 Hz, 3H)
^{13}C NMR (CD_3OD) (δ ppm) (75 MHz)		170.61, 166.91, 162.82, 139.70, 137.14, 128.00, 114.65, 107.79, 76.08, 32.59, 19.58
DEPT (135°) (CD_3OD)	CH :	137.14, 114.65, 76.08
	CH_2 :	32.59
	CH_3 :	19.58
EIMS *m/z* (% relative intensity):		222 (4), 126 (100), 85 (22)

Band 3 was obtained as a white solid (1.4 mg). Its chromatogram showed one UV-active spot on normal phase TLC with the R_f value of 0.30 using 6% methanol in dichloromethane (5 runs) as a mobile phase. Its ^{1}H NMR spectral data indicated that it was **N30**.

Band 4 was obtained as a yellow gum (4.5 mg), which showed one spot under UV-S on normal phase TLC with the R_f value of 0.13 using 6% methanol in dichloromethane (4 runs) as a mobile phase. The ^{1}H NMR data suggested that none of major components. Thus, no attempted purification was carried out.

Subfraction MC-33 showed no UV-active spots on normal phase TLC using 6% methanol in dichloromethane (4 runs) as a mobile phase. Its ^{1}H NMR spectrum showed none of aromatic proton signals. Thus, it was not further investigated.

Subfraction MC-4 appeared two spots under UV-S on normal phase TLC with the R_f values of 0.10 and 0.45 using 4% methanol in dichloromethane as a mobile phase (2 runs). Furthermore, its chromatogram showed five UV-active spots on reverse phase TLC with the R_f values of 0.21, 0.31, 0.42, 0.46 and 0.58 using 20%

methanol in water as a mobile phase. Further separation by column chromatography over reverse phase silica gel was performed. Elution was conducted initially with 20% methanol in water and gradually enriched with methanol until pure methanol. Subfractions, which contained similar components, were combined and evaporated to dryness under reduced pressure to give two subfractions, as shown in **Table 87.**

Table 87 Subfractions obtained from **subfraction MC-4** by column chromatography over reverse phase silica gel

Subfraction	Eluent	Weight (mg)	Physical appearance
MC-41	20-80% MeOH/H_2O	8.4	Yellow solid
MC-42	80% MeOH/H_2O - 100% MeOH	5.6	Yellow solid

Subfraction MC-41 showed two spots under UV-S on normal phase TLC with the R_f values of 0.13 and 0.38 using 5% methanol in dichloromethane (2 runs) followed by 10% methanol in dichloromethane as mobile phases. Further purification by precoated TLC using 6% methanol in dichloromethane (4 runs) followed by 10% methanol in dichloromethane (2 runs) as mobile phases afforded two bands.

Band 1 was a white solid (3.2 mg), which showed one spot under UV-S on normal phase TLC with the R_f value of 0.35 using 10% methanol in dichloromethane as a mobile phase. Its ^{1}H NMR data indicated that it was **N31.**

Band 2 was a yellow solid (1.9 mg), which showed one spot under UV-S on normal phase TLC with the R_f value of 0.15 using 10% methanol in dichloromethane as a mobile phase. Because the ^{1}H NMR data indicated that it was a mixture, no further investigation was pursued.

Subfraction MC-42 showed many inseparable spots under UV-S on normal phase TLC using 5% methanol in dichloromethane (2 runs) followed by 10%

methanol in dichloromethane as mobile phases. Its ^{1}H NMR spectrum displayed none of major components. Therefore, further investigation was not conducted.

Fraction MD showed one major UV-active spot on normal phase TLC with the R_f value of 0.13 using 10% methanol in dichloromethane (3 runs) as a mobile phase. Further separation by column chromatography over Sephadex LH20 using 100% MeOH as eluent was performed. All subfractions were examined by TLC, combined on the basis of their chromatogram characteristics and then evaporated to dryness under reduced pressure to afford three subfractions, as shown in **Table 88**.

Table 88 Subfractions obtained from **fraction MD** by column chromatography over Sephadex LH20

Subfraction	Eluent	Weight (mg)	Physical appearance
MD-1	100% MeOH	5.8	Yellow gum
MD-2	100% MeOH	3.5	Yellow solid
MD-3	100% MeOH	1.7	Yellow gum

Subfraction MD-1 showed no spots under UV-S on normal phase TLC using 12% methanol in dichloromethane (3 runs) as a mobile phase. Its ^{1}H NMR spectrum showed none of major components. Thus, no attempted investigation was performed.

Subfraction MD-2 (N32) melted at 232.0-232.7 °C and displayed one spot under UV-S on normal phase TLC with the R_f value of 0.15 using 12% methanol in dichloromethane (3 runs) as a mobile phase.

$[\alpha]_D^{27}$	-70.11 (c = 1.65, MeOH)
UV(MeOH) λ_{max} nm (log ε)	217 (4.95), 246 (4.54), 323 (4.31)
FT-IR (neat) ν_{cm-1}	3394 (O-H stretching), 1668 (C=O stretching), 1608 and 1550 (C=C stretching)

^{1}H NMR (CD_3OD) (δ ppm) (300 MHz)	7.56 (*d*, *J* = 9.0 Hz, 1H), 6.84 (*d*, *J* = 9.0 Hz, 1H), 4.73 (*m*, 1H), 3.38 (*dd*, *J* = 15.0, 3.0 Hz, 1H), 2.80 (*dd*, *J* = 15.0, 9.0 Hz, 1H), 1.50 (*d*, *J* = 6.0 Hz, 3H)
^{13}C NMR (CD_3OD) (δ ppm) (75 MHz)	169.00, 159.00, 142.28, 134.24, 131.12, 115.27, 106.70, 76.43, 28.94, 19.56
DEPT (135°) (CD_3OD)	CH : 131.12, 115.27, 76.43
	CH_2 : 28.94
	CH_3 : 19.56

Subfraction MD-3 appeared as a long tail under UV-S on normal phase TLC using 12% methanol in dichloromethane (3 runs) as a mobile phase. Because of low quantity, it was not further isolated.

Fraction ME showed no spots under UV-S on normal phase TLC using 12% methanol in dichloromethane (3 runs) as a mobile phase. Its ^{1}H NMR spectrum displayed none of major components and none of aromatic proton signals. Thus, no further investigation was carried out.

CHAPTER 4.3
RESULTS AND DISCUSSION

One new compound (**N26**) was isolated from the broth extract together with seven known compounds (**N21-N25, N27** and **N28**). Four additional known compounds (**N29-N32**) were obtained from the mycelial extract. The structures were identified by spectroscopic methods.

4.3.1 Compound N21

N21 was obtained as a yellow gum. The UV spectrum showed maximum absorption bands of a conjugated double bond at λ_{max} 243 and 306 nm. The IR spectrum exhibited an absorption band at 1730 cm^{-1} for a carbonyl group. The ^{1}H NMR spectral data (**Figure 53**) (**Table 89**) were similar to those of **N15** except that a signal of the chelated hydroxy proton (δ_H 11.06, *s*, 1H) in **N15** was replaced, in **N21**, by a methoxy signal (δ_H 3.95, *s*, 3H). The presence of the methoxyl group was supported by a methoxyl resonance at δ_C 56.17 in the ^{13}C NMR spectrum (**Figure 54**) (**Table 89**). The methoxyl group was then located at C-8 (δ_C 161.26), *peri* position to the carbonyl group. Its HMBC correlation (**Table 90**) with C-8 and signal enhancement of an aromatic proton (δ_H 6.92, *d*, J = 8.7 Hz, H-7) after irradiation of 8-OCH_3 in the NOEDIFF experiment (**Table 90**) confirmed above assignment. **N21** gave almost identical optical rotation to that of (*R*)-(-)-mellein methyl ether, $[\alpha]_D^{27}$ of **N21** = -232.73 (c = 0.50, $CHCl_3$) and $[\alpha]_D$ of (*R*)-(-)-mellein methyl ether = -259.00 (c = 0.50, $CHCl_3$) (Dimitriadis, C., *et al.* 1997). Therefore, **N21** was assigned as (*R*)-(-)-mellein methyl ether which was previously isolated from *Apiospora montagnei* (Klemke *et al.*, 2004).

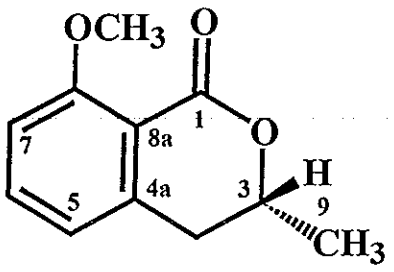

Table 89 The NMR data of **N21** and **(*R*)-(-)-mellein methyl ether** in $CDCl_3$

Position	N21		(*R*)-(-)-Mellein methyl ether [a]	
	δ_H (mult., J_{Hz})	δ_C (C-Type)	δ_H (mult., J_{Hz})	δ_C (C-Type)
1	-	162.57 (C=O)	-	162.7 (C=O)
3	4.56 (*qt*, 6.3, 4.2)	74.08 (CH)	4.55 (*m*)	74.1 (CH)
4	2.87 (*d*, 4.2)	36.11 (CH_2)	2.87 (*m*)	36.1 (CH_2)
4a	-	141.95 (C)	-	141.9 (C)
5	6.79 (*d*, 7.2)	119.17 (CH)	6.80 (*d*, 7.3)	119.1 (CH)
6	7.45 (*dd*, 8.7, 7.2)	134.39 (CH)	7.45 (*m*)	134.4 (CH)
7	6.92 (*d*, 8.7)	110.91 (CH)	6.92 (*d*, 8.5)	110.8 (CH)
8	-	161.26 (C)	-	161.1 (C)
8-OCH_3	3.95 (*s*)	56.17 (CH_3)	3.95 (*s*)	56.1 (CH_3)
8a	-	113.93 (C)	-	113.6 (C)
9	1.48 (*d*, 6.3)	20.69 (CH_3)	1.48 (*d*, 6.1)	20.7 (CH_3)

[a] Dimitriadis *et al.*, 1997.

Table 90 The HMBC, COSY and NOE data of **N21** in $CDCl_3$

Position	HMBC	COSY	NOE
H-3	-	H-4, Me-9	H-4, Me-9
H-4	C-3, C-4a, C-5, C-8a	H-3	H-3, H-5, Me-9
H-5	C-4, C-7, C-8a	H-6	H-4, H-6
H-6	C-4a, C-8	H-5, H-7	H-5, H-7
H-7	C-5, C-8a	H-6	H-6, 8-OCH_3
8-OCH_3	C-8	-	H-7
Me-9	C-3, C-4	H-3	H-3, H-4

4.3.2 Compound N32

N32 was obtained as a yellow solid and melted at 232.0-232.7 °C. The UV and IR spectra were almost identical to those of **N15**. The ^{1}H NMR spectral data (**Figure 55**) (**Table 91**) were similar to those of **N15** except for the presence of two *ortho*-coupled aromatic protons [δ_H 7.56 (*d*, *J* = 9.0 Hz, 1H) and 6.84 (*d*, *J* = 9.0 Hz, 1H)] which were attributed to H-6 and H-7, respectively, on the basis of HMBC correlations of H-6/C-4a (δ_C 134.24), C-5 (δ_C 142.48) and C-8 (δ_C 159.00) and those of H-7/C-1 (δ_C 169.00), C-5, C-8 and C-8a (δ_C 106.70) (**Table 92**). Since there are no other signals, the substituent at C-5 must be a hydroxyl group. The resonance effect of 8-OH caused higher field shift of C-5. The observed optical rotation of **N32** ($[\alpha]_D^{27}$ -70.11, c = 1.65, MeOH) was almost identical to that of (*R*)-(-)-5-hydroxymellein ($[\alpha]_D^{20}$ -72.00, c = 1.65, MeOH) (Devys *et al.*, 1994), indicating that they possessed the same absolute configuration. Therefore, **N32** was assigned as (*R*)-(-)-5-hydroxymellein, which was previously isolated from *Botryosphaeria obtusa* (Venkatasubbbaiah and Chilton, 1990).

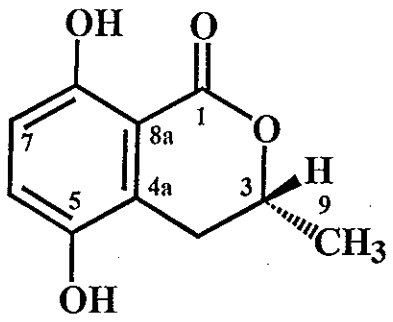

Table 91 The NMR data of **N32** in CD_3OD and **(*R*)-(-)-5-hydroxymellein** in acetone-d_6

Position	N32		(*R*)-(-)-5-Hydroxymellein [a]
	δ_H (mult., J_{Hz})	δ_C (C-Type)	δ_H (mult., J_{Hz})
1	-	169.00 (C=O)	-
3	4.73 (*m*)	76.43 (CH)	4.74 (*m*)
4	a: 3.38 (*dd*, 15.0, 3.0) b: 2.80 (*dd*, 15.0, 9.0)	28.94 (CH_2)	a: 3.18 (*dd*, 17.0, 3.0) b: 2.63 (*dd*, 17.0, 11.0)
4a	-	134.24 (C)	-
5-OH	-	142.48 (C)	8.35 (*brs*)

Table 91 Continued

Position	N32		(*R*)-(-)-5-Hydroxymellein [a]
	δ_H (mult., J_{Hz})	δ_C (C-Type)	δ_H (mult., J_{Hz})
6	7.56 (*d*, 9.0)	131.12 (CH)	7.10 (*d*, 9.0)
7	6.84 (*d*, 9.0)	115.27 (CH)	6.69 (*d*, 9.0)
8-OH	-	159.00 (C)	10.30 (*s*)
8a	-	106.70 (C)	-
9	1.50 (*d*, 6.0)	19.56 (CH_3)	1.48 (*d*, 7.0)

[a] Venkatasubbaiah and Chilton, 1990.

Table 92 The HMBC, COSY and NOE data of **N32** in CD_3OD

Position	HMBC	COSY	NOE
H-3	-	H_{ab}-4, Me-9	H_{ab}-4, Me-9
H_a-4	C-4a, C-5, C-8a, C-9	H-3, H_b-4	H-3, H_b-4, Me-9
H_b-4	C-3, C-4a, C-5, C-8a, C-9	H-3, H_a-4	H-3, H_a-4, Me-9
H-6	C-4a, C-5, C-8	H-7	H-7
H-7	C-1, C-5, C-8, C-8a	H-6	H-6
Me-9	C-3, C-4	H-3	H-3, H_{ab}-4

4.3.3 Compound N31

N31 was obtained as a white solid and melted at 245.5-246.3 °C with $[\alpha]_D^{27}$ -52.55 (c = 0.02, MeOH). The UV and IR spectra were almost identical to those of **N32**. The ^{1}H NMR spectral data (**Figure 58**) (**Table 93**) were similar to those of **N32** with the difference in the chemical shift of H-6. The signal of H-6 (δ_H 7.90, *d*, J = 8.7 Hz) in **N31** appeared at much lower field than that (δ_H 7.56, *d*, J = 9.0 Hz) in **N32**. The ^{13}C NMR spectrum (**Figure 59**) (**Table 93**) displayed two carbonyl carbons at δ_C 170.16 and 166.91. The carbon resonance at δ_C 170.16 was assigned as C-1 on the basis of HMBC correlations of H-7 (δ_H 6.84, *d*, J = 8.7 Hz)/C-1, C-5 (δ_C 128.00) and C-8a (δ_C 107.79) (**Table 94**). These results indicated the presence of a carboxyl group at C-5. The LREI-MS (**Figure 57**) showed the molecular formula $C_{11}H_{10}O_5$, supporting the attachment of the carboxyl group at C-5. Therefore, **N31** was assigned

as 5-carboxymellein, which was previously isolated from *Halorosellinia oceanica* (Chinworrungsee *et. al.*, 2001).

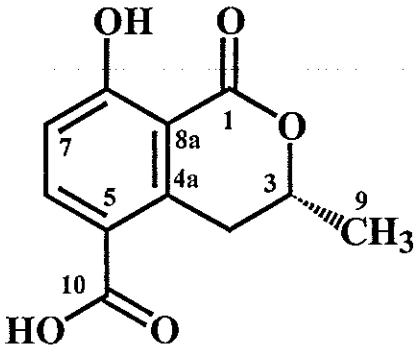

Table 93 The NMR data of **N31** in CD_3OD and **5-carboxymellein** (δ_H in acetone-d_6, δ_C in DMSO-d_6)

Position	N31		5-Carboxymellein	
	δ_H (mult., J_{Hz})	δ_C (C-Type)	δ_H[a] (mult., J_{Hz})	δ_C[b] (C-Type)
1	-	170.61 (C=O)	-	169.5 (C=O)
3	4.68 (*m*)	76.08 (CH)	4.60 (*m*)	75.4 (CH)
4	a: 3.74 (*dd*, 17.4, 3.3) b: 2.97 (*dd*, 17.4, 11.7)	32.59 (CH_2)	a: 3.70 (*m*) b: 2.90 (*m*)	32.2 (CH_2)
4a	-	139.70 (C)	-	143.4 (C)
5	-	128.00 (C)	-	120.1 (C)
6	7.90 (*d*, 8.7)	137.14 (CH)	7.96 (*d*, 8.0)	138.4 (CH)
7	6.84 (*d*, 8.7)	114.65 (CH)	6.86 (*d*, 8.0)	115.5 (CH)
8-OH	-	162.82 (C)	11.60 (*brs*)	163.9 (C)
8a	-	107.79 (C)	-	109.1 (C)
9	1.49 (*d*, 6.3)	19.58 (CH_3)	1.46 (*d*, 6.0)	20.4 (CH_3)
10	-	166.91 (C=O)	-	167.2 (C=O)

[a] Anderson *et al.*, 1983.
[b] Chinworrungsee *et al.*, 2001.

Table 94 The HMBC, COSY and NOE data of **N31** in CD_3OD

Position	HMBC	COSY	NOE
H-3	-	H_{ab}-4, Me-9	H_{ab}-4, Me-9
H_a-4	C-4a, C-5, C-8a, C-9	H-3, H_b-4	H-3, H_b-4, Me-9
H_b-4	C-3, C-4a, C-5, C-8a, C-9	H-3, H_a-4	H-3, H_a-4, Me-9

Table 94 Continued

Position	HMBC	COSY	NOE
H-6	C-4a, C-5, C-8	H-7	H-7
H-7	C-1, C-5, C-8, C-8a	H-6	H-6
Me-9	C-3, C-4	H-3	H-3, H_{ab}-4

4.3.4 Compound N23

N23 was obtained as a white solid and melted at 259.7-260.5 °C. The UV spectrum showed a maximum absorption band at λ_{max} 237 nm. The IR spectrum exhibited absorption bands due to hydroxyl (3393 cm^{-1}), ester carbonyl (1736 cm^{-1}), 5-membered lactam carbonyl (1698 cm^{-1}) and ketone carbonyl (1642 cm^{-1}) groups. The ester carbonyl, 5-membered lactam carbonyl and ketone carbonyl resonances at δ_C 169.73 (C-30), 174.53 (C-1) and 210.41 (C-17), respectively, in ^{13}C NMR spectrum (**Figure 61**) (**Table 95**) supported the IR data. The ^1H NMR spectral data (**Figure 60**) (**Table 95**) were similar to those of **N6** except for the splitting pattern of phenyl protons and an additional signal of the methyl protons (δ_H 2.18, *s*, 3H) of an acetoxyl group. **N23** possessed a monosubstituted benzene ring instead of 4-methoxybenzene ring in **N6**, according to the characteristic proton resonances of the monosubstituted benzene, [δ_H 7.28 (*m*, 1H), 7.23 (*m*, 2H) and 7.12 (*dd*, J = 6.6, 1.5 Hz, 2H)]. HMBC correlations (**Table 96**) of the oxymethine proton, H-21 (δ_H 5.74, *t*, J = 2.4 Hz), with C-1, C-4 (δ_C 50.65), C-8 (δ_C 45.15), C-19 (δ_C 127.68) and C-30, that of methyl protons, Me-31 (δ_H 2.18), with C-30 and the ^1H chemical shift of H-21 linked the acetoxyl group at C-21 (δ_C 75.85). Irradiation of H-21 enhanced signal intensity of H-13 (δ_H 5.77, *dd*, J = 15.6 and 9.6 Hz), indicating that they were located at the same α-face. In addition, the remaining absolute configuration was identical to that in **N6** according to NOEDIFF experiment (**Table 96**). **N23** gave almost identical optical rotation to that of cytochalasin O, $[\alpha]_D^{27}$ of **N23** = -38.20 (c = 0.80, MeOH) and $[\alpha]_D^{20}$ of cytochalasin O = -39.00 (c = 0.80, MeOH) (Merifield and Thomas, 1999). Therefore, **N23** was assigned as cytochalasin O which was previously isolated from *Hypoxylon terricola* Mill (Edwards *et al.*, 1989).

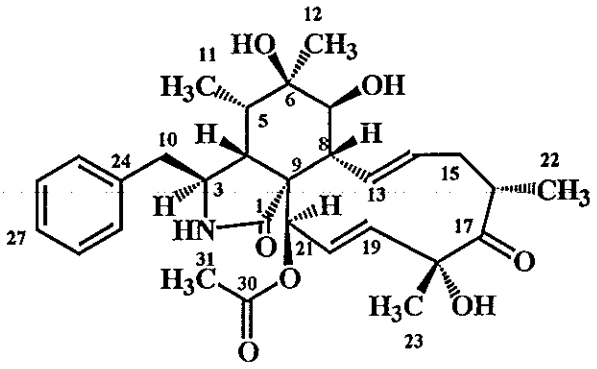

Table 95 The NMR data of **N23** and **cytochalasin O** in $CDCl_3$

Position	N23		Cytochalasin O
	δ_H (mult., J_{Hz})	δ_C (C-Type)	δ_H[a] (mult., J_{Hz})
1	-	174.53 (C=O)	-
2-NH	5.67 (*s*)	-	5.74 (*s*)
3	3.53 (*brt*, 8.4)	54.08 (CH)	3.54 (*m*)
4	2.05 (*dd*, 5.7, 2.4)	50.65 (CH)	2.19-1.97 (*m*)
5	1.66 (*m*)	36.82 (CH)	2.19-1.97 (*m*)
6	-	57.04 (C)	-
7	2.67 (*d*, 5.7)	62.54 (CH)	3.07-2.88 (*m*)
8	2.47 (*dd*, 9.9, 5.7)	45.15 (CH)	3.07-2.88 (*m*)
9	-	55.09 (C)	-
10	2.73 (*d*, 7.2)	45.88 (CH_2)	3.07-2.88 (*m*)
11	0.83 (*d*, 7.2)	12.55 (CH_3)	1.05 (*d*, 7.5)
12	1.13 (*s*)	19.58 (CH_3)	1.22 (*s*)
13	5.77 (*dd*, 15.6, 9.6)	130.86 (CH)	5.59 (*dd*, 15.0, 9.0)
14	5.20 (*ddd*, 15.6, 10.8, 4.8)	131.80 (CH)	5.32 (*ddd*, 15.0, 11.0, 5.0)
15	a: 2.40 (*m*) b: 1.90 (*m*)	37.92 (CH_2)	a: 2.59-2.44 (*m*) b: 2.19-1.97 (*m*)
16	2.65 (*m*)	42.28 (CH)	2.74 (*m*)
17	-	210.41 (C=O)	-
18	-	77.76 (C)	-
19	5.07 (*dd*, 15.6, 2.4)	127.68 (CH)	5.15 (*dd*, 15.0, 2.0)
20	6.03 (*dd*, 15.6, 2.4)	131.84 (CH)	6.15 (*dd*, 16.0, 3.0)
21	5.74 (*t*, 2.4)	75.85 (CH)	5.49 (*m*)
22	1.14 (*d*, 6.6)	19.31 (CH_3)	1.19 (*d*, 7.5)
23	1.45 (*s*)	24.23 (CH_3)	1.50 (*s*)
24	-	136.97 (C)	-
25, 29	7.12 (*dd*, 6.6, 1.5)	129.16 (CH)	7.36-7.10 (*m*)
26, 28	7.23 (*m*)	127.14 (CH)	7.36-7.10 (*m*)
27	7.28 (*m*)	128.97 (CH)	7.36-7.10 (*m*)
30	-	169.73 (C=O)	-
31	2.18 (*s*)	20.76 (CH_3)	2.23 (*s*)

[a] Merifield and Thomas, 1999.

Table 96 The HMBC, COSY and NOE data of **N23** in $CDCl_3$

Position	HMBC	COSY	NOE
2-NH	C-3, C-9	-	-
H-3	C-1, C-5	H-4, H_2-10	Me-11
H-4	C-3, C-5, C-6, C-9, C-10, C-21	H-3, H-5	-
H-5	C-3, C-4, C-6, Me-11, Me-12	H-4, Me-11	H-4
H-7	C-6, C-8, Me-12	H-8	-
H-8	C-1, C-7, C-9, C-13, C-14, C-21	H-7, H-13	-
H_2-10	C-3, C-4, C-24, C-25, C-29	H-3	-
Me-11	C-4, C-5, C-6	H-5	H-3, H-5, Me-12
Me-12	C-5, C-6, C-7	-	-
H-13	C-7, C-14, C-15	H-8, H-14	H-7, H_b-15
H-14	C-8, C-15	H-13, H_a-15, H_b-15	H-8, H_b-15, H-16
H_a-15	C-13, C-14, C-16, C-17, C-22	H-14, H_b-15	-
H_b-15	C-13, C-14, C-16, C-17, C-22	H-14, H_a-15	-
H-16	C-15, C-22	Me-22	-
H-19	C-17, C-18, C-20, C-21, C-23	H-20, H-21	-
H-20	C-18, C-19, C-21	H-19, H-21	H-21
H-21	C-1, C-4, C-8, C-9, C-18, C-19, C-20, C-30	H-19, H-20	H-4, H-13, H-20
Me-22	C-15, C-16, C-17	H-16	-
Me-23	C-17, C-18, C-19, C-20	-	-
H-25, H-29	C-10, C-26, C-27, C-28	H-26, H-28	-
H-26, H-28	C-24, C-25, C-29	H-25, H-29	-
H-27	C-25	-	-
Me-31	C-30	-	Me-11, H-21

4.3.5 Compound N22

N22 was obtained as a white solid and melted at 267.0-267.3 °C. The UV and IR spectra were almost identical to those of **N23**. The ^1H NMR spectral data (**Figure 62**) (**Table 97**) were similar to those of **N23** except that the singlet methyl signal (δ_H 1.13) in **N23** was replaced, in **N22**, by signals of two geminal olefinic protons, H_{ab}-12 (δ_H 5.30, *brs* and 5.09, *brs*). These indicated that the gem-disubstituted alkene moiety was connected to C-6 (δ_C 147.58). HMBC correlations (**Table 98**) of H_{ab}-12 with C-5 (δ_C 32.67), C-6 and C-7 (δ_C 69.84) supported the assignment. The observed optical rotation of **N22** ($[\alpha]_D^{27}$ -31.05, c = 0.33, $CHCl_3$) was almost identical to that of cytochalasin D ($[\alpha]_D^{20}$ -28.00, c = 0.33, $CHCl_3$)

(Merifield and Thomas, 1999), indicating that they possessed the same absolute configuration. Therefore, **N22** was assigned as cytochalasin D which was previously isolated from *Hypoxylon terricola* Mill (Edwards *et al.*, 1989).

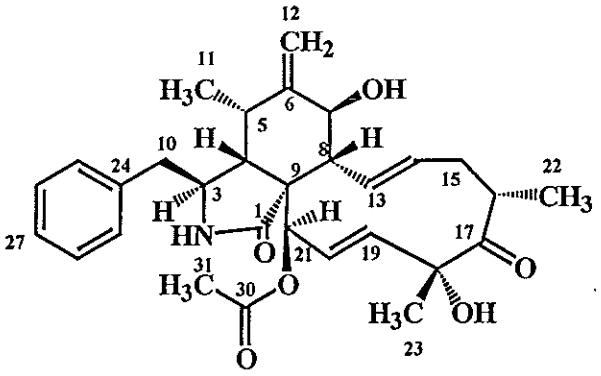

Table 97 The NMR data of **N22** and **cytochalasin D** in $CDCl_3$

Position	N22		Cytochalasin D	
	δ_H (mult., J_{Hz})	δ_C (C-Type)	δ_H[a] (mult., J_{Hz})	δ_C[b] (C-Type)
1	-	173.50 (C=O)	-	174.9 (C=O)
2-NH	5.60 (*brs*)	-	5.52 (*s*)	-
3	3.24 (*m*)	53.57 (CH)	3.23 (*m*)	54.0 (CH)
4	2.15 (*dd*, 6.6, 3.6)	50.00 (CH)	2.16 (*m*)	50.0 (CH)
5	2.75 (*m*)	32.67 (CH)	2.89-2.63 (*m*)	33.1 (CH)
6	-	147.58 (C)	-	151.4 (C)
7	3.81 (*d*, 10.8)	69.84 (CH)	3.81 (*d*, 11.0)	71.2 (CH)
8	2.85 (*m*)	47.00 (CH)	2.89-2.63 (*m*)	47.8 (CH)
9	-	50.90 (C)	-	54.4 (C)
10	a: 2.83 (*m*) b: 2.68 (*m*)	45.29 (CH_2)	2.89-2.63 (*m*)	45.5 (CH_2)
11	0.94 (*d*, 6.6)	13.65 (CH_3)	0.96 (*d*, 7.0)	13.6 (CH_3)
12	a: 5.30 (*brs*) b: 5.09 (*brs*)	114.43 (CH_2)	a: 5.40-5.27 (*m*) b: 5.14 (*m*)	112.2 (CH_2)
13	5.69 (*dd*, 15.6, 9.9)	130.61 (CH)	5.70 (*m*)	132.1 (CH)
14	5.34 (*ddd*, 15.6, 10.5, 4.8)	134.12 (CH)	5.40-5.27 (*m*)	132.7 (CH)
15	a: 2.51 (*dd*, 12.6, 10.5) b: 2.02 (*dd*, 12.6, 4.8)	37.75 (CH_2)	a: 2.52 (*q*, 11.0) b: 2.02 (*dd*, 13.0, 4.0)	38.6 (CH_2)
16	2.74 (*m*)	42.34 (CH)	2.89-2.63 (*m*)	42.4 (CH)
17	-	210.27 (C=O)	-	210.7 (C=O)
18-OH	-	77.12 (C)	-	78.3 (C)
19	5.14 (*dd*, 15.6, 2.4)	127.63 (CH)	5.14 (*m*)	127.7 (CH)
20	6.10 (*dd*, 15.6, 2.4)	132.30 (CH)	6.12 (*dd*, 16.0, 3.0)	133.7 (CH)

Table 97 Continued

Position	N22		Cytochalasin D	
	δ_H (mult., J_{Hz})	δ_C (C-Type)	δ_H[a] (mult., J_{Hz})	δ_C[b] (C-Type)
21	5.63 (*t*, 2.4)	77.71 (CH)	5.70 (*m*)	77.9 (CH)
22	1.20 (*d*, 6.9)	19.37 (CH_3)	1.20 (*d*, 7.0)	19.4 (CH_3)
23	1.51 (*s*)	24.18 (CH_3)	1.50 (*s*)	24.6 (CH_3)
24	-	137.23 (C)	-	138.3 (C)
25, 29	7.13 (*dd*, 8.1, 1.5)	129.09 (CH)	7.37-7.10 (*m*)	129.9 (CH)
26, 28	7.27 (*m*)	127.09 (CH)	7.37-7.10 (*m*)	126.8 (CH)
29	7.32 (*td*, 8.1, 1.5)	128.93 (CH)	7.37-7.10 (*m*)	128.7 (CH)
30	-	169.68 (C=O)	-	170.3 (C=O)
31	2.26 (*s*)	20.82 (CH_3)	2.27 (*s*)	20.6 (CH_3)

[a] Merifield and Thomas, 1999.
[b] Steyn *et al.*, 1982.

Table 98 The HMBC, COSY and NOE data of **N22** in $CDCl_3$

Position	HMBC	COSY	NOE
H-3	C-1, C-4	H-4, H_{ab}-10	H_{ab}-10, Me-11, H-25, H-29
H-4	C-1, C-3, C-5, C-6, C-10, C-11, C-21	H-3, H-5	H-3, H_{ab}-10, Me-11
H-5	C-4, C-11	H-4	-
H-7	C-5, C-6, C-12, C-13	H-8	H_a-12, H-13
H-8	C-1, C-6, C-7, C-13, C-14, C-21	H-7, H-13	-
H_a-10	C-3	H-3, H_b-10	-
H_b-10	C-3, C-4, C-24, C-25, C-29	H-3, H_a-10	-
Me-11	C-4, C-5, C-6	H-5	H-3, H-4, H-5, H_b-12
H_a-12	C-5, C-6, C-7	-	H-7, H-8, H_b-12
H_b-12	C-5, C-6, C-7	-	Me-11, H_a-12
H-13	C-8, C-14, C-15	H-8, H-14	H-7, H-20
H-14	C-8, C-15	H-13, H_a-15, H_b-15	H-8, H_b-15
H_a-15	C-13, C-14, C-16, C-17, C-22	H-14, H_b-15, H-16	H-13, H_b-15
H_b-15	C-13, C-14, C-16, C-17, C-22	H-14, H_a-15	H-14, H_a-15, H-16, Me-22
H-16	C-22	H_a-15, Me-22	-
H-19	C-18, C-20, C-23	H-20, H-21	Me-23, Me-31
H-20	C-18, C-19, C-21	H-19, H-21	H-21
H-21	C-1, C-4, C-8, C-19, C-20, C-30	H-19, H-20	H-4, H-20

Table 98 Continued

Position	HMBC	COSY	NOE
Me-22	C-15, C-16, C-17	H-16	H_b-15, H-16
Me-23	C-17, C-18, C-19	-	H-16, H-19
H-25, H-29	C-24, C-26, C-27, C-28	-	-
H-26, H-28	C-26, C-27, C-28	-	-
H-27	C-25, C-26, C-28, C-29	-	-
Me-31	C-30	-	-

4.3.6 Compound N24

N24 was obtained as a colorless gum. The UV and IR spectra were almost identical to those of **N22**. The ^{1}H NMR spectral data (**Figure 64**) (**Table 99**) were similar to those of **N22** with the difference in chemical shift of the oxymethine proton, H-21 (δ_H 4.07, *brs*), and the absence of the methyl signal of the acetoxyl group. These indicated that the acetoxyl group in **N22** was replaced, in **N24**, by a hydroxyl group. The appearance of H-21 in **N24** at much higher field confirmed the above conclusion. The observed optical rotation of **N24** ($[\alpha]_D^{27}$ +23.70, c = 0.23, EtOH) was almost identical to that of zygosporin D ($[\alpha]_D^{25}$ +20.60, c = 0.23, EtOH), indicating that they possessed the same absolute configuration. Therefore, **N24** was assigned as zygosporin D which was previously isolated from *Metarrhizium anisopliae* (Fujii *et al.*, 2000).

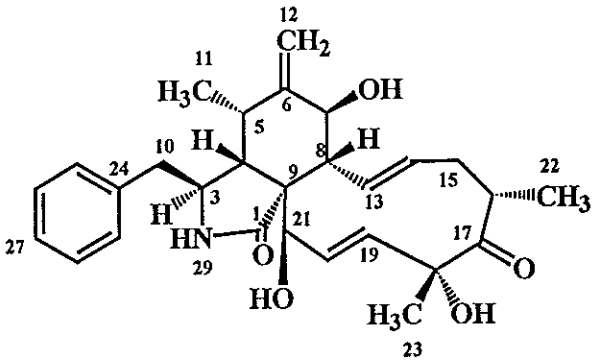

Table 99 The NMR data of **N24** and **zygosporin D** in $CDCl_3$

Position	N24		Zygosporin D[a]	
	δ_H (mult., J_{Hz})	δ_C (C-Type)	δ_H (mult., J_{Hz})	δ_C (C-Type)
1	-	175.00 (C=O)	-	175.0 (C=O)
2-NH	5.45 (*brs*)	-	5.53 (*s*)	-
3	3.29 (*ddd*, 8.5, 4.5, 4.0)	53.48 (CH)	3.29 (*ddd*, 8.3, 4.3, 3.8)	53.5 (CH)
4	2.56 (*m*)	50.22 (CH)	2.57 (*m*)	50.0 (CH)
5	1.90 (*m*)	32.91 (CH)	2.90-2.80 (*m*)	32.9 (CH)
6	-	148.22 (C)	-	148.1 (C)
7	3.79 (*d*, 10.5)	69.76 (CH)	3.79 (*d*, 10.7)	69.7 (CH)
8	2.84 (*t*, 10.5)	45.64 (CH)	2.83 (*dd*, 10.7, 10.2)	45.6 (CH)
9	-	54.32 (C)	-	54.2 (C)
10	a: 2.88 (*dd*, 14.0, 4.0) b: 2.57 (*m*)	45.39 (CH_2)	a: 2.88 (*dd*, 13.6, 3.5) b: 2.55 (*m*)	45.3 (CH_2)
11	1.10 (*d*, 6.5)	13.81 (CH_3)	1.11 (*d*, 6.8)	13.9 (CH_3)
12	a: 5.31 (*s*) b: 5.11 (*s*)	113.99 (CH_2)	a: 5.31 (*s*) b: 5.11 (*s*)	114.0 (CH_2)
13	5.65 (*dd*, 15.0, 10.5)	131.09 (CH)	5.65 (*dd*, 15.9, 10.2)	127.0 (CH)
14	5.27 (*ddd*, 15.0, 11.0, 5.5)	133.67 (CH)	5.27 (*ddd*, 15.9, 10.8, 5.4)	130.9 (CH)
15	a: 2.48 (*ddd*, 13.0, 11.5, 11.0) b: 2.00 (*ddd*, 13.0, 5.5, 2.0)	37.72 (CH_2)	a: 2.48 (*ddd*, 13.0, 11.0, 10.8) b: 2.00 (*ddd*, 13.0, 5.4, 1.6)	37.7 (CH_2)
16	2.72 (*ddq*, 11.5, 2.0, 6.5)	42.37 (CH)	2.72 (*ddq*, 11.0, 1.6, 6.5)	42.3 (CH)
17	-	210.00 (C=O)	-	210.2 (C=O)
18-OH	4.71 (*brs*)	77.21 (C)	-	77.7 (C)
19	5.42 (*dd*, 16.0, 2.5)	127.16 (CH)	5.41 (*dd*, 16.2, 2.6)	133.7 (CH)
20	6.21 (*dd*, 16.0, 2.5)	137.01 (CH)	6.21 (*dd*, 16.2, 2.4)	137.1 (CH)
21	4.07 (*brs*)	76.52 (CH)	4.05 (*dd*, 2.6, 2.4)	76.4 (CH)
22	1.19 (*d*, 6.5)	19.38 (CH_3)	1.19 (*d*, 6.8)	19.4 (CH_3)
23	1.54 (*s*)	24.24 (CH_3)	1.55 (*s*)	24.2 (CH_3)
24	-	137.32 (C)	-	137.3 (C)
25, 29	7.12 (*d*, 7.0)	129.19 (CH)	7.12 (*m*)	129.2 (CH)
26, 28	7.25 (*m*)	127.15 (CH)	7.26 (*m*)	127.1 (CH)
27	7.31 (*t*, 7.0)	128.90 (CH)	7.32 (*m*)	128.9 (CH)

[a] Fujii *et al.*, 2000.

Table 100 The HMBC, COSY and NOESY data of **N24** in $CDCl_3$

Position	HMBC	COSY	NOESY
2-NH	C-3, C-4, C-9	-	-
H-3	C-4, C-5	H-4, H_{ab}-10	H_a-10, Me-11
H-4	C-3, C-5, C-8, C-9, C-10	-	Me-11
H-5	-	-	-
H-7	C-6, C-12, C-13	H-8	-
H-8	C-1, C-7, C-9, C-13, C-14, C-21	H-7, H-13	-
H_a-10	-	H-3, H_b-10	-
H_b-10	C-3, C-4, C-25, C-29	H-3, H_a-10	-
Me-11	C-4, C-5, C-6	H-5	H-3, H_a-10
H_a-12	C-5, C-7	-	H_b-12
H_b-12	C-5, C-7	-	Me-11, H_a-12
H-13	C-8, C-15	H-8, H-14	-
H-14	C-8, C-15	H-13, H_a-15, H_b-15	H_b-15
H_a-15	C-13, C-14, C-16, C-22	H-14, H_b-15, H-16	H_b-15
H_b-15	C-13, C-14, C-16, C-22	H-14, H_a-15	H_a-15
H-16	C-17, C-22	H_a-15, Me-22	Me-22
H-19	C-18, C-20, C-21	H-20, H-21	Me-23
H-20	C-18, C-21	H-19, H-21	-
H-21	-	-	H-13, H_a-15, H-20
Me-22	C-15, C-16, C-17	H-16	H_b-15, H-16
Me-23	C-17, C-18, C-19	-	H-16
H-25, H-29	C-10, C-27	H-26	-
H-26, H-28	C-24, C-25	H-25, H-27	-
H-27	-	-	-

4.3.7 Compound N26

N26 was obtained as a colorless gum with $[\alpha]_D^{27}$ -19.17 (c = 0.90, $CHCl_3$). The UV spectrum showed maximum absorption bands at 223, 251 and 334 nm, indicating the presence of a conjugation chromophore. Its IR spectrum showed absorption bands at 3371 and 1686 cm^{-1} for hydroxyl and carbonyl groups, respectively. The HREI-MS showed the molecular formula $C_{13}H_{19}NO_4$. The ^1H NMR spectrum (**Figure 67**) (**Table 101**) showed signals for three aromatic protons of a 1,2,4-trisubstituted benzene [δ_H 7.81 (*d*, J = 8.1 Hz, 1H), 6.56 (*d*, J = 1.5 Hz, 1H) and 6.52 (*dd*, J = 8.1 and 1.5 Hz, 1H)], one oxymethine proton (δ_H 3.62, *dd*, J = 10.5 and 2.4 Hz, 1H), two nonequivalent methylene protons [δ_H 2.80 (*dd*, J = 13.5 and 2.4 Hz,

1H), and 2.50 (*dd*, J = 13.5 and 10.5 Hz, 1H)], one methoxyl group (δ_H 3.86, *s*, 3H) and two methyl groups (δ_H 1.29, *s*, 3H and 1.26, *s*, 3H). The aromatic protons at δ_H 7.81, 6.56 and 6.52 were attributed to H-6, H-3 and H-5, respectively, on the basis of their multiplicity and J values. The ester carbonyl resonance at δ_C 168.10 in the ^{13}C NMR spectrum (**Figure 68**) (**Table 101**) confirmed the presence of this functional group in the IR spectrum. ^3J HMBC correlations of both Me-13 (δ_H 3.86) and H-6 with C-12 (δ_C 168.10) indicated the presence of a methyl ester moiety at C-1 (δ_C 109.50). The COSY spectrum (**Table 101**) revealed that the oxymethine proton, H-8 (δ_H 3.62), was coupled with the nonequivalent methylene protons, H_{ab}-7 (δ_H 2.80 and 2.50). In the HMBC spectrum (**Table 101**), Me-10 (δ_H 1.29) and Me-11 (δ_H 1.26) correlated with C-8 (δ_C 78.62) and C-9 (δ_C 72.64), thus constructing a 2,3-dihydroxy-3-methylbutyl side chain. The attachment of this side chain at C-2 (δ_C 145.71) was established by HMBC correlations of H_{ab}-7/C-1, C-2 and C-3 (δ_C 117.15). The substituent at C-4 (δ_C 150.61) was then assigned as an amino group according to the chemical shift of C-4 and the molecular formula. Therefore, **N26** was determined as a new methyl aminobenzoate.

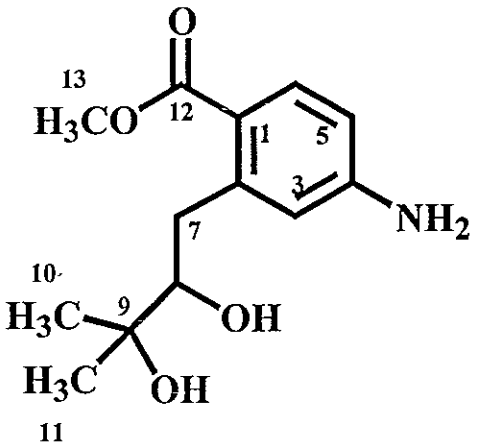

Table 101 The NMR data of **N26** in $CDCl_3$

Position	N26		HMBC	COSY	NOE
	δ_H (mult., J_{Hz})	δ_C (C-Type)			
1	-	109.50 (C)	-	-	-
2	-	145.71 (C)	-	-	-
3	6.56 (*d*, 1.5)	117.15 (CH)	C-1, C-4, C-5, C-7	H-5	H_{ab}-7, H-8
4	-	150.61 (C)	-	-	-
5	6.52 (*dd*, 8.1, 1.5)	117.40 (CH)	C-1, C-3, C-4, C-6, C-12	H-3, H-6	H-6
6	7.81 (*d*, 8.1)	131.70 (CH)	C-2, C-4, C-5, C-12	H-5	H-5
7	a: 2.80 (*dd*, 13.5, 2.4)	38.35 (CH_2)	C-2, C-3, C-8	H_b-7, H-8	H-3, H-8 Me-10, Me11
	b: 2.50 (*dd*, 13.5, 10.5)		C-2, C-3, C-8, C-9	H_a-7, H-8	H-3, Me-10, Me-11
8	3.62 (*dd*, 10.5, 2.4)	78.62 (CH)	C-2, C-9, C-10, C-11	H_{ab}-7,	H-3, H_a-7, Me-10
9	-	72.64 (C)	-	-	-
10	1.29 (*s*)	26.45 (CH_3)	C-8, C-9, C-11	-	H_{ab}-7, H-8
11	1.26 (*s*)	23.82 (CH_3)	C-8, C-9, C-10	-	H_{ab}-7, H-8
12	-	168.10 (C=O)	-	-	-
13	3.86 (*s*)	51.46 (CH_3)	C-12	-	-

4.3.8 Compound N28

N28 was obtained as a white solid and melted at 182.0-182.6 °C. The UV spectrum showed maximum absorption bands of a conjugation chromophore at 222, 236, 311 and 330 nm. Its IR spectrum showed an absorption band at 3392 cm^{-1} for a hydroxyl group. The LREI-MS (**Figure 69**) showed the molecular formula $C_{10}H_8N_2O$. The ^1H NMR spectral data (**Figure 70**) (**Table 102**) revealed characteristic signals of a 4-substituted quinoline [δ_H 8.86 (*d*, J = 4.5 Hz, 1H), 8.45 (*dd*, J = 8.4 and 1.2 Hz, 1H), 8.12 (*dd*, J = 8.4 and 1.2 Hz, 1H), 7.80 (*ddd*, J = 8.4, 6.6 and 1.2 Hz, 1H)], 7.72 (*d*, J = 4.5 Hz, 1H) and 7.64 (*ddd*, J = 8.4, 6.6 and 1.2 Hz, 1H)] and one downfield proton (δ_H 8.77, *s*). The ^{13}C NMR spectrum (**Figure 71**) (**Table 102**) showed one additional methine carbon (δ_C 150.04) apart from carbon resonances of the 4-substituted quinoline (δ_C 153.45, 152.02, 141.54, 133.78, 133.10, 131.37,

129.41, 128.10 and 123.05). These data together with the molecular formula established a substituent at C-4 to be a carboxaldehyde oxime. HMBC correlations (**Table 102**) of H-9 (δ_H 8.77) of the carboxaldehyde oxime with C-3 (δ_C 123.05), C-4 (δ_C 141.54) and C-4a (δ_C 129.41) together with signal enhancement of H-3 (δ_H 7.72) and H-5 (δ_H 8.45) upon irradiation of H-9 supported the assigned location of this functional group. Therefore, **N28** was assigned as 4-quinolinecarboxaldehyde oxime which was previously isolated from the genera of myxobacteria (Boehlendorf *et al.*, 1996).

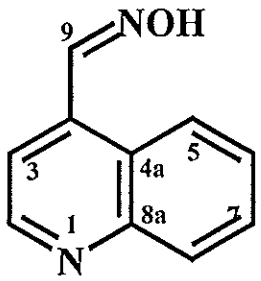

Table 102 The NMR data of **N28** in $CDCl_3$+CD_3OD

Position	N28		HMBC	COSY	NOE
	δ_H (mult., J_{Hz})	δ_C (C-Type)			
2	8.86 (*d*, 4.5)	153.45 (CH)	C-3, C-4, C-8a	H-3	H-3
3	7.72 (*d*, 4.5)	123.05 (CH)	C-2, C-4a, C-9	H-2	H-2, H-9
4	-	141.54 (C)	-	-	-
4a	-	129.41 (C)	-	-	-
5	8.45 (*dd*, 8.4, 1.2)	128.10 (CH)	C-4, C-7, C-4a, C-8a	H-6, H-7	H-6, H-9
6	7.64 (*ddd*, 8.4, 6.6, 1.2)	131.37 (CH)	C-4a, C-8	H-5, H-7, H-8	-
7	7.80 (*ddd*, 8.4, 6.6, 1.2)	133.78 (CH)	C-5, C-8a	H-5, H-6, H-8	-
8	8.12 (*dd*, 8.4, 1.2)	133.10 (CH)	C-4a, C-6	H-6, H-7	-
8a	-	152.02 (C)	-	-	
9	8.77 (*s*)	150.04 (CH)	C-3, C-4, C-4a	-	H-3, H-5

4.3.9 Compound N25

N25 was obtained as a yellow solid and melted at 102.5-102.9 °C. The UV and IR spectra were almost identical to those of **N28**. The ^{1}H NMR spectral data (**Figure 72**) (**Table 103**) were similar to those of **N28** except for the absence of carboxaldehyde oxime. Comparison of the ^{13}C NMR data (**Table 103**) with those of **N28** showed analogy of the chemical shifts except for those of C-4 (δ_C 118.80) and C-9 (δ_C 115.50). These suggested that the carboxadehyde oxime in **N28** was replaced by a cyano group in **N25**. This was confirmed by ^{3}J HMBC cross peaks (**Table 103**) of H-3 (δ_H 7.75, *d*, J = 4.5 Hz)/C-4a (δ_C 125.06) and C-9. Thus, **N25** was elucidated as a dehydration derivative of **N28** which was previously reported (Ferles *et al.*, 1979).

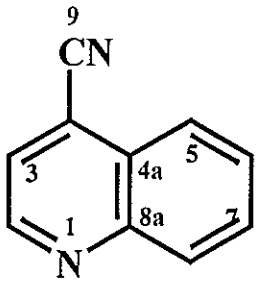

Table 103 The NMR data of **N25** in $CDCl_3$

Position	N25		HMBC	COSY
	δ_H (mult., J_{Hz})	δ_C (C-Type)		
2	9.06 (*d*, 4.5)	149.42 (CH)	C-3, C-4, C-8a	H-3
3	7.75 (*d*, 4.5)	124.79 (CH)	C-4a, C-9	H-2
4	-	118.80 (C)	-	-
4a	-	125.06 (C)	-	-
5	8.22 (*dd*, 8.5, 1.0)	124.98 (CH)	C-4, C-4a, C-7, C-8a	H-6, H-7
6	7.79 (*td*, 8.5, 1.0)	129.21 (CH)	C-4a, C-8	H-5, H-7, H-8
7	7.89 (*td*, 8.5, 1.0)	131.17 (CH)	C-5, C-8a	H-5, H-6, H-8
8	8.23 (*d*, 8.5, 1.0)	130.45 (CH)	C-4a, C-6	H-6, H-7
8a	-	148.20 (C)	-	-
9	-	115.50 (C)	-	-

4.3.10 Compound N27

N27 was obtained as a yellow gum. The UV spectrum showed maximum absorption bands at 222, 275 and 284 nm, indicating the presence of a conjugation chromophore. Its IR spectrum showed absorption bands at 3370 for amino and hydroxyl groups, 1675 and 1644 cm^{-1} for lactam carbonyl groups. The ^{1}H NMR spectral data (**Figure 74**) (**Table 104**) showed characteristic signals of a *para*-disubstituted aromatic protons [δ_H 7.08 (*d*, J = 8.5 Hz, 2H) and 6.80 (*d*, J = 8.5 Hz, 2H)], two methine protons [δ_H 4.22 (*dd*, J = 10.0 and 3.5 Hz, 1H) and 4.08 (*t*, J = 8.0 Hz, 1H)] and four methylene groups [δ_H 3.64 (*m*, 1H), 3.57 (*td*, J = 13.0 and 3.0 Hz, 1H), 3.51 (*dd*, J = 14.5 and 3.5 Hz, 1H), 2.74 (*dd*, J = 14.5 and 10.0 Hz, 1H), 2.34 (*m*, 1H), 2.02 (*m*, 1H), 1.97 (*m*, 1H) and 1.90 (*m*, 1H)]. The HMQC data together with integration suggested the signal at δ_H 5.70 (*s*) for NH group. In the ^{13}C NMR spectrum (**Figure 75**) (**Table 104**), signals of two lactam carbonyl carbons at δ_C 169.45 (C-2) and 165.13 (C-5) supported the IR data. These results together with HMBC cross peaks (**Table 105**) of 4-NH/C-3 (δ_C 56.23), C-5 (δ_C 165.13) and C-6 (δ_C 59.14) and H-6 (δ_H 4.08)/C-2 and C-7 (δ_C 28.35) established a diketopiperazine skeleton. In the COSY spectrum, H_{ab}-7 (δ_H 2.34 and 2.02) were coupled with H-6 and H_{ab}-8 (δ_H 1.97 and 1.90). H_{ab}-8 were further coupled with H_{ab}-9 (δ_H 3.64 and 3.57). Ring closure between the nitrogen atom (1-N) and C-9 (δ_C 45.42) to form a pyrrolidine was established according to the down-field chemical shift value of H_{ab}-9 and C-9. The COSY cross peaks (**Table 105**) of, H_{ab}-10 (δ_H 3.51 and 2.74) with H-3 (δ_H 4.22), HMBC cross peaks of H_b-10/C-3, C-11 (δ_C 127.57), C-12 and C-16 (δ_C 130.34) connected the *para*-hydroxybenzyl moiety with C-3 of the diketopiperazine skeleton. **N27** gave almost identical optical rotation to that of cyclo(L-Pro-L-Tyr), $[\alpha]_D^{27}$ of **N27** = -88.59 (c = 0.50, MeOH) and $[\alpha]_D^{30}$ of cyclo(L-Pro-L-Tyr) = -92.00 (c = 0.50, MeOH) (Arunrattiyakorn *et al.*, 2006). Therefore, **N27** was assigned as cyclo(L-Pro-L-Tyr) which was previously isolated from *Jaspis digonoxea*. (Rudi *et al.*, 1994).

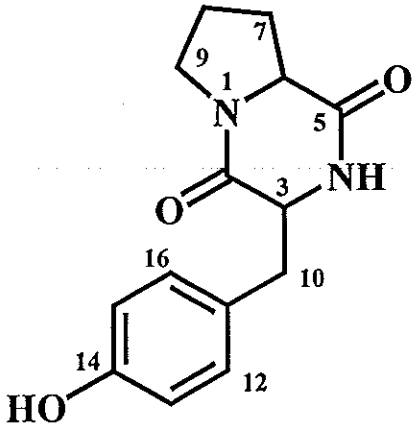

Table 104 The NMR data of **N27** and **cyclo(L-Pro-L-Tyr)** in $CDCl_3$

Position	N27		Cyclo(L-Pro-L-Tyr)	
	δ_H (mult., J_{Hz})	δ_C (C-Type)	δ_H[a] (mult., J_{Hz})	δ_C[b] (C-Type)
2	-	169.45 (C=O)	-	169.0 (C=O)
3	4.22 (*dd*, 10.0, 3.5)	56.23 (CH)	4.20 (*dd*, 9.8, 3.9)	59.3 (CH)
4-NH	5.70 (*s*)	-	-	-
5	-	165.13 (C=O)	-	165.0 (C=O)
6	4.08 (*t*, 8.0)	59.14 (CH)	4.06 (*m*)	59.5 (CH)
7	a: 2.34 (*m*)	28.35 (CH_2)	a: 2.30 (*m*)	28.3 (CH_2)
	b: 2.02 (*m*)		b: 1.92 (*m*)	
8	a: 1.97 (*m*)	22.52 (CH_2)	a: 1.98 (*m*)	22.2 (CH_2)
	b: 1.90 (*m*)		b: 1.89 (*m*)	
9	a: 3.64 (*m*)	45.42 (CH_2)	a: 3.61 (*m*)	45.2 (CH_2)
	b: 3.57 (*td*, 13.0, 3.0)		b: 3.53 (*m*)	
10	a: 3.51 (*dd*, 14.5, 3.5)	35.98 (CH_2)	a: 3.44 (*dd*, 14.5, 3.9)	36.2 (CH_2)
	b: 2.74 (*dd*, 14.5, 10.0)		b: 2.76 (*dd*, 14.5, 9.8)	
11	-	127.57 (C)	-	126.0 (C)
12, 16	7.08 (*d*, 8.5)	130.34 (CH)	7.02 (*d*, 8.6)	130.2 (CH)
13, 15	6.80 (*d*, 8.5)	116.15 (CH)	6.75 (*d*, 8.6)	116.0 (CH)
14-OH	-	155.26 (C)	6.95 (*s*)	156.0 (C)

[a] Arunrattiyakorn *et al.*, 2006.
[b] Rudi *et al.*, 1994.

Table 105 The HMBC, COSY and NOE data of **N27** in $CDCl_3$

Position	HMBC	COSY	NOE
H-3	C-5, C-10, C-11	H_{ab}-10	H_a-10, H-12, H-16
4-NH	C-3, C-5, C-6	-	-
H-6	C-2, C-7	H_{ab}-7	H_a-7
H_a-7	-	H-6, H_b-7, H_b-8	H-6, H_b-7, H_a-8
H_b-7	C-8, C-9	H_a-7, H_b-8, H_a-9	H-6, H_a-7
H_a-8	-	H_a-7, H_b-8, H_{ab}-9	H_{ab}-7, H_b-8
H_b-8	C-6, C-7, C-9	H_a-7, H_a-8, H_{ab}-9	H_a-8
H_a-9	C-3	H_{ab}-8, H_b-9	H_b-10
H_b-9	C-7, C-8	H_{ab}-8, H_a-9	H_b-10
H_a-10	-	H-3, H_b-10	H-3, H_b-10, H-12, H-16
H_b-10	C-3, C-5, C-11, C-12, C-16	H-3, H_a-10,	H_a-10, H-12, H-16
H-12, H-16	C-10, C-13, C-14, C-15	H-13, H-15	H-3, H_{ab}-10
H-13, H-15	C-11, C-14	H-12, H-16	H-12, H-16

4.3.11 Compound N29

N29 was obtained as a white solid and melted at 247.8-248.1 °C. The UV spectrum showed a maximum absorption band at 247 nm. The IR spectrum showed an absorption band at 3362 cm^{-1} for a hydroxyl group. The ^1H NMR spectral data (**Figure 76**) (**Table 106**) consisted of the signals for *trans*-olefinic protons [δ_H 5.23 (*dd, J* = 15.0 and 6.0 Hz, 1H) and 5.16 (*dd, J* = 15.0 and 6.0 Hz, 1H)], one olefinic protons of a trisubstituted alkene [δ_H 5.35 (*brd, J* = 3.0 Hz, 1H)], two oxymethine protons [δ_H 4.08 (*m*, 1H) and 3.63 (*brs*, 1H)], six methine protons [δ_H 2.06 (*m*, 1H), 1.97 (*m*, 1H), 1.92 (*m*, 1H), 1.87 (*m*, 1H), 1.48 (*m*, 1H) and 1.30 (*m*, 1H)], seven methylene groups [δ_H 2.14 (*dd, J* = 12.0 and 9.0 Hz, 1H), 1.87 (*m*, 1H), 1.78 (*m*, 2H), 1.66 (*m*, 2H), 1.58 (*m*, 2H), 1.55 (*m*, 2H), 1.44 (*m*, 1H), 1.33 (*m*, 1H) and 1.26 (*m*, 2H)] and six methyl groups [δ_H 1.09 (*s*, 3H), 1.02 (*d, J* = 9.0 Hz, 1H), 0.91 (*d, J* = 9.0 Hz, 1H), 0.84 (*d, J* = 6.0 Hz, 1H), 0.82 (*d, J* = 6.0 Hz, 1H) and 0.60 (*s*, 3H)]. The ^{13}C NMR spectrum (**Figure 77**) (**Table 106**) showed one sp^2 quaternary (δ_C 144.01), three sp^2 methine (δ_C 135.37, 132.19 and 117.54), one oxyquaternary (δ_C 75.97), two oxymethine (δ_C 73.67 and 67.74), six methine (δ_C 55.99, 54.76, 43.77, 42.81, 40.39 and 33.08), seven methylene (δ_C 39.45, 39.22, 32.96, 30.85, 29.69, 22.89

and 22.05), two quaternary (δ_C 43.45 and 37.15) and six methyl (δ_C 21.11, 19.95, 19.63, 18.83, 17.59 and 12.33) carbons. These signals indicated the presence of an ergostane-type side-chain with a 22*E*,24*R*-configuration (Migliuolo *et al.*, 1990 and Yue *et al.*, 2001). Two carbons of the trisubstituted alkene resonating in the sp^2 region at δ_C 117.54 and 144.01 were attributed to C-7 and C-8, respectively, on the basis of ^3J HMBC correlations (**Table 107**) of H-7 (δ_H 5.35)/C-5 (δ_C 75.97), C-9 (δ_C 43.77) and C-14 (δ_C 54.76). HMBC cross peaks of Me-18 (δ_H 1.09)/C-1 (δ_C 30.85), C-5 (δ_C 75.97) and C-9 (δ_C 43.77) and those of Me-19 (δ_H 0.60)/C-12 (δ_C 39.22), C-13 (δ_C 43.45), C-14 and C-17 (δ_C 55.99) supported the location of Me-18 and Me-19 at C-10 (δ_C 37.15) and C-13, respectively. The following COSY experiment (**Table 107**) confirmed the presence of 2-substituted-*E*-5,6-dimethylhepten-3-enyl side chain attached at C-17. The methine proton, H-20 (δ_H 2.06), was coupled with the methyl protons, Me-21 (δ_H 1.02). The *trans*-olefinic proton, H-22 (δ_H 5.16), was coupled with H-20 and the other *trans*-olefinic proton, H-23 (δ_H 5.23). The methine proton, H-24 (δ_H 1.87), was coupled with H-23, Me-28 (δ_H 0.91) and H-25 (δ_H 1.48). The methine proton, H-25, was coupled with H-24, Me-26 (δ_H 0.82) and Me-27 (δ_H 0.84). Since there was no other proton signal, the substituents at C-3 (δ_C 67.74), C-5 and C-6 (δ_C 73.67) must be hydroxyl groups. The ^{13}C chemical shifts of these carbons supported this assignment. Irradiation of H-20, in the NOEDIFF experiment (**Table 107**), enhanced the signal of Me-19, indicating their *cis*-relationship. Irradiation of Me-18 enhanced signal intensity of H_a-4 (δ_H 2.14), but not H-6 (δ_H 3.63) and further irradiation of H_a-4 affected Me-18, but not H-3 (δ_H 4.08). These indicated *cis* relationship of H_a-4/Me-18 and *trans* relationship of H_a-4/H-3 and Me-18/H-6. No signal enhancement of Me-19, upon irradiation of H-14 (δ_H 1.92), established *trans* relationship of H-14/Me-19. **N29** gave almost identical optical rotation to that of cerevisterol, $[\alpha]_D^{27}$ of **N29** = -77.75 (c = 0.16, pyridine) and $[\alpha]_D^{25}$ of cerevisterol = -75.00 (c = 0.16, pyridine). Thus, they had the same absolute configuration. Therefore, **N29** was assigned as cerevisterol which was previously isolated from *Spongionella gracilis* (Piccialli and Sica, 1987).

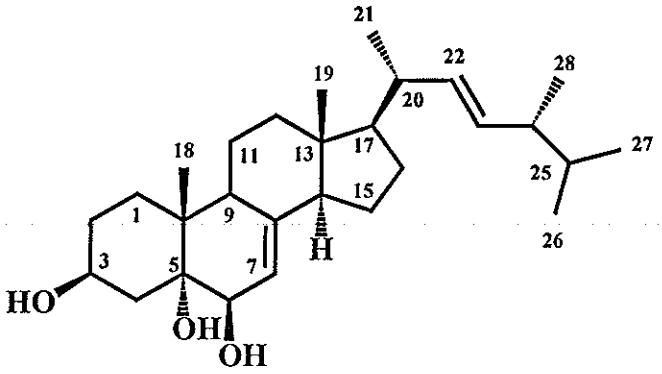

Table 106 The NMR data of **N29** and **cerevisterol** in $CDCl_3$

Position	N29		Cerevisterol[a]	
	δ_H (mult., J_{Hz})	δ_C (C-Type)	δ_H (mult., J_{Hz})	δ_C (C-Type)
1	1.66 (*m*)	32.96 (CH_2)	-	33.9 (CH_2)
2	a: 1.87 (*m*)	30.85 (CH_2)	-	32.6 (CH_2)
	b: 1.44 (*m*)			
3	4.08 (*m*)	67.74 (CH)	4.08 (*m*)	67.6 (CH)
4	a: 2.14 (*dd*, 12.0, 9.0)	39.45 (CH_2)	a: 2.14 (*dd*, 12.8, 12.8)	41.9 (CH_2)
	b: 1.78 (*m*)		b: 1.78 (*dd*, 12.8, 4.9)	
5	-	75.97 (C)	-	76.2 (C)
6	3.63 (*brs*)	73.67 (CH)	3.63 (*brs*)	74.3 (CH)
7	5.35 (*brd*, 3.0)	117.54 (CH)	5.35 (*brd*, 4.9)	120.5 (CH)
8	-	144.01 (C)	-	141.6 (C)
9	1.97 (*m*)	43.77 (CH)	-	43.8 (CH)
10	-	37.15 (C)	-	38.1 (C)
11	1.58 (*m*)	22.05 (CH_2)	-	22.5 (CH_2)
12	a: 1.78 (*m*)	39.22 (CH_2)	-	40.0 (CH_2)
	b: 1.33 (*m*)			
13	-	43.45 (C)	-	43.8 (C)
14	1.92 (*m*)	54.76 (CH)	-	55.3 (CH)
15	1.55 (*m*)	22.89 (CH_2)	-	23.5 (CH_2)
16	1.26 (*m*)	29.69 (CH_2)	-	28.5 (CH_2)
17	1.30 (*m*)	55.99 (CH)	-	56.2 (CH)
18	1.09 (*s*)	18.83 (CH_3)	1.08 (*s*)	18.8 (CH_3)
19	0.60 (*s*)	12.33 (CH_3)	0.59 (*s*)	12.6 (CH_3)
20	2.06 (*m*)	40.39 (CH)	-	40.8 (CH)
21	1.02 (*d*, 9.0)	21.11 (CH_3)	1.04 (*d*, 6.9)	21.5 (CH_3)
22	5.16 (*dd*, 15.0, 6.0)	135.37 (CH)	5.15 (*dd*, 14.8, 7.9)	136.2 (CH)
23	5.23 (*dd*, 15.0, 6.0)	132.19 (CH)	5.20 (*dd*, 14.8, 6.9)	132.2 (CH)
24	1.87 (*m*)	42.81 (CH)	-	43.2 (CH)
25	1.48 (*m*)	33.08 (CH)	-	33.4 (CH)
26	0.82 (*d*, 6.0)	19.63 (CH_3)	0.82 (*d*, 6.9)	20.2 (CH_3)
27	0.84 (*d*, 6.0)	19.95 (CH_3)	0.84 (*d*, 6.9)	19.9 (CH_3)
28	0.91 (*d*, 9.0)	17.59 (CH_3)	0.91 (*d*, 6.9)	17.9 (CH_3)

[a] Piccialli and Sica, 1987.

Table 107 The HMBC, COSY and NOE data of **N29** in $CDCl_3$

Position	HMBC	COSY	NOE
H_2-1	-	-	-
H_{ab}-2	C-2	H_2-1, H-3	-
H-3	C-2, C-4	H_{ab}-2, H_{ab}-4	-
H_a-4	C-3, C-5	-	Me-18
H_b-4	-	-	-
H-6	C-5, C-7, C-8, C-10	H-7	H-7
H-7	C-5, C-9, C-14	H-6, H-14	H-6
H-9	-	-	-
H_2-11	C-8, C-9, C-10	H-9, H_{ab}-12	-
H_{ab}-12	C-13, C-19	-	-
H-14	-	H-7, H_2-15	-
H_2-15	C-8, C-13	H-14, H_2-16	-
H_2-16	-	H_2-15, H-17	-
H-17	C-13, C-19, C-20	-	-
Me-18	C-1, C-5, C-9, C-10	-	H_a-4
Me-19	C-12, C-13,C-14, C-17	-	-
H-20	C-13	Me-21	H_b-12, Me-19, Me-21
	-	-	
Me-21	C-17, C-20, C-22	H-20	-
H-22	C-20, C-21	H-20, H-23	-
H-23	C-20, C-22, C-28	H-22, H-24	-
H-24	C-22, C-23, C-25, C-26, C-27, C-28	H-23, H-25, Me-28	-
H-25	C-24, C-28	H-24, Me-26, Me-27	-
Me-26	C-24, C-25	H-25	-
Me-27	C-24, C-25	H-25	-
Me-28	C-23, C-24, C-25	H-24	H-23

4.3.12 Compound N30

N30 was obtained as a white solid and melted at 311.2-311.8 °C. The UV spectrum showed a maximum absorption band at λ_{max} 258 nm. The IR spectrum exhibited absorption bands at 1657 and 1622 cm^{-1} for lactam carbonyl groups. The ^1H NMR spectrum (**Figure 78**) (**Table 108**) showed only signals for *cis*-olefinic protons [δ_H 7.40 (*d*, J = 7.5 Hz, 1H) and 5.62 (*d*, J = 7.5 Hz, 1H)]. The ^{13}C NMR spectrum (**Figure 79**) (**Table 108**) displayed two carbonyls (δ_C 164.98 and 151.18) and two methine carbons (δ_C 141.14 and 99.35). HMBC correlations (**Table 108**) of H-5 (δ_H

5.62)/C-4 (δ_C 164.98) and C-6 (δ_C 141.14) and those of H-6 (δ_H 7.40)/C-2 (δ_C 151.18), C-4 and C-5 (δ_C 99.35) indicated that **N30** was uracil which was previously isolated from *Tryblidiopycnis* sp. (Huang *et al.*, 2006).

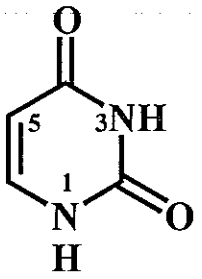

Table 108 The NMR data of **N30** in CD_3OD and **uracil** in DMSO-d_6

Position	N30		HMBC	Uracil[a]
	δ_H (mult., J_{Hz})	δ_C (C-Type)		δ_H (mult., J_{Hz})
1-NH	-	-	-	11.03 (*s*)
2	-	151.18	-	-
3-NH	-	-	-	10.84 (*brs*)
4	-	164.98	-	-
5	5.62 (*d*, 7.5)	99.35	C-4, C-6	5.44 (*d*, 7.0)
6	7.40 (*d*, 7.5)	141.14	C-2, C-4, C-5	7.38 (*d*, 7.0)

[a] Huang and Liu, 2002.

PART V

CHEMICAL CONSTITUENTS FROM THE ENDOPHYTIC FUNGUS *XYLARIA* SP. PSU-D14

CHAPTER 5.1
INTRODUCTION

5.1.1 Introduction

Chemical constituents of the genus *Xylaria* are summarized in Table 59. The endophytic fungus *Xylaria* sp. PSU-D14 was isolated from the leaves of *Garcinia dulcis*, collected in Songkhla Province, Thailand, in 2004. This fungus was deposited as PSU-D14 at the Department of Microbiology, Faculty of Science, Prince of Songkla University. The ethyl acetate extract from the culture broth of this endophytic fungus exhibited antifungal activity against *Candida albicans* ATCC90028 (CA) with the MIC value of 128 μg/ml.

CHAPTER 5.2
EXPERIMENTAL

5.2.1 Fermentation and extraction

The fermentation and extraction was performed using the same procedure as those of *Botryosphaeria mamane* PSU-M76. The crude EtOAc extracts from the culture broth and mycelia were obtained in 650.0 mg and 140.0 mg, respectively, both as a brown gum.

5.2.2 Purification of the broth extract

The broth extract showed many UV-active spots on normal phase TLC using 4% methanol in dichloromethane (2 runs) as a mobile phase. It was further separated by column chromatography over Sephadex LH20 using 100% MeOH as eluent. Fractions, which contained similar components, were combined and evaporated to dryness under reduced pressure to give eight fractions, as shown in **Table 109**.

Table 109 Fractions obtained from **the broth extract** by column chromatography over Sephadex LH20

Fraction	Eluent	Weight (mg)	Physical appearance
A	100% MeOH	4.6	Brown gum
B	100% MeOH	30.2	Brown gum
C	100% MeOH	204.3	Brown gum
D	100% MeOH	203.6	Brown gum mixed with yellow solid
E	100% MeOH	129.5	Brown gum mixed with yellow solid
F	100% MeOH	17.1	Yellow gum
G	100% MeOH	46.2	Brown solid
H	100% MeOH	13.1	Brown gum

Fraction A showed no UV-active spots on normal phase TLC using 4% methanol in dichloromethane (3 runs) as a mobile phase. Its ^{1}H NMR spectrum displayed proton signals at high field region. Thus, no attempted investigation was performed.

Fraction B demonstrated a long tail under UV-S using 4% methanol in dichloromethane (3 runs) as a mobile phase. In addition, its chromatogram showed many spots after dipping the normal phase TLC in ASA reagent and subsequently heating. It was further separated by column chromatography over Sephadex LH20 using 100% MeOH as eluent. All subfractions were examined by TLC, combined on the basis of their chromatogram characteristics and then evaporated to dryness under reduced pressure to afford three subfractions, as shown in **Table 110**.

Table 110 Subfractions obtained from **fraction B** by column chromatography over Sephadex LH20

Subfraction	Eluent	Weight (mg)	Physical appearance
B1	100% MeOH	6.7	Brown gum
B2	100% MeOH	19.7	Brown gum
B3	100% MeOH	2.8	Brown gum

Subfraction B1 showed no UV-active spots on normal phase TLC using 4% methanol in dichloromethane (2 runs) as a mobile phase and displayed no spots after dipping the normal phase TLC in ASA reagent and subsequently heating. Its ^{1}H NMR spectrum displayed proton signals at high field region. Therefore, further investigation was not conducted.

Subfraction B2 displayed many spots under UV-S on normal phase TLC using 4% methanol in dichloromethane (2 runs) as a mobile phase and showed many inseparable spots after dipping the normal phase TLC in ASA reagent and subsequently heating. The ^{1}H NMR data indicated that it contained many compounds. Thus, it was not further purified.

Subfraction B3 displayed no spots under UV-S on normal phase TLC using 4% methanol in dichloromethane (2 runs) as a mobile phase and displayed a long tail after dipping the normal phase TLC in ASA reagent and subsequently heating. The ^{1}H NMR spectrum demonstrated none of major components. Therefore, further investigation was not performed.

Fraction C contained many spots under UV-S on normal phase TLC using 2% methanol in dichloromethane (3 runs) as a mobile phase. It was further separated by column chromatography over Sephadex LH20 using 100% MeOH as eluent. All subfractions were examined by TLC, combined on the basis of their chromatogram characteristics and then evaporated to dryness under reduced pressure to afford four subfractions, as shown in **Table 111**.

Table 111 Subfractions obtained from **fraction C** by column chromatography over Sephadex LH20

Subfraction	Eluent	Weight (mg)	Physical appearance
C1	100% MeOH	13.0	Brown gum
C2	100% MeOH	34.0	Brown gum
C3	100% MeOH	128	Brown gum mixed with yellow solid
C4	100% MeOH	27.6	Brown gum

Subfraction C1 showed no UV-active spots on normal phase TLC using 4% methanol in dichloromethane (2 runs) as a mobile phase. The ^{1}H NMR spectrum displayed proton signals at high field region. Therefore, further investigation was not performed.

Subfraction C2 displayed a long tail under UV-S on normal phase TLC using 4% methanol in dichloromethane (2 runs) as a mobile phase and displayed many spots after dipping the normal phase TLC in ASA reagent and subsequently heating. Its ^{1}H NMR spectrum showed none of major proton signals. Thus, it was not further purified.

Subfraction C3 showed many UV-active spots on normal phase TLC using 4% methanol in dichloromethane (2 runs) as a mobile phase. Further purification by flash column chromatography over silica gel using a gradient system of methanol-dichloromethane was performed. Subfractions, which contained similar components, were combined and evaporated to dryness under reduced pressure to afford six subfractions, as shown in **Table 112.**

Table 112 Subfractions obtained from **subfraction C3** by flash column chromatography over silica gel

Subfraction	Eluent	Weight (mg)	Physical appearance
C3-1	100% CH_2Cl_2 - 1% MeOH/CH_2Cl_2	4.7	Yellow gum
C3-2	1% MeOH/CH_2Cl_2	8.3	Yellow gum
C3-3	2-10% MeOH/CH_2Cl_2	28.7	Yellow gum
C3-4	10-40% MeOH/CH_2Cl_2	42.0	Yellow gum mixed with yellow solid
C3-5	50-80% MeOH/CH_2Cl_2	8.1	Yellow gum
C3-6	100% MeOH	38.6	Brown gum

Subfraction C3-1 showed no UV-active spots on normal phase TLC using 4% methanol in dichloromethane (2 runs) as a mobile phase and showed no definite spots after dipping the normal phase TLC in ASA reagent and subsequently heating. Its ^1H NMR spectrum showed none of major components. Thus, no attempted separation was carried out.

Subfraction C3-2 showed a long tail under UV-S on normal phase TLC using 4% methanol in dichloromethane (2 runs) as a mobile phase. When using 30% ethyl acetate in light petroleum (2 runs) as a mobile phase, the chromatogram showed two spots after dipping the normal phase TLC in ASA reagent and subsequently heating with the R_f values of 0.58 and 0.65. Further separation by column chromatography over silica gel using a gradient system of ethyl acetate-light

petroleum followed by a gradient system of methanol-ethyl acetate was performed. Fractions, which contained similar components, were combined and evaporated to dryness under reduced pressure to give three subfractions, as shown in **Table 113.**

Table 113 Subfractions obtained from **subfraction C3-2** by column chromatography over silica gel

Subfraction	Eluent	Weight (mg)	Physical appearance
C3-2-1	10-30% EtOAc/Light petroleum	0.6	Pale-yellow gum
C3-2-2	50% EtOAc/Light petroleum - 100% EtOAc	3.7	Yellow gum
C3-2-3	2% MeOH/EtOAc - 100% MeOH	3.5	Yellow gum

Subfraction C3-2-1 displayed no spots under UV-S on normal phase TLC using 20% ethyl acetate in light petroleum (3 runs) as a mobile phase. According to the appearance of proton signals at high field, it was not further investigated.

Subfraction C3-2-2 showed many spots after dipping the normal phase TLC in ASA reagent and subsequently heating using 20% ethyl acetate in light petroleum (3 runs) as a mobile phase. Its ^{1}H NMR spectrum displayed none of major components. Thus, no attempted separation was conducted.

Subfraction C3-2-3 displayed a long tail after dipping the normal phase TLC in ASA reagent and subsequently heating using 20% ethyl acetate in light petroleum (3 runs) as a mobile phase. Its ^{1}H NMR spectrum showed none of major components. Thus, no attempted separation was carried out.

Subfraction C3-3 showed many inseparable spots after dipping the normal phase TLC in ASA reagent and subsequently heating using 50% ethyl acetate

in light petroleum (2 runs) as a mobile phase. The ^{1}H NMR data indicated that it contained many compounds. Thus, it was not further purified.

Subfraction C3-4 showed two spots with the R_f values of 0.08 and 0.35 after dipping the normal phase TLC in ASA reagent and subsequently heating using 4% methanol in dichloromethane (2 runs) as a mobile phase. When using 50% ethyl acetate in light petroleum (3 runs) as a mobile phase, the chromatogram showed four spots with the R_f values of 0.08, 0.20, 0.30 and 0.58 after dipping the normal phase TLC in ASA reagent and subsequently heating. Further separation by column chromatography over silica gel using a gradient system of ethyl acetate-light petroleum followed by a gradient system of methanol-ethyl acetate was performed. Fractions, which contained similar components, were combined and evaporated to dryness under reduced pressure to give three subfractions, as shown in **Table 114.**

Table 114 Subfractions obtained from **subfraction C3-4** by column chromatography over silica gel

Subfraction	Eluent	Weight (mg)	Physical appearance
C3-4-1	30-80% EtOAc/Light petroleum	3.1	Pale-yellow gum
C3-4-2	100% EtOAc - 60% MeOH/EtOAc	10.6	Yellow gum
C3-4-3	80% MeOH/EtOAc - 100% MeOH	23.2	Yellow gum mixed with yellow solid

subfraction C3-4-1 showed no definite spots after dipping the normal phase TLC in ASA reagent and subsequently heating using 60% ethyl acetate in light petroleum (3 runs). Its ^{1}H NMR data suggested none of major components. Thus, no attempted investigation was carried out.

Subfraction C3-4-2 showed three spots with the R_f values of 0.08, 0.20 and 0.30 after dipping the normal phase TLC in ASA reagent and subsequently

heating using 60% ethyl acetate in light petroleum (3 runs). Its ^{1}H NMR data suggested that it contained sugars as major components. Thus, no attempted investigation was performed.

Subfraction C3-4-3 displayed one major spot with the R_f value of 0.63 after dipping the normal phase TLC in ASA reagent and subsequently heating using 60% ethyl acetate in light petroleum (3 runs). The ^{1}H NMR data indicated the presence of a mixture of **N33** and other components. Therefore, further investigation was not conducted.

Subfraction C3-5 showed many inseparable spots after dipping the normal phase TLC in ASA reagent and subsequently heating using 4% methanol in dichloromethane (2 runs) as a mobile phase. Its ^{1}H NMR spectrum displayed none of major components. Thus, further purification was not conducted.

Subfraction C3-6 demonstrated a long tail after dipping the normal phase TLC in ASA reagent and subsequently heating using 4% methanol in dichloromethane (2 runs) as a mobile phase. When using 70% ethyl acetate in light petroleum (6 runs) as a mobile phase, the chromatogram showed many spots after dipping the normal phase TLC in ASA reagent and subsequently heating. Further separation by column chromatography over silica gel using a gradient system of ethyl acetate-light petroleum followed by a gradient system of methanol-ethyl acetate was performed. Fractions, which contained similar components, were combined and evaporated to dryness under reduced pressure to obtained three subfractions, as shown in **Table 115.**

Table 115 Subfractions obtained from **subfraction C3-6** by column chromatography over silica gel

Subfraction	Eluent	Weight (mg)	Physical appearance
C3-6-1	50% EtOAc/Light petroleum - 10% MeOH/EtOAc	23.0	Pale-yellow gum
C3-6-2	30-70% MeOH/EtOAc	5.7	Yellow gum
C3-6-3	100% MeOH	5.6	Yellow gum

Subfraction C3-6-1 displayed many spots after dipping the normal phase TLC in ASA reagent and subsequently heating using 70% ethyl acetate in light petroleum (2 runs). The ^{1}H NMR data indicated the presence of a mixture of **N33** and other components. Therefore, further investigation was not carried out.

Subfraction C3-6-2 displayed one major spot with the R_f value of 0.60 after dipping the normal phase TLC in ASA reagent and subsequently heating using 70% ethyl acetate in light petroleum (2 runs). The ^{1}H NMR data indicated the presence of **N33** as a major component. Therefore, further investigation was not conducted.

Subfraction C3-6-3 displayed a long tail after dipping the normal phase TLC in ASA reagent and subsequently heating using 70% ethyl acetate in light petroleum (2 runs). Its ^{1}H NMR spectrum displayed none of major components. Therefore, further investigation was not performed.

Subfraction C4 showed many UV-active spots on normal phase TLC using 4% methanol in dichloromethane (2 runs) as a mobile phase and showed many spots after dipping the normal phase TLC in ASA reagent and subsequently heating. Therefore, further investigation was not conducted.

Fraction D demonstrated many spots under UV-S on normal phase TLC using 2% methanol in dichloromethane (3 runs) as a mobile phase. It was further separated by column chromatography over Sephadex LH20 using 100% MeOH as eluent. All subfractions were examined by TLC, combined on the basis of their chromatogram characteristics and then evaporated to dryness under reduced pressure to afford four subfractions, as shown in **Table 116.**

Table 116 Subfractions obtained from **fraction D** by column chromatography over Sephadex LH20

Subfraction	Eluent	Weight (mg)	Physical appearance
D1	100% MeOH	6.9	Brown gum
D2	100% MeOH	62.1	Brown gum
D3	100% MeOH	128.0	Brown gum mixed with yellow solid
D4	100% MeOH	5.1	Brown gum mixed with yellow solid

Subfraction D1 showed no spots after dipping the normal phase TLC in ASA reagent and subsequently heating using 2% methanol in dichloromethane (2 runs) as a mobile phase. Its ^{1}H NMR spectrum displayed none of major components. Thus, no attempted investigation was performed.

Subfraction D2 showed many spots after dipping the normal phase TLC in ASA reagent and subsequently heating using 2% methanol in dichloromethane (2 runs) as a mobile phase. Further purification by column chromatography over silica gel using a gradient system of methanol-dichloromethane was performed. Subfractions, which contained similar components, were combined and evaporated to dryness under reduced pressure to afford three subfractions, as shown in **Table 117.**

Table 117 Subfractions obtained from **subfraction D2** by column chromatography over silica gel

Subfraction	Eluent	Weight (mg)	Physical appearance
D2-1	100% CH_2Cl_2 - 10% MeOH/CH_2Cl_2	10.7	Yellow gum
D2-2	20-80% MeOH/CH_2Cl_2	34.2	Yellow gum mixed with yellow solid
D2-3	100% MeOH	16.0	Yellow gum

Subfraction D2-1 showed many spots after dipping the normal phase TLC in ASA reagent and subsequently heating using 2% methanol in dichloromethane (2 runs) as a mobile phase. The ^{1}H NMR data indicated that it contained many compounds. Thus, further purification was not conducted.

Subfraction D2-2 displayed many spots after dipping the normal phase TLC in ASA reagent and subsequently heating using 2% methanol in dichloromethane (2 runs) as a mobile phase. The ^{1}H NMR data indicated the presence of a mixture of **N33** and other components. Therefore, further investigation was not performed.

Subfraction D2-3 displayed a long tail after dipping the normal phase TLC in ASA reagent and subsequently heating using 2% methanol in dichloromethane (2 runs) as a mobile phase. Its ^{1}H NMR spectrum displayed none of major components. Therefore, further investigation was not performed.

Subfraction D3 showed many spots after dipping the normal phase TLC in ASA reagent and subsequently heating using 2% methanol in dichloromethane (2 runs) as a mobile phase. Further purification by column chromatography over silica gel using a gradient system of methanol-dichloromethane was performed. Subfractions, which contained similar components, were combined

and evaporated to dryness under reduced pressure to afford six subfractions, as shown in **Table 118.**

Table 118 Subfractions obtained from **subfraction D3** by column chromatography over silica gel

Subfraction	Eluent	Weight (mg)	Physical appearance
D3-1	100% CH_2Cl_2 - 2% MeOH/CH_2Cl_2	16.3	Yellow gum
D3-2	2-8% MeOH/CH_2Cl_2	27.8	Yellow solid
D3-3	10-12% MeOH/CH_2Cl_2	36.9	Yellow gum
D3-4	15-20% MeOH/CH_2Cl_2	24.5	Yellow solid
D3-5	20-40% MeOH/CH_2Cl_2	7.5	Yellow solid
D3-6	40% MeOH/CH_2Cl_2 - 100% MeOH	14.7	Brown gum

Subfraction D3-1 showed many spots after dipping the normal phase TLC in ASA reagent and subsequently heating using 100% dichloromethane (4 runs) as a mobile phase. The ^{1}H NMR data indicated that it contained many components. Thus, further purification was not pursued.

Subfraction D3-2 (N33) melted at 187.5-188.0 °C and showed one spot with the R_f value of 0.43 after dipping the normal phase TLC in ASA reagent and subsequently heating using 100% dichloromethane (2 runs) followed by 2% methanol in dichloromethane (2 runs) as mobile phases.

$[\alpha]_D^{27}$	-60.56 (c = 0.19, MeOH)
FT-IR (neat) ν_{cm-1}	3415 (O-H stretching), 1715 and 1709 (C=O stretching), 1564 (C=C stretching)
^{1}H NMR ($CDCl_3$+CD_3OD) (δ ppm) (300 MHz)	9.65 (*s*, 1H), 6.06 (*brd*, *J* = 2.4 Hz, 1H), 4.07 (*d*, *J* = 11.1 Hz, 1H), 3.30 (*d*, *J* = 11.1 Hz,

	1H), 2.40 (*m*, 1H), 2.38 (*m*, 1H), 2.13 (*t*, *J* = 13.5 Hz, 1H), 2.10 (*m*, 1H), 2.03 (*m*, 1H), 2.02 (*m*, 1H), 1.96 (*m*, 1H), 1.94 (*dd*, *J* = 12.3, 4.5 Hz, 1H), 1.83 (*m*, 1H), 1.56 (*dd*, *J* = 13.5, 6.0 Hz, 1H), 1.25 (*m*, 1H), 1.20 (*t*, *J* = 12.6 Hz, 1H), 1.04 (*d*, *J* = 6.9 Hz, 3H), 1.00 (*m*, 1H), 0.99 (*d*, *J* = 6.6 Hz, 3H), 0.82 (*d*, *J* = 6.6 Hz, 3H)
^{13}C NMR ($CDCl_3$+CD_3OD) (δ ppm) (75 MHz)	206.44, 177.62, 148.69, 130.62, 75.25, 66.49, 66.22, 59.11, 47.68, 41.21, 31.99, 31.16, 29.84, 27.81, 27.60, 26.50, 22.49, 20.98, 17.21
DEPT (135°) ($CDCl_3$+CD_3OD)	CH : 206.44, 130.62, 47.68, 41.21, 41.19, 31.16, 27.60
	CH_2 : 66.49, 31.99, 29.84, 27.81, 26.50
	CH_3 : 22.49, 20.98, 17.21
EIMS *m/z* (% relative intensity):	332 (24), 314 (37), 301 (39), 284 (100), 256 (43), 241 (45), 166 (55), 147 (62), 121 (47)

Subfraction D3-3 showed many spots after dipping the normal phase TLC in ASA reagent and subsequently heating using 100% dichloromethane (2 runs) followed by 2% methanol in dichloromethane (2 runs) as mobile phases. Its ^{1}H NMR data suggested that it contained a mixture of sugars and **N33**. Therefore, it was not further separated.

Subfraction D3-4 showed three spots with the R_f values of 0.08, 0.15 and 0.35 after dipping the normal phase TLC in ASA reagent and subsequently heating using 100% dichloromethane (2 runs) followed by 2% methanol in dichloromethane (2 runs) as mobile phases. Further purification by column chromatography over silica gel using a gradient system of methanol-dichloromethane was performed. Subfractions, which contained similar components, were combined

and evaporated to dryness under reduced pressure to afford four subfractions, as shown in **Table 119**.

Table 119 Subfractions obtained from **subfraction D3-4** by column chromatography over silica gel

Subfraction	Eluent	Weight (mg)	Physical appearance
D3-4-1	100% CH_2Cl_2 - 2% MeOH/CH_2Cl_2	1.0	Yellow gum
D3-4-2	2-8% MeOH/CH_2Cl_2	4.8	Yellow solid
D3-4-3	10-12% MeOH/CH_2Cl_2	12.1	Yellow solid
D3-4-4	15-20% MeOH/CH_2Cl_2	5.8	Yellow solid

Subfraction D3-4-1 showed no spots after dipping the normal phase TLC in ASA reagent and subsequently heating using 5% methanol in dichloromethane (5 runs) as a mobile phase. Its ^{1}H NMR data suggested that it contained sugars as major components. Thus, further purification was not performed.

Subfraction D3-4-2 (N34) melted at 103.1-103.6 °C and showed one spot with the R_f value of 0.07 after dipping the normal phase TLC in ASA reagent and subsequently heating using 5% methanol in dichloromethane (5 runs) as a mobile phase.

$[\alpha]_D^{27}$	+26.57 (c = 0.36, MeOH)
UV(MeOH) λ_{max} nm (log ε)	220 (3.45), 281 (2.95)
FT-IR (neat) ν_{cm-1}	3348 (O-H stretching), 1609 and 1588 (C=C stretching)
^{1}H NMR (Acetone-d_6) (δ ppm) (500 MHz)	7.07 (*t*, *J* = 7.5 Hz, 1H), 6.71 (*dd*, *J* = 7.5, 1.5 Hz, 1H), 6.70 (*dd*, *J* = 7.5, 1.5 Hz, 1H), 4.99 (*d*, *J* = 11.0 Hz, 1H), 4.93 (*d*, *J* = 4.0 Hz, 1H), 4.61 (*d*, *J* = 11.0 Hz, 1H), 3.82 (*dd*, *J* = 12.0, 2.5 Hz, 1H),

		3.70 (*m*, 1H), 3.69 (*dd*, *J* = 12.0, 6.0 Hz, 1H), 3.61 (*t*, *J* = 9.0 Hz, 1H), 3.42 (*dd*, *J* = 9.0, 4.0 Hz, 1H), 3.36 (*t*, *J* = 9.0 Hz, 1H), 2.68 (*dd*, *J* = 14.0, 7.5 Hz, 1H), 2.62 (*dd*, *J* = 14.0, 7.5 Hz, 1H), 1.58 (*sextet*, *J* = 7.5 Hz, 2H), 0.96 (*t*, *J* = 7.5 Hz, 3H)
^{13}C NMR (Acetone-d_6) (δ ppm) (125 MHz)		157.88, 143.97, 129.67, 122.43, 121.72, 114.82, 99.56, 75.32, 73.74, 73.35, 71.87, 63.41, 62.90, 35.83, 25.69, 14.35
DEPT (135°) (Acetone-d_6)	CH :	129.67, 114.82, 99.56, 75.32, 73.74, 73.35, 71.87
	CH_2 :	63.41, 62.90, 35.83, 25.69
	CH_3 :	14.39
FAB *m/z* (% relative intensity):		328 (1), 297 (12), 149 (100), 133 (21), 121 (34)

Subfraction D3-4-3 showed three spots with the R_f values of 0.07, 0.15 and 0.40 after dipping the normal phase TLC in ASA reagent and subsequently heating using 5% methanol in dichloromethane (5 runs) as a mobile phase. Further separation by column chromatography over Sephadex LH20 using 100% MeOH as eluent was performed. All subfractions were examined by TLC, combined on the basis of their chromatogram characteristics and then evaporated to dryness under reduced pressure to afford three subfractions, as shown in **Table 120**.

Table 120 Subfractions obtained from **subfraction D3-4-3** by column chromatography over Sephadex LH20

Subfraction	Eluent	Weight (mg)	Physical appearance
D3-4-31	100% MeOH	1.3	Yellow solid
D3-4-32	100% MeOH	7.9	Pale-yellow solid
D3-4-33	100% MeOH	2.7	Yellow solid

Subfraction D3-4-31 showed no spots after dipping the normal phase TLC in ASA reagent and subsequently heating using 70% ethyl acetate in light

petroleum (3 runs) as a mobile phase. Its ^{1}H NMR spectrum displayed none of major components. Thus, further purification was not performed.

Subfraction D3-4-32 showed two spots with the R_f values of 0.07 and 0.15 after dipping the normal phase TLC in ASA reagent and subsequently heating using 70% ethyl acetate in light petroleum (3 runs) as a mobile phase. Further separation by column chromatography over Sephadex LH20 using 100% MeOH as eluent was performed. All subfractions were examined by TLC, combined on the basis of their chromatogram characteristics and then evaporated to dryness under reduced pressure to afford three subfractions, as shown in **Table 121.**

Table 121 Subfractions obtained from **subfraction D3-4-32** by column chromatography over Sephadex LH20

Subfraction	Eluent	Weight (mg)	Physical appearance
D3-4-321	100% MeOH	1.6	White solid
D3-4-322	100% MeOH	5.6	Yellow solid
D3-4-323	100% MeOH	0.6	Yellow gum

Subfraction D3-4-321 showed no spots after dipping the normal phase TLC in ASA reagent and subsequently heating using 80% ethyl acetate in light petroleum (3 runs) as a mobile phase. Its ^{1}H NMR spectrum displayed none of major components. Thus, further purification was not conducted.

Subfraction D3-4-322 showed three UV-active spots on normal phase TLC with the R_f values of 0.15, 0.28 and 0.43 using 80% ethyl acetate in light petroleum (3 runs) as a mobile phase. Further purification by precoated TLC with 70% ethyl acetate in light petroleum as a mobile phase (6 runs) afforded three bands.

Band 1 was obtained as a white solid (1.2 mg), which showed one spot under UV-S on normal phase TLC with the R_f value of 0.38 using 70% ethyl acetate in light petroleum as a mobile phase (6 runs). The ^{1}H NMR data suggested that it was a mixture. Because of the minute amount, it was not further investigated.

Band 2 was obtained as a yellow solid (1.7 mg), which showed one spot under UV-S on normal phase TLC with the R_f value of 0.20 using 70% ethyl acetate in light petroleum as a mobile phase (6 runs). Its ^{1}H NMR spectral data indicated that it was **N34**.

Band 3 (N35) was obtained as a white solid (1.5 mg), which melted at 103.4-104.1 °C and showed one spot under UV-S on normal phase TLC with the R_f value of 0.15 using 70% ethyl acetate in light petroleum as a mobile phase (6 runs).

$[\alpha]_D^{27}$	+35.40 (c = 0.20, MeOH)
UV(MeOH) λ_{max} nm (log ε)	217 (4.53), 276 (3.87)
FT-IR (neat) ν_{cm-1}	3344 (O-H stretching), 1602 and 1584 (C=C stretching)
^{1}H NMR (Acetone-d_6) (δ ppm) (500 MHz)	7.17 (*dd*, *J* = 8.5, 2.0 Hz, 1H), 7.13 (*t*, *J* = 8.5, Hz, 1H), 6.87 (*dd*, *J* = 8.5, 2.0 Hz, 1H), 5.35 (*d*, *J* = 4.0 Hz, 1H), 4.79 (*d*, *J* = 12.0 Hz, 1H), 4.56 (*d*, *J* = 12.0 Hz, 1H), 3.91 (*d*, *J* = 9.5 Hz, 1H), 3.84 (*dd*, *J* = 11.5, 2.0 Hz, 1H), 3.80 (*m*, 1H), 3.73 (*dd*, *J* = 11.5, 5.5 Hz, 1H), 3.59 (*dd*, *J* = 9.5, 4.0 Hz, 1H), 3.48 (*t*, *J* = 9.5 Hz, 1H), 2.70 (*t*, *J* = 7.5 Hz, 2H), 1.58 (*m*, 2H), 0.95 (*t*, *J* = 7.5 Hz, 3H)
^{13}C NMR (Acetone-d_6) (δ ppm) (125 MHz)	156.86, 140.91, 128.61, 127.31, 122.73, 112.62, 98.99, 73.30, 72.67, 71.70, 69.69, 60.86, 54.73, 33.96, 24.04, 12.35
DEPT (135°) (Acetone-d_6)	CH : 127.31, 122.73, 112.62, 98.99, 73.30, 72.67, 71.70, 69.69
	CH_2 : 60.86, 54.73, 33.96, 24.04
	CH_3 : 12.35
EIMS *m/z* (% relative intensity):	328 (1), 166 (35), 148 (100), 133 (11)

Subfraction D3-4-323 appeared as a long tail after dipping the normal phase TLC in ASA reagent and subsequently heating using 80% ethyl acetate in light petroleum (3 runs) as a mobile phase. Because of low quantity, it was not further isolated.

Subfraction D3-4-33 showed no definite spots after dipping the normal phase TLC in ASA reagent and subsequently heating using 70% ethyl acetate in light petroleum (3 runs) as a mobile phase. Its ^{1}H NMR spectrum displayed none of major components. Thus, no further investigation was carried out.

Subfraction D3-4-4 showed many inseparable spots after dipping the normal phase TLC in ASA reagent and subsequently heating using 5% methanol in dichloromethane (5 runs) as a mobile phase. Its ^{1}H NMR spectrum displayed none of major components. Therefore, further investigation was not conducted.

Subfraction D3-5 showed many spots after dipping the normal phase TLC in ASA reagent and subsequently heating using 100% dichloromethane (2 runs) followed by 2% methanol in dichloromethane (2 runs) as mobile phases. The ^{1}H NMR spectral data and chromatogram on normal phase TLC indicated the presence of a mixture of **N33** and other components. Therefore, it was not further separated.

Subfraction D3-6 showed many spots after dipping the normal phase TLC in ASA reagent and subsequently heating using 100% dichloromethane (2 runs) followed by 2% methanol in dichloromethane (2 runs) as mobile phases. Its ^{1}H NMR spectrum showed none of major components. Thus, no attempted investigation was carried out.

Subfraction D4 showed one major spot with the R_f value of 0.13 after dipping the normal phase TLC in ASA reagent and subsequently heating using 2% methanol in dichloromethane (2 runs) as a mobile phase. The ^{1}H NMR data indicated the presence of **N33** as a major component. Therefore, further investigation was not conducted.

Fraction E showed many spots after dipping the normal phase TLC in ASA reagent and subsequently heating using 4% methanol in dichloromethane (3 runs) as a mobile phase. It was further separated by column chromatography over Sephadex LH20 using 100% MeOH as eluent. Subfractions, which contained similar components, were combined and evaporated to dryness under reduced pressure to give three subfractions, as shown in **Table 122.**

Table 122 Subfractions obtained from **fraction E** by column chromatography over Sephadex LH20

Subfraction	Eluent	Weight (mg)	Physical appearance
E1	100% MeOH	3.8	Brown gum
E2	100% MeOH	104.5	Brown gum mixed with yellow solid
E3	100% MeOH	20.5	Brown gum

Subfraction E1 showed no definite spots after dipping the normal phase TLC in ASA reagent and subsequently heating using 100% dichloromethane (2 runs) as a mobile phase. Its ^{1}H NMR spectrum displayed none of major components. Thus, further purification was not performed.

Subfraction E2 displayed many spots after dipping the normal phase TLC in ASA reagent and subsequently heating using 4% methanol in dichloromethane (2 runs) as a mobile phase. Further separation by column chromatography over silica gel using a gradient system of methanol-dichloromethane was performed. Fractions, which contained similar components, were combined and evaporated to dryness under reduced pressure to give three subfractions, as shown in **Table 123.**

Table 123 Subfractions obtained from **subfraction E2** by column chromatography over silica gel

Subfraction	Eluent	Weight (mg)	Physical appearance
E2-1	100% CH_2Cl_2 - 20% MeOH/CH_2Cl_2	8.4	Yellow gum
E2-2	30-60% MeOH/CH_2Cl_2	15.4	Yellow gum
E2-3	70% MeOH/CH_2Cl_2 - 100% MeOH	68.5	Yellow gum

Subfraction E2-1 showed no spots after dipping the normal phase TLC in ASA reagent and subsequently heating using 4% methanol in dichloromethane (3 runs) as a mobile phase. Its ^{1}H NMR spectrum displayed none of major components. Therefore, further investigation was not conducted.

Subfraction E2-2 showed one major spot with the R_f value of 0.43 after dipping the normal phase TLC in ASA reagent and subsequently heating using 4% methanol in dichloromethane (3 runs) as a mobile phase. The ^{1}H NMR spectral data and chromatogram on normal phase TLC indicated the presence of a mixture of **N33** and other components. Therefore, it was not further separated.

Subfraction E2-3 showed one major spot with the R_f value of 0.43 after dipping the normal phase TLC in ASA reagent and subsequently heating using 4% methanol in dichloromethane (3 runs) as a mobile phase. It was further separated by column chromatography over Sephadex LH20 using 100% MeOH as eluent. All subfractions were examined by TLC, combined on the basis of their chromatogram characteristics and then evaporated to dryness under reduced pressure to afford three subfractions, as shown in **Table 124**.

Table 124 Subfractions obtained from **subfraction E2-3** by column chromatography over Sephadex LH20

Subfraction	Eluent	Weight (mg)	Physical appearance
E2-31	100% MeOH	19.9	Yellow gum
E2-32	100% MeOH	23.1	Yellow gum
E2-33	100% MeOH	35.4	Yellow gum

Subfraction E2-31 showed one major spot with the R_f value of 0.20 after dipping the normal phase TLC in ASA reagent and subsequently heating using 20% ethyl acetate in light petroleum (3 runs) as a mobile phase. The ^{1}H NMR spectral data and chromatogram on normal phase TLC indicated the presence of **N33** as a major component. Therefore, it was not further separated.

Subfraction E2-32 showed a long tail after dipping the normal phase TLC in ASA reagent and subsequently heating using 20% ethyl acetate in light petroleum (3 runs) as a mobile phase. The ^{1}H NMR spectral data and chromatogram on normal phase TLC indicated the presence of a mixture **N33, N34** and other components. Therefore, it was not further investigated.

Subfraction E2-33 showed many inseparable spots after dipping the normal phase TLC in ASA reagent and subsequently heating using 20% ethyl acetate in light petroleum (3 runs) as a mobile phase. Its ^{1}H NMR spectrum displayed none of major components. Thus, no attempted separation was performed.

Subfraction E3 displayed a long tail after dipping the normal phase TLC in ASA reagent and subsequently heating using 4% methanol in dichloromethane (2 runs) as a mobile phase. When using 40% ethyl acetate in light petroleum as a mobile phase, the chromatogram showed many spots after dipping the normal phase TLC in ASA reagent and subsequently heating. Further separation by column chromatography over silica gel using a gradient system of ethyl acetate-light petroleum followed by a gradient system of methanol-ethyl acetate was performed.

Subfractions, which contained similar components, were combined and evaporated to dryness under reduced pressure to give three subfractions, as shown in **Table 125.**

Table 125 Subfractions obtained from **subfraction E3** by column chromatography over silica gel

Subfraction	Eluent	Weight (mg)	Physical appearance
E3-1	20-50% EtOAc/Light petroleum	4.1	Yellow gum
E3-2	70% EtOAc/Light petroleum - 20% MeOH/EtOAc	3.6	Yellow gum
E3-3	30% MeOH/EtOAc - 100% MeOH	11.0	Yellow gum

Subfraction E3-1 showed one spot with the R_f value of 0.60 after dipping the normal phase TLC in ASA reagent and subsequently heating using 20% ethyl acetate in light petroleum as a mobile phase. The ^1H NMR spectrum showed none of major proton signals. Because of the minute amount, it was not further investigated.

Subfraction E3-2 showed one spot with the R_f value of 0.48 after dipping the normal phase TLC in ASA reagent and subsequently heating using 20% ethyl acetate in light petroleum as a mobile phase. The ^1H NMR data indicated that it contained many compounds. Thus, it was not further purified.

Subfraction E3-3 showed one major spot with the R_f value of 0.10 after dipping the normal phase TLC in ASA reagent and subsequently heating using 20% ethyl acetate in light petroleum as a mobile phase. The ^1H NMR spectral data indicated the presence of **N33** as a major component. Therefore, it was not further separated.

Fraction F showed one major UV-active spot with the R_f value of 0.63 on normal phase TLC using 4% methanol in dichloromethane (3 runs) as a mobile phase. The ^1H NMR data indicated the presence of **N36** as a major component. Thus, no attempted investigation was performed.

Fraction G (N36) melted at 44.7-45.3 °C and showed one UV-active spot on normal phase TLC with the R_f value of 0.63 using 4% methanol in dichloromethane (3 runs) as a mobile phase.

$[\alpha]_D^{27}$		+11.00 (c = 0.19, CH_2Cl_2)
UV(MeOH) λ_{max} nm (log ε)		221 (4.92), 271 (4.72), 345 (4.28)
FT-IR (neat) ν_{cm-1}		3060 (O-H stretching), 1648 (C=O stretching), 1580 (C=C stretching)
^1H NMR ($CDCl_3$+CD_3OD) (δ ppm) (300 MHz)		11.71 (*s*, 1H), 7.35 (*t*, *J* = 9.0 Hz, 1H), 6.49 (*d*, *J* = 9.0 Hz, 1H), 6.43 (*d*, *J* = 9.0 Hz, 1H), 4.57 (*m*, 1H), 2.75 (*dd*, *J* = 18.0, 12.0 Hz, 1H), 2.66 (*dd*, *J* = 18.0, 3.0 Hz, 1H), 1.51 (*d*, *J* = 6.0 Hz, 3H)
^{13}C NMR ($CDCl_3$+CD_3OD) (δ ppm) (75 MHz)		198.57, 161.68, 138.18, 109.07, 107.38, 73.80, 43.75, 20.72
DEPT (135°) ($CDCl_3$+CD_3OD)	CH :	138.18, 109.07, 107.38, 73.80
	CH_2 :	43.75
	CH_3 :	20.72

Fraction H showed many UV-active spots on normal phase TLC using 100% dichloromethane (2 runs) as a mobile phase. Further separation by column chromatography over Sephadex LH20 using 100% MeOH as eluent was performed. Subfractions, which contained similar components, were combined and evaporated to dryness under reduced pressure to give three subfractions, as shown in **Table 126.**

Table 126 Subfractions obtained from **fraction H** by column chromatography over Sephadex LH20

Subfraction	Eluent	Weight (mg)	Physical appearance
H1	100% MeOH	1.4	Brown gum
H2	100% MeOH	5.0	Yellow gum
H3	100% MeOH	7.0	Brown-orange gum

Subfraction H1 showed many UV-active spots on normal phase TLC using 100% dichloromethane (3 runs) as a mobile phase. The ^{1}H NMR data suggested that it was a mixture. Because of the minute amount, it was not further investigated.

Subfraction H2 showed many UV-active spots on normal phase TLC using 100% dichloromethane (3 runs) as a mobile phase. The ^{1}H NMR data suggested that it was a mixture of **N15** and other components. Thus, it was not further purified.

Subfraction H3 showed no UV-active spots on normal phase TLC using 100% dichloromethane (3 runs) as a mobile phase and showed no definite spots after dipping the normal phase TLC in ASA reagent and subsequently heating. The ^{1}H NMR spectrum showed none of major components. Thus, no further investigation was pursued.

5.2.3 Purification of the mycelial extract

The crude extract showed many UV-active spots on normal phase TLC using 4% methanol in dichloromethane (2 runs) as a mobile phase. It was separated by column chromatography over Sephadex LH20 using 100% MeOH as eluent. All fractions were examined by TLC, combined on the basis of their chromatogram characteristics and then evaporated to dryness under reduced pressure to give four fractions, as shown in **Table 127**.

Table 127 Fractions obtained from **the mycelial extract** by column chromatography over Sephadex LH20

Fraction	Eluent	Weight (mg)	Physical appearance
MA	100% MeOH	40.1	Brown gum
MB	100% MeOH	41.5	Brown gum
MC	100% MeOH	50.7	Brown gum mixed with brown solid
MD	100% MeOH	14.6	Brown gum

Fraction MA displayed a long tail after dipping the normal phase TLC in ASA reagent and subsequently heating using 6% methanol in dichloromethane (3 runs) as a mobile phase. The ^{1}H NMR data indicated that the major components might be a mixture of long chain hydrocarbons. Therefore, it was not further investigated.

Fraction MB showed many definite spots after dipping the normal phase TLC in ASA reagent and subsequently heating using 6% methanol in dichloromethane (3 runs) as a mobile phase. Its ^{1}H NMR spectral data indicated the presence of **N33** as a major component. Therefore, further investigation was not conducted.

Fraction MC showed four spots with the R_f values of 0.20, 0.25, 0.35 and 0.85 after dipping the normal phase TLC in ASA reagent and subsequently heating using 6% methanol in dichloromethane (3 runs) as a mobile phase. This fraction was separated by column chromatography over silica gel using a gradient system of methanol-dichloromethane. All subfractions were examined by TLC, combined on the basis of their chromatogram characteristics and then evaporated to dryness under reduced pressure to give three subfractions, as shown in **Table 128**.

Table 128 Subfractions obtained from **fraction MC** by column chromatography over silica gel

Subfraction	Eluent	Weight (mg)	Physical appearance
MC-1	100% CH_2Cl_2 - 10% MeOH/CH_2Cl_2	8.5	Yellow gum
MC-2	10% MeOH/CH_2Cl_2	9.7	Yellow gum
MC-3	10-40% MeOH/CH_2Cl_2	28.5	Brown gum mixed with brown solid

Subfraction MC-1 showed no spots after dipping the normal phase TLC in ASA reagent and subsequently heating using 100% dichloromethane followed by 2% methanol in dichloromethane as mobile phases. Its ^{1}H NMR spectrum displayed proton signals at high field region. Therefore, it was not further purified.

Subfraction MC-2 displayed many spots after dipping the normal phase TLC in ASA reagent and subsequently heating using 100% dichloromethane followed by 2% methanol in dichloromethane as mobile phases. Its ^{1}H NMR spectrum showed none of major components. Thus, no attempted investigation was carried out.

Subfraction MC-3 showed many definite spots after dipping the normal phase TLC in ASA reagent and subsequently heating using 4% methanol in dichloromethane (3 runs) as a mobile phase. Its ^{1}H NMR spectral data indicated the presence of **N33** as a major component. Therefore, it was not further investigated.

Fraction MD showed many definite spots after dipping the normal phase TLC in ASA reagent and subsequently heating using 6% methanol in dichloromethane (3 runs) as a mobile phase. The ^{1}H NMR data indicated that it was a mixture of **N33** and other components. Thus, no attempted investigation was performed.

CHAPTER 5.3
RESULTS AND DISCUSSION

Two new compounds (**N34** and **N35**) were isolated from the broth extract together with two known compounds (**N33** and **N36**). The structures were identified by spectroscopic methods.

5.3.1 Compound N33

N33 was obtained as a yellow solid and melted at 187.5-188.0 °C. The UV spectrum showed no absorption bands in the region of 200-400 nm. The IR spectrum showed absorption bands at 3415 cm^{-1} for a hydroxyl group and 1715 and 1709 cm^{-1} for carbonyl groups. The molecular formula $C_{20}H_{28}O_4$ was deduced from the HREI-MS. The ^1H NMR spectrum (**Figure 81**) (**Table 129**) showed characteristic signals of one aldehyde proton (δ_H 9.65, *s*, 1H), one olefinic proton of a trisubstituted alkene (δ_H 6.06, *brd*, J = 2.4 Hz, 1H), one oxymethylene group [δ_H 4.07 (*d*, J = 11.1 Hz, 1H) and 3.30 (*d*, J = 11.1 Hz, 1H)], four methine protons [δ_H 2.39 (*m*, 1H), 2.06 (*m*, 1H), 2.03 (*m*, 1H) and 1.83 (*m*, 1H)], four methylene groups [δ_H 2.13 (*t*, J = 13.5 Hz, 1H), 2.05 (*m*, 1H), 1.96 (*m*, 1H), 1.94 (*dd*, J = 12.3 and 4.5 Hz, 1H), 1.56 (*dd*, J = 13.5 and 6.0 Hz, 1H), 1.25 (*m*, 1H), 1.20 (*t*, J = 12.6, 1H) and 1.02 (*m*, 1H)], one isopropyl side chain [δ_H 2.38 (*m*, 1H), 1.04 (*d*, J = 6.9 Hz, 3H) and 0.99 (*d*, J = 6.6 Hz, 3H)] and one secondary methyl group (δ_H 0.82, *d*, J = 6.6 Hz, 1H). An aldehyde carbonyl resonance at δ_C 206.44 in the ^{13}C NMR spectrum (**Figure 82**) (**Table 129**) supported the ^1H NMR data. In addition, its ^{13}C NMR spectrum showed one carboxylic (δ_C 177.62), four quaternary (δ_C 148.69, 75.25, 66.22 and 59.11), six methine (δ_C 130.62, 47.68, 41.21, 31.16, 41.19 and 27.60), five methylene (δ_C 66.49, 31.99, 29.84, 27.81 and 26.50), three methyl (δ_C 22.49, 20.98 and 17.21) carbons. These evidence suggested that **N33** has a unique tetracyclic diterpene core containing a norbornene system (Chiba *et al.*, 2006). HMBC correlations (**Table 130**) of the methine proton (δ_H 2.38, H-14) of the isopropyl unit/C-2 (δ_C 130.62) and C-18 (δ_C

177.62) and those of the olefinic proton (δ_H 6.06, H-2) of the trisubstituted alkene/C-4 (δ_C 29.84), C-6 (δ_C 75.25), C-7 (δ_C 66.22), C-14 (δ_C 27.60) and C-18 established the attachment of the isopropyl group at C-1 (δ_C 148.69) and carboxylic acid at C-6. The aldehyde proton (δ_H 9.65, H-17) and the hydroxymethylene protons (δ_H 4.07 and 3.30, H_{ab}-19) were located at C-5 (δ_C 59.11) and C-7, respectively, on the basis of ^3J HMBC correlations of H-17/C-4, C-5 and C-13 (δ_C 41.19) and those of H_{ab}-19/C-3 (δ_C 47.68), C-6 and C-8 (δ_C 27.81). The methyl group (δ_H 0.82, Me-20) was attached at C-10 on the basis of HMBC correlations of the methyl protons with C-9 (δ_C 41.21), C-10 (δ_C 31.16) and C-11 (δ_C 31.99). Enhancement of H-13 (δ_H 2.03) and Me-20 signals were not observed when H-9 (δ_H 1.83) was irradiated in the NOEDIFF experiment (**Table 130**), indicating *trans* relationship of H-9/H-13 and H-9/Me-20. The observed optical rotation of **N33** ($[\alpha]_D^{27}$ -60.56, c = 0.19, MeOH) was almost identical to that of sordaricin ($[\alpha]_D$ -58.40, c = 0.19, MeOH) (Mander and Thomson, 2005), indicating that they possessed the same absolute configuration. Therefore, **N33** was sordaricin, which was previously isolated from *Podospora pleiospora* (Weber *et al.*, 2005).

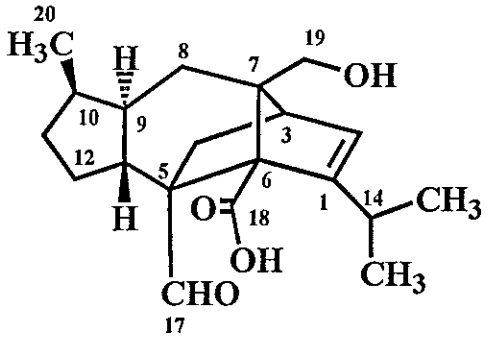

Table 129 The NMR data of **N33** in $CDCl_3$+CD_3OD and **sordaricin** in pyridine-d_5

Position	N33		Sordaricin[a]	
	δ_H (mult., J_{Hz})	δ_C (C-Type)	δ_H (mult., J_{Hz})	δ_C (C-Type)
1	-	148.69 (C)	-	148.9 (C)
2	6.06 (*brd*, 2.4)	130.62 (CH)	6.13 (*d*, 3.1)	130.9 (CH)
3	2.40 (*m*)	47.68 (CH)	2.97 (*t*, 3.8)	47.1 (CH)
4	a: 1.94 (*dd*, 12.3, 4.5) b: 1.20 (*t*, 12.6)	29.84 (CH_2)	a: 1.95 (*m*) b: 1.48 (*d*,12.5)	32.4 (CH_2)

Table 129 Continued

Position	N33		Sordaricin[a]	
	δ_H (mult., J_{Hz})	δ_C (C-Type)	δ_H (mult., J_{Hz})	δ_C (C-Type)
5	-	59.11 (C)	-	59.4 (C)
6	-	75.25 (C)	-	67.5 (C)
7	-	66.22 (C)	-	66.9 (C)
8	a: 2.13 (*t*, 13.5)	27.81 (CH_2)	a: 2.50-2.20 (*m*)	29.7 (CH_2)
	b: 1.56 (*dd*, 13.5, 6.0)		b: 1.95 (*m*)	
9	1.83 (*m*)	41.21 (CH)	1.95 (*m*)	42.0 (CH)
10	2.10 (*m*)	31.16 (CH)	2.50-2.20 (*m*)	31.6 (CH)
11	a: 2.02 (*m*)	31.99 (CH_2)	a: 2.50-2.20 (*m*)	26.9 (CH_2)
	b: 1.25 (*m*)		b: 1.74 (*m*)	
12	a: 1.96 (*m*)	26.50 (CH_2)	1.95 (*m*)	29.1 (CH_2)
	b: 1.00 (*m*)			
13	2.03 (*m*)	41.19 (CH)	1.95 (*m*)	41.9 (CH)
14	2.38 (*m*)	27.60 (CH)	2.72 (*sep*, 6.7)	28.2 (CH)
15	1.04 (*d*, 6.9)	20.98 (CH_3)	1.08 (*m*)	21.3 (CH_3)
16	0.99 (*d*, 6.6)	22.49 (CH_3)	1.08 (*m*)	22.7 (CH_3)
17	9.65 (*s*)	206.44 (CH)	10.24 (*s*)	204.8 (CH)
18	-	177.62 (C)	8.85 (*brs*)	176.0 (C)
19	a: 4.07 (*d*, 11.1)	66.49 (CH_2)	4.37 (*d*, 10.5)	73.8 (CH_2)
	b: 3.30 (*d*, 11.1)		4.20 (*d*, 10.5)	
20	0.82 (*d*, 6.6)	17.21 (CH_3)	0.80 (*d*, 6.6)	17.7 (CH_3)

[a] Mander and Thomson, 2005.

Table 130 The HMBC, COSY and NOE data of **N33** in $CDCl_3$+CD_3OD

Position	HMBC	COSY	NOE
H-2	C-1, C-3, C-6, C-14, C-18	H-3	H-3, H_b-4, Me-15, H_{ab}-19
H-3	C-1, C-2, C-5	H-2, H_{ab}-4	H-2, H_{ab}-4, H-17, H_{ab}-19
H_a-4	C-2, C-3, C-5, C-6, C-7, C-9, C-17	H-3, H_b-4	H-3, H_b-4, H-17
H_b-4	C-2, C-3, C-5, C-6, C-9, C-17	H-3, H_a-4	H-2, H-3, H_a-4
H_a-8	C-3, C-6, C-7, C-9	-	-
H_b-8	C-3, C-6, C-7, C-9	-	H-3, H-9, H_b-19
H-9	C-4, C-8, C-10, C-12, C-13, C-20	-	-
H-10	-	Me-20	-
H_a-11	-	H-10, H_b-11, H_{ab}-12	-
H_b-11	C-9, C-10, C-12, C-20	H-10, H_a-11, H_{ab}-12	-
H_a-12	-	H_{ab}-11, H_b-12	-
H_b-12	C-4, C-10, C-11	H_{ab}-11, H_a-12	-
H-14	C-2, C-15, C-16, C-18	-	-
Me-15	C-1, C-2, C-14, C-16	H-14	-

Table 130 Continued

Position	HMBC	COSY	NOE
Me-16	C-1, C-14, C-15	H-14	-
H-17	C-4, C-5, C-7, C-9	-	H-3, H_b-4
H_a-19	C-3, C-6, C-8	H_b-19	H-2, H-3, H_b-19
H_b-19	C-3, C-6, C-8	H_a-19	H-2, H-3, H_a-19
Me-20	C-10, C-11, C-13	H-10	-

5.3.2 Compound N34

N34 was obtained as a colorless solid and melted at 103.1-103.6 °C with $[\alpha]_D^{27}$ +26.57 (c = 0.36, MeOH). The UV spectrum showed maximum absorption bands of a benzene chromophore at λ_{max} 220 and 281 nm. The IR spectrum exhibited an absorption band at 3348 cm^{-1} for a hydroxyl group. The HREI-MS showed the molecular formula $C_{16}H_{24}O_7$. The ^1H NMR spectral data (**Figure 84**) (**Table 131**) showed three aromatic protons of a 1,2,3-trisubstituted benzene [δ_H 7.07 (*t*, J = 7.5 Hz, 1H), 6.71 (*dd*, J = 7.5 and 1.5 Hz, 1H) and 6.70 (*dd*, J = 7.5 and 1.5 Hz, 1H)], two nonequivalent oxymethylene protons [δ_H 4.99 (*d*, J = 11.0 Hz, 1H) and 4.61 (*d*, J = 11.0 Hz, 1H)], one propyl side chain [δ_H 2.68 (*dd*, J = 14.0 and 7.5 Hz, 1H), 2.62 (*dd*, J = 14.0 and 7.5 Hz, 1H), 1.58 (*sextet*, J = 7.5 Hz, 2H) and 0.96 (*t*, J = 7.5 Hz, 3H) and characteristic signals of a glucose moiety: one anomeric proton (δ_H 4.93, *d*, J = 4.0 Hz, 1H), two nonequivalent oxymethylene protons [δ_H 3.82 (*dd*, J = 12.0 and 2.5 Hz, 1H) and 3.69 (*dd*, J = 12.0 and 6.0 Hz, 1H)] and four oxymethine protons [δ_H 3.70 (*m*, 1H), 3.61 (*t*, J = 9.0 Hz, 1H), 3.42 (*dd*, J = 9.0 and 4.0 Hz, 1H) and 3.36 (*t*, J = 9.0 Hz, 1H)]. The appearance of the anomeric proton as a *doublet* with small coupling constant of 4.0 Hz indicated that the glucose unit must be an α-glucopyranose. The aromatic protons at δ_H 6.70, 7.07 and 6.71 were assigned as H-4, H-5 and H-6, respectively, on the basis of their multiplicity and the coupling constants. ^3J HMBC correlations (**Table 131**) from H_{ab}-8 (δ_H 2.68 and 2.62) of the propyl side chain to C-2 (δ_C 122.43) and C-4 (δ_C 121.72) and signal enhancement of H_{ab}-8 after irradiation of H-4 in the NOEDIFF experiment (**Table 131**) established the attachment of the propyl group at C-3 (δ_C 143.97). The nonequivalent oxymethylene

protons, H_{ab}-7 (δ_H 4.99 and 4.61), gave HMBC cross peaks with C-1′ (δ_C 99.56) of the α-glucopyranose moiety, C-1 (δ_C 157.88), C-2 and C-3, thus connecting this group with C-2 of the 1,2,3-trisubstituted benzene and forming an ether linkage with C-1′ of the glucose unit. Signal enhancement of both H-1′ and H_{ab}-8 upon irradiated of H_{ab}-7 in the NOEDIFF experiment supported the assigned location. The substituent at C-1 must be a hydroxyl group according to its ^{13}C chemical shift. Thus, **N34** was determined as a new naturally occurring α-glucoside.

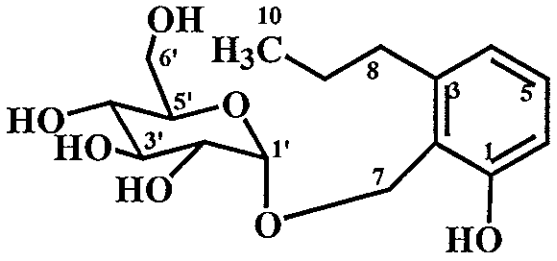

Table 131 The NMR data of **N34** in acetone-d_6

Position	N34		HMBC	COSY	NOE
	δ_H (mult., J_{Hz})	δ_C (C-Type)			
1	-	157.88 (C)	-	-	-
2	-	122.43 (C)	-	-	-
3	-	143.97 (C)	-	-	-
4	6.70 (*dd*, 7.5, 1.5)	121.72 (CH)	C-3, C-5, C-6, C-8	H-5	H-5, H_{ab}-8
5	7.07 (*t*, 7.5)	129.67 (CH)	C-1, C-3, C-4	H-4, H-6	H-4, H-6
6	6.71 (*dd*, 7.5, 1.5)	114.82 (CH)	C-1, C-2, C-4, C-5	H-5	H-5
7	a: 4.99 (*d*, 11.0) b: 4.61 (*d*, 11.0)	63.41 (CH_2)	C-1, C-1′, C-2, C-3	H_b-7 H_a-7	H_b-7, H_{ab}-8 H-1′, H_a-7
8	a: 2.68 (*dd*, 14.0, 7.5) b: 2.62 (*dd*, 14.0, 7.5)	35.83 (CH_2)	C-2, C-3, C-4, C-9, C-10	H_2-9	H-4, H_b-7
9	1.58 (*sextet*, 7.5)	25.69 (CH_2)	C-3, C-8, C-10	H_{ab}-8, Me-10	H_{ab}-8, Me-10
10	0.96 (*t*, 7.5)	14.35 (CH_3)	C-8, C-9	H_2-9	H_2-9
1′	4.93 (*d*, 4.0)	99.56 (CH)	C-2′, C-5′, C-7	H-2′	H-2′, H_b-7
2′	3.42 (*dd*, 9.0, 4.0)	73.35 (CH)	C-3′	H-1′, H-3′	H-1′
3′	3.61 (*t*, 9.0)	75.32 (CH)	C-2′, C-4′	H-2′, H-4′	-

Table 131 Continued

Position	N34		HMBC	COSY	NOE
	δ_H (mult., J_{Hz})	δ_C (C-Type)			
4′	3.36 (*t*, 9.0)	71.87 (CH)	C-5′, C-6′	H-3′, H-5′	-
5′	3.70 (*m*)	73.74 (CH)	C-3′	H-4′, H_a-6′	-
6′	a: 3.82 (*dd*, 12.0, 2.5)	62.90 (CH_2)	C-4′, C-5′	H_b-6′	-
	b: 3.69 (*dd*, 12.0, 6.0)			H_a-6′	

5.3.3 Compound N35

N35 was obtained as a colorless solid and melted at 103.4-104.1 °C with $[\alpha]_D^{27}$ +35.40 (c = 0.20, MeOH). The UV and IR were almost identical to those of **N34**. The HREI-MS showed that they had the same molecular formula. The significant difference in the ^{1}H NMR spectrum (**Figure 87**) (**Table 132**) was the chemical shift of H-1′ of the α-glucose moiety (δ_H 4.93 in **N34** and δ_H 5.35 in **N35**). The ^3J HMBC cross peak (**Table 132**) from H-1′ to C-1 (δ_C 156.86) established an ether linkage between the anomeric carbon (δ_C 98.99, C-1′) and the oxyaromatic carbon (C-1), but not the oxyaliphatic C-7 as found in **N34**. The irradiation of H-1′ of the α-glucopyranose unit enhanced signal intensity of H-6 (δ_H 7.17, *dd*, J = 8.5, 2.0 Hz, 1H), indicating that the α-glucopyranose was located at C-1, not at C-7 (δ_C 54.73). The hydroxymethyl protons [H_{ab}-7, δ_H 4.79 (*d*, J = 12.0 Hz, 1H) and 4.56 (*d*, J = 12.0 Hz, 1H)] and the propyl side chain were located at C-2 (δ_C 128.61) and C-3 (δ_C 140.91), respectively, on the basis of ^3J HMBC correlations of H_{ab}-7/C-1 and C-3 and those of H_2-8 (δ_H 2.70, *t*, J = 7.5 Hz, 2H)/C-2 and C-4 (δ_C 122.73). Thus, **N35**, a new naturally occurring α-glucoside, differed from **N34** in the location of the glucose unit.

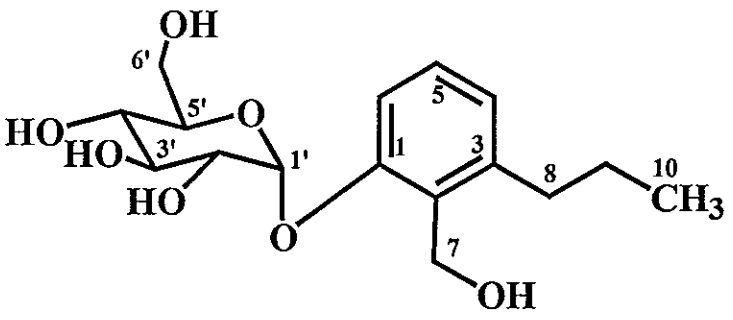

Table 132 The NMR data of **N35** in acetone-d_6

Position	N35		HMBC	COSY	NOE
	δ_H (mult., J_{Hz})	δ_C (C-Type)			
1	-	156.86 (C)	-		-
2	-	128.61 (C)	-	-	-
3	-	140.91 (C)	-	-	-
4	6.87 (*dd*, 8.5, 2.0)	122.73 (CH)	C-2, C-3, C-5, C-6, C-8	H-5, H-6	-
5	7.13 (*t*, 8.5)	127.31 (CH)	C-1, C-3, C-4	H-4, H-6	-
6	7.17 (*dd*, 8.5, 2.0)	112.62 (CH)	C-1, C-2, C-4	H-4, H-5	-
7	a: 4.79 (*d*, 12.0)	54.73 (CH_2)	C-1, C-2, C-3	H_b-7	H_b-7
	b: 4.56 (*d*, 12.0)		C-1	H_a-7	-
8	2.70 (*t*, 7.5)	33.96 (CH_2)	C-2, C-3, C-4, C-9, C-10	H_2-9	H-4, Me-10
9	1.58 (*m*)	24.04 (CH_2)	C-3, C-8, C-10	H_2-8, Me-10	Me-10
10	0.95 (*t*, 7.5)	12.35 (CH_3)	C-8, C-9	H_2-9	H_2-9
1′	5.35 (*d*, 4.0)	98.99 (CH)	C-1, C-2′, C-5′	H-2′	H-2′, H-6
2′	3.59 (*dd*, 9.5, 4.0)	71.70 (CH)	C-3′, C-4′	H-1′, H-3′	H-1′, H-4′
3′	3.91 (*t*, 9.5)	73.30 (CH)	C-2′, C-4′, C-5′	H-2′, H-4′	-
4′	3.48 (*t*, 9.5)	69.69 (CH)	C-3′, C-5′, C-6′	H-5′, H-3′	H-2′
5′	3.80 (*m*)	72.67 (CH)	C-4′, C-6′	H-4′, H_{ab}-6′	-
6′	a: 3.84 (*dd*, 11.5, 2.0)	60.86 (CH_2)	C-5′	H-5′, H_b-6′	-
	b: 3.73 (*dd*, 11.5, 5.5)			H-5′, H_a-6′	

5.3.4 Compound N36

N36 was obtained as a brown solid and melted at 44.7-45.3 °C. The UV maximum absorption bands at λ_{max} 221, 271 and 345 nm revealed the presence of a conjugate chromophore. The IR spectrum showed absorption bands at 3060 and 1648 cm^{-1} for hydroxyl and ketone carbonyl groups, respectively. The ^1H NMR spectrum (**Figure 89**) (**Table 133**) revealed signals for one chelated hydroxy proton (δ_H 11.71, *s*, 1H), a 1,2,3-trisubstituted benzene [δ_H 7.35 (*t*, J = 9.0 Hz , 1H), 6.49 (*d*, J = 9.0 Hz, 1H) and 6.43 (*d*, J = 9.0 Hz, 1H)], one oxymethine proton (δ_H 4.57, *m*, 1H), two nonequivalent methylene protons [δ_H 2.75 (*dd*, J = 18.0 and 12.0 Hz, 1H) and 2.66 (*dd*, J = 18.0 and 3.0 Hz, 1H)] and one methyl group (δ_H 1.51, *d*, J = 6.0 Hz, 3H). A ketone carbonyl resonance at δ_C 198.57 in the ^{13}C NMR spectrum (**Figure 90**) (**Table 133**) supported the IR data. The chelated hydroxyl group (δ_H 11.71) was placed at C-8 (δ_C 161.68), *peri* position to the ketone carbonyl group C-1 (δ_C 198.57).

In addition, the aromatic protons at δ_H 6.43, 7.35 and 6.49 were assigned as H-5, H-6 and H-7, respectively, on the basis of their multiplicity, coupling constants and HMBC correlations. In the COSY spectrum (**Table 134**), H-3 (δ_H 4.57) was coupled with H_{ab}-2 (δ_H 2.75 and 2.66) and Me-9 (δ_H 1.51). These results together with ^3J HMBC cross peaks (**Table 134**) of H-3/C-1 and C-4a (δ_C 161.68) indicated that C-3 (δ_C 73.80) and C-4a joined together with an ether linkage to form a chroman-4-one skeleton having a methyl group at C-3. **N36** gave almost identical optical rotation to that of 2,3-dihydro-5-hydroxy-2-methyl-*4H*-1-benzopyran-4-one, $[\alpha]_D^{27}$ of **N36** = +11.00 (c = 0.19, CH_2Cl_2) and $[\alpha]_D^{25}$ of 2,3-dihydro-5-hydroxy-2-methyl-*4H*-1-benzopyran-4-one = +6.00 (c = 0.19, CH_2Cl_2). Therefore, **N36** was assigned as 2,3-dihydro-5-hydroxy-2-methyl-*4H*-1-benzopyran-4-one which was previously isolated from *Nodulisporium* sp. 7080 (Dai *et al.*, 2006).

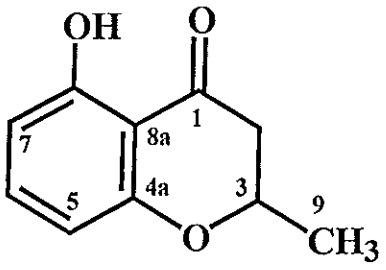

Table 133 The NMR data of **N36** in $CDCl_3$+CD_3OD and **2,3-dihydro-5-hydroxy-2-methyl-*4H*-1-benzopyran-4-one** in $CDCl_3$

Position	N36		2,3-Dihydro-5-hydroxy-2-methyl-*4H*-1-benzopyran-4-one[a]	
	δ_H (mult., J_{Hz})	δ_C (C-Type)	δ_H (mult., J_{Hz})	δ_C (C-Type)
1	-	198.57 (C=O)	-	198.5 (C=O)
2	a: 2.75 (*dd*, 18.0, 12.0) b: 2.66 (*dd*, 18.0, 3.0)	43.75 (CH_2)	a: 2.73 (*dd*, 17.1, 12.0) b: 2.66 (*dd*, 17.1, 3.7)	43.8 (CH_2)
3	4.57 (*m*)	73.80 (CH)	4.56 (*m*)	73.8 (CH)
4a	-	161.68 (C)	-	161.7 (C)
5	6.43 (*d*, 9.0)	107.38 (CH)	6.41 (*dd*, 8.3, 1.0)	107.3 (CH)
6	7.35 (*t*, 9.0)	138.18 (CH)	7.33 (*t*, 8.3)	138.2 (CH)
7	6.49 (*d*, 9.0)	109.07 (CH)	6.48 (*dd*, 8.3, 1.0)	109.1 (CH)
8-OH	11.71 (*s*)	161.68 (C)	11.70 (*s*)	162.1 (C)
8a		108.00 (C)		108.0 (C)
9	1.51 (*d*, 6.0)	20.72 (CH_3)	1.50 (*d*, 6.3)	20.8 (CH_3)

[a] Gray *et al.*, 1999.

Table 134 The HMBC, COSY and NOE data of **N36** in $CDCl_3$+CD_3OD

Position	HMBC	COSY	NOE
H_{ab}-2	C-1, C-3, C-9	H-3	H-3, Me-9
H-3	C-1, C-4a, C-9	H_{ab}-2, Me-9	H_{ab}-2, Me-9
H-5	C-1, C-4a, C-7	H-6	H-6
H-6	C-4a, C-5, C-8	H-5, H-7	H-5, H-7
H-7	C-5	H-6	H-6
8-OH	C-7, C-8, C-8a	-	-
Me-9	C-2, C-3	H-3	H_{ab}-2, H-3

PART VI

CHEMICAL CONSTITUENTS FROM THE ENDOPHYTIC FUNGUS *XYLARIA* SP. PSU-D65

CHAPTER 6.1
INTRODUCTION

6.1.1 Introduction

Metabolites of the genus *Xylaria* are summarized in Table **59**. The endophytic fungus *Xylaria* sp. PSU-D65 was isolated from the leaves of *Garcinia dulcis*, collected in Songkhla Province, Thailand, in 2004. This fungus was deposited as PSU-D65 at the Department of Microbiology, Faculty of Science, Prince of Songkla University. The ethyl acetate extract from the culture broth of this endophytic fungus exhibited antibacterial activity against *Staphylococcus aureus* ATCC25923, methicillin-resistant *S. aureus*, *Escherichia coli* ATCC25922 and *Pseudomonas aeruginosa* ATCC27853 and antifungal activity against *Cryptococcus neoformans* ATCC90113 with equal MIC values of 128 μg/ml.

CHAPTER 6.2
EXPERIMENTAL

6.2.1 Fermentation and extraction

The fermentation and extraction was performed using the same procedure as those of *Eutypella scoparia* PSU-D44. The crude EtOAc extract from the culture broth was obtained a brown gum (270.2 mg).

6.2.2 Purification of the broth extract

The ethyl acetate extract of the culture filtrate showed three UV-active spots on normal phase TLC with the R_f values of 0.28, 0.51 and 0.57 using 2% methanol in dichloromethane as a mobile phase (3 runs). Further purification by flash column chromatography over silica gel using a gradient system of methanol-dichloromethane was performed. Fractions with the similar chromatogram were combined and evaporated to dryness under reduced pressure to afford five fractions, as shown in **Table 135**.

Table 135 Fractions obtained from **the broth extract** by column chromatography over silica gel

Subfraction	Eluent	Weight (mg)	Physical appearance
A	100% CH_2Cl_2 - 3% MeOH/CH_2Cl_2	7.0	Yellow gum
B	3% MeOH/CH_2Cl_2	63.2	Yellow gum mixed with yellow solid
C	5-10% MeOH/CH_2Cl_2	14.4	Yellow gum mixed with yellow solid

Table 135 Continued

Subfraction	Eluent	Weight (mg)	Physical appearance
D	20-80% MeOH/CH_2Cl_2	25.1	Yellow gum
E	100% MeOH	128.4	Yellow gum

Fraction A showed no UV-active spots on normal phase TLC using 100% dichloromethane (2 runs) as a mobile phase. Its ^{1}H NMR spectrum displayed proton signals at high field region. Thus, no attempted investigation was performed.

Fraction B was separated into two parts: a white solid (21.4 mg) (**N37**) and a yellow solution (**Ys**), upon standing at room temperature. **N37** melted at 217.2-218.0 °C and showed one UV-active spot on normal phase TLC with the R_f value of 0.55 using 100% dichloromethane (4 runs) followed by 1% methanol in dichloromethane (2 runs) as mobile phases.

$[\alpha]_D^{27}$		+305.00 (c = 1.03, $CHCl_3$)
UV (MeOH) λ_{max} nm (log ε)		235 (4.43), 291 (4.46), 326 (3.83)
FT-IR (neat) ν_{cm-1}		1706 and 1664 (C=O stretching), 1616 (C=C stretching)
^{1}H NMR ($CDCl_3$) (δ ppm) (300 MHz)		6.14 (*s*, 1H), 5.55 (*s*, 1H), 4.04 (*s*, 3H), 3.98 (*s*, 3H), 3.62 (*s*, 3H), 3.03 (*dd*, *J* = 16.5, 13.2 Hz, 1H), 2.85 (*m*, 1H), 2.43 (*dd*, *J* = 16.5, 4.5 Hz, 1H), 0.96 (*d*, *J* = 6.6 Hz, 3H)
^{13}C NMR ($CDCl_3$) (δ ppm) (75 MHz)		197.01, 192.45, 170.79, 169.54, 164.61, 157.76, 105.16, 104.86, 97.28, 90.75, 89.50, 57.00, 56.66, 56.38, 40.05, 36.43, 14.23
DEPT (135°) ($CDCl_3$)	CH :	104.86, 89.50, 36.43
	CH_2 :	40.05
	CH_3 :	57.00, 56.66, 56.38, 14.23
EIMS *m/z* (% relative intensity):		352 (42), 321 (35), 310 (37), 207 (83), 149 (55), 138 (77), 83 (63), 69 (100)

The yellow solution (**Ys**) showed two UV-active spots on normal phase TLC with the R_f values of 0.55 and 0.63 using 100% dichloromethane (4 runs) followed by 1% methanol in dichloromethane (2 runs) as mobile phases. When using 30% ethyl acetate in light petroleum (6 runs) as a mobile phase, the chromatogram showed two UV-active spots on normal phase TLC with the R_f values of 0.13 and 0.23. Further purification by precoated TLC with 70% ethyl acetate in light petroleum as a mobile phase (6 runs) afforded two bands.

Band 1 (N38) was obtained as a white solid (2.5 mg), melting at 193.5-194.1 °C. It showed one spot under UV-S on normal phase TLC with the R_f value of 0.23 using 30% ethyl acetate in light petroleum as a mobile phase (6 runs).

$[\alpha]_D^{27}$		+364.00 (c = 1.00, acetone)
UV (MeOH) λ_{max} nm (log ε)		251(4.52), 286 (4.78), 316 (4.15)
FT-IR (neat) ν_{cm-1}		1700 and 1659 (C=O stretching), 1620 (C=C stretching)
^{1}H NMR ($CDCl_3$) (δ ppm) (300 MHz)		6.24 (*d*, *J* = 3.0 Hz, 1H), 6.05 (*d*, *J* = 3.0 Hz, 1H), 5.54 (*s*, 1H), 3.91 (*s*, 3H), 3.90 (*s*, 3H), 3.63 (*s*, 3H), 3.06 (*dd*, *J* = 18.0, 12.0 Hz, 1H), 2.76 (*m*, 1H), 2.40 (*dd*, *J* = 18.0, 6.0 Hz, 1H), 0.96 (*d*, *J* = 9.0 Hz, 3H)
^{13}C NMR ($CDCl_3$) (δ ppm) (75 MHz)		197.33, 192.50, 176.09, 171.31, 170.39, 159.13, 104.78, 104.43, 93.34, 89.95, 88.55, 56.61, 56.11, 56.08, 40.10, 36.58, 14.26
DEPT (135°) ($CDCl_3$)	CH :	104.78, 93.34, 88.55, 36.58
	CH_2 :	40.10
	CH_3 :	56.61, 56.11, 56.08, 14.26
EIMS *m/z* (% relative intensity):		318 (100), 287 (97), 276 (57), 250 (42), 181 (45), 138 (60)

Band 2 was obtained as a white solid (36.4 mg), which showed one spot under UV-S on normal phase TLC with the R_f value of 0.13 using 60% ethyl

acetate in light petroleum as a mobile phase (6 runs). Its ^{1}H NMR spectral data indicated that it was **N37.**

Fraction C showed a long tail under UV-S on normal phase TLC using 100% dichloromethane (4 runs) followed by 1% methanol in dichloromethane (2 runs) as mobile phases. When using 30% ethyl acetate in light petroleum (6 runs) as a mobile phase, the chromatogram showed three UV-active spots on normal phase TLC with the R_f values of 0.08, 0.28 and 0.60. Further separation by column chromatography over silica gel using a gradient system of ethyl acetate-light petroleum followed by a gradient system of methanol-ethyl acetate was performed. Subfractions, which contained similar components, were combined and evaporated to dryness under reduced pressure to give three subfractions, as shown in **Table 136.**

Table 136 Subfractions obtained from **fraction C** by column chromatography over silica gel

Subfraction	Eluent	Weight (mg)	Physical appearance
C1	10-70% EtOAc/Light petroleum	5.1	Yellow gum
C2	70% EtOAc/Light petroleum-1% MeOH/EtOAc	6.3	Yellow gum
C3	5% MeOH/EtOAc-100% MeOH	2.9	Yellow gum

Subfraction C1 showed no UV-active spots on normal phase TLC using 40% ethyl acetate in light petroleum (8 runs) as a mobile phase. The ^{1}H NMR data indicated that it contained many compounds. Thus, it was not further purified.

Subfraction C2 displayed one major UV-active spot on normal phase TLC using 40% ethyl acetate in light petroleum (8 runs) as a mobile phase with the R_f value of 0.30. The ^{1}H NMR data indicated the presence of **N22** as a major component. Therefore, further investigation was not conducted.

Subfraction C3 showed many UV-active spots on normal phase TLC using 40% ethyl acetate in light petroleum (8 runs) as a mobile phase. Its ^{1}H NMR spectrum displayed none of major components. Thus, further purification was not performed.

Fraction D showed a long tail under UV-S on normal phase TLC using 100% dichloromethane (4 runs) followed by 1% methanol in dichloromethane (2 runs) as mobile phases. When using 30% ethyl acetate in light petroleum (6 runs) as a mobile phase, the chromatogram showed two UV-active spots on normal phase TLC with the R_f values of 0.05 and 0.23. Further separation by column chromatography over silica gel using a gradient system of ethyl acetate-light petroleum followed by a gradient system of methanol-ethyl acetate was performed. Subfractions, which contained similar components, were combined and evaporated to dryness under reduced pressure to give four subfractions, as shown in **Table 137.**

Table 137 Subfractions obtained from **fraction D** by column chromatography over silica gel

Subfraction	Eluent	Weight (mg)	Physical appearance
D1	20% EtOAc/Light petroleum - 100% EtOAc	4.6	Yellow gum
D2	2% MeOH/EtOAc	2.4	Yellow gum
D3	5-80% MeOH/EtOAc	8.1	Yellow gum
D4	100% MeOH	7.9	Brown gum

Subfraction D1 showed no UV-active spots on normal phase TLC using 30% ethyl acetate in light petroleum (4 runs) as a mobile phase. The ^{1}H NMR data indicated that it contained many compounds. Thus, it was not further investigated.

Subfraction D2 showed two UV-active spots on normal phase TLC with the R_f values of 0.18 and 0.33 using 50% ethyl acetate in light petroleum (3 runs)

as a mobile phase. The ^{1}H NMR data suggested that it was a mixture. Because of the minute amount, it was not further investigated.

Subfraction D3 showed one spot under UV-S on normal phase TLC with the R_f value of 0.10 using 50% ethyl acetate in light petroleum as a mobile phase (3 runs). Its ^{1}H NMR spectral data indicated that it was **N37**.

Subfraction D4 showed a long tail under UV-S on normal phase TLC using 50% ethyl acetate in light petroleum (3 runs) as a mobile phase. Its ^{1}H NMR spectrum displayed none of major components. Thus, further purification was not performed.

Fraction E showed a long tail under UV-S on normal phase TLC using 5% methanol in dichloromethane (2 runs) as a mobile phase. Its ^{1}H NMR spectrum displayed none of major components. Thus, further purification was not conducted.

CHAPTER 6.3
RESULTS AND DISCUSSION

Two known compounds (**N37** and **N38**) were isolated from the broth extract. The structures were identified by spectroscopic methods.

6.3.1 Compound N37

N37 was obtained as a white solid, melting at 217.2-218.0 °C. The UV spectrum showed maximum absorption bands at λ_{max} 235, 291 and 326 nm, indicating the presence of a conjugation chromophore. The IR spectrum exhibited absorption bands at 1706 and 1664 cm^{-1} for ketone carbonyl and conjugated ketone carbonyl groups, respectively. The HREI-MS showed the molecular formula $C_{17}H_{17}ClO_6$. The ^1H NMR spectrum (**Figure 92**) (**Table 138**) showed characteristic signals of one aromatic proton (δ_H 6.14, *s*, 1H) of a pentasubstituted benzene, one olefinic proton of a trisubstituted alkene (δ_H 5.55, *s*, 1H), one methine proton (2.85, *m*, 1H), two nonequivalent methylene protons [δ_H 3.03 (*dd*, J = 16.5 and 13.2 Hz, 1H) and 2.43 (*dd*, J = 16.5 and 4.5 Hz, 1H)], three methoxyl groups [δ_H 4.04 (*s*, 3H), 3.98 (*s*, 3H) and 3.62 (*s*, 3H)] and one methyl group (δ_H 0.96, *d*, J = 6.6 Hz, 3H). Carbon resonances of an α, β-unsaturated ketone moiety (δ_C 197.02, 170.79 and 104.86) and the ketone carbonyl carbon (δ_C 192.45), in the ^{13}C NMR spectrum (**Figure 93**) (**Table 138**), supported the IR data. In addition, its ^{13}C NMR spectrum showed six quaternary (δ_C 169.54, 164.61, 157.76, 105.16, 97.28 and 90.75), two methine (δ_C 89.50 and 36.43), one methylene (δ_C 40.05), three methoxyl (δ_C 57.00, 56.66 and 56.38) and one methyl (δ_C 14.23) carbons. The olefinic proton (δ_H 5.55) of the trisubstituted alkene was attributed to H-2′ on the basis of HMBC correlations with C-2 (δ_C 90.75), C-1′ (δ_C 170.79), C-3′ (δ_C 197.02) and C-4′ (δ_C 40.05). One of the methoxyl groups resonating at δ_H 3.62 was located at C-1′ due to its HMBC correlation with C-1′. Signal enhancement of H-2′ resonance after irradiation of 1′-OCH_3, in the NOEDIFF experiment, supported the above assignment. In the COSY spectrum (**Table 139**), The

methine proton (δ_H 2.85, H-5′) was coupled with the nonequivalent methylene protons (δ_H 3.03 and 2.43, H_{ab}-4′) and the methyl protons (δ_H 0.96, Me-6′). These results together with the ^3J HMBC correlations of H_b-4′/C-2, C-2′ (δ_C 104.86) and C-6′ (δ_C 14.23), H-5′/C-3 (δ_C 192.45) and Me-6′/C-2 and C-4′ (δ_C 40.05) constructed a cyclohexenone ring having the ketone carbonyl and methyl groups at C-2 and C-5′, respectively. The methoxyl groups resonating at δ_H 3.98 and 4.04 were located at C-4 (δ_C 157.76) and C-6 (δ_C 164.61) of the pentasubstituted benzene, respectively, on the basis of the following ^3J HMBC correlations (**Table 139**): 4-OCH_3/C-4 and 6-OCH_3/C-6. The aromatic proton (δ_H 6.14) was attributed to H-5 due to ^3J HMBC cross peaks with C-3a (δ_C 105.16) and C-7 (δ_C 97.28). Signal enhancement of 4-OCH_3 and 6-OCH_3 upon irradiation of H-5 in the NOEDIFF experiment (**Table 139**) supported above assignment. A ^4J HMBC cross peak of H-5/C-3 indicated that the previous ketone carbonyl group was also linked at C-3a of the aromatic ring. The chemical shifts of C-7a (δ_C 169.54) and C-2 indicated that these carbons were oxycarbons. According to the molecular formula and the X-ray data (**Figure 94**), the C-2 and C-7a joined together with an ether linkage to form a 3-oxobenzofuran moiety which had a spiro-cyclohexenone ring at C-2. Consequently, the substituent at C-7 must be a chlorine atom. In the previous literature, griseofulvin and epigriseofulvin showed $[\alpha]_D^{24}$ +339.00 (c = 1.03, $CHCl_3$) and $[\alpha]_D$ +83.00 (c = 1.00, $CHCl_3$), respectively (Taub *et al.*, 1963). The observed optical rotation of **N37** ($[\alpha]_D^{27}$ +305.00, c = 1.03, $CHCl_3$) was almost identical to that of griseofulvin, indicating that they possessed the same absolute configuration. Therefore, **N37** was identified as griseofulvin, which was previously isolated from *Penicillium griseofulvin* (MacMillan, 1953).

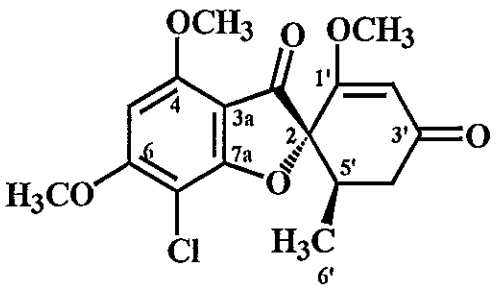

Table 138 The NMR data of **N37** and **griseofulvin** in $CDCl_3$

Position	N37		Griseofulvin[a]
	δ_H	δ_C	δ_C
2	-	90.75 (C)	90.1 (C)
3	-	192.45 (C=O)	191.2 (C=O)
3a	-	105.16 (C)	104.1 (C)
4	-	157.76 (C)	157.6 (C)
4-OCH_3	3.98 (*s*)	56.38 (CH_3)	57.5 (CH_3)
5	6.14 (*s*)	89.50 (CH)	91.2 (CH)
6	-	164.61 (C)	169.6 (C)
6-OCH_3	4.04 (*s*)	57.00 (CH_3)	56.6 (CH_3)
7	-	97.28 (C)	95.3 (C)
7a	-	169.54 (C)	164.5 (C)
1′	-	170.79 (C)	170.3 (C)
1′-OCH_3	3.62 (*s*)	56.66 (CH_3)	57.1 (CH_3)
2′	5.55 (*s*)	104.86 (CH)	104.7 (CH)
3′	-	197.02 (C=O)	195.6 (C=O)
4′	a: 2.43 (*dd*, 16.5, 4.5) b: 3.03 (*dd*, 16.5, 13.2)	40.05 (CH_2)	39.5 (CH_2)
5′	2.85 (*m*)	36.43 (CH)	35.4 (CH_2)
6′	0.96 (*d*, 6.6)	14.23 (CH_3)	13.8 (CH_3)

[a] Levine *et al.*, 1975.

Table 139 The HMBC, COSY and NOE data of **N37** in $CDCl_3$

Position	HMBC	COSY	NOE
4-OCH_3	C-4	-	H-5
H-5	C-3, C-3a, C-4, C-6, C-7	-	4-OCH_3, 6-OCH_3
6-OCH_3	C-6	-	H-5
1′-OCH_3	C-1′	-	H-2′
H-2′	C-2, C-1′, C-3′, C-4′	-	1′-OCH_3
H_a-4′	C-2, C-3′, C-5′, C-6′	H_b-4′, H-5′	H_b-4′, H-5′, Me-6′
H_b-4′	C-2, C-2′, C-3′, C-5′, C-6′	H_a-4′, H-5′	H_a-4′, Me-6′
H-5′	C-2, C-3, C-4′	H_{ab}-4′, Me-6′	H_a-4′, Me-6′
Me-6′	C-2, C-4′, C-5′	H-5′	H_{ab}-4′, H-5′

6.3.2 Compound N38

N38 was obtained as a white solid, melting at 193.5-194.1 °C. The UV and IR spectra were almost identical to those of **N37**. The HREI-MS showed the molecular formula $C_{17}H_{18}O_6$. The ^1H NMR spectral data (**Figure 96**) (**Table 140**) were similar to those of **N37** except for the presence of two *meta*-coupled aromatic protons [δ_H 6.05 (*d*, *J* = 3.0 Hz, 1H) and 6.24 (*d*, *J* = 3.0 Hz, 1H)] which were attributed to H-5 and H-7, respectively, on the basis of HMBC correlations (**Table 141**) of H-5/C-3a (δ_C 104.43), C-4 (δ_C 159.13), C-6 (δ_C 170.39) and C-7 (δ_C 88.55) and those of H-7/C-3a, C-5 (δ_C 93.34), C-6 and C-7a (δ_C 176.09). This evidence together with the molecular formula supported that the chloride atom at C-7 in **N37** was replaced, in **N38**, by an aromatic proton. In the previously literature, dechlorogriseofulvin and epidechlorogriseofulvin displayed $[\alpha]_D^{19}$ +390.00 (c = 1.00, acetone) (MacMillan, 1953) and $[\alpha]_D^{20}$ +28.50 (c = 0.20, acetone) (Jarvis *et al.*, 1996), respectively. The observed optical rotation of **N38** ($[\alpha]_D^{27}$ +364.00, c = 1.00, acetone) was almost identical to that of dechlorogriseofulvin, indicating that they possessed the same absolute configuration. Therefore, **N38** was assigned as dechlorogriseofulvin, which was previously isolated from *Penicillium griseofulvin* (MacMillan, 1953).

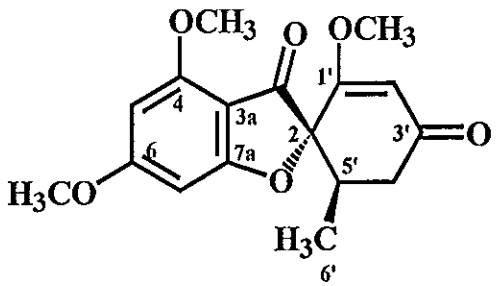

Table 140 The NMR data of **N38** and **dechlorogriseofulvin** in $CDCl_3$

Position	N38		Dechlorogriseofulvin[a]
	δ_H	δ_C	δ_C
2	-	89.95 (C)	91.0 (C)
3	-	192.50 (C=O)	191.9 (C=O)
3a	-	104.43 (C)	105.5 (C)
4	-	159.13 (C)	159.3 (C)
4-OCH_3	3.91 (*s*)	56.11 (CH_3)	57.1 (CH_3)
5	6.05 (*d*, 3.0)	93.34 (CH)	90.7 (CH)
6	-	170.39 (C)	171.4 (C)
6-OCH_3	3.90 (*s*)	56.08 (CH_3)	56.4 (CH_3)
7	6.24 (*d*, 3.0)	88.55 (CH)	96.9 (CH)
7a	-	176.09 (C)	176.3 (C)
1′	-	171.31 (C)	170.6 (C)
1′-OCH_3	3.63 (*s*)	56.61 (CH_3)	56.6 (CH_3)
2′	5.54 (*s*)	104.78 (CH)	105.4 (CH)
3′	-	197.33 (C=O)	195.5 (C=O)
4′	a: 2.40 (*dd*, 18.0, 6.0) b: 3.06 (*dd*, 18.0, 12.0)	40.10 (CH_2)	40.5 (CH_2)
5′	2.76 (*m*)	36.58 (CH)	36.8 (CH)
6′	0.96 (*d*, 9.0)	14.26 (CH_3)	14.3 (CH_3)

[a] Sato *et al.*, 1976.

Table 141 The HMBC, COSY and NOE data of **N38** in $CDCl_3$

Position	HMBC	COSY	NOE
4-OCH_3	C-4	-	H-5
H-5	C-3a, C-4, C-6, C-7	H-7	4-OCH_3, 6-OCH_3
6-OCH_3	C-6	-	H-5, H-7
H-7	C-3a, C-5, C-6, C-7a	H-5	6-OCH_3
1′-OCH_3	C-1′	-	H-2′
H-2′	C-2, C-1′, C-3′, C-4′	-	1′-OCH_3
H_a-4′	C-3′, C-5′, C-6′	H_b-4′, H-5′	H_b-4′, H-5′
H_b-4′	C-2, C-2′, C-3′, C-5′, C-6′	H_a-4′, H-5′	H_a-4′, Me-6′
H-5′	C-2, C-3	H_{ab}-4′, Me-6′	H_a-4′, Me-6′
Me-6′	C-2, C-4′, C-5′	H-5′	H_{ab}-4′, H-5′

PART VII

CHEMICAL CONSTITUENTS FROM THE ENDOPHYTIC FUNGUS *PHOMOPSIS* SP. PSU-A56

CHAPTER 7.1
INTRODUCTION

7.1.1 Introduction

Various types of compounds were isolated from the genus *Phomopsis* (**Table 142**). Some of them showed interesting biological activities (**Table 142**). Chemical constituents isolated from the genus *Phomopsis* were summarized by Miss Ubonta Sommart in 2007. Therefore, only additional constituents based on SciFinder Scholar database and some missing information are reported in **Table 142**.

The endophytic fungus *Phomopsis* sp. PSU-A56 was isolated from the leaves of *Garcinia atroviridis*, collected in Yala Province, Thailand, in 2005. This fungus was deposited as PSU-A56 at the Department of Microbiology, Faculty of Science, Prince of Songkla University. The ethyl acetate extract from the culture broth of this endophytic fungus exhibited antibacterial and antifungal activities against *Escherichia coli* ATCC25922 (EC) and *Cryptococcus neoformans* ATCC90113 (CN) with MIC values of 320 and 640 μg/ml, respectively.

Table 142 Compounds isolated from the *Phomopsis* genus

Scientific name	Compound	Activity	References
P. amygdali *Niigata*	(+)-Menthol, **134** (+)-7-Hydroxymenthol, **135** (+)-(6*S*)-Hydroxymenthol, **136** (-)-*p*-Menthanetriol, **137**	-	Sassa *et al.*, 2003
	Fusicoccin R, **138** Fusicoccin S, **139** 3α-Hydroxyfusicoccin J, **140** Phomopsiol, **141**	Germination-stimulating activity toward lettuce seed	Tajima *et al.*, 2004

Table 142 Continued

Scientific name	Compound	Activity	References
P. cassiae	Ethyl 2,4-dihydroxy-5,6-dimethylbenzoate, **142** Phomopsilactone, **143**	Antifungal and cytotoxicity against human cervical tumor cell line	Silva *et al.*, 2005
	(7*S*,9*S*,10*S*)-3,9,12-Trihydroxycalamenene, **144** (7*S*,9*R*,10*S*)-3,9,12-Trihydroxycalamenene, **145** (7*S*,10*S*)-3,12-Dihydroxycalamenene, **146** 3,12-Dihydroxycadalene, **147** 3,11,12-Trihydroxycadalene, **148**	Antifungal and cytotoxicity	Silva *et al.*, 2006
P. helianthi	*trans*-4,6-Dihydroxymellein, **149** *cis*-4,6-Dihydroxymellein, **150**	Phytotoxic	Avantaggiato *et al.*, 1999.
P. juniperovora	1-Hydroxy-3-methoxy-6-methylanthraquinone, **151** 1,7-Dihydroxy-3-methoxy-6-methylanthraquinone, **152** 1-Hydroxy-3,7-dimethoxy-6-methylanthraquinone, **153** Stemphylin, **154**	-	Wheeler *et al.*, 1975
P. leptostromiformis	Roridin A, **155**	Hepatotoxicity	Samples *et al.*, 1984

Table 142 Continued

Scientific name	Compound	Activity	References
	Phomopsin A, **156**	-	Mackay *et al.*, 1986 Culvenor *et al.*, 1989
P. oblonga	Orsellinic acid, **157** Tyrosol, **39** (-)-5-Methylmellein, **158** Nectriapyrone, **159** (-)-5-Carboxymellein, **73** Oblongolide A, **160** Phomopsolide A, **161** Phomopsolide B, **162** 5-Methyluracil, **163** 2-Furoic acid, **164** 3-Nitropropanoic acid, **165** Portensterol, **166** (+)-Mellein, **167**	Boring and feeding deterrent activity for elm bark beetles	Claydon *et al.*, 1985
	Phomopsolide A, **161** Phomopsolide B, **162** 6-(4-Hydroxy-3-oxo-1-pentenyl)2*H*-pyran-2-one, **168**	Boring and feeding deterrent activity for elm bark beetles	Grove 1985
P. paspelli	Cytochalasin H, **169** Cytochalasin J, **170**	-	Patwardhan *et al.*, 1974
	Cytochalasin H, **169**	Antiinflam-matory	Deshmukh *et al.*, 1978

Table 142 Continued

Scientific name	Compound	Activity	References
	Oblongolide M, **185** Oblongolide I, **186** Oblongolide J, **187** Oblongolide K, **188** Phomopsolide B, **162** Alternariol, **189** Alternariol monomethyl ether, **190** Alternariol dimethyl ether, **191** Ergosterol, **44** 5α,8α-Epidioxyergosterol, **192** 4-[5-(1-Hydroxyethyl)furan-2-yl]-4-oxobutanoic acid, **193**		
	Phomoxanthone A, **194** Cytochalasin L-696474, **195** 21-*O*-Deacetylcytochalasin L-696474, **196**	Biological activities against bacteria and phytopatho-genic fungi	Elsaesser *et al.*, 2005

Structures of the metabolites from *Phomopsis* genus

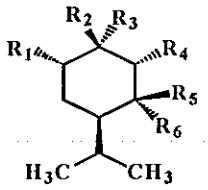

134: $R_1 = R_2 = R_4 = R_5 = H$, $R_3 = CH_3$, $R_6 = OH$: (+)-Menthol

135: $R_1 = R_2 = R_4 = R_5 = H$, $R_3 = CH_2OH$, $R_6 = OH$: (+)-7-Hydroxymenthol

136: $R_1 = R_6 = OH$, $R_2 = R_4 = R_5 = H$, $R_3 = CH_3$: (+)-(6*S*)-Hydroxymenthol

137: $R_1 = R_6 = H$, $R_2 = CH_3$, $R_3 = R_4 = R_5 = OH$: (-)-*p*-Menthanetriol

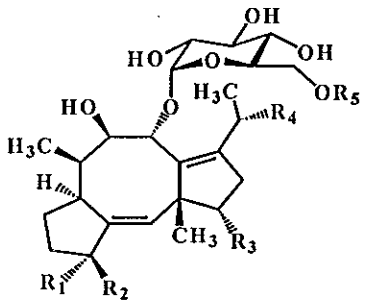

138: $R_1 = R_3 = OH$, $R_2 = CH_2OCH_3$, $R_4 = CH_2OAc$, $R_5 =$ 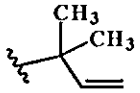 : Fusicoccin R

139: $R_1 = CH_2OH$, $R_2 = OH$, $R_3 = R_5 = H$, $R_4 = CH_3$: Fusicoccin S

140: $R_1 = R_3 = OH$, $R_2 = CH_2OCH_3$, $R_4 = CH_3$, R5 = 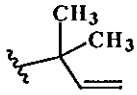 : 3α-Hydroxyfusicoccin J

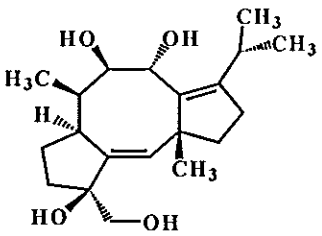

141: Phomopsiol

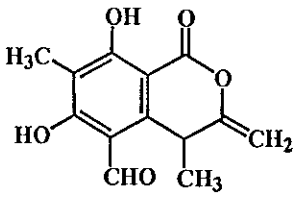

143: Phomopsilactone

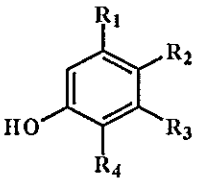

142: $R_1 = OH$, $R_2 = CO_2Et$, $R_3 = R_4 = CH_3$: Ethyl 2,4-dihydroxy-5,6-dimethylbenzoate

157: $R_1 =$ OH, $R_2 = CO_2H$, $R_3 = CH_3$, $R_4 = H$: Orsellinic acid

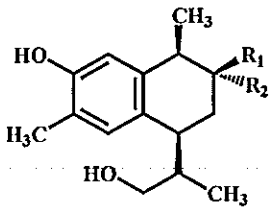

144: R_1 = OH, R_2 = H: (7*S*,9*S*,10*S*)-3,9,12-Trihydroxycalamenene
145: R_1 = H, R_2 = OH : (7*S*,9*R*,10*S*)-3,9,12-Trihydroxycalamenene
146: R_1 = R_2 = H: (7*S*,10*S*)-3,12-Dihydroxycalamenene

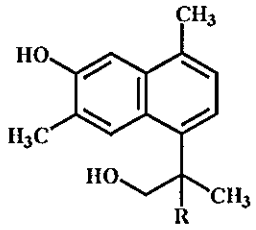

147: R = H: 3,12-Dihydroxycadalene
148: R = OH: 3,11,12-Trihydroxycadalene

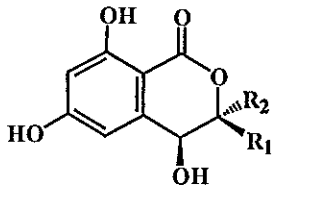

149: R_1 = H, R_2 = CH_3 : *trans*-4,6-Dihydroxymellein
150: R_1 = CH_3, R_2 = H : *cis*-4,6-Dihydroxymellein

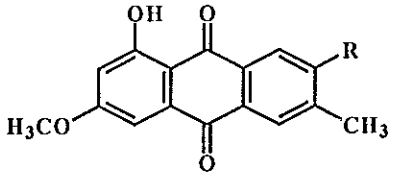

151: R = H : 1-Hydroxy-3-methoxy-6-methylanthraquinone
152: R = OH : 1,7-Dihydroxy-3-methoxy-6-methylanthraquinone
153: R = OCH_3 : 1-Hydroxy-3,7-dimethoxy-6-methylanthraquinone

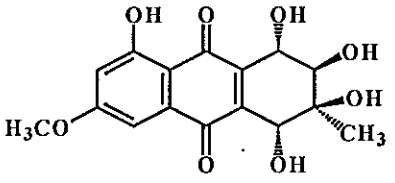

154: Stemphylin

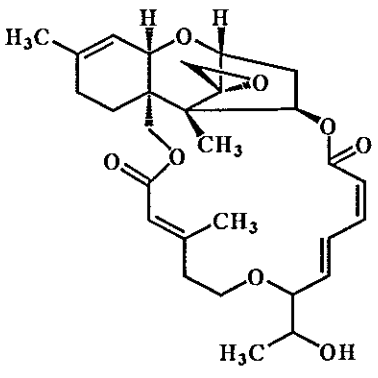

155: Roridin A

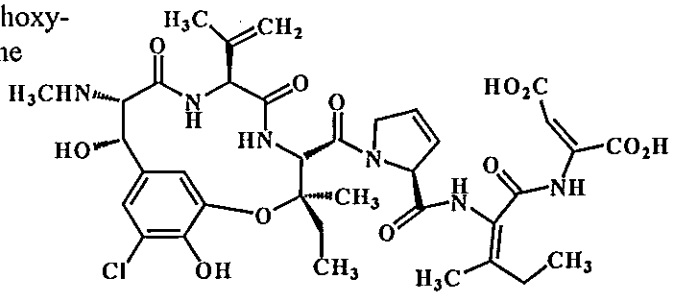

156: Phomopsin A

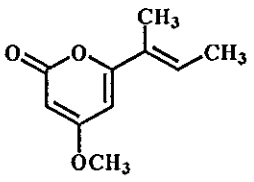

159: Nectriapyrone

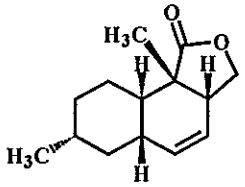

160: Oblongolide A

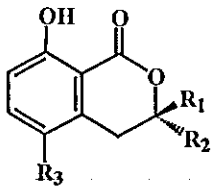

158: R_1 = H, R_2 = R_3 = CH_3 : (-)-5-Methylmellein
167: R_1 = CH_3, R_2 = R_3 = H : (+)-Mellein

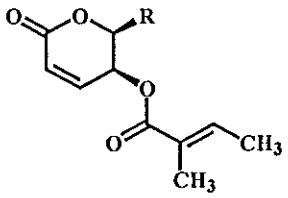

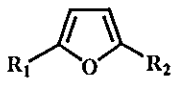

164: R_1 = H, R_2 = CO_2H : 2-Furoic acid

161: R = 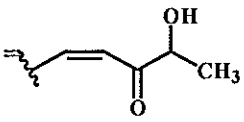 : Phomopsolide A

193: R_1 = $CHOHCH_3$, R_2 = 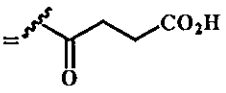

: 4-[5-(1-Hydroxyethyl)furan-2-yl]-4-oxobutanoic acid

162: R = 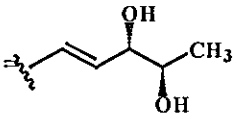 : Phomopsolide B

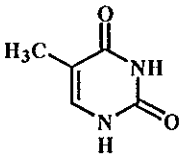

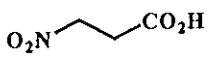

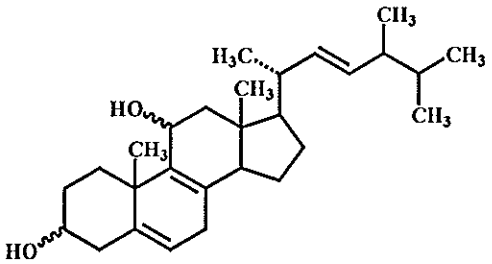

163: 5-Methyluracil **165:** 3-Nitropropanoic acid

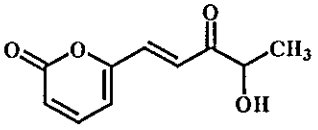

166: Portensterol

168: 6-(4-Hydroxy-3-oxo-1-pentenyl)2*H*-pyran-2-one

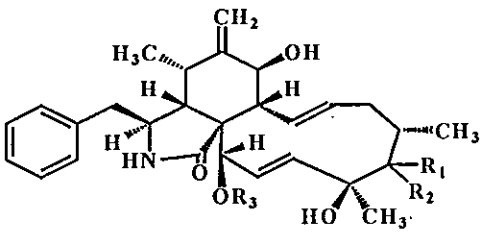

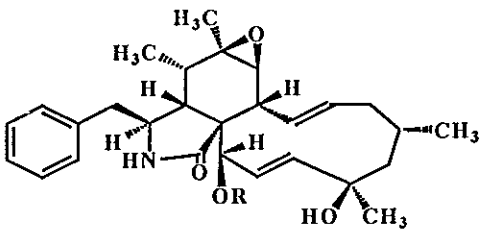

169: R_1 = R_2 = H, R_3 = Ac : Cytochalasin H
170: R_1 = R_2 = R_3 = H : Cytochalasin J

171: R = Ac : Epoxycytochalasin H
172: R = H : Epoxycytochalasin J

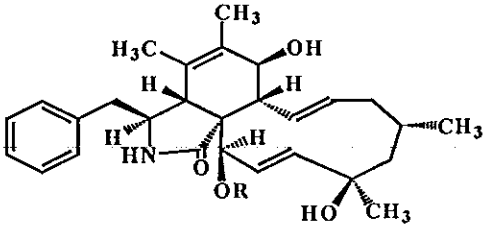

173: R = Ac : Cytochalasin N
174: R = H : Cytochalasin O

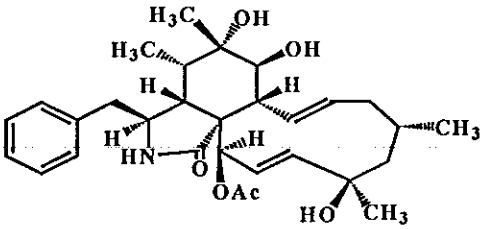

175: Cytochalasin P

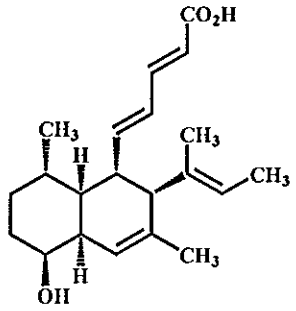

176: Phomopsidine

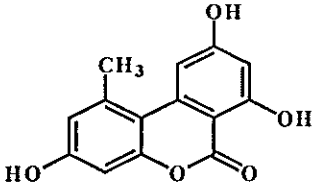

189: Alternariol

190: Alternariol monomethyl ether
OCH_3 at C-3, C-7 or C-9

191: Alternariol dimethyl ether
OCH_3 at C-3 and C-7, C-3 and C-9 or C-7 and C-9

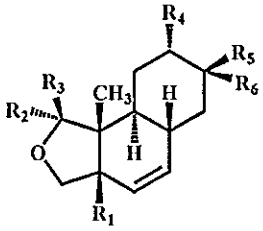

177: $R_1 = R_5 = OH$, $R_2+R_3 = O$, $R_4 = H$, $R_6 = CH_3$: Oblongolide B
178: $R_1 = OH$, $R_2+R_3 = O$, $R_4 = R_5 = H$, $R_6 = CH_3$: Oblongolide C
179: $R_1 = R_4 = H$, $R_2+R_3 = O$, $R_5 = OH$, $R_6 = CH_3$: Oblongolide D
180: $R_1 = OH$, $R_2+R_3 = O$, $R_4 = R_5 = H$, $R_6 = CH_2OH$: Oblongolide E
181: $R_1 = R_4 = R_5 = H$, $R_2+R_3 = O$, $R_6 = CH_2OH$: Oblongolide F
182: $R_1 = R_4 = R_5 = H$, $R_2+R_3 = O$,$R_6 = CH_2OAc$: Oblongolide G
183: $R_1 = R_5 = H$, $R_2+R_3 = O$, $R_4 = OH$, $R_6 = CH_3$: Oblongolide H
184: $R_1 = R_4 = R_5 = H$, $R_2 = n$-BuO, $R_3 = Ac$, $R_6 = CH_2OAc$: Oblongolide L
185: $R_1 = R_4 = R_5 = H$, $R_2 = OH$, $R_3 = Ac$, $R_6 = CH_2OAc$: Oblongolide M

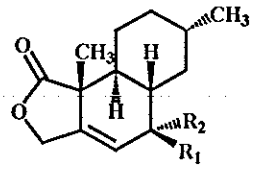

186: $R_1+R_2 = O$: Oblongolide I

187: $R_1 = OH$, $R_2 = H$: Oblongolide J

188: $R_1 = H$, $R_2 = OH$: Oblongolide K

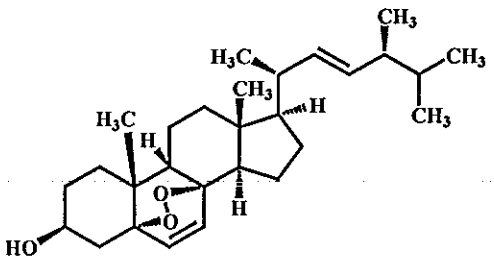

192: 5α,8α-Epidioxyergosterol

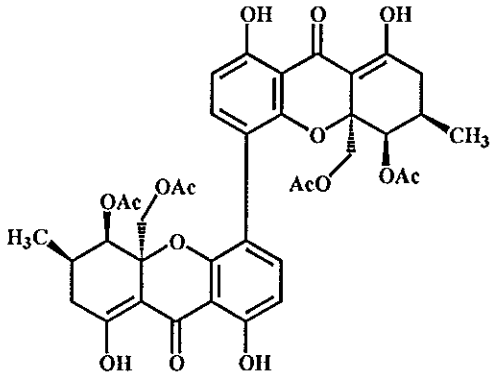

194: Phomoxanthone A

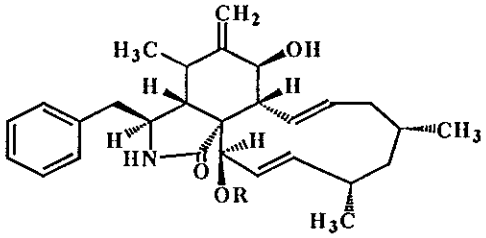

195: R = Ac : Cytochalasin L-696474

196: R = H : 21-*O*-Deacetylcytochalasin L-696474

CHAPTER 7.2
EXPERIMENTAL

7.2.1 Fermentation and extraction

The fermentation and extraction was performed using the same procedure as those of *Botryosphaeria mamane* PSU-M76. The crude EtOAc extracts from the culture broth and mycelia were obtained in 2.84 g and 506.2 mg, respectively, both as a brown gum. The crude mycelial extract was not further investigated because its ^{1}H NMR spectrum indicated the presence of a mixture of long-chain hydrocarbons.

7.2.2 Purification of the broth extract

The broth extract showed three UV-active spots on normal phase TLC with the R_f values of 0.13, 0.45 and 0.83 using 100% dichloromethane (2 runs) as a mobile phase. It was further separated by column chromatography over Sephadex LH20 using 100% MeOH as eluent. Fractions, which contained similar components, were combined and evaporated to dryness under reduced pressure to give five fractions, as shown in **Table 143**.

Table 143 Fractions obtained from **the broth extract** by column chromatography over Sephadex LH20

Fraction	Eluent	Weight (g)	Physical appearance
A	100% MeOH	0.2649	Brown solid
B	100% MeOH	2.5968	Brown-red solid
C	100% MeOH	0.0360	Brown solid
D	100% MeOH	0.1141	Brown gum
E	100% MeOH	0.0275	Brown gum

Fraction A showed four spots under UV-S on normal phase TLC with the R_f values of 0.05, 0.13, 0.43 and 0.58 using 2% methanol in dichloromethane as a mobile phase (3 runs). Further separation by column chromatography over silica gel using a gradient system of methanol-dichloromethane was performed. Subfractions, which contained similar components, were combined and evaporated to dryness under reduced pressure to give four subfractions, as shown in **Table 144.**

Table 144 Subfractions obtained from **fraction A** by column chromatography over silica gel

Subfraction	Eluent	Weight (mg)	Physical appearance
A1	100% CH_2Cl_2 - 6% MeOH/CH_2Cl_2	6.8	Pale-yellow gum
A2	6-10% MeOH/CH_2Cl_2	92.1	Yellow gum mixed with yellow solid
A3	10-20% MeOH/CH_2Cl_2	20.4	Yellow gum
A4	20% MeOH/CH_2Cl_2 - 100% MeOH	106.3	Brown gum

Subfraction A1 showed no UV-active spots on normal phase TLC using 4% methanol in dichloromethane (3 runs) as a mobile phase. Its ^{1}H NMR spectrum displayed proton signals at high field region. Thus, no attempted investigation was performed.

Subfraction A2, upon standing at room temperature, was separated into two parts: a white solid (55.4 mg) and a yellow solution. Both showed one UV-active spot on normal phase TLC with the R_f value of 0.50 using 4% methanol in dichloromethane (3 runs) as a mobile phase. Its ^{1}H NMR spectral data indicated the presence of **N22** as a major component. Thus, it was not further investigated.

Subfraction A3 showed two UV-active spots on normal phase TLC with the R_f values of 0.28 and 0.35 using 4% methanol in dichloromethane (3 runs) as

a mobile phase. It was further separated by column chromatography over Sephadex LH20 using 100% MeOH as eluent. All subfractions were examined by TLC, combined on the basis of their chromatogram characteristics and then evaporated to dryness under reduced pressure to afford three subfractions, as shown in **Table 145.**

Table 145 Subfractions obtained from **subfraction A3** by column chromatography over Sephadex LH20

Subfraction	Eluent	Weight (mg)	Physical appearance
A3-1	100% MeOH	5.7	Pale-yellow gum
A3-2	100% MeOH	5.8	Yellow gum
A3-3	100% MeOH	8.6	Yellow gum

Subfraction A3-1 demonstrated no UV-active spots using 2% methanol in dichloromethane (3 runs) as a mobile phase. In addition, its chromatogram showed no spots after dipping the normal phase TLC in ASA reagent and subsequently heating. Its ^{1}H NMR spectrum displayed proton signals at high field region. Therefore, it was not further investigated.

Subfraction A3-2 showed no UV-active spots on normal phase TLC using 2% methanol in dichloromethane (3 runs) as a mobile phase and showed many inseparable spots after dipping the normal phase TLC in ASA reagent and subsequently heating. Its ^{1}H NMR spectrum displayed none of major components. Thus, no attempted investigation was carried out.

Subfraction A3-3 displayed many spots under UV-S on normal phase TLC using 2% methanol in dichloromethane (3 runs) as a mobile phase and showed many inseparable spots after dipping the normal phase TLC in ASA reagent and subsequently heating. Its ^{1}H NMR spectrum displayed none of aromatic proton signal. Thus, no attempted investigation was performed.

Subfraction A4 showed two overlapping UV-active spots on normal phase TLC using 4% methanol in dichloromethane (3 runs) as a mobile phase. Its ^{1}H NMR spectrum displayed proton signals at high field region. Thus, it was not further purified.

Fraction B was separated into two parts: a white solid (241.5 mg) (**N39**) and a brown solution (**Bs**), upon standing at room temperature. **N39** melted at 151.8-152.4 °C and showed one UV-active spot on normal phase TLC with the R_f value of 0.23 using 100% dichloromethane as a mobile phase (5 runs).

$[\alpha]_D^{27}$		-95.33 (c = 0.33, EtOH)
UV(MeOH) λ_{max} nm (log ε)		257 (4.33)
FT-IR (neat) ν_{cm-1}		3402 (O-H stretching), 1648 (C=O stretching), 1608 (C=C stretching)
^{1}H NMR ($CDCl_3$+CD_3OD) (δ ppm) (300 MHz)		5.25 (*d*, *J* = 2.1 Hz, 1H), 4.51 (*d*, *J* = 6.6 Hz, 1H), 4.48 (*d*, *J* = 6.6 Hz, 1H), 3.76 (*s*, 3H), 3.30 (*d*, *J* = 2.1 Hz, 1H), 1.63 (*s*, 3H)
^{13}C NMR ($CDCl_3$+CD_3OD) (δ ppm) (75 MHz)		194.11, 172.75, 97.92, 68.74, 60.25, 59.54, 56.50, 18.79
DEPT (135°) ($CDCl_3$+CD_3OD)	CH :	97.92, 68.74, 60.25
	CH_3 :	56.50, 18.79
EIMS *m/z* (% relative intensity):		170 (41), 141 (100), 125 (91), 113 (26), 85 (25)

The brown solution (**Bs**) showed seven UV-active spots on normal phase TLC with the R_f values of 0.10, 0.20, 0.23, 0.55, 0.65, 0.70 and 0.88 using 2% methanol in dichloromethane (3 runs) as a mobile phase. Further separation by column chromatography over silica gel using a gradient system of methanol-dichloromethane was performed. Subfractions, which contained similar components, were combined and evaporated to dryness under reduced pressure to give five subfractions, as shown in **Table 146.**

Table 146 Subfractions obtained from **fraction Bs** by column chromatography over silica gel

Subfraction	Eluent	Weight (g)	Physical appearance
Bs1	100% CH_2Cl_2	0.0064	Yellow gum
Bs2	100% CH_2Cl_2 - 3% MeOH/CH_2Cl_2	0.0601	Yellow solid
Bs3	3-5% MeOH/CH_2Cl_2	1.4005	Red gum mixed with white solid
Bs4	5% MeOH/CH_2Cl_2	0.3650	Red gum mixed with white solid
Bs5	8-80% MeOH/CH_2Cl_2	0.3185	Brown gum

Subfraction Bs1 showed no UV-active spots on normal phase TLC using 30% dichloromethane in light petroleum (3 runs) as a mobile phase. Its ^1H NMR spectrum displayed proton signals at high field region. Thus, no attempted investigation was carried out.

Subfraction Bs2 showed one UV-active spot on normal phase TLC with the R_f value of 0.50 using 30% dichloromethane in light petroleum (3 runs) as a mobile phase. Its ^1H NMR spectral data indicated the presence of **N15**. Thus, further investigation was not conducted.

Subfraction Bs3 showed four UV-active spots on normal phase TLC with the R_f values of 0.05, 0.23, 0.45 and 0.93 using 100% dichloromethane (6 runs) as a mobile phase. Further separation by column chromatography over silica gel was performed. Elution was conducted with gradient systems of dichloromethane-light petroleum and methanol-dichloromethane. Subfractions, which contained similar components, were combined and evaporated to dryness under reduced pressure to give eight subfractions, as shown in **Table 147**.

Table 147 Subfractions obtained from **fraction Bs3** by column chromatography over silica gel

Subfraction	Eluent	Weight (mg)	Physical appearance
Bs3-1	30-70% CH_2Cl_2/Light petroleum	352.5	Yellow solid
Bs3-2	100% CH_2Cl_2	3.7	Yellow gum
Bs3-3	100% CH_2Cl_2	4.6	Yellow gum
Bs3-4	1% MeOH/CH_2Cl_2	1.6	Yellow gum
Bs3-5	1-10% MeOH/CH_2Cl_2	5.2	Yellow gum
Bs3-6	10-20% MeOH/CH_2Cl_2	10.0	Orange gum mixed with orange solid
Bs3-7	30-80% MeOH/CH_2Cl_2	832.7	Brown-orange gum
Bs3-8	100% MeOH	11.3	Purple solid

Subfraction Bs3-1 showed one UV-active spot on normal phase TLC with the R_f value of 0.50 using 50% dichloromethane in light petroleum (2 runs) as a mobile phase. Its ^1H NMR spectral data indicated the presence of **N15**. Therefore, further investigation was not performed.

Subfraction Bs3-2 showed two UV-active spots on normal phase TLC with the R_f values of 0.35 and 0.50 using 50% dichloromethane in light petroleum (2 runs) as a mobile phase. Its ^1H NMR spectral data indicated the presence of a mixture of **N15** and **N40**. Therefore, further investigation was not carried out.

Subfraction Bs3-3 (N40) showed one UV-active spot on normal phase TLC with the R_f value of 0.35 using 50% dichloromethane in light petroleum (2 runs) as a mobile phase.

$[\alpha]_D^{27}$	-158.00 (c = 1.00, $CHCl_3$)
UV(MeOH) λ_{max} nm (log ε)	226 (4.20), 254 (3.76), 312 (3.25)

FT-IR (neat) ν_{cm-1}	3390 (O-H stretching), 1716 and 1682 (C=O stretching), 1592 (C=C stretching)
^{1}H NMR ($CDCl_3$) (δ ppm) (300 MHz)	11.83 (*s*, 1H), 8.13 (*d*, *J* = 9.0 Hz, 1H), 6.94 (*d*, *J* = 9.0 Hz, 1H), 4.67 (*m*, 1H), 3.88 (*s*, 3H), 3.87 (*dd*, *J* = 17.7, 3.3 Hz, 1H), 3.05 (*dd*, *J* = 17.7, 11.7 Hz, 1H), 1.56 (*d*, *J* = 6.3 Hz, 3H)
^{13}C NMR ($CDCl_3$) (δ ppm) (75 MHz)	170.03, 166.16, 165.51, 143.45, 138.46, 118.16, 116.23, 108.92, 75.61, 52.01, 32.61, 20.76
DEPT (135°) ($CDCl_3$)	CH : 138.47, 116.23, 75.61
	CH_2 : 32.61
	CH_3 : 52.01, 20.76

Subfraction Bs3-4 (N41) showed one UV-active spot on normal phase TLC with the R_f value of 0.18 using 50% dichloromethane in light petroleum (2 runs) as a mobile phase.

UV(MeOH) λ_{max} nm (log ε)	262 (4.71), 355 (3.70)
FT-IR (neat) ν_{cm-1}	1676 and 1653 (C=O stretching), 1602 (C=C stretching)
^{1}H NMR ($CDCl_3$) (δ ppm) (300 MHz)	6.54 (*qd*, *J* = 2.1, 1.8 Hz, 1H), 5.88 (*d*, *J* = 2.1 Hz, 1H), 3.81 (*s*, 3H), 2.07 (*d*, *J* = 1.8 Hz, 3H)
^{13}C NMR ($CDCl_3$) (δ ppm) (75 MHz)	187.36, 182.32, 158.82, 143.63, 133.83, 107.30, 56.22, 15.44
DEPT (135°) ($CDCl_3$)	CH : 133.83, 107.30
	CH_3 : 56.22, 15.44

Subfraction Bs3-5 showed no UV-active spots on normal phase TLC using 100% dichloromethane and 2% methanol in dichloromethane (2 runs) as mobile phases. The ^{1}H NMR spectrum displayed proton signals at high field region. Thus, no attempted investigation was performed.

Subfraction Bs3-6 showed two UV-active spots on normal phase TLC with the R_f values of 0.50 and 0.63 using 100% dichloromethane and 2% methanol in dichloromethane (2 runs) as mobile phases. Its ^{1}H NMR spectral data indicated that it was a mixture of **N17, N18** and **N40**. Therefore, it was not further investigated.

Subfraction Bs3-7 showed one major UV-active spot on normal phase TLC with the R_f value of 0.35 using 100% dichloromethane followed by 2% methanol in dichloromethane (2 runs) as mobile phases. The ^{1}H NMR data indicated the presence of **N39** as a major component. Therefore, it was not further investigated.

Subfraction Bs3-8 showed no UV-active spots on normal phase TLC using 100% dichloromethane followed by 2% methanol in dichloromethane (2 runs) as mobile phases. Its ^{1}H NMR spectrum showed none of major components. Thus, it was not further isolated.

Subfraction Bs4 showed one major UV-active spot on normal phase TLC with the R_f value of 0.23 using 100% dichloromethane (5 runs) as a mobile phase. Its ^{1}H NMR data suggested that it contained **N39** as a major component. Therefore, further investigation was not conducted.

Subfraction Bs5 showed two UV-active spots on normal phase TLC with the R_f values of 0.08 and 0.45 using 100% dichloromethane (5 runs) as a mobile phase. It was further separated by column chromatography over Sephadex LH20 using 100% MeOH as eluent. All subfractions were examined by TLC, combined on the basis of their chromatogram characteristics and then evaporated to dryness under reduced pressure to afford five subfractions, as shown in **Table 148**.

Table 148 Subfractions obtained from **subfraction Bs5** by column chromatography over Sephadex LH20

Subfraction	Eluent	Weight (mg)	Physical appearance
Bs5-1	100% MeOH	27.3	Brown gum
Bs5-2	100% MeOH	106.4	Brown gum
Bs5-3	100% MeOH	114.5	Brown gum
Bs5-4	100% MeOH	30.4	Brown solid
Bs5-6	100% MeOH	31.0	Brown solid mixed with brown gum

Subfraction Bs5-1 showed no UV-active spots on normal phase TLC using 4% methanol in dichloromethane (2 runs) as a mobile phase and showed no definite spots after dipping the normal phase TLC in ASA reagent and subsequently heating. Its ^{1}H NMR spectrum showed none of major proton signals. Thus, no attempted investigation was performed.

Subfraction Bs5-2 showed one major UV-active spot on normal phase TLC with the R_f value of 0.13 using 4% methanol in dichloromethane (2 runs) as a mobile phase. It was further separated by column chromatography over Sephadex LH20 using 100% MeOH as eluent. All subfractions were examined by TLC, combined on the basis of their chromatogram characteristics and then evaporated to dryness under reduced pressure to afford three subfractions, as shown in **Table 149.**

Table 149 Subfractions obtained from **subfraction Bs5-2** by column chromatography over Sephadex LH20

Subfraction	Eluent	Weight (mg)	Physical appearance
Bs5-21	100% MeOH	23.1	Yellow gum
Bs5-22	100% MeOH	77.4	Yellow gum
Bs5-23	100% MeOH	5.5	Browm gum

Subfraction Bs5-21 showed no UV-active spots on normal phase TLC using 4% methanol in dichloromethane (3 runs) as a mobile phase and showed no definite spots after dipping the normal phase TLC in ASA reagent and subsequently heating. Its ^{1}H NMR data suggested none of major components. Thus, no attempted investigation was carried out.

Subfraction Bs5-22 showed one major UV-active spot on normal phase TLC with the R_f value of 0.25 using 4% methanol in dichloromethane (3 runs) as a mobile phase. Its ^{1}H NMR data suggested that it contained sugars as major components. Thus, no attempted investigation was performed.

Subfraction Bs5-23 displayed many UV-active spots on normal phase TLC using 4% methanol in dichloromethane (3 runs) as a mobile phase. The ^{1}H NMR data indicated that it contained many compounds. Thus, it was not further purified.

Subfraction Bs5-3 showed two UV-active spots with the R_f values of 0.13 and 0.65 using 4% methanol in dichloromethane (3 runs) as a mobile phase. Further separation by column chromatography over Sephadex LH20 using 100% MeOH as eluent was performed. All subfractions were examined by TLC, combined on the basis of their chromatogram characteristics and then evaporated to dryness under reduced pressure to afford three subfractions, as shown in **Table 150**.

Table 150 Subfractions obtained from **subfraction Bs5-3** by column chromatography over Sephadex LH20

Subfraction	Eluent	Weight (mg)	Physical appearance
Bs5-31	100% MeOH	4.1	Brown gum
Bs5-32	100% MeOH	100.1	Brown gum
Bs5-33	100% MeOH	9.9	Brown-purple gum

Subfraction Bs5-31 showed no UV-active spots on normal phase TLC using 4% methanol in dichloromethane (3 runs) as a mobile phase and displayed as a

long tail under UV-S on reverse phase TLC using 20% methanol in water as a mobile phase. The ^{1}H NMR spectrum showed none of major proton signals. Thus, no attempted investigation was performed.

Subfraction Bs5-32 showed many UV-active spots on normal phase TLC using 4% methanol in dichloromethane (3 runs) as a mobile phase. Further purification by flash column chromatography over silica gel using a gradient system of methanol-dichloromethane was performed. Fractions, which contained similar components, were combined and evaporated to dryness under reduced pressure to give four subfractions, as shown in **Table 151.**

Table 151 Subfractions obtained from **subfraction Bs5-32** by flash column chromatography over silica gel

Subfraction	Eluent	Weight (mg)	Physical appearance
Bs5-321	100% CH_2Cl_2 - 5% MeOH/CH_2Cl_2	3.7	Yellow solid
Bs5-322	5-10% MeOH/CH_2Cl_2	2.6	Yellow gum
Bs5-323	10-30% MeOH/CH_2Cl_2	4.6	Yellow gum
Bs5-324	50% MeOH/CH_2Cl_2 - 100% MeOH	87.0	Brown gum

Subfraction Bs5-321 showed one UV-active spot on normal phase TLC with the R_f value of 0.45 using 2% methanol in dichloromethane (3 runs) as a mobile phase. The ^{1}H NMR data indicated that it was a mixture. Thus, no attempted separation was carried out.

Subfraction Bs5-322 showed two UV-active spots on normal phase TLC with the R_f values of 0.33 and 0.43 using 4% methanol in dichloromethane (4 runs) as a mobile phase. The ^{1}H NMR data suggested none of major components. Therefore, it was not further investigated.

Subfraction Bs5-323 (N42) displayed one major spot under UV-S on normal phase TLC with the R_f value of 0.18 using 4% methanol in dichloromethane (4 runs) as a mobile phase.

$[\alpha]_D^{27}$		+100.00 (c = 0.39, EtOH)
UV(MeOH) λ_{max} nm (log ε)		248 (4.79)
FT-IR (neat) ν_{cm-1}		3418 (O-H stretching), 1647 (C=O stretching), 1616 (C=C stretching)
^{1}H NMR ($CDCl_3$+CD_3OD) (δ ppm) (300 MHz)		5.43 (*s*, 1H), 4.49 (*s*, 1H), 4.13 (*s*, 1H), 3.81 (*s*, 3H), 1.15 (*s*, 3H)
^{13}C NMR ($CDCl_3$+CD_3OD) (δ ppm) (75 MHz)		196.48, 174.64, 99.43, 77.21, 75.07, 74.65, 56.81, 18.34
DEPT (135°) ($CDCl_3$+CD_3OD)	CH :	99.43, 75.07, 74.65
	CH_3 :	56.81, 18.34
EIMS *m/z* (% relative intensity):		170 (31), 141 (100), 125 (42), 114 (68), 86 (77)

Subfraction Bs5-324 displayed many inseparable spots under UV-S on normal phase TLC using 4% methanol in dichloromethane (4 runs) as a mobile phase. It was further acetylated with acetic anhydride (7.0 ml) in the presence of pyridine (1.0 ml). The mixture was stirred at room temperature for 24 hours. To the extract was added H_2O (20 ml), and the reaction mixture was extracted with ethyl acetate (3×20 ml). The ethyl acetate layer was consecutively washed with 10% hydrochloric acid (3×20 ml), 10% sodium bicarbonate (3×20 ml) and water (2×20 ml). The organic layer was dried over anhydrous Na_2SO_4, filtered and evaporated under reduced pressure to yield a yellow gum (97.6 mg), which displayed as a long tail under UV-S on normal phase TLC using 4% methanol in dichloromethane (4 runs) as a mobile phase. The ^{1}H NMR data suggested that it contained sugars as major components. Thus, no attempted purification was carried out.

Subfraction Bs5-33 showed no spots under UV-S on normal phase TLC using 4% methanol in dichloromethane (3 runs) as a mobile phase. The ^{1}H NMR

data suggested that it contained none of major components. Thus, no attempted purification was carried out.

Subfraction Bs5-4 showed one UV-active spot on normal phase TLC with the R_f value of 0.65 using 4% methanol in dichloromethane (2 runs) as a mobile phase. It was further separated by column chromatography over Sephadex LH20 using 100% MeOH as eluent. All subfractions were examined by TLC, combined on the basis of their chromatogram characteristics and then evaporated to dryness under reduced pressure to afford four subfractions, as shown in **Table 152.**

Table 152 Subfractions obtained from **subfraction Bs5-4** by column chromatography over Sephadex LH20

Subfraction	Eluent	Weight (mg)	Physical appearance
Bs5-41	100% MeOH	7.5	Yellow gum
Bs5-42	100% MeOH	6.0	Purple solid
Bs5-43	100% MeOH	10.5	Purple-brown gum
Bs5-44	100% MeOH	5.3	Brown gum

Subfraction Bs5-41 showed two UV-active spots on normal phase TLC with the R_f values of 0.13 and 0.50 using 4% methanol in dichloromethane (2 runs) as a mobile phase. Its ^{1}H NMR spectrum displayed none of major components. Therefore, further investigation was not conducted.

Subfraction Bs5-42 displayed many spots under UV-S on normal phase TLC using 4% methanol in dichloromethane (2 runs) as a mobile phase. The ^{1}H NMR data indicated that it contained many compounds. Thus, it was not further purified.

Subfraction Bs5-43 displayed two spots under UV-S on normal phase TLC with the R_f values of 0.25 and 0.50 using 4% methanol in dichloromethane (2

runs) as a mobile phase. The ^{1}H NMR data indicated the presence of a mixture of **N31** and other components. Therefore, it was not further separated.

Subfraction Bs5-44 showed no UV-active spots on normal phase TLC using 4% methanol in dichloromethane (2 runs) as a mobile phase. Its ^{1}H NMR spectrum displayed none of major components. Therefore, further investigation was not performed.

Subfraction Bs5-5 showed two UV-active spots on normal phase TLC with the R_f values of 0.30 and 0.65 using 4% methanol in dichloromethane (2 runs) as a mobile phase. It was further separated by column chromatography over Sephadex LH20 using 100% MeOH as eluent. All subfractions were examined by TLC, combined on the basis of their chromatogram characteristics and then evaporated to dryness under reduced pressure to afford three subfractions, as shown in **Table 153.**

Table 153 Subfractions obtained from **subfraction Bs5-5** by column chromatography over Sephadex LH20

Subfraction	Eluent	Weight (mg)	Physical appearance
Bs5-51	100% MeOH	4.4	Pale-yellow gum
Bs5-52	100% MeOH	21.2	Purple solid
Bs5-53	100% MeOH	4.8	Brown gum

Subfraction Bs5-51 showed no UV-active spots on normal phase TLC using 2% methanol in dichloromethane (3 runs) as a mobile phase. According to the appearance of proton signals at high field, it was not further investigated.

Subfraction Bs5-52 displayed two spots under UV-S on normal phase TLC with the R_f values of 0.28 and 0.58 using 2% methanol in dichloromethane (3 runs) as a mobile phase. Its ^{1}H NMR spectral data indicated that it contained **N31** as a major component. Therefore, further investigation was not conducted.

Subfraction Bs5-53 displayed no district spots under UV-S on normal phase TLC using 2% methanol in dichloromethane (3 runs) as a mobile phase. Its ^{1}H NMR data indicated none of major components. Thus, no attempted separation was performed.

Fraction C contained many spots under UV-S on normal phase TLC using 2% methanol in dichloromethane (3 runs) as a mobile phase. The ^{1}H NMR data indicated the presence of a mixture of **N17, N18** and **N40**. Therefore, it was not further separated.

Fraction D demonstrated four UV-active spots with the R_f values of 0.10, 0.15, 0.28 and 0.55 using 2% methanol in dichloromethane (2 runs) as a mobile phase. Further purification by column chromatography over silica gel using a gradient system of methanol-dichloromethane was performed. Subfractions, which contained similar components, were combined and evaporated to dryness under reduced pressure to give five subfractions, as shown in **Table 154**.

Table 154 Subfractions obtained from **fraction D** by column chromatography over silica gel

Subfraction	Eluent	Weight (mg)	Physical appearance
D1	100% CH_2Cl_2 - 10% MeOH/CH_2Cl_2	2.5	Brown gum
D2	10% MeOH/CH_2Cl_2	40.4	Brown-red gum
D3	30-50% MeOH/CH_2Cl_2	9.7	Brown gum
D4	50% MeOH/CH_2Cl_2	29.6	Brown solid
D5	70% MeOH/CH_2Cl_2 - 100% MeOH	23.5	Brown gum

Subfraction D1 showed no UV-active spots on normal phase TLC using 2% methanol in dichloromethane (2 runs) as a mobile phase. Its ^{1}H NMR

spectrum displayed none of major components. Thus, no attempted investigation was performed.

Subfraction D2 showed four UV-active spots on normal phase TLC with the R_f values of 0.20, 0.33, 0.50 and 0.65 using 2% methanol in dichloromethane (2 runs) as a mobile phase. The ^{1}H NMR data indicated the presence of **N39** as a major component. Therefore, further investigation was not conducted.

Subfraction D3 showed many inseparable UV-active spots on normal phase TLC using 2% methanol in dichloromethane (2 runs) as a mobile phase. Its ^{1}H NMR spectrum displayed none of major components. Thus, further purification was not conducted.

Subfraction D4 showed four UV-active spots on normal phase TLC with the R_f values of 0.05, 0.08, 0.20 and 0.33 using 2% methanol in dichloromethane (2 runs) as a mobile phase. Its ^{1}H NMR spectrum displayed none of major components. Therefore, no further investigation was pursued.

Subfraction D5 showed no definite UV-active spots on normal phase TLC using 2% methanol in dichloromethane (2 runs) as a mobile phase. The ^{1}H NMR spectrum displayed none of major components. Therefore, it was not further investigated.

Fraction E displayed two UV-active spots on normal phase TLC with the R_f values of 0.23 and 0.55 using 2% methanol in dichloromethane (2 runs) as a mobile phase. It was further separated by column chromatography over Sephadex LH20 using 100% MeOH as eluent. Subfractions, which contained similar components, were combined and evaporated to dryness under reduced pressure to give five subfractions, as shown in **Table 155.**

Table 155 Subfractions obtained from **fraction E** by column chromatography over Sephadex LH20

Subfraction	Eluent	Weight (mg)	Physical appearance
E1	100% MeOH	1.8	Yellow gum
E2	100% MeOH	10.7	Yellow gum
E3	100% MeOH	3.8	Yellow gum
E4	100% MeOH	4.2	Yellow gum
E5	100% MeOH	6.7	Brown gum

Subfraction E1 showed no definite spots under UV-S on normal phase TLC using 2% methanol in dichloromethane (3 runs) as a mobile phase. Because of the minute amount, it was not further investigated.

Subfraction E2 showed one major UV-active spot on normal phase TLC with the R_f value of 0.50 using 2% methanol in dichloromethane (3 runs) as a mobile phase. The ^{1}H NMR data indicated the presence of **N39** as a major component. Therefore, further investigation was not conducted.

Subfraction E3 showed no UV-active spots on normal phase TLC using 2% methanol in dichloromethane (3 runs) as a mobile phase. Its ^{1}H NMR spectrum displayed none of major components. Thus, further purification was not performed.

Subfraction E4 (N43) showed one UV-active spot on normal phase TLC with the R_f value of 0.28 using 2% methanol in dichloromethane (3 runs) as a mobile phase.

UV(MeOH) λ_{max} nm (log ε)	215 (3.72), 237 (3.66), 309 (3.30), 344 (3.04)
FT-IR (neat) ν_{cm-1}	3369 (O-H stretching), 1639 (C=O stretching), 1610 (C=C stretching)

^{1}H NMR ($CDCl_3$+CD_3OD) (δ ppm) (300 MHz)	13.63 (*s*, 1H), 6.62 (*d*, *J* = 2.4 Hz, 1H), 6.58 (*d*, *J* = 2.4 Hz, 1H), 6.26 (*d*, *J* = 2.1 Hz, 1H), 6.18 (*d*, *J* = 2.1 Hz, 1H), 2.82 (*s*, 3H)
^{13}C NMR ($CDCl_3$+CD_3OD) (δ ppm) (75 MHz)	183.20, 164.95, 164.08, 162.83, 160.30, 158.10, 144.53, 116.83, 113.14, 104.24, 101.65, 98.81, 94.53, 24.10
DEPT (135°) ($CDCl_3$+CD_3OD)	CH : 116.83, 101.65, 98.81, 94.53 CH_3 : 24.10

Subfraction E5 showed no UV-active spots on normal phase TLC using 2% methanol in dichloromethane (2 runs) as a mobile phase. The ^{1}H NMR spectrum displayed none of major components. Therefore, it was not further investigated.

CHAPTER 7.3
RESULTS AND DISCUSSION

Five known compounds (**N39-N43**) were isolated from the broth extract. The structures were identified by spectroscopic methods.

7.3.1 Compound N39

N39 was obtained as a white solid and melted at 151.8-152.4 °C. The UV spectrum showed maximum an absorption band at λ_{max} 257 nm, indicating the presence of a conjugated enone chromophore (Shino *et al.*, 2005). The IR spectrum exhibited absorption bands at 3402 cm^{-1} for a hydroxyl group and 1648 cm^{-1} for a conjugated ketone carbonyl group. The ^{1}H NMR spectral data (**Figure 98**) (**Table 156**) showed signals for two oxymethine protons [δ_H 4.51 (*d*, J = 6.6 Hz, 1H) and 3.30 (*d*, J = 2.1 Hz, 1H)], one olefinic proton (δ_H 5.25, *d*, J = 2.1 Hz, 1H), methoxy protons (δ_H 3.76, *s*, 3H) and methyl protons (δ_H 1.63, *s*, 3H). A signal at δ_H 4.48 (*d*, J = 6.6 Hz, 1H) which was coupled with the oxymethine proton at δ_H 4.51 was assigned to a hydroxy proton. This proton showed no correlation in the HMQC spectrum, thus supporting the above conclusion. The ^{13}C NMR spectrum (**Figure 99**) (**Table 156**) displayed resonances of an α, β-unsaturated ketone moiety with an alkoxyl group at β-position (δ_C 194.11, 172.75 and 97.92), one oxyquaternary (δ_C 59.54), two oxymethine (δ_C 68.74 and 60.25) and two methyl (δ_C 56.50 and 18.79) carbons. These data indicated the presence of an oxygenated cyclohexenone nucleus bearing hydroxyl, methoxyl and methyl substituents. The methoxyl (δ_H 3.76, 3-OCH_3) and methyl (δ_H 1.63, Me-7) groups were attached at C-3 (δ_C 172.75) and C-5 (δ_C 59.54), respectively, according to ^{3}J HMBC correlations (**Table 157**) of 3-OCH_3/C-3 and those of Me-7/C-4 (δ_C 68.74) and C-6 (δ_C 60.25). The COSY spectrum (**Table 157**) displayed a long-range coupling between H-2 (δ_H 5.25) and H-6 (δ_H 3.30). The chemical shift of H-6, C-4, C-5 and C-6 established the position of an epoxide functionality at C-5 and C-6 and the hydroxyl group at C-4. Irradiation of Me-7, in the

NOEDIFF experiment (**Table 157**), enhanced signal intensity of both H-4 (δ_H 4.51) and H-6, indicating their *cis* relationship. The observed optical rotation of **N39** ($[\alpha]_D^{27}$ -95.33, c = 0.33, EtOH) was almost identical to that of (4*S*,5*S*,6*S*)-5,6-epoxy-4-hydroxy-3-methoxy-5-methylcyclohex-2-en-1-one ($[\alpha]_D^{20}$ -100.00, c = 0.33, EtOH), suggesting that they possessed the same absolute configuration. The X-ray analysis (**Figure 100**) confirmed above conclusion. Therefore, **N39** was (4*S*,5*S*,6*S*)-5,6-epoxy-4-hydroxy-3-methoxy-5-methylcyclohex-2-en-1-one, which was previously isolated from ascomycetes Xylariaceae genus (Shiono *et al.*, 2005).

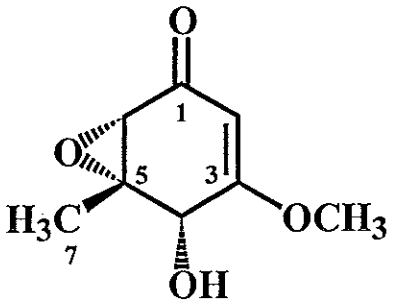

Table 156 The NMR data of **N39** in $CDCl_3$+CD_3OD and **(4*S*,5*S*,6*S*)-5,6-epoxy-4-hydroxy-3-methoxy-5-methylcyclohex-2-en-1-one** in acetone-d_6

Position	**N39**		**(4*S*,5*S*,6*S*)-5,6-Epoxy-4-hydroxy-3-methoxy-5-methyl-cyclohex-2-en-1-one** [a]	
	δ_H (mult., J_{Hz})	δ_C (C-Type)	δ_H (mult., J_{Hz})	δ_C (C-Type)
1	-	194.11 (C=O)	-	194.4 (C=O)
2	5.25 (*d*, 2.1)	97.92 (CH)	5.11 (*d*, 2.0)	98.6 (CH)
3	-	172.75 (C)	-	174.6 (C)
4	4.51 (*d*, 6.6)	68.74 (CH)	4.53 (*d*, 6.3)	69.6 (CH)
4-OH	4.48 (*d*, 6.6)	-	4.85 (*d*, 6.3)	-
5	-	59.54 (C)	-	60.8 (C)
6	3.30 (*d*, 2.1)	60.25 (CH)	3.11 (*d*, 2.0)	61.2 (CH)
7	1.63 (*s*)	18.79 (CH_3)	1.51 (*s*)	19.7 (CH_3)
3-OCH_3	3.76 (*s*)	56.50 (CH_3)	3.68 (*s*)	57.2 (CH_3)

[a] Shiono *et al.*, 2005.

Table 157 The HMBC, COSY and NOE data of **N39** in $CDCl_3$+CD_3OD

Position	HMBC	COSY	NOE
H-2	C-1, C-3, C-4, C-6	H-6	3-OCH_3
H-4	C-2, C-3, C-5, C-7	-	H-6, Me-7
H-6	C-1, C-2, C-5, C-7	H-2	Me-7
Me-7	C-4, C-6	-	H-4, H-6
3-OCH_3	C-2, C-3	-	H-2

7.3.2 Compound N42

N42 was obtained as a yellow gum. The UV, IR and ^{1}H NMR spectra (**Figure 101**) (**Table 158**) were almost identical to those of **N42**. The ^{13}C NMR spectral data (**Figure 102**) (**Table 158**) were similar to those of **N42** with the differences in chemical shift values of C-5 (δ_C 77.21) and C-6 (δ_C 75.07). These data established diol functional group at C-5 and C-6. HMBC data (**Table 159**) suggested the identical location of all substituents. Irradiation of Me-7 (δ_H 3.81, *s*, 3H), in the NOEDIFF experiment, enhanced signal intensity of H-4 (δ_H 4.13, *s*, 1H), but not H-6 (δ_H 4.49, *s*, 1H) (**Table 159**), indicating *cis* and *trans* relationship of Me-7/H-4 and Me-7/H-6, respectively. The observed optical rotation of **N42** ($[\alpha]_D^{27}$ +100.00, c = 0.39, EtOH) was almost identical to that of (4*R*,5*S*,6*R*)-4,5,6-trihydroxy-3-methoxy-5-methylcyclohex-2-en-1-one ($[\alpha]_D^{20}$ +110.00, c = 0.39, EtOH), suggesting that they possessed the same absolute configuration. Therefore, **N42** was assigned as (4*R*,5*S*,6*R*)-4,5,6-trihydroxy-3-methoxy-5-methylcyclohex-2-en-1-one which was previously isolated from ascomycetes Xylariaceae genus (Shiono *et al.*, 2005).

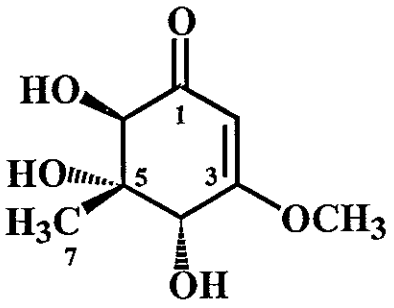

Table 158 The NMR data of **N42** in $CDCl_3$+CD_3OD and **(4*R*,5*S*,6*R*)-4,5,6-trihydroxy-3-methoxy-5-methylcyclohex-2-en-1-one** in acetone-d_6

Position	**N42**		**(4*R*,5*S*,6*R*)-4,5,6-Trihydroxy-3-methoxy-5-methylcyclohex-2-en-1-one**[a]	
	δ_H (mult., J_{Hz})	δ_C (C-Type)	δ_H (mult., J_{Hz})	δ_C (C-Type)
1	-	196.48 (C=O)	-	190.6 (C=O)
2	5.43 (*s*)	99.43 (CH)	5.31 (*s*)	100.6 (CH)
3	-	174.64 (C)	-	175.8 (C)
4	4.13 (*s*)	74.65 (CH)	4.23 (*s*)	73.8 (CH)
5-OH	-	77.21 (C)	5.05 (*brs*)	75.6 (C)
6	4.49 (*s*)	75.07 (CH)	4.44 (*d*, 2.0)	67.6 (CH)
6-OH	-	-	5.05 (*brs*)	-
7	1.15 (*s*)	18.34 (CH_3)	1.27 (*s*)	21.8 (CH_3)
3-OCH_3	3.81 (*s*)	56.81 (CH_3)	3.75 (*s*)	57.5 (CH_3)

[a] Shiono *et al.*, 2005.

Table 159 The HMBC and NOE data of **N42** in $CDCl_3$+CD_3OD

Position	HMBC	NOE
H-2	C-1, C-3, C-4, C-6	3-OCH_3
H-4	C-2, C-3, C-6, C-7	Me-7
H-6	C-1, C-4, C-7	-
Me-7	C-4, C-6	H-4
3-OCH_3	C-2, C-3	H-2

7.3.3 Compound N40

N40 was obtained as a yellow gum. The UV and IR spectra were almost identical to those of **N31**. The ^{1}H NMR spectral data (**Figure 103**) (**Table 160**) were similar to those of **N31** except for an additional signal for one methoxyl group (δ_H 3.88, *s*, 3H) in **N40**. The presence of the methoxyl group was supported by a carbon resonance of the methoxyl group at δ_C 52.01 in the ^{13}C NMR spectrum (**Figure 104**) (**Table 160**). The aromatic proton, H-6 (δ_H 8.13, *d*, J = 9.0 Hz, 1H), showed a ^3J HMBC correlation (**Table 161**) with an ester carbonyl carbon (C-10, δ_C 166.16) and 10-OCH_3 gave a ^3J HMBC correlation with the same carbon. These evidence constructed a methoxycarbonyl group at C-5 (δ_C 118.61). **N40** gave almost identical optical rotation to that of 5-methoxycarbonylmellein, $[\alpha]_D^{27}$ of **N40** =

-158.00 (c = 1.00, $CHCl_3$) and $[\alpha]_D^{22}$ of 5-methoxycarbonylmellein = -163.00 (c = 1.00, $CHCl_3$). Therefore, **N40** was assigned as 5-methoxycarbonylmellein which was previously isolated from *Hypoxylon mammatum* (Anderson *et al.*, 1983).

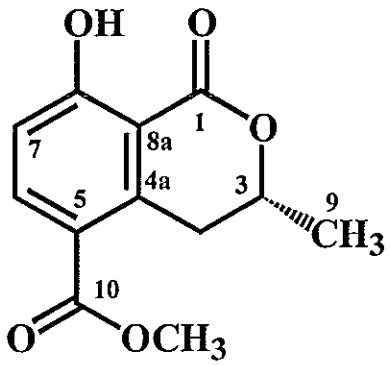

Table 160 The NMR data of **N40** and **5-methoxycarbonylmellein** in $CDCl_3$

Position	N40		5-Methoxycarbonylmellein [a]
	δ_H (mult., J_{Hz})	δ_C (C-Type)	δ_H (mult., J_{Hz})
1	-	170.03 (C=O)	-
3	4.67 (*m*)	75.61 (CH)	4.70 (*m*)
4	a: 3.87 (*dd*, 17.7, 3.3)	32.61 (CH_2)	a: 3.96 (*m*)
	b: 3.05 (*dd*, 17.7, 11.7)		b: 3.00 (*m*)
4a	-	143.45 (C)	-
5	-	118.61 (C)	-
6	8.13 (*d*, 9.0)	138.46 (CH)	8.15 (*d*, 7.0)
7	6.94 (*d*, 9.0)	116.23 (CH)	6.95 (*d*, 7.0)
8-OH	11.83 (*s*)	165.51 (C)	11.87 (*s*)
8a	-	108.92 (C)	-
9	1.56 (*d*, 6.3)	20.76 (CH_3)	1.55 (*d*, 6.0)
10	-	166.16 (C=O)	-
10-OCH_3	3.88 (*s*)	52.01 (CH_3)	3.90 (*s*)

[a] Anderson *et al.*, 1983.

Table 161 The HMBC, COSY and NOE data of **N40** in $CDCl_3$

Position	HMBC	COSY	NOE
H-3	-	H_{ab}-4, Me-9	H_a-4, Me-9
H_a-4	C-4a, C-5, C-8a, C-9	H-3, H_b-4	H-3, H_b-4, Me-9
H_b-4	C-3, C-4a, C-5, C-8a, C-9	H-3, H_a-4	H_a-4, Me-9
H-6	C-4a, C-5, C-8, C-10	H-7	H-7, 10-OCH_3
H-7	C-1, C-5, C-8, C-8a	H-6	H-6
Me-9	C-3, C-4	H-3	H-3, H_{ab}-4
10-OCH_3	C-10	-	-

7.3.4 Compound N41

N41 was obtained as a yellow gum. The UV and IR spectra were almost identical to those of **N16**. The ^{1}H NMR spectral data (**Figure 105**) (**Table 162**) were similar to those of **N16** except that the pentyl signal [δ_H 2.45 (*td*, J = 8.1 and 1.5 Hz, 2H), 1.54 (*m*, 2H), 1.37 (*m*, 2H), 1.34 (*m*, 2H) and 0.92 (*t*, J = 6.9 Hz, 3H)] in **N16** was replaced, in **N41**, by a methyl signal (δ_H 2.07, *d*, J = 1.8 Hz, 3H). The methyl group was then located at C-6 (δ_C 143.63). HMBC correlations (**Table 163**) between the methyl protons (δ_H 2.07, *d*, 1.8, 3H) and C-1 (δ_C 182.32), C-5 (δ_C 133.83) and C-6 (δ_C 143.63) and the signal enhancement of the olefinic proton, H-5 (δ_H 6.54, *qd*, J = 1.8 and 2.1 Hz), after irradiation of Me-7 in the NOEDIFF experiment (**Table 163**), confirmed the above assigned location. Therefore, **N41** was assigned as 2-methoxy-6-methyl-1,4-benzoquinone, which was previously isolated *Aspergillus* sp. (Sood *et al.*, 1982).

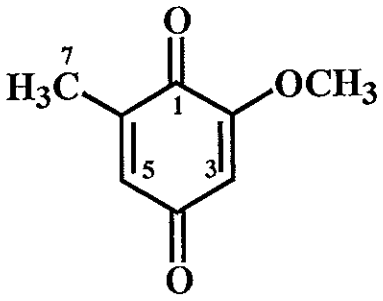

Table 162 The NMR data of **N41** and **2-methoxy-6-methyl-1,4-benzoquinone** in $CDCl_3$

Position	N41		2-Methoxy-6-methyl-1,4-benzoquinone[a]	
	δ_H (mult., J_{Hz})	δ_C (C-Type)	δ_H (mult., J_{Hz})	δ_C (C-Type)
1	-	182.32 (C=O)	-	181.0 (C=O)
2	-	158.82 (C)	-	158.0 (C)
2-OCH_3	3.81 (*s*)	56.22 (CH_3)	3.77 (*s*)	56.3 (CH_3)
3	5.88 (*d*, 2.1)	107.30 (CH)	5.83 (*s*)	107.2 (CH)
4	-	187.36 (C=O)	-	186.2 (C=O)
5	6.54 (*qd*, 2.1, 1.8)	133.83 (CH)	6.48 (*q*, 1.6)	133.8 (CH)
6	-	143.63 (C)	-	142.1 (C)
7	2.07 (*d*, 1.8)	15.44 (CH_3)	2.00 (*d*, 1.6)	15.0 (CH_3)

[a] Bernini *et al.*, 2006.

Table 163 The HMBC and NOE data of **N41** in $CDCl_3$

Position	HMBC	NOE
2-OCH_3	C-2	H-3
H-3	C-1, C-2, C-4, C-5	2-OCH_3
H-5	C-1, C-4, C-7	Me-7
Me-7	C-1, C-5, C-6	H-5

7.3.5 Compound N43

N43 was obtained as a yellow gum. The UV spectrum showed maximum absorption bands at 215, 237, 309 and 344 nm, indicating that **N43** had a xanthone chromophore. Its IR spectrum exhibited absorption bands due to a hydroxyl group at 3369 cm^{-1} and a ketone carbonyl group at 1654 cm^{-1}. The ^1H NMR spectrum (**Figure 107**) (**Table 164**) showed the characteristic signals for one chelated hydroxyl group (δ_H 13.63, *s*, 1H), two sets of the *meta*-aromatic protons [δ_H 6.62 (*d*, J = 2.4 Hz, 1H), 6.58 (*d*, J = 2.4 Hz, 1H) and 6.26 (*d*, J = 2.1 Hz, 1H), 6.18 (*d*, J = 2.1 Hz, 1H)] and one aromatic methyl group (δ_H 2.82, *s*, 3H). The ^{13}C NMR spectrum (**Figure 108**) (**Table 164**) showed one ketone carbonyl (δ_C 183.20), eight quaternary (δ_C 164.95, 164.08, 162.83, 160.30, 158.10, 144.53, 113.14 and 104.24), four methine (δ_C 116.83, 101.65, 98.81 and 94.53) and one methyl (δ_C 24.10) carbons. The chelated hydroxy proton (1-OH) was placed at C-1 (δ_C 164.08), *peri* position to the ketone carbonyl group (C-9), due to its HMBC correlations (**Table 165**) with C-1, C-2 (δ_C 98.81) and C-9a (δ_C 140.24). Two *meta*-aromatic protons (δ_H 6.18 and 6.26) were then attributed to H-2 and H-4, respectively, on the basis of a HMQC correlation of the aromatic protons at δ_H 6.18 with C-2 and a cross peak between H-2 and H-4 in the COSY spectrum. HMBC correlations of H-2/C-1, C-3 (δ_C 164.95), C-4 (δ_C 94.53) and C-9a and those of H-4/C-2, C-3, C-4a (δ_C 158.10), C-9 and C-9a supported above assignment. Other two *meta*-aromatic protons (δ_H 6.62 and 6.58) were assigned as H-5 and H-7, respectively, on the basis of their chemical shifts and HMBC correlations of H-5/C-6 (δ_C 162.83), C-7 (δ_C 116.83), C-8a (δ_C 113.14 and C-10a (δ_C 160.30) and those of H-7/C-5 (δ_C 101,65), C-8a and C-11 (δ_C 24.10). These results together with

HMBC cross peaks of the methyl protons (δ_H 2.82, Me-11) with C-7, C-8 (δ_C 144.53) and C-8a suggested the attachment of the methyl group at C-8. Signal enhancement of Me-11 after irradiation of H-7, in the NOEDIFF experiment (**Table 165**), confirmed the assigned location. Since there was no other signal, the substituents at C-3 and C-6 must be hydroxyl groups. Their ^{13}C chemical shifts supported the conclusion. Thus, **N43** was elucidated as 1,3,6-trihydroxy-8-methylxanthone which was previously isolated from *Ledebouria graminifolia* (Mutanyatta *et al.*, 2003).

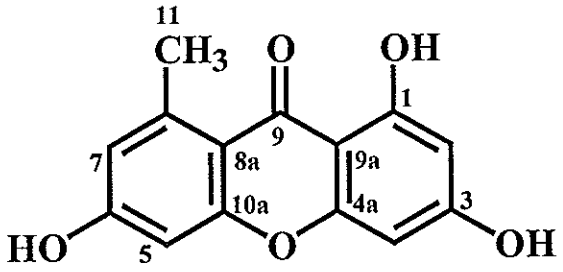

Table 164 The NMR data of **N43** in $CDCl_3$+CD_3OD and **1,3,6-trihydroxy-8-methylxanthone** in acetone-d_6

Position	N43		1,3,6-Trihydroxy-8-methylxanthone[a]	
	δ_H (mult., J_{Hz})	δ_C (C-Type)	δ_H (mult., J_{Hz})	δ_C (C-Type)
1-OH	13.63 (*s*)	164.08 (C)	13.60 (*s*)	164.9 (C)
2	6.18 (*d*, 2.1)	98.81 (CH)	6.16 (*d*, 1.9)	98.3 (CH)
3	-	164.95 (C)	-	165.9 (C)
4	6.26 (*d*, 2.1)	94.53 (CH)	6.30 (*d*, 1.9)	93.6 (CH)
4a	-	158.10 (C)	-	157.6 (C)
5	6.62 (*d*, 2.4)	101.65 (CH)	6.67 (*m*)	101.0 (CH)
6	-	162.83 (C)	-	164.1 (C)
7	6.58 (*d*, 2.4)	116.83 (CH)	6.67 (*m*)	117.1 (CH)
8	-	144.53 (C)	-	143.4 (C)
8a	-	113.14 (C)	-	111.3 (C)
9	-	183.20 (C=O)	-	182.1 (C=O)
9a	-	104.24 (C)	-	102.8 (C)
10a	-	160.30 (C)	-	160.0 (C)
11	2.82 (*s*)	24.10 (CH_3)	2.77 (*s*)	23.0 (CH_3)

[a] Mutanyatta *et al.*, 2003.

Table 165 The HMBC, COSY and NOE data of **N43** in $CDCl_3$+CD_3OD

Position	HMBC	COSY	NOE
1-OH	C-1, C-2, C-9a	-	-
H-2	C-1, C-3, C-4, C-9a	H-4	-
H-4	C-2, C-3, C-4a, C-9, C-9a	H-2	-
H-5	C-6, C-7, C-8a, C-10a	H-7	-
H-7	C-5, C-8a, C-11	H-5	Me-11
Me-11	C-7, C-8, C-8a	-	H-7

REFERENCES

Abate, D., Abraham, W-R. and Meyer, H. 1997. Cytochalasins and Phytotoxins from the Fungus *Xylaria obovata*. Phytochemistry 44(8), 1443-1448.

Adeboya, M.O., Edwards, R.L., Laessoee, T. and Maitland, D.J. 1995. Metabolites of the Higher Fungi. Part 27. Berteric Acid, Cameronic Acid, and Malaysic Acid, Three New Polysubstituted Fatty Acids Related to Cubensic Acid from Species of the Fungus Genus *Xylaria*. J. Chem. Res., Synop. 9, 356-357.

Adeboya, M.O., Edwards, R.L., Lassoee, T., Maitland, D.J., Shields, L. and Whalley, A.J.S. 1996a. Metabolites of the Higher Fungi. Part 29. Maldoxin, Maldoxone, Dihydromaldoxin, Isodihydromaldoxin and Dechlorodihydro-maldoxin. A Spirocyclohexadienone, a Depsidone and Three Diphenyl Ethers: Key in the Depsidone Biosynthetic Pathway from a Member of the Fungus Genus *Xylaria*. J. Chem. Soc., Perkin Trans. I: Organic and Bio-Organic Chemistry 12, 1419-1425.

Adeboya, M.O., Edwards, R.L., Laessoee, T., Maitland, D.J. and Whalley, A.J.S. 1996b. Metabolites of the Higher Fungi. Part 30. *threo*- and *erythro*-Telfairic Acid and 2,3-Didehydrotelfairic Anhydride from the Fungus *Xylaria telfairii*. Liebigs Ann. 9, 1437-1441.

Anderson, J.R., Edwards, R.L. and Whalley, A.J.S. 1983. Metabolites of the Higher Fungi. Part 21. 3-Methyl-3,4-dihydroisocoumarins and Related Compounds from the Ascomycete Family Xylariaceae. J. Chem. Soc., Perkin Trans. I, 2185-2192.

Arunrattiyakorn, P., Nitoda, T. and Kanzaki, H. 2006. Enzymatic Conversion-based Method for Screening Cyclic Dipeptide-producing Microbes. Peptides 27, 633-639.

Asha, K.N., Chowdhury, R., Hasan, C.M. and Rashid, M.A. 2004. Steroids and Polyketides from *Uvaria hamiltonii* Stem Bark. Acta Pharm. 54, 57-63.

Avantaggiato, G., Solfrizzo, M., Tosi, L., Zazzerini, A., Fanizzi, F.P. and Visconti, A. 1999. Isolation and Characterization of Phytotoxic Compounds Produced by *Phomopsis helianthi*. Nat. Toxins. 7(3), 119-127.

Behr, D., Wahlberg, I., Nishida, T. and Enzell, C.R. 1978. Tobacco Chemistry. 45. (2*E*,6*S*)-2,6-Dimethyl-2,7-octadiene-1,6-diol, a New Monoterpenoid from Greek Tobacco. Acta Chem. Scand. B32(3), 228-229.

Beno, M.A. and Christoph, G.G. 1976. X-ray Crystal Structure of Cytochalasin H, a Potent New [11]Cytochalasan Toxin. J. Chem. Soc., Chem. Commun. 10, 344-345.

Bernini,R., Mincione, E., Barontini, M., Fabrizi, G., Pasqualetti, M. and Tempesta, S. 2006. Convenient Oxidation of Alkylated Phenols and Methoxytoluenes to Antifungal 1,4-Benzoquinones with Hydrogen Peroxide (H_2O_2)/Methyl-trioxorhenium (CH_3ReO_3) Catalytic System in Neutral Ionic Liquid. Tetrahedron 62, 7733-7737.

Bieber, L.W., Chiappeta, A.D.A., De Moraes E Souza, M.A., Generino, R.M. and Neto, P.R. 1990. Simple Synthesis of Primin and Its Analogues via Lithiation of Protected Guaiacol. J. Nat. Prod. 53(3), 706-709.

Boehlendorf, B., Forche, E., Bedorf, N., Gerth, K., Irschik, H., Jansen, R., Kunze, B., Trowitzsch-Kienast, W., Reichenbach, H. and Hoefle, G. 1996. Antibiotics from Gliding Bacteria. Part LXXIII. Indole and Quinoline Derivatives as Metabolites of Tryptophan in Myxobacteria. Liebigs Ann. 1, 49-53.

Boonphong, S., Kittakoop, P., Isaka, M., Pittayakhajonwut, D., Tanticharoen, M. and Thebtaranonth, Y. 2001. Multiplolides A and B, New Antifungal 10-Membered Lactones from *Xylaria multiplex*. J. Nat. Prod. 64(7), 965-967.

Cafeu, M.C., Silva, G.H., Teles, H.L., Bolzani, V. Da S., Araujo, A.R., Young, M.C. M. and Pfenning, L.H. 2005. Antifungal Compounds of *Xylaria* sp., an Endophytic Fungus Isolated from *Palicourea marcgravii* (Rubiaceae). Quim. Nova 28(6), 991-995.

Chiba, S., Kitamura, M. and Narasaka, K. 2006. Synthesis of (-)-Sordarin. J. Am. Chem. Soc. 128, 6931-6937.

Chinworrungsee, M., Kittakoop, P., Isaka, M., Chanphen, R., Tanticharoen, M. and Thebtaranonth, Y. 2002. Halorosellins A and B, Unique Isocoumarin Glucosides from the Marine Fungus *Halorosellinia oceanica*. J. Chem. Soc., Perkin Trans. I, 2473–2476.

Chinworrungsee, M., Kittakoop, P., Isaka, M., Rungrod, A., Tanticharoen, M. and Thebtaranonth, Y. 2001. Antimalarial Halorosellinic Acid from the Marine Fungus *Halorosellinia oceanica*. Bioorg. Med. Chem. Lett. 11(15), 1965-1969.

Claydon, N., Grove, J.F. and Pople, M. 1985. Elm Bark Beetle Boring and Feeding Deterrents from *Phomopsis oblonga*. Phytochemistry 24(5), 937-943.

Cole, R.J., Wells, J.M., Cox, R.H. and Cutler, H.G. 1981. Isolation and Biological Properties of Deacetylcytochalasin H from *Phomopsis* sp. J. Agric. Food. Chem. 29(1), 205-206.

Cole, R.J., Wilson, D.M., Harper, J.L., Cox, R.H., Cochran, T.W., Cutler, H.G. and Bell, D.K. 1982. Isolation and Identification of Two New [11]Cytochalasins from *Phomopsis sojae*. J. Agric. Food. Chem. 30(2), 301-304.

Culvenor, C.C.J., Edgar, J.A., Mackay, M.F., Gorst-Allman, C.P., Marasas, W.F.O., Steyn, P.S., Vleggaar, R. and Wessels, P.L. 1989. Structure Elucidation and

Absolute Configuration of Phomopsin A, a Hexapeptide Mycotoxin Produced by *Phomopsis leptostromiformis*. Tetrahedron 45(8), 2351-2372.

Curci, R., Fiorentino, M., Troisi, L., Edwards, J.O. and Pater, R.H. 1980. Epoxidation of Alkenes by Dioxirane Intermediates Generated in the Reaction of Potassium Caroate with Ketones. J. Org. Chem. 45(23), 4758-4760.

Dagne, E., Gunatilaka, A.A.L., Asmellash, S., Abate, D., Kingston, D.G.I., Hofmann, G.A. and Johnson, R.K. 1994. Two New Cytotoxic Cytochalasins from *Xylaria obovata*. Tetrahedron 50(19), 5615-5620.

Dai, J., Krohn, K., Floerke, U., Draeger, S., Schulz, B., Kiss-Szikszai, A., Antus, S., Kurtan, T. and van Ree, T. 2006. Metabolites from the Endophytic Fungus *Nodulisporium* sp. from *Juniperus cedre*. Eur. J. Org. Chem. 3498-3506.

Dai, J., Krohn, K., Gehle, D., Kock, I., Floerke, U., Aust, H-J., Draeger, S., Schulz, B. and Rheinheimer, J. 2005. Active Secondary Metabolites from Fungi, 22. New Oblongolides Isolated from the Endophytic Fungus *Phomopsis* sp. from *Melilotus dentata* from the Shores of the Baltic Sea. Eur. J. Org. Chem. 18, 4009-4016.

Davis, R.A., Watters, D. and Healy, P.C. 2005a. The Isolation and Synthesis of 3-Chloro-4-hydroxyphenylacetamide Produced by a Plant-associated Microfungus of the Genus *Xylaria*. Tetrahedron Lett. 46(6), 919-921.

Davis, R.A. 2005b. Isolation and Structure Elucidation of the New Fungal Metabolite (-)-Xylariamide A. J. Nat. Prod. 68(5), 769-772.

Davis, R.A. and Pierens, G.K. 2006. ^{1}H and ^{13}C NMR Assignments for Two New Xanthones from the Endophytic Fungus *Xylaria* sp. FRR 5657. Magn. Reson. Chem. 44(10), 966-968.

Deshmukh, P.G., Mujumdar, A.M. and Pendse, G.S. 1978. Preliminary Pharmacological Studies on Cytochalasin H. Indian Drugs 15(5), 76-83.

Dettrakul, S., Kittakoop, P., Isaka, M., Nopichai, S., Suyarnsestakorn, C., Tanticharoen, M. and Thebtaranonth, Y. 2003. Antimycobacterial Pimarane Diterpenes from the Fungus *Diaporthe* sp. Bioorg. Med. Chem. Lett. 13, 1253-1255.

Devys, M., Barbier, M., Bousquet, J-F. and Kollmann, A. 1994. Isolation of the (-)-(3*R*)-5-Hydroxymellein from the Fungus *Septoria nodorum*. Phytochemistry 35(3), 825-826.

Deyrup, S.T., Gloer, J.B., O'Donnell, K. and Wicklow D.T. 2007. Kolokosides A-D: Triterpenoid Glycosides from a Hawaiian Isolate of *Xylaria* sp. J. Nat. Prod. 70(3), 378-382.

Dimitriadis, C., Gill, M. and Harte, M.F. 1997. The First Stereospecific Approach to Both Enantiomers of Mellein. Tetrahedron: Asymmetry 8(13), 2153-2158.

Edwards, R.L., Maitland, D.J. and Whalley, A.J.S. 1989. Metabolites of the Higher Fungi. Part 24. Cytochalasin N, O, P, Q, and R. New Cytochalasins from the Fungus *Hypoxylon terricola* Mill. J. Chem. Soc., Perkin Trans. I: Organic and Bio-Organic Chemistry (1972-1999) 1, 57-65.

Edwards, R.L., Maitland, D.J. and Whalley, A.J.S. 1991. Metabolites of the Higher Fungi. Part 26. Cubensic Acid, 3,7,11,15-Tetrahydroxy-18-(hydroxymethyl)-2,4,6,10,14,16,20-heptamethyldocosa-4*E*,8*E*,12*E*,16*E*-tetraenoic acid, a Novel Polysubstituted C22 Fatty Acid from the Fungus *Xylaria cubensis* (Mont.) Fr. with Substituents and Substitution Pattern Similar to the Macrolide Antibiotics. J. Chem. Soc., Perkin Trans. I: Organic and Bio-Organic Chemistry (1972-1999) 6, 1411-1417.

Edwards, R.L., Maitland, D.J., Oliver, C.L., Pacey, M.S., Shields, L. and Whalley, A.J.S. 1999. Metabolites of the Higher Fungi. Part 31. Longianone, a $C_7H_6O_4$ Spiro Bicyclic Lactone from the Fungus *Xylaria longiana* (Rehm.). J. Chem. Soc., Perkin Trans. I: Organic and Bio-Organic Chemistry 6, 715-720.

Edwards, R.L., Maitland, D.J., Pittayakhajonwut, P. and Whalley, A.J.S. 2001. Metabolites of the Higher Fungi. Part 33. Grammicin, a Novel Bicyclic $C_7H_6O_4$ Furanopyranol from the Fungus *Xylaria grammica* (Mont.) Fr. J. Chem. Soc., Perkin Trans. I 11, 1296-1299.

Elsaesser, B., Krohn, K., Floerke, U., Root, N., Aust, H-J., Draeger, S., Schulz, B., Antus, S. and Kurtan, T. 2005. X-ray Structure Determination, Absolute Configuration and Biological Activity of Phomoxanthone A. Eur. J. Org. Chem. (21), 4563-4570.

Espada, A., Rivera-Sagredo, A., De La Fuente, J.M., Hueso-Rodriguez, J.A. and Elson, S.W. 1997. New Cytochalasins from the Fungus *Xylaria hypoxylon.* Tetrahedron 53(18), 6485-6492.

Evidente, A., Sparapano, L., Bruno, G. and Motta, A. 2002. Sphaeropsidins D and E, Two Other Pimarane Diterpenes, Produced in Vitro by the Plant Pathogenic Fungus *Sphaeropsis sapinea* f. sp. *cupressi.* Phytochemistry 59, 817–823.

Ferles, M. and Kocian, O. 1979. Quinoline and Isoquinoline Derivatives. V. Reduction of 2-, 3- and 4-Quinolinecarbonitrile and 3- and 4-Quinoline-carbonitrile Methyl Methosulfates with Triethylammonium Formate. Collect. Czech. Chem. Commun. 44(7), 2238-2242.

Fujii, Y., Tani, H., Ichinoe, M. and Nakajima, H. 2000. Zygosporin D and Two New Cytochalasins Produced by the Fungus *Metarrhizium anisopliae.* J. Nat. Prod. 63, 132-135.

Garson, M.J., Staunton, J. and Jones, P.G. 1984. New Polyketide Metabolites from *Aspergillus melleus*: Structural and Stereochemical Studies. J. Chem. Soc., Perkin Trans. I, 1021-1026.

Gray, L.E., Gardner, H.W., Weisleder, D. and Leib, M. 1999. Production and Toxicity of 2,3-Dihydro-5-hydroxy-2-methyl-4*H*-1-benzopyran-4-one by *Phialophora gregata*. Phytochemistry 50, 1337-1340.

Grove, J.F. 1985. Metabolic Products of *Phomopsis oblonga*. Part 2. Phomopsolide A and B, Tiglic Esters of Two 6-Substituted 5,6-Dihydro-5-hydroxypyran-2-ones. J. Chem. Soc., Perkin Trans. I: Organic and Bio-Organic Chemistry (1972-1999) 4, 865-869.

Gunatilaka, A.A.L., Leslie, Berger, J.M., Evans, R., Miller, J.S., Wisse, J.H., Neddermann, K.M., Bursuker, I. and Kingston, D.G.I. 2001. Isolation, Synthesis, and Structure-activity Relationships of Bioactive Benzoquinones from *Miconia lepidota* from the Suriname Rainforest. J. Nat. Prod. 64, 2-5.

Healy, P.C., Hocking, A., Tran-Dinh, N., Pitt, J.I., Shivas, R.G., Mitchell, J.K., Kotiw, M. and Davis, R.A. 2004. Xanthones from a Microfungus of the Genus *Xylaria*. Phytochemistry 65(16), 2373-2378.

Huang, X. and Liu, Z. 2002. Solid-phase Synthesis of 4(1*H*)-Quinolone and Pyrimidine Derivatives Based on a New Scaffold-polymer-bound Cyclic Malonic Acid Ester. J. Org. Chem. 67, 6731-6737.

Huang, H-R., Xia, X-K., She, Z-G., Lin, Y-C., Vrijmoed, L.L.P. and Jones, E.BG. 2006. A New Chloromonoterpene from the Mangrove Endophytic Fungus *Tryblidiopycnis* sp. (4275). J. Asian Nat. Prod. Res. 8(7), 609-612.

Isaka, M., Jaturapat, A., Kladwang, W., Punya, J., Lertwerawat, Y., Tanticharoen, M. and Thebtaranonth, Y. 2000. Antiplasmodial Compounds from the Wood-decayed Fungus *Xylaria* sp. BCC 1067. Planta Med. 66(5), 473-475.

Izawa, Y., Hirose, T., Shimizu, T., Koyama, K. and Natori, S. 1989. Six New 10-Phenyl-[11]-cytochalasans, Cytochalasins N-S from *Phomopsis* sp. Tetrahedron 45(8), 2323-2335.

Jaime, C., Sanchez-Ferrando, F. and Segura, C. 1991. 4,5-Disubstituted 2-Hexenoic and 2-Pentenoic Acids and Esters. A Proton NMR and MM2 Study. An. Quim. 87(5), 669-674.

Jarvis, B.B., Zhou, Y., Jiang, J., Wang, S., Sorenson, W.G, Hintikka, E-L., Nikulin, M., Parikka, P., Etzel, R.A. and Dearborn, D.G. 1996. Toxigenic Molds in Water-damaged Buildings: Dechlorogriseofulvins from *Memnoniella echinata*. J. Nat. Prod. 59(6), 553-554.

Jayasuriya, H., Herath, K.B., Ondeyka, J.G., Polishook, J.D., Bills, G.F., Dombrowski, A.W., Springer, M.S., Siciliano, S., Malkowitz, L., Sanchez, M., Guan, Z., Tiwari, S., Stevenson, D.W., Borris, R.P. and Singh, S.B. 2004. Isolation and Structure of Antagonists of Chemokine Receptor (CCR5). J. Nat. Prod. 67(6), 1036-1038.

Klemke, C., Kehraus, S., Wright, A.D. and Koenig, G.M. 2004. New Secondary Metabolites from the Marine Endophytic Fungus *Apiospora montagnei*. J. Nat. Prod. 67(6), 1058-1063.

Kimura, Y., Mizuno, T., Nakajima, H. and Hamasaki, T. 1992. Altechromones A and B, New Plant Growth Regulators Produced by the Fungus, *Alternaria* sp. Biosci. Biotechnol. Biochem. 56(10), 1664-1665.

Levine, S.G., Hicks, R.E., Gottlieb, H.E. and Wenkert, E. 1975. Carbon-13 Nuclear Magnetic Resonance Spectroscopy of Naturally Occurring Substances. XXX. Griseofulvin. J. Org. Chem. 40(17), 2540-2542.

Lin, Y., Wu, X., Feng, S., Jiang, G., Zhou, S., Vrijmoed, L.L.P. and Jones, E.B.G. 2001a. A Novel N-Cinnamoylcyclopeptide Containing an Allenic Ether from the Fungus *Xylaria* sp. (strain #2508) from the South China Sea. Tetrahedron Lett. 42(3), 449-451.

Lin, Y., Wu, X., Feng, S., Jiang, G., Luo, J., Zhou, S., Vrijmoed, L.L., Jones, E.B., Krohn, K., Steingrover, K. and Zsila, F. 2001b. Five Unique Compounds: Xyloketals from Mangrove Fungus *Xylaria* sp. from the South China Sea Coast. J. Org. Chem. 66(19), 6252-6256.

Liu, X., Xu, F., Zhang, Y., Liu, L., Huang, H., Cai, X., Lin, Y. and Chan, W. 2006a. Xyloketal H from the Mangrove Endophytic Fungus *Xylaria* sp. 2508. Russ. Chem. Bull. 55(6), 1091-1092.

Liu, X-H., Xu, F., Zhang, Y., Liu, L-H., Huang, H-R., She, Z-G., Lin, Y-C. and Chan, W. 2006b. Crystal Structure of 3*S*-Hydroxy-7-melleine. J. Chem. Phys. 19(5), 423-427.

Liu, X.H., Xu, F., Lin, Y.C., Chan, W.L. and Zhou, Z.Y. 2006c. 2-Hexylidene-3-methylsuccinic Acid. Acta Crystallogr. Sect. E: Struct. Rep. Online. E62(6), 2419-2420.

Mackay, M.F., Van Donkelaar, A. and Culvenor, C.C.J. 1986. The X-ray Structure of Phomopsin A, a Hexapeptide Mycotoxin. J. Chem. Soc., Chem. Commun. 15, 1219-1221.

Macmillan, J. 1953. Griseofulvin. VII. Dechlorogriseofulvin. J. Chem. Soc. 1697-1702.

Mander, L.N. and Thomson, R.J. 2005. Total Synthesis of Sordaricin. J. Org. Chem. 70, 1654-1670.

Merifield, E. and Thomas, E.J. 1999. Total Synthesis of Cytochalasin D: Total Synthesis and Full Structural Assignment of Cytochalasin O. J. Chem. Soc., Perkin Trans. I, 3269-3283.

Migliuolo, A., Notaro, G., Piccialli, V. and Sica, D. 1990. New Tetrahydroxylated Sterols from the Marine Sponge *Spongia officinalis*. J. Nat. Prod. 53(6), 1414-1424.

Morikawa, H., Kasai, R., Otsuka, H., Hirata, E., Shinzato, T., Aramato, M. and Takeda, Y. 2004. Terpenic and Phenolic Glycosides from Leaves of *Breynia officinalis* HEMSL. Chem. Pharm. Bull. 52(9), 1086-1090.

Mutanyatta, J., Matapa, B.G., Shushu, D.D. and Abegaz, B.M. 2003. Homoisoflavonoids and Xanthones from the Tubers of Wild and in Vitro Regenerated *Ledebouria graminifolia* and Cytotoxic Activities of Some of the Homoisoflavonoids. Phytochemistry 62, 797-804.

Namikoshi, M., Kobayashi, H., Yoshimoto, T. and Hosoya, T. 1997. Phomopsidin, a New Inhibitor of Microtubule Assembly Produced by *Phomopsis* sp. Isolated from Coral Reef in Pohnpei. J. Antibiot. 50(10), 890-892.

Patwardhan, S.A., Pandey, R.C., Dev, S. and Pendse, G.S. 1974. Toxic Cytochalasins of *Phomopsis paspalli*, a Pathogen of Kodo Millet. Phytochemistry 13(9), 1985-1988.

Piccialli, V. and Sica, D. 1987. Four New Trihydroxylated Sterols from the Sponge *Spongionella gracilis*. J. Nat. Prod. 50(5), 915-920.

Pittayakhajonwut, P., Suvannakad, R., Thienhirun, S., Prabpai, S., Kongsaeree, P. and Tanticharoen, M. 2005. An Anti-herpes Simplex Virus-type 1 Agent from *Xylaria mellisii* (BCC 1005). Tetrahedron Lett. 46(8), 1341-1344.

Quang, D.N., Bach, D.D., Hashimoto, T. and Asakawa, Y. 2006. Chemical Constituents of the Vietnamese Inedible Mushroom *Xylaria intracolorata.* Nat. Prod. Res. 20(4), 317-321.

Rudi, A., Kashman, Y., Benayahu, Y. and Schleyer, M. 1994. Amino Acid Derivatives from the Marine Sponge *Jaspis digonoxea.* J. Nat. Prod. 57(6), 829-832.

Rukachaisirikul, V., Kamkaew, M., Sukavisit, D., Phongpaichit, S., Sawangchote, P. and Taylor, W.C. 2003. Antibacterial Xanthones from the Leaves of *Garcinia nigrolineata.* J. Nat. Prod. 66, 1531-1535.

Samples, D., Hill, D.W., Bridges, C.H. and Camp, B.J. 1984. Isolation of a Mycotoxin (roridin A) from *Phomopsis* spp. Vet. Hum. Toxicol. 26(1), 21-23.

Sassa, T., Ishizaki, A., Nukina, M., Ikeda, M. and Sugiyama, T. 1998. Isolation and Identification of New Antifungal Macrophorins E, F and G as Malonyl Meroterpenes from *Botryosphaeria berengeriana*, Biosci. Biotechnol. Biochem. 62(11), 2260-2262.

Sassa, T., Kenmoku, H., Sato, M., Murayama, T. and Kato, N. 2003. (+)-Menthol and Its Hydroxy Derivatives, Novel Fungal Monoterpenols from the Fusicoccin-Producing Fungi, *Phomopsis amygdali* F6a and Niigata 2. Biosci., Biotechnol., Biochem. 67(3), 475-479.

Sato, Y., Oda, T. and Urano, S. 1976. Griseofulvin Biosynthesis: New Evidence of Two Acetate-dispositions in the Ring A from ^{13}C Nuclear Magnetic Resonance Studies. Tetrahedron Lett. 44, 3971-3974.

Schneider, G., Anke, H. and Sterner, O. 1995. Xylarin, an Antifungal *Xylaria* Metabolite with an Unusual Tricyclic Uronic Acid Moiety. Nat. Prod. Lett. 7(4), 309-316.

Schneider, G., Anke, H. and Sterner, O. 1996. Xylaramide, a New Antifungal Compound, and Other Secondary Metabolites from *Xylaria longipes*. Biosci. 51(11/12), 802-806.

Shan, R., Stadler, M., Sterner, O. and Anke, H. 1996a. New Metabolites with Nematicidal and Antimicrobial Activities from the Ascomycete *Lachnum papyraceum* (Karst.) Karst. VIII. Isolation, Structure Determination and Biological Activities of Minor Metabolites Structurally Related to Mycorrhizin A. J. Antibiot. 49(5), 447-452.

Shan, R., Anke, H., Stadler, M. and Sterner, O. 1996b. Papyracillic Acid, a New Penicillic Acid Analog from the Ascomycete *Lachnum papyraceum*. Tetrahedron 52(30), 10249-10254.

Shan, R., Stadler, M., Anke, H. and Sterner, O. 1997a. New Metabolites with Nematicidal and Antimicrobial Activities from the Ascomycete *Lachnum papyraccum* (Karst.) Karst. 10. The Reactivity of the Fungal Toxin Papyracillic Acid. Tetrahedron 53(17), 6209-6214.

Shan, R., Stadler, M., Anke, H. and Sterner, O. 1997b. Naphthalenone and Phthalide Metabolites from *Lachnum papyraceum*, J. Nat. Prod. 60(8), 804-805.

Shiono, Y., Murayama, T., Takahashi, K., Okada, K., Katohda, S. and Ikeda, M. 2005. Three Oxygenated Cyclohexenone Derivatives Produced by an Endophytic Fungus. Biosci. Biotechnol. Biochem. 69(2), 287-292.

Silva, G.H., Teles, H.L., Trevisan, H.C., Bolzani, Vanderlan, da S., Young, M.C.M., Pfenning, L.H., Eberlin, M.N., Haddad, R., Costa-Neto, C.M. and Araujo,

A.R. 2005. New Bioactive Metabolites Produced by *Phomopsis cassiae*, an Endophytic Fungus in *Cassia spectabilis*. J. Braz. Chem. Soc. 16(6B), 1463-1466.

Silva, G.H., Teles, H.L., Zanardi, L.M., Marx Young, M.C., Eberlin, M.N., Hadad, R., Pfenning, L.H., Costa-Neto, C.M., Castro-Gamboa, I., Bolzani, V. da S. and Araujo, A.R. 2006. Cadinane Sesquiterpenoids of *Phomopsis cassiae*, an Endophytic Fungus Associated with *Cassia spectabilis* (Leguminosae). Phytochemistry 67(17), 1964-1969.

Singh, S.B., Zink, D., Polishook, J., Valentino, D., Shafiee, A., Silverman, K., Felock, P., Teran, A., Vilella, D., Hazuda, D.J. and Lingham, R.B. 1999. Structure and Absolute Stereochemistry of HIV-1 Integrase Inhibitor Integric Acid. A Novel Eremophilane Sesquiterpenoid Produced by a *Xylaria* sp. Tetrahedron Lett. 40(50), 8775-8779.

Smith, C.J., Morin, N.R., Bills, G.F., Dombrowski, A.W., Salituro, G.M., Smith, S. K., Zhao, A. and MacNeil, D.J. 2002. Novel Sesquiterpenoids from the Fermentation of *Xylaria persicaria* are Selective Ligands for the NPY Y5 Receptor. J. Org. Chem. 67(14), 5001-5004.

Sood, R.S., Roy, K., Reddy, G.C.S., Reden, J. and Ganguli, B.N. 1982. 3-Methoxy-2,5-toluquinone from *Aspergillus* sp. HPL Y-30,212. Fermentation, Isolation, Characterization and Biological Properties. J. Antibiot. 35(8), 985-987.

Srebnik, M. and Mechoulam, R. 1983. A Facile Method for Regiospecific Hydroxylation of Resorcinol Diethers. Synthesis, 1046-1048.

Stadler, M., Anke, H., Arendholz, W.R., Hansske, F., Anders, U., Sterner, O. and Bergquist, K.E. 1993a. Lachnumon and Lachnumol A, New Metabolites with Nematicidal and Antimicrobial Activities from the Ascomycete *Lachnum*

papyraceum (Karst.) Karst. I. Producing Organism, Fermentation, Isolation and Biological Activities. J. Antibiot. 46(6), 961-967.

Stadler, M., Anke, H., Bergquist, K.E. and Sterner, O. 1993b. Lachnumon and Lachnumol A, New Metabolites with Nematicidal and Antimicrobial Activities from the Ascomycete *Lachnum papyraceum* (Karst.) Karst. II. Structural Elucidation. J. Antibiot. 46(6), 968-971.

Stadler, M. and Anke, H. 1995a. Metabolites with Nematicidal and Antimicrobial Activities from the Ascomycete *Lachnum papyraceum* (Karst.) Karst. V. Production, Isolation and Biological Activities of Bromine-containing Mycorrhizin and Lachnumon Derivatives and Four Additional New Bioactive Metabolites. J. Antibiot. 48(2), 149-153.

Stadler, M. and Anke, H. 1995b. New Metabolites with Nematicidal and Antimicrobial Activities from the Ascomycete *Lachnum papyraceum* (Karst.) Karst. VI. Structure Determination of Non-halogenated Metabolites Structurally Related to Mycorrhizin A. J. Antibiot. 48(2), 154-157.

Stadler, M. and Anke, H. 1995c. New Metabolites with Nematicidal and Antimicrobial Activities from the Ascomycete *Lachnum papyraceum* (Karst.) Karst. VII. Structure Determination of Brominated Lachnumon and Mycorrhizin A Derivatives. J. Antibiot. 48(2), 158-161.

Stadler, M., Anke, H. and Sterner, O. 1995d. Metabolites with Nematicidal and Antimicrobial Activities from the Ascomycete *Lachnum papyraceum* (Karst.) Krast. III. Production of Novel Isocoumarin Derivatives, Isolation, and Biological Activities. J. Antibiot. 48(3), 262-266.

Stadler, M. and Anke, H. 1995e. New Metabolites with Nematicidal and Antimicrobial Activities from the Ascomycete *Lachnum papyraceum* (Karst.)

Karst. IV. Structural Elucidation of Novel Isocoumarin Derivatives. J. Antibiot. 48(3), 267-270.

Steyn, P.S., Van Heerden, F.R. and Rabie, C.J. 1982. Cytochalasins E and K, Toxic Metabolites from *Aspergillus clavatus*. J. Chem. Soc., Perkin Trans. I: Organic and Bio-Organic Chemistry (1972-1999) 2, 541-544.

Tajima, N., Nukina, M., Kato, N. and Sassa, T. 2004. Novel Fusicoccins R and S, and the Fusicoccin S Aglycon (Phomopsiol) from *Phomopsis amygdali* Niigata 2-A, and Their Seed Germination-stimulating Activity in the Presence of Abscisic Acid. Biosci., Biotechnol., Biochem. 68(5), 1125-1130.

Taub, D., Kuo, C.H., Slates, H.L. and Wendler, N.L. 1963. Total Synthesis of Griseofulvin and Its Optical Antipode. Tetrahedron 19, 1-17.

Tomioka, T., Izawa, Y., Koyama, K. and Natori, S. 1987. Three New 10-Phenyl[11]cytochalasans, Cytochalasins N, O and P from *Phomopsis* sp. Chem. Pharm. Bull. 35(2), 902-905.

Veiga, T.A.M., Silva, S.C., Francisco, A-C., Filho, E.R., Vieira, P.C., Fernandes, J.B., Silva, M.F.G.F., Mueller, M.W. and Lotina-Hennsen, B. 2007. Inhibition of Photophosphorylation and Electron Transport Chain in Thylakoids by Lasiodiplodin, a Natural Product from *Botryosphaeria rhodina*. J. Agric. Food. Chem. 55(10), 4217-4221.

Venkatasubbaiah, P. and Chilton, W.S. 1990. Phytotoxins of Plant Pathogens. Part IV. Phytotoxins of *Botryosphaeria obtusa*. J. Nat. Prod. 53(6), 1628-1630.

Wang, X-N., Tan, R-X. and Liu, J-K. 2005. Xylactam, a New Nitrogen-containing Compound from the Fruiting Bodies of Ascomycete *Xylaria euglossa*. J. Antibiot. 58(4), 268-270.

Weber, R.W.S., Meffert, A., Anke, H. and Sterner, O. 2005. Production of Sordarin and Related Metabolites by the Coprophilous Fungus *Podospora pleiospora* in Submerged Culture and in Its Natural Substrate. Mycol. Res. 109 (5), 619-626.

Wheeler, M.M., Wheeler, D.M.S. and Peterson, G.W. 1975. Anthraquinone Pigments from the Phytopathogen *Phomopsis juniperovora*. Phytochemistry 14(1), 288-289.

Wu, X-Y., Li, M-L., Hu, G-P., Lin, Y-C. and Vrijmoed, L.L.P. 2002. Metabolites of the Endophyte Fungus No. 2508 in the Mangrove Tree from the South China Seacoast. Zhongshan Daxue Xuebao, Ziran Kexueban 41(3), 34-36.

Wu, X., Liu, X., Jiang, G., Lin, Y., Chan, W. and Vrijmoed, L.L.P. 2005a. Xyloketal G, a Novel Metabolite from the Mangrove Fungus *Xylaria* sp. 2508. Chem. Nat. Compd. 41(1), 27-29.

Wu, X.Y., Liu, X.H., Lin, Y.C., Luo, J.H., She, Z.G., Li, H., Chan, W.L., Antus, S., Kurtan, T., Elsasser, B. and Krohn, K. 2005b. Xyloketal F: A Strong L-Calcium Channel Blocker from the Mangrove Fungus *Xylaria* sp. (#2508) from the South China Sea Coast. Eur. J. Org. Chem. 19, 4061-4064.

Yue, J-M., Chen, S-N., Lin, Z-W. and Sun, H-D. 2001. Sterols from the Fungus *Lactarium volemus*. Phytochemistry 56, 801-806.

APPENDIX

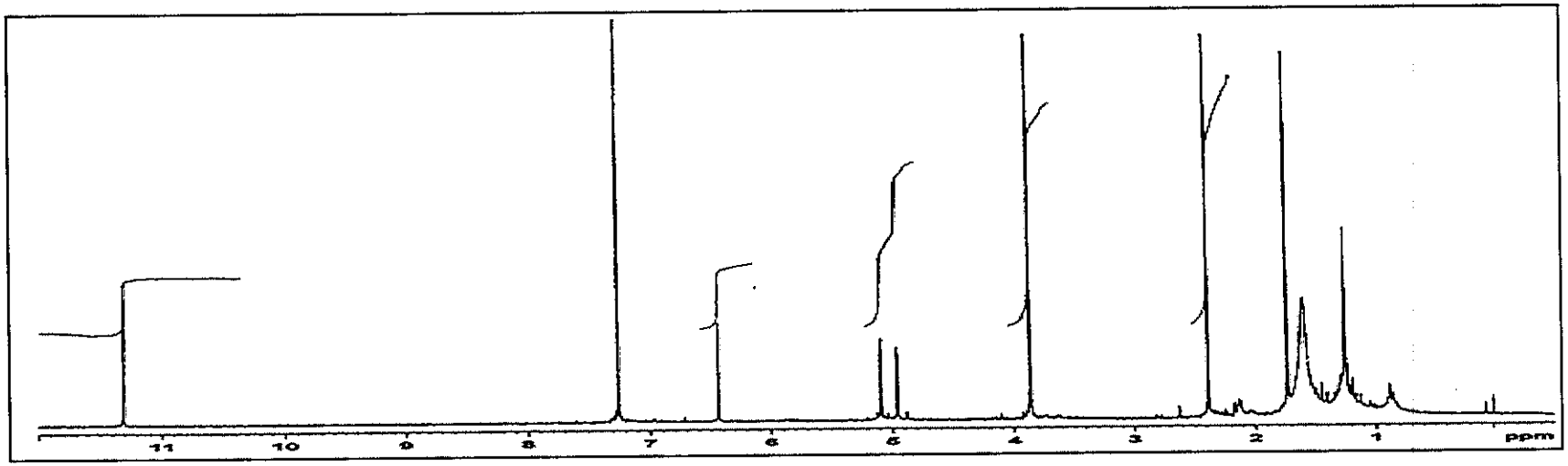

Figure 1 ^{1}H NMR (300 MHz) ($CDCl_3$) spectrum of compound **N1**

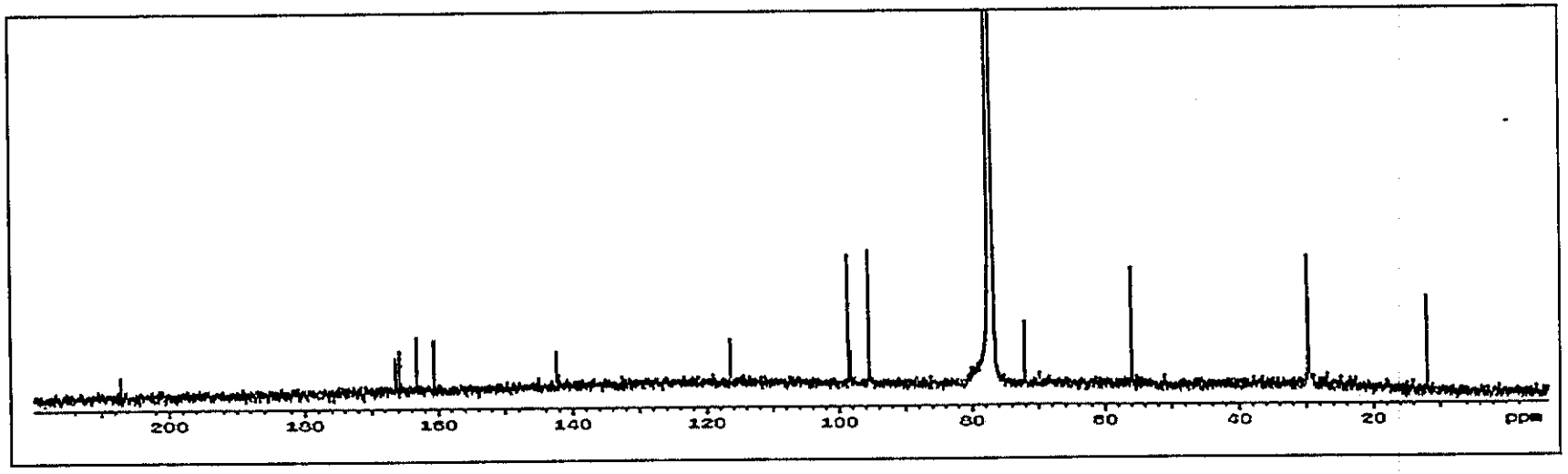

Figure 2 ^{13}C NMR (125 MHz) ($CDCl_3$) spectrum of compound **N1**

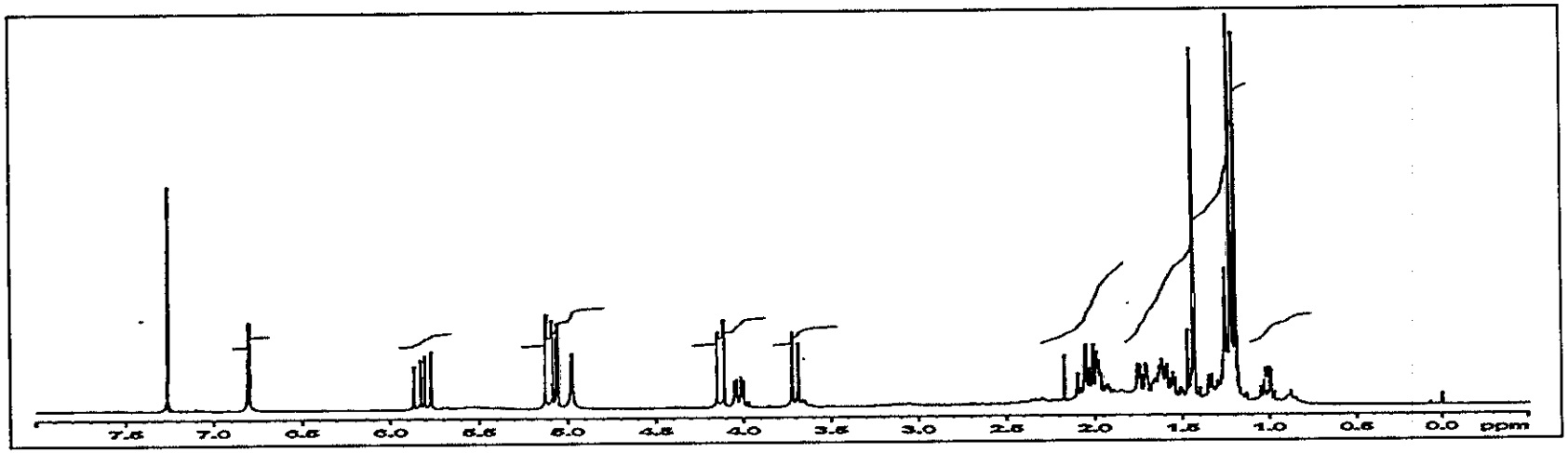

Figure 3 ^{1}H NMR (300 MHz) ($CDCl_3$) spectrum of compound N3

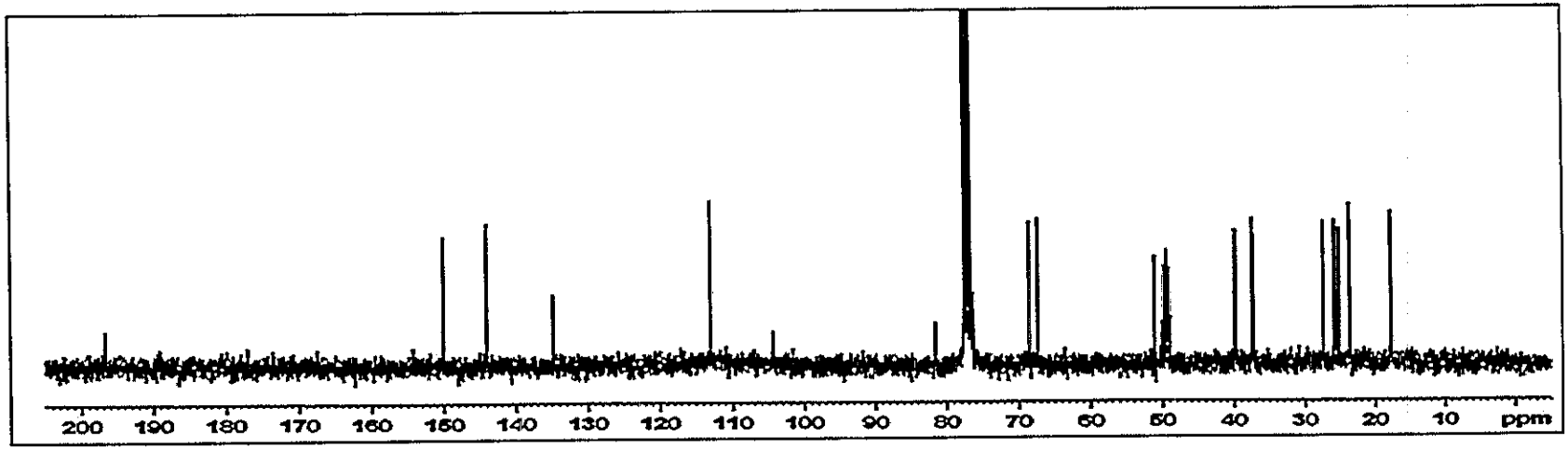

Figure 4 ^{13}C NMR (75 MHz) ($CDCl_3$) spectrum of compound N3

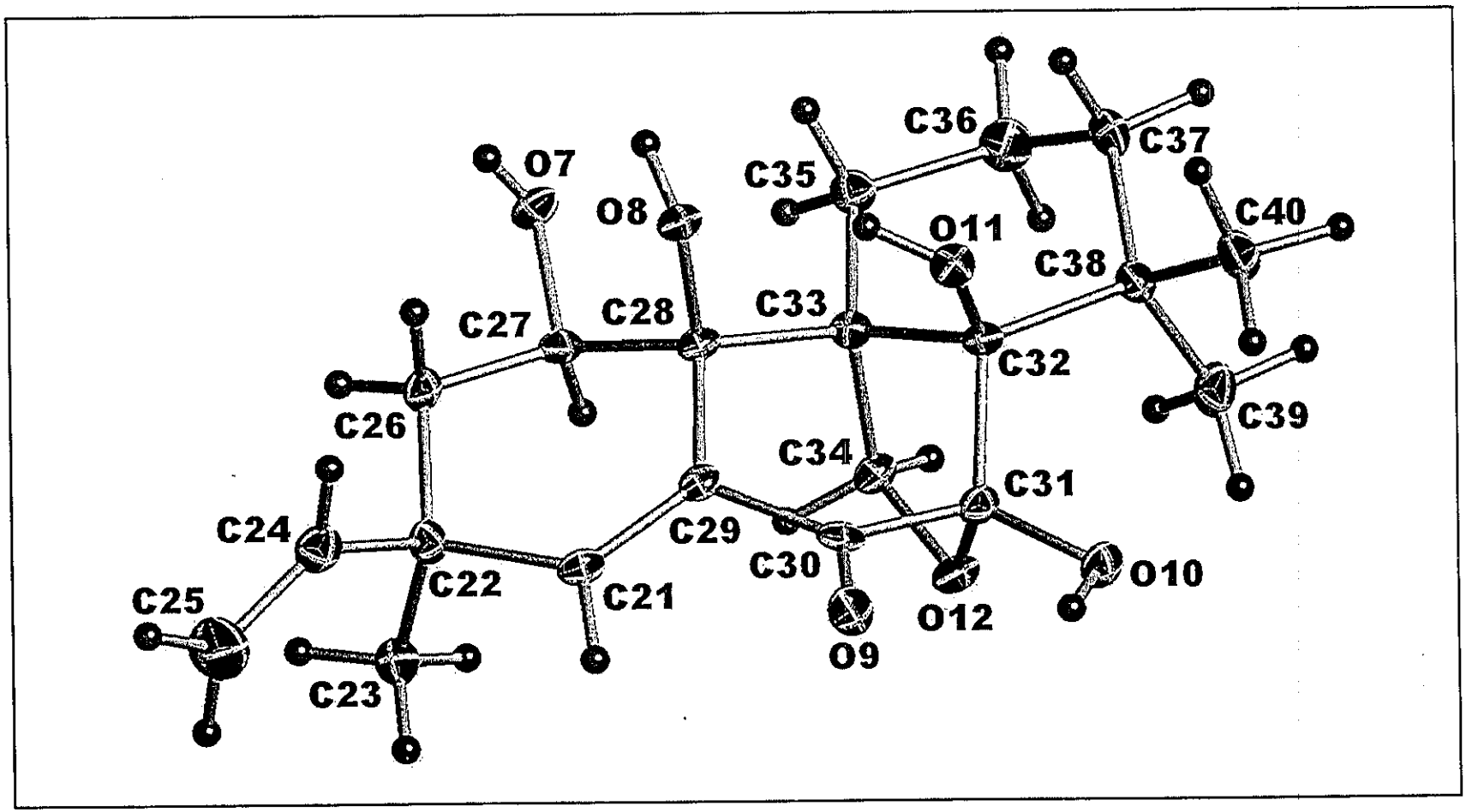

Figure 5 X-ray structure of compound N3

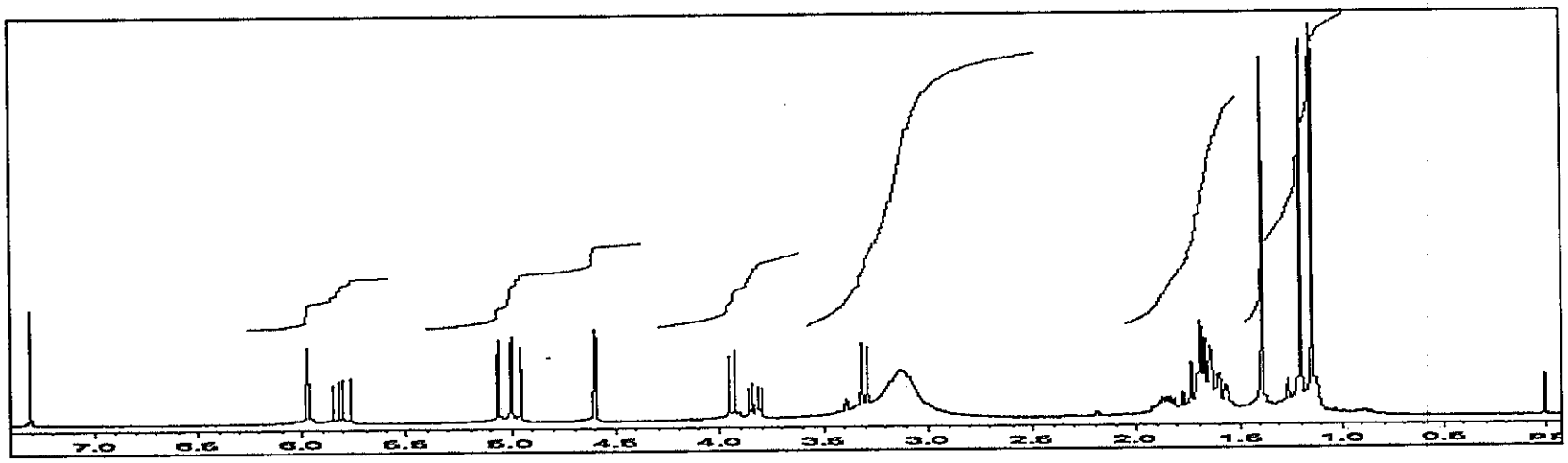

Figure 6 ^{1}H NMR (300 MHz) ($CDCl_3$) spectrum of compound **N4**

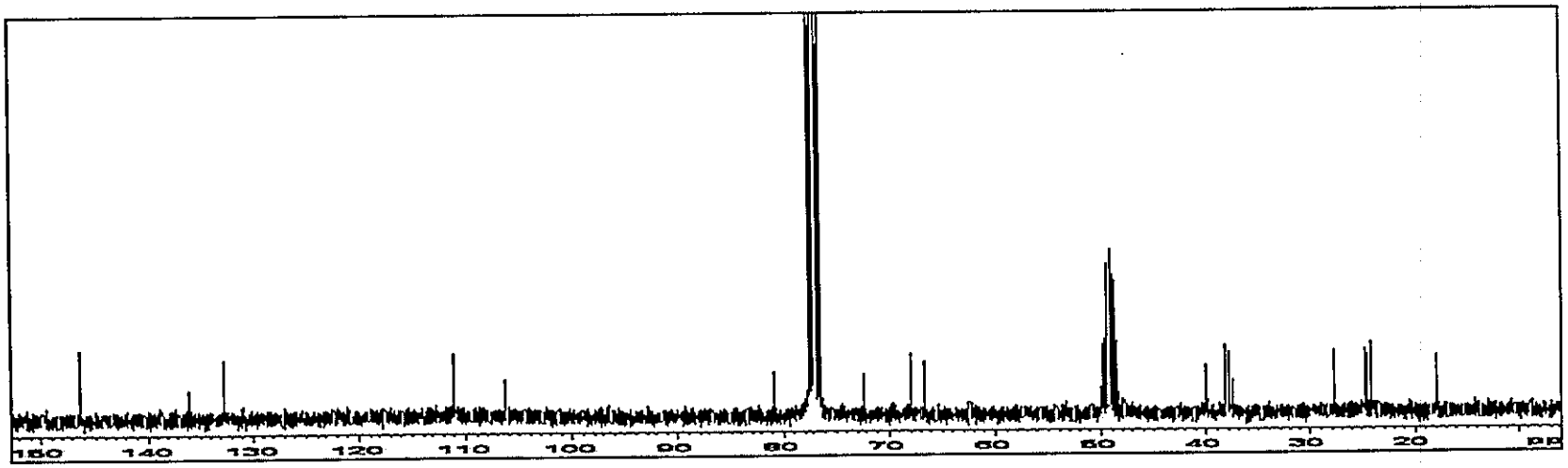

Figure 7 ^{13}C NMR (75 MHz) ($CDCl_3$) spectrum of compound **N4**

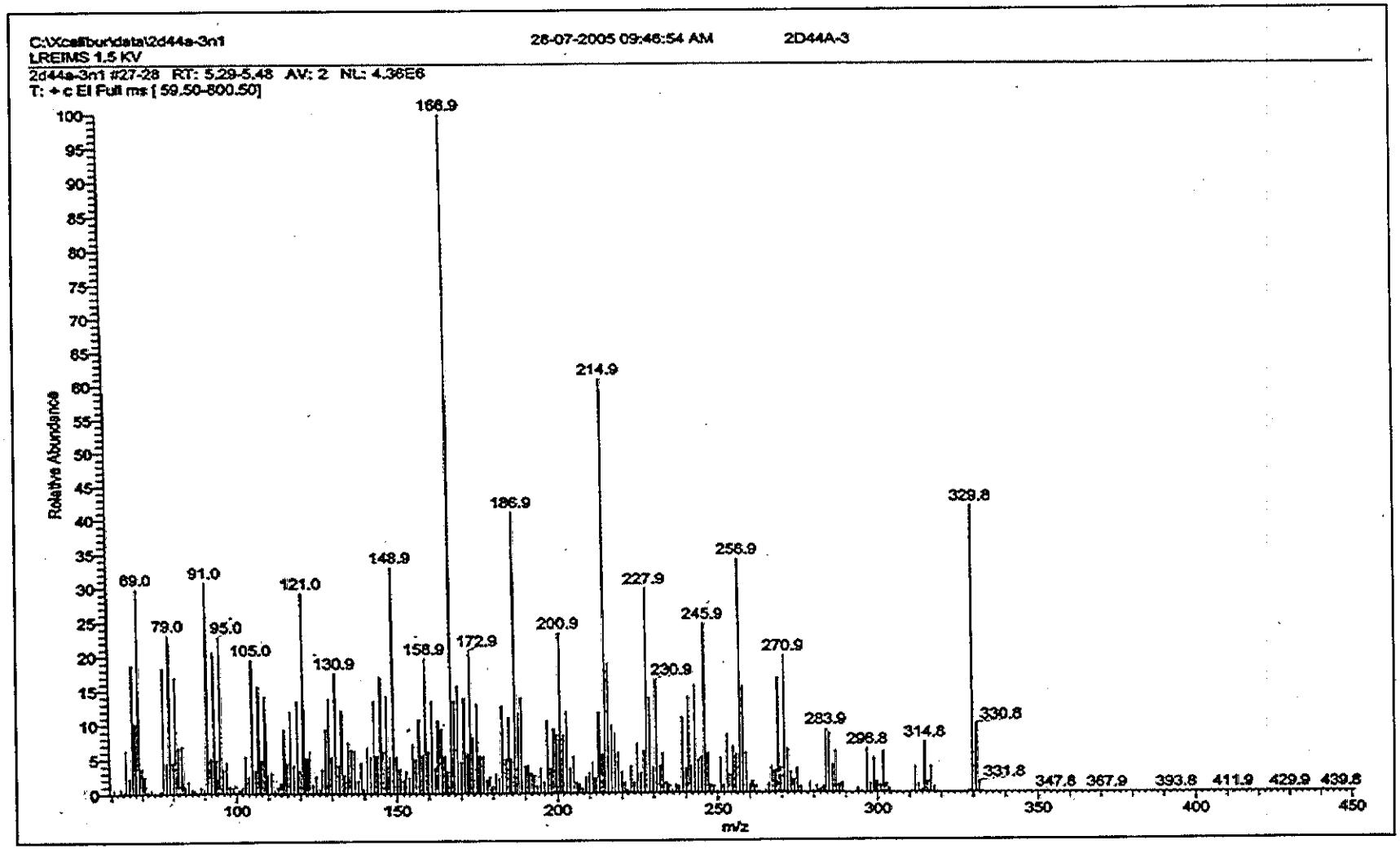

Figure 8 Mass spectrum of compound N2

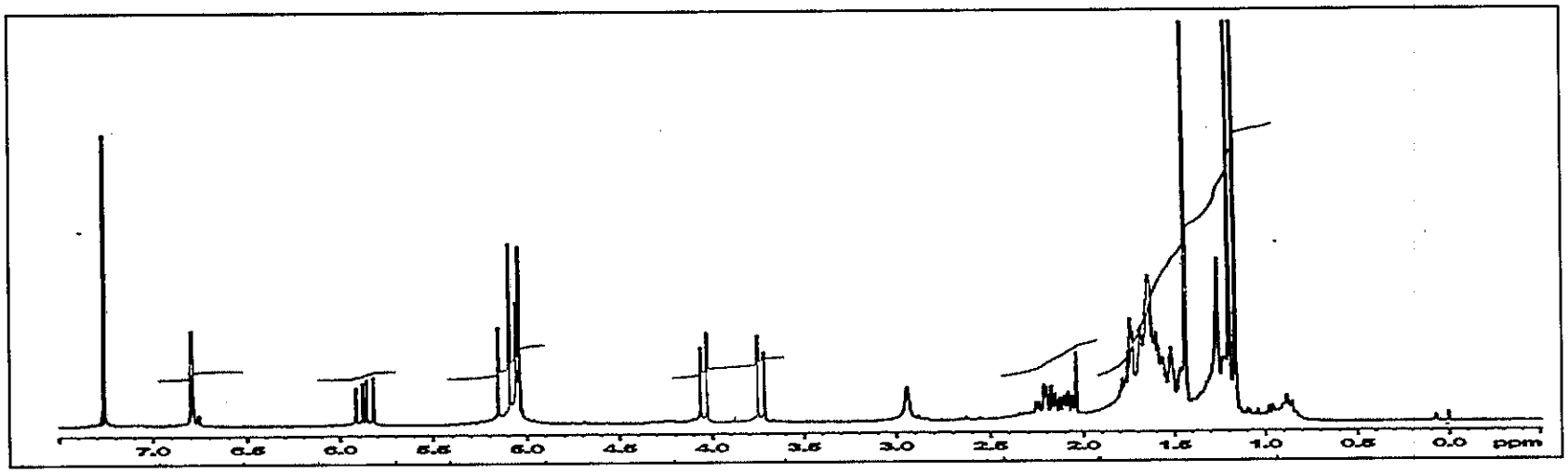

Figure 9 ^{1}H NMR (300 MHz) ($CDCl_3$) spectrum of compound N2

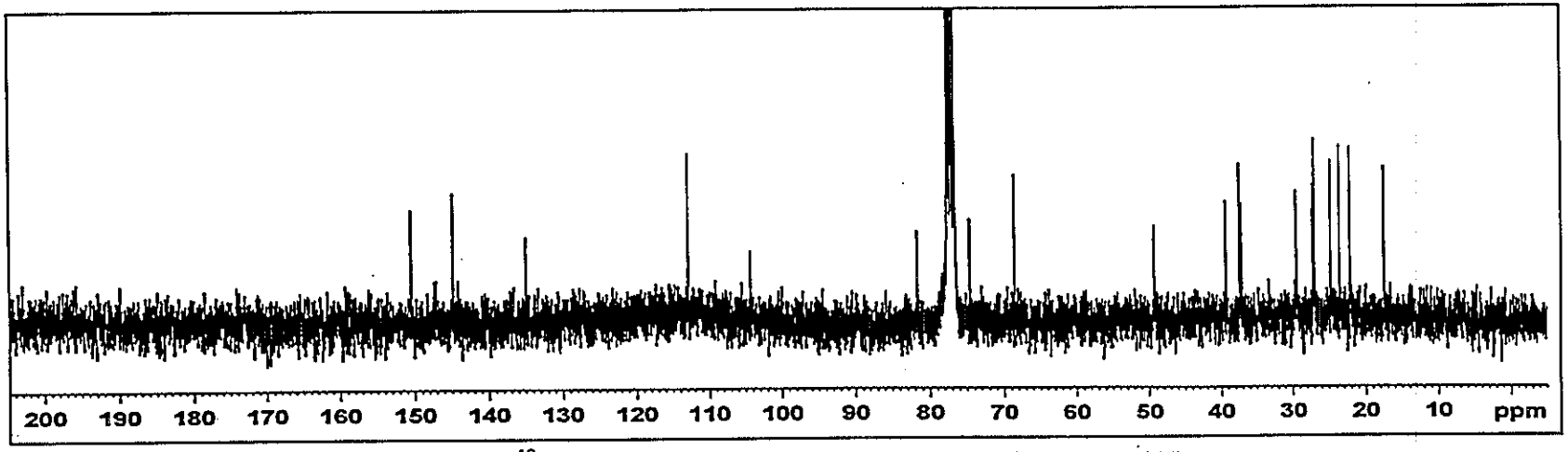

Figure 10 ^{13}C NMR (75 MHz) ($CDCl_3$) spectrum of compound N2

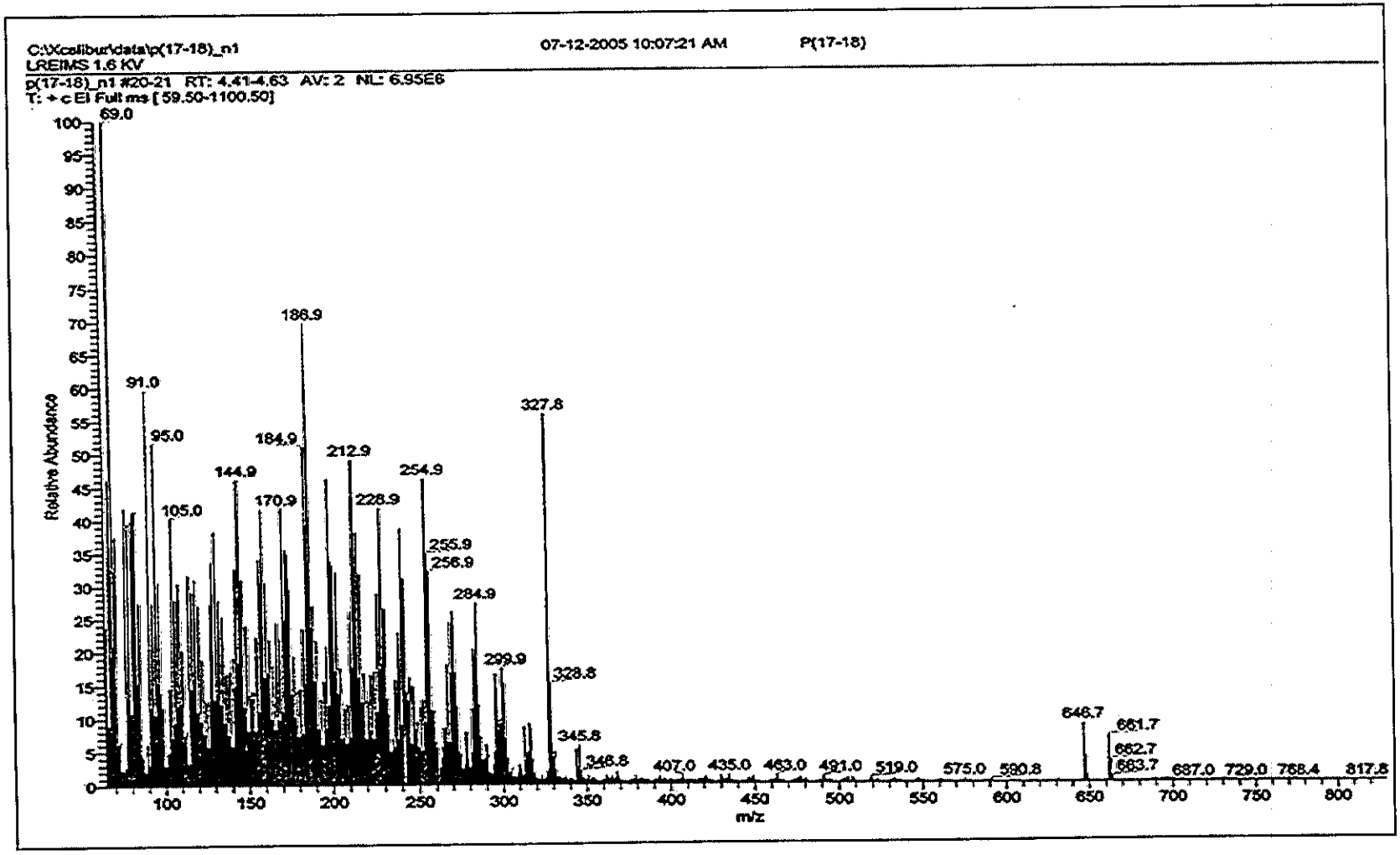

Figure 11 Mass spectrum of compound N5

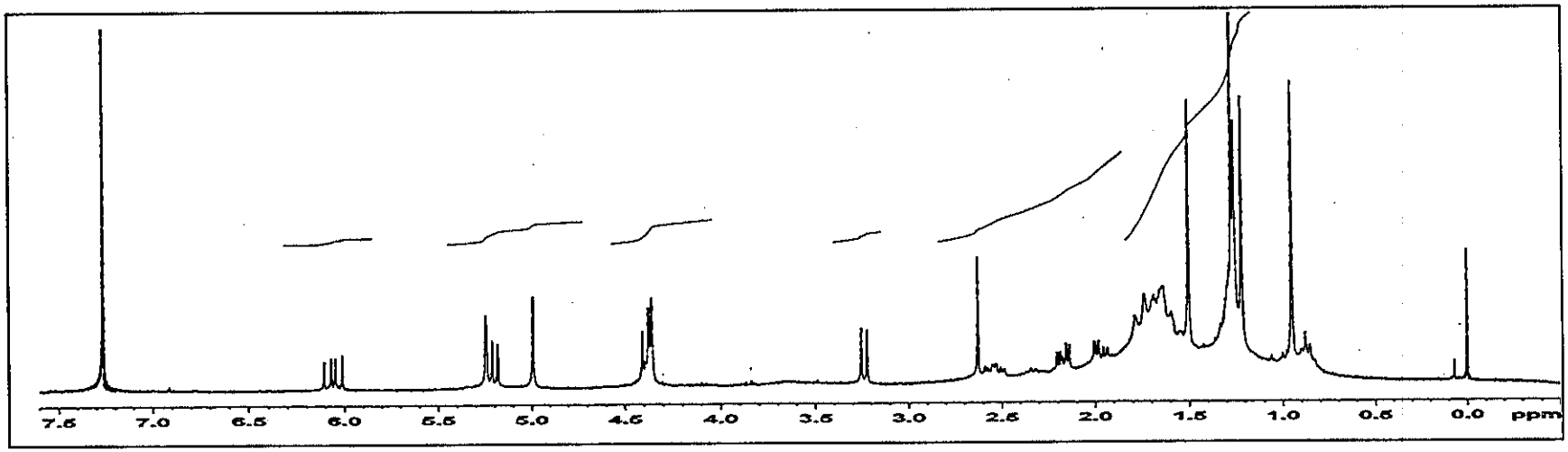

Figure 12 ^{1}H NMR (300 MHz) ($CDCl_3$) spectrum of compound **N5**

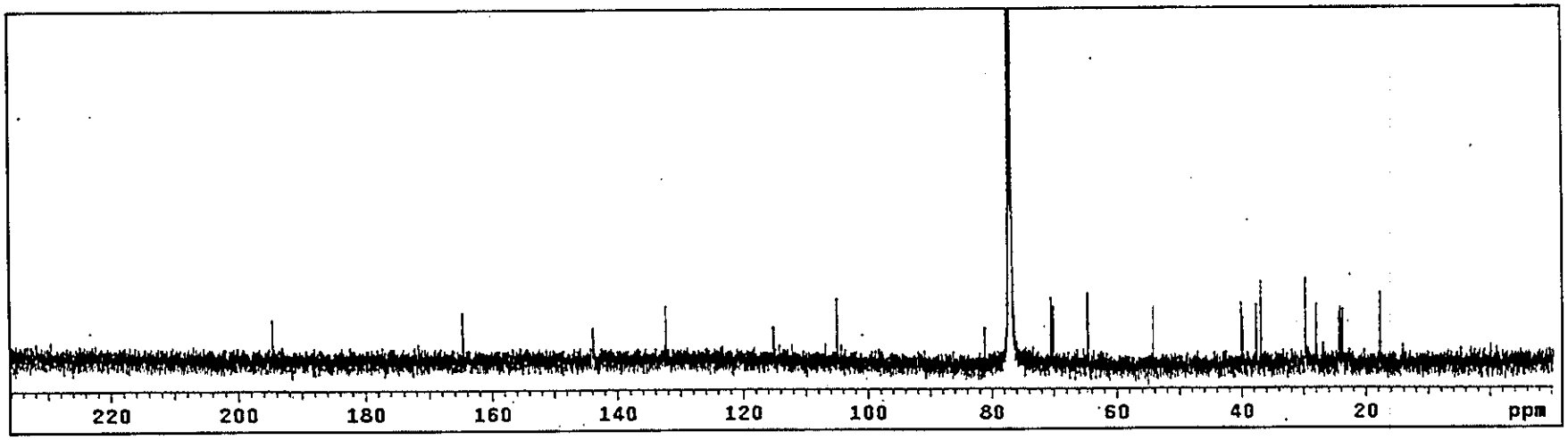

Figure 13 ^{13}C NMR (125 MHz) ($CDCl_3$) spectrum of compound **N5**

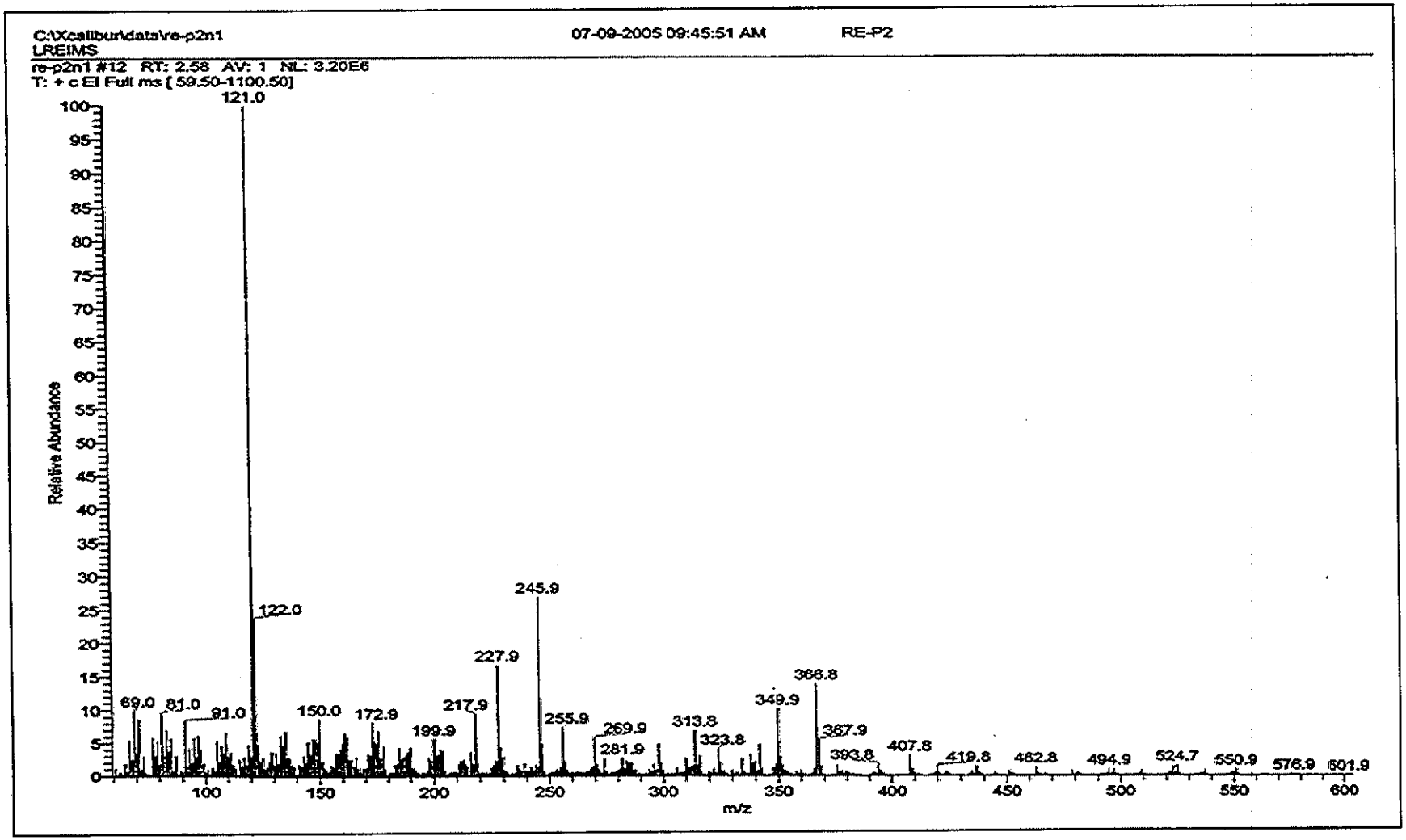

Figure 14 Mass spectrum of compound N7

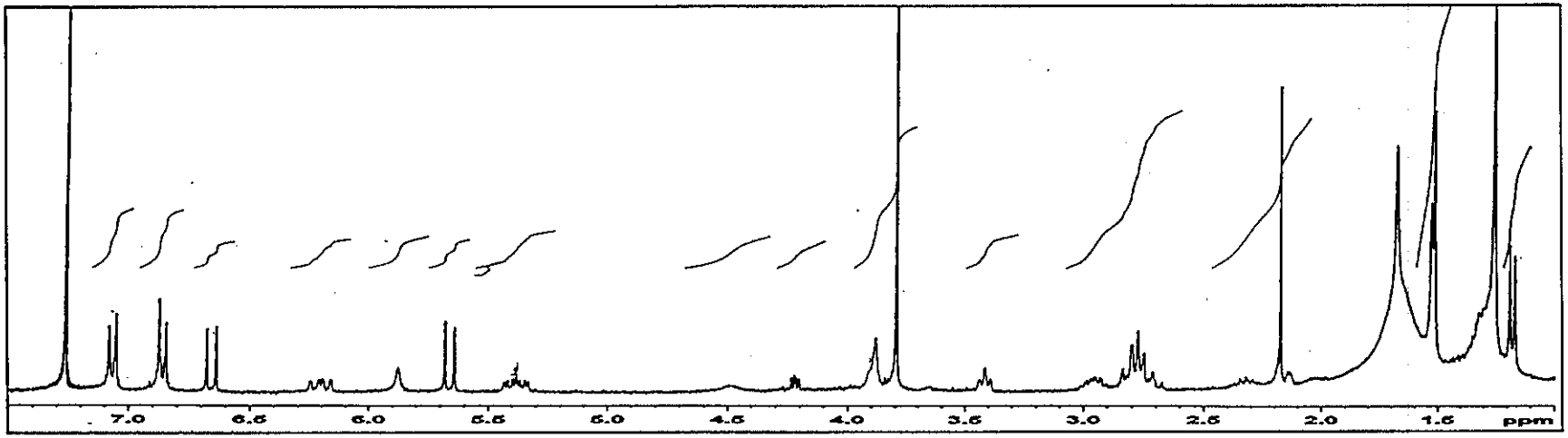

Figure 15 ^{1}H NMR (300 MHz) ($CDCl_3$) spectrum of compound **N7**

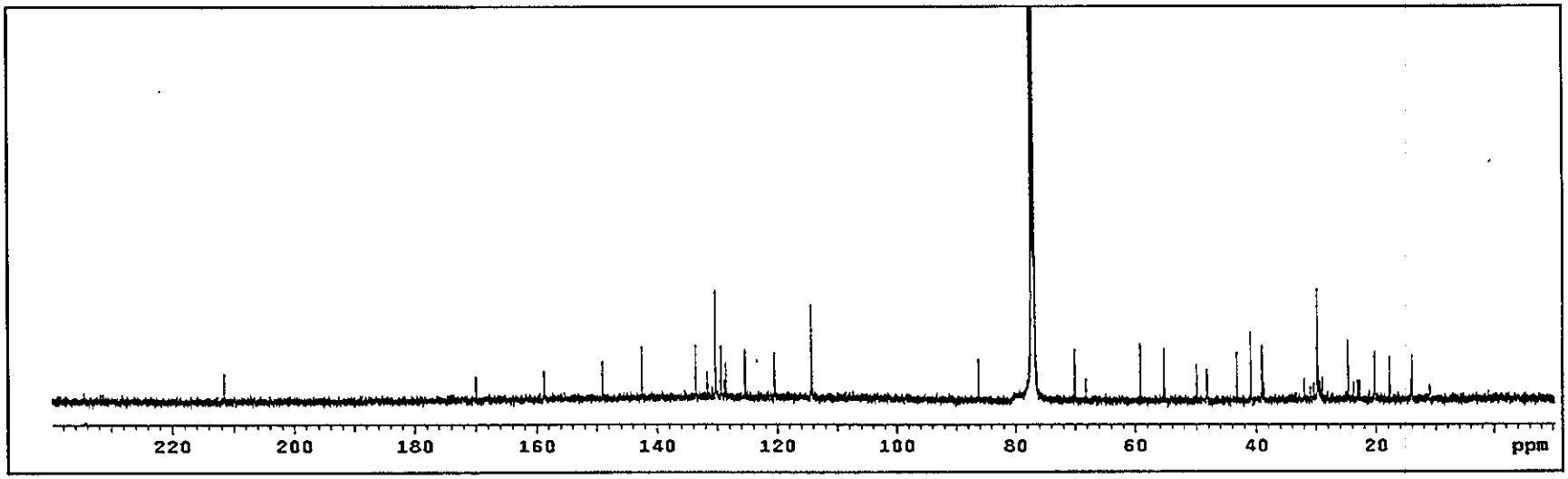

Figure 16 ^{13}C NMR (125 MHz) ($CDCl_3$) spectrum of compound **N7**

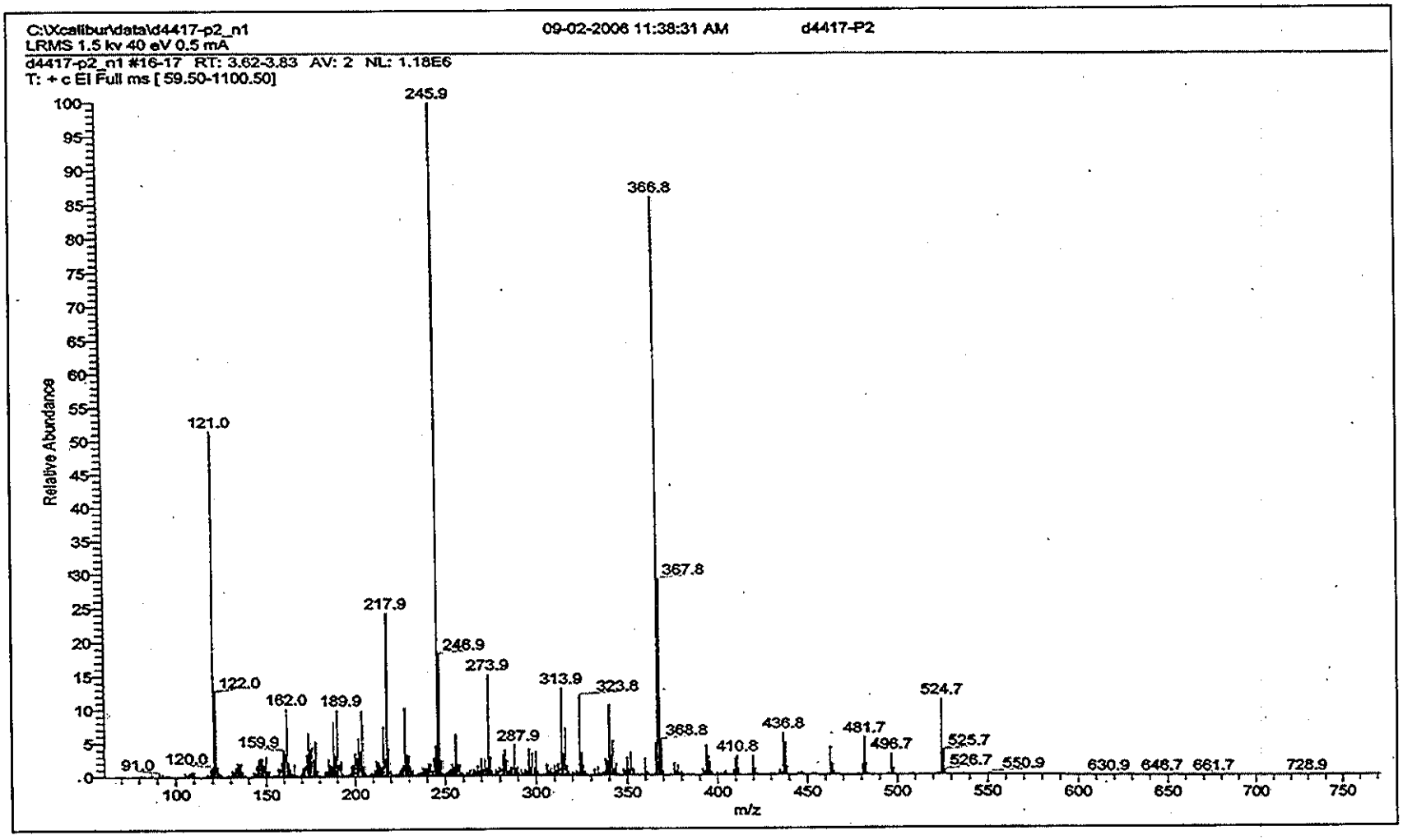

Figure 17 Mass spectrum of compound **N6**

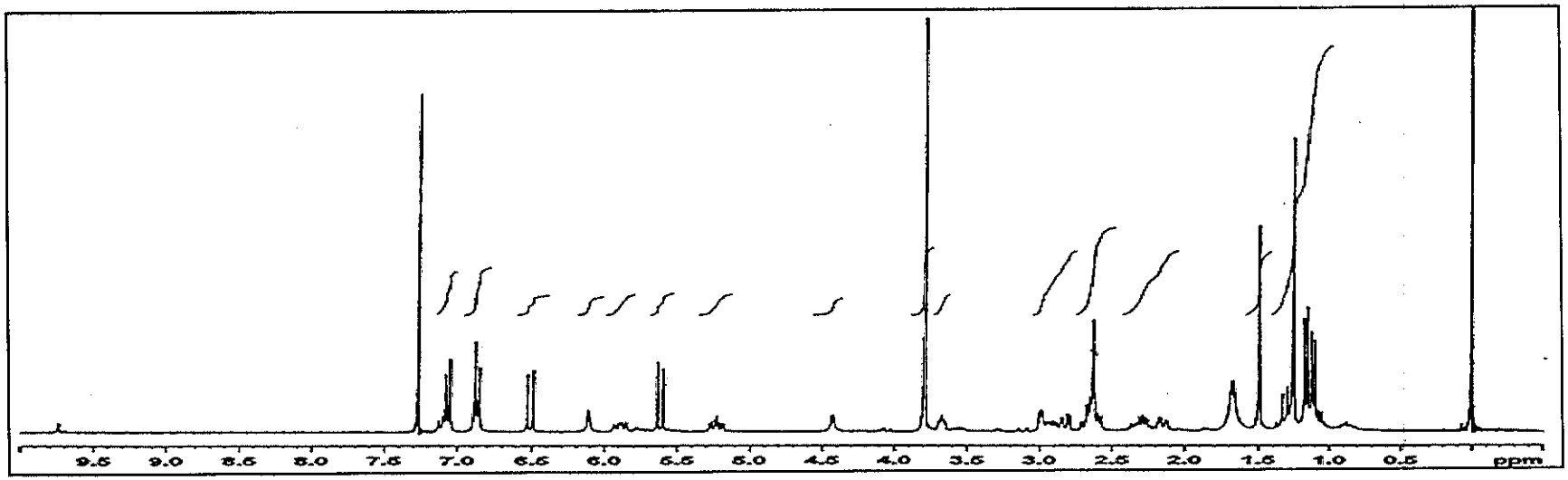

Figure 18 ^{1}H NMR (300 MHz) ($CDCl_3$) spectrum of compound **N6**

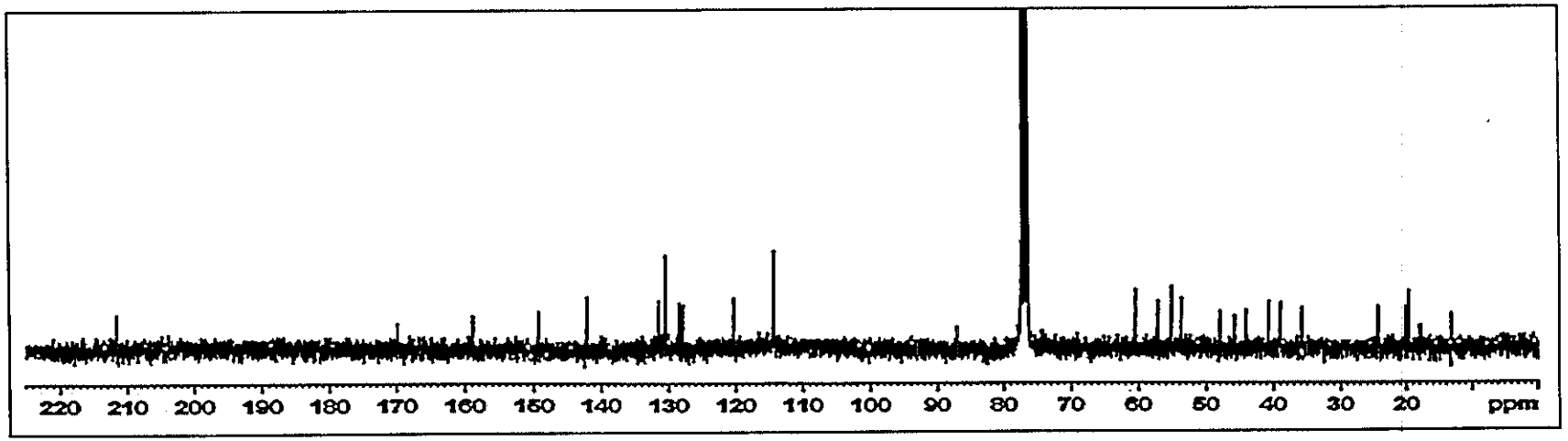

Figure 19 ^{13}C NMR (75 MHz) ($CDCl_3$) spectrum of compound **N6**

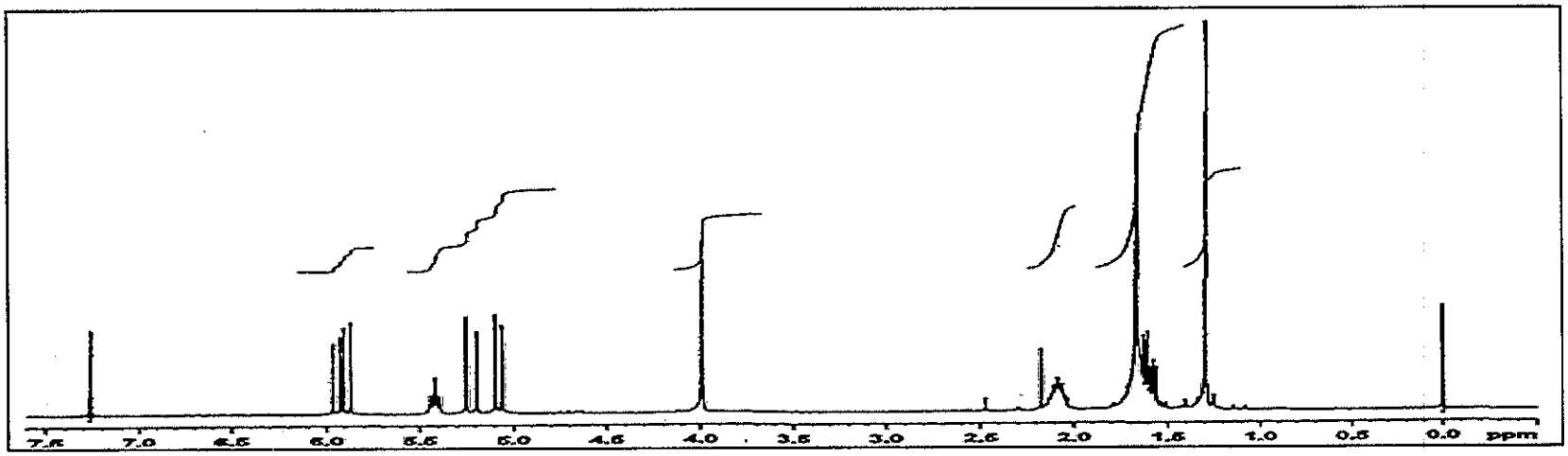

Figure 20 ^{1}H NMR (300 MHz) ($CDCl_3$) spectrum of compound **N8**

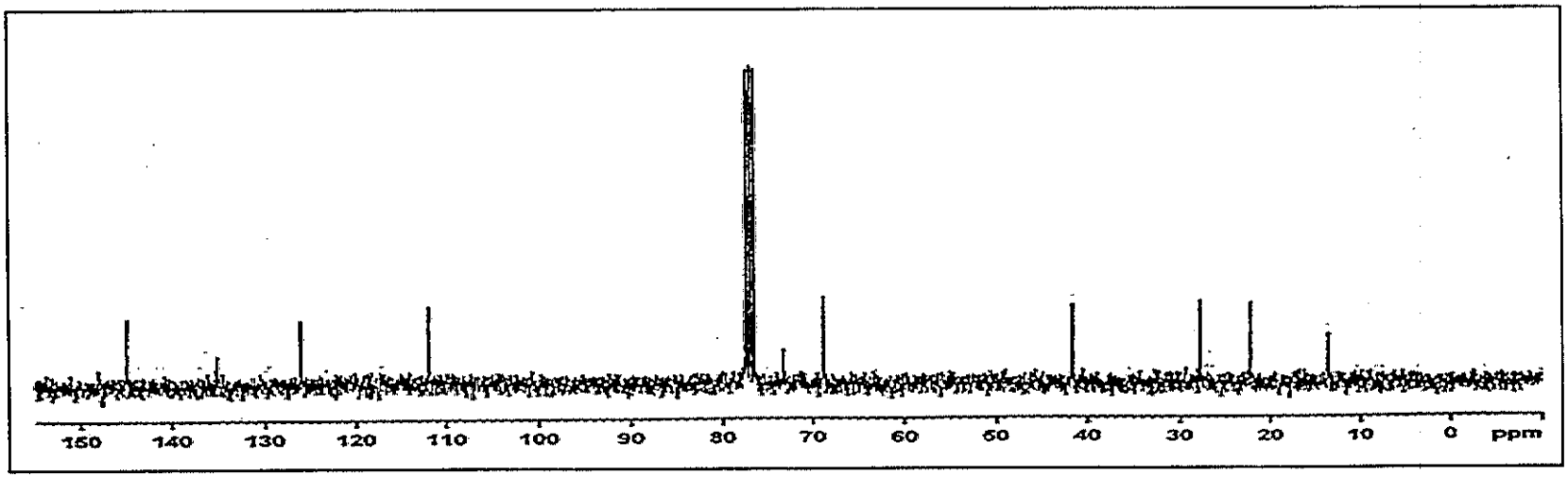

Figure 21 ^{13}C NMR (75 MHz) ($CDCl_3$) spectrum of compound **N8**

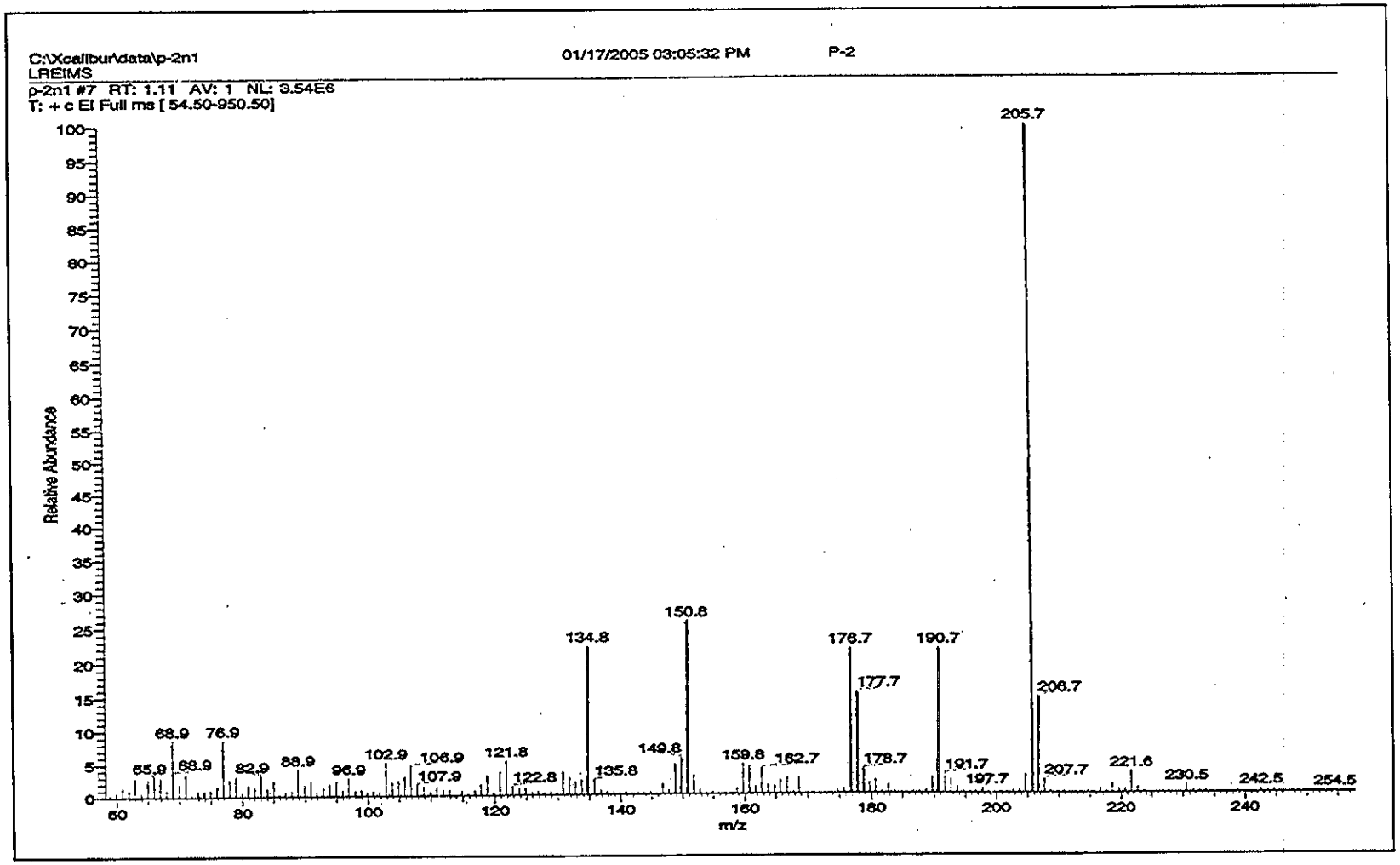

Figure 22 Mass spectrum of compound **N12**

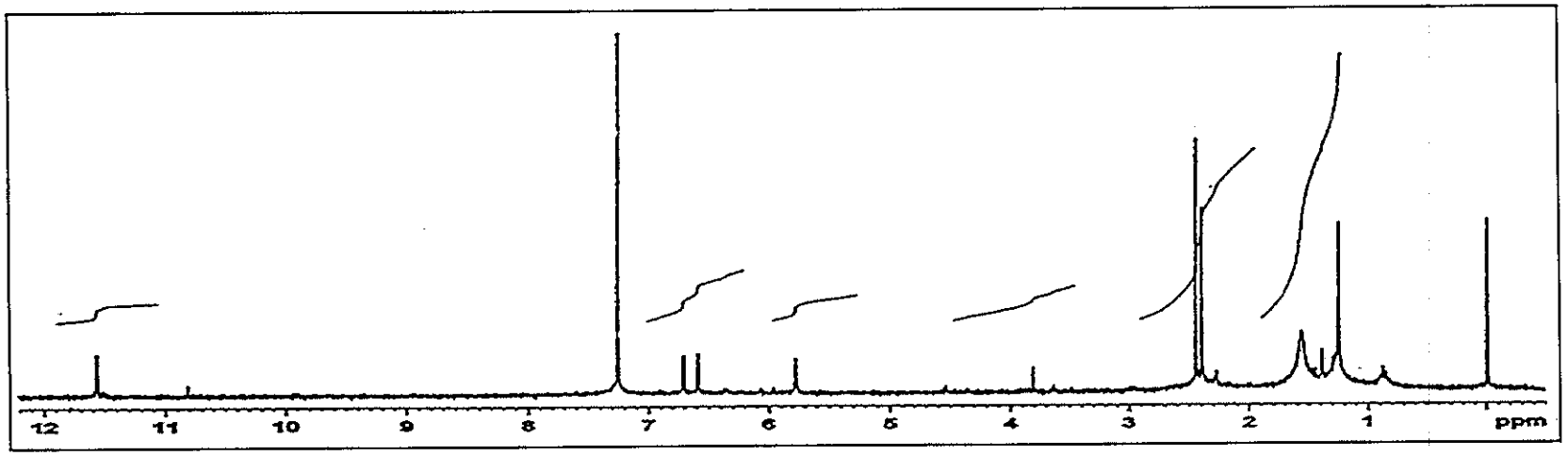

Figure 23 ^{1}H NMR (300 MHz) ($CDCl_3$) spectrum of compound **N12**

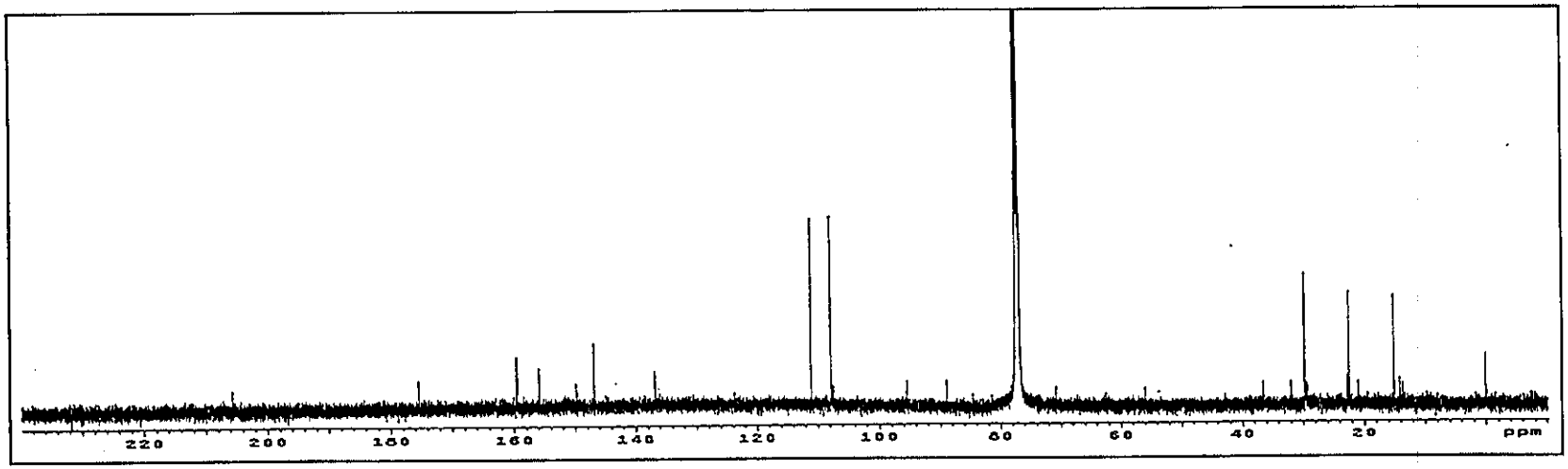

Figure 24 ^{13}C NMR (125 MHz) ($CDCl_3$) spectrum of compound **N12**

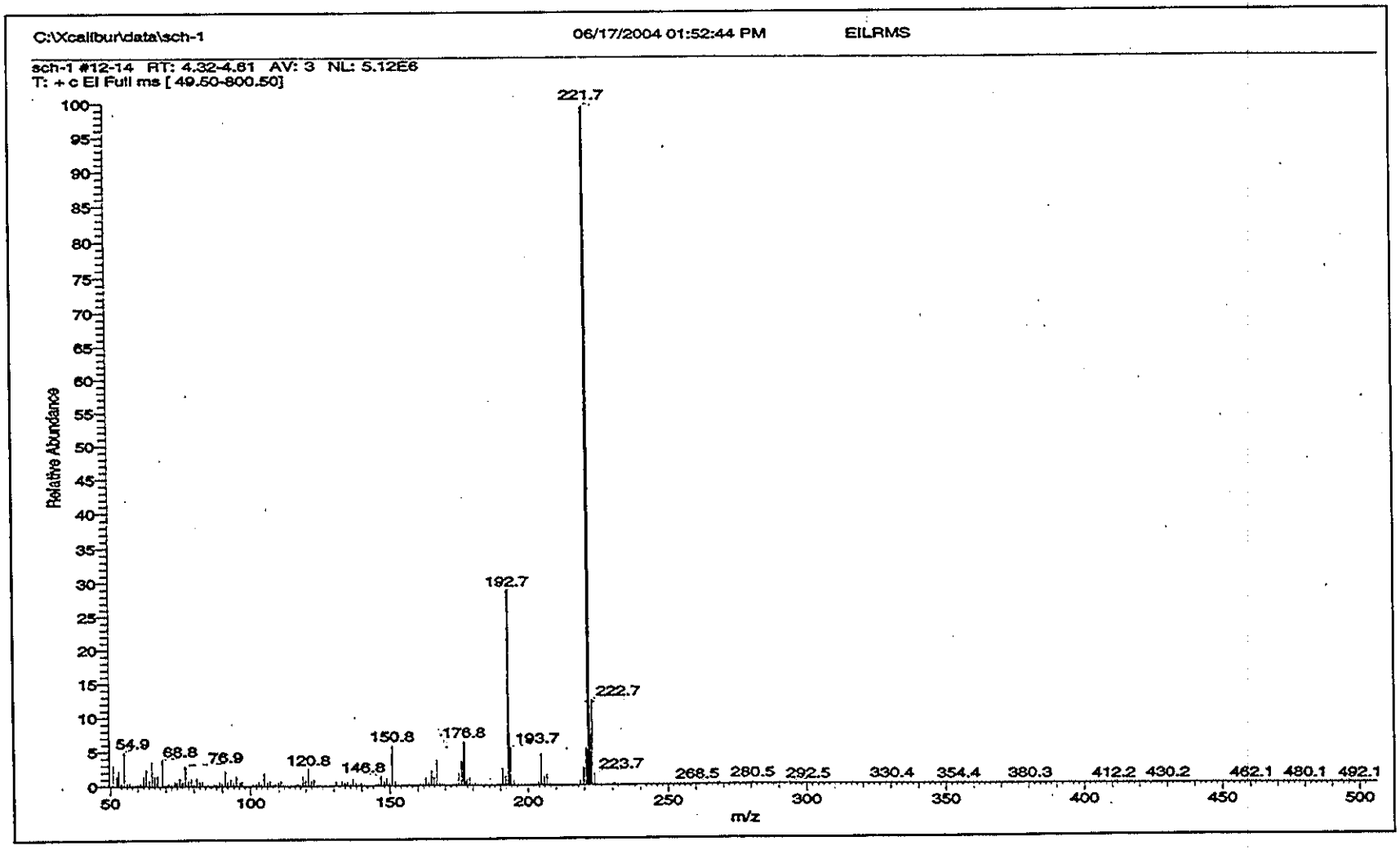

Figure 25 Mass spectrum of compound N13

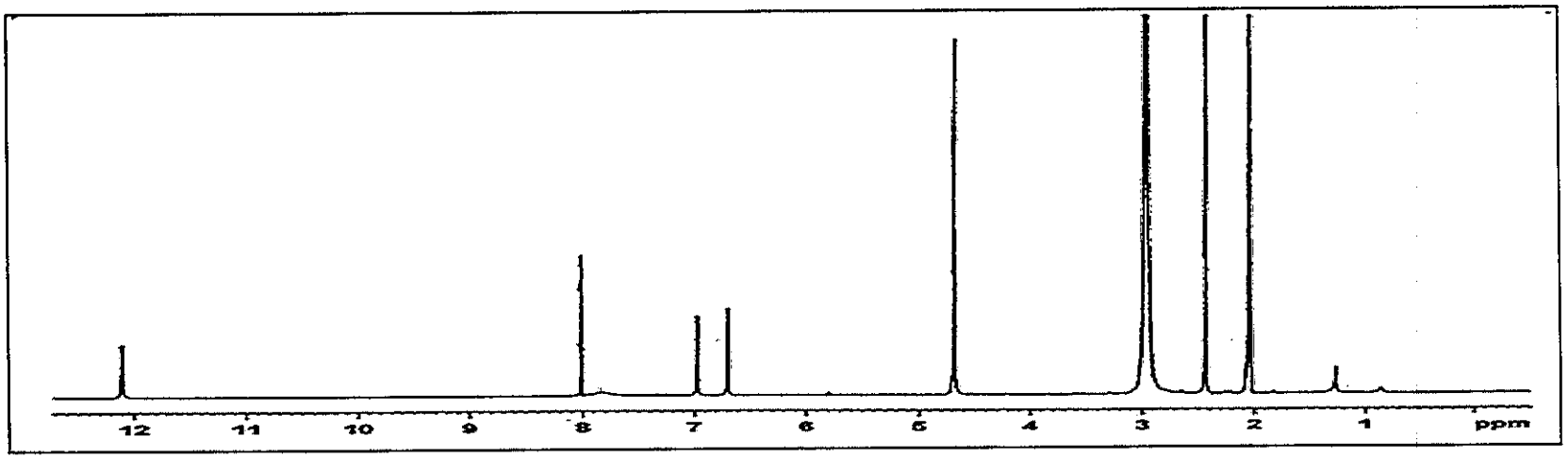

Figure 26 ^{1}H NMR (300 MHz) (Acetone-d_6) spectrum of compound **N13**

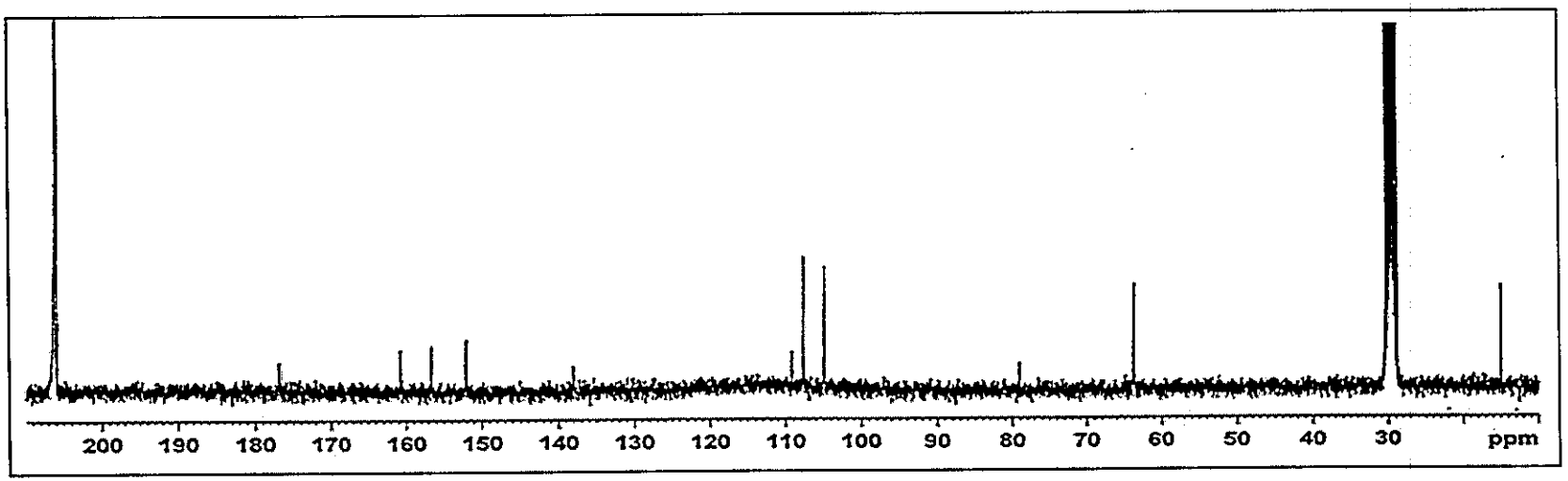

Figure 27 ^{13}C NMR (75 MHz) (Acetone-d_6) spectrum of compound **N13**

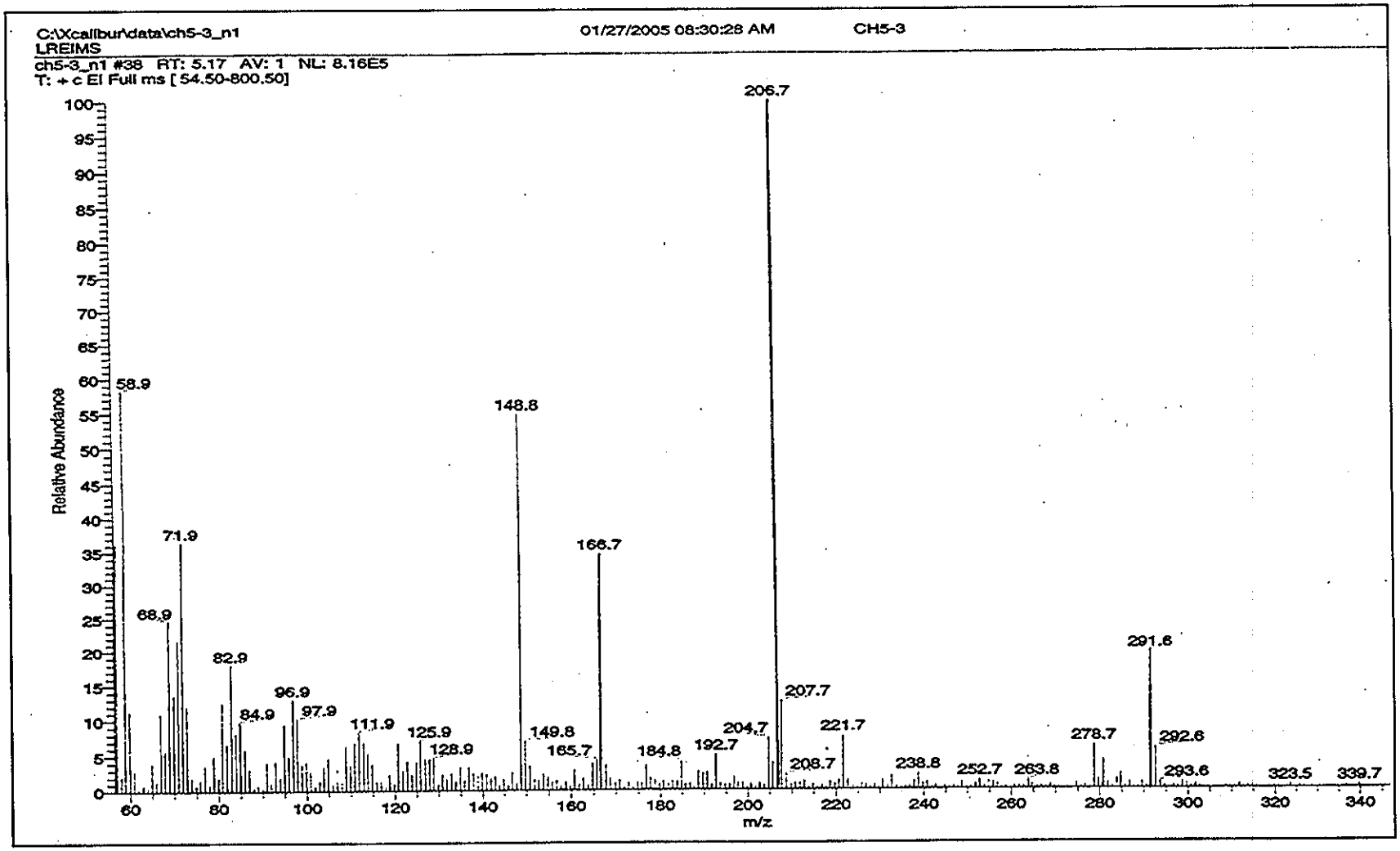

Figure 28 Mass spectrum of compound N9

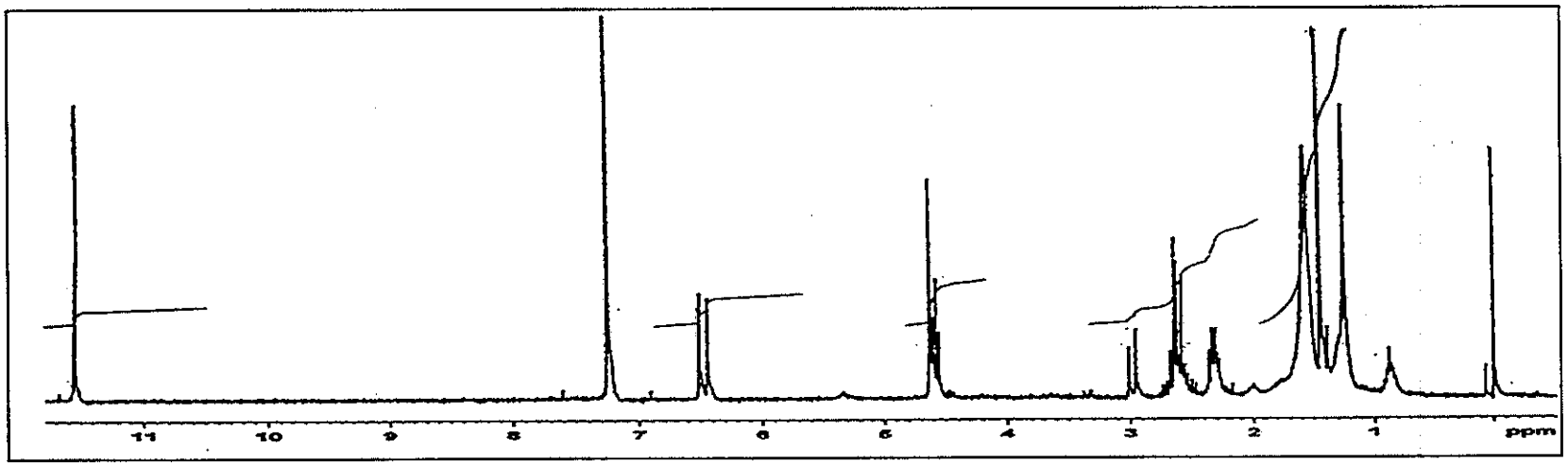

Figure 29 ^{1}H NMR (300 MHz) ($CDCl_3$) spectrum of compound N9

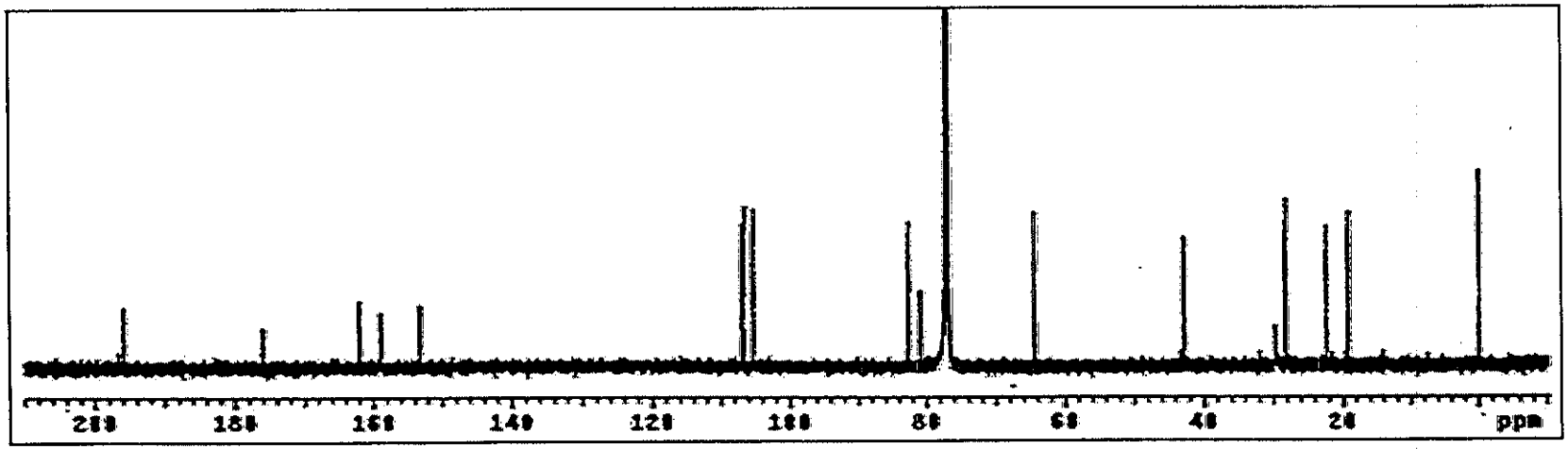

Figure 30 ^{13}C NMR (125 MHz) ($CDCl_3$) spectrum of compound N9

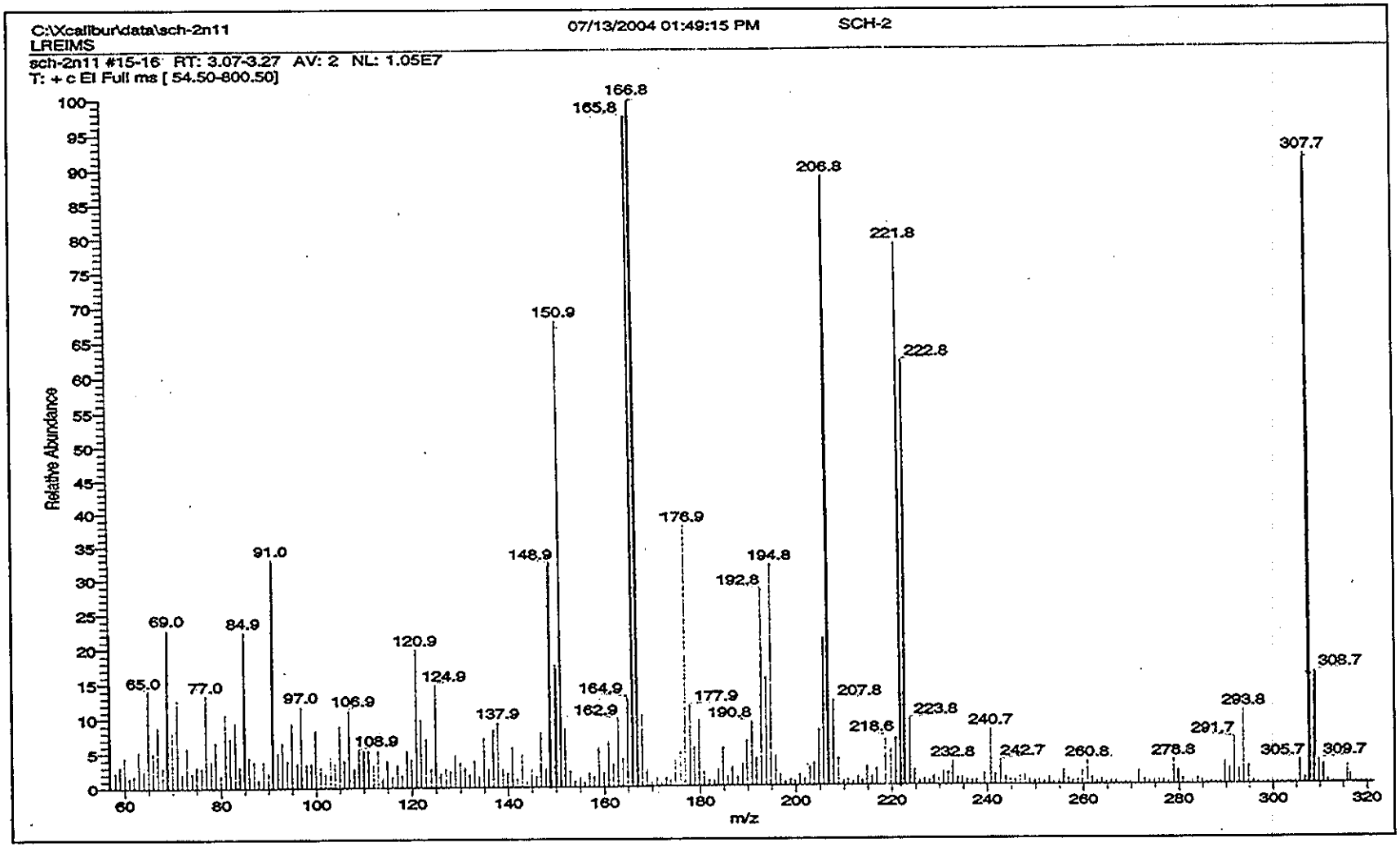

Figure 31 Mass spectrum of compound N11

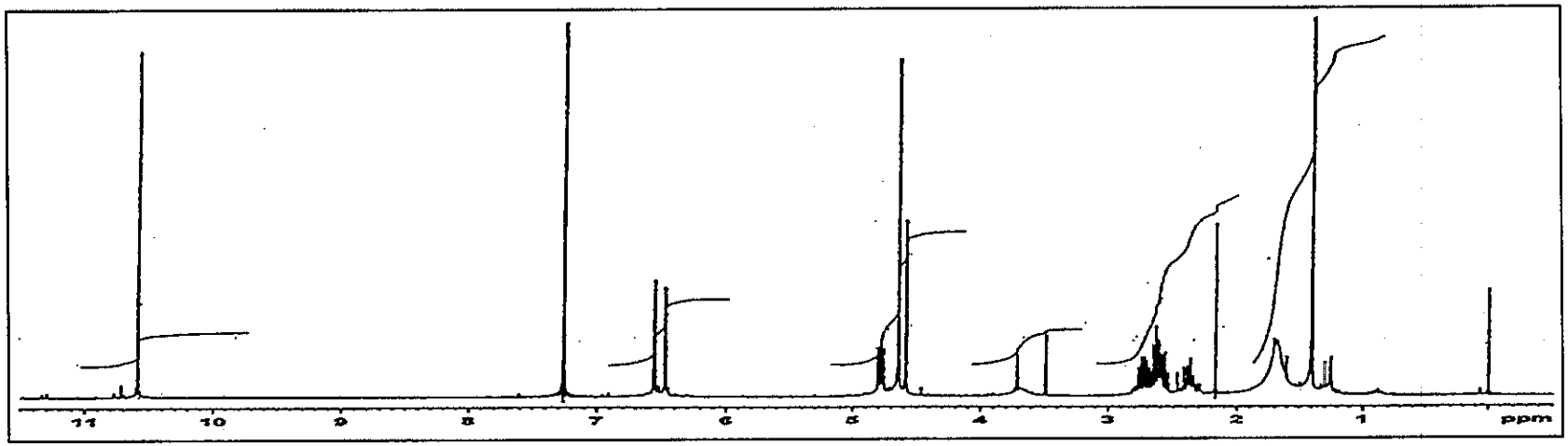

Figure 32 ^{1}H NMR (300 MHz) ($CDCl_3$) spectrum of compound **N11**

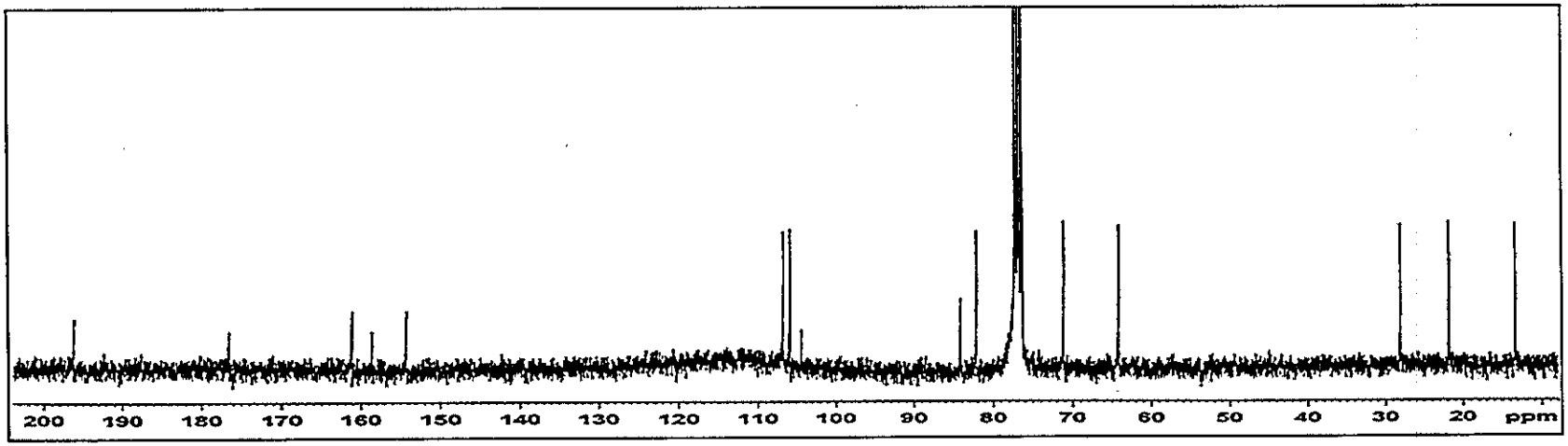

Figure 33 ^{13}C NMR (125 MHz) ($CDCl_3$) spectrum of compound **N11**

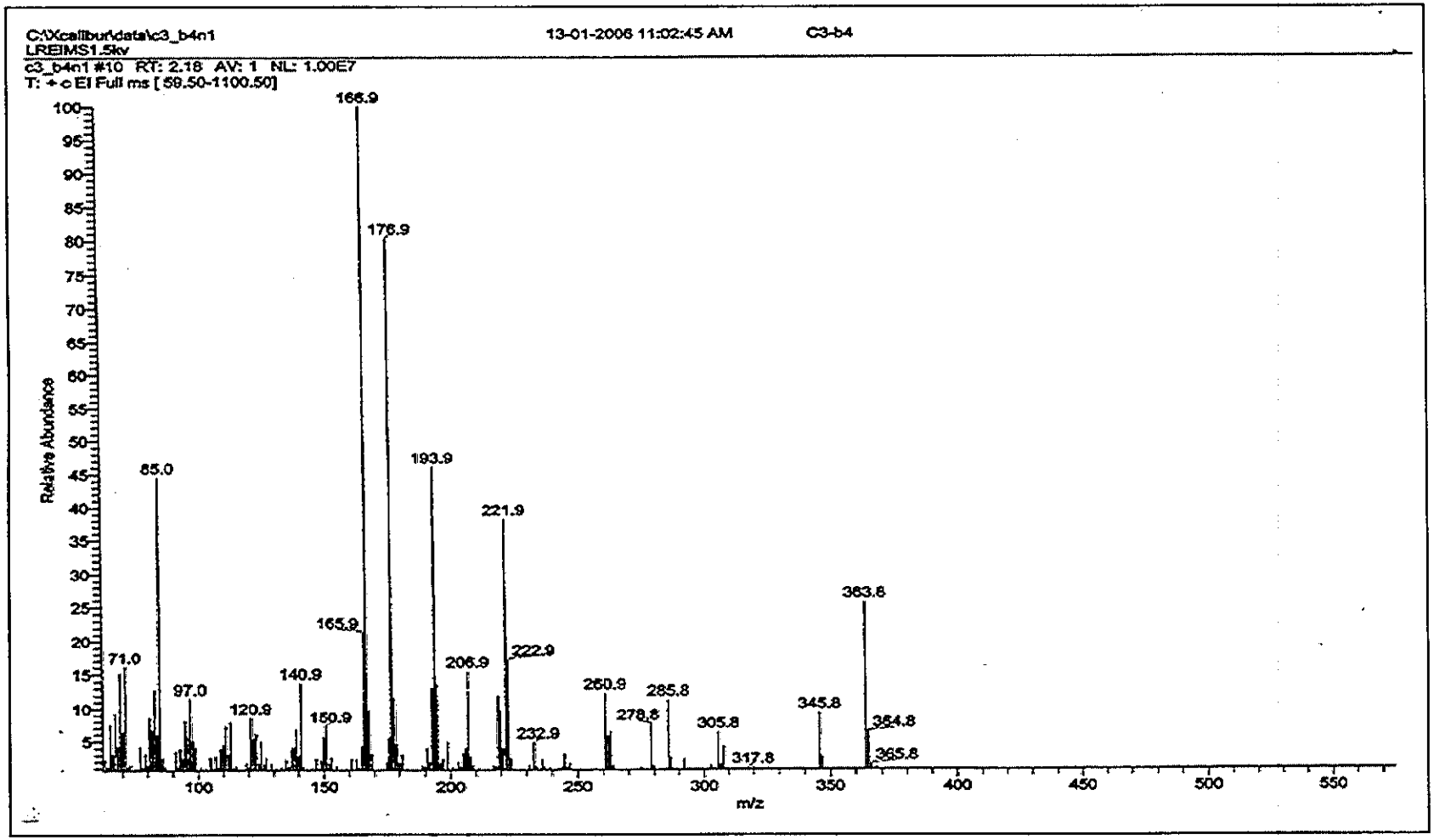

Figure 34 Mass spectrum of compound **N10**

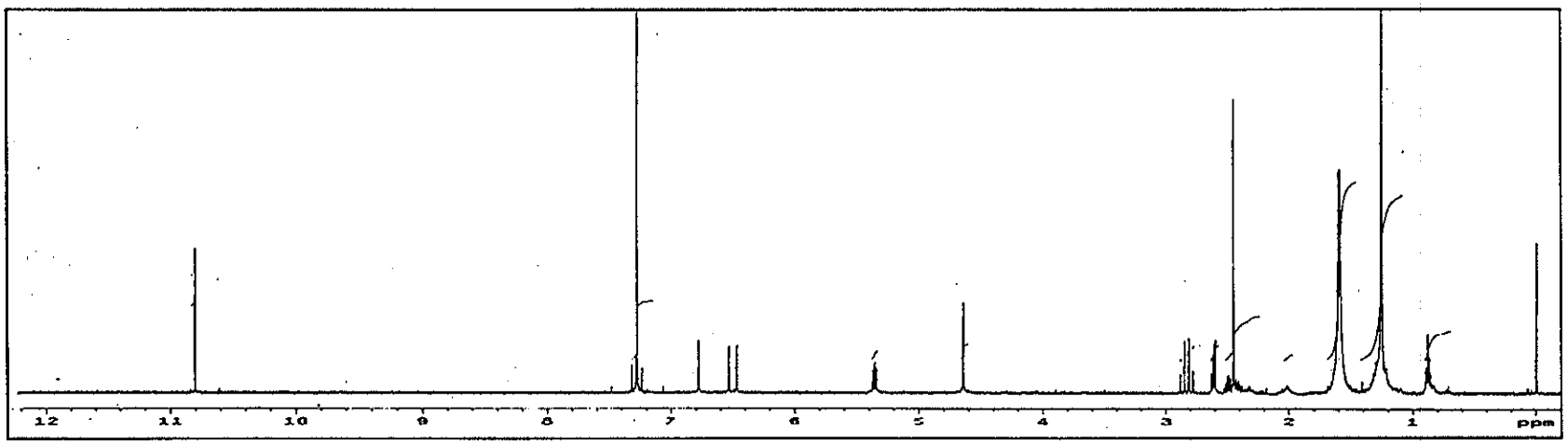

Figure 35 ^{1}H NMR (500 MHz) ($CDCl_3$) spectrum of compound **N10**

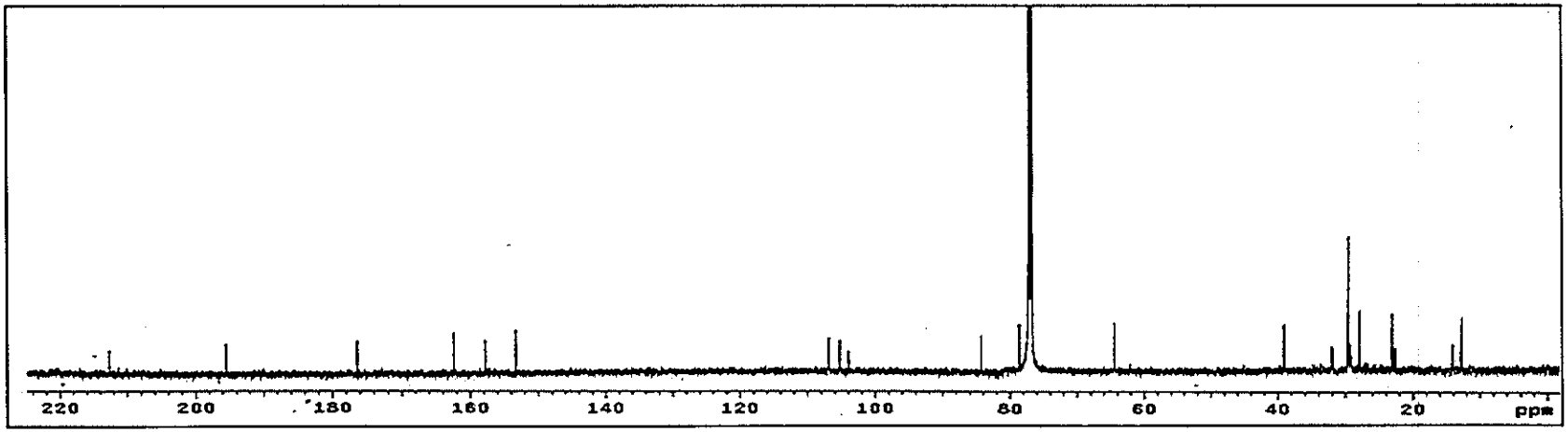

Figure 36 ^{13}C NMR (125 MHz) ($CDCl_3$) spectrum of compound **N10**

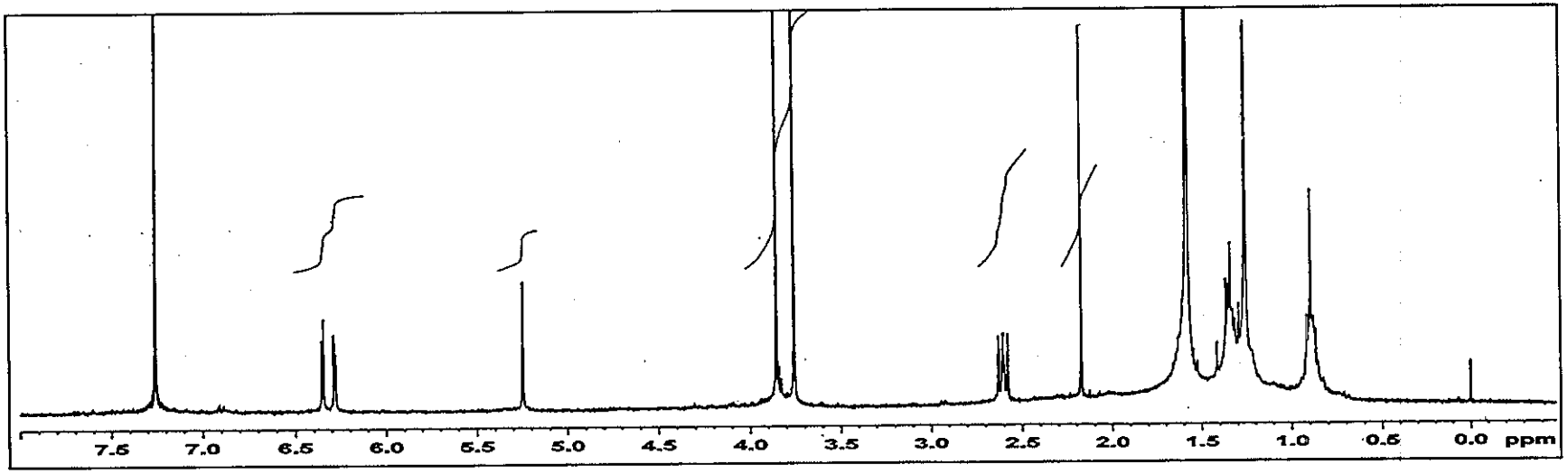

Figure 37 ^{1}H NMR (300 MHz) ($CDCl_3$) spectrum of compound **N14**

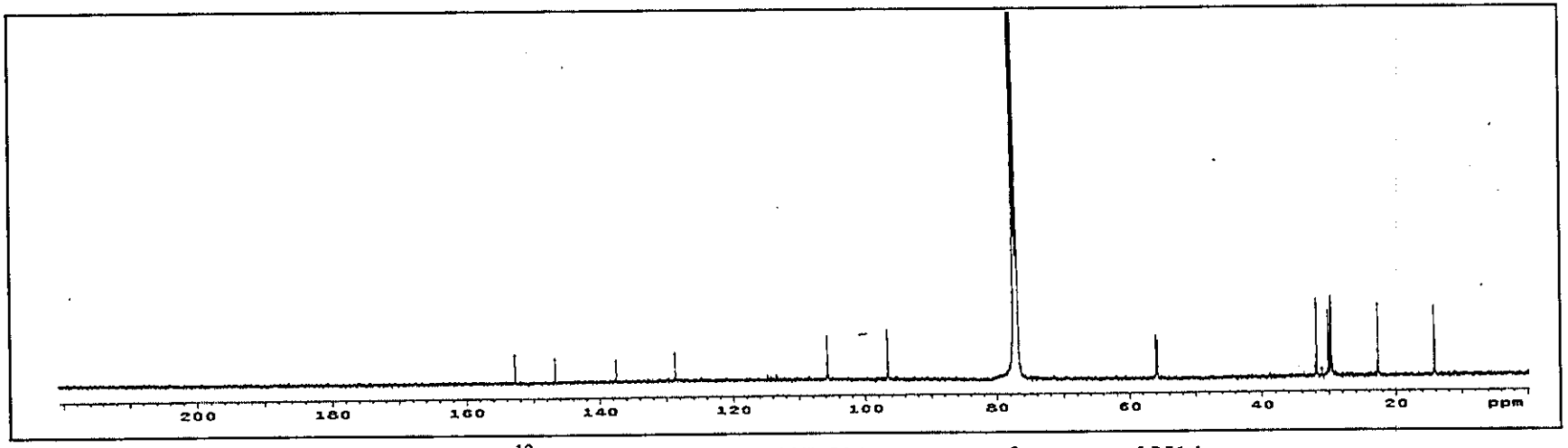

Figure 38 ^{13}C NMR (125 MHz) ($CDCl_3$) spectrum of compound **N14**

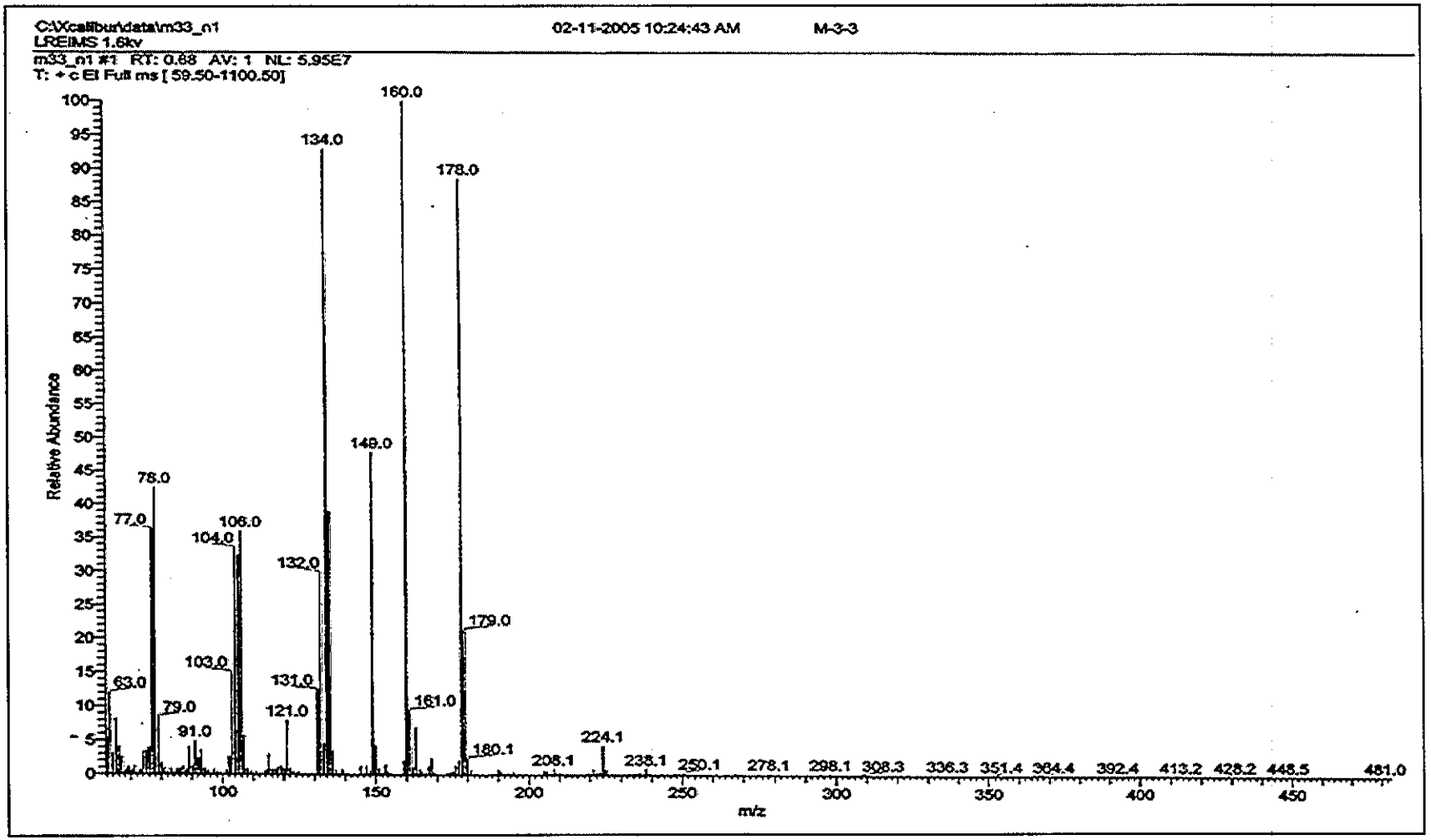

Figure 39 Mass spectrum of compound **N15**

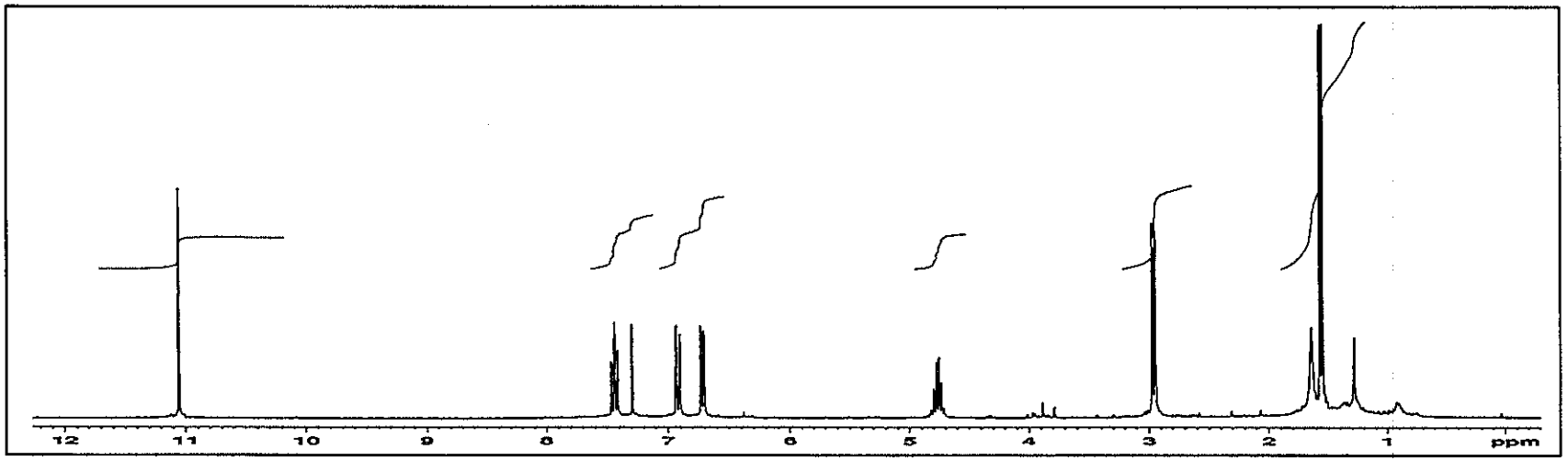

Figure 40 ^{1}H NMR (300 MHz) ($CDCl_3$) spectrum of compound **N15**

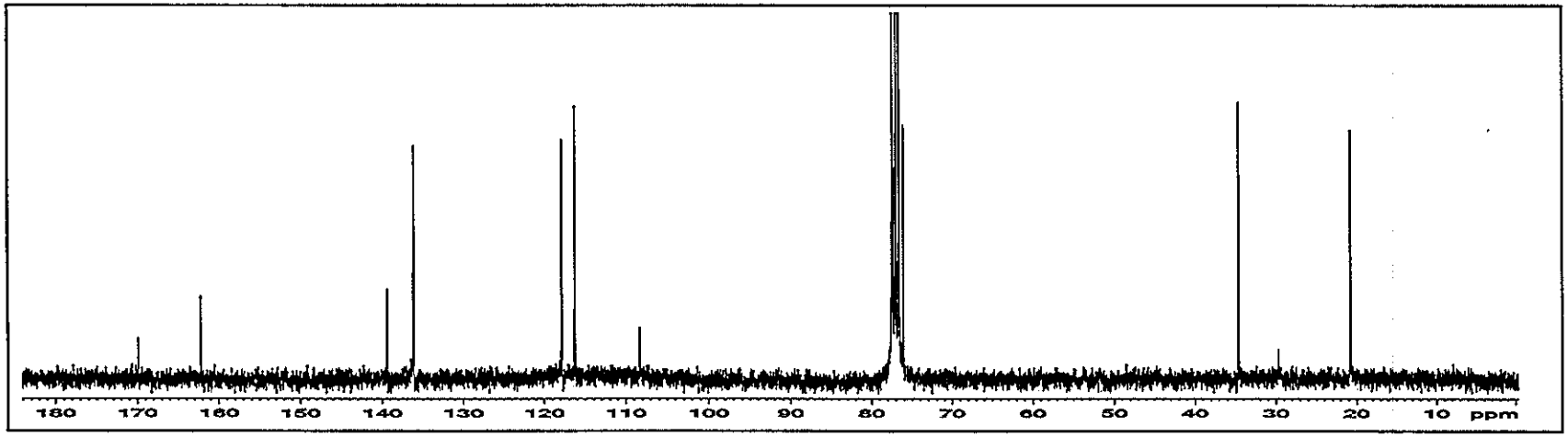

Figure 41 ^{13}C NMR (75 MHz) ($CDCl_3$) spectrum of compound **N15**

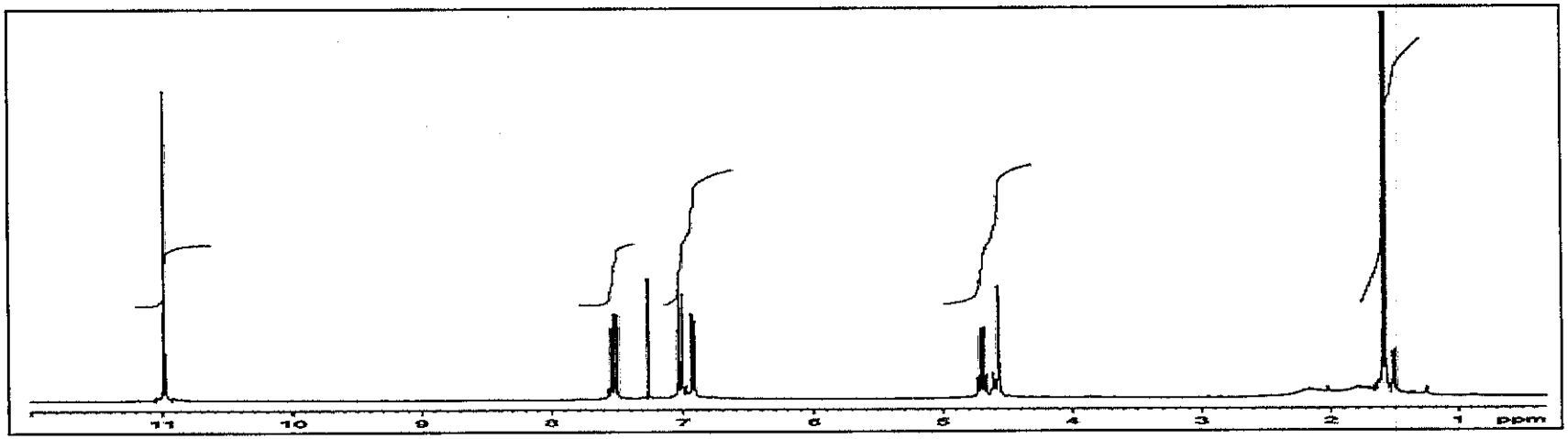

Figure 42 ^{1}H NMR (300 MHz) ($CDCl_3$) spectrum of compound **N17**

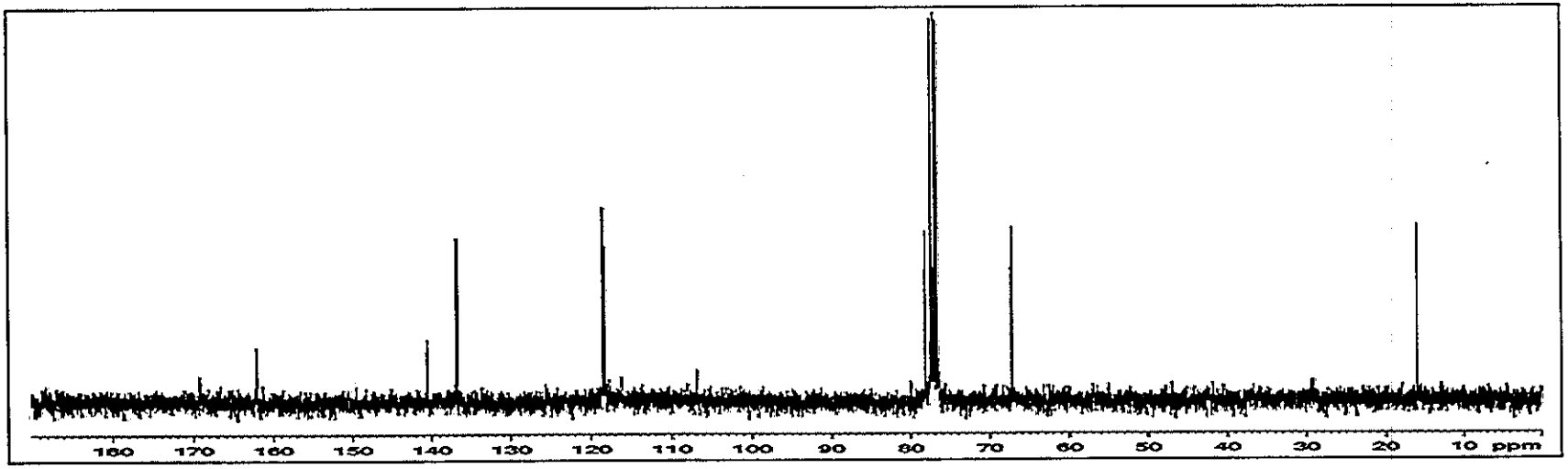

Figure 43 ^{13}C NMR (75 MHz) ($CDCl_3$) spectrum of compound **N17**

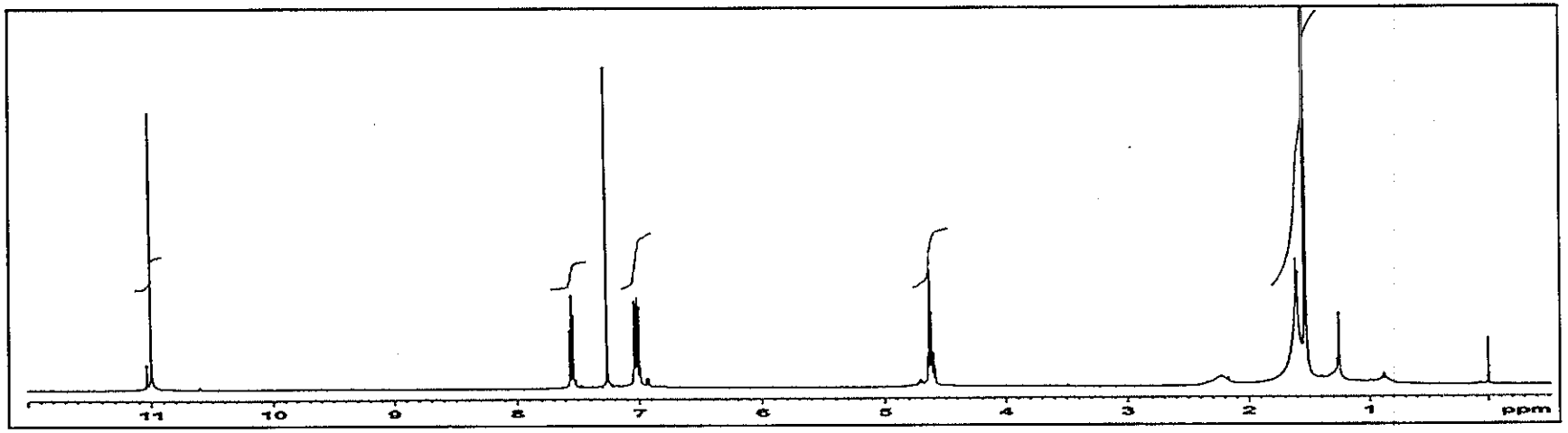

Figure 44 ^{1}H NMR (500 MHz) ($CDCl_3$) spectrum of compound **N18**

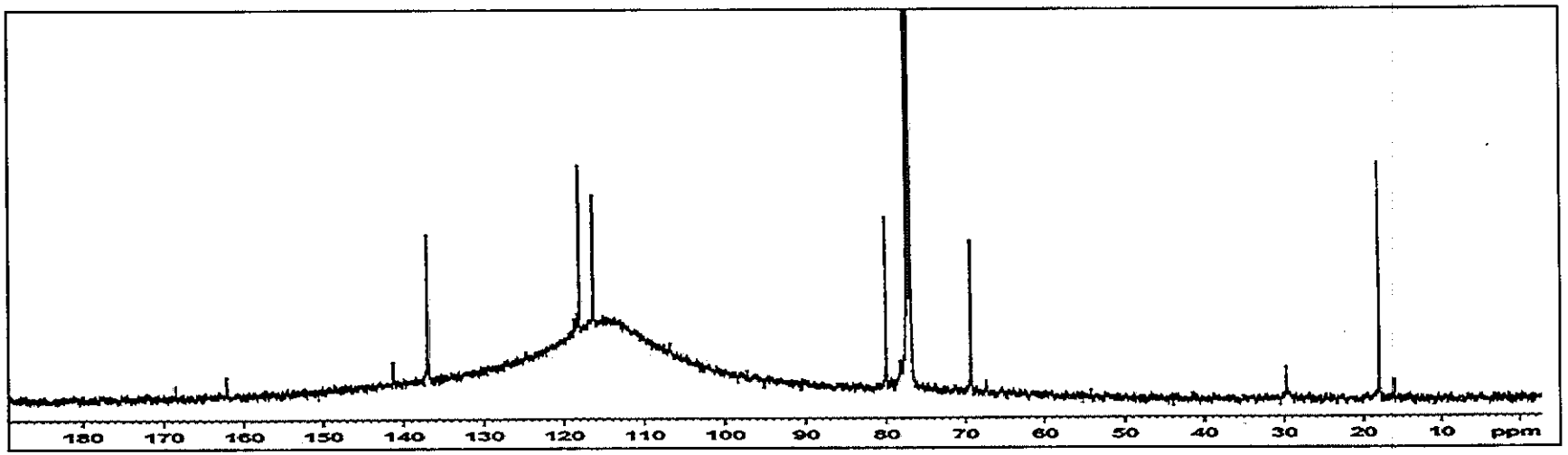

Figure 45 ^{13}C NMR (125 MHz) ($CDCl_3$) spectrum of compound **N18**

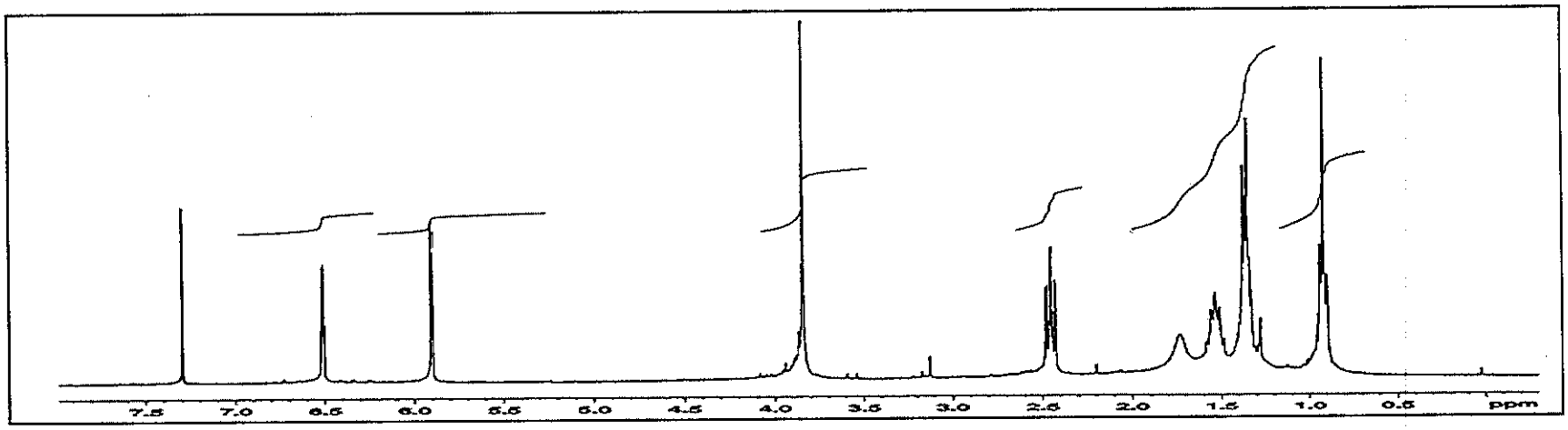

Figure 46 ^{1}H NMR (300 MHz) ($CDCl_3$) spectrum of compound **N16**

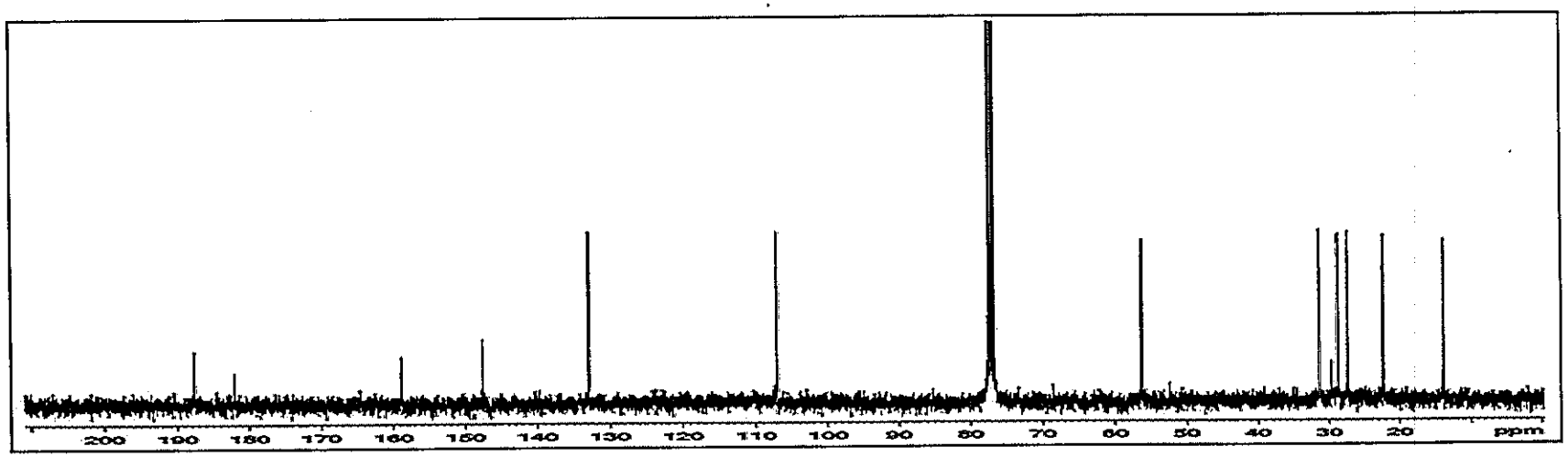

Figure 47 ^{13}C NMR (75 MHz) ($CDCl_3$) spectrum of compound **N16**

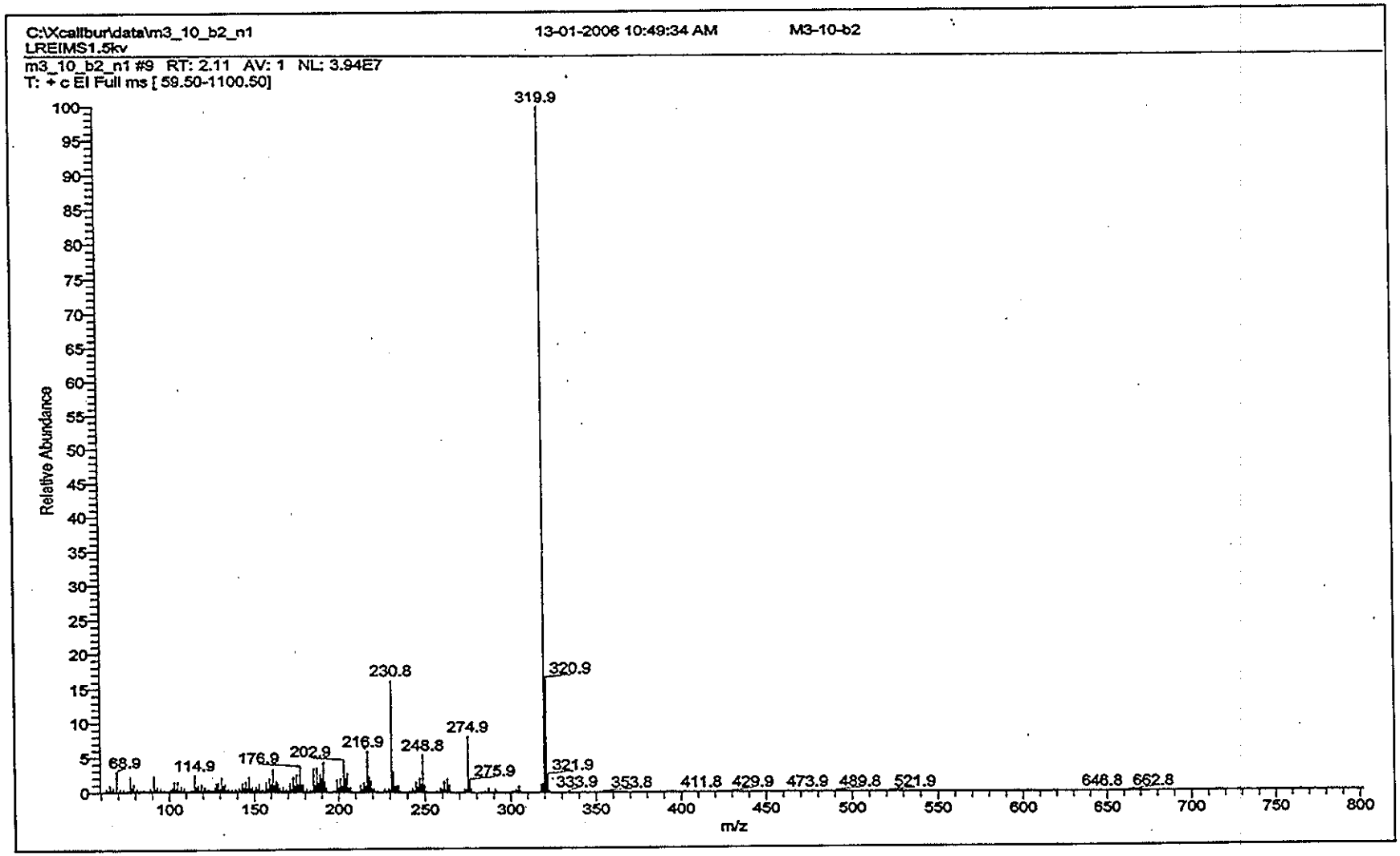

Figure 48 Mass spectrum of compound **N19**

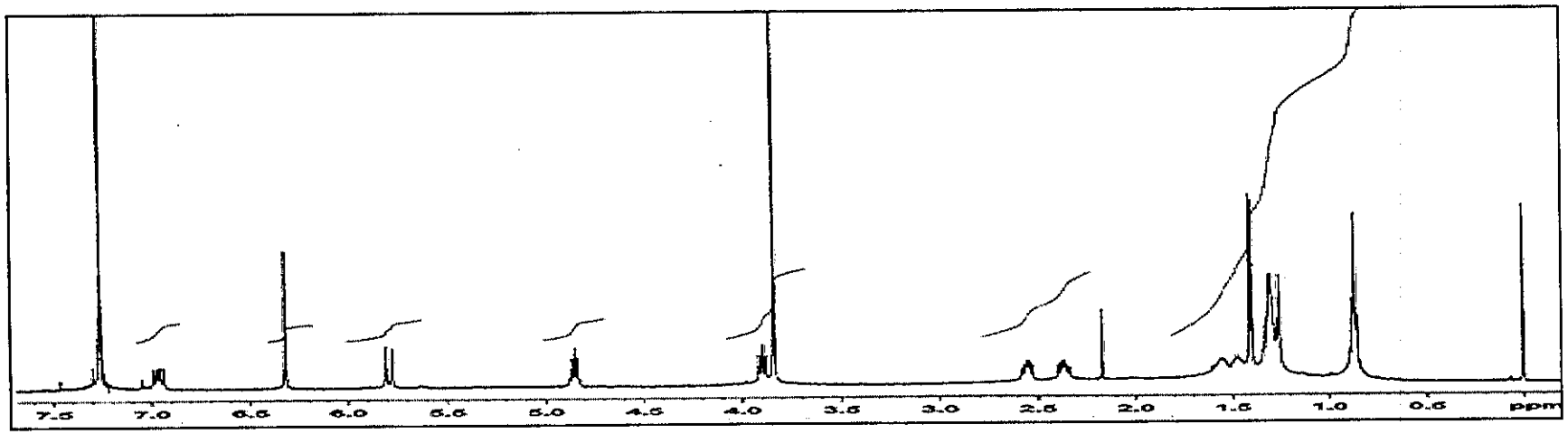

Figure 49 ^{1}H NMR (500 MHz) ($CDCl_3$) spectrum of compound **N19**

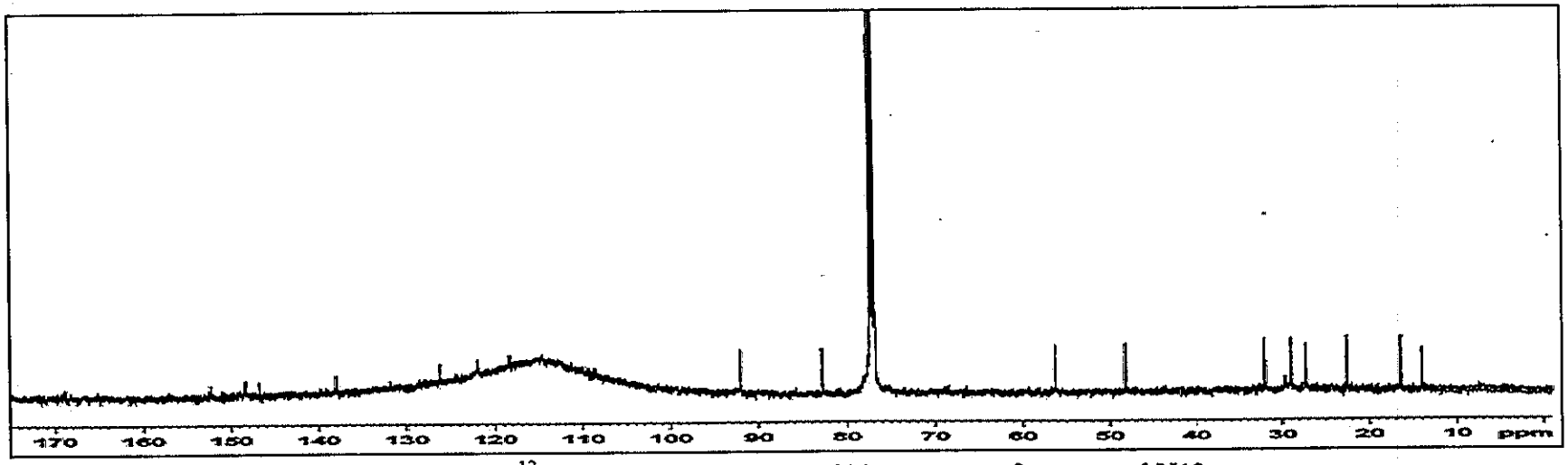

Figure 50 ^{13}C NMR (125 MHz) ($CDCl_3$) spectrum of compound **N19**

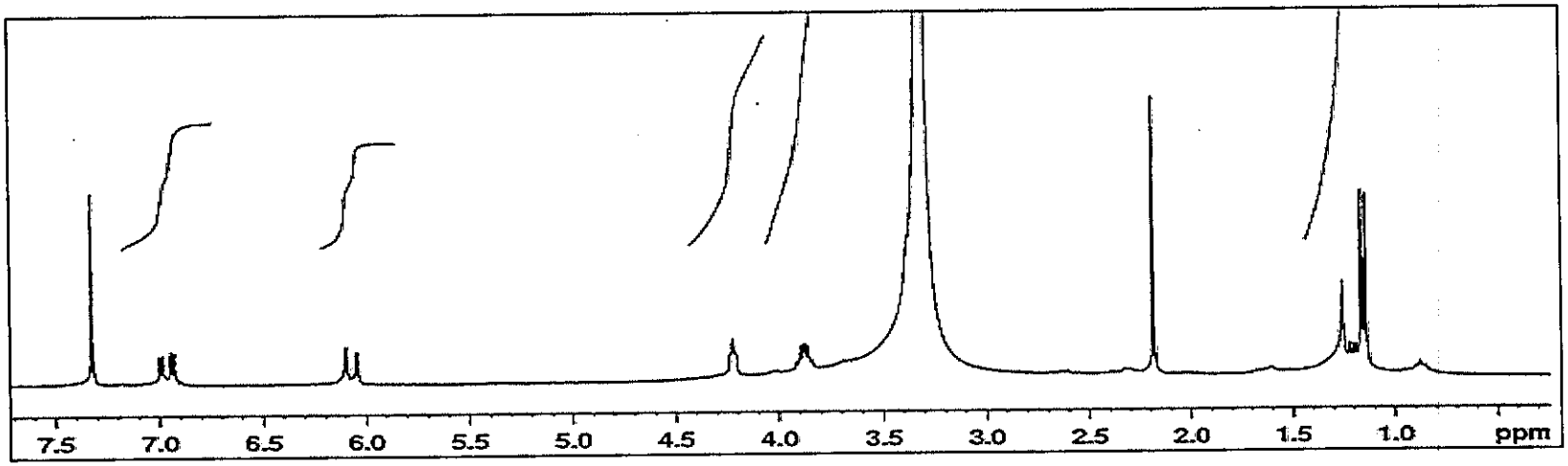

Figure 51 ^{1}H NMR (300 MHz) ($CDCl_3$+CD_3OD) spectrum of compound **N20**

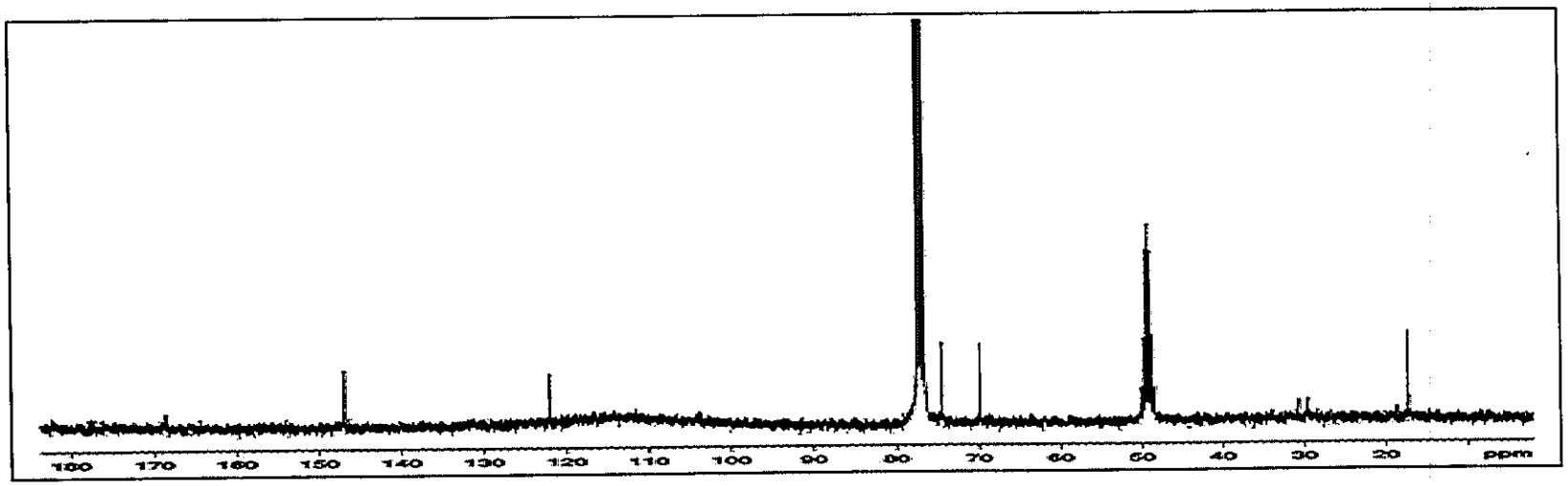

Figure 52 ^{13}C NMR (125 MHz) ($CDCl_3$+ CD_3OD) spectrum of compound **N20**

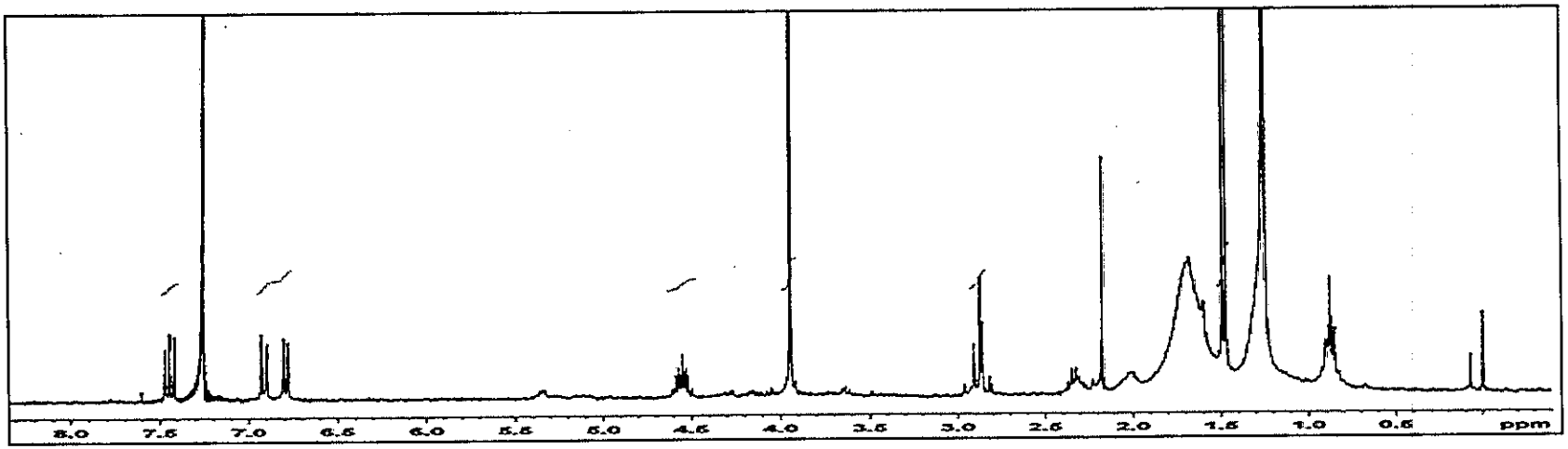

Figure 53 ^{1}H NMR (300 MHz) ($CDCl_3$) spectrum of compound **N21**

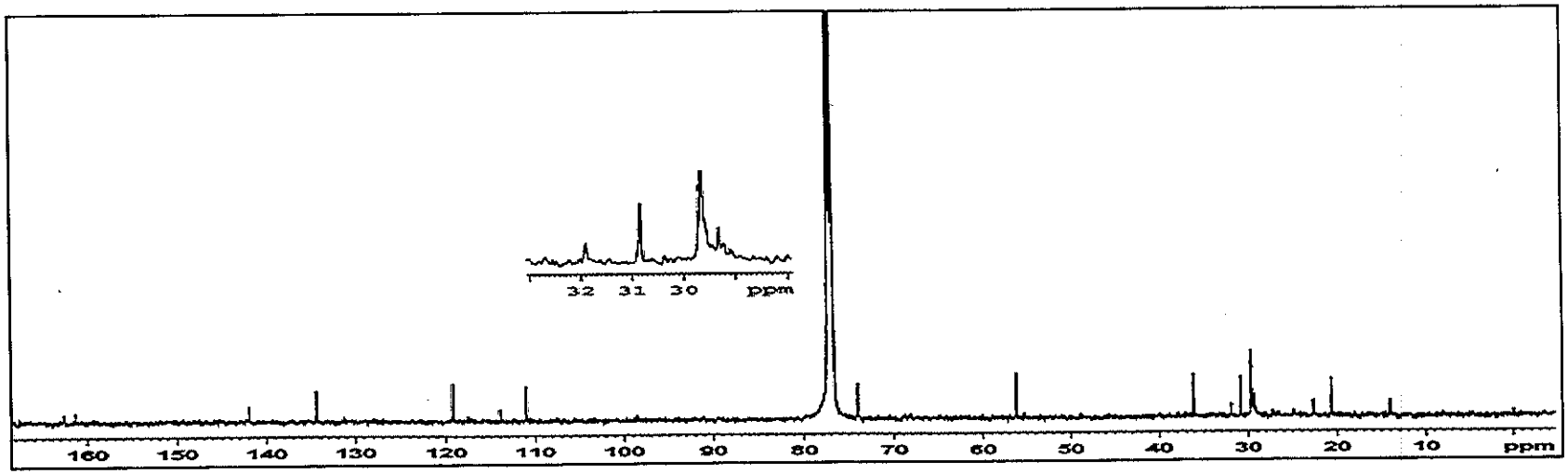

Figure 54 ^{13}C NMR (75 MHz) ($CDCl_3$) spectrum of compound **N21**

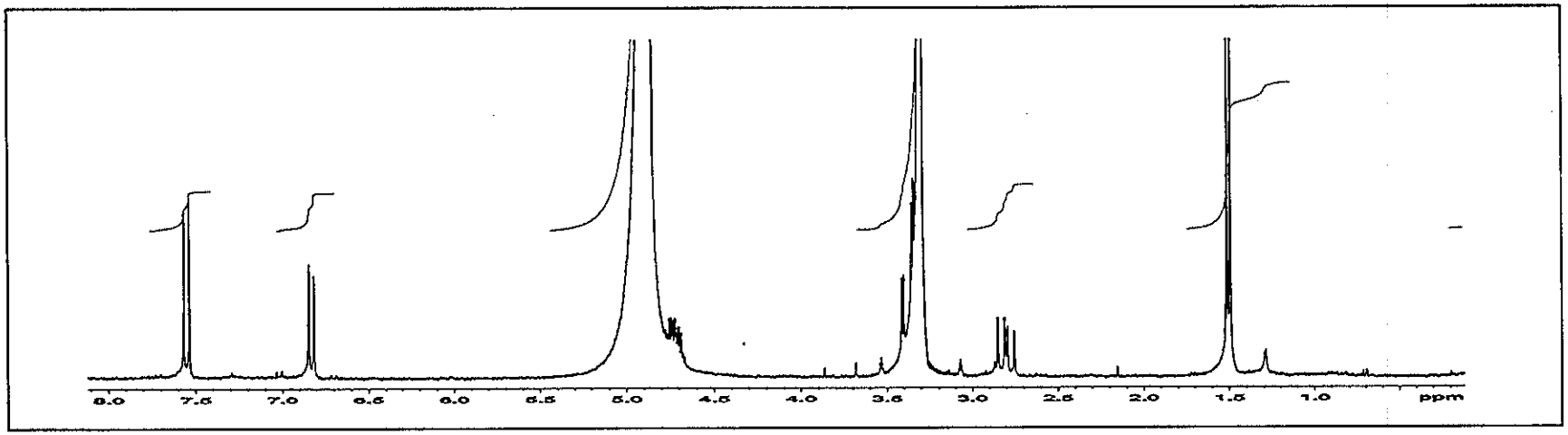

Figure 55 ^{1}H NMR (300 MHz) (CD_3OD) spectrum of compound **N32**

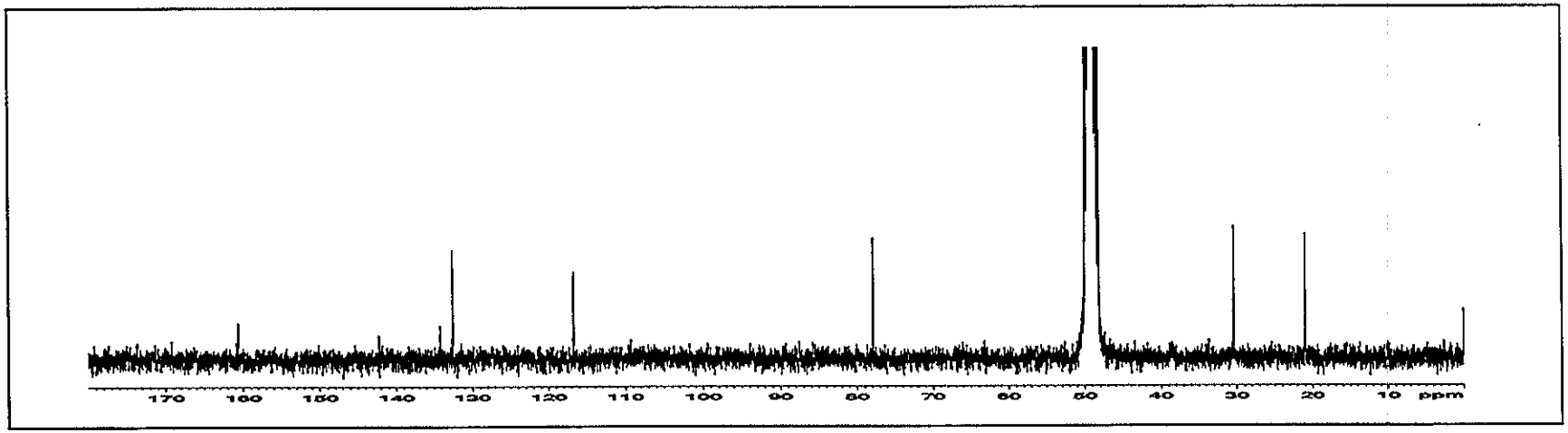

Figure 56 ^{13}C NMR (75 MHz) (CD_3OD) spectrum of compound **N32**

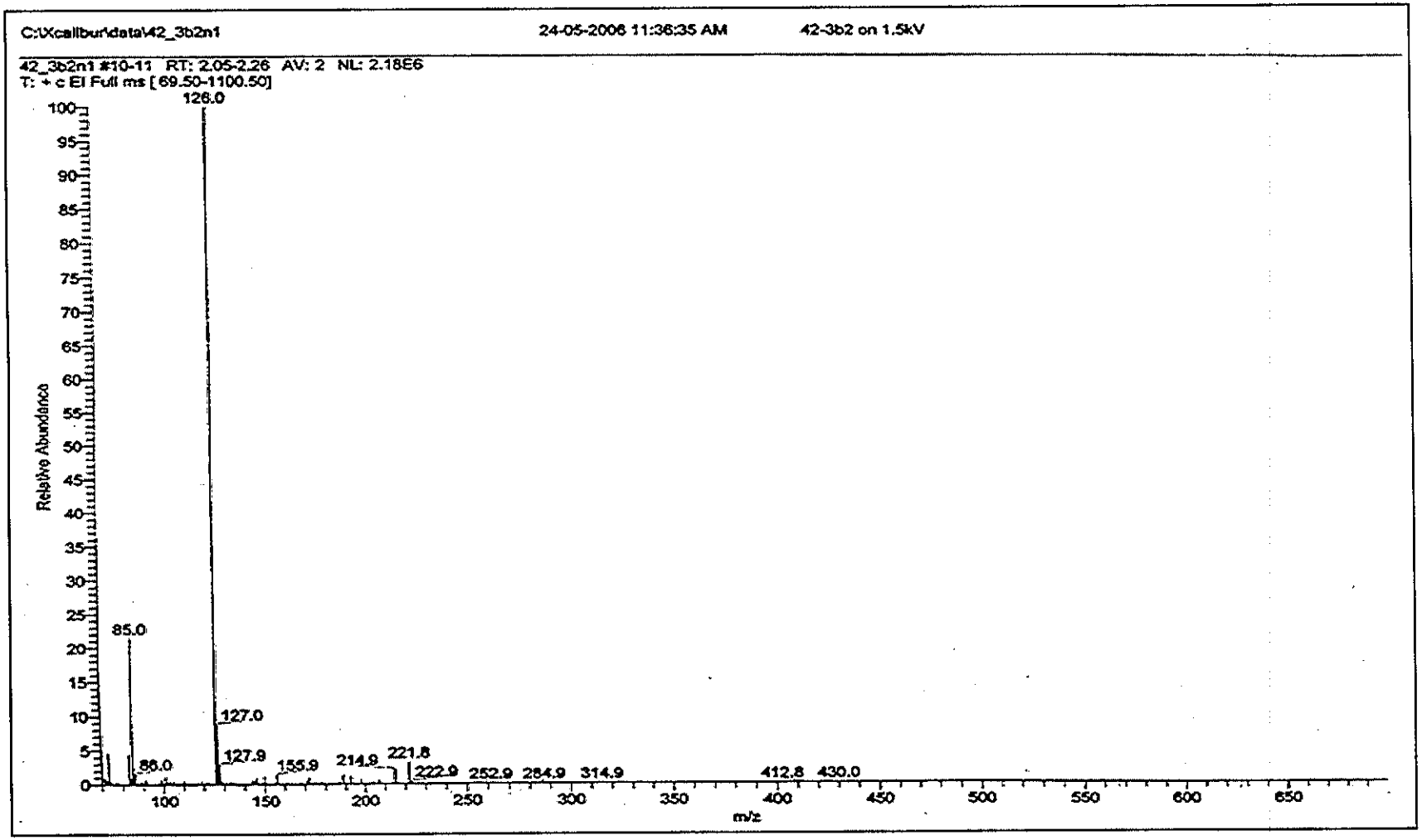

Figure 57 Mass spectrum of compound N31

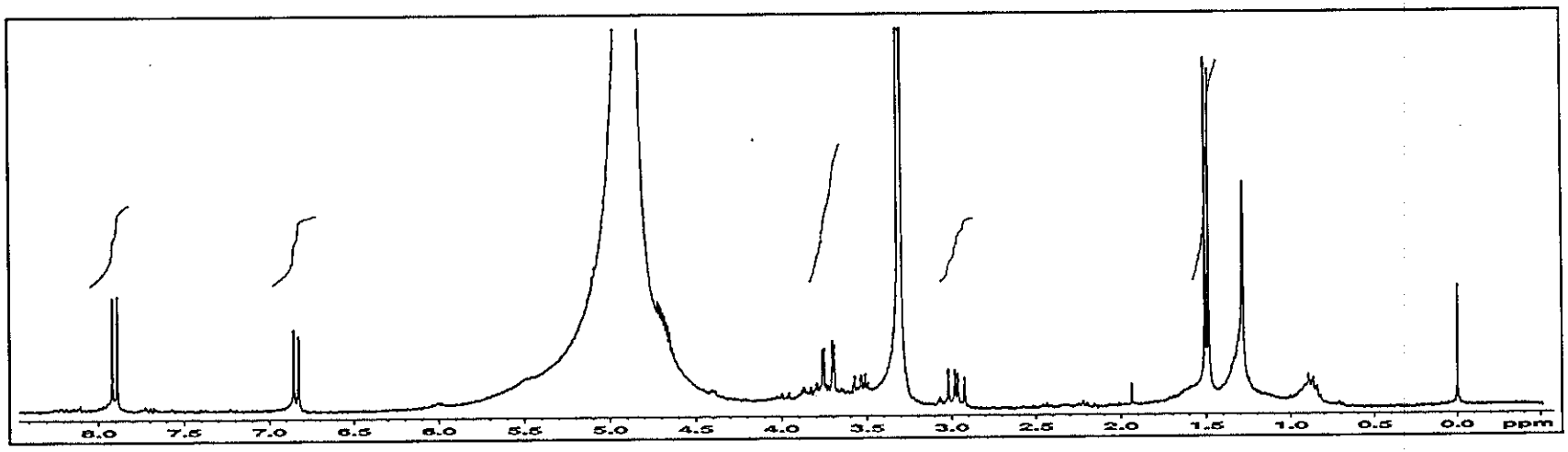

Figure 58 ^{1}H NMR (300 MHz) (CD_3OD) spectrum of compound **N31**

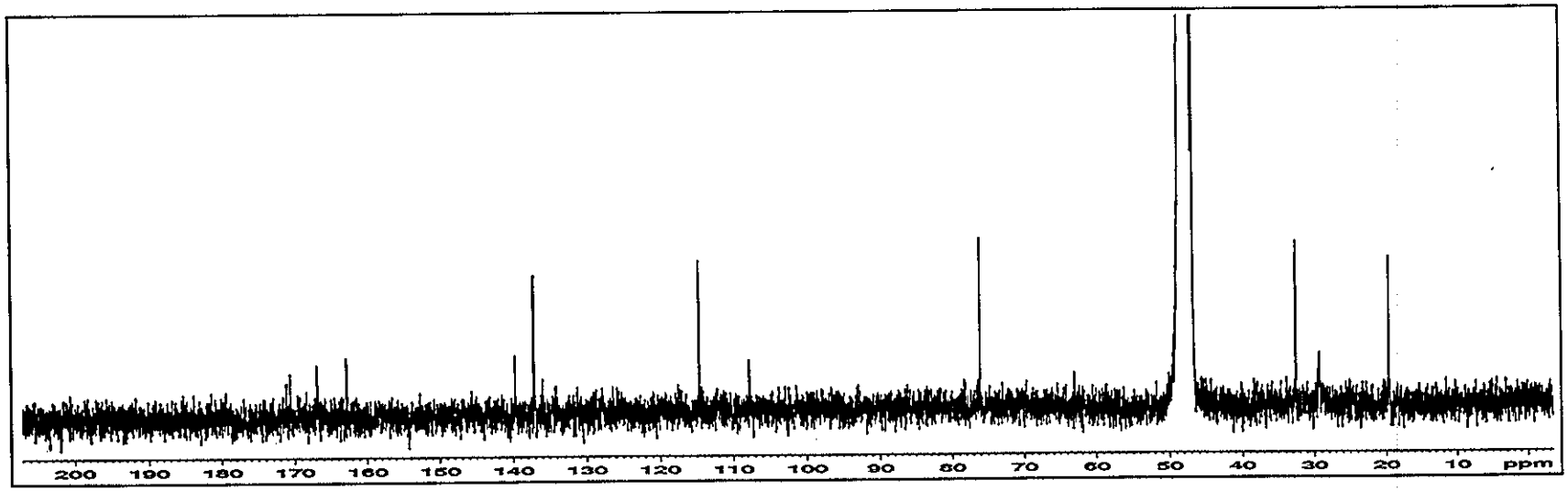

Figure 59 ^{13}C NMR (75 MHz) (CD_3OD) spectrum of compound **N31**

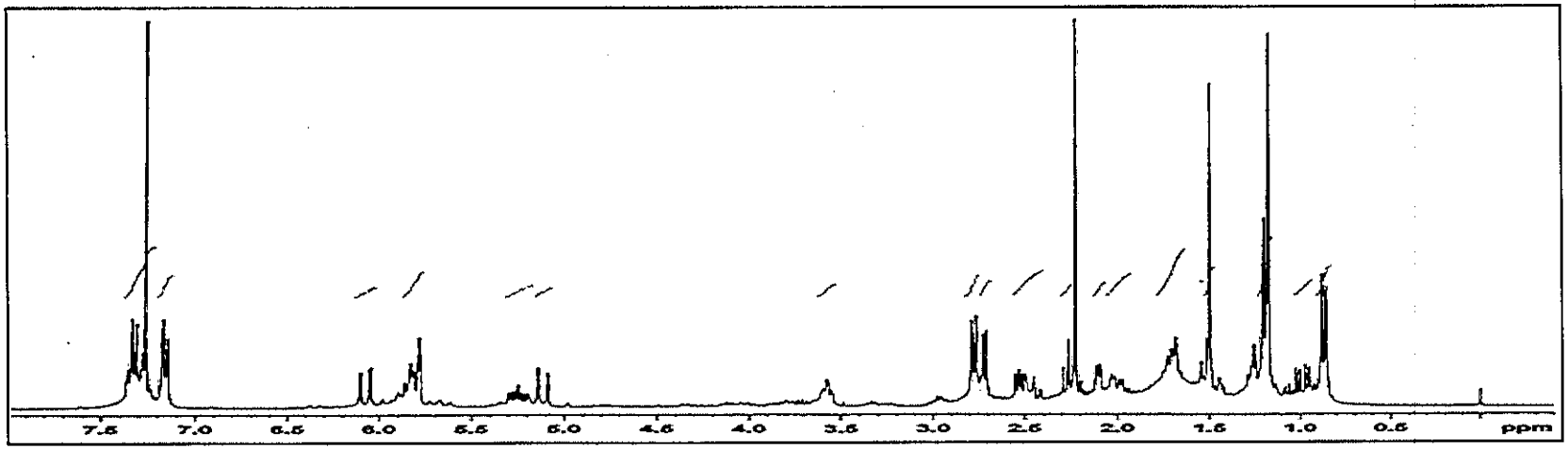

Figure 60 ^{1}H NMR (300 MHz) ($CDCl_3$) spectrum of compound **N23**

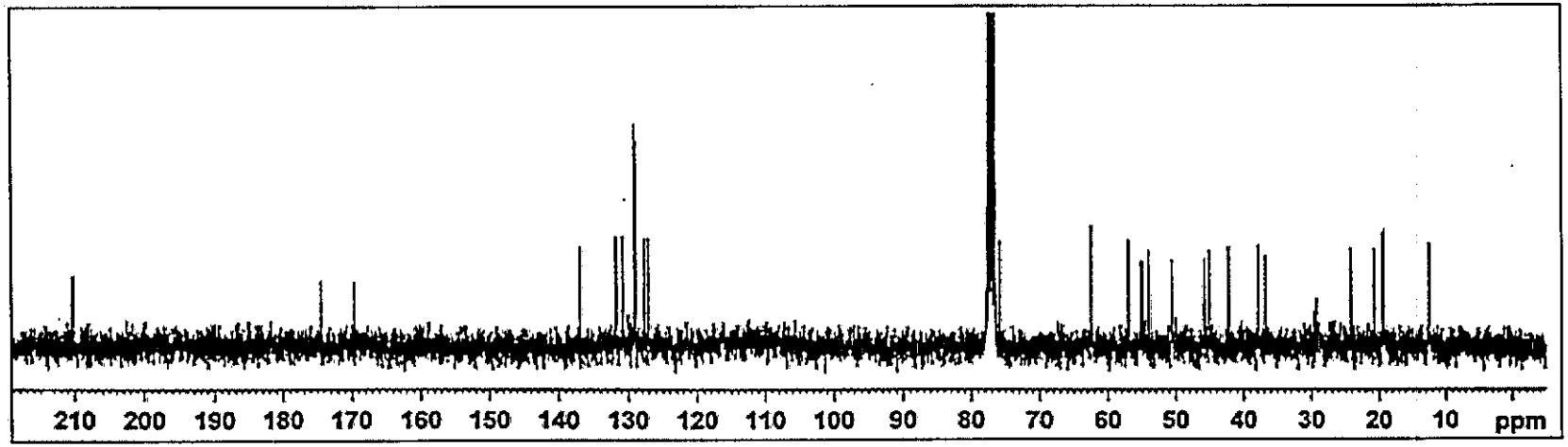

Figure 61 ^{13}C NMR (75 MHz) ($CDCl_3$) spectrum of compound **N23**

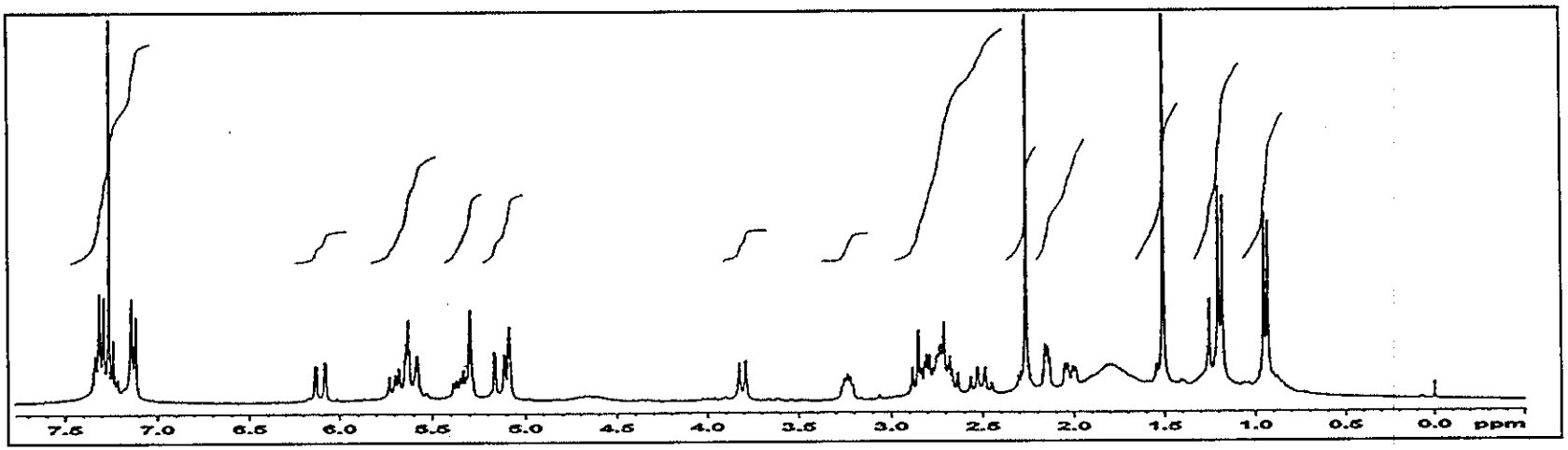

Figure 62 ^{1}H NMR (300 MHz) ($CDCl_3$) spectrum of compound **N22**

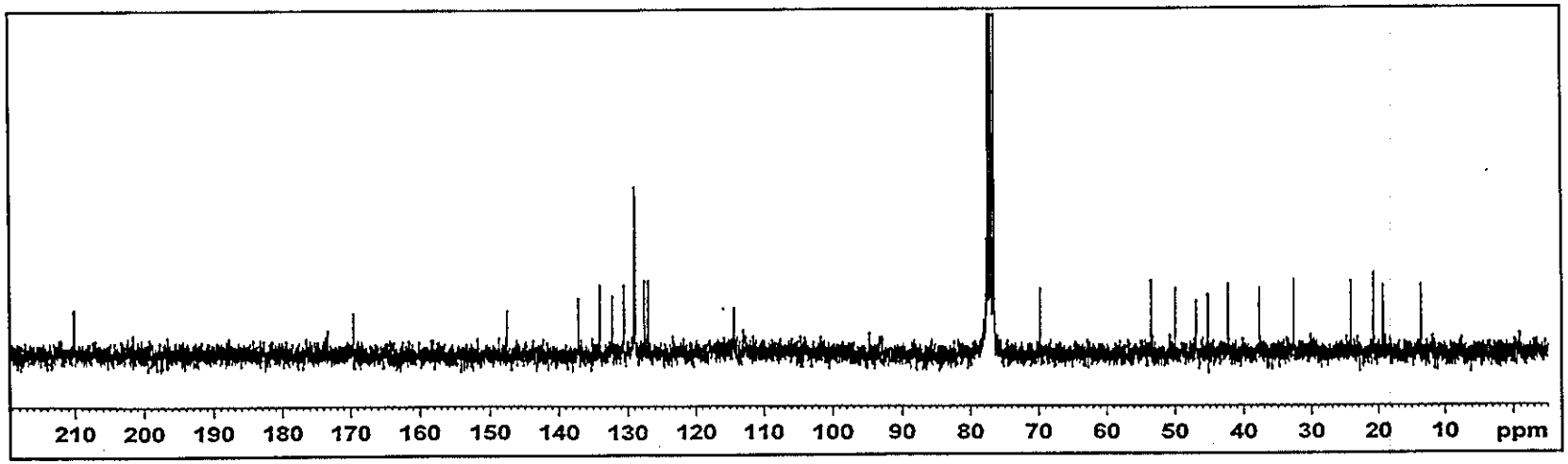

Figure 63 ^{13}C NMR (75 MHz) ($CDCl_3$) spectrum of compound **N22**

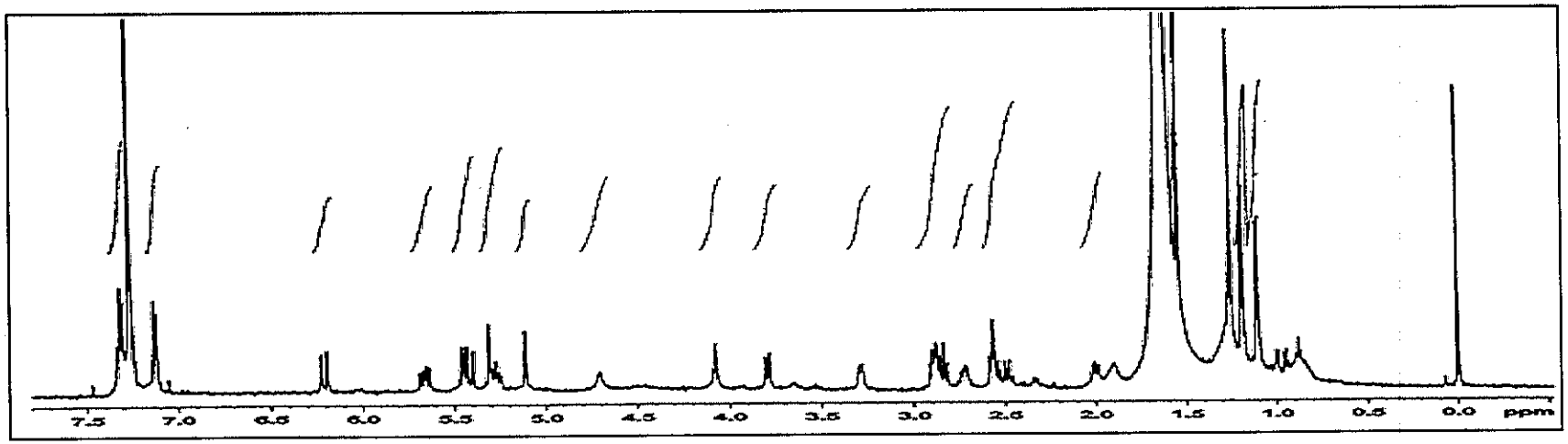

Figure 64 ^{1}H NMR (500 MHz) ($CDCl_3$) spectrum of compound **N24**

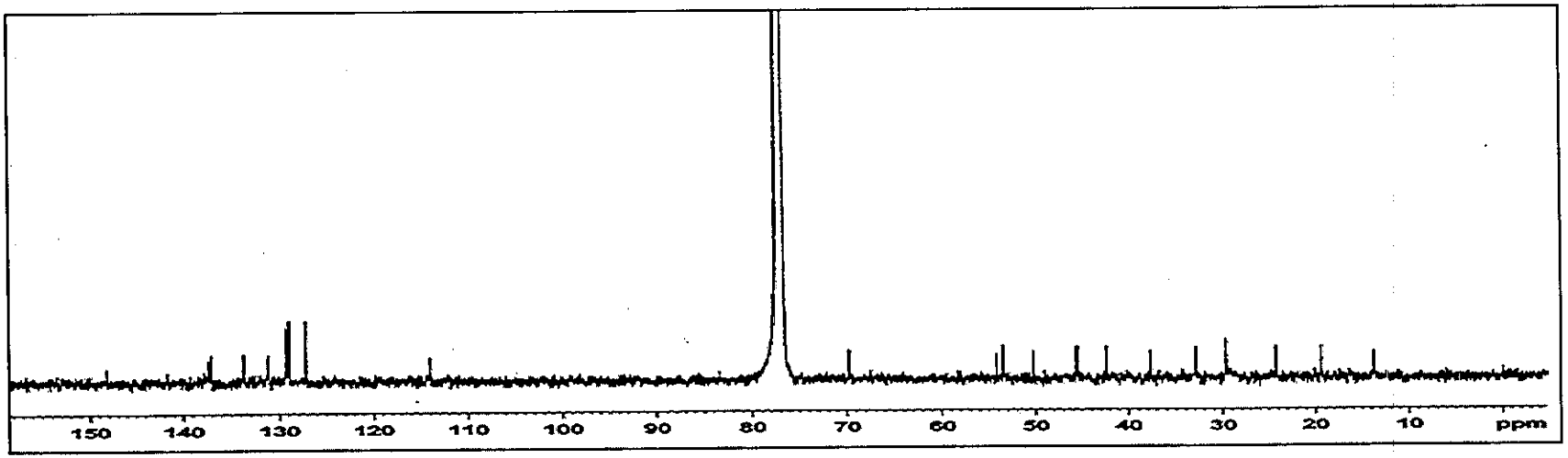

Figure 65 ^{13}C NMR (125 MHz) ($CDCl_3$) spectrum of compound **N24**

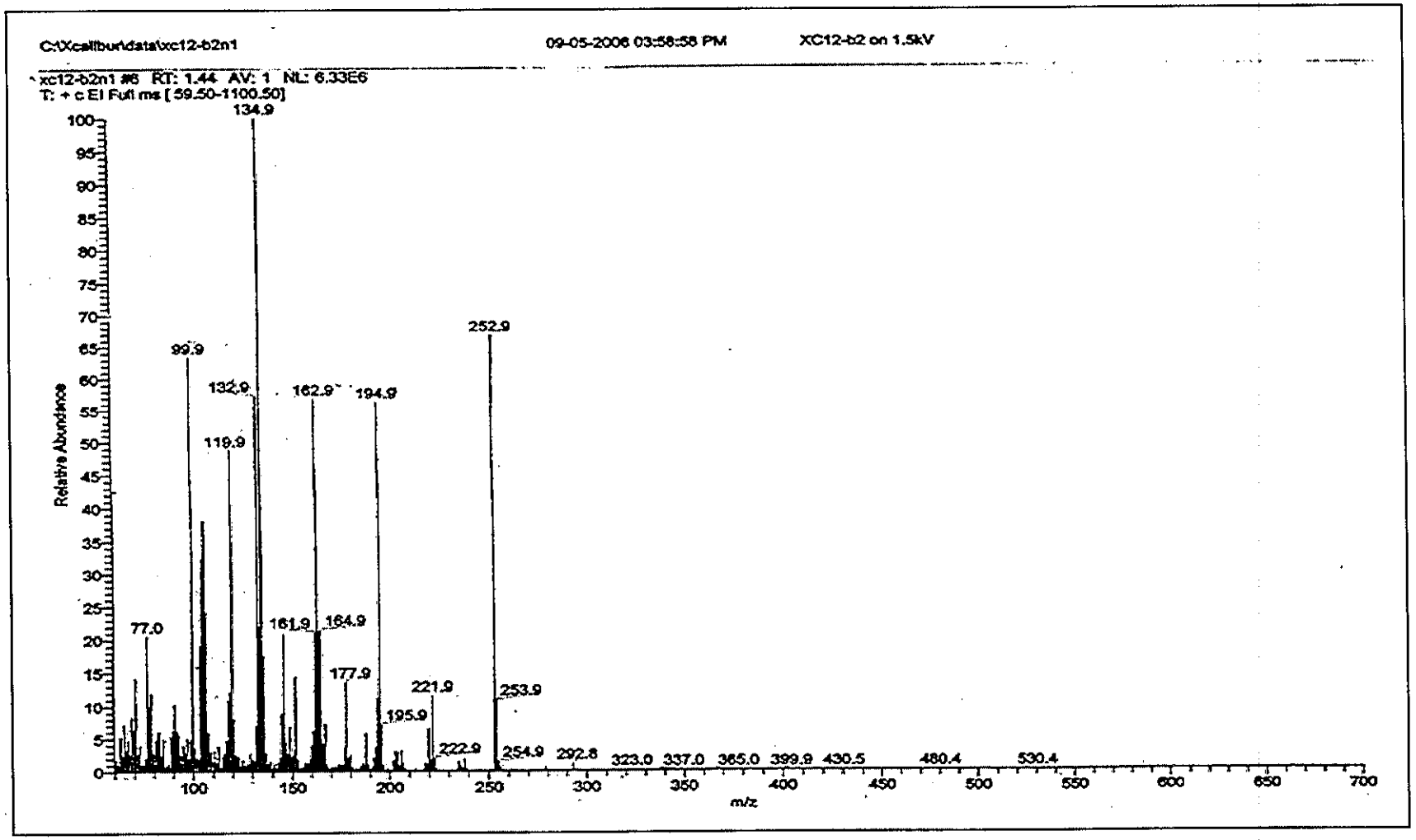

Figure 66 Mass spectrum of compound **N26**

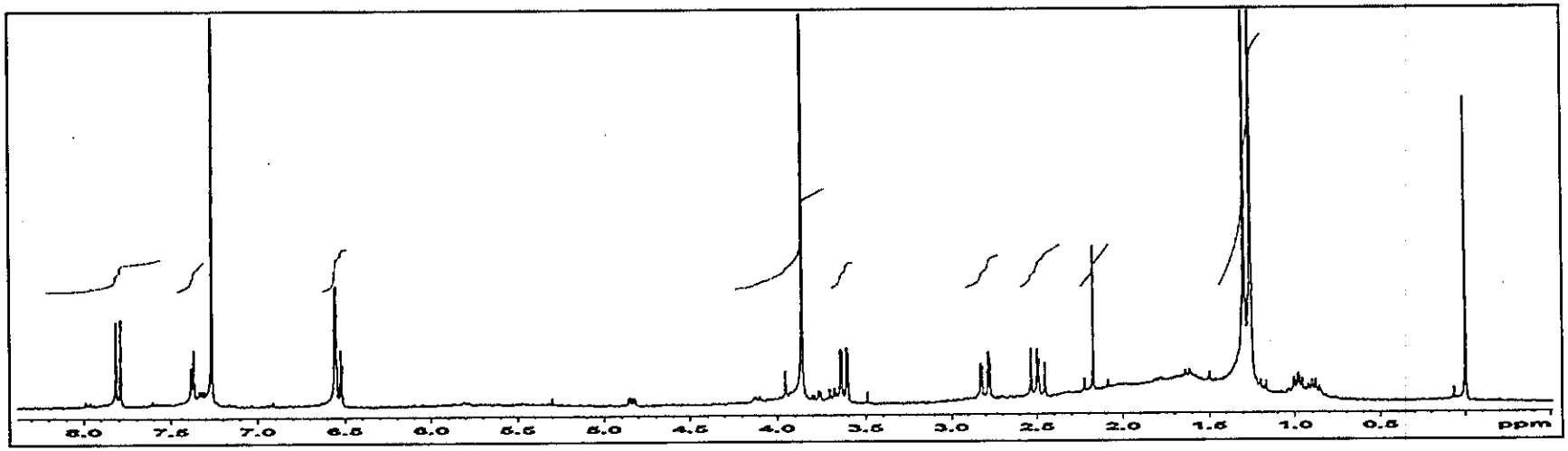

Figure 67 ^{1}H NMR (500 MHz) ($CDCl_3$) spectrum of compound **N26**

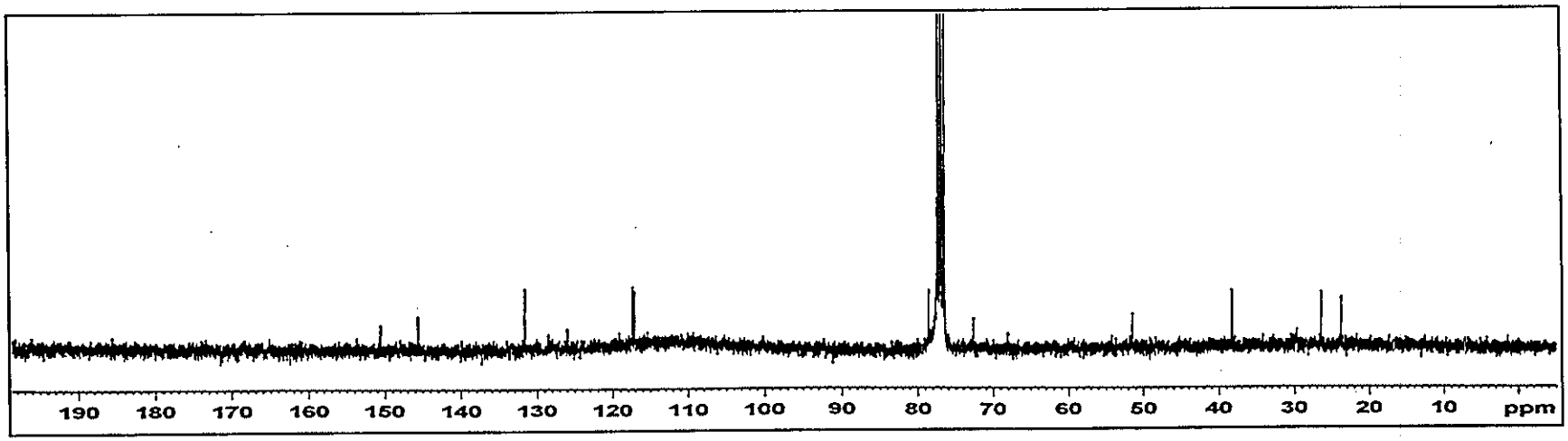

Figure 68 ^{13}C NMR (125 MHz) ($CDCl_3$) spectrum of compound **N26**

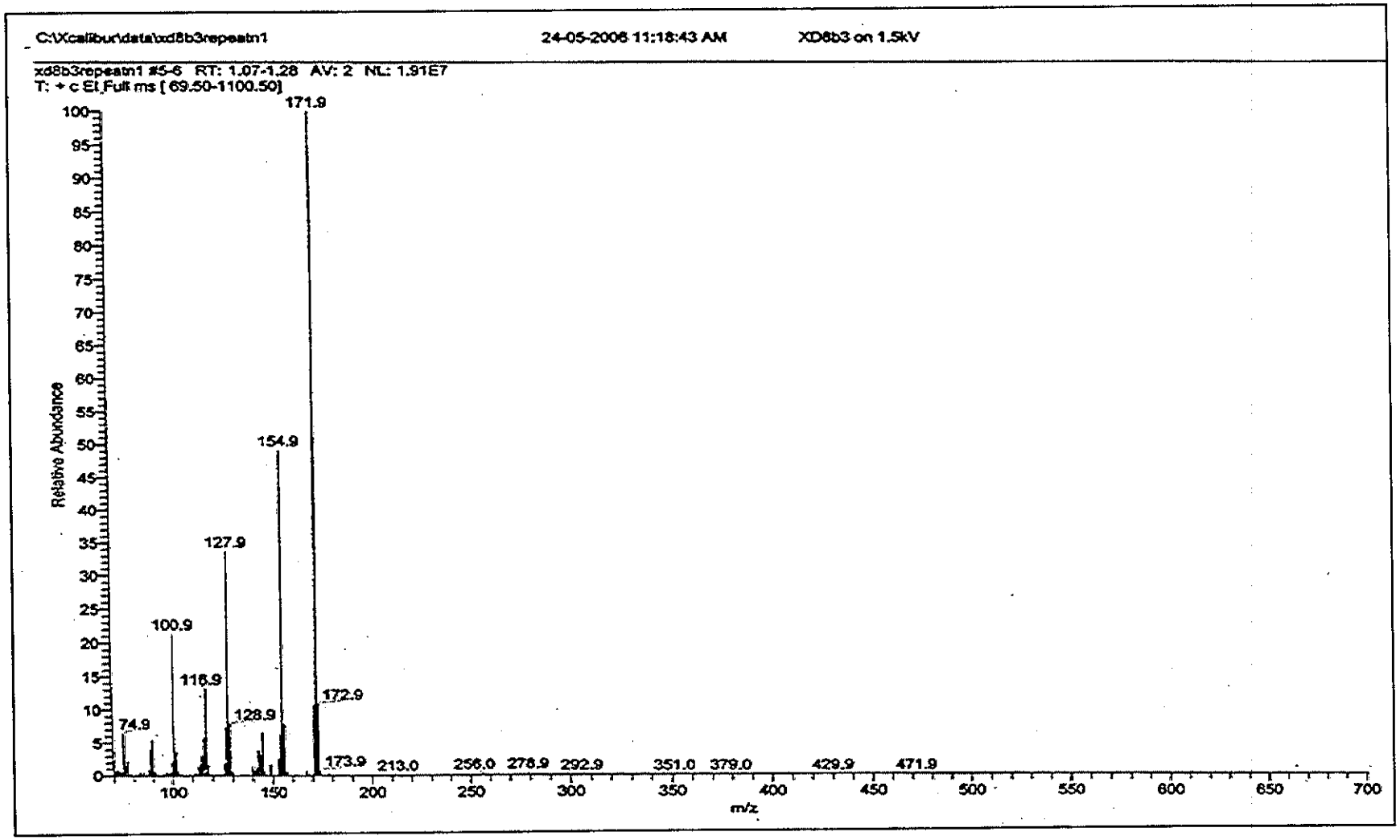

Figure 69 Mass spectrum of compound **N28**

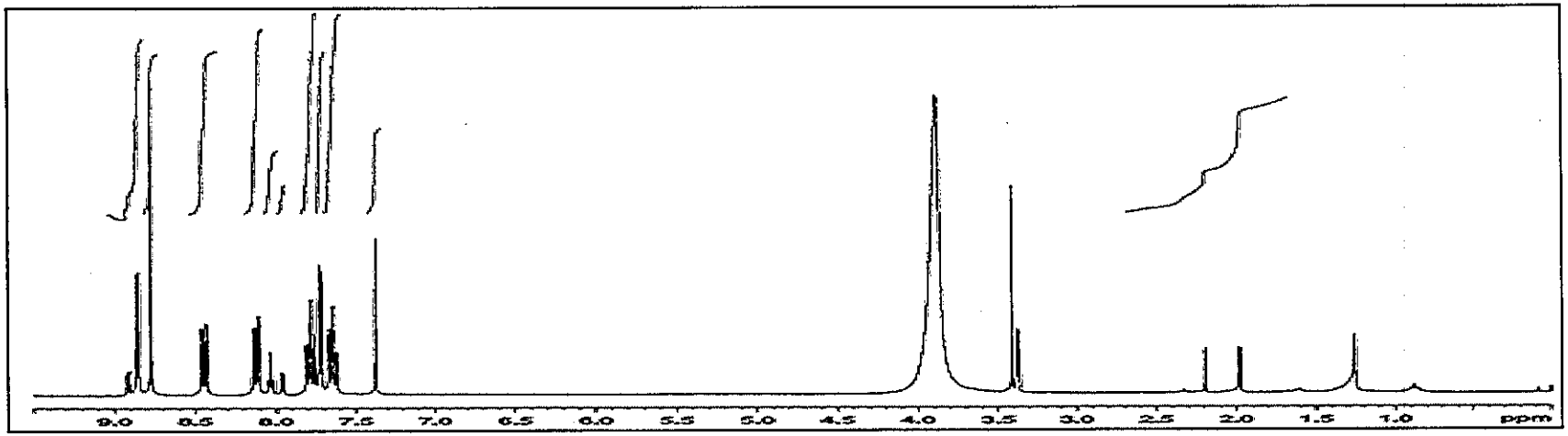

Figure 70 ^{1}H NMR (300 MHz) ($CDCl_3$+CD_3OD) spectrum of compound **N28**

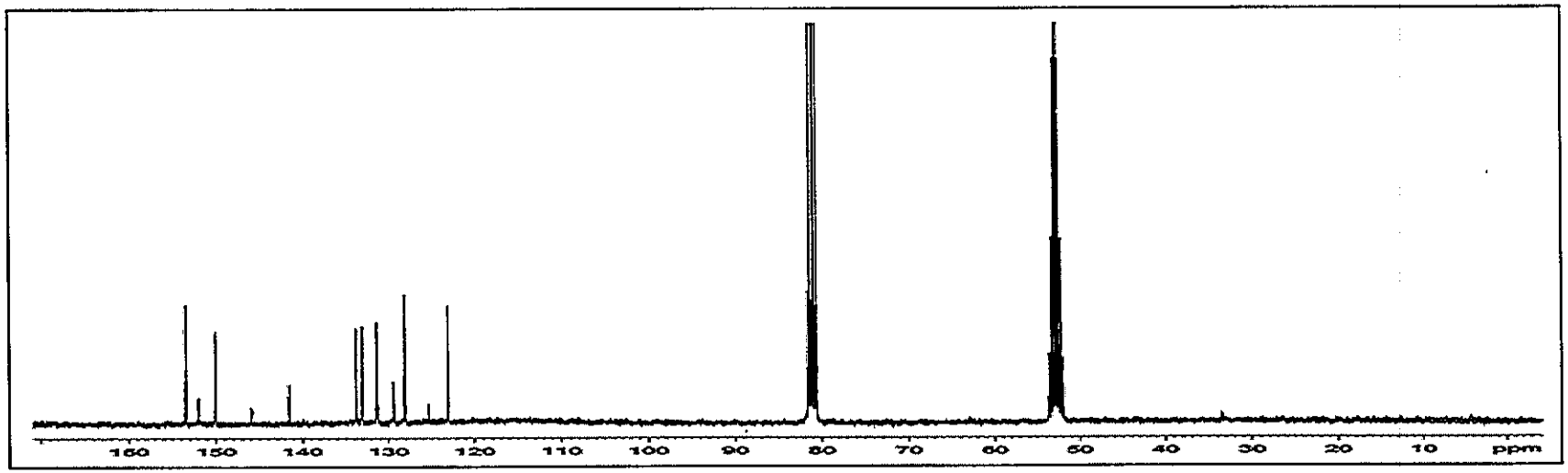

Figure 71 ^{13}C NMR (75 MHz) ($CDCl_3$+CD_3OD) spectrum of compound **N28**

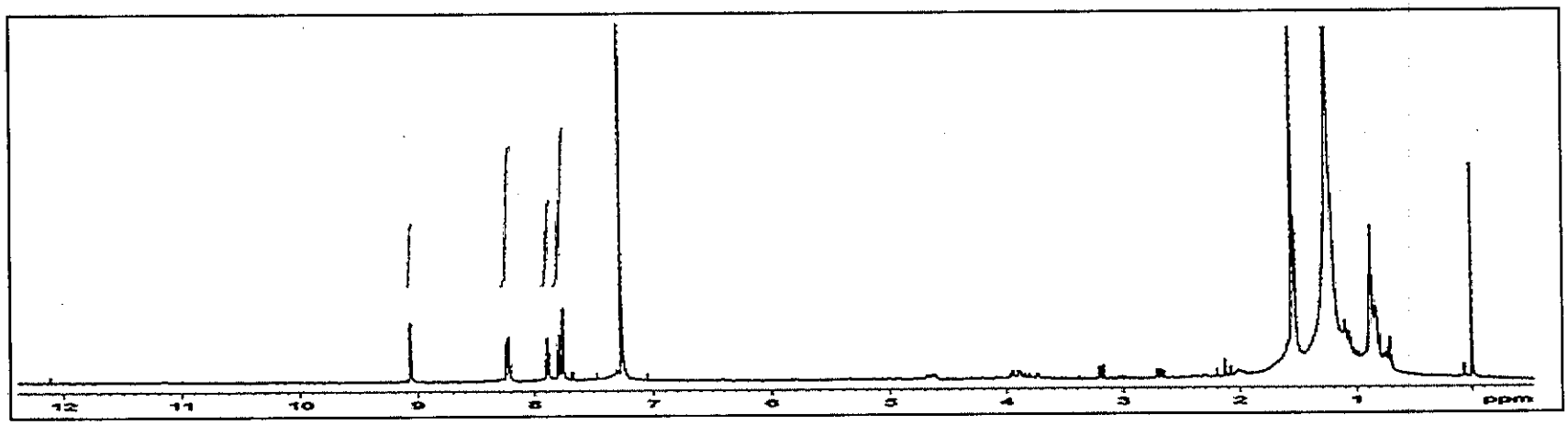

Figure 72 ^{1}H NMR (500 MHz) ($CDCl_3$) spectrum of compound **N25**

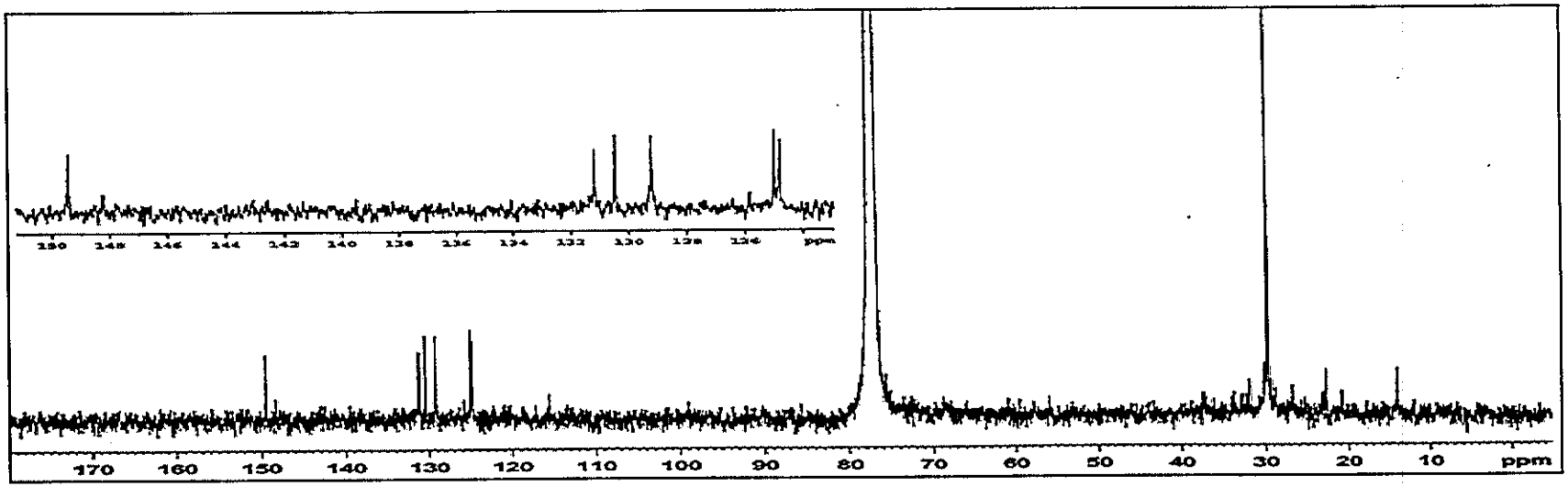

Figure 73 ^{13}C NMR (125 MHz) ($CDCl_3$) spectrum of compound **N25**

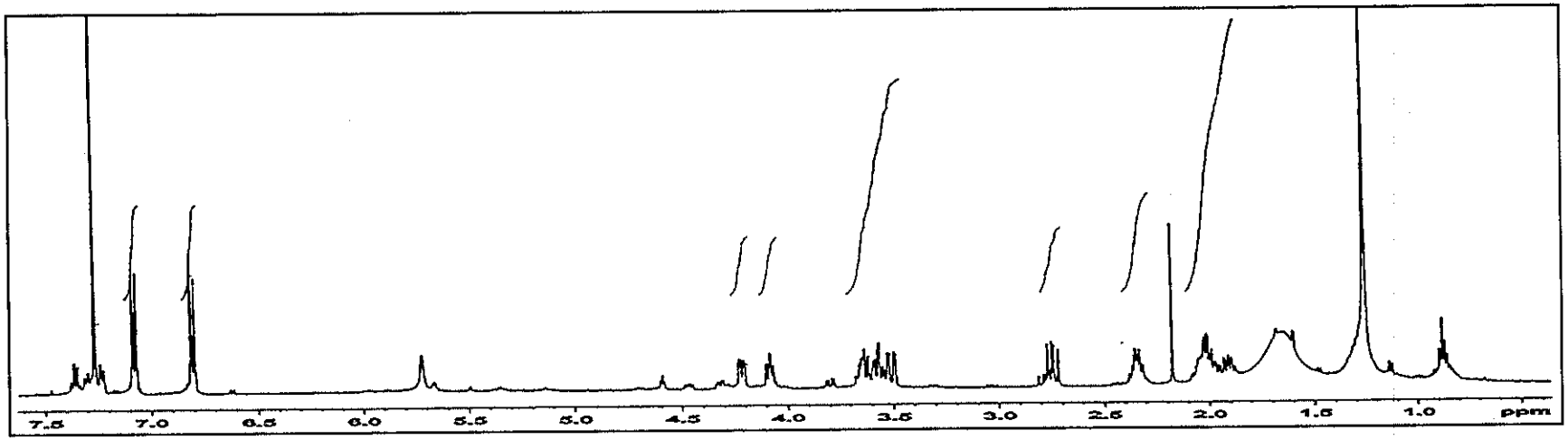

Figure 74 ^{1}H NMR (500 MHz) ($CDCl_3$) spectrum of compound **N27**

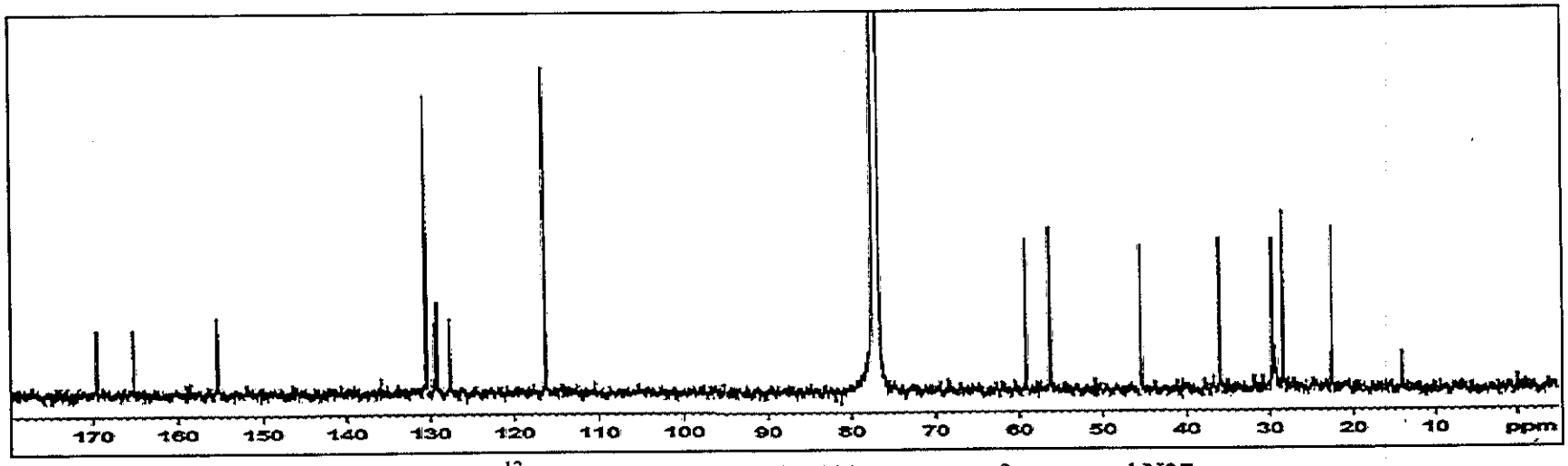

Figure 75 ^{13}C NMR (125 MHz) ($CDCl_3$) spectrum of compound **N27**

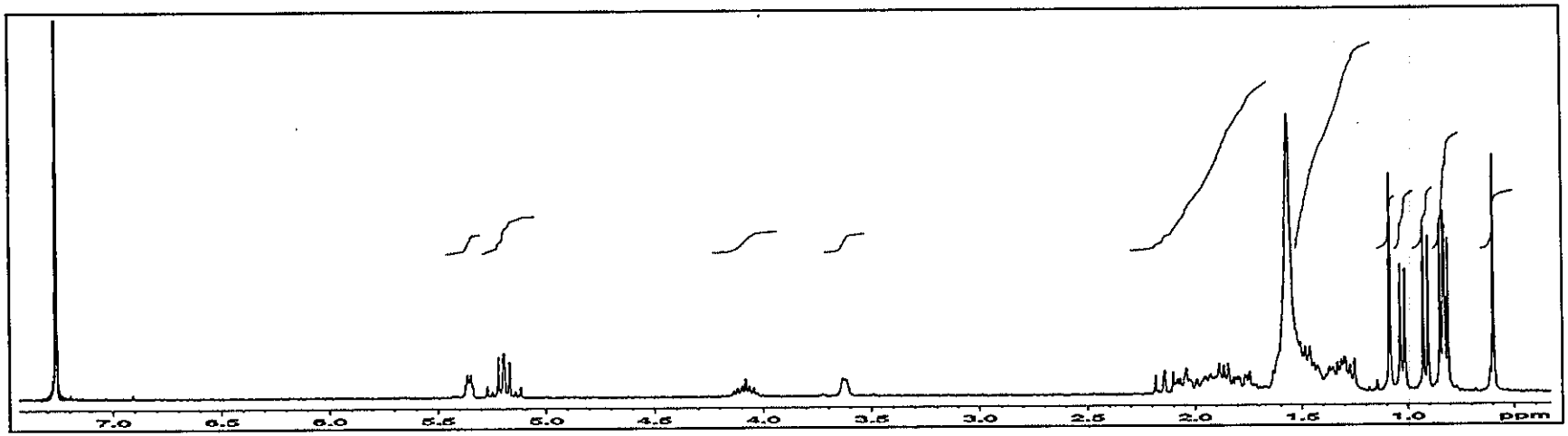

Figure 76 ^{1}H NMR (300 MHz) ($CDCl_3$) spectrum of compound **N29**

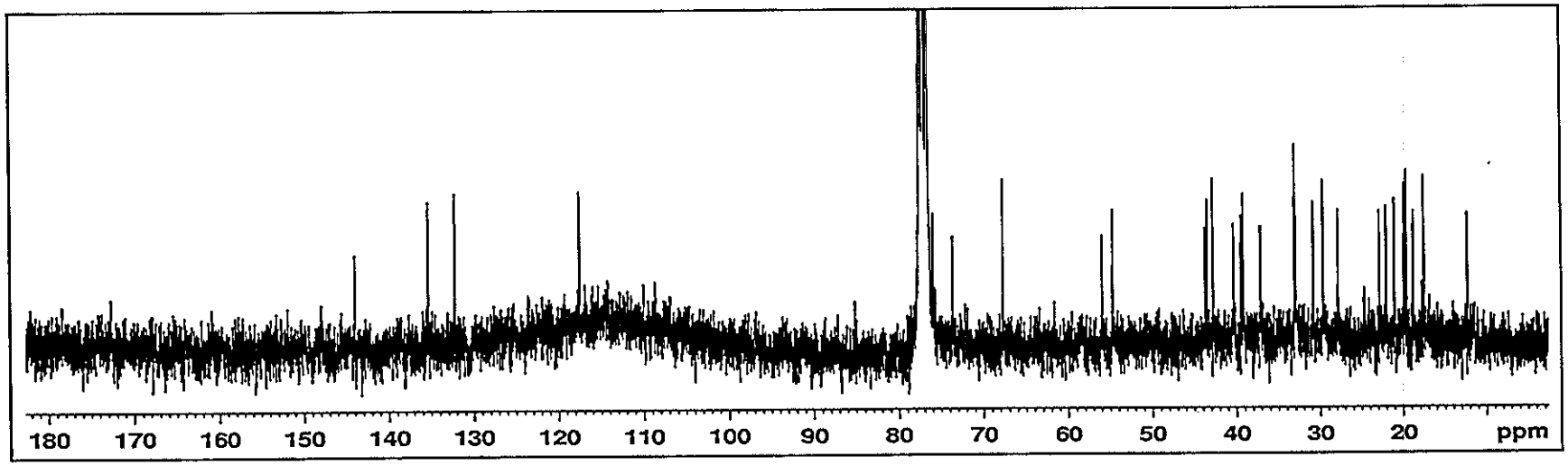

Figure 77 ^{13}C NMR (75 MHz) ($CDCl_3$) spectrum of compound **N29**

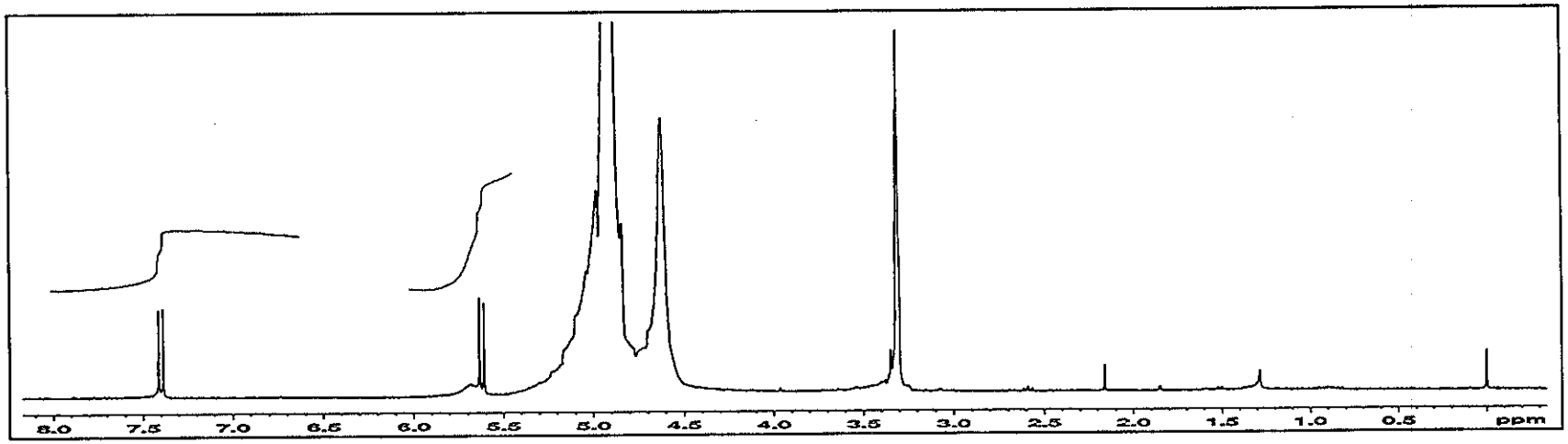

Figure 78 ^{1}H NMR (300 MHz) (CD_3OD) spectrum of compound **N30**

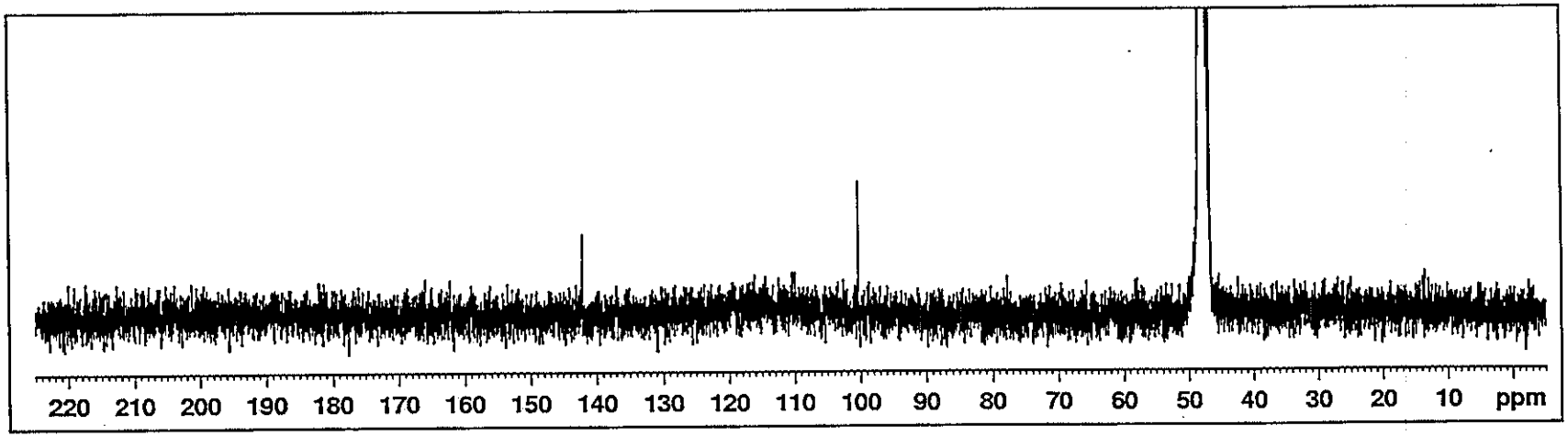

Figure 79 ^{13}C NMR (75 MHz) (CD_3OD) spectrum of compound **N30**

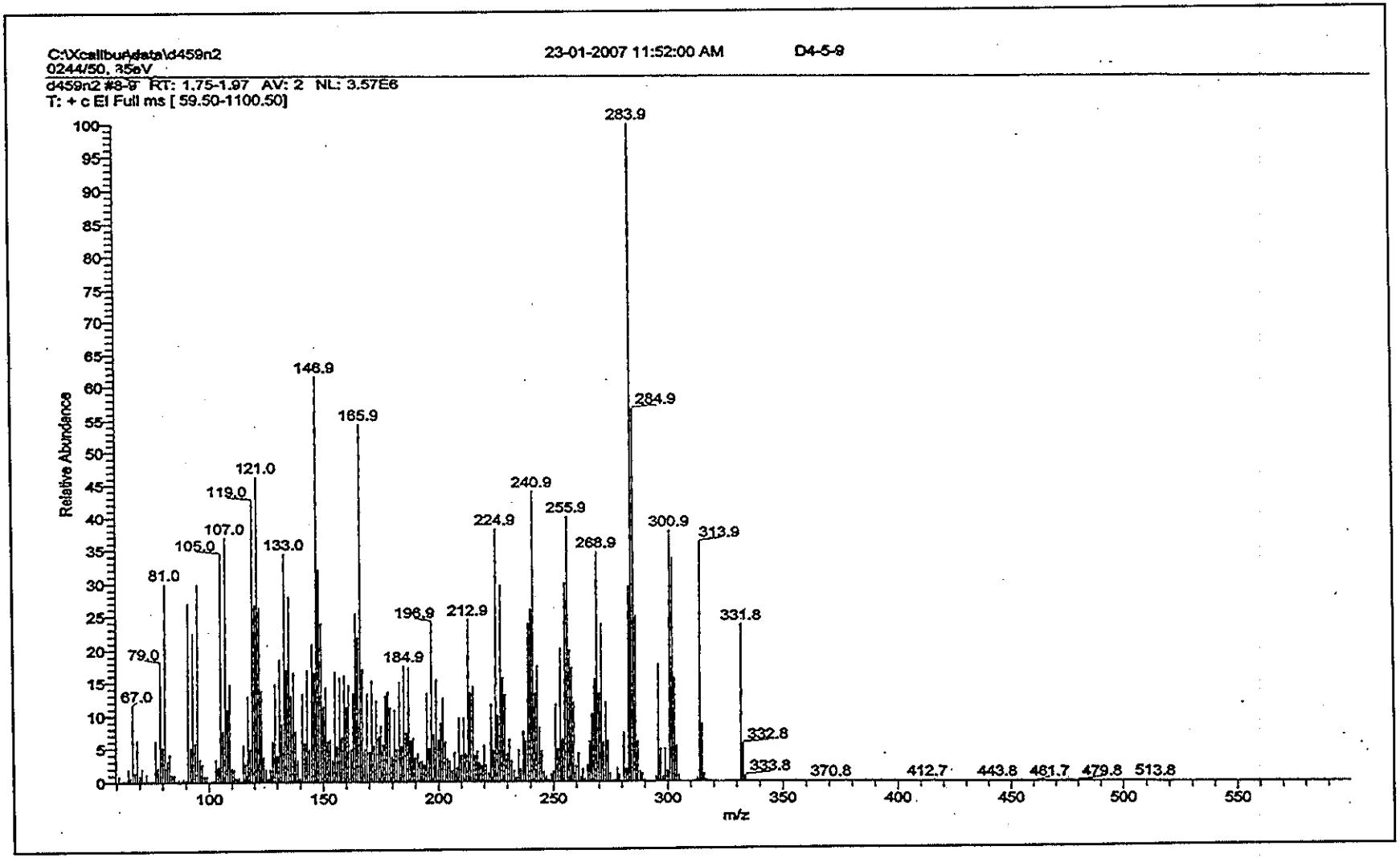

Figure 80 Mass spectrum of compound N33

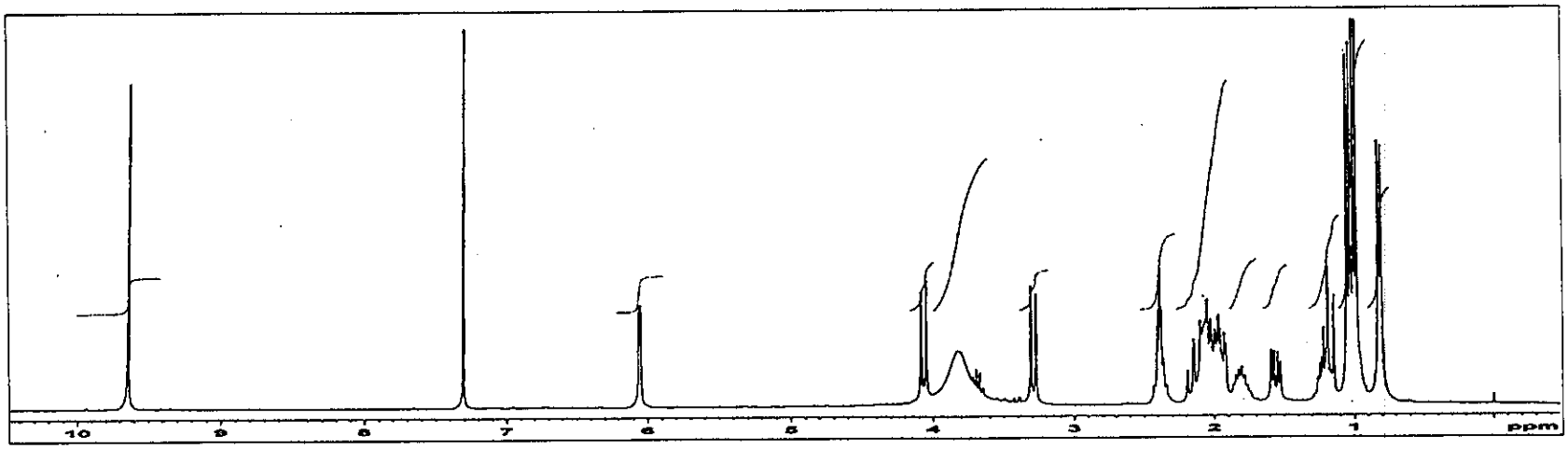

Figure 81 ^{1}H NMR (300 MHz) ($CDCl_3$+CD_3OD) spectrum of compound **N33**

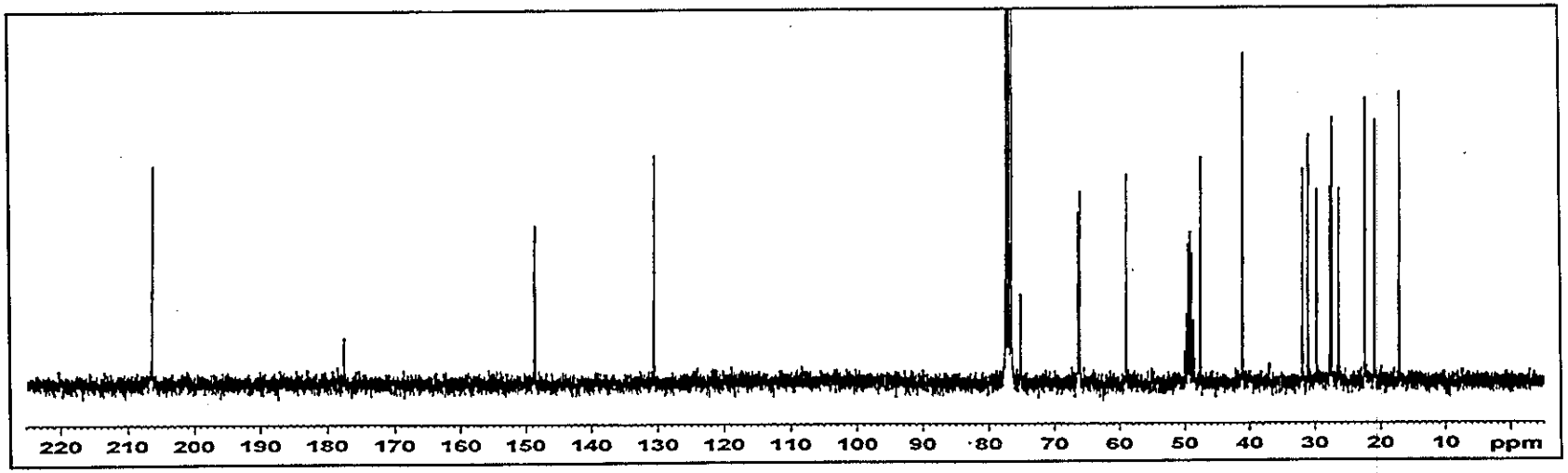

Figure 82 ^{13}C NMR (75 MHz) ($CDCl_3$+CD_3OD) spectrum of compound **N33**

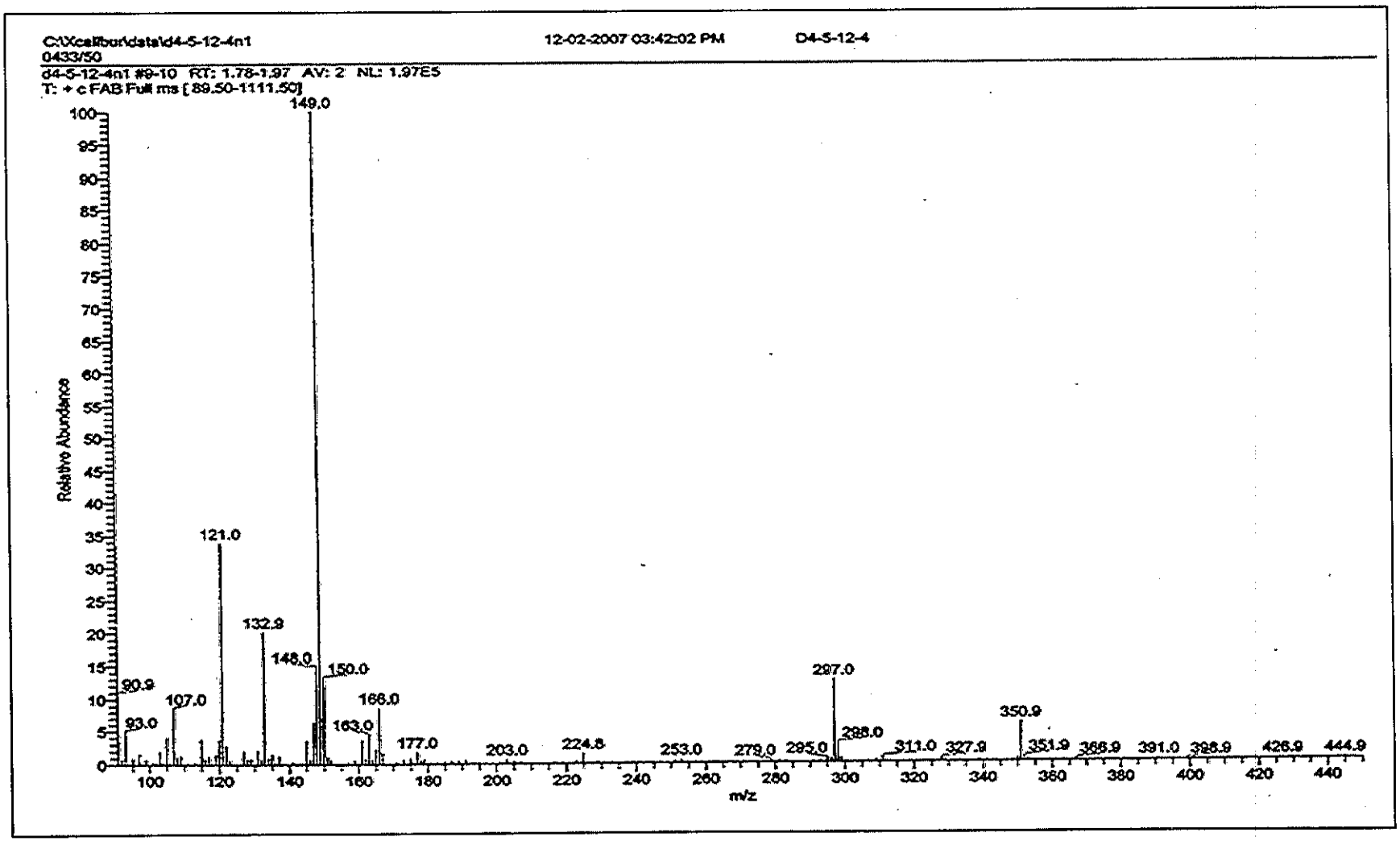

Figure 83 Mass spectrum of compound N34

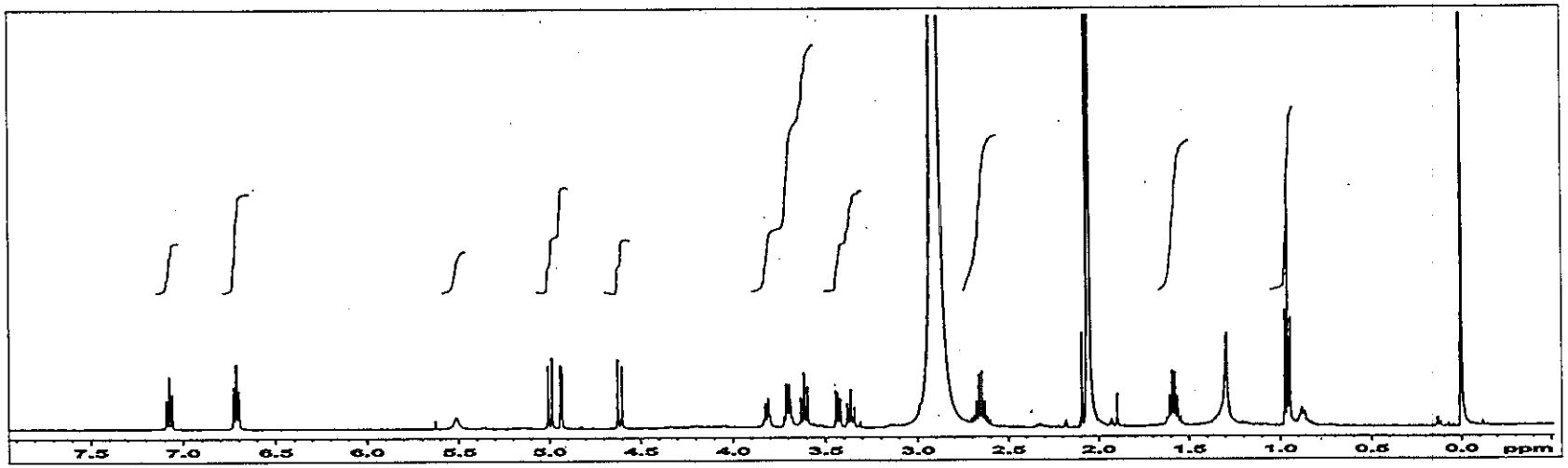

Figure 84 ^{1}H NMR (500 MHz) (Acetone-d_6) spectrum of compound N34

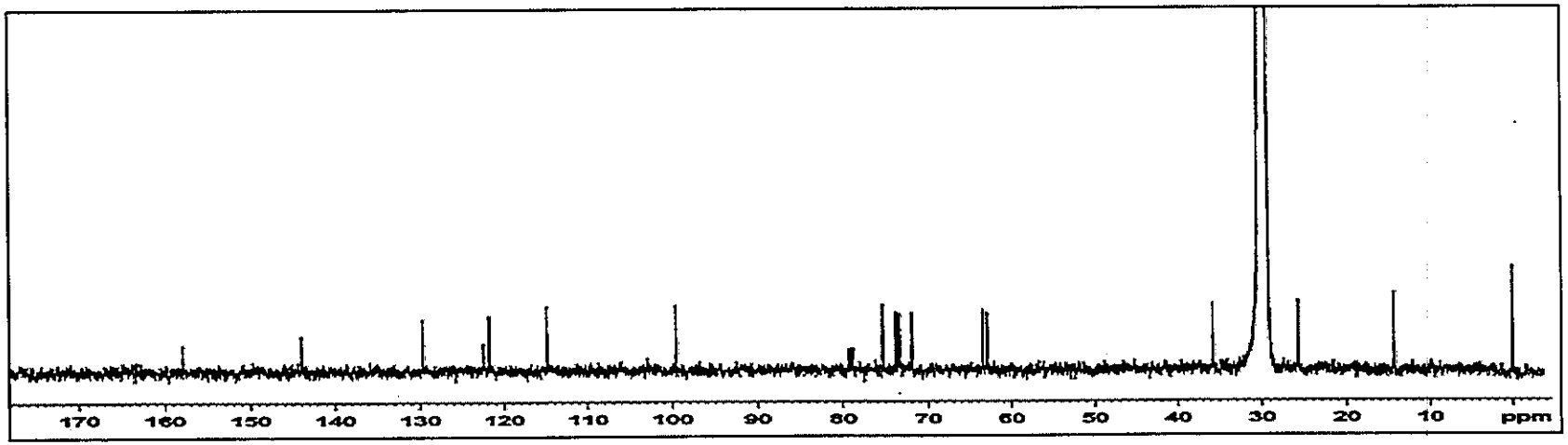

Figure 85 ^{13}C NMR (125 MHz) (Acetone-d_6) spectrum of compound N34

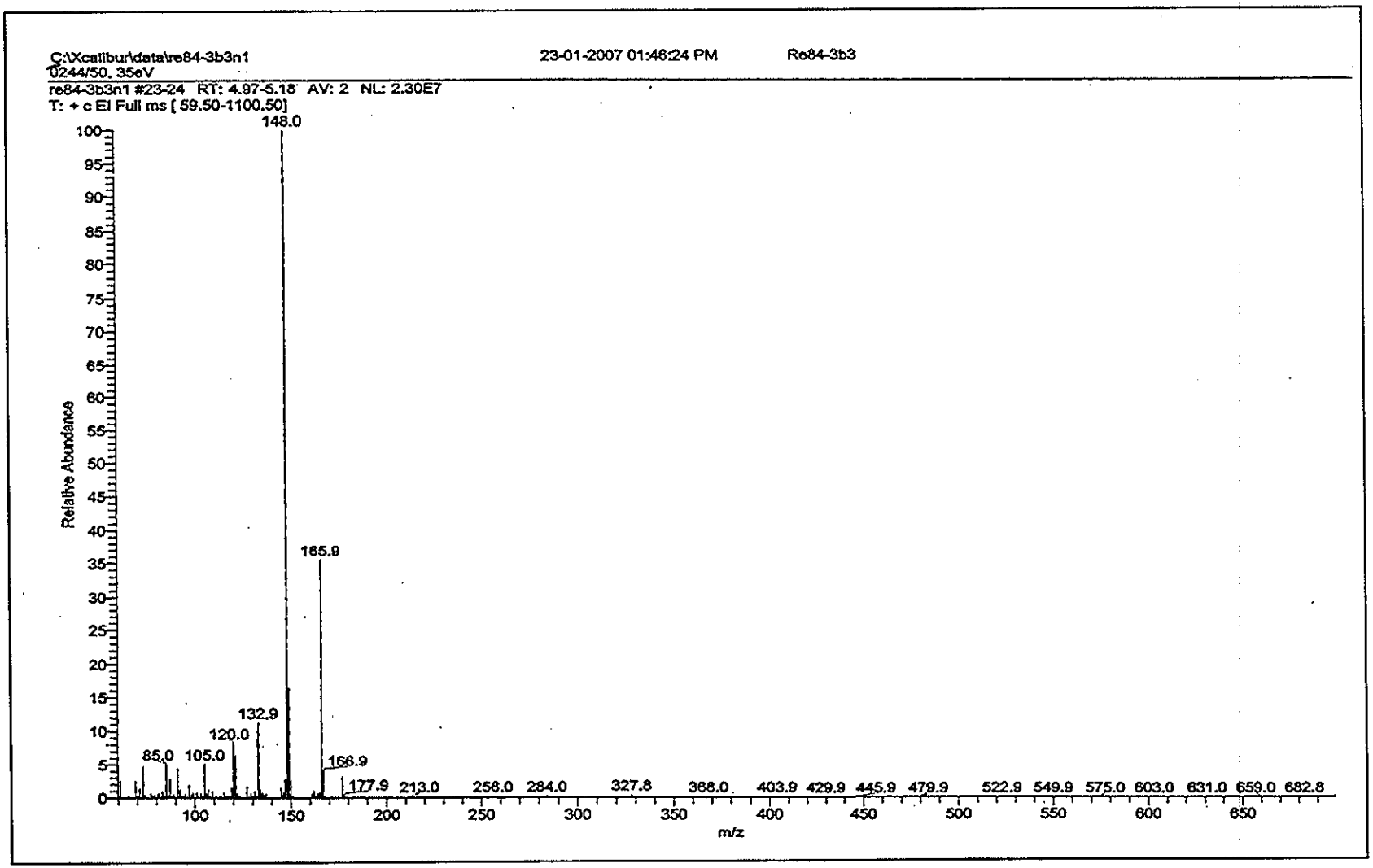

Figure 86 Mass spectrum of compound N35

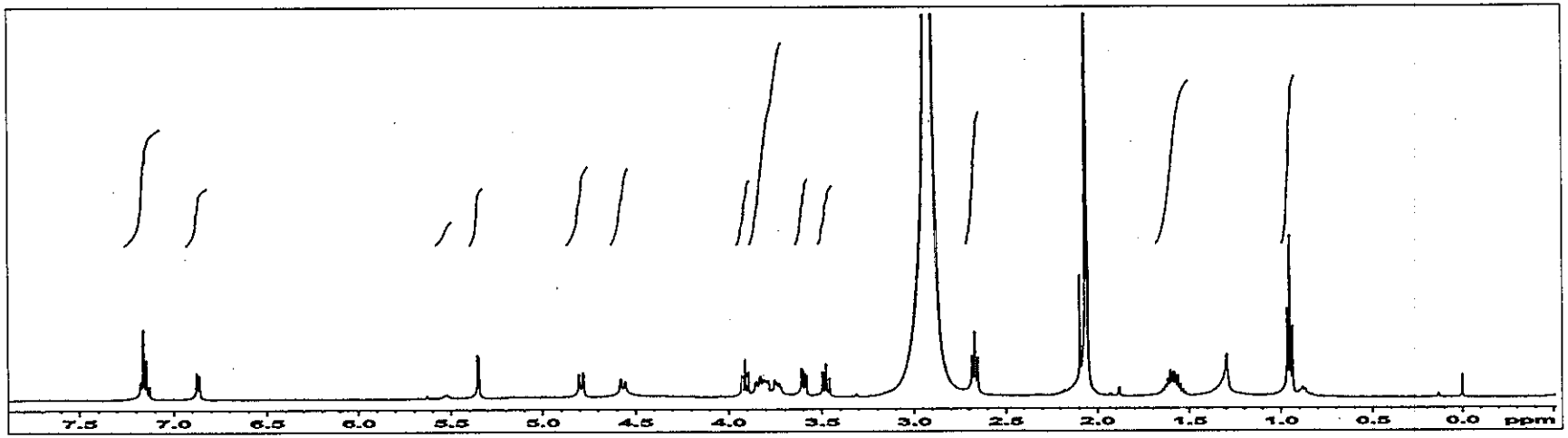

Figure 87 ^{1}H NMR (500 MHz) (Acetone-d_6) spectrum of compound **N35**

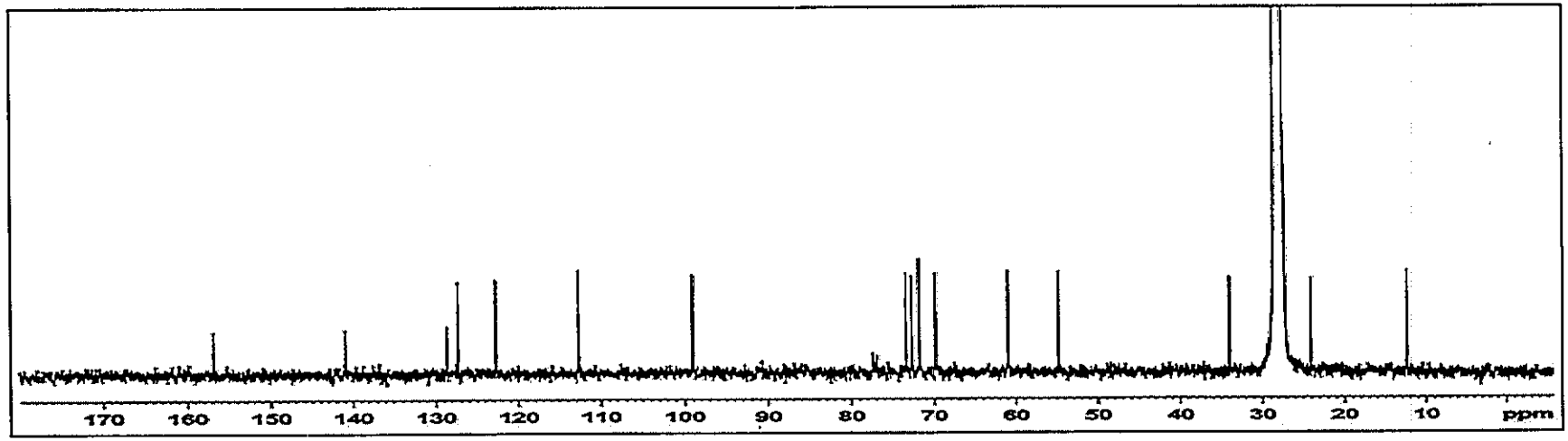

Figure 88 ^{13}C NMR (125 MHz) (Acetone-d_6) spectrum of compound **N35**

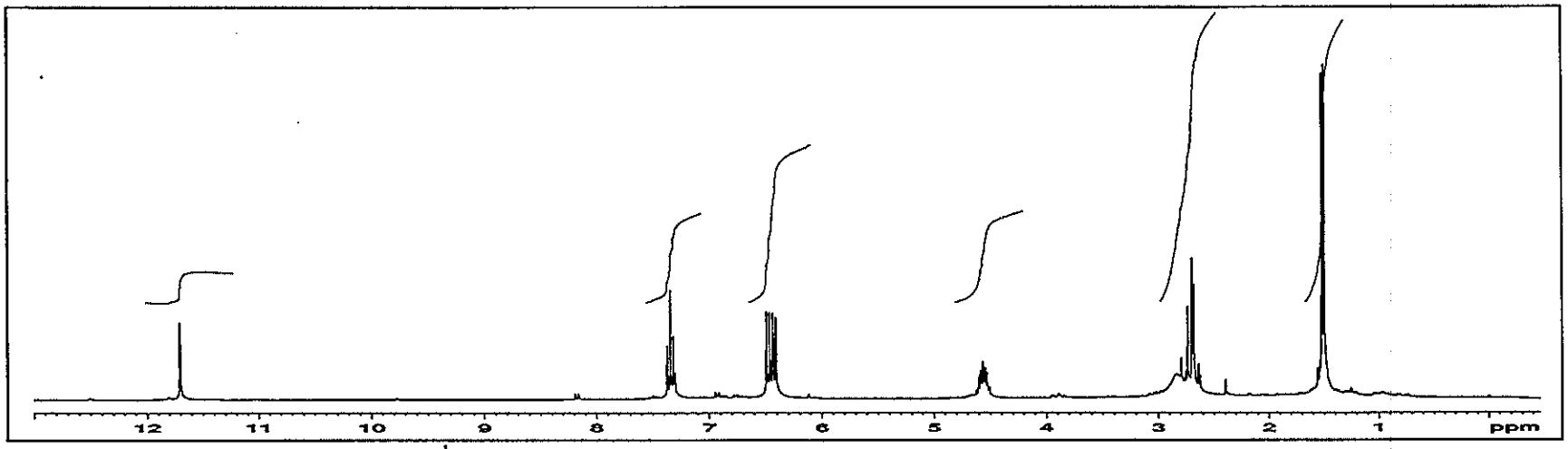

Figure 89 ^{1}H NMR (300 MHz) ($CDCl_3$+CD_3OD) spectrum of compound **N36**

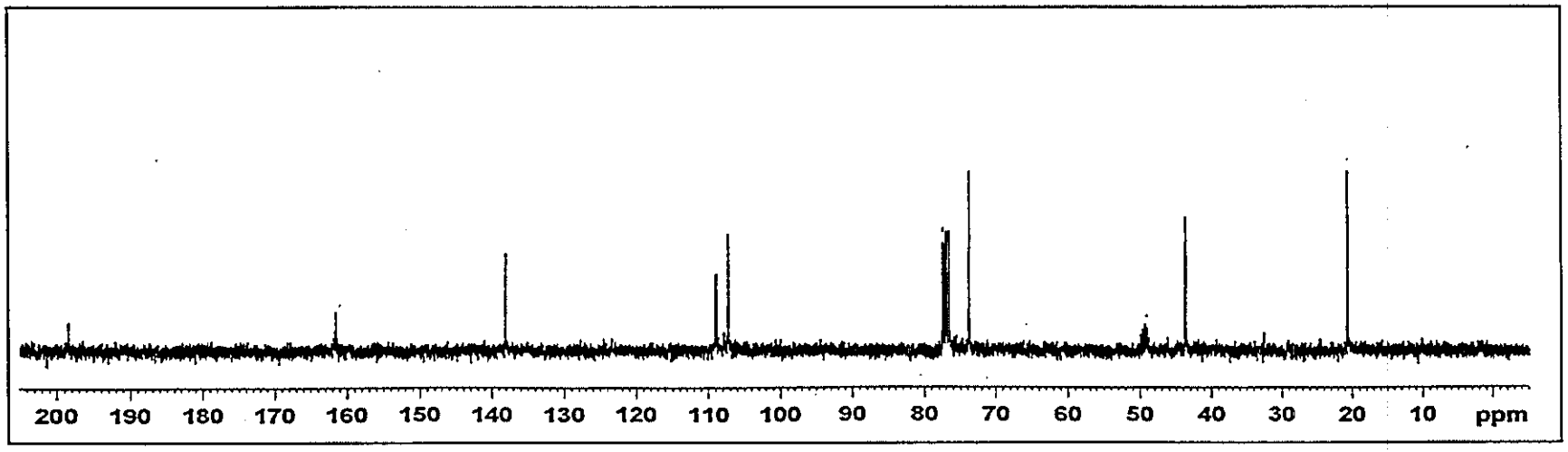

Figure 90 ^{13}C NMR (75 MHz) ($CDCl_3$+CD_3OD) spectrum of compound **N36**

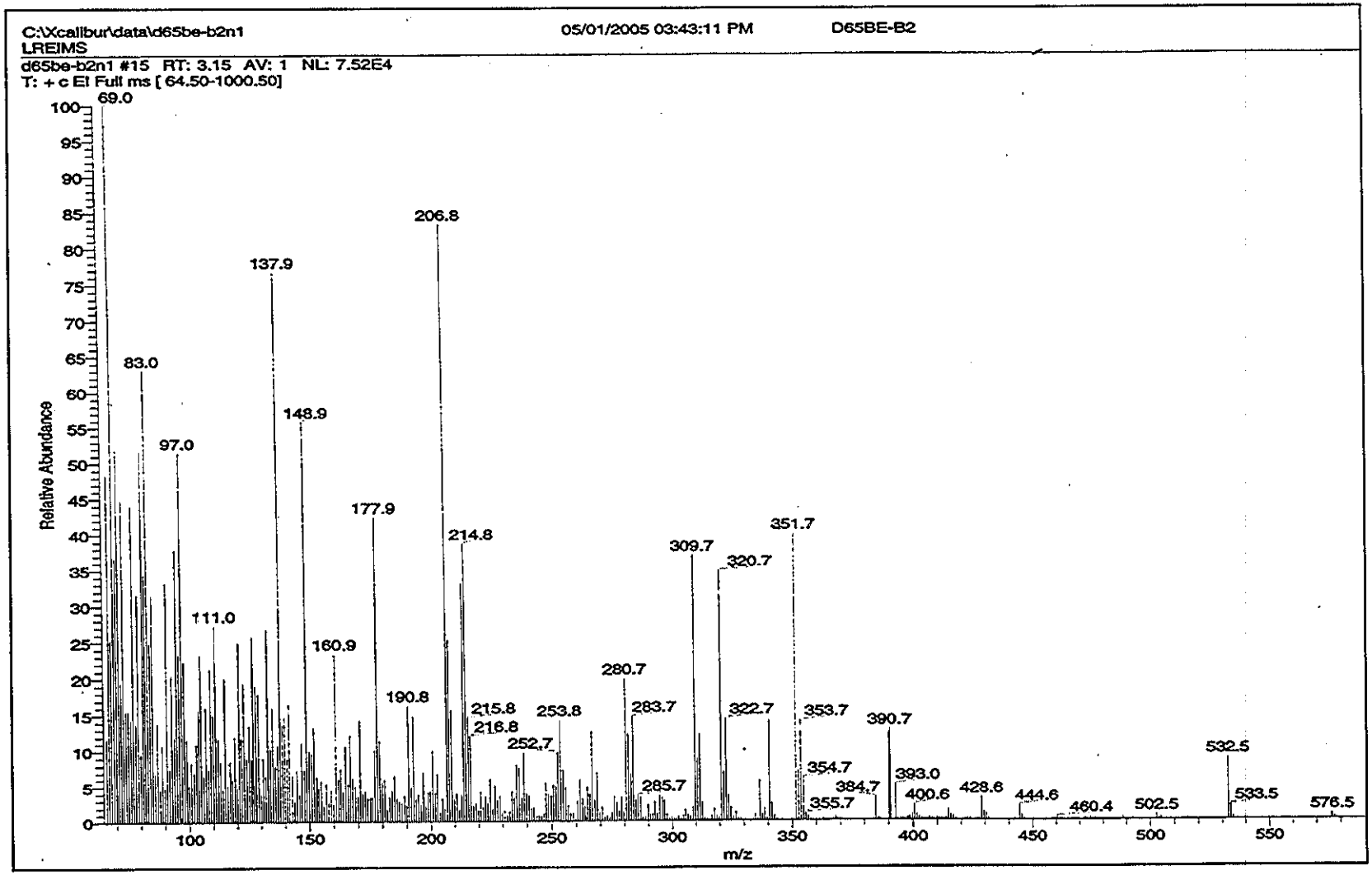

Figure 91 Mass spectrum of compound N37

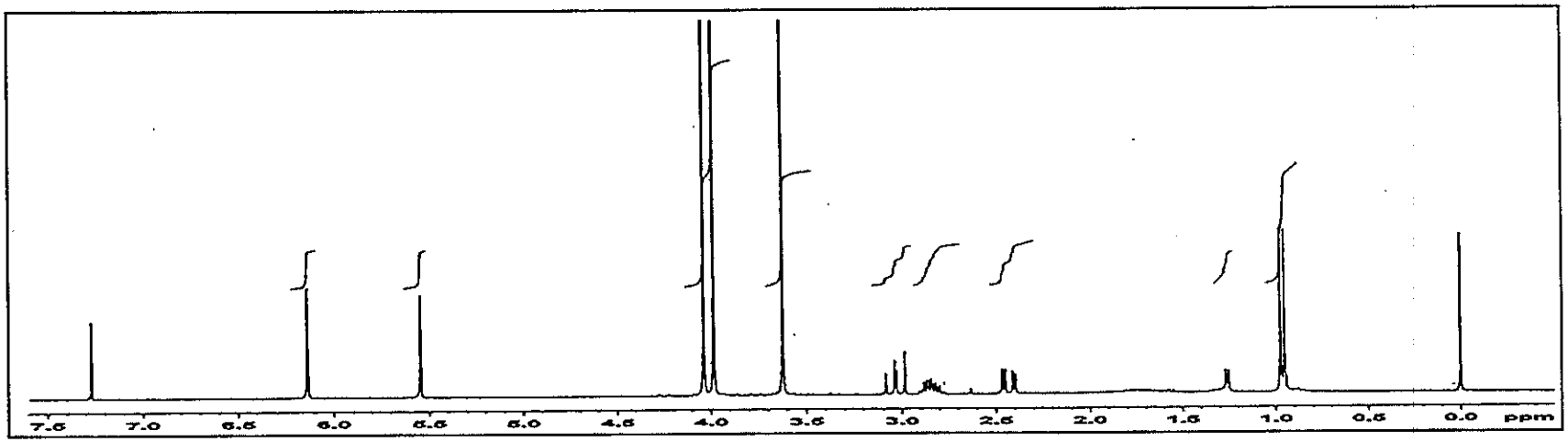

Figure 92 ^{1}H NMR (300 MHz) ($CDCl_3$) spectrum of compound **N37**

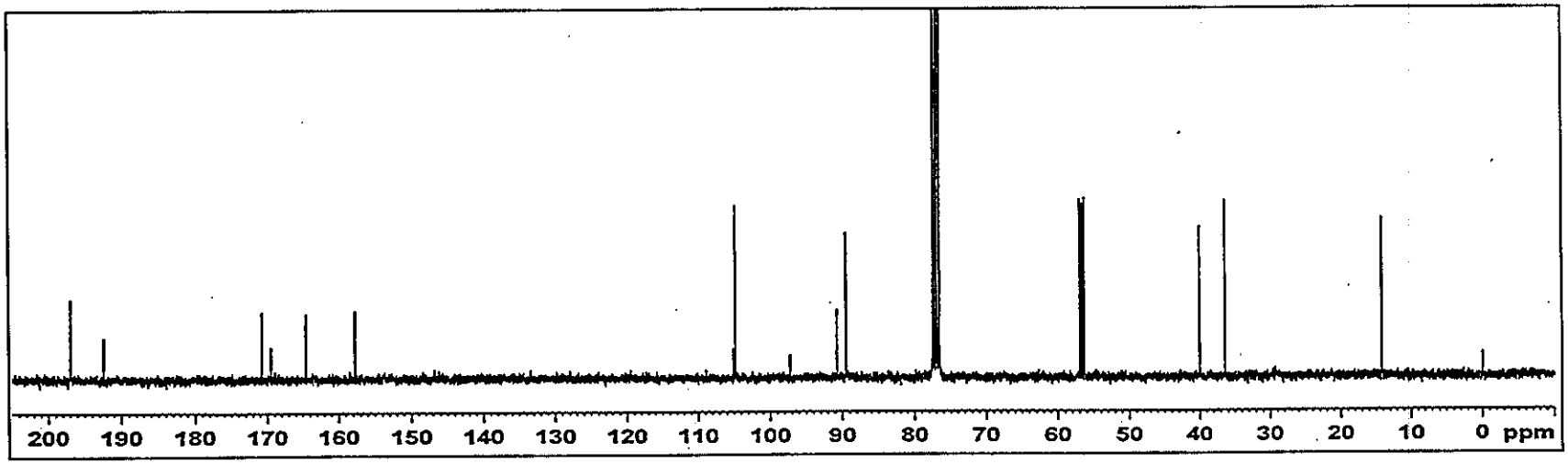

Figure 93 ^{13}C NMR (75 MHz) ($CDCl_3$) spectrum of compound **37**

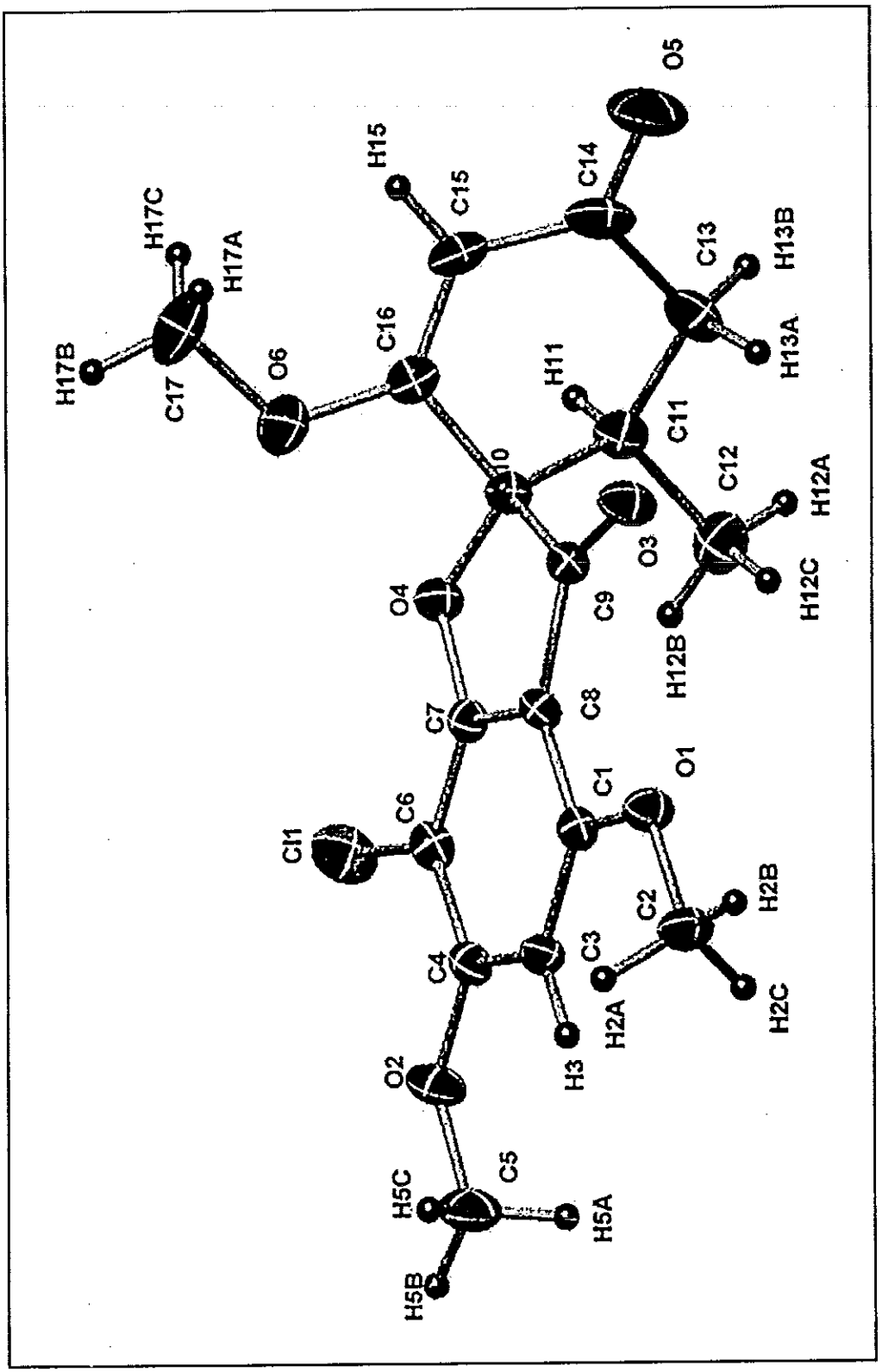

Figure 94 X-ray structure of compound N37

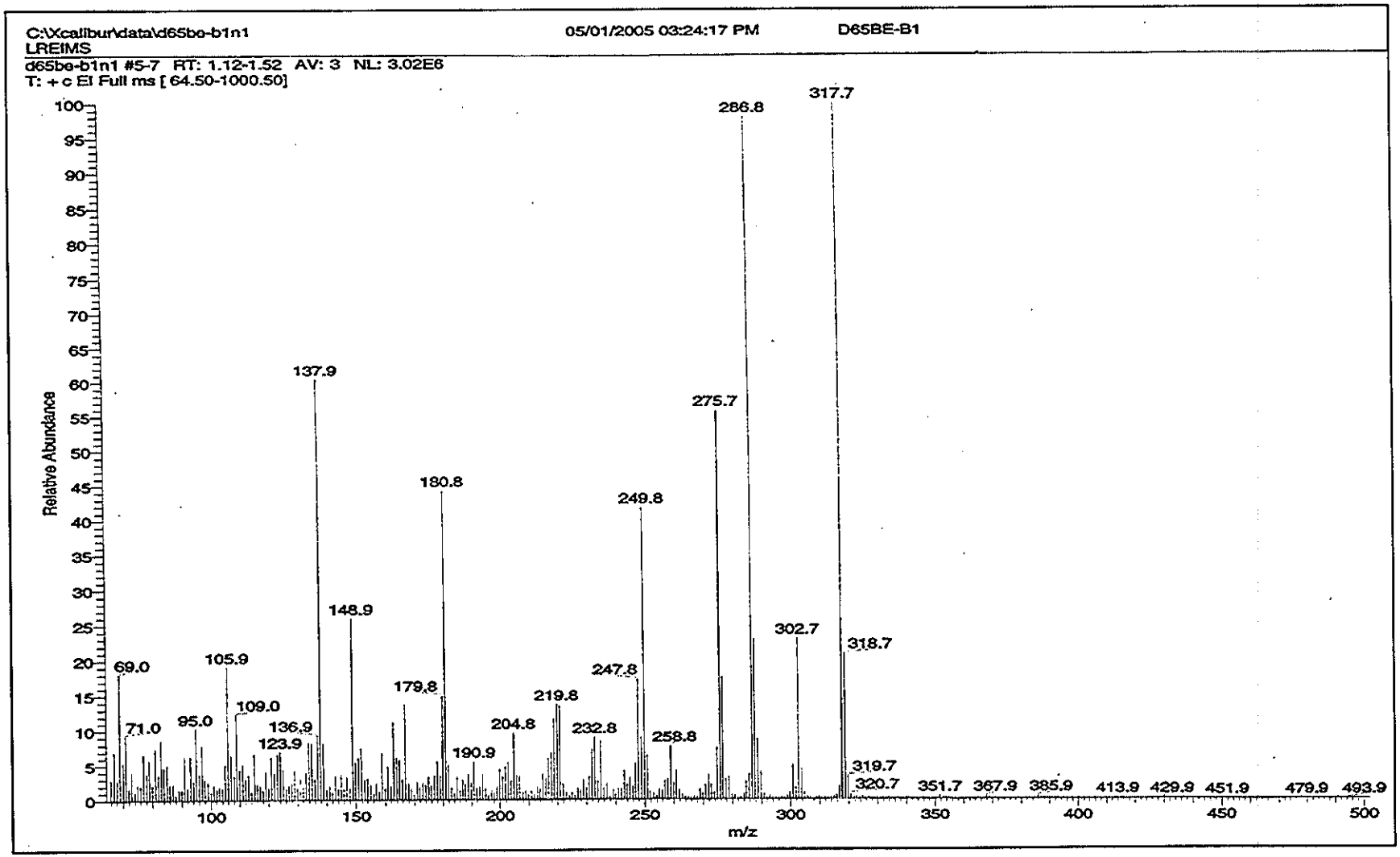

Figure 95 Mass spectrum of compound **N38**

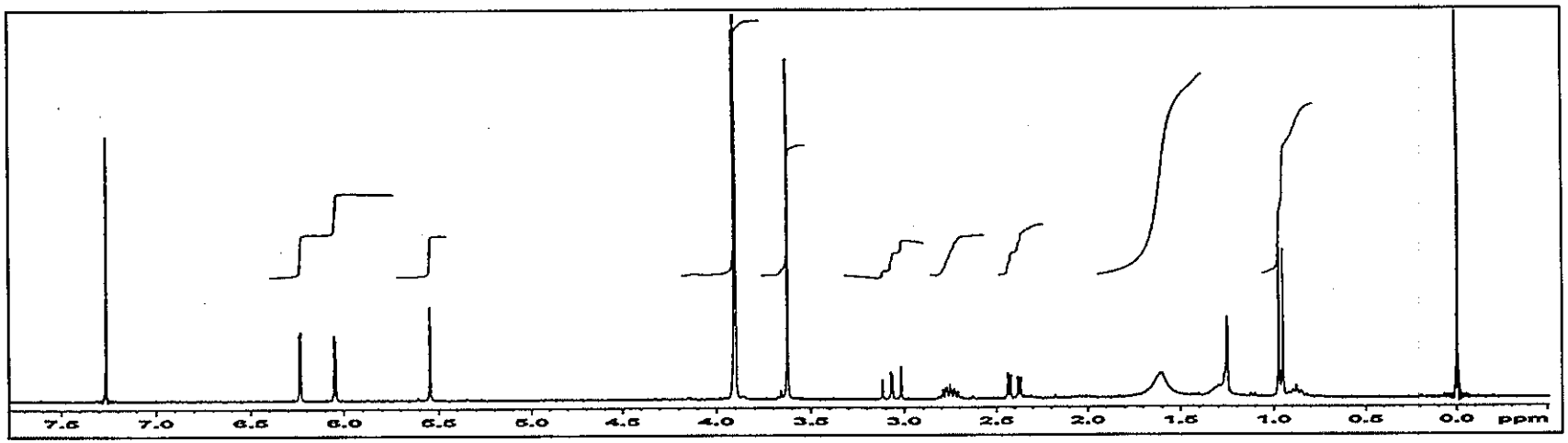

Figure 96 ^{1}H NMR (300 MHz) ($CDCl_3$) spectrum of compound **N38**

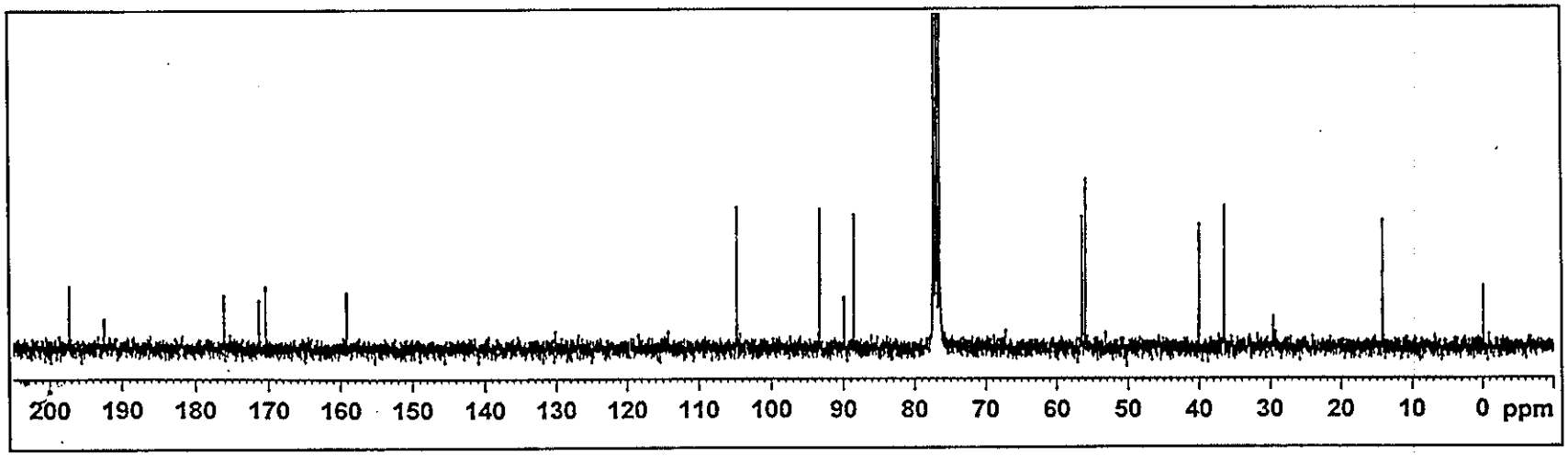

Figure 97 ^{13}C NMR (75 MHz) ($CDCl_3$) spectrum of compound **N38**

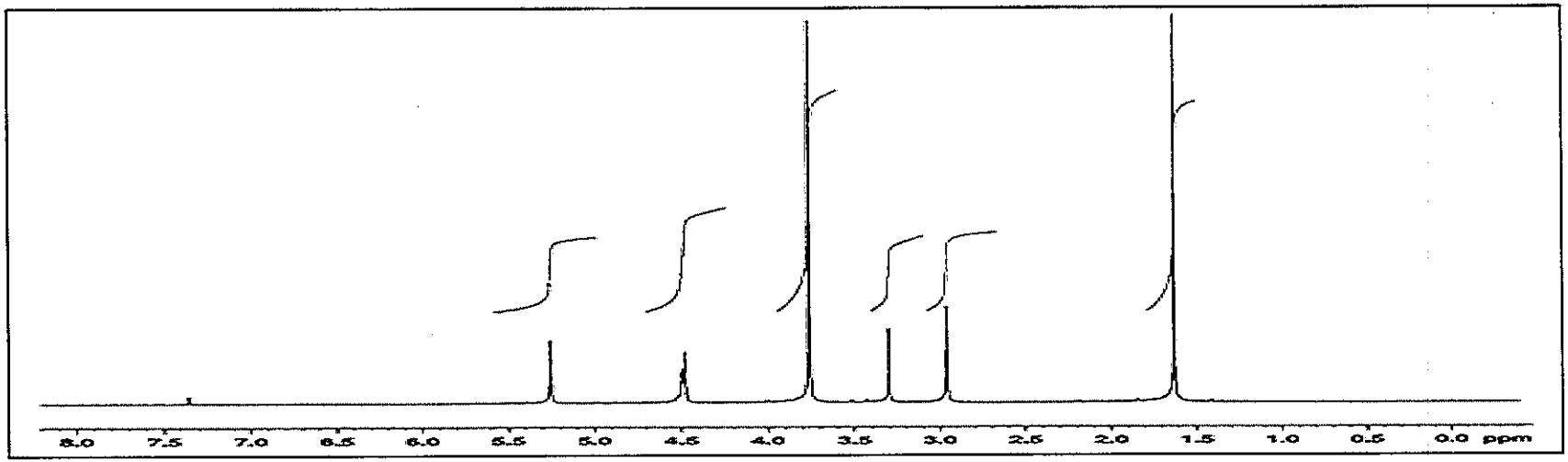

Figure 98 ^{1}H NMR (300 MHz) ($CDCl_3$+CD_3OD) spectrum of compound **N39**

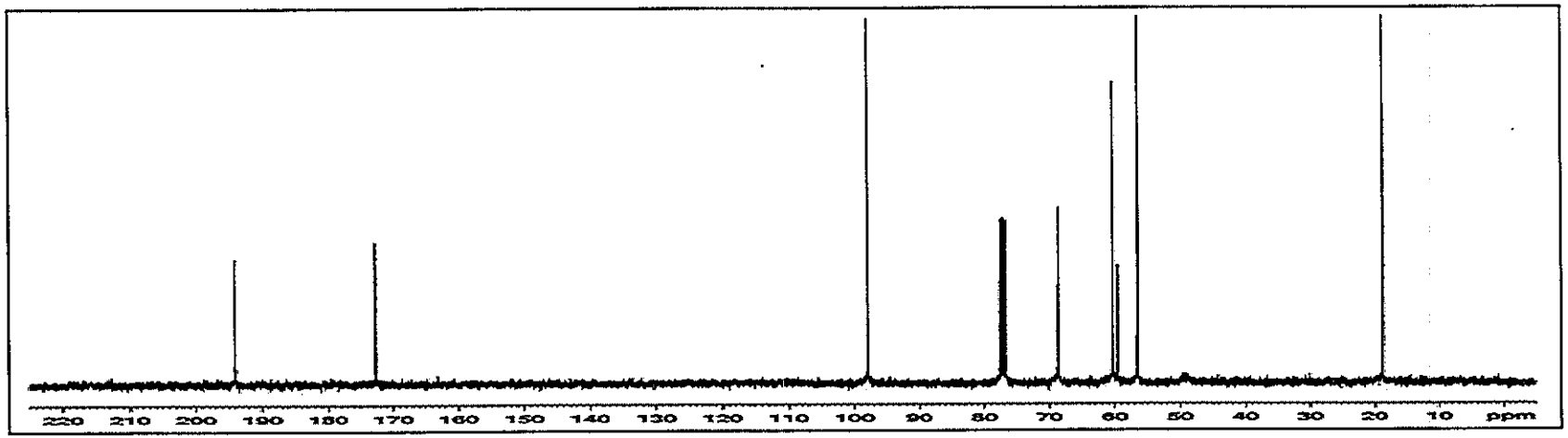

Figure 99 ^{13}C NMR (75 MHz) ($CDCl_3$+CD_3OD) spectrum of compound **N39**

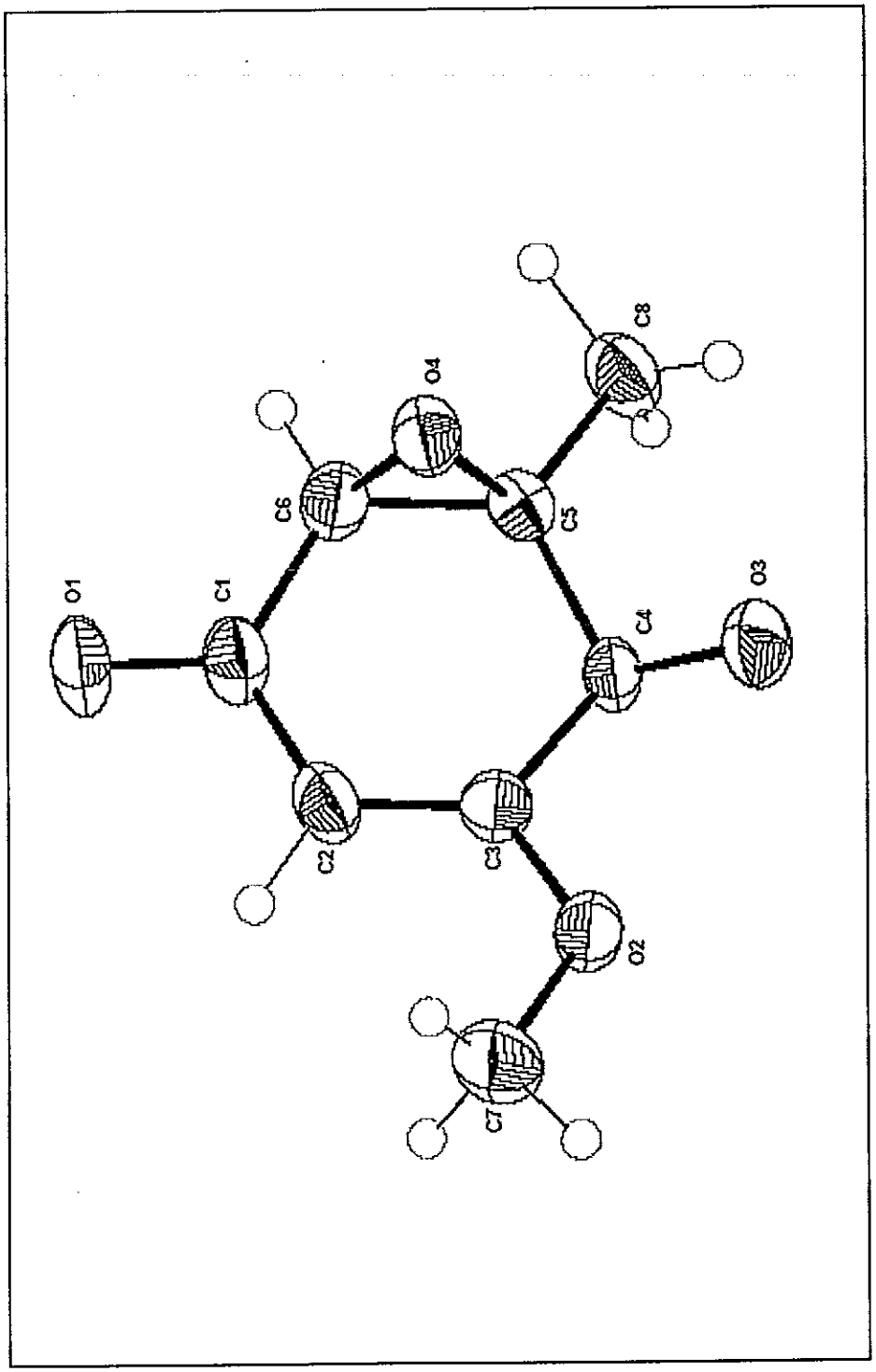

Figure 100 X-ray structure of compound N39

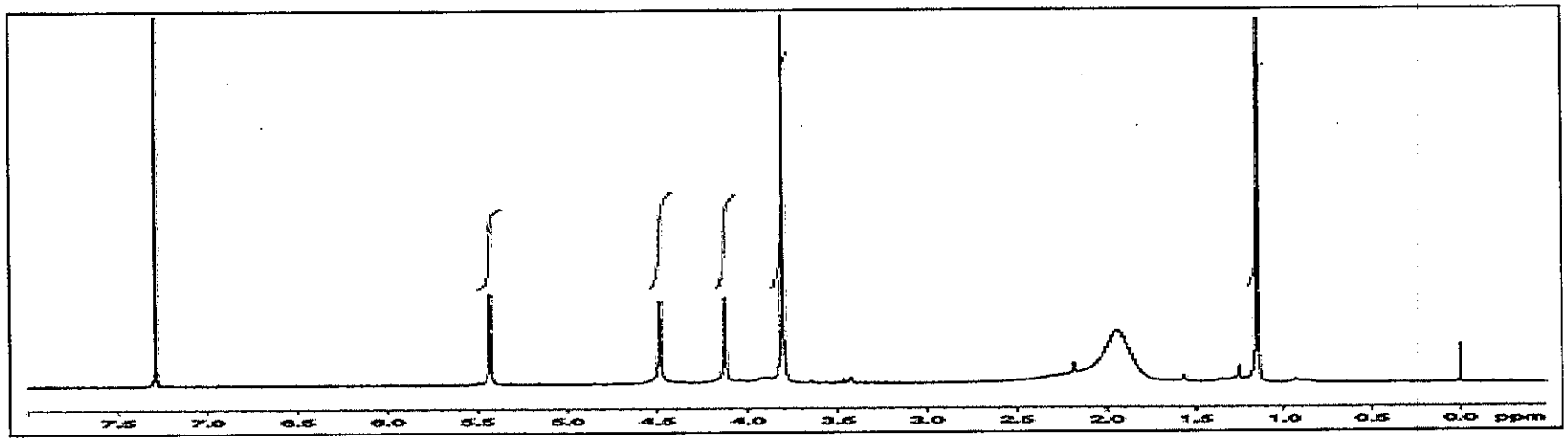

Figure 101 ^{1}H NMR (300 MHz) ($CDCl_3$+CD_3OD) spectrum of compound **N42**

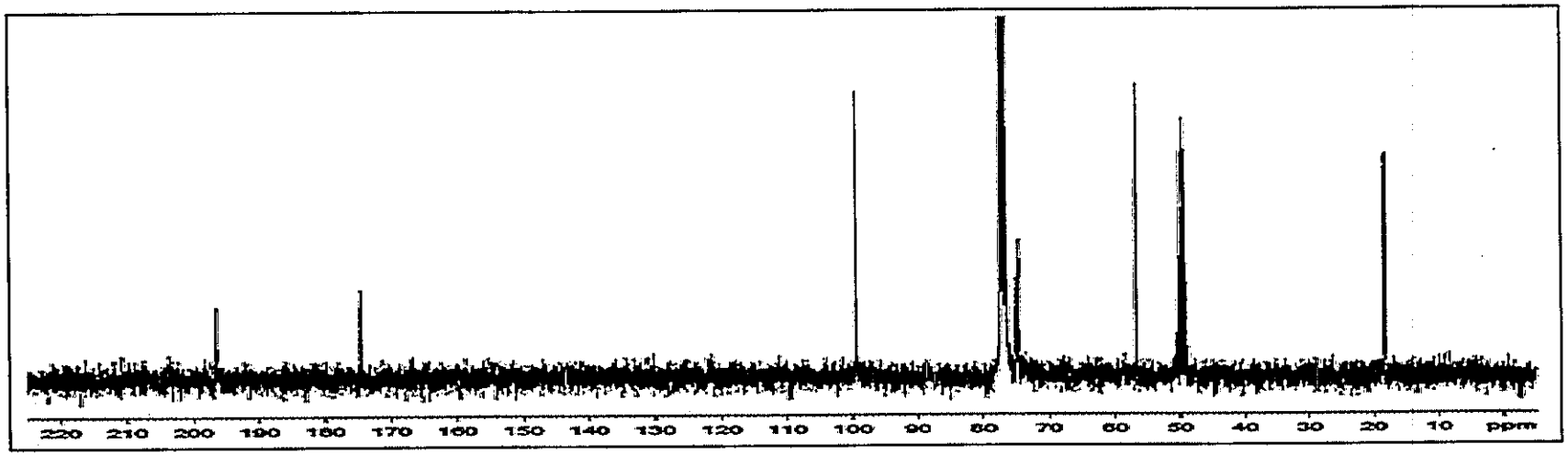

Figure 102 ^{13}C NMR (75 MHz) ($CDCl_3$+CD_3OD) spectrum of compound **N42**

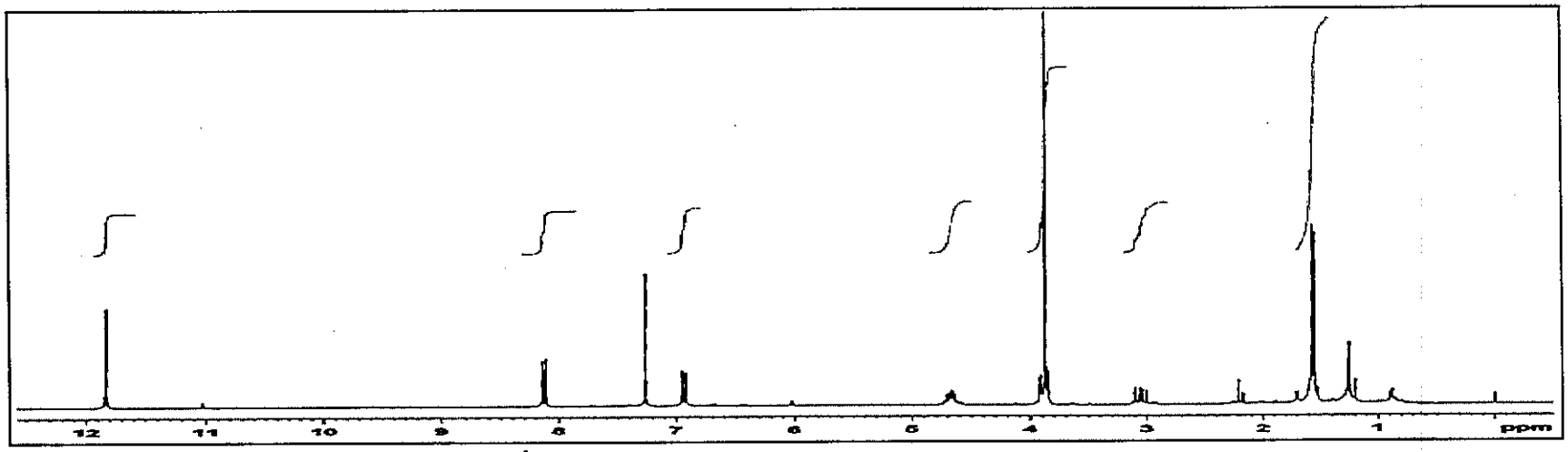

Figure 103 ^{1}H NMR (300 MHz) ($CDCl_3$) spectrum of compound **N40**

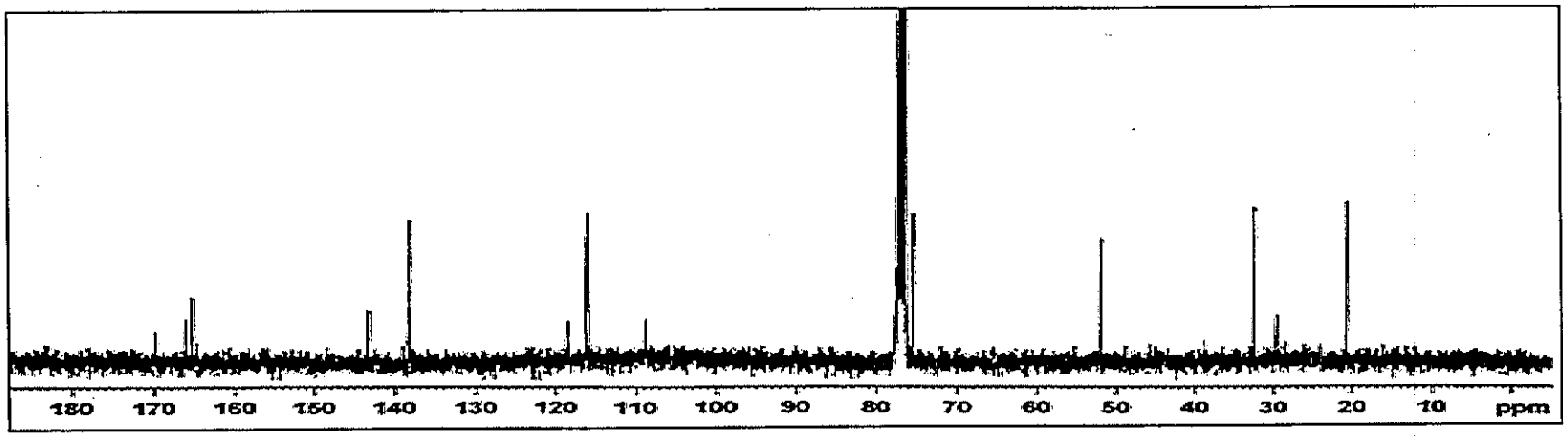

Figure 104 ^{13}C NMR (75 MHz) ($CDCl_3$) spectrum of compound **N40**

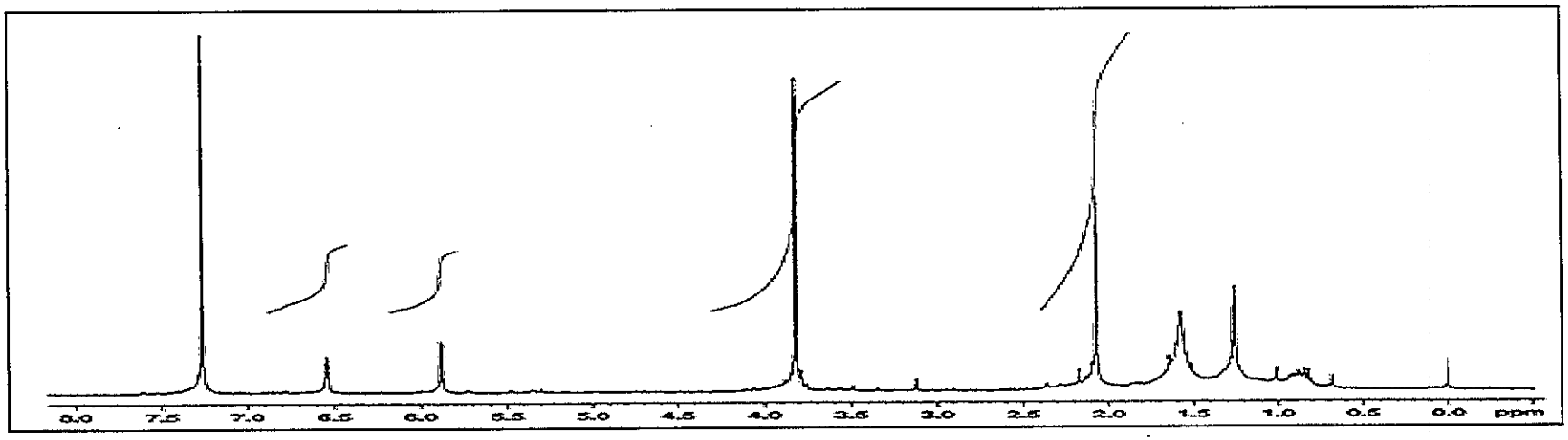

Figure 105 ^{1}H NMR (300 MHz) ($CDCl_3$) spectrum of compound **N41**

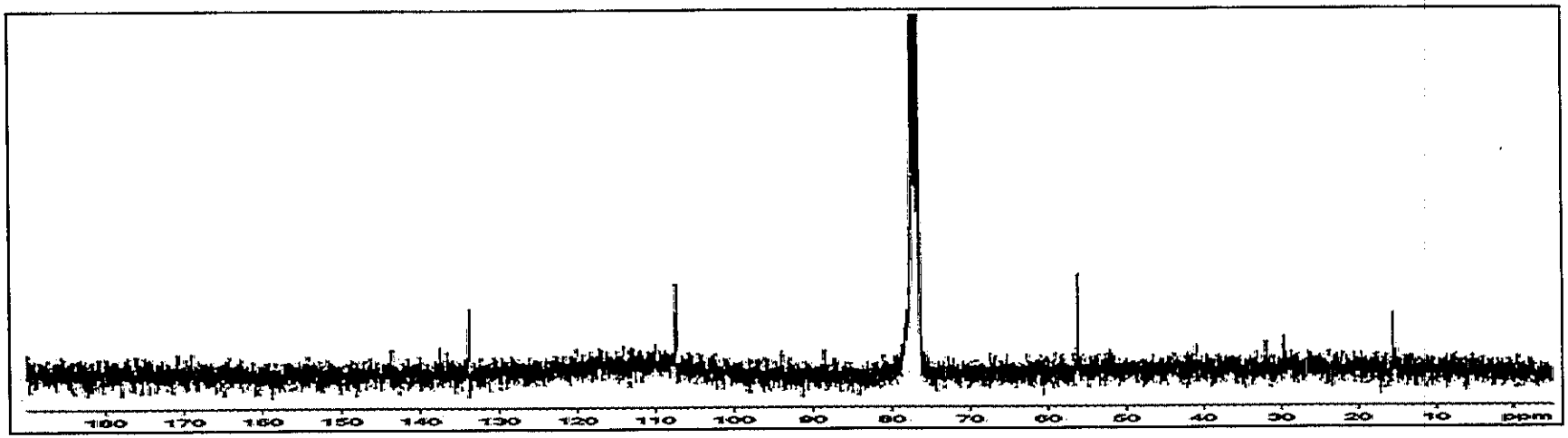

Figure 106 ^{13}C NMR (75 MHz) ($CDCl_3$) spectrum of compound **N41**

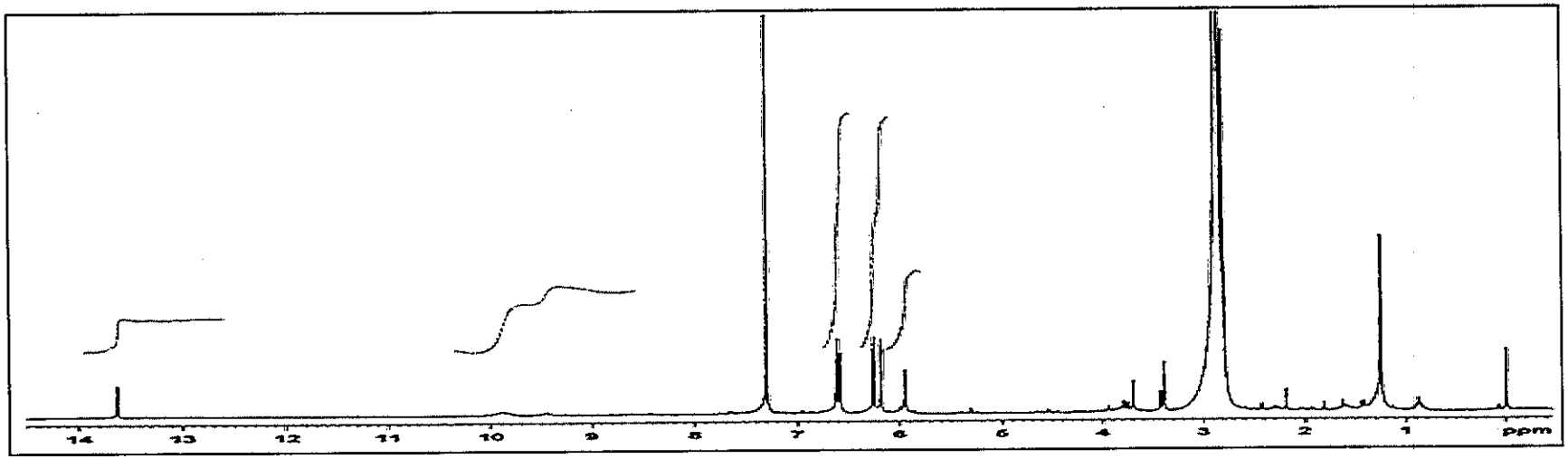

Figure 107 ^{1}H NMR (300 MHz) ($CDCl_3$+CD_3OD) spectrum of compound **N43**

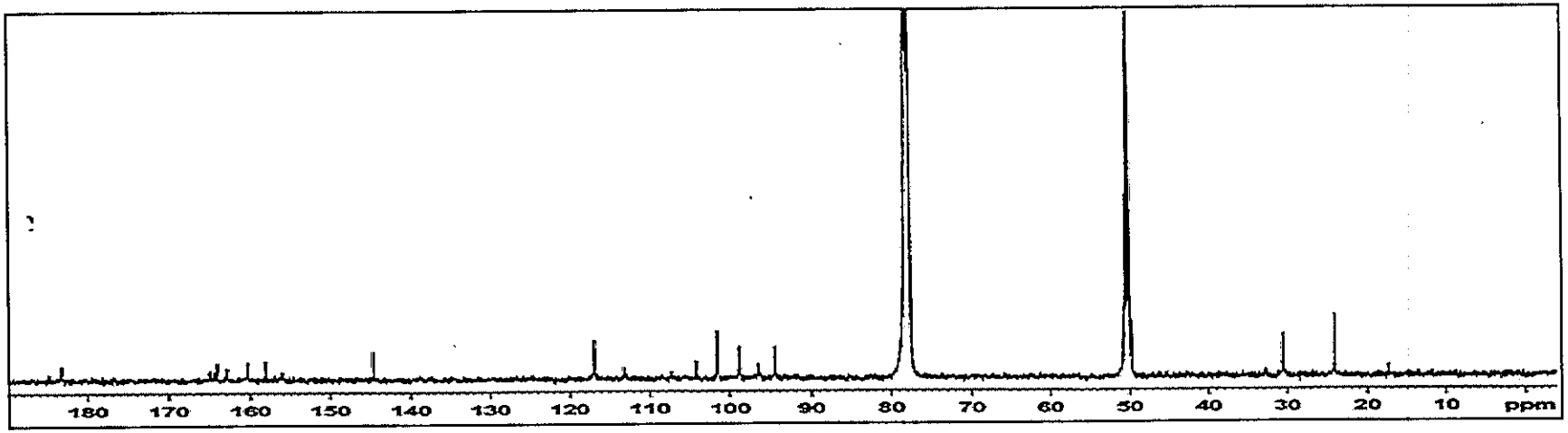

Figure 108 ^{13}C NMR (75 MHz) ($CDCl_3$+CD_3OD) spectrum of compound **N43**

VITAE

Name Miss Wipapan Pongcharoen

Student ID 4823006

Educational Attainment

Degree	Name of Institution	Year of Graduation
B.Sc (2nd Hons.) (Chemistry)	Thaksin University	2002
M.Sc. (Organic Chemistry)	Prince of Songkla University	2004

Scholarship Awards during Enrolment

1. The Royal Golden Jubilee Ph.D. Program of the Thailand Research Fund (Grant No. PHD/0218/2547)
2. The Center for Innovation in Chemistry: Postgraduate Education and Research Program in Chemistry (PERCH-CIC)

List of Publications and Proceedings

Publications

1. Panthong, K., Pongcharoen, W., Phongpaichit, S. and Taylor, W.C. 2006. Tetraoxygenated Xanthones from the Fruits of *Garcinia cowa*. Phytochemistry. 67, 999-1004.
2. Pongcharoen, W., Rukachaisirikul, V., Phongpaichit, S., Rungjindamai, N. and Sakayaroj, J. 2006. Pimarane Diterpene and Cytochalasin Derivatives from the Endophytic Fungus *Eutypella scoparia* PSU-D44. J. Nat. Prod. 69, 856-858.
3. Rukachaisirikul, V., Chantaruk, S., Pongcharoen, W., Isaka, M. and Lapanun, S. 2006. Chromone Derivatives from the Filamentous Fungus *Lachnum* sp. BCC 2424. J. Nat. Prod. 69, 980-982.

4. Pongcharoen, W., Rukachaisirikul, V., Phongpaichit, S. and Sakayaroj, J. 2007. A New Dihydrobenzofuran Derivative from the Endophytic Fungus *Botryosphaeria mamane* PSU-M76. Chem. Pharm. Bull. 55, 1404-1405.
5. Pongcharoen, W., Rukachaisirikul, V., Isaka, M. and Sriklung, K. 2007. Cytotoxic Metabolites from the Wood-decayed Fungus *Xylaria* sp. BCC 9653. Chem. Pharm. Bull. 55, 1647-1648.
6. Pongcharoen, W., Rukachaisirikul, V., Phongpaichit, S., Kühn, T., Pelzing, M., Sakayaroj, J. and Taylor, W.C. 2008. Metabolites from the Endophytic Fungus *Xylaria* sp. PSU-D14. Phytochemistry. *in press*.

Proceedings

1. Pongcharaen, W., Panthong. K. and Rukachaisirikul, V. 2004. Chemical Constituents from the Fruits of *Garcinia cowa*. Proceeding of the 30th Congress on Science and Technology of Thailand, October 19-21, 2004. pp. 85. (Oral Presentation)
2. Pongcharoen, W., Rukachaisirikul, V., Pakawatchai, C., Phongpaichit, S., Rungjindamai, N. and Sakayaroj, J. 2005. Chemical Constituents from the Endophytic Fungus *Eutypella scoparia* PSU-D44. Proceeding of the 31st Congress on Science and Technology of Thailand, October 18-20, 2005. pp. 130-131. (Oral Presentation)
3. Pongcharoen, W., Rukachaisirikul, V., Phongpaichit, S., Rungjindamai, N. and Sakayaroj, J. 2006. Chemical Constituents from the Endophytic Fungus *Botryosphaeria mamane* PSU-M76. Proceeding of the 32nd Congress on Science and Technology of Thailand, October 10-12, 2006. pp 177. (Poster Presentation)
4. Pongcharoen, W., Rukachaisirikul, V. and Isaka, M. 2007. Chemical Constituents from the Fungus *Xylaria* sp. BCC 9653. Proceeding of the PERCH-CIC Congress V, May 6-9, 2007. pp. 205. (Poster Presentation)
5. Pongcharoen, W., Rukachaisirikul, V., Phongpaichit, S. and Sakayaroj, J. 2007. Chemical Constituents from the Endophytic Fungus *Xylaria* sp. PSU-D14. Proceeding of the 33rd Congress on Science and Technology of Thailand, October 18-20, 2007. pp. 170. (Poster Presentation)

6. Pongcharoen, W., Rukachaisirikul, V., Phongpaichit, S. and Sakayaroj, J. 2007. Chemical constituents from the endophytic fungus *Xylaria* sp. PSU-D14. Proceeding of the RGJ-Ph.D. Congress IX. April 4-6, 2008. pp. 249. (Poster Presentation)